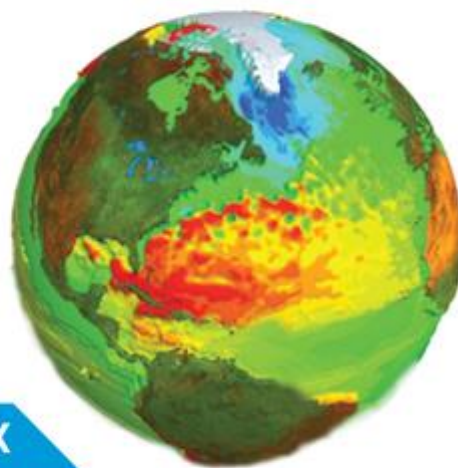


Radar Altimetry Tutorial

brat



BROADVIEW RADAR ALTIMETRY TOOLBOX

October 2018
Issue 3a

V. Rosmorduc, J. Benveniste, E. Bronner, S. Dinardo, O. Lauret, C. Maheu, M. Milagro, N. Picot,
A. Ambrozio, R. Escolà, A. Garcia-Mondejar, E. Schrama, M. Restano, M. Terra-Homem

J. Benveniste, N. Picot, Editors

Radar Altimetry Tutorial

Introduction

Predicting climate, monitoring mean sea level, river and lake levels, global warming, El Niño and La Niña events, marine currents and ocean circulation, tides, geoid estimates, wind, wave and marine meteorology models, ice sheet topography and sea ice extent, etc. Radar altimetry can provide such a wealth of information -- and more -- from its measurements.

This Radar Altimetry Tutorial describes applications, examples (data use cases) and techniques, including standard data processing, as well as the various satellite missions that have carried, are carrying or will carry a radar altimeter onboard, plus a range of altimetry products (data, software and documentation).

A Broadview Radar Altimetry Toolbox is also available. This is a collection of tools and documents designed to facilitate the use of radar altimetry data. It can read most distributed radar altimetry data, from ERS-1 & 2, Topex/Poseidon, Geosat Follow-on, Jason-1 and 2, Envisat, CryoSat-2 to the Sentinel-3 mission, and can perform processing and data editing, extraction of statistics, and visualisation of results.

Acknowledgements & Contributors

Background

The Broadview Radar Altimetry Toolbox (BRAT) and the Radar Altimetry Tutorial (RAT) were originally produced by CLS and S&T in 2006-2011 under contract with ESA and CNES (the toolbox name at the time was called Basic Radar Altimetry Toolbox). Since April 2015 under ESA contract within the SEOM program, with additional support from CNES, the current consortium formed by DEIMOS Engenharia S.A., isardSAT UK, and TU Delft is continuing the work, updating the content of the tutorial and redesigning and improving the toolbox.

Citation

If using this tutorial, please cite:

Rosmorduc, V., J. Benveniste, E. Bronner, S. Dinardo, O. Lauret, C. Maheu, M. Milagro, N. Picot, A. Ambrozio, R. Escolà, A. Garcia-Mondejar, M. Restano, E. Schrama, M. Terra-Homem Radar Altimetry Tutorial; J. Benveniste and N. Picot (Eds), <http://www.altimetry.info>, 2016.

Authors

V. Rosmorduc (CLS), J. Benveniste (ESA), O. Lauret (CLS), C. Maheu (Akka), M. Milagro (SERCO), N. Picot (CNES), A. Ambrozio (DEIMOS), R. Escolà (isardSAT), A. Garcia-Mondejar (isardSAT), M. Restano (SERCO), E. Schrama (TU Delft), M. Terra-Homem (Deimos Engenharia)

Editors

J. Benveniste (ESA), N. Picot (CNES)

Scientific committee

G. Goni (NOAA, USA), S. Laxon (UCL, UK), J.M. Lefèvre (Mètèo France, France), C. Maes (IRD, New Caledonia), F. Remy (Legos/CNRS, France), J. Tournadre (Ifremer, France)

Acknowledgements

Thanks to M. Ablain, L. Amarouche, L. Carrère, J. Dorandeu, J.P. Dumont, P. Escudier, S. Guinehut, S. Labroue, F. Lefèvre, F. Mercier, P. Schaeffer, P. Thibaut, O.Z. Zanifè (CLS) for inputs and advices.

Table of Contents

Radar Altimetry Tutorial.....	1
Acknowledgements & Contributors.....	2
1 Toolbox	6
1.1 Download Now.....	6
1.2 Current Release	6
1.3 Toolbox Design	7
1.4 BRAT Data samples	8
2 Code Access	9
3 Data Access.....	10
4 Webs / Documents.....	12
4.1 Documentation	12
4.2 Software.....	12
5 An overview of Altimetry	13
5.1 How altimetry works	14
5.1.1 Basic Principle	15
5.1.2 From radar pulse to altimetry measurements	16
5.1.3 Frequencies used & their impacts	26
5.1.4 High-precision altimetry with satellites working together	29
5.1.5 Delay-Doppler (or SAR) Altimetry	31
5.2 Data Flow	33
5.2.1 Data acquisition	34
5.2.2 Data processing.....	34
5.2.3 Data qualification: "CalVal"	60
5.3 Future technology improvements	62
5.3.1 Ka-band altimeter	63
5.3.2 Interferometers	64
5.3.3 Constellations.....	68
5.3.4 GNSS altimetry.....	69
5.4 SAR Tutorial	71
5.4.1 On-board	71
5.4.2 Resolution cells.....	74
5.4.3 Ground processing steps	75
5.4.4 Product levels.....	77
6 Thematic Use Cases	80
6.1 Geodesy & geophysics	82
6.1.1 Bathymetry estimate from altimetry	82
6.1.2 Geodesy	85
6.1.3 Other geophysical applications	87

6.1.4	Tsunamis.....	88
6.2	Ocean applications.....	90
6.2.1	Large-scale ocean circulation.....	90
6.2.2	Ocean currents and eddies: mesoscale ocean applications.....	92
6.2.3	Operational oceanography	94
6.2.4	Tides	95
6.2.5	Mean Sea Level	98
6.2.6	Open Ocean - SAR	101
6.3	Ice: Land and sea ice	104
6.3.1	Land Ice	105
6.3.2	Sea ice.....	108
6.4	Climate	115
6.4.1	El Niño - Southern Oscillation (ENSO).....	115
6.4.2	North Atlantic Oscillation (NAO).....	117
6.4.3	Decadal oscillations	119
6.4.4	Seasons	119
6.4.5	Sea Level CCI.....	120
6.5	Atmosphere, wind & waves.....	121
6.5.1	Wind & waves as seen by altimetry.....	121
6.5.2	Cyclones, hurricanes and typhoons.....	123
6.5.3	Rain.....	125
6.6	Hydrology and land applications	128
6.6.1	Lake level monitoring	129
6.6.2	Land applications	130
6.6.3	River monitoring.....	130
6.6.4	Inland Water – SAR.....	132
6.7	Coastal applications.....	135
6.7.1	Coastal Ocean - SAR & SARIn.....	135
6.8	Examples of altimetry data use.....	142
6.8.1	Western boundary currents: The Gulf Stream and its seasonal variations	142
6.8.2	Ocean eddies as seen by satellite altimetry: the Kuroshio current.....	144
6.8.3	Geostrophic velocities: The Antarctic Circumpolar Current, due East around the Earth	147
6.8.4	The North Western Mediterranean Sea by using coastal dedicated products	148
6.8.5	The Agulhas current by using coastal dedicated products	152
6.8.6	The Florida Keys currents by using coastal dedicated products	160
6.8.7	Ice applications: Combined altimetry and radiometry for sea ice classification.....	165
6.8.8	Ice caps applications: Altimetry for observing polar ice caps.....	167
6.8.9	Ice applications: CryoSat over continental ice.....	170
6.8.10	Ice applications: CryoSat over sea ice.....	172
6.8.11	Monitoring El Niño: Rossby and Kelvin waves	177
6.8.12	Mean sea level.....	179

6.8.13	Seasonal distribution of Significant Wave Height.....	182
6.8.14	Observing wind and waves: hurricane Katrina.....	184
6.8.15	Temporal water surface height variations in enclosed areas: the Amazon Basin	186
6.8.16	Monitoring Aral Sea level:	189
6.8.17	Land applications: Monitoring continental surfaces	194
6.8.18	Altimetric waveforms to monitor lakes level: Lake Issyk-kul.....	196
6.8.19	Altimetry for lake/reservoir studies by using hydrology dedicated products.	201
6.8.20	Altimetry for wetland studies by using hydrology dedicated products.....	211
6.8.21	Use of the GOCE toolbox (GUT) in oceanography along with altimetry	215
7	Missions	220
7.1	Past missions	221
7.1.1	Skylab	222
7.1.2	GEOS 3.....	223
7.1.3	Seasat	224
7.1.4	Geosat	225
7.1.5	ERS-1.....	226
7.1.6	Topex/Poseidon	234
7.1.7	Geosat Follow-On.....	247
7.1.8	ERS-2.....	248
7.1.9	Envisat	256
7.1.10	Jason-1.....	272
7.2	Current missions.....	289
7.2.1	Jason-2.....	290
7.2.2	CryoSat-2.....	302
7.2.3	HaiYang-2.....	311
7.2.4	Saral	315
7.2.5	Jason-3	322
7.2.6	Sentinel-3.....	327
7.3	Future altimetry missions	333
7.3.1	Jason-CS / Sentinel-6.....	334
7.3.2	SWOT.....	336
7.4	Altimetry in planetary missions.....	339
7.4.1	MARSIS - Mars.....	339
7.4.2	SHARAD - Mars	342
7.4.3	RIME – Jupiter Moons.....	344
7.4.4	SRS - Venus.....	346
8	Glossary	348

1 Toolbox

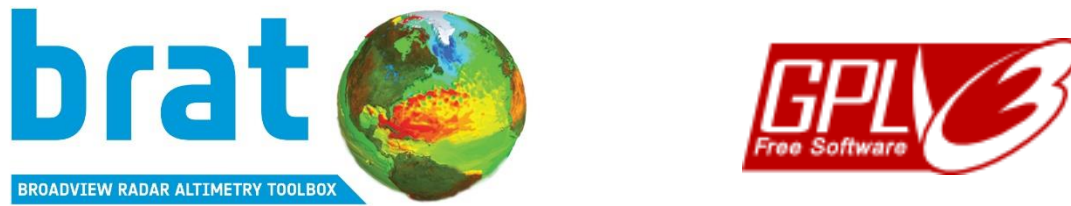


Figure 1.1. BRAT logo under GPL license

The Broadview Radar Altimetry Toolbox is a tool designed to use radar altimetry data. It is available in 32-bit and 64-bit versions for Windows, Mac OS X and Linux. The Broadview Radar Altimetry Tutorial and Toolbox is a joint project between ESA and CNES to develop an open source tool (GPL-3) freely available to all the altimetry community.

The toolbox is able to:

- to read all altimetry data from official data centres, from ERS-1 and 2, Topex/Poseidon, Geosat Follow-on, Jason-1, Envisat, Jason-2, Cryosat and Sentinel-3, from Sensor Geophysical Data Record to gridded merged data
- to do some processing and computations
- to visualise the results

1.1 Download Now

- Download the auto-installer (<http://www.altimetry.info/install>) for Linux, MacOS or Windows
- User manual (pdf, 3.5 MB, http://www.altimetry.info/filestorage/brat_user_manual.pdf)
- For installing the toolbox please read the quick installation details (<http://www.altimetry.info/filestorage/INSTALL>) or read the installation section of the user manual
- To test the toolbox, you can download data samples (<http://www.altimetry.info/toolbox/brat-data-samples/>)
- See also the section 6.8, for examples of altimetry uses with BRAT (mostly)
- Practical material can be downloaded from <http://www.altimetry.info/radar-altimetry-tutorial/training-material/>

1.2 Current Release

The current version of the Broadview Radar Altimetry Toolbox is v4.2.1, released in June 2018.

The following improvements have been added to BRAT:

- Dimensions consistency check of all operation parameters
- Correction of map distance tool for all latitudes and projections
- Improved visualization of X axis, supporting multiple dimensions
- Support user defined variables for filtering parameters
- Addition of aliases for SIR_SAR_2

- Support information accessible from about box
- Updated licensing information

See the [complete change log \(http://www.altimetry.info/filestorage/README\)](http://www.altimetry.info/filestorage/README) for full details of the changes in the different versions.

To report any bug with the software, please use the toolbox [GitHub account bugs \(https://github.com/BRAT-DEV/main/issues\)](https://github.com/BRAT-DEV/main/issues) form (preferred way) or send us an email via the [Helpdesk \(http://www.altimetry.info/helpdesk/\)](http://www.altimetry.info/helpdesk/). If you have any questions or suggestions for improvements please contact us using the [Helpdesk](http://www.altimetry.info/helpdesk/), and also check out the [Forums \(http://www.altimetry.info/?forum=altimetry-forum-2\)](http://www.altimetry.info/?forum=altimetry-forum-2) in case that someone has already experienced the same problem.

1.3 Toolbox Design

The Broadview Radar Altimetry Toolbox can be divided into four main components:

1. Data reading (also called “ingestion”)
 1. Processing routine functions
 2. Visualisation functions
 3. Graphic User Interface (GUI)

The structure is onionskin: each layer using the previous ones, and being available to be used without the ones above (e.g. you use the processing routines, which read data with the data ingestion tools, without using either the visualisation or the GUI). The GUI is using the other layers, and is available for current versions of Windows and Linux operating systems.

The **reading** (or “ingestion”) tools are a data dictionary, based on handbooks and data structures. They free the users of looking at each and every data format, byte by byte, to be able to read their products. The user can select several data files to work on them at the same time. They can be combined if they are of the same kind (same level, same mission or format). Once a dataset is chosen, the user is able to select a geographical area subset chosen by its minimum and maximum longitude and latitude, and/or a temporal subset by its start and end dates, and this for any type of data.

Processing functions are also available, to combine data fields (e.g. addition/subtraction needed to compute sea surface height from satellite altitude, altimetric range and corrections), select them (e.g. data editing to edit out-of-range values), etc. Such formulas can be saved for future use. The toolbox processed outputs are saved in NetCDF, and can be exported in either NetCDF, ASCII or GeoTIFF (with a Google Earth export feature). All processing is made through command files where all the parameters are indicated (even when using the GUI, with which the files are automatically generated).

Once processed, the BRAT outputs can be **visualised**, whether one parameter against one other or against two others (typically, classical maps, including several cartographic projections, but also dispersion plots, or waveforms). For all modes, title and comments can be written by the user. The user is able to choose a colour scale among a pre-defined set. A “do-your-own colour scale” tool is also provided. Plots can be saved in raster (.gif, .png, .tif, .jpg) format.

The **graphic user interface** is an interactive interface, to provide the user with an easy-to-use tool. It enables to use all the above components without writing a single line of programme or command files. In that frame, users are able to save the data context for future work: they are able to save their set preferences for future uses, under a user-defined name, the area, period, mission, colour scale, type of visualisation and the parameters combinations they might have defined.

1.4 BRAT Data samples

Here are samples of data read by the toolbox

- **Level 1B and 2 data**
 - [Envisat](#) (54 MB) (updated April 2011)
 - [ERS-1](#) (OPRs) (178 KB)
 - [ERS-2](#) (OPRs) (144 KB)
 - [ERS-2](#) (WAPs) (5.8 MB)
 - [GFO](#) (GDRs) (182 KB)
 - [Jason-1](#) (16 MB)
 - [Jason-2](#) (32 MB)
 - [Topex/Poseidon](#) (GDR-M) (327 KB)
 - [Topex waveforms](#) (16 MB)
 - [Cryosat 2](#) (15.4 MB) (updated April 2011)
- **Higher-level data**
 - [River & Lake](#) (ESA) (6 KB)
 - [Aviso](#) (level 3 and 4) (39 MB)
 - [Podaac](#) (level 3) (633 KB)
- **Datasets used in training kits**
 - [CryoSat 2 and Sentinel 3 from SARvatore GPOD](#) (150MB)
 - [TUDelft training](#) (230MB)
 - [4th ESA Advanced Training on Ocean Remote Sensing](#) (25 MB)
 - [25YPRA training](#) (105MB)

For more data of the kind, please contact the relevant data distribution centre (see the [Data product fact sheets](#) for names and links).

2 Code Access



Figure 2.1 Github logo

BRAT is an open source software with a GPL-3 license type. Its source code is publicly available online in a dedicated [GitHub repository](#). Contributions from the altimetry community to the code are encouraged and everyone can propose new code to be committed to the master branch via the [pull requests feature](#) from GitHub. If you have tailored the code, or added new functionality to the tool for your work, chances are that there are others that would find it useful as well. We therefore urge you to share your work with the whole community and use the GitHub features for collaborative coding. You can also check out useful discussions with other users of the tool in our portal [Forum](#).

In order to access the code it is required to [create an account](#) on GitHub, for which only a valid email is required. The account is completely free and does not require any additional information. The BRAT repository is public and all code can be seen by any GitHub user, however if you wish to contribute to the code, after creating the account, you will need to request to be a member of the [BRAT project](#), which will then allow you to create branches, perform commits and raise pull requests. Each pull request shall be reviewed and discussed with the author by a panel of specialists. This panel of specialists controls the final decision on the merging of the changes to the master branch for incorporation into the next release of the software.

In addition any bugs found in the code can be raised on BRAT's GitHub [integrated issue tracking system](#) by anyone with a GitHub account, where the developers will provide feedback to the issues raised. Issues and suggestions for improvements of the tool can also be raised via our [Helpdesk](#).

You can find information about the installation and compilation steps [here](#).

3 Data Access

Name	Mission	Level	Organisation	Access	
Sentinel-3 Operations Data Hub	Sentinel-3	L1A-L1BS-L1B-L2	ESA - COPERNICUS	web	Registration
CODA Copernicus Online Data Access	Sentinel-3	L1A-L1BS-L1B-L2	EUMETSAT - COPERNICUS	web	Registration
Sea Level CCI	Multimission Merged	L3-L4	ESA	web	Registration
EOPI	CryoSat-2	FBR-L1B-L2	ESA	form	Registration
EOPI	Envisat	L2/GDR	ESA	form	Registration
EOPI	ERS-1 ERS-2	GDR REAPER	ESA	form	Registration
AVISO	Jason-2	L2/IGDR-PISTACH	CNES	ftp	Anonymous
	Jason-1	L1 -L2	CNES	ftp	Anonymous
	Jason-2	L1 -L2	CNES	ftp	Anonymous
	SARAL	L1 -L2-L3	CNES	ftp	Anonymous
	HY-2	L2	CNES	ftp	
	Topex-Poseidon	L2	CNES	ftp	Anonymous
RADS	Geosat	L2	DEOS-TU Delft	web	Registration
	ERS-1	L2	DEOS-TU Delft	web	Registration
	ERS-2	L2	DEOS-TU Delft	web	Registration
	Topex/Poseidon	L2	DEOS-TU Delft	web	Registration
	GFO-1	L2	DEOS-TU Delft	web	Registration
	Jason-1	L2	DEOS-TU Delft	web	Registration
	Enviat	L2	DEOS-TU Delft	web	Registration
	Jason-2	L2	DEOS-TU Delft	web	Registration
	CryoSat-2	L2	DEOS-TU Delft	web	Registration
	SARAL	L2	DEOS-TU Delft	web	Registration
	Jason-2	L2	DEOS-TU Delft	web	Registration
Sentinel-3	L2	DEOS-TU Delft	web	Registration	
PO.DAAC	Jason-3	L2/GPS-OGDR	NASA	ftp	Anonymous
	SARAL	L2	NASA	ftp	Anonymous
	TOPEX	L1B-L2	NASA	ftp	Anonymous
	Jason-2	L2	NASA	ftp	Anonymous
	Multimission	L4 dynamic topo	NASA	ftp	Anonymous
	Multimission	L4 SSH grid	NASA	ftp	Anonymous
	GEOS3	L2	NASA	ftp	Anonymous
	Envisat and Jason-2	L2 ALES	NASA	ftp	Anonymous
Jason-1	L2	NASA	ftp	Anonymous	

ODES: Online Data Extraction Service	Different missions	L2	CNES	web	Registration
AVISO Ssalto/Duacs	Multimission	L3	CNES	ftp	Registration
AVISO	Jason-2	L2/IGDR-PISTACH	CNES	ftp	Anonymous
	Jason-1	L1 -L2	CNES	ftp	Anonymous
	Jason-2	L1 -L2	CNES	ftp	Anonymous
	SARAL	L1 -L2-L3	CNES	ftp	Anonymous
	HY-2	L2	CNES	ftp	Anonymous
	Topex-Poseidon	L2	CNES	ftp	Anonymous
CTOH Center for Topographic studies of the Ocean and Hydrosphere	ERS-2	L2	CNES	form	Registration
	Envisat, Jason-1 and Jason-2	L2 CTOH	CNES	web	Free access
	, CryoSat-2	L2	CNES	form	Registration
	ERS-1, ERS-2, Envisat, TOPEX, Jason-1, Jason-2, CryoSat-2 SARAL	WET Tropospheric correction	U. Porto	form	Registration
Haiyang-2 data center	HY-2	L2-L3	NSOAS	form	Registration
CCAR	Multimission	L3	University of Colorado	web	Free access
CERSAT	Envisat, Jason, Topex, Merged	L3 Rain	Ifremer	ftp	Anonymous

4 Webs / Documents

4.1 Documentation

- [\(M\)SLA and \(M\)ADT Near-Real Time and Delayed Time Products AVISO](#)
- [Jason-1 Sea Surface Height Anomaly Product – JPL/PO.DAAC User’s Reference Manual PO.DAAC](#)
- [TOPEX/POSEIDON Sea Surface Height Anomaly Product – JPL/PO.DAAC User’s Reference Manual PO.DAAC](#)
- [Level 3 rain products from dual frequency altimeters: RAIN-ALT products – User Manual CERSAT](#)
- [Altimeter & Microwave Radiometer ERS Products – User Manual CERSAT](#)
- [Altimeter waveform product ALT.WAP compact user guide ESA](#)
- [EnviView User Guide ESA](#)
- [RA2-MWR Product Handbook ESA](#)
- [Guide to programs to read and write Envisat altimetry products ESA](#)
- [User handbook for POSEIDON Waveforms product AVISO](#)
- [CryoSat product Handbook ESA](#)
- [Sentinel 3 user handbook ESA](#)

4.2 Software

- [Broadview Radar Altimetry Toolbox CNES/ESA](#)
- [PublicReadBinairies AVISO](#)
- [SSHA software PO.DAAC](#)
- [OPR reading software CERSAT](#)
- [Modified Chelton-Wentz model DEOS](#)
- [EnviView ESA](#)
- [Envisat L2 RA2-MWR Products Read and Write Software ESA](#)
- [Convert programs for waveforms POSEIDON products AVISO](#)

5 An overview of Altimetry

This Radar Altimetry Tutorial describes applications, examples (data use cases) and techniques, including standard data processing, as well as the various satellite missions that have carried, are carrying or will carry a radar altimeter onboard, plus a range of altimetry products (data, software and documentation).

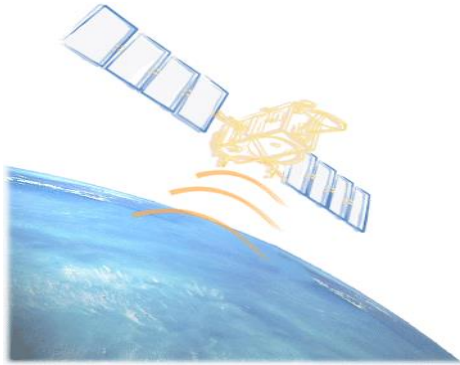


Figure 5.1. Altimeter illustration

Altimetry is basically a technique for measuring height. Satellite radar altimetry measures the time taken by a radar pulse to travel from the satellite antenna to the surface and back to the satellite receiver. Moreover, this measurement yields a wealth of other information that can be used for a wide range of applications.

Further information on radar:

- http://www.alphalpha.org/radar/intro_e.html
- www.radartutorial.eu
- <http://en.wikipedia.org/wiki/Radar>

Further information on radar remote sensing:

- <http://www.nrcan.gc.ca/earth-sciences/geomatics/satellite-imagery-air-photos/satellite-imagery-products/educational-resources/9309>
- <http://rst.gsfc.nasa.gov/>
- <http://www.r-s-c-c.org/>
- <http://ceos.org/about-ceos/publications-2/>

5.1 How altimetry works

Altimetry satellites basically determine the distance from the satellite to a target surface by measuring the satellite-to-surface round-trip time of a radar pulse. However, this is not the only measurement made in the process, and a lot of other information can be extracted from altimetry.

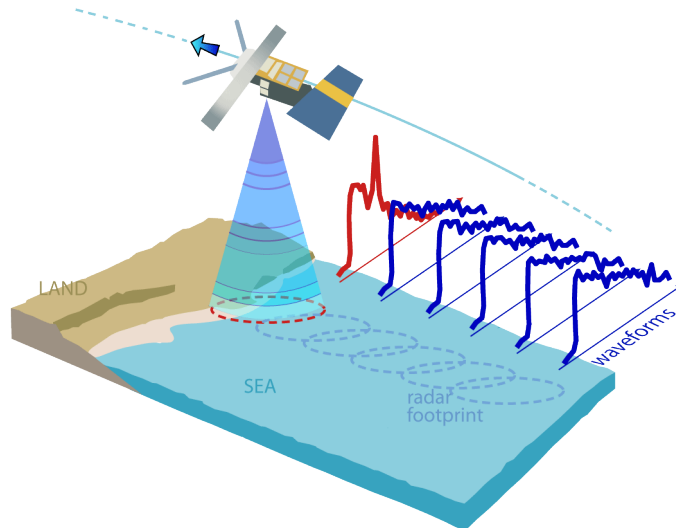


Figure 5.2. Altimeter received waveforms in sea to land transition illustration (COASTALT portal)

The principle is that the altimeter emits a radar wave and analyses the return signal that bounces off the surface. Surface height is the difference between the satellite's position on orbit with respect to an arbitrary reference surface (the Earth's centre or a rough approximation of the Earth's surface: the reference ellipsoid) and the satellite-to-surface range (calculated by measuring the time taken for the signal to make the round trip). Besides surface height, by looking at the return signal's amplitude and waveform, we can also measure wave height and wind speed over the oceans and, more generally, backscatter coefficient and surface roughness for most surfaces off which the signal is reflected.

If the altimeter emits in two frequencies, the comparison between the signals, with respect to the frequencies used, can also generate interesting results (rain rate over the oceans, detection of crevasses over ice shelves, etc.).

To obtain measurements accurate to within a few centimetres over a range of several hundred kilometres requires an extremely precise knowledge of the satellite's orbital position. Thus several locating systems are usually carried on-board altimetry satellites. Any interference with the radar signal also needs to be taken into account. Water vapour and electrons in the atmosphere, sea state and a range of other parameters can affect the signal round-trip time, thus distorting range measurements. We can correct for these interference effects on the altimeter signal by measuring them with supporting instruments, or at several different frequencies, or by modelling them.

Altimetry thus requires a lot of information to be taken into account before being able to use the data. Data processing is also a major part of altimetry, producing data of different levels optimised for different uses at the highest levels.

Further information:

Chelton, D.B., J.C. Ries, B.J. Haines, L.L. Fu, P.S. Callahan, *Satellite Altimetry, Satellite altimetry and Earth sciences*, L.L. Fu and A. Cazenave Ed., Academic Press, 2001

5.1.1 Basic Principle

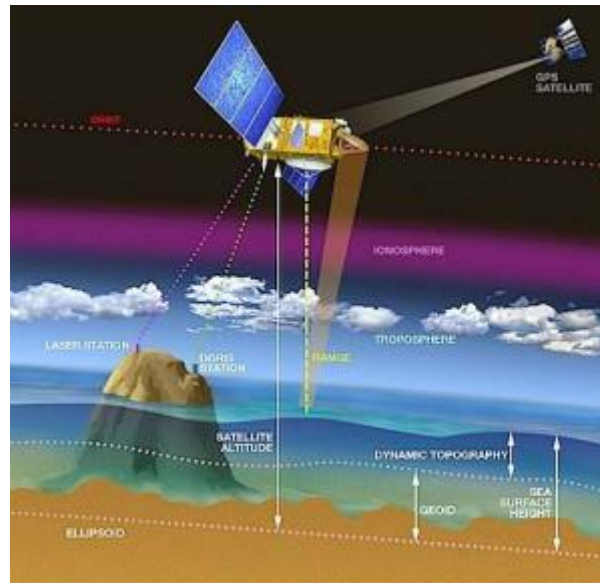


Figure 5.3. The principle of altimetry (Credits CNES/D. Ducros)

Satellite-to-surface distance: Range

Radar altimeters on board satellites transmit signals at high frequencies (over 1,700 pulses per second) to Earth and receive echoes from the surface (the ‘waveform’). They are analysed to derive a precise measurements of the time taken to make the round trip between the satellite and the surface. These time measurements, scaled to the speed of light (the speed at which electromagnetic waves travel), yields the **range R** measurements (see From radar pulse to altimetry measurements for Further details).

However, as electromagnetic waves travel through the atmosphere, they can be decelerated by water vapour or ionisation. Once these phenomena have been corrected for, the final range can be estimated with great accuracy (see Data processing).

The ultimate aim is to measure surface height relative to a terrestrial reference frame. This requires independent measurements of the satellite’s orbital trajectory, i.e. exact latitude, longitude and altitude coordinates.

Satellite Altitude

The critical orbital parameters for satellite altimeter missions are altitude, inclination and period. The altitude of a satellite depends upon a number of constraints (e.g. inclination, atmospheric drag, gravity forces acting on the satellite, area of the world to be mapped, etc). The period, or ‘repeat orbit’ is the time needed for the satellite to pass over the same position on the ground, uniformly sampling the Earth’s surface. Inclination gives the highest latitude at which the satellite can take measurements.

The **altitude of a satellite (S)** is the satellite’s distance with respect to an arbitrary reference (e.g. the reference ellipsoid, a rough approximation of the Earth’s surface). It depends upon a number of constraints (e.g. inclination, atmospheric drag, gravity forces acting on the satellite, area of the world to be mapped, etc). The satellite can be tracked in a number of ways so as to measure its altitude with

the greatest possible accuracy and thus determine its precise orbit, accurate to within 1 or 2 cm. The main techniques used are:

- Doppler shift, to accurately determine the satellite's velocity on its orbit, using dynamic orbitography models to deduce the satellite's trajectory relative to Earth (e.g. DORIS, or PRARE instruments),
- GPS or similar systems can also be used,
- laser tracking is also used, often for calibration.

Surface height

The **surface height (H)**, is the satellite's distance at a given instant from the reference surface, so:

$$(\text{corrected}) \text{ Height} = \text{Altitude} - (\text{corrected}) \text{ Range} \quad \text{Eq. 1}$$

For the ocean, the sea surface height (or SSH) integrates effects such as:

- The sea surface height which would exist without any perturbing factors (wind, currents, tides, etc.). This surface, known as the **geoid**, is determined by gravity variations around the world, which are in turn due to major mass and density differences on the seafloor. For example, a denser rock zone on the seafloor would deform sea level by tens of metres, and be visible as a hill on the geoid.
- The ocean circulation, or **dynamic topography**, which comprises
 - the permanent stationary component (permanent circulation linked to Earth's rotation, permanent winds, etc.). The mean effect is of the order of one metre.
 - and a highly variable component (due to wind, eddies, seasonal variations, etc.).

To derive the dynamic topography, the easiest way would be to subtract the geoid height from SSH. In practice, mean sea level is subtracted instead, to yields the variable part (sea level anomalies) of the ocean signal.

5.1.2 From radar pulse to altimetry measurements

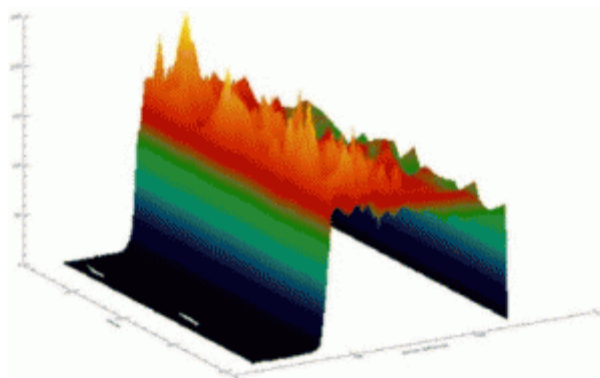


Figure 5.4. Poseidon-2 (Jason-1 altimeter) first waveforms. (Credits CNES)

A radar altimeter measures surface characteristics with a high degree of accuracy. This implies high precision in the radar measurements and therefore requires performance far greater than a

conventional radar, in particular for classic radar range measurements. The radar altimeter emits a pulse towards the Earth's surface. The time which elapses from the transmission of a pulse to the reception of its echo reflected off the Earth's surface is proportional to the satellite's altitude. Some theoretical details of the principle of radar applied to altimetry will help better understand the different behaviours and characteristics of the pulse in function of irregularities on the surface encountered. The magnitude and shape of the echoes (or waveforms) also contain information about the characteristics of the surface which caused the reflection. The best results are obtained over the ocean, which is spatially homogeneous and has a surface which conforms with known statistics. Surfaces which are not homogeneous, which contain discontinuities or significant slopes, such as some land surfaces, make accurate interpretation more difficult. Even in the best case (the ocean), the pulse should last no longer than 70 picoseconds to achieve an accuracy of a few centimetres. Technically, this means that the emission power should be greater than 200 kW and that the radar will have to switch every few nanoseconds. These problems are solved by the full deramp technique, making it possible to use only 5 W for emission. The range resolution of the altimeter is about half a metre (3.125 ns) but the range measurement performance over the ocean is about one order of magnitude greater than this. This is achieved by fitting the shape of the sampled echo waveform to a model function which represents the form of the echo.

5.1.2.1 On-board reception and tracking

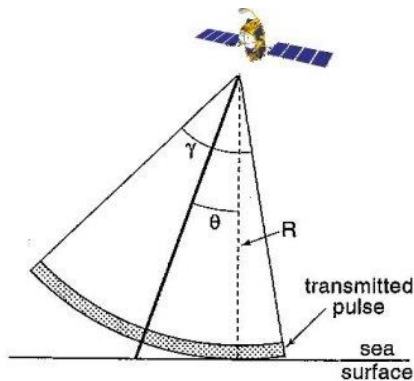


Figure 5.5. Altimeter transmission geometry, R represents the distance from the satellite to the sea surface, γ represents the pointing angle and θ the pitch angle

The altimeter transmits a short pulse of microwave radiation with known power toward the surface. The pulse interacts with the rough surface and part of the incident radiation reflects back to the altimeter. This is a straightforward concept but more difficult to understand in all details.

The antenna altimeter emits a spherical microwave radiation with known one or two frequencies (13.575 GHz for the Ku-band and 3.2 GHz for the S-band of Envisat), toward the surface (water or land) on a nadir direction comprised in a 1.29°-cone (in Ku-band for Envisat). On the basis of this radiation, the altimeter emits pulses, but they are not as narrow as with a laser, rather it leaves the antenna as a widening beam, getting wider the further it travels.

These pulses are frequency linearly modulated signals and are emitted at regular intervals defined by the Pulse Repetition Frequency (PRF): 1795 Hz for Envisat. In order to reduce the reflection sequencing of the wave on the ground surface.

- First, when the reception mode is activated by the on-board tracking system, a low power noise signal is received corresponding to parasite reflection of the pulse in the ionosphere and atmosphere, in addition to the instrument electronic noise.
- When the leading edge of the radar pulse hits the ground, the returned signal rises up, the footprint being a disc linearly spreading with time, which makes the corresponding return signal increase up to a maximum corresponding to the passage of the rear edge of the pulse 'through' the ground surface. In case of a perfectly flat surface, this rise would be linear.
- After the rear edge of the pulse passed 'through' the ground level, the footprint turns to a ring with increasing radius and constant area. Then the returned signal to the altimeter decreases

due mostly to antenna pattern decay and antenna mispointing, till vanishing down to the noise level or being cut by reception gate.

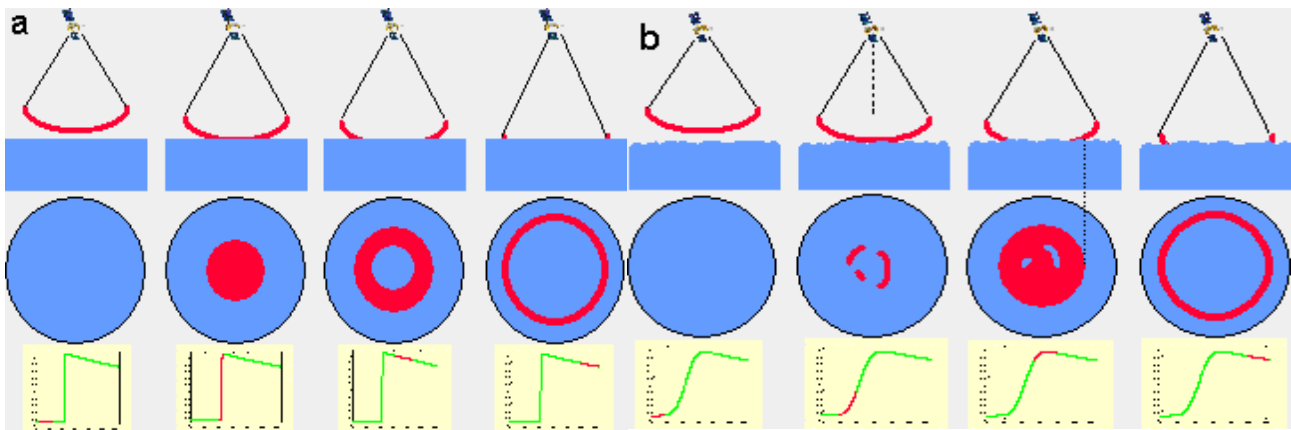


Figure 5.6. The radar altimeter receives the reflected wave (or echo), which varies in intensity over time. Where the sea surface is flat (a), the reflected wave's amplitude increases sharply from the moment the leading edge of the radar signal strikes the surface. However, in sea swell or rough seas (b), the wave strikes the crest of one wave and then a series of other crests which cause the reflected wave's amplitude to increase more gradually. We can derive ocean wave height from the information in this reflected wave since the slope of the curve representing its amplitude over time is proportional to wave height.

Significant return signal is available from reflecting surfaces situated up to 18 km off nadir, which makes the exploitation of altimetric data particularly delicate in case of strong variations of the surface reflectivity.

On-board acquisition and tracking

In order to keep the waveforms well centred in range and power in the analysis window and to better adjust these parameters for the echoes to come, the on-board altimeter calculator makes a brief processing of the radar echoes that the receiver has just recorded. It anticipates the settings for $n+1$ echoes from the n , $n-1$, $n-2$, etc. treatment echoes. When this on-board tracking function is not able to adjust these parameters under critical conditions, the altimeter loses lock. Then, it goes in its acquisition phase, searching for the signal, locking onto it and stabilizing the tracking loops. This acquisition sequence lasts from 0.6 seconds (for Envisat) to 3 seconds and there's no data during this, until the tracking is properly reinitialised.

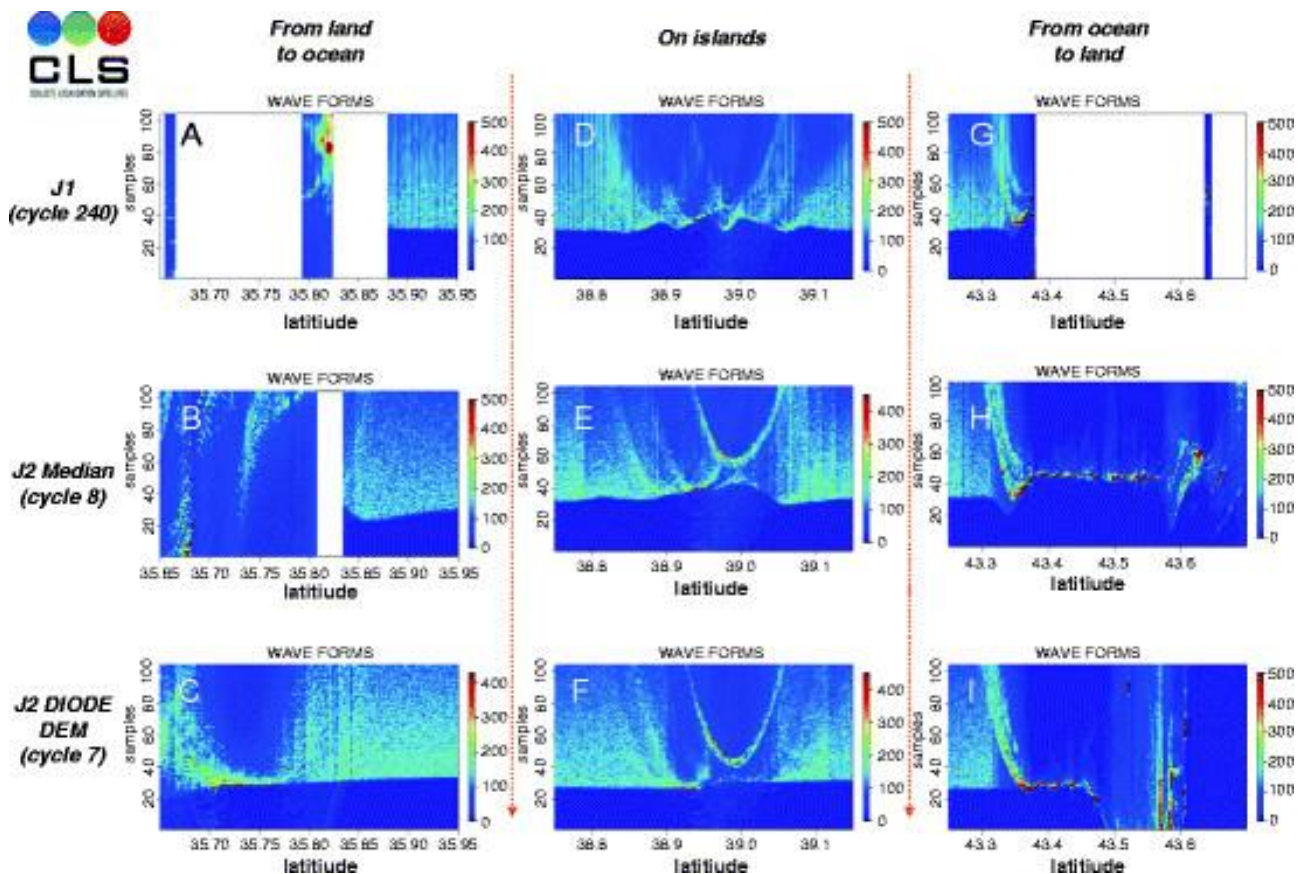


Figure 5.7. Jason-1 and Jason-2 waveforms over various land/ocean and ocean/land transitions over the Mediterranean Sea from Algeria to France via Ibiza Island (pass 187). The top subplot shows the Jason-1 waveforms, collected with the Split Gate on-board Tracker. The middle and bottom subplots show Jason-2 waveforms, collected with the Median Tracker and the DIODE/DEM tracker, respectively. In each subplot, three transitions are considered: 1st column: a land/ocean transition over the Algerian coasts (latitude 35.73°); 2nd column: orbit segment over Ibiza Island (latitudes $38.95\text{--}38.975^\circ$); 3rd column: an ocean/land transition over the French coast (latitude 43.366°) (Credits CLS)

The Poseidon-3 altimeter (Jason-2) is equipped with an open-loop tracking technique for which a Digital Elevation Model (DEM) has been developed. The altimeter's onboard memory contains the elevation values of areas overlaid by the ground tracks. These data, combined with DORIS data, are used to position the radar echo receiving window in advance, in order to anticipate the contrasts of the topography and to give priority to measurements over water. This technique prevents the altimeter from losing track as sometimes occurs with a conventional tracking loop, and enables measurements to be acquired close to the shoreline or on continental waters.

For the RA-2 altimeter (Envisat), an innovative tracking algorithm, known as Model Free Tracker (MFT) concentrates its effort in maintaining the earliest part of radar echoes within the tracking window, independently of its shape. In particular, the MFT will decide whether the range window is using the adequate resolution, whether the resolution could be increased, or decreased, based on the Signal to Noise Ratio (SNR) of the on-board waveform position compared to reference values stored in the on-board memory. When the radar echo is about to move out of the tracking window, due for example to a sudden change in the surface elevation, the window is broadened to recapture the echo.

This allows uninterrupted radar operation over all type of surfaces and its boundaries (see Frequencies used & their impacts).

5.1.2.2 Full-Deramp Technique

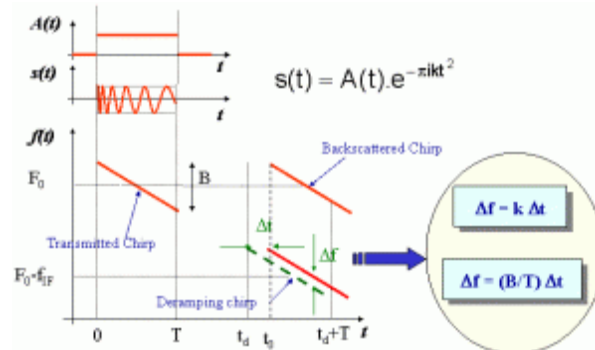


Figure 5.8. Deramp signals

The radar emits a modulated chirp $s(t)$ of duration T in a frequency-band B towards the Earth's surface, then, with a delay corresponding to the estimated return time of the emitted chirp, another which is slightly shifted in frequency. By mixing the returning and deramping chirps, the frequency shift can be estimated, which, using Fourier transforms, gives the time delay.

To obtain a resolution of 3.125 ns, pulses of this duration can be used; this is the approach used in laser ranging systems. Maintaining the strength of the return signal requires a certain amount of energy in the pulse, and with such short duration pulses a very high transmit power is required. The approach commonly used in radar systems is to inject a short pulse into a dispersive delay line, which spreads the energy over time, generating a frequency modulated or chirp signal. When the echo is received, the radar passes the signal through an inverse matched filter which compresses the chirp signal back to a short pulse. This technique is called pulse compression. The compressed time resolution is inversely proportional to the chirp bandwidth.

A radar range resolution of 3.125 ns would require a very high radio frequency bandwidth, of the order of several hundred megahertz. To generate chirp signals of this bandwidth, the frequency of the signals from the dispersive delay line has to be multiplied. This entails difficulties in the receiver matched filter as the corresponding frequency division is not possible. Even if such a filter were available, video signal handling at a similar high bandwidth would be necessary.

To circumvent this problem, the full-deramp technique is used in combination with linear FM (Frequency Modulation) pulse compression. The return echo signal consists of many discrete chirps, each reflected from a different facet of the ocean surface, with slightly different delay times. The full-deramp concept consists in mixing this incoming signal with a replica of the transmitted chirp, slightly shifted in frequency. The deramp mixer generates signals which are the frequency difference between its two inputs. As both inputs have the same rate of frequency change, the output frequencies are constant tones. The input signals are linear so there is a mapping of time offset onto frequency offset. As a result, targets with a different range give echoes at different frequencies. Therefore, the range discriminator can be implemented with a bank of contiguous filters. The translation from the time domain to the frequency domain simplifies the signal processing stages as they are able to work with much-reduced bandwidth.

5.1.2.3 Altimetry measurements over the ocean

The basic schematic outlines of a return echo over the ocean are as follows:

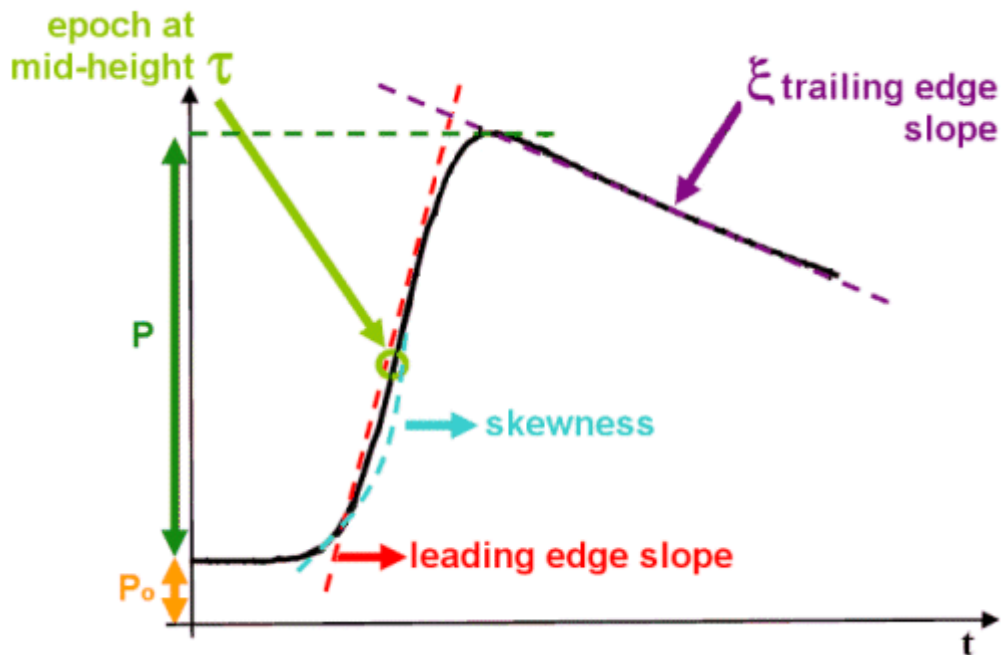


Figure 5.9. Parts of a waveform

Over an ocean surface, the echo waveform has a characteristic shape that can be described analytically (the Brown model). From this shape, six parameters can be deduced, by comparing the real (averaged) waveform with the theoretical curve providing the best fitting:

- epoch at mid-height: this gives the time delay of the expected return of the radar pulse (estimated by the tracker algorithm) and thus the time the radar pulse took to travel the satellite-surface distance (or ‘range’) and back again.
- P : the amplitude of the useful signal. This amplitude with respect to the emission amplitude gives the backscatter coefficient, σ_0 .
- P_0 : thermal noise
- leading edge slope: this can be related to the significant wave height (SWH)
- skewness: the leading edge curvature
- trailing edge slope: this is linked to any mispointing of the radar antenna (i.e. any deviation from nadir of the radar pointing).

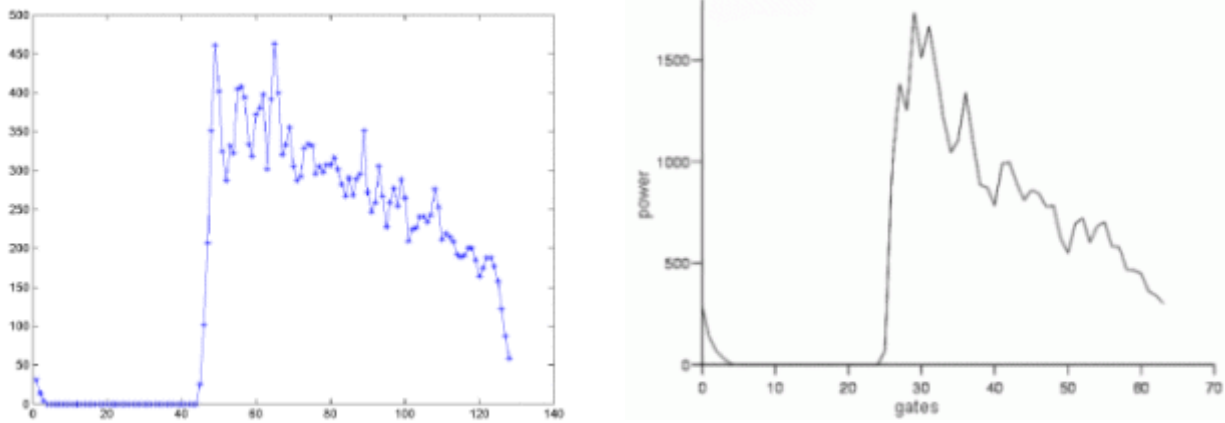


Figure 5.10. Example of real Envisat (left) and Topex (right) waveforms over the ocean.

References:

- Brown, G. S., The Average Impulse Response of a rough surface and its applications, *IEEE Trans. Antennas Propag.*, 25, 1977.
- Hayne, G. S., Radar Altimeter Mean Return Waveforms from Near-Normal-Incidence Ocean surface scattering, *IEEE Trans. Antennas Propag.* AP-28, 687-692, 1980.

5.1.2.4 Continental ice waveforms

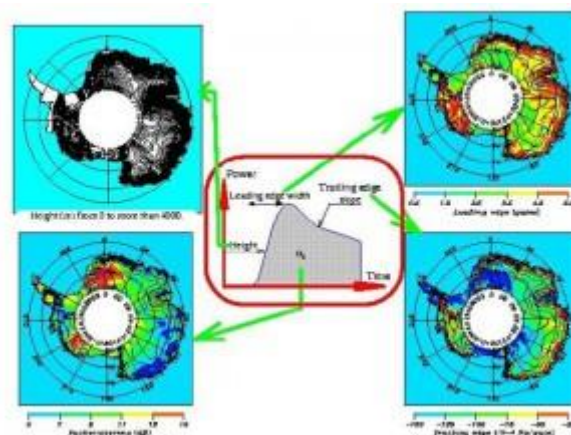


Figure 5.11. a waveform over ice, and the parameters that can be extracted from it. (Credits LEGOS/CNRS)

The echo waveform over ice enable to retrieve several parameters:

- epoch at mid-height: this gives the time delay of the expected return of the radar pulse (estimated by the tracker algorithm), and thus the time the radar pulse took to travel the satellite-surface distance (or 'range') and back again.
- backscatter coefficient, σ_0 .
- leading edge amplitude
- leading edge width: this is related to the penetration into the medium and the surface roughness of the target.
- trailing edge slope: this gives information on antenna mispointing, and also on the signal penetration into the medium.

All altimeter data for ice sheets must be post-processed to produce accurate surface elevation measurements. This post-processing is called ‘retracking’ and is required because the leading edge of the ice-sheet return waveform deviates from the on-board altimeter tracking gate, causing an error in the telemetered range measurement.

5.1.2.5 Altimetric measurements over land

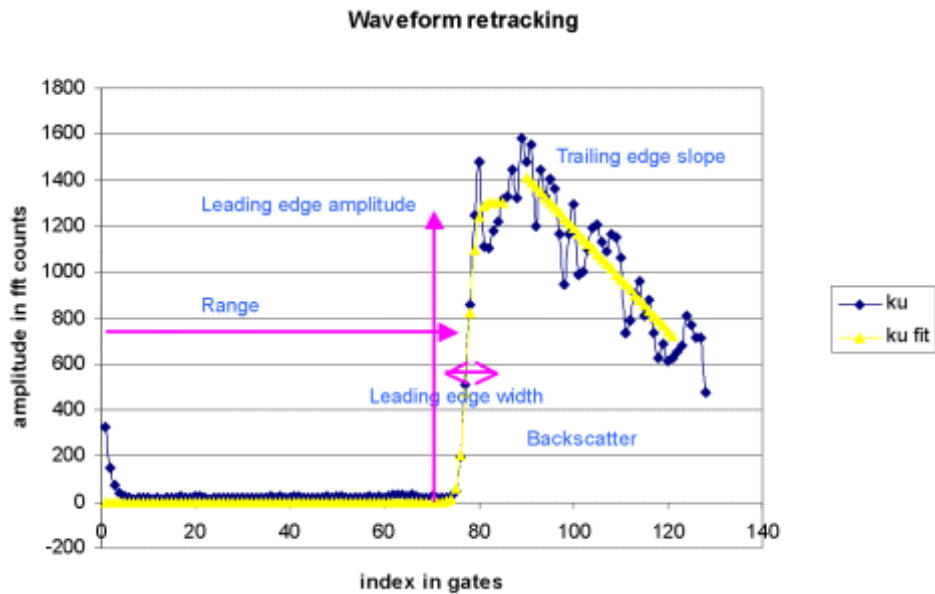


Figure 5.12. Envisat’s ‘ICE2’ retracker: Continental ice retracking can also be used successfully on continental surfaces

The continental lands are composed of a variety of surfaces which reflect the signal back with different intensities depending on each surface properties. The altimeter footprint is frequently composed of and contaminated by a multiplicity of surfaces. Thus, waveforms on these surfaces include a wide variety of configurations which are difficult to classify and process. Altimeter data over land must be post-processed in another way than the Brown model because the leading edge of the terrain return waveform deviates from the on-board altimeter tracking gate, causing a significant error in the telemetered range measurement.

Analyses from waveforms over heterogeneous surfaces enable to retrieve several parameters and deduce other interesting characteristics.

Thus, the backscatter coefficient (σ_0) is used to characterize the surface: a low value for mountainous regions and a high value on flat surfaces or wetlands. The backscatter coefficient can also be related to the dates when a surface is completely frozen when the ice breaks up and fast-ice duration. The leading edge width is related to the penetration into the medium and the surface roughness of the target.

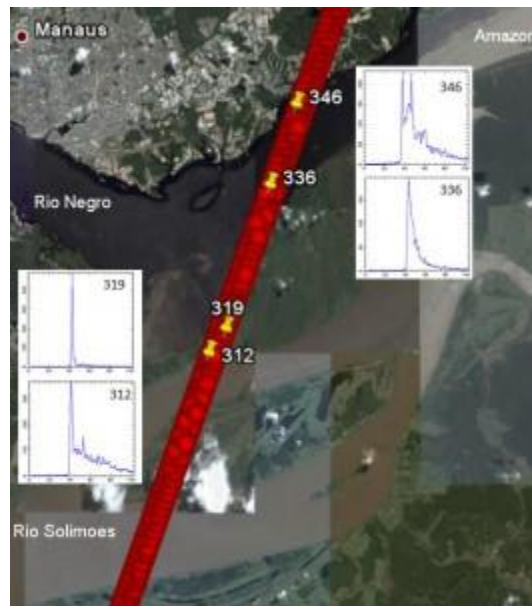


Figure 5.13. Jason-2 waveforms on Amazon river: specular waveform (n°319) result of the return signal from very reflective surfaces like water bodies, multi-peaked waveforms result of heterogeneous targets in the footprint.

The parameters extracted from the waveforms over continental surfaces are similar to the ones for ice:

- epoch at mid-height: this gives the time delay of the expected return of the radar pulse (estimated by the tracker algorithm), and thus the time the radar pulse took to travel the satellite-surface distance (or ‘range’) and back again.
- backscatter coefficient (or σ_0): gives information on the nature of the surface.
- leading edge amplitude.
- leading edge width: this is related to the penetration into the medium and the surface roughness of the target.
- trailing edge slope: this gives information on antenna mispointing, and also on the signal penetration into the medium.

For Ku and S band, the backscatter is low in mountainous regions (e.g. e.g. <7 dB in Ku band, <14 dB in S band) as a direct result of the presence of topographic slopes. For both bands, the backscatter values are high on very flat surfaces, such as deserts, large river basins or wetlands (e.g. >15 dB in Ku band and >20 dB in S band), due to the specularity of the return radar echo.

The leading edge width values are high in desert areas due to the strong penetration of the wave and the dunes generated by the winds. Low values, related to weak penetration, correspond to dense vegetated areas, such as tropical or boreal forests, or to large river basins or flooded regions. In contrast to the backscatter coefficient, the use of only one frequency gives a characteristic signature on continental surfaces, providing good discrimination of forests, deserts, etc.

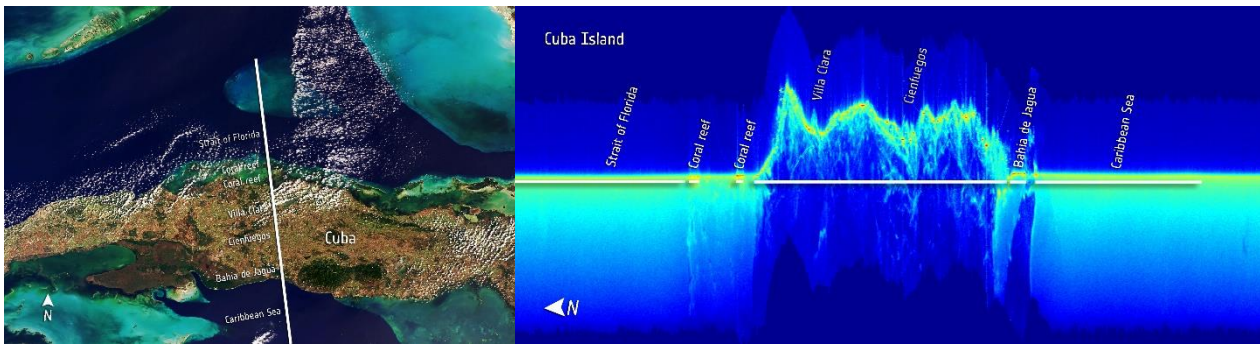


Figure 5.14. Examples of real waveforms (from the CryoSat-2 SIRAL altimeter), over the isle of Cuba. (Credits ESA)

5.1.2.6 Envisat RA-2 individual echoes or Burst mode

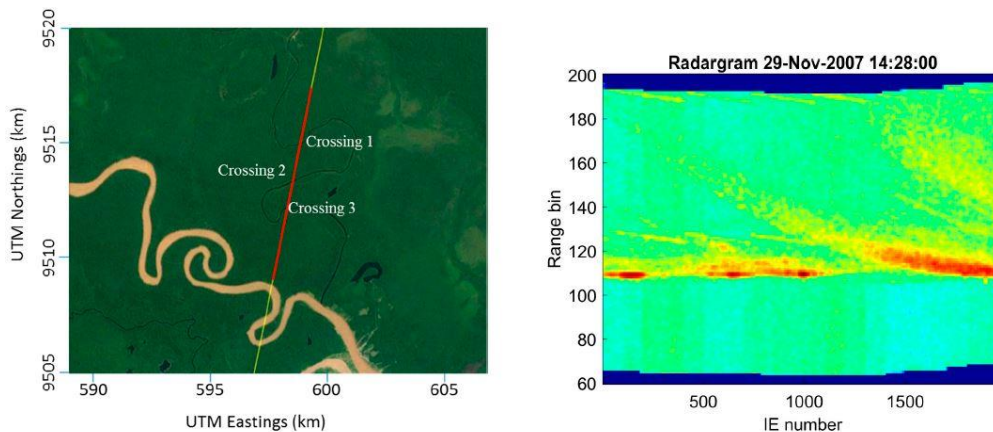


Figure 5.15. Rio Nahuapa and Envisat Nominal track (IE coverage highlighted in red). (left) and Radargram (right), from Ron Abileah, 2017.

The altimeter transmits pulses at regular intervals (defined by the Pulse Repetition Frequency: 1795 per second for Envisat) toward the Earth’s surface. During nominal operation, the on-board tracker averages them by groups of 100 echoes (typically every 50 ms). Then, the averages are transmitted to ground.

But during the telemetry burst mode (only for the Ku-band), the RA-2 altimeter has the capability to provide a limited amount of individual, unaveraged echo at the full PRF rate (1 second every 3 minutes). These raw data are sampled before the Fast Fourier Transform module and are stored into an internal buffer memory in parallel to the normal averaging. Since the collected individual echoes have not been processed in the frequency domain on-board, the processing is reproduced on-ground (See Roca, 2007 for further details).

These individual echoes with higher spatial resolution are interesting as they give access to very detailed information encoded in them and can give insight on some feature that cannot be seen with the averaged data. They particularly demonstrate that the use of un-averaged echoes when possible can provide better surface information. They are available as a dedicated-data product (in RA-2 level2 products, RA2_MWS_2P)).

Further information:

- Roca M., Martinez, D. Reche M. ,The RA-2 individual echoes processing description and some scientific results, Envisat Symposium, Montreux, 2007.
- Gommenginger C., and al., New scientific applications for ocean, coastal, land and ice remote sensing with Envisat radar altimeter individual echoes. Fifteen Years of Progress in Radar Altimetry, Venice, 2006.
- Zanife, O.Z. Roca, M. Remy, F. and al., Envisat Radar Altimeter Individual Echoes, Fifteen Years of Progress in Radar Altimetry, Venice, 2006.
- Ron Abileah, Andrea Scozzari, Stefano Vignudelli Envisat RA-2 Individual Echoes: A Unique Dataset for a Better Understanding of Inland Water Altimetry Potentialities, Remote Sens. 2017, 9, 605

5.1.2.7 Footprint size

The ground footprint size is an important notion to better understand what the altimeter can really observe and measure. The footprint of an antenna is traditionally defined to be the area on the sea surface within the field of view subtended by the beamwidth of the antenna gain pattern. A radar pulse is not narrow such as with a laser, rather it leaves the antenna as a widening beam, getting wider the further it travels.

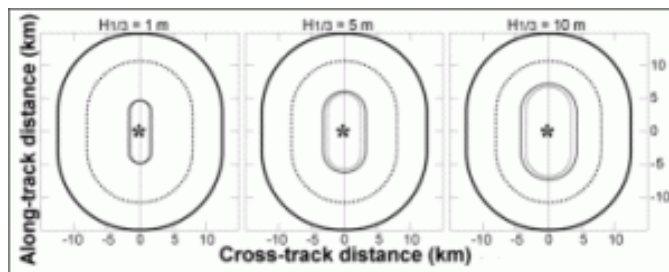


Figure 5.16. The oval footprint characteristics for SWH of 1, 5 and 10 m for 1-second averages of altimeter measurements of nadir mean sea level from orbit heights of 1 336 km (solid lines) and 785 km (dashed lines). (Credits CNES)

The beam illuminates a circle of ocean or land surfaces with a 3 to 5 km wide, depending on the sea state, the wave height or the corrugated land. A calm sea or a flat land surface affords a narrower footprint (typically 2 km) than if the sea is very rough (typically 10 km). Significant return signal is available from reflecting surfaces situated up to 18 km off nadir, which makes the exploitation of altimetric data particularly delicate in case of strong variations of the surface reflectivity.

The returning echoes are a blend of thousands of little echoes from within the footprint, some coming from the troughs of waves, some coming up from wave peaks. With waves up to many metres in height, this creates a mish-mash of echoes from varying heights.

5.1.3 Frequencies used & their impacts

Several different frequencies are used for radar altimeters. The choice depends upon regulations, mission objectives and constraints, technical possibilities — and impossibilities. Each frequency band has its advantages and disadvantages.

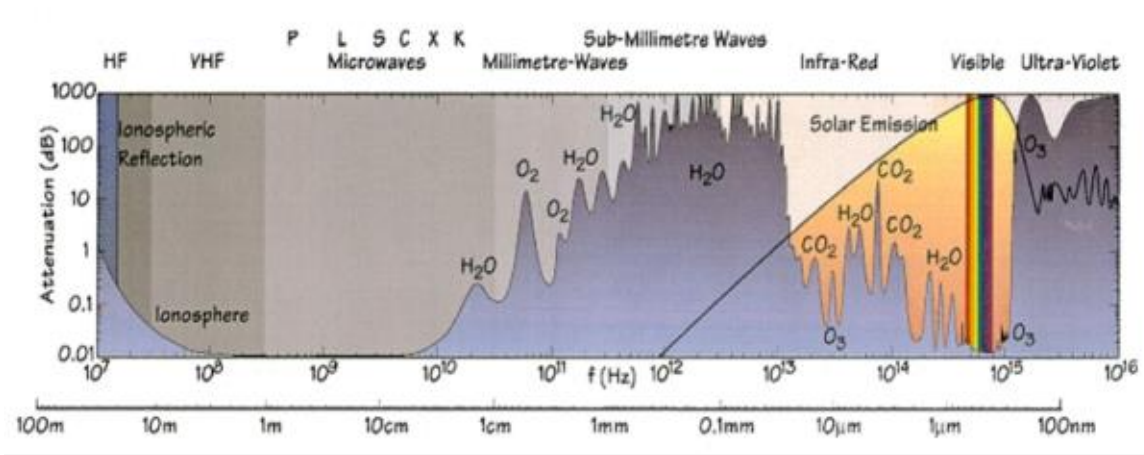


Figure 5.17. Electromagnetic spectrum with different bands indicated. (Credits ESA)

Ku band (13.6 GHz)

Ku band is the most commonly-used frequency (used for Topex/Poseidon, Jason-1, Envisat, ERS, etc). It is the best compromise between the capabilities of the technology (relating to power emitted), the available bandwidth (determined by international regulations for specific applications), sensitivity to atmospheric perturbations, and perturbation by ionospheric electrons.

C band (5.3 GHz)

C band is known to be more sensitive than Ku to ionospheric perturbation, and less sensitive to the effects of atmospheric liquid water. Its main function is to enable correction of the ionospheric delay in combination with the Ku-band measurements. To obtain the best results, an auxiliary band like this must also be as far as possible from the main one.

S band (3.2 GHz)

S band is also used in combination with the Ku-band measurements, for the same reasons as the C band.

Ka band (35 GHz)

Signal frequencies in the Ka band enable better observation of ice, rain, coastal zones, land masses (forests, etc.) and wave heights. Due to international regulations governing the use of electromagnetic wave bandwidth, a larger bandwidth is available than for other frequencies, thus enabling higher resolution, especially near the coast. It is also better reflected on ice. However, attenuation due to water or water vapour in the troposphere is high, meaning that no measurements are produced when the rain rate is higher than 1.5 mm/h.

Dual-frequency altimeters

Using two frequencies is a way of estimating the content of ionospheric electrons, thus correcting the altimeter range from the delay these electrons induce. Other uses of these two simultaneous measurements can be made, such as estimation of rain rates.

A varying bandwidth

For the Envisat satellite, the RA-2 has three different bandwidths for the same central Ku-band frequency. Each bandwidth corresponds to a proper resolution, which is better with an increasing bandwidth:

- a first bandwidth at 320 MHz with resolution of 47 cm and the returned power is recorded in 128 tracking gates spaced at 3.125 ns
- a 80 MHz bandwidth with resolution of 190 cm and a tracking gate width of 12.5 ns
- a 20 MHz bandwidth with resolution of 750 cm and a tracking gate width of 50 ns

The change of the resolution is done autonomously by the instrument, in function to the topographic features observed. If the instrument is on the maximum resolution (320 MHz bandwidth) and the surface type changes, the resolution will autonomously change (from 320 MHz to 80 MHz and then to 20 MHz) in order to maintain always the echo within the tracking window, avoiding, as it happened on ERS-2 RA, to lose track. Only under critical conditions, over abrupted terrains, when the 20 MHz window width is not enough to hold the echo, the track is lost until it lock on again, a few moments later.

5.1.4 High-precision altimetry with satellites working together

In many ways, the orbit of an altimetry satellite is a compromise. But one point that deserves special attention is getting the right balance between spatial and temporal resolution: a satellite that revisits the same spot frequently covers fewer points than a satellite with a longer orbital cycle. One solution is to operate several satellites together.

Ocean

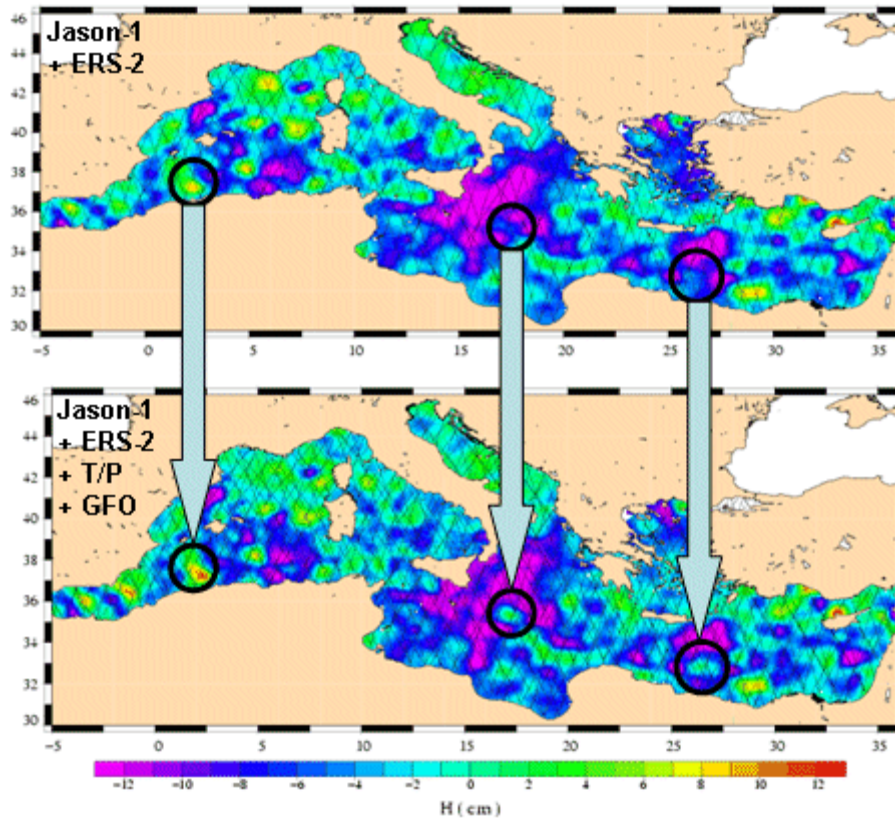
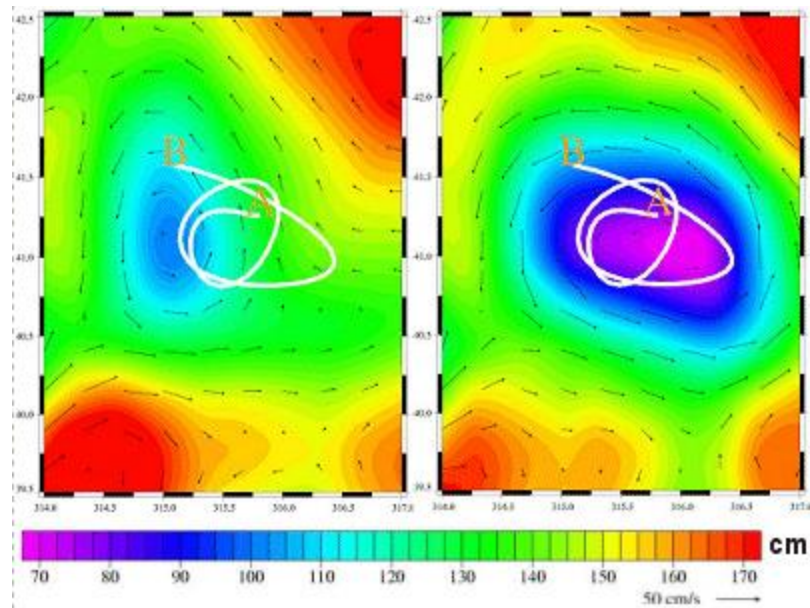


Figure 5.18. Sea level anomaly maps over the Mediterranean from 11 June 2003, made from Jason-1 + ERS-2 (top) and Jason-1+ERS-2+T/P+GFO (bottom). Merging the data from the four satellites shows eddies (circles) that are invisible, or barely visible with two satellites and much better resolved with four. (CreditsCLS)

Topex/Poseidon-ERS and Jason-Envisat are fine examples of how altimetry satellites can operate together. Topex/Poseidon and Jason-1 follow a repeat cycle of ten days designed to monitor ocean variations, so they pass over the same points fairly frequently but their ground tracks are some 315 kilometres apart at the equator – wider than the average span of an ocean eddy. On the other hand, ERS-2 and Envisat only revisit the same point on the globe every 35 days but the maximum distance between two tracks at the equator is just 80 kilometres. Other combinations are possible, but at least two altimetry satellites are required to map the ocean and monitor its movements precisely, particularly at scales of 100 to 300 kilometres (mesoscale). With four altimetry satellites available (Jason-1, Envisat or ERS-2, Topex/Poseidon and GFO), the resolution of sea surface height measurements is greatly enhanced. At least three satellites are needed to observe eddies and mesoscale phenomenon, especially in the Mediterranean.

Figure 5.19. Buoy trajectory (white line, from 14 to 28 May 2003, from A to B) and merged absolute dynamic topography in the Gulf Stream on 21 May 2003. Left with 'only' two satellites, right with four satellites. The left-hand map corresponds more closely to the eddy revealed by the buoy's path. (Credits CLS)



Hydrology

For hydrology applications, more satellites primarily mean that a larger number of lakes and rivers can be observed.

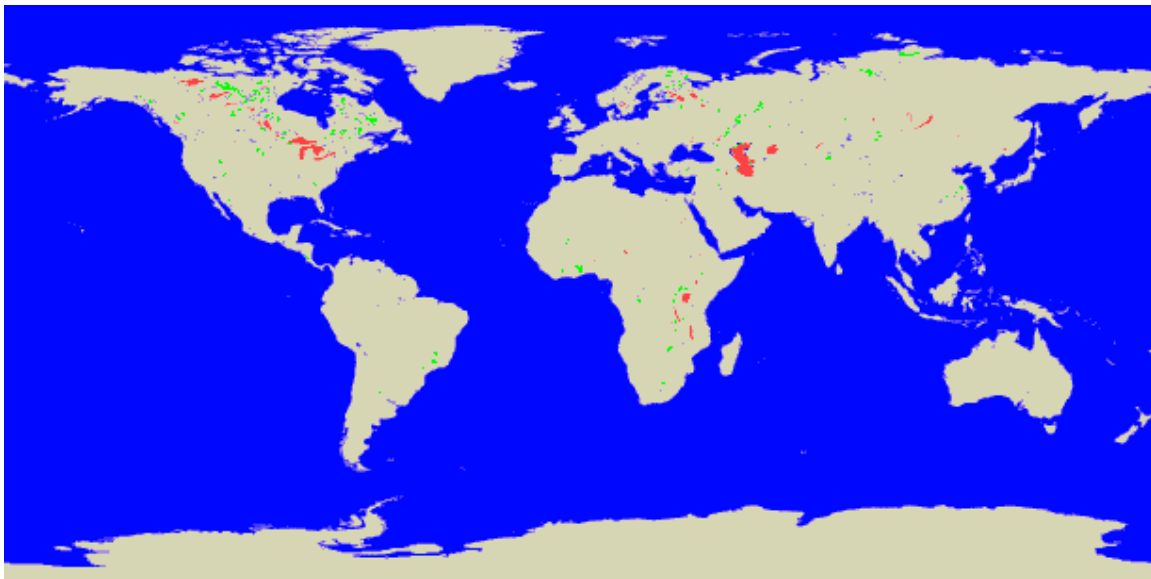


Figure 5.20. Number of lakes seen by ERS (or Envisat) (215 lakes of more than 100km²) and Topex/Poseidon (43 lakes) (Credits DMU)

Ice and land

Over ice and land, the main advantage is the denser coverage. On some surfaces, and with some satellites (e.g. Envisat and CryoSat over ice caps), some data combinations are possible.

Further information:

- Report of the High-Resolution Ocean Topography Science Working Group Meeting, Dudley B. Chelton, Ed., March 2001.
- Ducet, N., P.-Y. Le Traon, and G. Reverdin, Global high resolution mapping of ocean circulation from Topex/Poseidon and ERS-1 and -2, *J. Geophys. Res.*, 105 (C8), 19477-19498, 2000.
- Pascual, A., Y. Faugère, G. Larnicol, P-Y Le Traon, Improved description of the ocean mesoscale variability by combining four satellite altimeters. *Geophys. Res. Lett.*, 33, L02611, doi:10.1029/2005GL024633, 2006.

5.1.5 Delay-Doppler (or SAR) Altimetry

The Delay Doppler/SAR altimeter differs from a conventional radar altimeter in that it exploits coherent processing of groups of transmitted pulses. It is not pulse-limited like classical radar altimeters, so the full Doppler bandwidth is exploited to make the most efficient use of the power reflected from the surface.

Delay Doppler/SAR altimeter “stares” at each resolved along-track cell as the radar passes overhead for as long as that particular cell is illuminated. Note that each cell is viewed over a larger fraction of the antenna beam than the pulse-limited; thus more data is gathered, which leads to substantial benefits (e.g. it uses most of the power received).

The Delay Doppler/SAR altimetry processes the data such that they could be seen as having been acquired from a synthetic aperture antenna. This along track processing increases resolution and offers a multilook processing with the two independent dimensions: along-track and across-track (range).

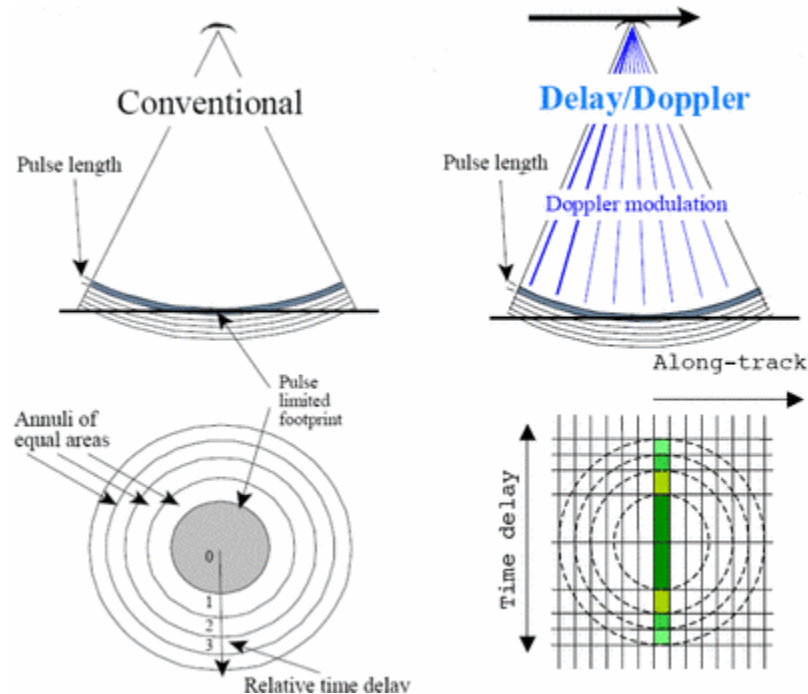


Figure 5.21. Comparison between conventional radar altimeter (far-left) and Delay Doppler/SAR (near-left) altimetry. (Credits R.K. Raney, Johns Hopkins University Applied Physics Laboratory)

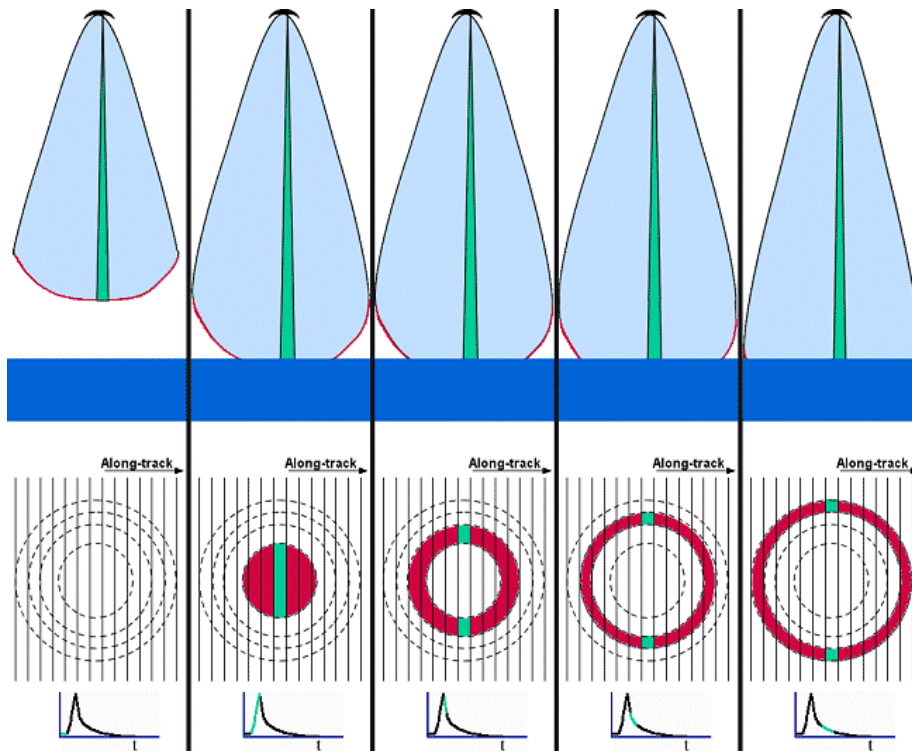


Figure 5.22. Theoretical “step-by-step” building of a SAR-altimetry waveform (for a single Doppler beam). Contrary to the classical altimeter, the lighted area is not a surface-constant ring, but only part of it, which explain the peakier shape of the echo. Several such beams are used at the same time (Using material from R.K. Raney, Johns Hopkins University Applied Physics Laboratory)

The Delay Doppler/SAR mode altimeter offers many potential improvements over conventional altimetry for measurements over the oceans, coastal zones and inland waters using retracker adapted to the specific nature of Delay Doppler/SAR altimeter echoes.

CryoSat-2 and Sentinel-3 operate a Delay Doppler/SAR mode altimeter , and Sentinel-6 mission will.

5.2 Data Flow

The mission ground segments are a vital component of satellite operations. They are responsible for turning the satellite telemetry into usable data products. They encompass ground support facilities which control instruments, process data and provide user services and expert altimetry support.

Step 0 Data acquisition

First of all, the data from the satellites have to be downlinked to the ground stations.

Step 1 Raw telemetry (level 0) and level 1 data

Raw telemetry downlinked to the ground stations is forwarded to the quality control and processing centres. Telemetry is then processed to obtain level 1 data, i.e., data that are timed and located, expressed in the appropriate units, and checked for quality.

Step 2 Level 1 data and level 2 geophysical data

Level 1 data are corrected for instrument errors, errors due to atmospheric signal propagation and perturbations caused by surface reflection. Geophysical corrections are then applied (solid earth, ocean and pole tides, etc.). Moreover, precise orbit determination (POD) can be performed to provide the highest accuracy.

Step 3 Data validation and qualification

The geophysical data are validated for quality assurance. Validation involves precise quality controls and monitoring of instrument drift. This step is an integral part of the processing sequence before giving the go-ahead to generate science products and distribute them to users.

Step 4 Level 3 and level 4 data: “value-added products”

Level 3 data are validated (off-record data are edited), along-track data. Further computation is performed on level 2 geophysical data (e.g. SSH or SLA). There may be cross-calibration between missions. Level 4 are multi-satellite (cross-calibrated), gridded data.

See Missions for information about their dedicated ground segments.

5.2.1 Data acquisition



Figure 5.23. Kiruna ground station (Credits ESA)

Data acquisition from the different altimetry satellites is performed by each agency. Several ground stations exist around the world (e.g. Kiruna, Sweden for the European Space Agency, Aussaguel, France for CNES, Poker Flats and Wallops for NASA, etc). They collect raw data from the satellites and send them to the control and processing centres.

Altimetry data processing also demands several external datasets, in particular to deal with the corrections required for processing the highest quality data.

5.2.2 Data processing

Transforming raw altimetry data into an easily usable form involves a great deal of data processing.

Numerous elements are included in altimetry data. Some come from the altimeter, some from the other onboard instruments, or other instruments; others from models, or a combination of all the former. Classic altimetry data processing (i.e. mostly dedicated to ocean applications), as performed by the ground segments includes:

Further information:

- [Envisat RA-2/MWR Level 2 User Manual](#) (pdf zipped version, 3 MB), Edition 1.2, June 2006
- [Aviso and PoDaac User Handbook – IGDR and GDR Jason-1 Products](#), (pdf version, 1.7 MB), SMM-MU-M5-OP-13184-CN, Edition 5.0, September 2015
- [Aviso User Handbook: Merged Topex/Poseidon Products](#), (pdf version, 900 KB), AVI-NT-02-101-CN, Edition 3.0, July 1996
- [RA/ATSR products – User Manual](#), (pdf, 2.9 MB), C2-MUT-A-01-IF, Edition 2.3, July 2001
- [OSTM/Jason-2 Product Handbook](#) (13th January 2017 Issue 1 rev 11)
- [CryoSat product Handbook](#)
- [Sentinel 3 user handbook](#)

5.2.2.1 Altimeter measurements

Altimeter measurements are deduced from the waveforms, i.e. the radar echoes (see How altimetry works for further details).

Altimetric range

The range is the distance from the satellite's centre of mass to the surface of the Earth, as measured by the altimeter. Thus, the altimeter measurements are referred as 'range' or 'altimeter range', not height. This is the principal measurement made by the radar altimeters. The range is estimated from the echo waveforms as part of the processing known as retracking. This measurement is not the altitude, it is still only a measurement of distance.

If the altimeter is a two-frequency instrument, there will be a range computed for both frequencies. However, the Ku band range is used for most applications.

Significant Wave Height

Significant wave height is computed from the slope of the return radar pulse (the gradient of the leading edge of the radar echo, known as the leading-edge slope), after reflection on the surface.

If the altimeter is a dual-frequency instrument, there will be a Significant Wave Height computed for both frequencies.

Backscatter coefficient (Sigma-naught)

The backscatter coefficient, σ_0 , is computed from the power of the altimeter's return pulse.

If the altimeter is a dual-frequency instrument, there will be a backscatter coefficient computed for both frequencies.

Wind speed

The backscatter coefficient can be related to wind speed. Empirical models have established a relationship between the wind speed, the sea surface backscatter coefficient and significant wave height. Wind speed is calculated from the mathematical relationship with the Ku-band backscatter coefficient and the significant wave height. The wind speed model function is evaluated for 10 metres above the sea surface, and is considered to be accurate to 2 m/s

5.2.2.1.1 Altimetric range

An altimeter operates by sending out a short pulse of radiation and measuring the time required for the pulse to return from the sea surface. This measurement, called the altimeter range, gives the distance between the instrument and the sea surface, provided that the velocity of the propagation of the pulse and the precise arrival time are known.

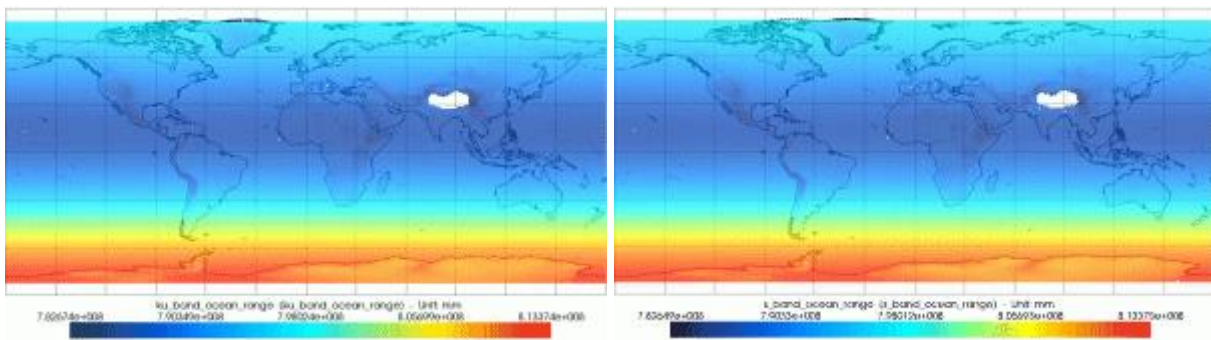


Figure 5.24. Altimetric range in Ku and S band (from Envisat GDR cycle 40) measurements. These maps are drawn using the BRAT.

The dual frequency altimeters perform range measurements at the two frequencies, enabling measurements of the range and the total electron content. While both range measurements are usually provided in (I)GDRs, the Ku band range measurement has much higher accuracy than the C or S band measurement. The range reported in (I)GDRs has already been corrected for a variety of calibration and instrument effects, including calibration errors, pointing angle errors, centre of gravity motion, and terms related to the altimeter acceleration such as Doppler shift and oscillator drift. The sum total of these corrections also appears on the (I)GDR for each frequency ranges.

5.2.2.1.2 Significant Wave Height

Significant wave height is computed from the slope of the return radar pulse (the gradient of the leading edge of the radar echo, so called the leading-edge slope), after reflection on the surface.

If the altimeter is a two-frequency instrument, there will be a Significant Wave Height computed for both frequencies.

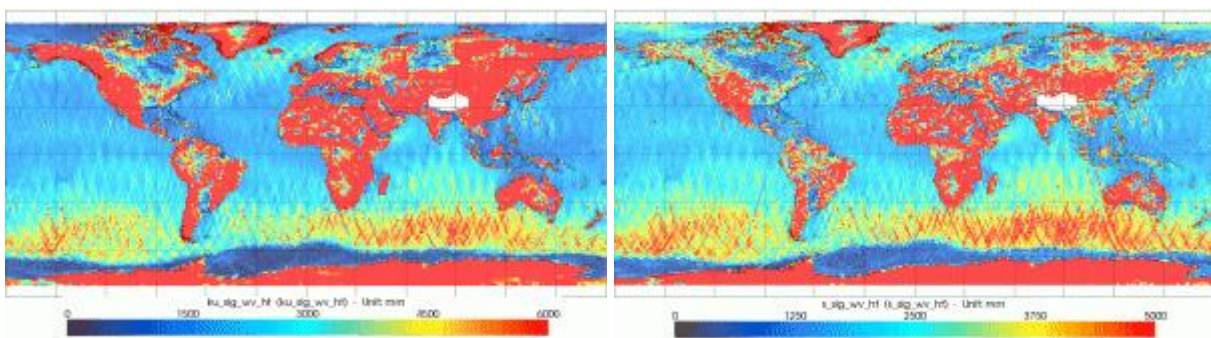


Figure 5.25. Significant wave heights in Ku and S band (from Envisat GDR cycle 40) measurements. The algorithm is computing on the whole Earth, even if the output is not meaningful outside ocean. These maps are drawn using the BRAT.

Significant wave height is a variable used in marine meteorology that matches the mean height of the third of the highest waves. However, a wave in a hundred reaches one and a half this value, and some can even reach twice this. Heights once at the coast are difficult to predict, since they depend on submarine reliefs. Significant wave heights measured during storms or hurricanes can be over 18 m: 18.3 m for a winter storm in the North Atlantic in December 2007, 16.9 m for Katrina in August 2005, 17.1 m for Hurricane Luis in September 1995, or 17.9 m for Ivan in September 2004.

5.2.2.1.3 Backscatter Coefficient

The backscatter coefficient, σ_0 , is computed from the power of the return pulse of the altimeter. It can be related to wind speed. Empirical models establish a relation between the wind speed, and the sea surface backscatter coefficient and significant wave height. It can also provide information about the surface upon which the radar wave reflected (e.g. snow or bare earth, even the kind of ice, the fact there are crevasses in ice shelves,...)

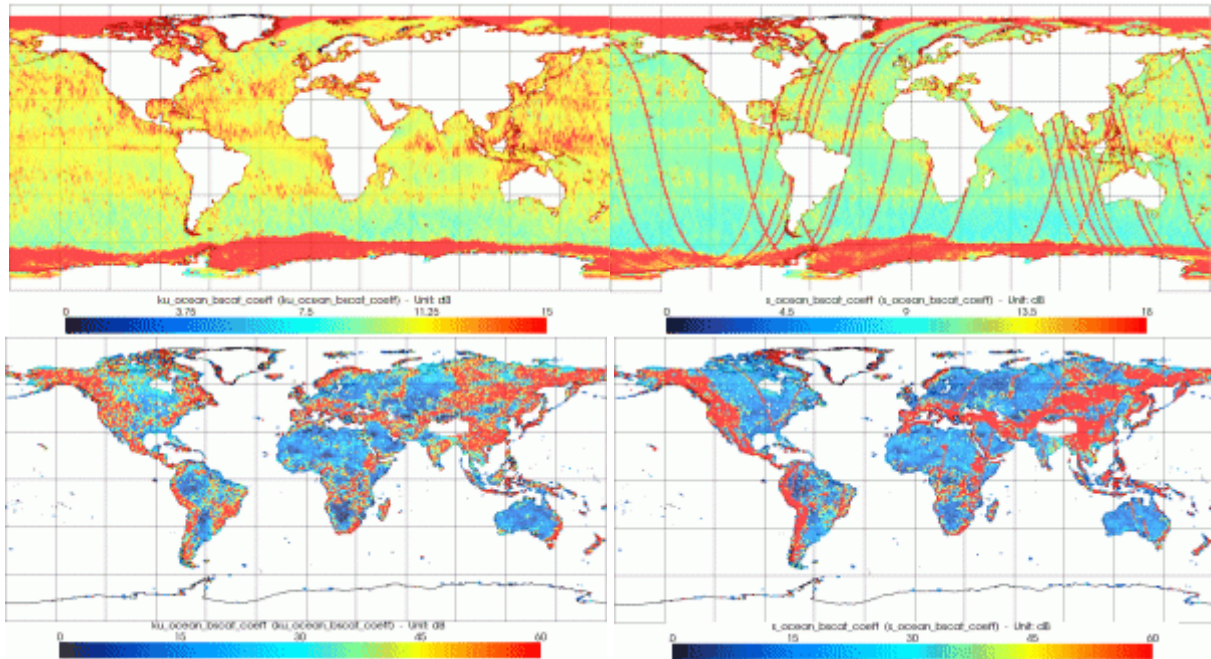


Figure 5.26. σ_0 in Ku and S band (from Envisat GDR cycle 40) measurements (top over ocean, bottom over lands). Water, ices and lands give very different values of these backscatter coefficients, since those surfaces have different reflexivity. These maps are drawn using the BRAT.

5.2.2.1.4 Wind Speed

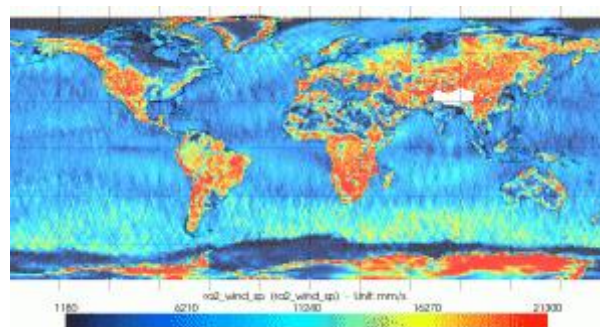


Figure 5.27. Wind speed modulus as computed from Envisat data (GDR cycle 40). Since wind speeds higher than 20 m/s can not be measured reliably, the algorithm used at that time in Envisat data is making a plateau at 21 m/s. The algorithm is computing on the whole Earth, even if the output is not meaningful outside ocean. This map is drawn using the BRAT

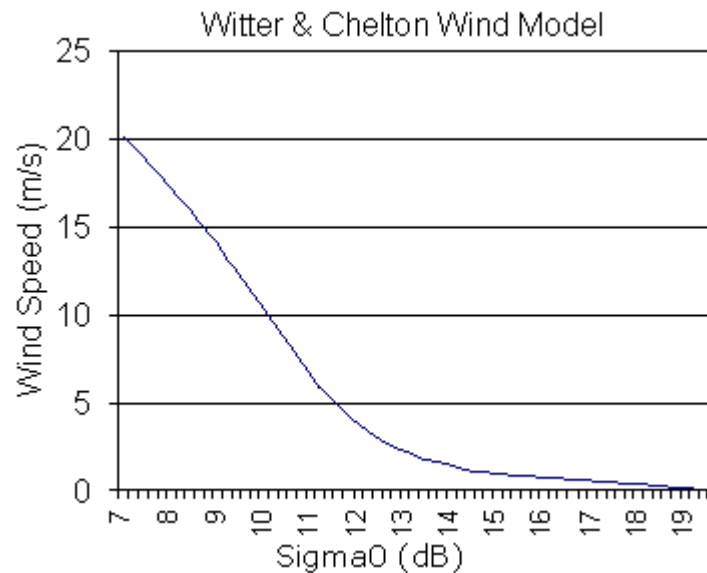


Figure 5.28. Winter & Chelton wind model

The backscatter coefficient can be related to wind speed. The model functions developed to date for altimeter wind speed have all been purely empirical. The model function establishes a relation between the wind speed, and the sea surface backscatter coefficient and significant wave height. A wind speed is calculated through a mathematical relationship with the Ku-band backscatter coefficient and the significant wave height, using the Vandemark and Chapron algorithm. The wind speed model function is evaluated for 10 metres above the sea surface, and is considered to be accurate to 2 m/s.

5.2.2.2 Orbit Determination

The ability to precisely determine a satellite's position on orbit is a key factor in the quality of altimetry data. Besides measurements acquired by the location systems onboard the satellites, which are cross-calibrated, we now rely on increasingly accurate orbit determination models.

Different products require different levels of accuracy. Data generated within three hours are based on a preliminary orbit from the Diode onboard navigator (DORIS). On the other hand, data generated 30 days post acquisition require the most accurate orbit possible and therefore demand more orbit data and more time for calculations. Expected accuracy on the radial orbit component is 20 cm rms for three-hour data, 2.5 cm rms for three-day data, and 1.5 cm for 30-day data. The ultimate aim is to achieve centimetre accuracy.

To achieve the goal of an orbit error of just one centimetre, we need a detailed knowledge of the satellite and its variations – due to manoeuvres, fuel consumption, solar panel orientation and so on – so that we can precisely model the forces acting on it (attraction, atmospheric drag, etc.). We also need to determine the gravity field very precisely. The geodesy missions (Champ, Grace, and Goce) will help us to improve our understanding of these factors.

Orbit choice

For dedicated missions like Topex/Poseidon and Jason-1, orbit precision is the most important criteria. A high-altitude orbit is chosen to attenuate the effects of the Earth's gravity potential, which are not known with great accuracy for lower orbits. The orbit must not be too close to the poles, because the Earth's gravity potential is also less well understood there. A high revisit capability is in

order, to enable ocean signals to be observed. And being able to overfly any absolute calibration sites is also an advantage. For multi-instrument missions like ERS and Envisat, the compromise must take into account any other intended observations (ice, in particular).

Conversely, the higher the orbit, the more power will be needed for the radar emission, in order to get back a strong enough signal, and the more vulnerable it will be to solar winds and cosmic particles. Lastly, to observe as much ocean as possible, an orbit close to the poles will be required.

The inclination of a satellite’s orbit is the angular distance of the orbital plane with respect to the Earth’s equatorial plane. An inclination of, e.g., 90 degrees indicates a polar orbit (this is the case with ESA’s Earth-observing Envisat satellite), in which the satellite passes nearly above both poles of the planet on each revolution. An inclination of 66 degrees, like the CNES/NASA Topex/Poseidon satellite, implies that the orbits sample from 66° North to 66° South, so as to cover most of the world’s oceans. There are different types of orbits: sun-synchronous, geosynchronous, geostationary, prograde, retrograde, etc. A sun-synchronous orbit (also called a heliosynchronous orbit) such as Envisat’s combines altitude and inclination in such a way that the satellite passes over any given point of the Earth’s surface at the same local solar time. Envisat, for instance, crosses the equator fourteen times a day, always at 10:00 local time. This is achieved by having the orbital plane of the satellite’s orbit precess (rotate) approximately one degree eastward each day, to keep pace with the Earth’s revolution around the sun. With a sun-synchronous orbit, observation of the ground is improved as the surface is always illuminated at the same Sun angle when viewed from the satellite. Sun-synchronous satellite orbits are retrograde (they orbit the Earth in an opposite direction to the Earth’s spin rotation). However, as 24 hours is the period of some tidal constituents, these will thus always be observed at the same stage of their cycle. Topex/Poseidon, in contrast, has a non-sun-synchronous and prograde orbit and a repeat period of 9.916 days (i.e. the satellite passes vertically over the same location, to within 1 km, every ten days). Envisat’s repeat cycle is 35 days. A satellite can be accurately tracked in a number of ways. The DORIS system on board Topex/Poseidon and Envisat, for instance, uses a worldwide network of ground beacons, transmitting to the satellite. It was developed by CNES. DORIS uses the Doppler shift on the beacon signals to accurately determine the velocity of the satellite on its orbit, and dynamic orbitography models to deduce the satellite’s trajectory relative to Earth.

Orbit selection

The factors to be considered for selecting the orbit for each instrument include:

Table 5.1 Factors considered on the orbit selection

Requirement	Influence Factors	Orbital Parameter
observation frequency	swath width; revisit time	altitude
global access	maximum latitude; spacing between ground-tracks	inclination, altitude
regular ground pattern	synchronous or drifting orbit	altitude
regular illumination conditions	sun-synchronism	inclination and altitude
aliasing of solar tides	sun-synchronism	inclination and altitude
aliasing of all tides	repeat period	altitude

Table 5.1 Factors considered on the orbit selection

Requirement	Influence Factors	Orbital Parameter
accessibility of celestial sphere	orbital precession	inclination and altitude
discontinuities in orbit	orbit maintenance frequency	altitude
mission lifetime	orbital decay	gross altitude
instrument spatial resolution / radar transmitter power		gross altitude
radar PRF (pulse repetition frequency)		altitude range
Permanent cold radiator surfaces	sun-synchronism	inclination and altitude

Some of these are fundamental and have an impact on the overall design of the system. In particular, the selection of a sun- or non-sun-synchronous orbit is of primary importance. The total altitude range is also critical to the design. After that, there is a certain degree of freedom in the choice of parameters. Previous mission orbits may also determine the choice of orbit (e.g. Jason-1 on the tracks of Topex/Poseidon, Envisat on those of ERS-2).

Orbit maintenance

The orbit maintenance requirements for altimetry missions are usually that the deviation of the actual ground track from the nominal one is kept below 1 km and that the mean local nodal crossing time matches the nominal one to better than to within five minutes. The orbit maintenance strategy aims for minimum disturbance of the payload operation. In-plane manoeuvres are used for altitude adjustment to compensate for the effects of air-drag. This altitude decay control affects the ground-track repeatability, mainly in the equatorial regions. The frequency of these manoeuvres is determined by the rate of orbital decay, which in turn is determined by the air density, and this is a function of solar activity. The nominal rate for these in-plane manoeuvres is nominally twice a month. They will do not interrupt the operations of most sensors. Out-of-plane corrections are used to correct rectify the steady drift of inclination mainly caused by solar and lunar gravity perturbations. The solar wind also influences inclination, but its contribution is typically an order of magnitude smaller than the one given made by solar and lunar gravity. Inclination drift degrades ground-track maintenance at high latitudes. The drift rate does not depend on air density and corrections are required every few months. As they are out-of-plane they require a 90-degree rotation of the spacecraft, to align the thrusters with the required thrust direction, so these manoeuvres will be performed in during the eclipse to avoid the risk of optical sensors viewing the sun.

5.2.2.3 Geophysical corrections

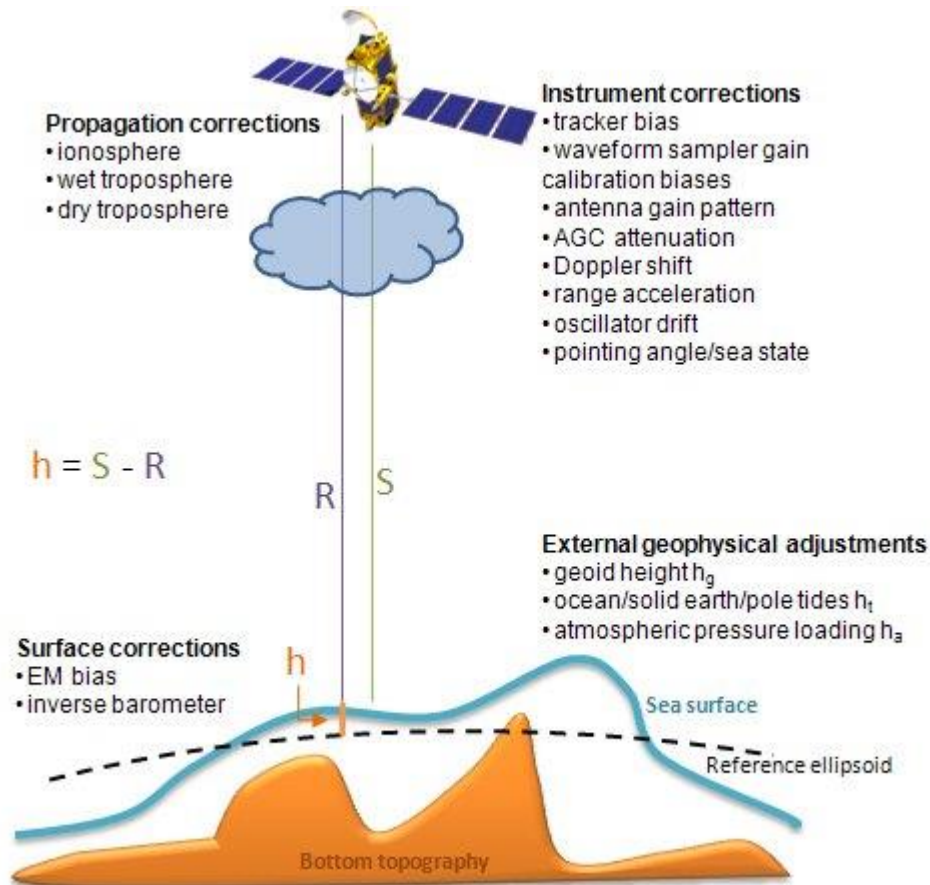


Figure 5.29. Altimetry corrections illustration

The following corrections are computed:

Geophysical corrections

- Ocean tides
Corrections for solid earth and sea surface height variations due to the attraction of the Sun and Moon. Calculated by models.
Order of magnitude: 1 m in mid-ocean, up to 15-20 m near some shorelines.
- Solid earth tides
Corrections for solid earth variations due to the attraction of the Sun and Moon. Calculated by models.
Order of magnitude: 50 cm.
- Pole tides
Corrections for variations due to the attraction of the Sun and Moon. Calculated by models.
Order of magnitude: 2 cm.
- Tidal loading
Corrections for height variations due to changes in tide-induced forces acting on the Earth's surface. Calculated by models.
Order of magnitude: 30 cm

Propagation corrections

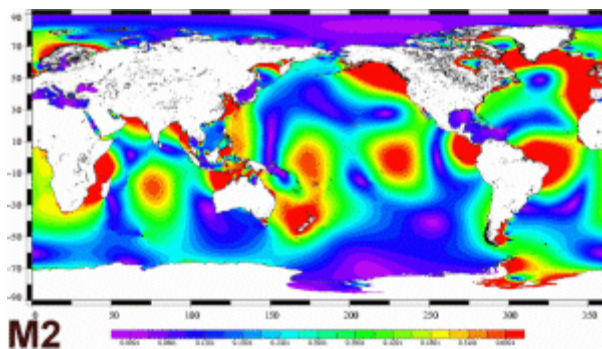
- Ionosphere
Correction for the path delay in the radar return signal due to the atmosphere's electron content. Calculated by combining radar altimeter measurements acquired at two separate frequencies (C-band and Ku-band for Topex and Jason-1, Ku-band and S-band for Envisat).
Order of magnitude: 0 to 50 cm
- Wet troposphere
Correction for the path delay in the radar return signal due to cloud liquid water and water vapour in the atmosphere. Calculated from radiometer measurements and/or meteorological models.
Order of magnitude: 0 to 50 cm
- Dry troposphere
Correction for the path delay in the radar return signal due to dry gases in the atmosphere. Calculated from meteorological models.
Order of magnitude: 2.3 m

Surface corrections

- Inverse barometer
Correction for variations in sea surface height due to atmospheric pressure variations (atmospheric loading). Calculated from meteorological models.
Order of magnitude: about 15 cm, depending on atmospheric pressure
- Electromagnetic bias
Correction for bias in measurements introduced by varying reflectivity of wave crests and troughs. Correction calculated from models. Bias uncertainty is currently the biggest factor in altimeter error budgets.
Order of magnitude: from 0 to 50 cm, depending on wave heights

5.2.2.3.1 Ocean tides

The combined attraction of the Moon and the Sun is behind the tides and their variations. Ocean tides represent more than 80% of the variability of the surface in the open ocean. In most regions of the world oceans, the tides periods are semidiurnal or diurnal (periods near 0.5 or 1 day) so they are shorter than the repeat periods of an altimeter satellite orbit. Tidal corrections are very important for oceanographic studies because tidal signals contaminate the low-frequency part of raw altimetric signals.



The standard deviations of tidal variations in the open ocean are 10-60 cm with larger values near coastal regions (they can reach 10 metres in some ports) and in marginal seas. Tidal variations are thus larger in magnitude than the 5-30 cm standard deviations of the dynamic sea surface height. In this respect, ocean tides can be regarded as noise and must therefore be removed to estimate the dynamic sea surface height. It is imperative that the tide model used

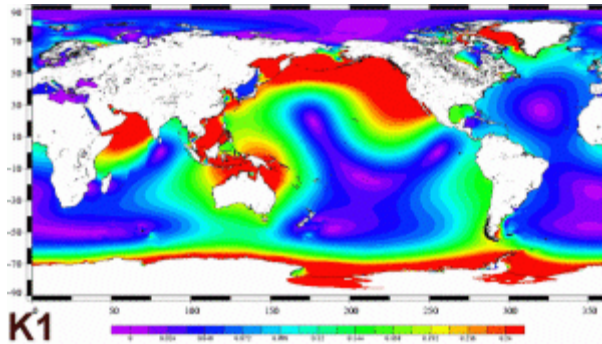


Figure 5.30. Amplitude in metres of the two main tide components from FES2004 model, one semi-diurnal (top, M2 wave), the other diurnal (bottom, K1 wave). While M2 is clearly dominant on the French coasts (two tides per day), K1 is dominant in the China Sea where there is only one tide per day. (Credits CLS/Legos)

to correct the altimeter data be accurate. If errors in the tide model are large compared with oceanographic variability at the alias frequencies, then oceanographic applications will be compromised at these frequencies. Prior to the launch of Topex/Poseidon, knowledge of tides over the global ocean was based primarily on hydrodynamical models. The accuracies of these models were limited by some uncertainties and were constrained by empirically determined ocean tides from a worldwide network of coastal and inland tide gauges and bottom pressure gauges. Tides errors exceeded 10 cm in many areas of the world ocean.

The altimeter data at the aliased tidal periods have been analysed to extract estimates of tidal amplitudes and phases at the altimeter satellites locations. These empirical estimates have been assimilated into sophisticated hydrodynamical and statistical models to estimate the tides globally with high spatial resolution. One of the important accomplishments of the altimeter missions has been the global estimation of tides to an accuracy of 2-3 cm.

Further information:

- Le Provost C., Ocean tides, Satellite altimetry and Earth sciences, L.L. Fu and A. Cazenave Ed., Academic Press, 2001
- Ray, R., A Global Ocean Tide Model From TOPEX/Poseidon Altimetry/ GOT99.2 – NASA/TM-1999-209478. Greenbelt, MD, Goddard Space Flight Center/NASA: 58, 1999.
- Lebedev, S., A. Sirota, D. Medvedev, et al., Exploiting satellite altimetry in coastal ocean through the ALTICORE project, Russ. J. Earth Sci., 10, ES1002, 2008 doi:10.2205/2007ES000262.

5.2.2.3.2 Pole tides

The ocean pole tide is the ocean response to the variation of both the solid Earth and the oceans to the centrifugal potential that is generated by small perturbations to the Earth's rotation axis.

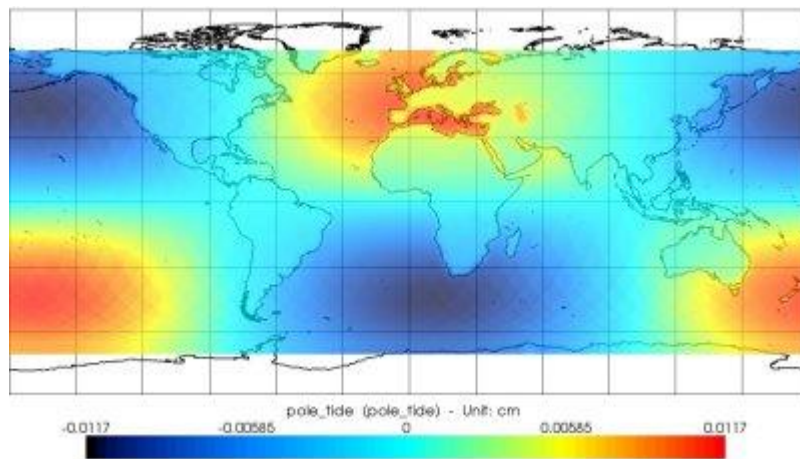


Figure 5.31. Amplitude in cm of the pole tide correction during the Jason-1 cycle 223 computed from an equilibrium model. This map is drawn using the BRAT from the Jason-1 GDR products. A Loess filter (value of 31) is applied to obtain a fully coloured plot.

These small perturbations to the Earth's rotation axis primarily occur at periods of 433 days (called the Chandler wobble) and annually. These periods are long enough for the pole tide displacement to be considered to be in equilibrium with the forcing centrifugal potential. Results from satellite altimetry demonstrate that the long-wavelength component of the geocentric pole tide deformations at the Chandler period is consistent with the theoretical self-consistent equilibrium response and can explain 70% of variations of the theoretical classical equilibrium response [Desai, 2002].

The pole tide is easily computed as described in Wahr [1985]. Modelling the pole tide requires knowledge of proportionality constants, the so-called Love numbers, and a time series of perturbations to the Earth's rotation axis, a quantity that is now measured routinely with space techniques.

Further information:

- Desai S. D., Observing the pole tide with satellite altimetry , *J. Geophys. Res.*, 107(C11), 3186, doi:10.1029/2001JC001224, 2002.
- Wahr J. M., Deformation induced by polar motion, *J. Geophys. Res.*, 90(B11): 9363 – 9368, 1985.

5.2.2.3.3 Ionosphere corrections

This correction takes into account the path delay in the radar return signal due to electron content in the atmosphere. Calculated by combining radar altimeter measurements acquired at two separate frequencies (C-band and K_u -band for Topex and Jason-1, K_u -band and S-band for Envisat) or from DORIS measurements (Topex/Poseidon, Jason-1 and Envisat).

Its order of magnitude can reach 0 to 50 cm.

The ionosphere is the uppermost layer of the atmosphere (ranging between about 60 and 800 km), distinct from the other layers by the fact it is ionized. The electrons that interfere with the radar wave propagation have their highest concentration between about 250 and 400 km. Ionization of this region of the atmosphere is attributed mostly to extreme-ultraviolet radiation from the Sun. Seasonal variations, as well as 11-year variations (corresponding to the solar cycle) can be seen. Number of sunspots, episodic X rays and solar particle fluxes associated with solar flares can also occur. Significant disturbances are also measured in particular during geomagnetic storms caused by the

interaction between the solar wind and the Earth's magnetic field (The solar wind consists of a constant stream of charged particles flowing outward from the Sun. Most of these particles are deflected by the Earth's magnetic field. But some get through to the ionosphere and interact with the atmosphere).

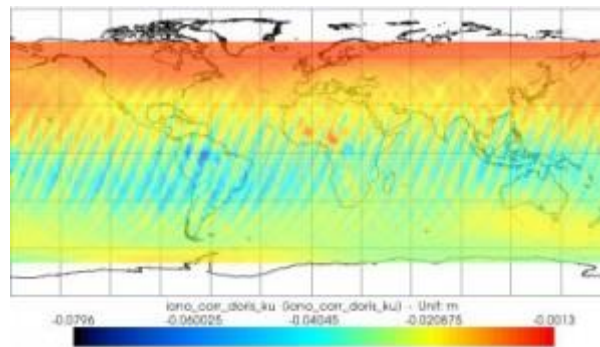


Figure 5.32. Amplitudes in metres of the ionospheric correction derived from Doris measurements. This map is drawn using the BRAT from the Jason-1 GDR products. A Loess filter (value of 31) is applied to obtain a fully coloured plot

The propagation velocity of a radio pulse is slowed by an amount proportional to the density of free electrons of the Earth's ionosphere, also known as the total electron content (TEC, measured by the total electron content units, $1 \text{ TECU} = 10^{16} \text{ el. m}^{-2}$). The retardation of velocity is inversely proportional to frequency squared. For instance, it causes the altimeter to slightly over-estimate the range to the sea surface by typically 0.2 to 20 cm at 13.6 GHz. The amount varies from day to night (very few free electrons at night), from summer to winter, and as a function of the solar cycle (fewer during solar minimum). For treatments of this correction, see Chelton et al. [2001], Imel [1994], and Callahan [1984].

Because this effect is dispersive, measurement of the range at two frequencies allows it to be estimated. Under typical ocean conditions of 2-metre significant wave height the Ku band ionospheric range correction that is determined from the dual frequency measurements from the altimeter is expected to have an accuracy of $\pm 0.5 \text{ cm}$.

References:

- Chelton *et al.*, Satellite Altimetry, *Satellite altimetry and Earth sciences*, L.L. Fu and A. Cazenave Ed., Academic Press, 2001.
- Imel, D., Evaluation of the Topex/Poseidon dual-frequency ionosphere correction, *J. Geophys. Res.*, 99, 24, 895-906, 1994.
- Callahan, P.S., Ionospheric variations affecting altimeter measurements: A brief synopsis, *Mar.Geod.*, 8, 249-263, 1984.

5.2.2.3.4 Wet troposphere correction

The wet troposphere correction is the correction for the path delay in the radar return signal due to cloud liquid water and water vapour in the atmosphere. It is calculated from radiometer measurements and meteorological models.

Its order of magnitude is about 0 to 50 cm with an annual cycle amplitude of up to 20 cm.

It is usually computed over oceans with simultaneous radiometric measurements (see the JMR: Jason-1 Microwave Radiometer). However, such radiometric measurements generally fail over land or near

the coasts and may be superseded by a correction computed from meteorological model outputs (GDP+, NCEP or ECMWF models).

In addition to its limited geographical coverage, this correction suffers from the fact that the altitude of the water body is not taken into account: the atmosphere column reaches the sea level everywhere and is thus too thick!

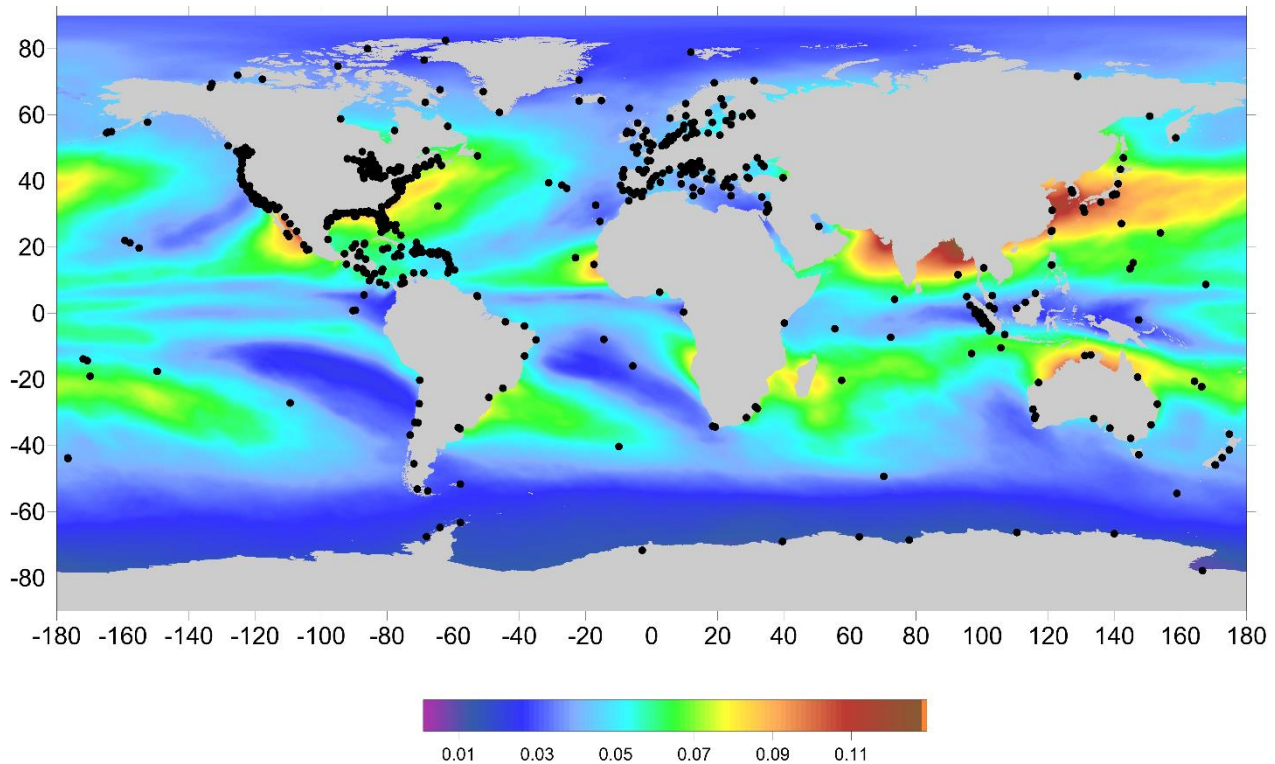


Figure 5.33. Location of the global set of GNSS coastal and island stations (black dots) used in the GPD+(GNSS-derived path delay Plus algorithms) computations. The background picture is the map of the standard deviation of the wet tropospheric correction, in metres, computed from two years of ECMWF model fields. (Credits University of Porto)

An error of 10 m in the thickness of the atmosphere column corresponds to an error of 1 mm in the correction. Consequently, the correction is often overestimated for non-ocean areas. When the surface altitude with a DEM (Digital Elevation Model) is taken into account in the meteorological models, the correction is more accurate.

Therefore, the precise estimation of the altitude of the reflecting continental surface appears as the key factor for an accurate computation of the propagation delay through the troposphere. Some projects are underway to improve this wet troposphere correction near the coasts and over land using the altitude value deduced from the altimetric measurement itself.

Further information:

- Desportes, C., Obligis, E., Eymard, L., On the wet tropospheric correction for altimetry in coastal regions, in *Geosc. and Remote Sensing*, Vol.45, Issue 7, Part 1,2139-2149, 2007.
- Mercier, F., Zanife, O.Z, Improvement of the Topex/Poseidon altimetric data processing for hydrological purposes, *15 years of progress in radar altimetry Symposium*, Venice, Italy, 2006.

5.2.2.3.5 Dry troposphere correction

This correction for the dry gas component of the atmosphere refraction takes into account the path delay in the radar return signal due to the atmosphere. It is by far the largest adjustment that must be applied to altimeter measurement (since its order of magnitude is about 2.3 m) but its temporal variations are low (a few centimetres only).

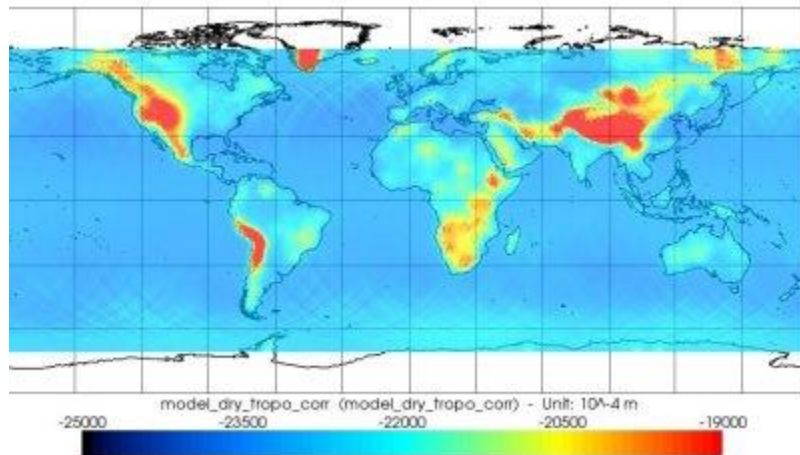


Figure 5.34. Amplitude in metres of the dry troposphere correction computed from the ECMWF atmospheric pressures and model for the Jason-1 cycle 223. This map is drawn using the BRAT from the Jason-1 GDR products. A Loess filter (value of 31) is applied to obtain a fully coloured plot.

The dry tropospheric range correction in units of cm can be approximated by the Saastamoinen formula:

$$\Delta R_{\text{dry}} = -0.02277 P_0 * (1 + 0.0026 \cos^2 \varphi) \quad \text{Eq. 2}$$

where P_0 is the sea level pressure in Pascal and φ the latitude. Thus, the dry tropospheric range delay is proportional to sea level pressure and also depends on the latitude. A sea level pressure error of 5 mbar corresponds to a range error of about 1 cm.

Since it is not possible to estimate the sea level pressure from space, the dry troposphere correction must be obtained from meteorological models.

5.2.2.3.6 Inverse barometer

The Inverse Barometer (IB) correction accounts for variations in sea surface height due to atmospheric pressure variations (atmospheric loading). It can reach about ± 15 cm and it is calculated from meteorological models.

The response of the sea surface to changes in atmospheric pressure has a large effect on measured sea surface height.

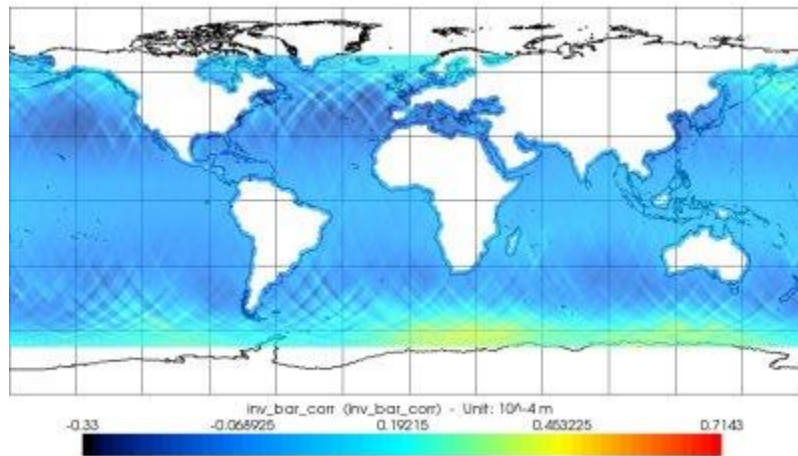


Figure 5.35. Amplitude in metres of Inverse Barometer correction computed from ECMWF atmospheric pressures during the Jason-1 cycle 223. This map is drawn using the BRAT from the Jason-1 GDR products. A Loess filter (value of 20) is applied to obtain a fully coloured plot but it makes some artificial data on coastal areas.

The inverse barometer correction IB can be easily computed from the dry troposphere correction obtained from the sea level pressure P_0 :

$$IB \text{ (mm)} = -9.948 * (\Delta R_{\text{dry}} \text{ (mbars)} - 1013.3) \quad \text{Eq. 3}$$

[from Aviso and PoDaac User Handbook – IGDR and GDR Jason-1 Product, 2008].

A 1 mbar atmospheric pressure change corresponds to a linear response of the sea level of about 1 cm.

Further information:

- C. Wunsch and D. Stammer, Atmospheric loading and the oceanic inverted barometer effect, *Reviews of Geophys.*, 35(1), 79-107, 1997.
- J. Willebrand, S.. Philander, R.. Pacanowski, The oceanic response to large-scale atmospheric disturbances, *J. Phys.Oceanography* 10, 411-429, 1980
- R.M. Ponte, P. Gaspar, Regional analysis of the inverted barometer effect over the global ocean using Topex/Poseidon data and model results, *J. Geophys. Res.*, 104 (C7), 15587-15601, 1999.
- D. Stammer, C. Wunsch, R.M. Ponte, De-aliasing of global high frequency barotropic motions in altimeter observations, *Geophys.Res.Lett.*, 27(8), 1175-1178, 2000.
- L. Carrère, F. Lyard, Modelling the barotropic response of the global ocean to atmospheric wind and pressure forcing – comparisons with observations , *Geophys.Res.Lett.*, 30(6), pp 1275, 2003.

5.2.2.3.7 Electromagnetic bias

The electromagnetic bias is originated in measurements by the different reflectivity of wave crests and troughs. The correction used is derived from models. Bias uncertainty is currently the biggest factor in altimeter error budgets.

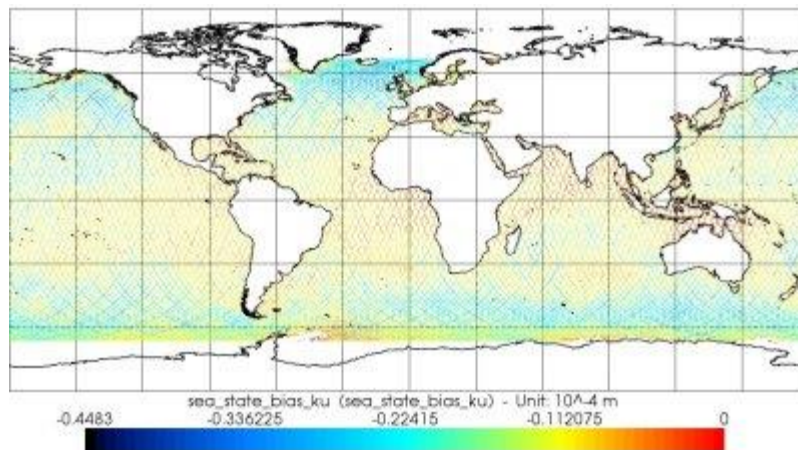


Figure 5.36. Amplitude in metres of the sea state bias correction computed from empirical model for the Ku-band, here for the Jason-1 cycle 223. This map is drawn using the BRAT from the Jason-1 GDR products.

The sea surface elements do not contribute equally to the radar return: troughs of waves tend to reflect altimeter pulses better than crests. Thus the centroid of the mean reflecting surface is shifted away from mean sea level towards the troughs of the waves. Consequently, the shift leads the altimeter to over-estimate the height of the satellite above the sea surface.

The nature of the sea state bias has been investigated using airborne radars and laser systems capable of determining, for various sea states, the strength of the vertically reflected signal as a function of the displacement of the reflecting area from mean sea level. The state bias is given as a function of wind speed and the skewness and kurtosis of the probability distribution of sea surface elevation due to the waves on the sea surface.

The electromagnetic bias is the difference between the mean height of the sea surface specular facets and the mean sea level. It is smaller towards the crests and larger towards the troughs [Yaplee, 1971]. In other words, the wave troughs are better reflectors than the crests. As a result, the mean height of the sea surface specular facets is below the mean sea level. The difference between the mean height of the specular facets and the mean sea level is the EMB.

References:

- Yaplee, B.S., and al., Nanoseconds radar observations of the ocean surface from a stable platform. IEEE Trans. Geosci.Electron. GE-9 171-174 , 1971.

5.2.2.4 Instrumental errors

The following corrections can be computed (depending on the satellites):

- USO correction (Ultra-Stable Oscillator)
Correction for drift of onboard oscillators used to generate the internal clock needed for sending radar pulses. The degree of the drift depends on the oscillator frequency.
Order of magnitude: 1 cm
- Centre of Gravity (CoG)
Correction for variations in the satellite's centre of gravity, due to fuel consumption, solar panel orientation and other factors (the presence of this correction depends on the satellite).

- Correction tables
Corrections for instrument and algorithm effects that cannot be modelled. These tables are derived from altimeter simulations (the presence of this correction depends on the satellite).
Order of magnitude: a few centimetres
- Applied to Waveforms (before retracking)
Correction for effects due to filters used to eliminate certain frequencies in the return radar signal.
Order of magnitude: a few centimetres

5.2.2.5 Reference surfaces

Reference ellipsoids and geoids are typically used to compute estimates (e.g. sea surface height with respect to WGS-84 ellipsoid) and can be included as additional information. Most are specific to the ocean.

Reference ellipsoid

The reference ellipsoid is an arbitrary reference surface that is a rough approximation of the Earth's shape, which is basically a sphere 'flattened' at its poles. The length of one of the axes at the equator is chosen so that the ellipsoid coincides with mean sea level at this latitude. It is the first-order definition of the non-spherical shape of the Earth as an ellipsoid of revolution.

Geoid

The marine geoid is the shape of the sea surface assuming the complete absence of perturbing forces (tides, wind, currents, etc.). The geoid reflects the Earth's gravitational field (it is an equipotential surface) and varies in height by as much as 100 metres over distances of several thousand kilometres due to the uneven mass distribution within the planet's crust, mantle and core. Other, less pronounced irregularities are also visible over smaller distances. These reflect the ocean bottom topography.

The marine geoid can be estimated also using altimetry measurements of sea surface height.

The absolute dynamic topography, used to derive ocean currents, can be defined as the mean sea surface height with respect to the geoid.

Mean sea surface

The Mean Sea Surface represents the sea level due to constant phenomena. It is the sum of the geoid and the Mean Dynamic Topography (that includes the permanent stationary component of ocean dynamic topography).

The Mean Sea Surface is computed from altimetry, averaging data over several years.

Sea level anomalies (also called sea surface height anomalies) are sea surface heights with respect to the Mean Sea Surface (MSS). It is not to be confused with what is usually called 'Mean Sea Level' (MSL), which is a measure of the sea level variations over time (see [Applications: Ocean: Mean Sea Level](#)).

A mean profile can also be used, which is the mean of the sea surface along the tracks of a specific satellite (whereas MSS can be computed from several satellites)

Mean dynamic topography

The Mean Dynamic Topography is the permanent stationary component of ocean dynamic topography.

This mean circulation is not produced directly from altimetry data, which rather provide the mean sea surface, consisting of the marine geoid plus the sea elevation due to the mean oceanic. We, therefore, have to combine altimetry data with other data (*in-situ*, gravimetric satellites, etc), to determine the geoid precisely, and by subtracting it, compute the mean circulation.

The relation between those three reference surfaces (each one referenced to a Reference ellipsoid) can be formalized as follow:

Mean Sea Surface (MSS) = Geoid + Mean Dynamic Topography (MDT)

Quantities computed from altimetric heights can be thus defined:

Sea Surface Height (SSH) is the sea surface height with respect to the Reference ellipsoid

Dynamic topography (or Absolute Dynamic Topography, ADT; sometimes called Sea Surface Topography — which can be misleading with Sea Surface Temperature, however) is the sea surface height with respect to the geoid

Sea Level Anomalies (SLA, also called SSHA, Sea Surface Height Anomalies) is the sea surface height with respect to a Mean Sea Surface or a Mean profile

So,

$$\text{SSH} = (\text{Altitude} - \text{Range} - \text{corrections}) = \text{geoid} + \text{ADT} = \text{MSS} + \text{SLA/SSHA} = \text{geoid} + \text{MDT} + \text{SLA/SSHA} \quad \text{Eq. 4}$$

Bathymetry

Bathymetry is the measurement of the ocean depths. Although it has no direct use in altimetry data processing, it can be useful in shallow water (since ocean altimetry is not as effective there), or for comparing with ocean features such as currents.

Bathymetry can be computed using, among other things, altimetry sea surface height measurements (via the geoid).

5.2.2.5.1 Reference ellipsoid

The reference ellipsoid is an arbitrary reference surface that is a raw approximation of the Earth's shape, which is basically a sphere "flattened" at its poles. The length of one of the axes at the Equator is chosen so that the ellipsoid coincides at this latitude with the mean sea level. It is the first-order definition of the non-spherical shape of the Earth as an ellipsoid of revolution. To first order, it accounts for over 90% of the geoid.

The reference ellipsoid is basically a convenience so that users don't have to work with larger numbers, and to get more precision in calculations. Sea surface height measurements from the centre

of the Earth are on the order of 6000 km. By removing a reference surface, the heights relative to the ellipsoid are on the order of 100 metres. Thus, one can gain several digits of accuracy in numerical calculations.

In fact, any reference surface could be used. A sphere would work, but sea surface height differences from this surface could be as large as 20 km, thus one would lose precision than by using an ellipsoid.

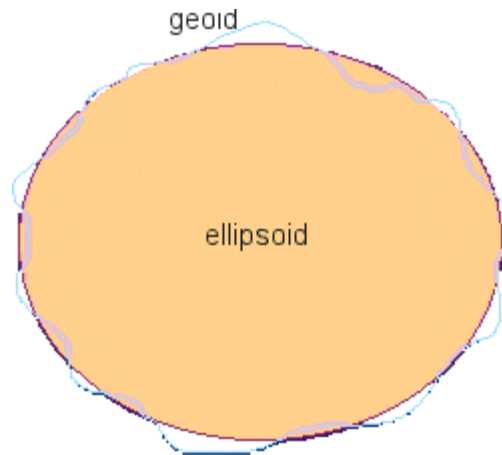


Figure 5.37. Schematic of the Reference ellipsoid with respect to the geoid.

In altimetry, the Topex/Poseidon and the WGS84 ellipsoids are typically used:

For Topex/Poseidon, Jason-1, Jason-2 (T/P ellipsoid):

- radius: 6378136.3 m
- inverse Earth flattening coefficient: 298.257

For ERS-1, ERS-2, Envisat (WGS84):

- radius: 6378137 m
- inverse Earth flattening coefficient: 298.257223563

5.2.2.5.2 Geoid

The marine geoid (actually geoid undulation, but called simply geoid) is a distance above the reference ellipsoid. It is an equipotential surface of the Earth's gravitational field that is closely associated with the location of the mean sea surface.

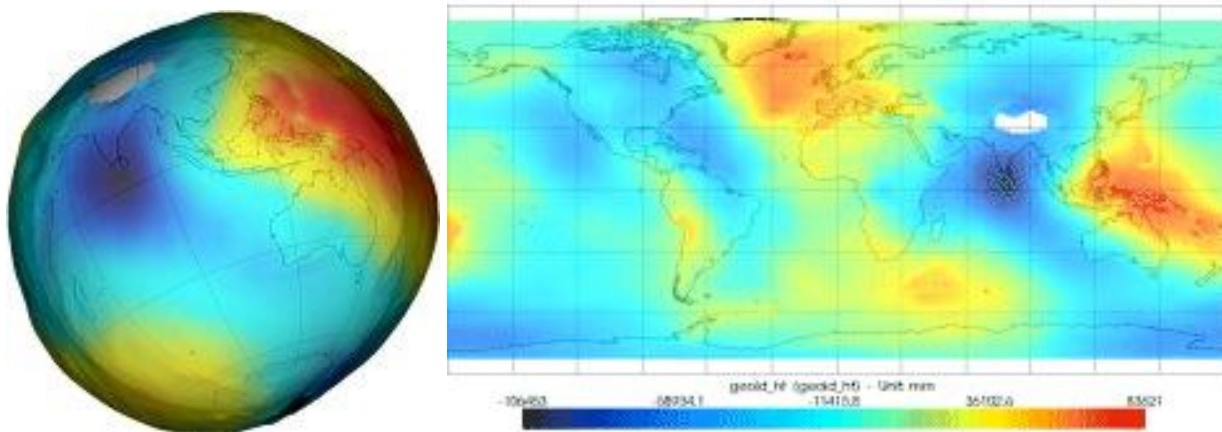


Figure 5.38. Geoid height (more properly geoid undulation) from Envisat GDR, in a 3D and in a plate carrée projection. These maps are drawn using the BRAT.

The reference ellipsoid is a bi-axial ellipsoid of revolution. The centre of the ellipsoid is ideally at the centre of mass of the Earth although the centre is usually placed at the origin of the reference frame in which a satellite orbit is calculated and tracking station positions are given. The separation between the geoid and the reference ellipsoid is the geoid undulation.

The geoid undulation, over the entire Earth, has a root mean square value of 30.6 m with extreme values of approximately 83 m and -106 m. Although the geoid undulations are primarily long wavelength phenomena, short wavelength changes in the geoid undulation are seen over seamounts, trenches, ridges, etc., in the oceans. The calculation of a high resolution geoid requires high resolution surface gravity data in the region of interest as well as a potential coefficient model that can be used to define the long and medium wavelengths of the Earth's gravitational field. For ocean circulation studies, it is important that the long wavelength part of the geoid be accurately determined. Thanks in particular to gravity missions, new geopotential models (EGM96 and EGM2008) have become available as an improvement of the initial JGM3 and OSU91A models (JGM3 is described in [Tapley et al., 1994]; OSU91A is described in [Rapp et al., 1991].)

References:

- Rapp, R. H. et al., 1991, Consideration of Permanent Tidal Deformation in the Orbit Determination and Data Analysis for the TOPEX/POSEIDON Mission, *NASA Tech. Memorandum 100775*, Goddard Space Flight Center, Greenbelt, MD.
- Rapp, R. H., Y. M. Wang, and N. K. Pavlis, 1991, The Ohio State 1991 geopotential and Sea Surface Topography Harmonic Coefficient Models, *Rpt. 410, Dept. of Geodetic Science and Surveying*, The Ohio State University, Columbus, OH.
- Tapley, B. D. et al., 1994, Accuracy Assessment of the Large Scale Dynamic Ocean Topography from TOPEX/POSEIDON Altimetry, *J. Geophys. Res.*, 99 (C12), 24, 605-24, 618.

5.2.2.5.3 Mean Sea surface

The Mean Sea Surface represents the sea level due to constant phenomena. It is the addition of the geoid and the Mean Dynamic Topography (that includes the permanent stationary component of the ocean dynamic topography).

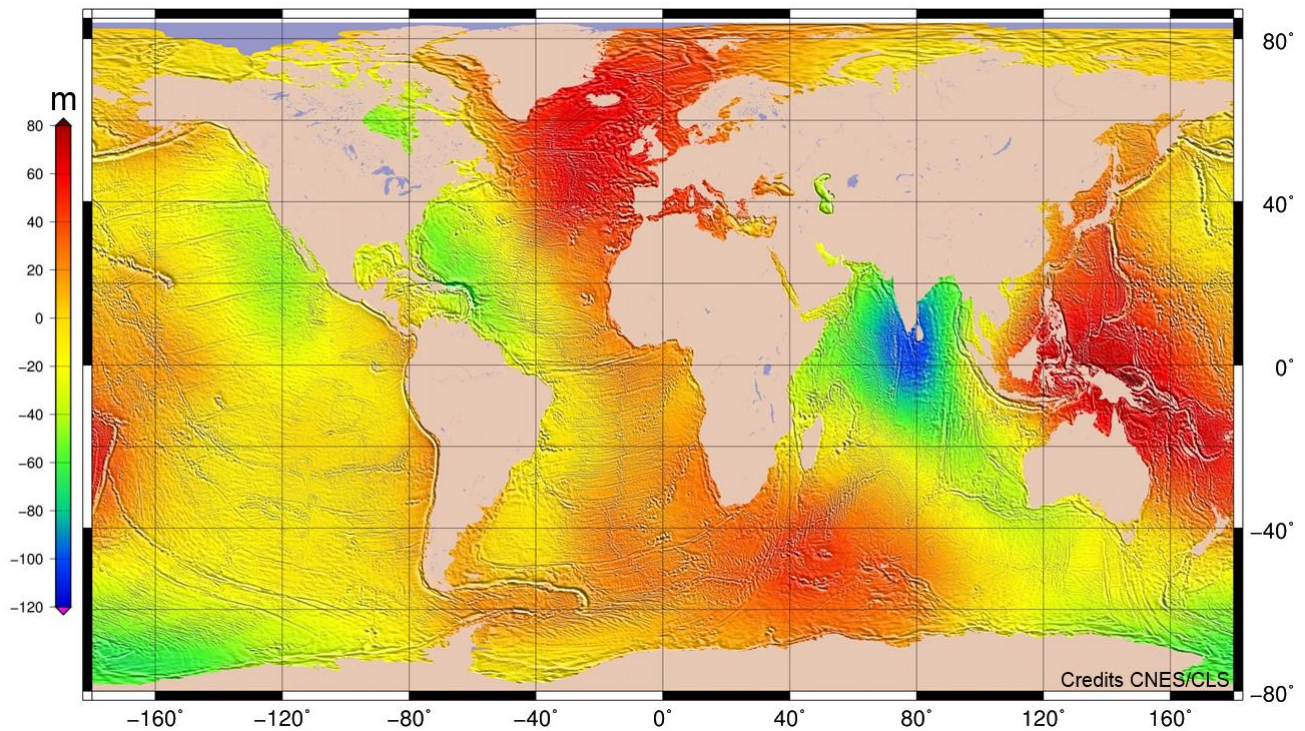


Figure 5.39. Mean Sea Surface MSS_CNES_CLS15. Credits CNES/CLS. It has been computed using a 20-year period of altimetry data

A Mean Sea Surface shows the mean shape of the sea surface during the period covered by the altimetry data. It corresponds to the sum of geoid + mean ocean circulation (it is corrected from seasonal variations). The relief of this surface reveals:

- on a scale of thousands metres, undulations of hundreds of metres due to differences in densities into the mantle;
- on medium wavelengths, currents and water masses of varying densities, leading to sea level variations of several metres;
- on short wavelengths, the heterogeneous distribution of matter concerning earth's surface layer and ocean's bottom topography, that implies geoid undulations of several metres.

A Mean Sea Surface (MSS) represents the position of the ocean surface averaged over an appropriate time period to remove annual, semi-annual, seasonal, and spurious sea surface height signals. A MSS is given as a grid with spacing consistent with the altimeter and other data used in the generation of the grid values. The MSS grid can be useful for data editing purposes; for the calculation of along track and cross track geoid gradients; for the calculation of gridded gravity anomalies, for geophysical studies; for a reference surface to which sea surface height data from different altimeter missions can be reduced, etc.

Longer time spans of data that become available in the future, along with improved data handling techniques could improve the current MSS models. Care must be given to the retention of high frequency signal and the reduction of high frequency noise.

5.2.2.5.4 Mean dynamic topography

The Mean Dynamic Topography is the permanent stationary component of the ocean dynamic topography.

This mean circulation is not an immediate product of altimetry data. Those data give more the mean sea surface, which contains the marine geoid plus the sea elevation due to the mean oceanic. So we have to combine altimetric data with others (in-situ, gravimetric satellites...), to precisely determine the geoid, and by subtracting it, compute the mean circulation.

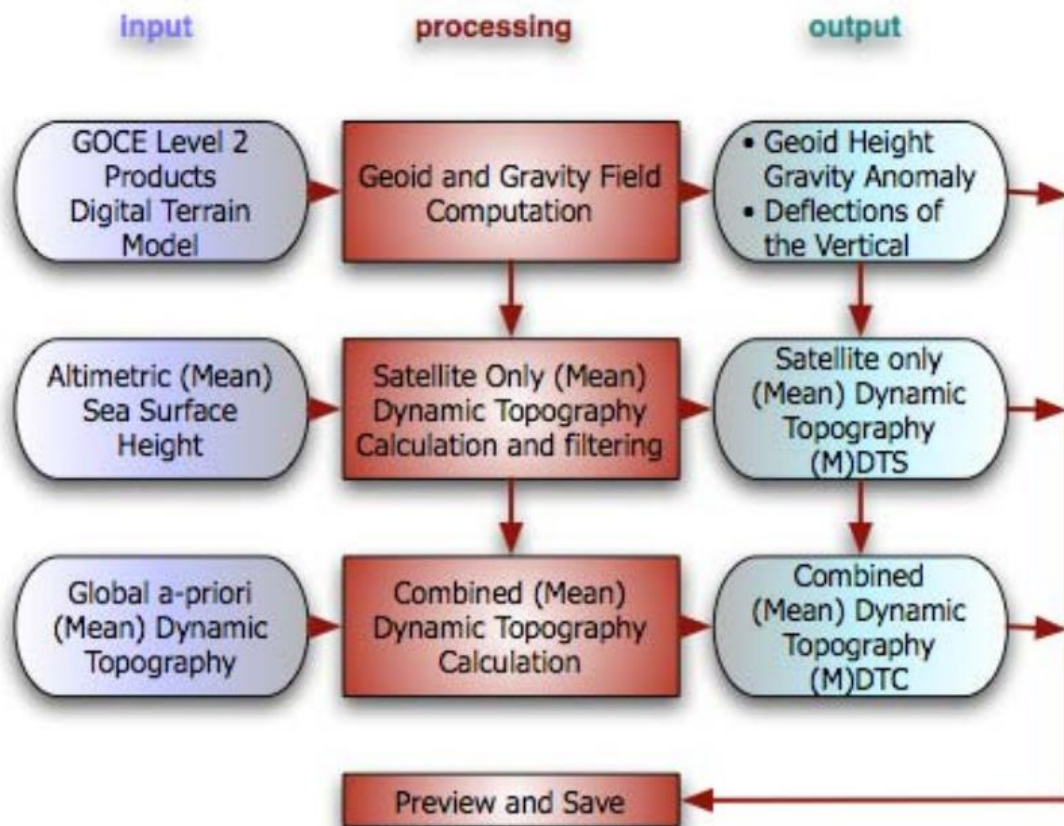


Figure 5.40. GOCE User Toolbox Workflow (Credits DTU)

The MDT computation can be performed with the GOCE User Toolbox [Bingham et al 2015]

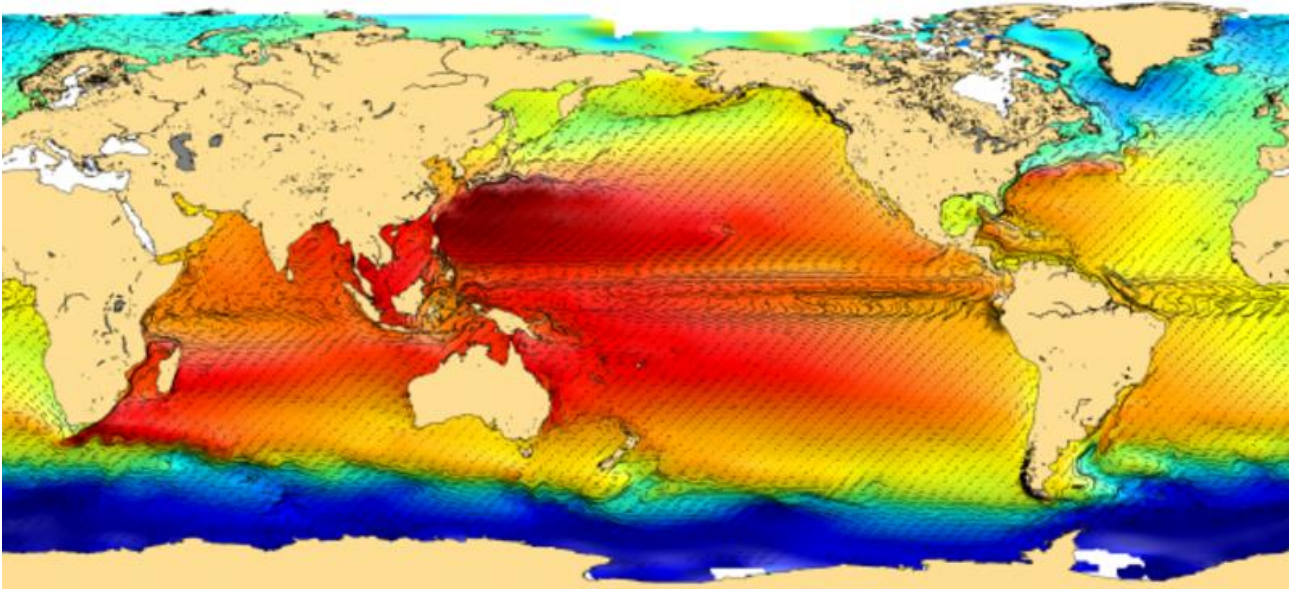


Figure 5.41. Mean dynamic topography, i.e. oceanic relief corresponding to permanent ocean circulation. Arrows are proportional to current speed. (Credits CNES/CLS)

5.2.2.5.5 Bathymetry

Bathymetry is the measurement of the ocean depths. Although it has no direct use for altimetry data processing, it can be useful for shallow water (since ocean altimetry is not at its best there), or to compare with some ocean features, like currents.

Bathymetry can be computed using among other things altimetry sea surface heights (via the geoid) measurement (see [Use Cases: Geophysics: Bathymetry](#)).

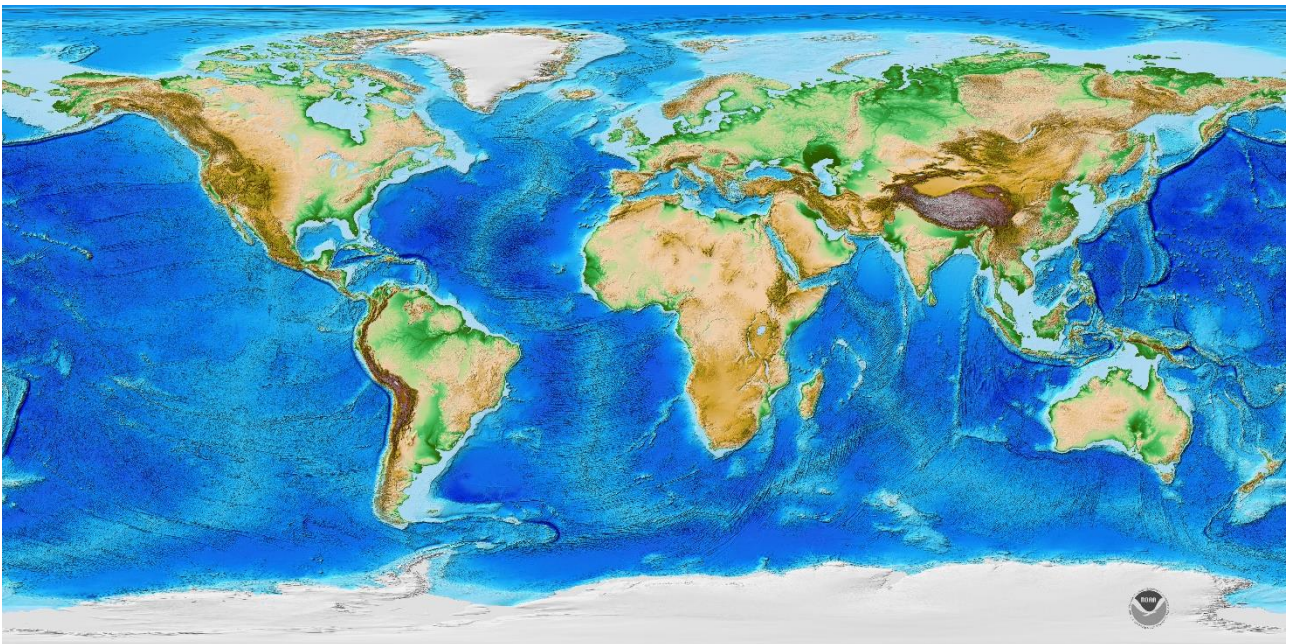


Figure 5.42. ETOPO1 Amante, C. and B.W. Eakins, 2009. ETOPO1 1 Arc-Minute Global Relief Model: Procedures, Data Sources and Analysis. NOAA Technical Memorandum NESDIS NGDC-24. National Geophysical Data Center, NOAA. doi:10.7289/V5C8276M

The (I)GDRs provide a parameter bathymetry that gives the ocean depth or land elevation of the data point. Ocean depths have negative values, and land elevations have positive values. This parameter is given to allow users to make their own “cut” for ocean depth. It is not a direct computation from the data within the same dataset.

5.2.2.6 Flags

In general, flagging consists of three parts: instrument flags (on/off), telemetry flags (preliminary flagging and editing) and data quality flags (geophysical processing flags).

- Telemetry flags are initially based on altimeter modes and concern checking of telemetry data quality. Only severely corrupted data are not processed. The flag setting used is designed to get a maximum of data into the Sensor Data Records. Science data are processed only when the altimeter is in a tracking mode.
- Quality flags involve residuals from smoothing or fits from the data themselves. Flag setting checks for gaps, exceeded limits and excessive changes. Among these flags, some have a general meaning, describing the measurement environment.
- Other flags indicate what type of surface is beneath the satellite (ocean, ice, solid earth, etc).
- Instrument flags tell us which instruments are on and/or which frequencies are used (mostly for Topex/Poseidon).

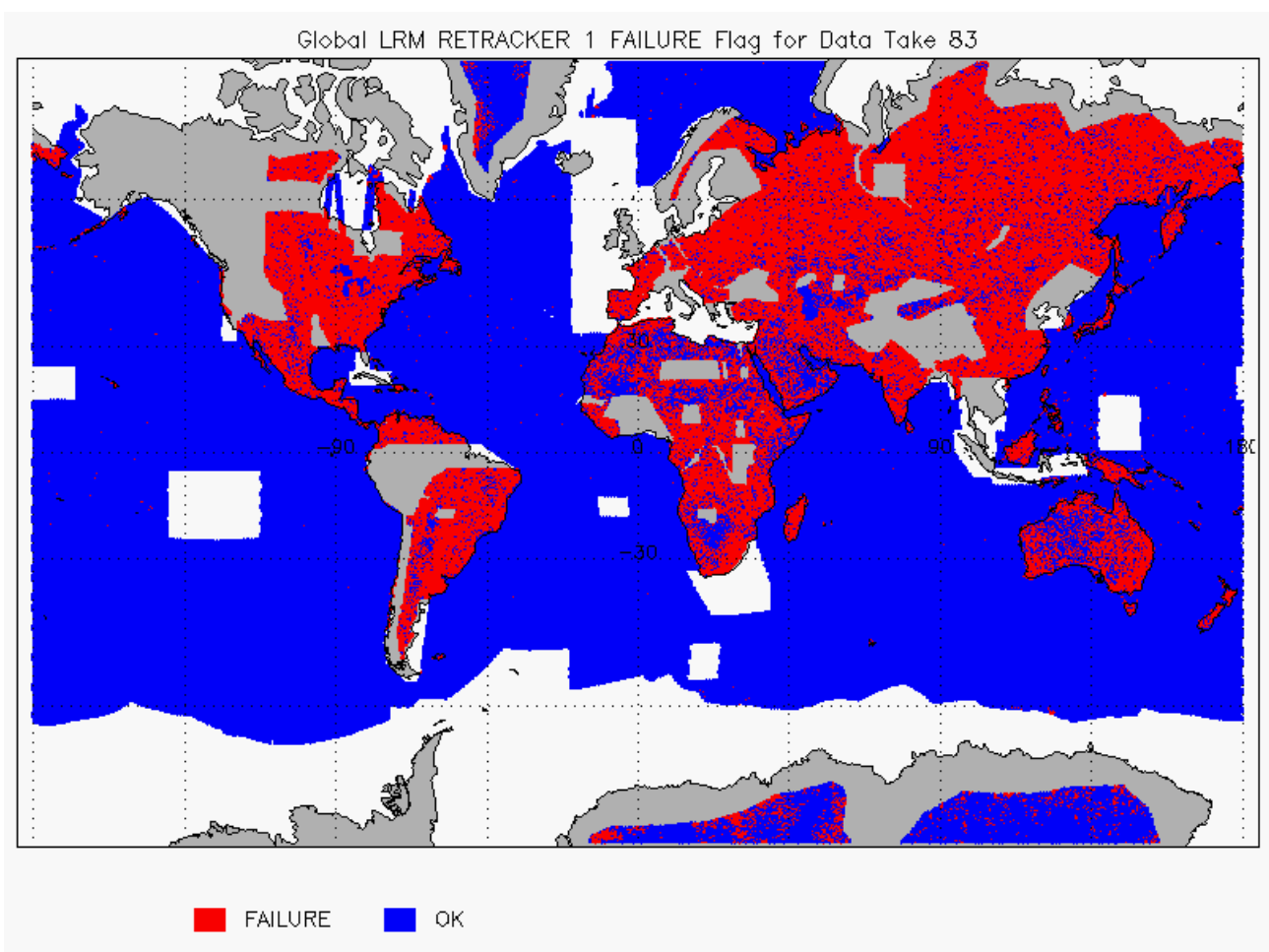


Figure 5.43. The CryoSat L2 Intermediate flag indicating the success or failure of the retracking process from 13/7/17 to 11/8/17. (Credits UCL)

5.2.2.7 Retracking

Retracking altimetry data is done by computing the departure of the waveform's leading edge from the altimeter tracking gate and correcting the satellite range measurement (and surface elevation) accordingly.

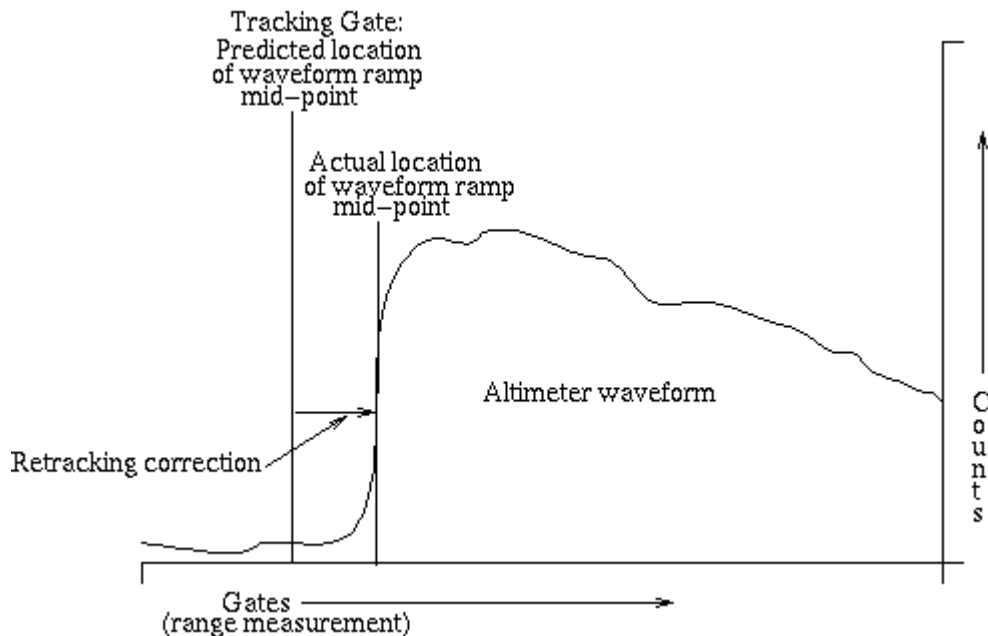


Figure 5.44. Typical ice sheet altimeter waveform illustrating the retracking correction that must be applied to compensate for deviation of the waveform's leading edge from the on-board altimeter tracking gate. (Credits NASA/GSFC)

The major stages in the acquisition and tracking of the waveforms are as follows. At regular intervals defined by the Pulse Repetition Frequency (PRF), frequency linearly modulated pulses are transmitted by the altimeter towards the Earth's surface. After reflection on the surface, the pulse is received back on board and mixed with a pulse similar to the emitted one which has been triggered by the tracker information. The mixed pulse, which is referred to as the 'individual echo', provides a sampled measurement of the return power as a function of time, distance or frequency. In order to reduce the statistical fluctuations (speckle) affecting the individual echoes and to perform real-time tracking (i.e. to maintain the signal inside an analysis window as far as range and power are concerned), these echoes are averaged on-board over a period which corresponds to the altimeter's duty cycle (typically 50 ms). The resulting signal is referred to as an 'averaged echo' or a 'waveform'. It is processed by the on-board tracking system to derive the range and power. In the case of Topex, the SWH information is also extracted. This information is then used as input for the tracking loop during the duty cycle that follows.

The acquisition and tracking functions are carried out by two subsystems. The first one performs acquisition of the waveforms, this is the Radio Frequency Unit (RFU). The second one processes the waveforms, this is the Processing and Control Unit (PCU).

Over topographic surfaces, a radar altimeter's on-board tracking system is unable to maintain the echo waveform at the nominal tracking position in the filter bank, due to rapid range variations. This results in an error in the telemetered range known as tracker offset. Retracking is the term used to describe a group of non-linear ground processing estimation techniques which attempt to determine the tracker offset from the telemetered echoes, and thereby estimate the range to the point of closest

approach on the surface. Peaky echoes from sea ice cause range tracking jitter, which also results in tracker offset.

For example, there are three independent retracking techniques used by Envisat RA2 over non-ocean surfaces:

- **Ice2 retracker**
The ice2 retracker was designed specifically for Envisat in order to extract parameters related to geophysical phenomena over land surfaces as well as water surfaces. This retracking fits a Brown-like model to the altimeter waveform.
The output parameters are: the leading-edge amplitude, the range, the leading-edge width, the trailing edge slope and the backscatter.
- **Sea-ice retracker**
The second retracker is a threshold retracker intended for use with data from sea ice, i.e. very specular or narrow-peaked echoes. From the parameterisation, a tracker offset is calculated. In addition, an estimate of the backscatter is made from the power in the filter bank. Although the given algorithm is general, only Envisat RA2 Ku-band calculations are currently done for sea ice.
The sea ice retracking algorithm uses a threshold to determine the leading-edge position calculated as a fraction, $T02_j$, of the peak amplitude A_{jsea} . The leading-edge position is taken as the point on the echo that first crosses the amplitude $T02_j A_{jsea}$, where the scaling factor is currently set to 0.5.
- **OCOG retracker**
The Offset Centre-of-Gravity (OCOG) retracker is most suited for continental ice data. The waveform pair is parameterised using the OCOG scheme. From the parameterisation, a tracker offset is calculated. In addition, an estimate of the backscatter is made from the power in the filter bank.
In OCOG retracking, the echo is replaced with a box that has the same centre of area as the echo. The box is defined by parameterisation of the waveform using three measurements, i) the position of the centre of area, ii) the width of the box, and iii) the amplitude of the box.
The leading edge position is taken as the point on the echo that first crosses the amplitude $T01_j A_{jocog}$, where $T01_j$ is an empirically determined threshold, currently set to 0.5.

5.2.2.8 High-Level processing

Once level 2 data (i.e data incorporating instrumental, atmospheric and geophysical corrections, and validated for quality assurance) have been processed, more advanced processing can be applied. This involves data qualification, pre-computing some parameters, re-projecting others, making a grid out of the along-track data, and even merging several different datasets from various satellites.

Selecting valid data

Processing high-level altimetry data begins with quality control, and validation of altimetry data and geophysical corrections. Only valid ocean data are selected. Editing criteria for each satellite is provided in the handbooks.

Applying altimetric corrections and computing physical parameters

Altimeter measurements have many potential sources of error. They need to be corrected for instrumental errors and geophysical influences (tides, atmospheric delays, etc). Then, by subtracting the range from the satellite's altitude, the (corrected) surface height can be obtained. Other parameters can also be derived, such as sea level anomalies, etc.

Reducing orbit error: multi-mission processing

Using multiple satellites together makes high-definition altimetry possible. The main point of multi-mission processing is to intercalibrate the different altimeters.

Multi-mission crossover differences are minimised by multi-satellite orbit error determination, or by adjusting less accurate orbits using a more precise mission as a reference. This is done for missions that do not have very accurate orbit determination (ERS and GFO) but also to remove biases and differences with the reference mission (T/P from February 2004, Envisat) [Le Traon et al., 1995], [Le Traon and Ogor, 1998]. Using the precision of the reference mission orbit, the orbit error can be estimated very accurately.

Mapping (or gridding) the along-track data

Altimetry data are, basically, along-track. For ease of use and compatibility with other datasets, they can be gridded, i.e. data along the track are interpolated and provided as points on a grid (e.g. data every $1/3^\circ$ in longitude and latitude).

References:

- Le Traon, P.-Y., F. Ogor, ERS-1/2 orbit improvement using Topex/Poseidon: The 2 cm challenge, *J. Geophys. Res.*, 103, C4, 8045-8057, 1998.
- Le Traon, P.-Y., P. Gaspar, F. Bouyssel, H. Makhmara, Using Topex/Poseidon data to enhance ERS-1 orbit, *J. Atm. Ocean. Tech.*, 12, 161-170, 1995.

5.2.3 Data qualification: "CalVal"

Calval (CALibration / VALidation) is what determines data quality. This step involves a series of quality controls designed to ensure a continuous supply of data.

Calval teams calibrate the satellite instruments and determine the parameters, corrections, biases and so on to be applied to measurements. In particular, this task involves validating and refining algorithms in close collaboration with processing system development teams and users. Once the mission is fully underway, Calval operations consist in determining data quality and keeping a check on instrument drift. Quality control is achieved through statistical data analysis, analyses at crossover points, and comparisons between orbit cycles. Data are also compared with other missions.

Calibration phase

Absolute calibration is the comparison of the engineering measurement with an independent measurement (e.g. buoy, tide gauge) of the same parameter (range, sea surface height, etc.). Absolute calibration provides one reference point for the complete altimetric time series, a decade after the absolute calibration of ERS-1. In relative calibration, two altimetry systems are compared through their global geophysical data products. Due to the huge number of globally-distributed measurements processed, relative calibration is significantly more precise than local absolute calibration. This is where the main benefit of this technique lies: to ensure consistency in two different but momentarily overlapping missions.

The altimeter's calibration and validation activities are normally organised by working teams with thematic responsibilities. Verification and absolute calibration of range and σ_0 are tasks of the In-flight Instrument Calibration Team, orbit validation is the task of the Precise Orbit Determination

Team, and relative calibration and product validation are the responsibility of the Cross-Calibration and Validation Team.

The altimetric measurement time series, being produced from different altimetric missions, will need to be inter-calibrated, within a required precision, in order to obtain a consistent multi-satellite data set. Inter-calibration, or so-called cross-calibration, is the determination of relative biases between the measurements of different altimeters.

Cross calibration activities are divided into product validation and algorithm verification. The objective behind product validation is to authorise the distribution of validated products to all users within weeks/months after launch. The geophysical processing algorithms also undergo a post-launch verification of real data with the aim of assessing algorithm performance, tuning processing parameters and applying relevant calibration coefficients at the end of the commissioning phase.

Data exploitation

After the Commissioning Phase, the Routine Exploitation phase begins, and continues until the end of the altimetry mission. The commissioning phase group is then required to formulate further recommendations at the completion of the phase (e.g. updating parameters in processors by applying new calibration values, updating algorithms, opportunity to reprocess commissioning phase data, proposed new products and algorithms, etc). During the routine phase these recommendations are taken on board, and new instrument or processing anomalies are investigated and solved.

5.3 Future technology improvements

Satellite altimetry has proven to be a valuable source of data for a broad range of applications. Looking beyond the missions in operational service today, future satellites will need to provide better spatial and temporal coverage so that we can study mesoscale variations and other phenomena more closely. For the medium term, consideration is now being given to altimetry missions capable of ‘scanning’ the ocean surface to acquire data at scales of a few tens of kilometres, passing over the same spots every few days. Other projects on the drawing board are based on constellations of dedicated, low-cost microsattellites. The use of ‘opportunity signals’ is also being considered, with the possibility of retrieving reflected signals transmitted by satellites in the Global Navigation Satellite System (GNSS).

Ka-band altimetry

A Ka-band (35 GHz) altimeter would be much less affected by the ionosphere than one operating at Ku-band, and would have greater performance in terms of vertical resolution, time decorrelation of echoes, spatial resolution and range noise. With the design of an adapted tracker algorithm, near-continuous altimetric tracking over all kinds of surface could be performed, which is especially important when approaching or leaving coasts. The main drawback is that Ka-band electromagnetic waves are sensitive to rain. However, this does not prevent them from acquiring a fairly high percentage of measurements, except for strong rain rates.

Altimeter-interferometers

An altimeter/interferometer would include several altimeters mounted on masts which would acquire measurements simultaneously, thus providing continuous, single- or multi-altimeter wide-area coverage.

Constellations

One of the ways to improve altimetry resolution is to use several satellites at the same time. Until now, this has been done with very different types of satellite. The use of several identical satellites in constellation could reduce costs (development costs, and launch costs too for micro-satellites launched by the same rocket).

GNSS altimetry

One approach being pursued to achieve maximum altimetry data coverage is to receive reflected signals transmitted by satellites in the Global Navigation Satellite System (GNSS), in particular from the Global Positioning System (GPS) constellation and its European civil counterpart, Galileo. This concept is based on a satellite in near-polar orbit (at an altitude of 400 to 500 km) retrieving signals emitted by multiple satellites and reflected by the ocean surface, then analysing these signals to compute sea surface height. This concept is currently still only in the study phase.

Further information:

- Special Issue on Satellite Altimetry: New Sensors and New Application, *Sensors*, Ge Chen and Graham D. Quartly ed., 2006
- Guijarro, J., R. Santoleri, B.B. Nardelli, L. Borgarelli, R. Croci, R. Venturini, G. Alberti, A. Caramagno, F. Pirondini, Innovative radar altimeter concepts, *Geoscience and Remote Sensing Symposium, 2003. IGARSS '03 Proceedings*, IEEE International, 2, 1080- 1082, 2003.

5.3.1 Ka-band altimeter

A Ka-band (35 GHz) altimeter would be much less affected by the ionosphere than one operating at Ku-band, and would have enhanced performance in terms of vertical resolution, time decorrelation of echoes, spatial resolution and range noise. With the design of an adapted tracker algorithm, near-continuous altimetric tracking above all kinds of surface could be performed, which is especially important when approaching or leaving coasts. The main drawback is that Ka-band electromagnetic waves are sensitive to rain. However, this does not prevent them from acquiring a fairly high percentage of measurements, except for strong rain rates.

Use of the Ka-band for an altimeter would provide:

- Low ionospheric attenuation—this can be considered as negligible, except for some exceptional ionospheric situations—and would therefore eliminate the need for a dual-frequency altimeter. The DORIS system can provide data for ionospheric corrections whenever there are significant perturbations.
- Higher pulse repetition frequency (4 kHz).
- The decorrelation time of sea echoes at Ka-band is shorter than at Ku-band. This makes it possible to increase significantly the number of independent echoes per second compared with Ku-band altimeters.
- Larger bandwidth (up to 500 MHz).
- The 500 MHz bandwidth that can be used at Ka-band provides a high vertical resolution (0.3 m) which is improved with respect to other altimeters (including Jason-1 and Envisat).
- Better description of sea surface roughness than at Ku-band
- The eight-millimetre wavelength is better suited to describing the slopes of small facets on the sea surface (capillary waves, etc.) and enables more accurate measurement of the backscatter coefficient over calm or moderate seas, thus leading to a noise reduction of a factor of two compared to Poseidon, for wave heights greater than 1 m.
- Lower radar penetration of snow and ice (penetration of snowpack is less than one centimetre at Ka-band, compared with five metres at Ku-band). The altimetric observation and height restitution thus correspond to a thin subsurface layer. This should improve measurements of snowpack with respect to ice aging in the surface layers of the polar ice caps. Moreover, ice grain size would also be measurable. Combined with better spatial resolution, Ka-band would therefore allow closer monitoring of sea and continental ice.

The one major drawback of Ka-band is that attenuation due to water or water vapour in the troposphere is high. Rain cells—which are often dense and frequent in the Tropics—will remain a constraining factor, since the radar wave can be attenuated by 2 dB in heavy rain. Typically, if the rain rate is higher than 1.5 mm/h, the radar echoes will be unusable (whereas at Ku-band, echoes are hardly affected at rain rates less than 3 mm/h). However, impact studies carried out on the basis of seven years of TMR data from Topex/Poseidon show that rain rates of over 1.5 mm/h only occur globally 10 per cent of the time. A Ka-band altimeter would therefore still be able to acquire measurements 90% of the time. If the satellite is on a sun-synchronous orbit, rain frequency will also have to be factored in (it rains most often in the Tropics between 6:00 and 12:00 a.m. and 6:00 and 12:00 p.m.). Conversely, this 1.5-mm/h threshold will also be likely to lead to more accurate mapping of rain cells over the ocean—one of the major remaining unknown factors in the global water budget—and yield more reliable climatology data.

Further information:

- Phalippou L., E. Caubet and E. Thouvenot, A Ka-band altimeter for future altimetry missions, IGARSS'2000, 2000.

- Remy F., B. Legresy and P. Vincent, New scientific opportunities from Ka-band altimetry, IGARSS'99, Hamburg, Germany, 1999.
- Jacques Verron and The AltiKa Mission Group, AltiKa: a Ka-band altimetry system for operational altimetry during the GMES period, 15 years of progress in radar altimetry symposium, Venice, 2006.
- Verron J., P. Bahurel and P. Vincent, AltiKa: Etude de la circulation océanique mèsechelle par altimétrie en bande Ka sur microsatellite, Research proposal to CNES, 2001.
- – Vincent, P., N. Steunou, E. Caubet, L. Phalippou, L. Rey, E. Thouvenot and J. Verron: AltiKa: a Ka-band Altimetry Payload and System for Operational Altimetry during the GMES Period, Sensors, Special Issue: Satellite Altimetry: New Sensors and New Applications, 2006.

5.3.2 Interferometers

An altimeter/interferometer would include several altimeters mounted on masts which would acquire measurements simultaneously, thus providing continuous, single- or multi-altimeter wide-area coverage.

The main limitations of standard nadir-pointing radar altimeters have been understood for a long time. They include the lack of coverage (intertrack distance of typically 150 km for the T/P / Jason tandem) and the spatial resolution (typically 2 km for T/P and Jason), expected to be a limiting factor for the determination of mesoscale phenomena in the deep ocean. In this context, various solutions using off-nadir radar interferometry have been proposed by Rodriguez et al. 2004 to provide a solution for oceanographic mission objectives. An initial approach is based on the Wide-Swath Ocean Altimeter (WSOA) which was intended to be implemented onboard Jason-2 in 2004 but has now been abandoned.



Figure 5.45 WSOA on a Jason satellite

An altimeter/interferometer would work as follows: each interferometer would send out and receive back a wave from the others.

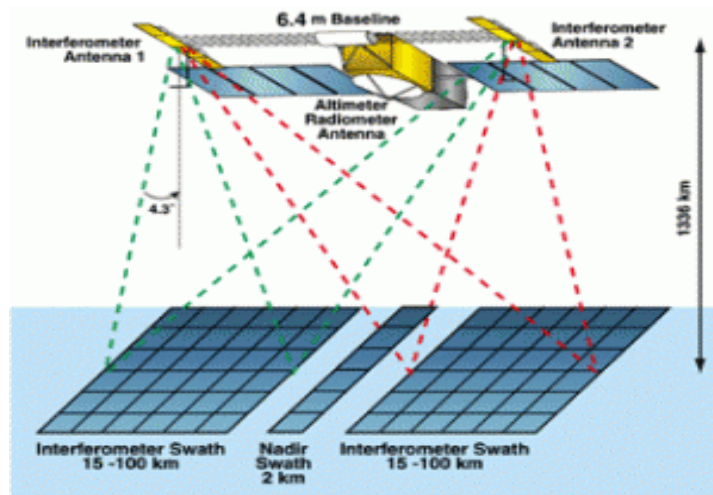


Figure 5.46. How the WSOA altimeter/interferometer works.

There are three factors underlying measurement uncertainty:

- Measurement noise, which depends on the antenna baseline: the longer the baseline, the less noise there is. This noise is reduced by mosaicking. The nadir-pointing altimeter also makes it possible to register pixels.
- The error related to ionospheric, tropospheric and sea-state bias effects. Here again, the radiometer's wide antenna lobe will enable tropospheric corrections to be extended reliably across a good proportion of the swath.
- The error induced by satellite roll and pitch, which has a direct impact on measurement geometry, by triangulation. This noise could be minimised by analysing and adjusting ascending and descending data at crossover points.

Final measurement accuracy could be as good as 3.2 cm rms per pixel in the mosaicked data (averaged to 15 km cells).

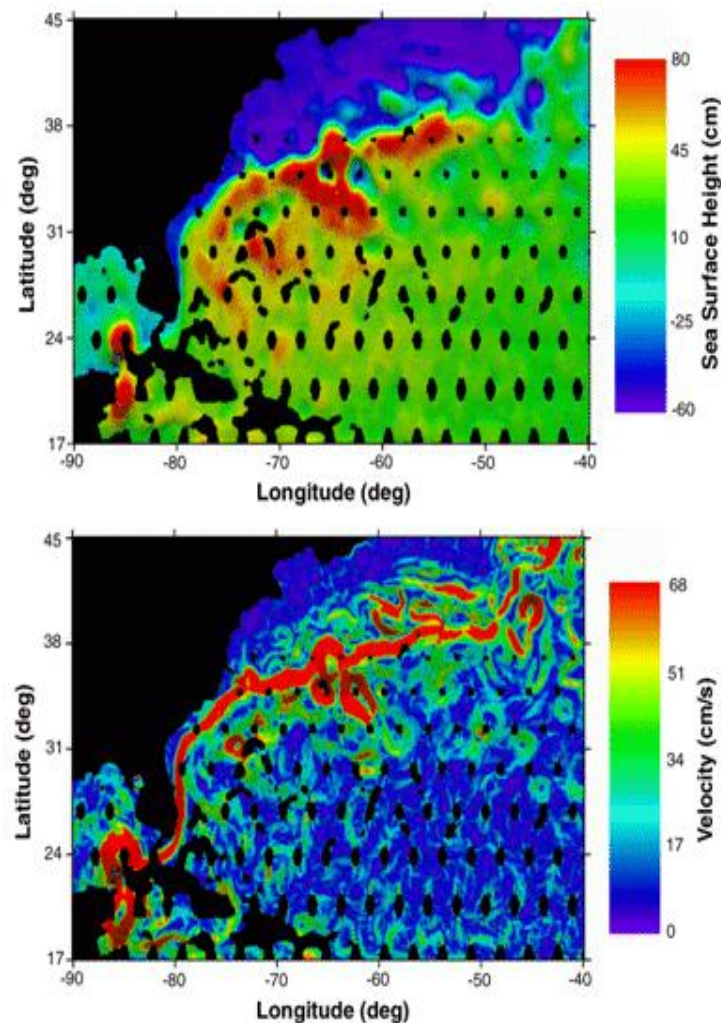


Figure 5.47. Example of WSOA measurements along a T/P-Jason-class orbit track.

This mosaic offers a huge advantage in terms of describing the dynamic topography at high resolution, since it allows us to measure sea surface gradient (between pixels) and, therefore, the geostrophic velocity. Simulations based on realistic model data yield an error of 4.7 cm/s rms (resp. 5.9) on the zonal velocity (resp. meridional velocity). Sampling simulations (based on a T/P-type orbit, since WSOA could be flown on the Jason satellite) show that the WSOA concept would require a constellation of four conventional nadir-pointing satellites in a repeating orbit. The instantaneous field of view would be wider than with a conventional altimeter, making it possible to cover coastal zones and to improve temporal resolution. The major drawback of such a system is that it involves intensive processing to improve accuracy.

The WSOA option for ocean monitoring was dropped from the Jason-2/OSTM spacecraft in the spring of 2005 because of concerns about programmatic risk to the core Jason-2/OSTM mission and due to cost overruns. It evolved in the SWOT KaRIn instrument to provide high-resolution measurements of SSH (Sea Surface Height) on approximately a 10 km grid across a 200 km swath centered on the satellite ground track.

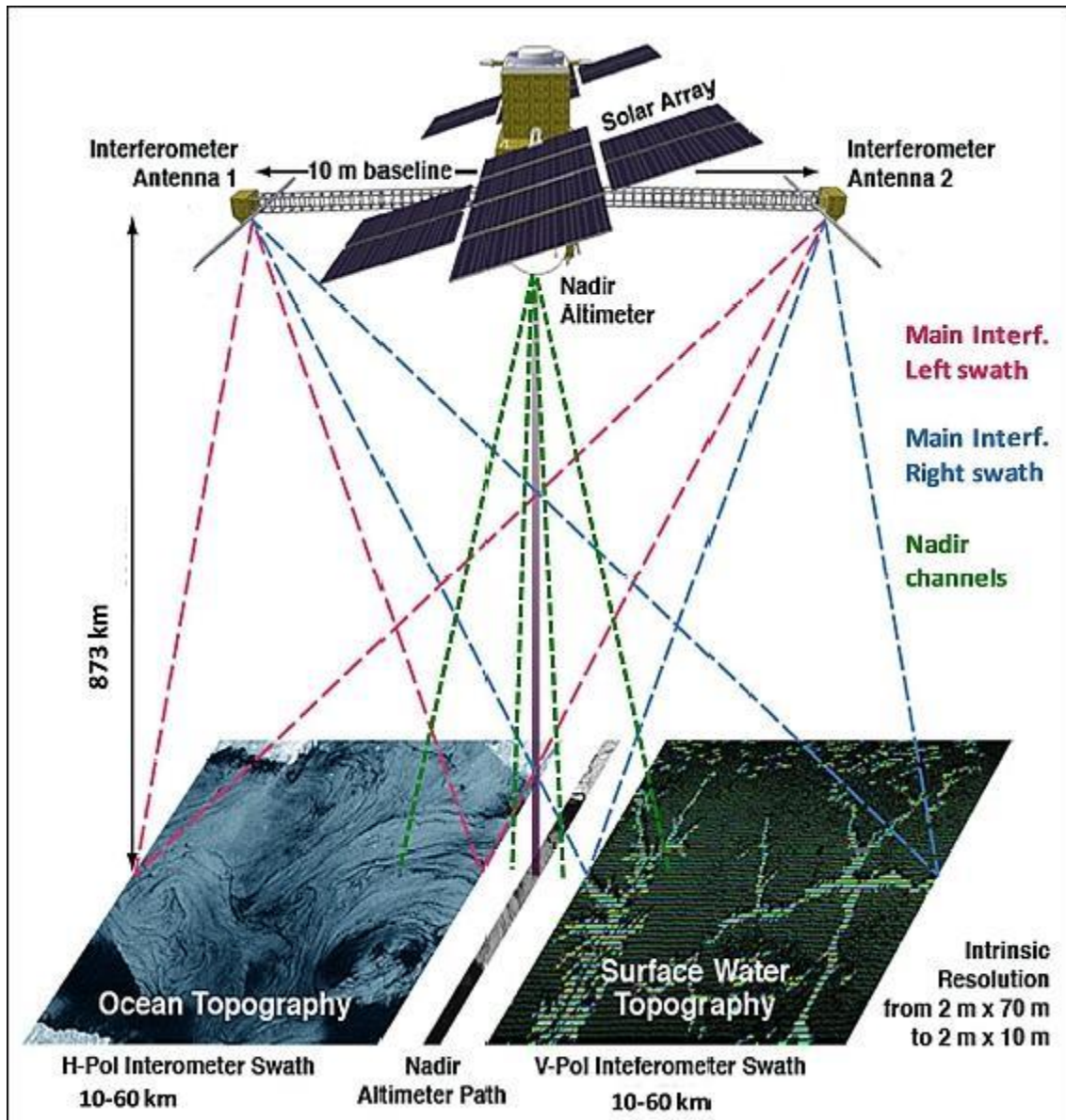


Figure 5.48. SWOT integrated measurement approach (NASA, CNES).

SWOT utilizes an integrated measurement approach, which includes the KaRIn system to observe in two off-nadir swaths, each of 50 km. KaRIn produces ocean and surface water heights and -co-registered weather imagery and elevations of 50 m and 1 km resolutions for hydrology and ocean communities, respectively. KaRIn includes an experimental nadir channel, either as a NNI (Near-Nadir Interferometer), or as a KNA (Ka-band Nadir Altimeter). The NNI is baselined. Both provide complimentary measurements to KaRIn and to support calibration and validation. The CNES-supplied Jason-heritage nadir altimeter specifically addresses SSH for long spatial wavelengths. The Jason-heritage microwave radiometer corrects the nadir altimeter range measurements for the wet tropospheric delay and the GPS and DORIS receivers, with the LRA (Laser Retroreflector Assembly), provide precision orbit determination.

Further information:

- Enjolras, V., P. Vincent, J.-C. Souyris, E. Rodriguez, L. Phalippou and A. Cazenave, Performances Study of Interferometric Radar Altimeters: from the Instrument to the Global Mission Definition, *Sensors*, 6, 164-192, 2006.
- Ernesto Rodríguez, "Surface Water and Ocean Topography Mission (SWOT), Science Requirements Document," NASA/JPL, March 19, 2009, URL: http://swot.jpl.nasa.gov/files/SWOT_science_reqs_final.pdf

5.3.3 Constellations

One of the ways to improve altimetry resolution is to use several satellites at the same time (see High-precision altimetry with satellites working together). Until now, this has been done with very different types of satellite. The use of several identical satellites in constellation could reduce costs (development costs, and launch costs too for micro-satellites launched by the same rocket).

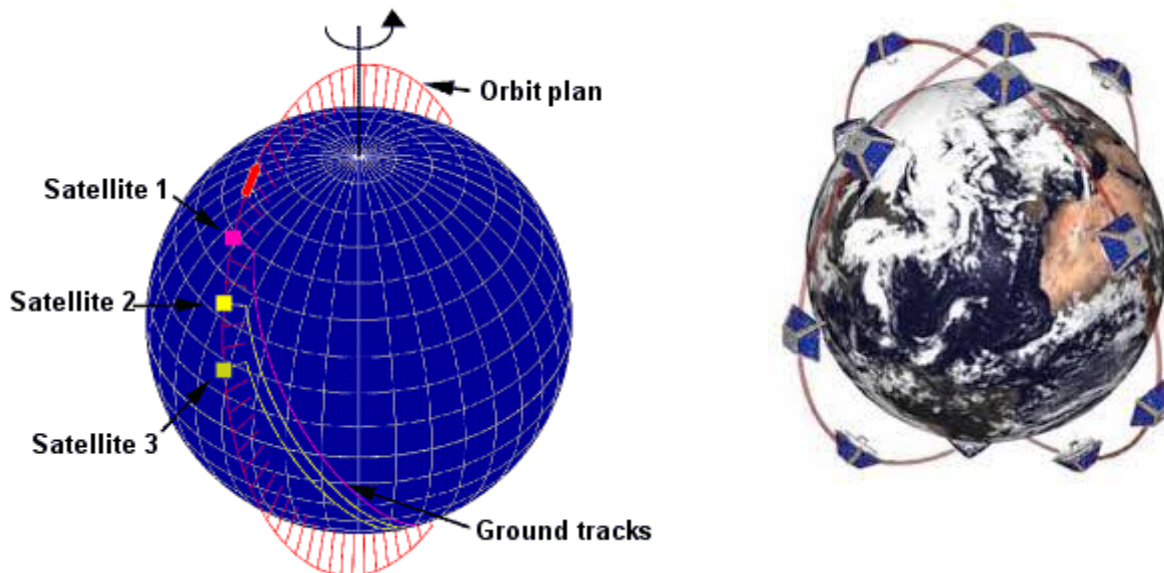


Figure 5.49. The WITTEX (Water Inclination Topography and Technology Experiment) altimetry satellite constellation project. (Credits John Hopkins University Applied Physics Laboratory) and GANDER (Global Altimeter Network Designed to Evaluate Risk) constellation of microsats in 2 orbit planes (SSTL)

The questions to be solved relate to the minimum number of satellites needed, their distribution in time and space, etc. The answers will depend in part on the applications favoured — and on the financing available.

Further information:

- Raney, R. Keith, and David L. Porter. "WITTEX: An innovative three-satellite radar altimeter concept." *IEEE Transactions on Geoscience and Remote Sensing* 39.11 (2001): 2387-2391.
- Allan, T., The story of GANDER, *Sensors*, 6, 249-259, 2006.

5.3.4 GNSS altimetry

One approach being pursued for achieving maximum altimetry data coverage is to receive reflected signals transmitted by satellites in the Global Navigation Satellite System (GNSS), in particular from the Global Positioning System (GPS) constellation and its future European civil counterpart, Galileo. This concept is based on a satellite on a low-earth orbit (at an altitude of 400 to 500 km) retrieving signals emitted by multiple satellites and reflected by the ocean surface, then analysing these signals to compute sea surface height. The concept is currently still only in the study phase.

The concept works as follows: a spaceborne GPS receiver receives a signal downlinked from a satellite in the constellation, then receives the return echo of the same signal reflected by the ocean surface. By measuring the delay between the two, we can calculate the sea surface height. The backscatter depends on the angle of incidence – the receiver only senses specular reflection – and on sea surface roughness. Consequently, the system only works well at low angles of incidence up to 10 degrees. Therefore signal returns will only be strong for GPS satellites ‘above’ the receiving satellite, which will number no more than ten at any one time. In fact, several return echoes above the same area on the ocean will have to be averaged (from 1 to 10 degrees) to reduce the noise. The main weakness of this concept is its accuracy: at an angle of incidence of 10 degrees, the sea surface height error would be several metres. The only way to improve accuracy would be to retrieve more return echoes from the same point on the ocean surface. That would depend on the number of satellites in the GNSS constellation, and the GPS constellation is not expected to expand significantly. On the other hand, the European Space Agency has developed its own GNSS, called Galileo, with the first satellite launched in 2011 and a total of 30 to be flying in the Fully Operational Capability (FOC) service. The highest accuracy at any given time would be 30 centimetres rms.

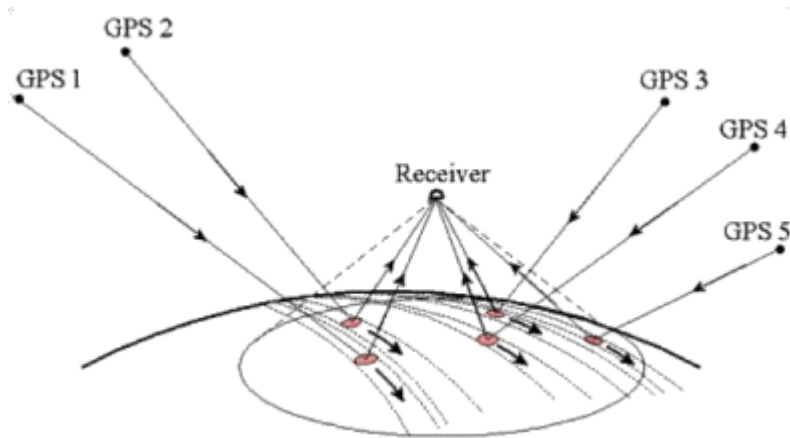


Figure 5.50. Reception of GPS signals by satellites of opportunity.

Simulations show that a single satellite receiving GPS signals, orbiting at an altitude of 400 kilometres, would cover the globe in 24 hours with a ground track spacing of 75 kilometres. In other words, the satellite would ‘see’ any given cell of 50 km² on the Earth’s surface 12 times in 10 days. On this basis, two satellites providing global coverage would make it possible to achieve sea surface height accuracy of 6 cm rms over an average of 10 days and at a resolution of 50 km². Eight satellites would offer the same level of accuracy, but at a resolution of 25 km².

The major advantage of this mission of opportunity concept is its low cost. Its main drawback is its accuracy, which only Galileo (or Glonass, the Russian satellite navigation system) could increase. It would complement conventional altimetry missions, which are still needed to track climatic variations over the oceans.

Fixed-location GPS receivers could also be installed along coastlines, for example on masts at a height of 200 metres, to deploy a high-quality network that would complement the ocean coverage provided by satellites carrying GPS receivers.

In December 2012 the Phase A studies of ESA's PAssive Reflectometry and Interferometry System In-orbit Demonstration (PARIS IoD) mission ended. PARIS is called an interferometric GNSS-R (iGNSS-R) system because the direct and the scattered signals are cross-correlated in order to use the whole signal's bandwidth, and improve the altimetric precision, despite the large bandwidth signals are not publicly available.

Further information

- Gleason, S., S. Hodgart, Y. Sun, C. Gommenginger, S. Mackin, M. Adjrak, M. Unwin, 2005, Detection and Processing of Bi-Statically Reflected GPS Signals From Low Earth Orbit for the Purpose of Ocean Remote Sensing, Accepted by IEEE Trans. Geosci. Remote Sensing.
- Martin-Neira, M., 1993, A Passive Reflectometry and Interferometry System (PARIS): Application to Ocean Altimetry, ESA Journal, vol. 17, pp. 331-355.

5.4 SAR Tutorial

5.4.1 On-board

The on board steps are similar to the ones in Low Resolution Mode. Some parts of the hardware are commonly shared between both modes. However the pulses need to be transmitted with a PRF high enough so they remain coherent. The PRF value would depend on the satellite orbit and the transmission pattern.

After a burst of pulses is successfully transmitted and received, some corrections should be applied before packing the data and send it to the ground station for further processing.

The Block diagrams of the SIRAL altimeter is shown below.

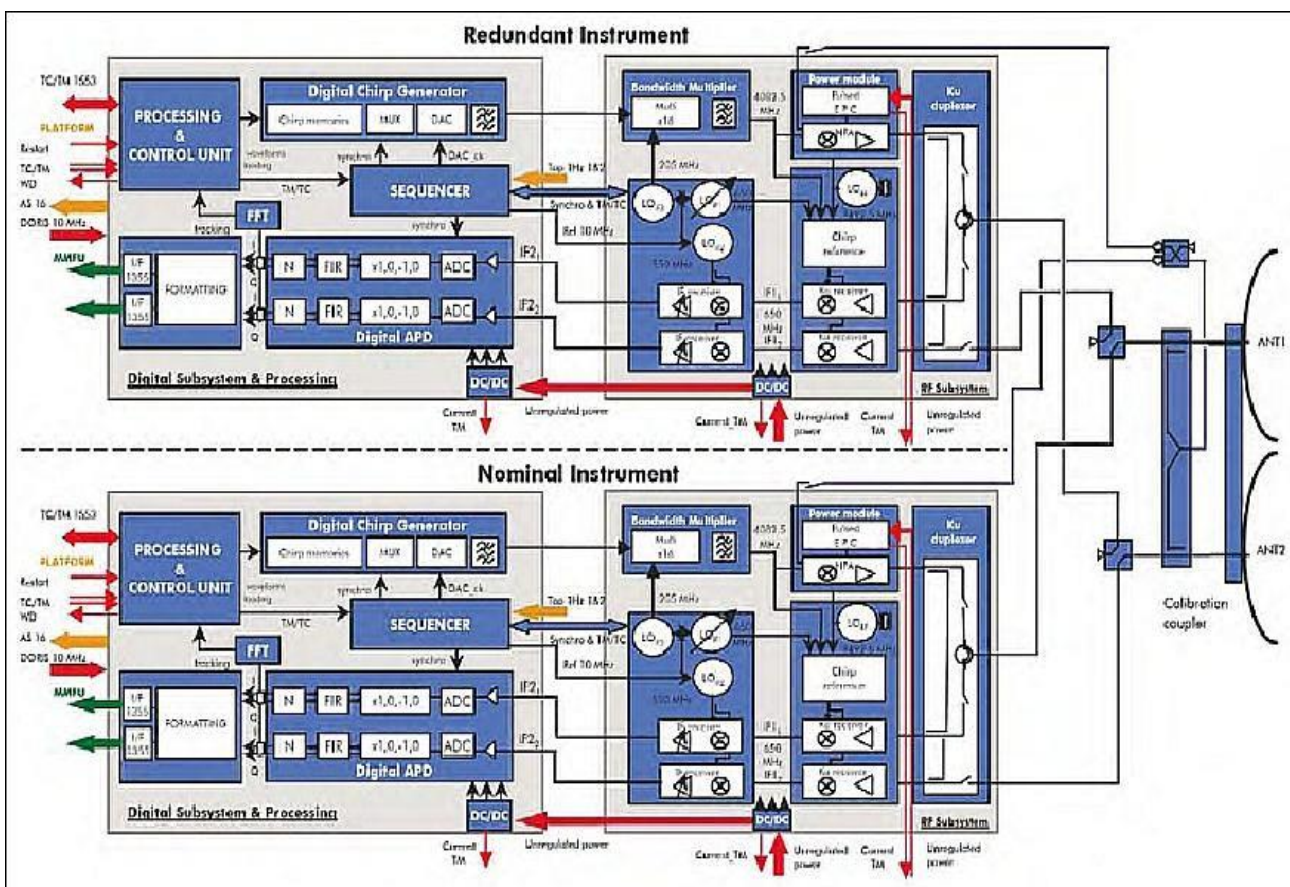


Figure 5.51. Block diagram of the SIRAL instrument. Credit: ESA

In this case, both LRM, SAR and SARIn data is received and routed to the Processing Unit. There the LRM pulses are transformed into range domain and averaged. The SAR pulses would remain in time domain and the Fourier transformation will be performed by the ground processor.

5.4.1.1 Transmission pattern

Alternatively to the classical altimeters, transmitted pulses in HR mode are grouped in bursts. The pulses within a burst have to be coherent. Thus, the PRI (Pulse Repetition Interval) has to be chosen accordingly.

Moreover, in order to exploit the concept of Delay-Doppler altimetry, these bursts have to be spaced enough so that the pulses are incoherent from burst to burst and they can be averaged later on to improve the SNR. Then another parameter comes up: the Burst Repetition Interval (BRI).

The following pictures show the transmission patterns from different Delay-Doppler altimeters.

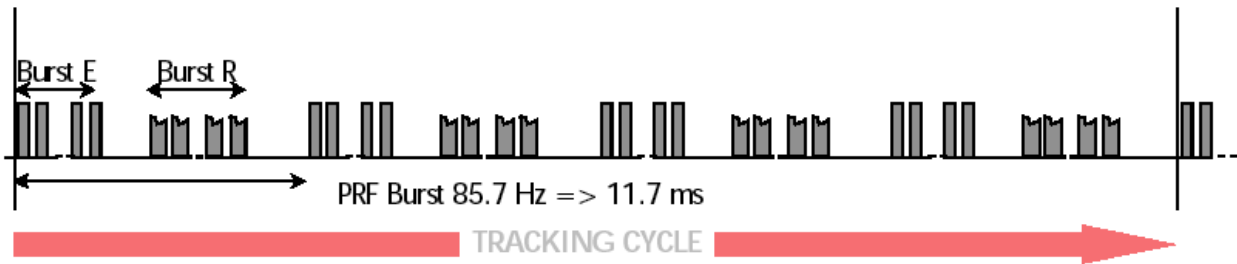


Figure 5.52 CryoSat-2 transmission pattern. Each burst is formed of 64 Ku-band pulses. Credit: ESA.

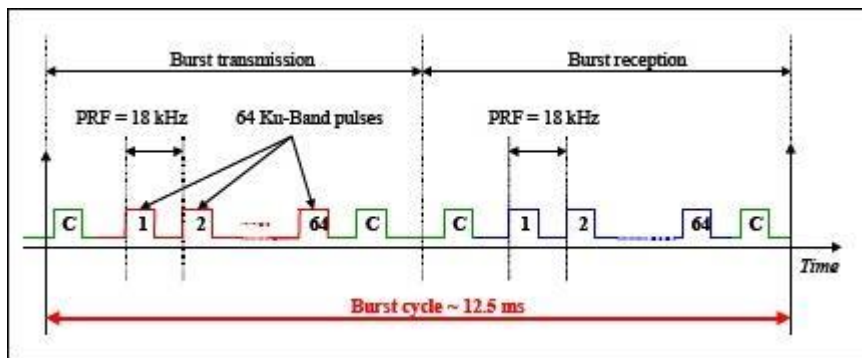


Figure 5.53. Sentinel-3 transmission pattern. Note that bursts include 2 C-band pulses here. These are used for ionospheric corrections. Credit: ESA

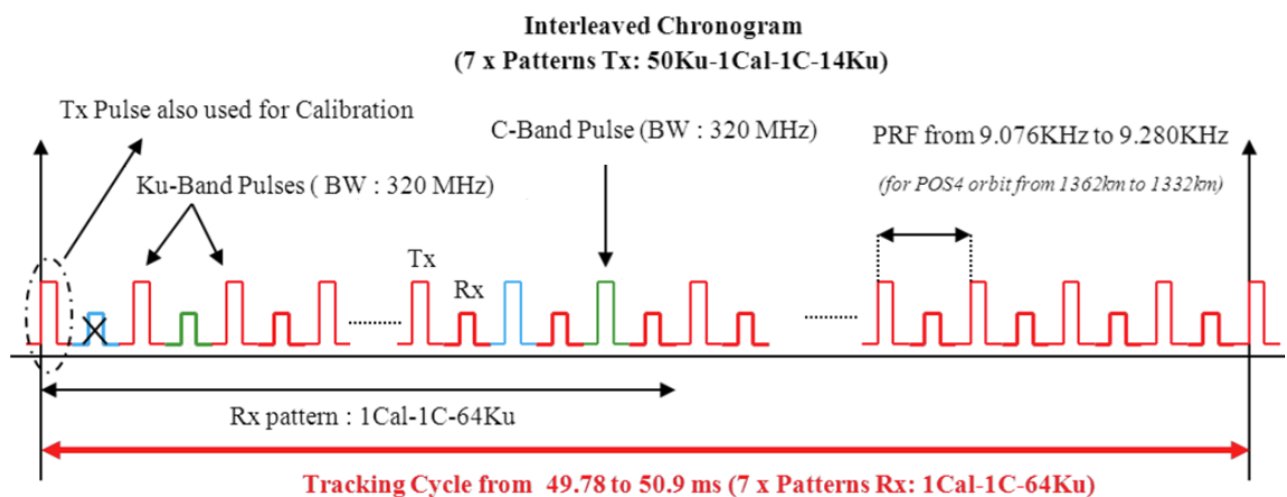


Figure 5.54. Sentinel-6 transmission pattern. Observe that no bursts are present and calibration pulses are also in the same transmission pattern as the Ku- and C-band pulses. Credit: ESA

5.4.1.2 Mode mask

CryoSat-2 and Sentinel-3 can switch between the Low Resolution Mode (LRM mode) and the High Resolution Mode (HR or SAR mode), depending on the scientific and/or user needs. In order to perform this switch autonomously, the altimeters carry a mode mask. This mode mask identifies, from the coordinates of the observed scenario, the mode that has to be operated at all times.

Figure below shows the CryoSat-2 mask, also including the interferometry mode called SARin.

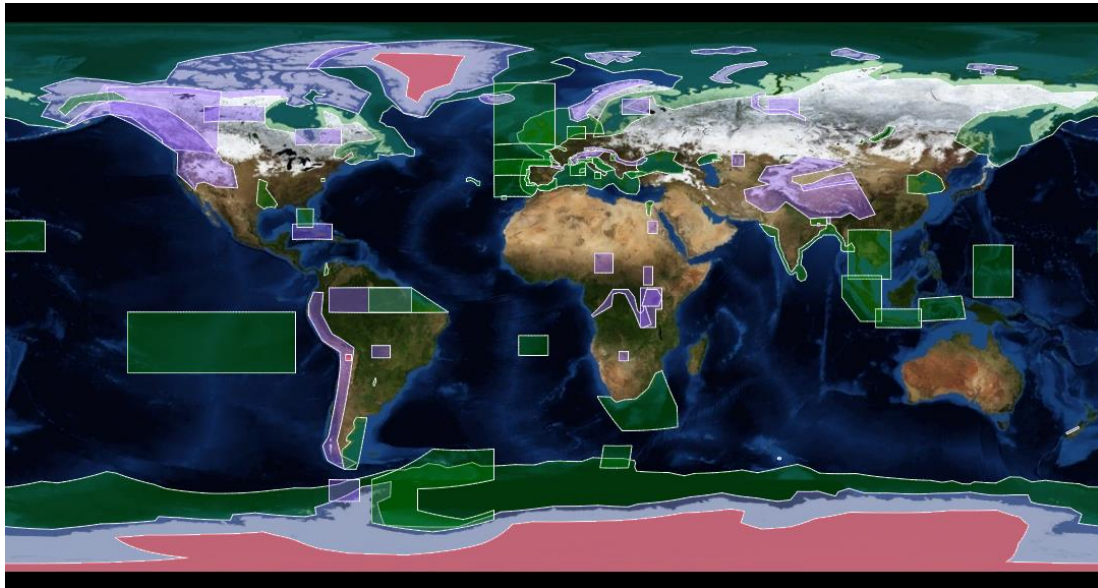


Figure 5.55. CryoSat-2 mode mask. SAR (green), SARin (purple) and LRM (red and others) operating modes. Credit: ESA

On the other hand, Sentinel-3 mode mask is:

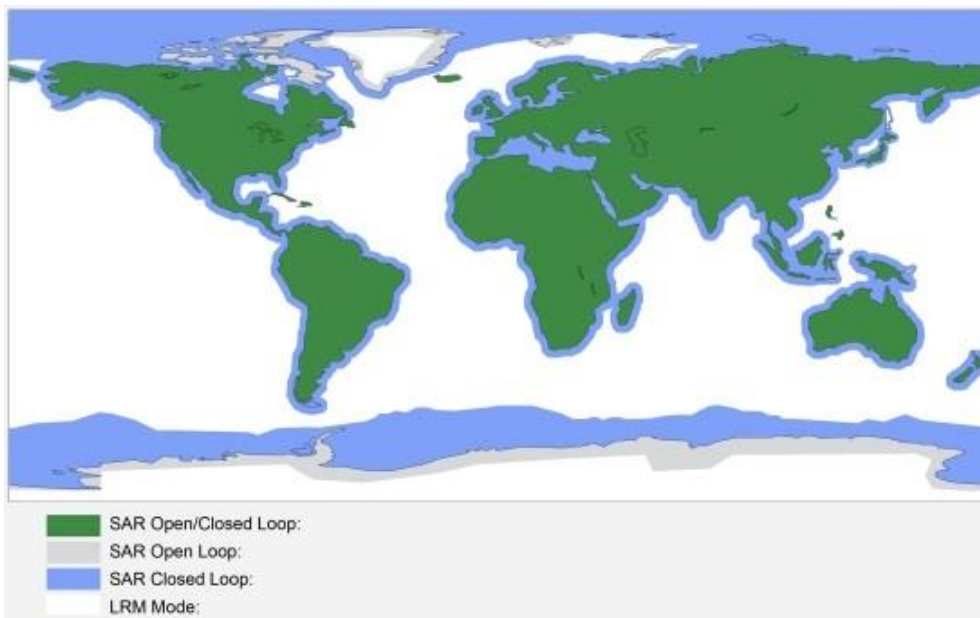


Figure 5.56. Sentinel-3 mode mask (2015, pre-launch). SAR open/closed loop (green), SAR open loop (grey), SAR closed loop (blue) and LRM Mode (white) operating areas. It currently operates in SAR mode everywhere. Credit: ESA

Alternatively, Sentinel-6 will perform a continuous transmission of pulses with a variable PRI such as both modes (LRM and SAR) can operate simultaneously. Thus, Sentinel-6 will not have a mode mask on-board (excluding calibration acquisitions). This new operating mode is called Interleaved mode.

5.4.2 Resolution cells

Each emitted pulse is reflected by the surface and is returned to the altimeter a few milliseconds later. As the illuminated area grows, the return signal strength grows rapidly until an annulus is formed. It then remains constant until the growing annulus (or ring) reaches the edge of the radar antenna beam, and then starts to diminish.

The signal acquired by the altimeter at each Ku-band burst is initially the same as in LRM. It is made up of a series of 64 elementary range measurements that correspond to ground resolution cells (i.e. concentric rings). The main difference, between LRM and SAR mode, is that the radar pulses of the same burst are correlated. The Pulse Repetition Frequency (PRF) and the altimeter phase coherence from pulse to pulse are key factors in the synthetic aperture process (i.e. the SAR process) to discriminate the along-track Doppler frequencies and to be able to have the reduced resolution cells.

Depending on the mission, the along and across track resolutions can vary.

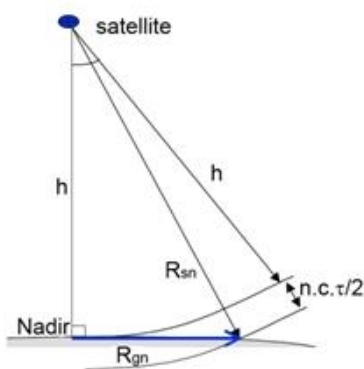


Figure 5.57. LRM Footprint (Credit: TAS-F)

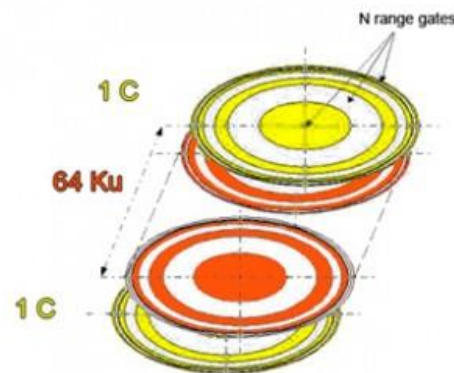


Figure 5.58. LRM Resolution Cell (Credit: TAS-F)

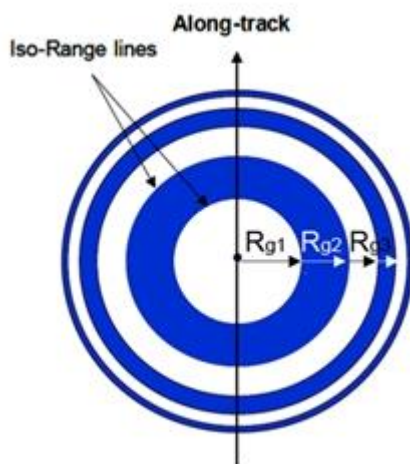


Figure 5.59. SAR Range Gates (Credit: TAS-F)

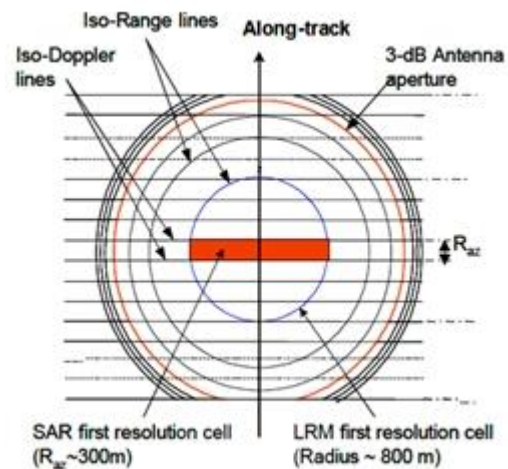


Figure 5.60. SAR Resolution Cell (Credit: TAS-F)

5.4.3 Ground processing steps

Once the data is telemetered to the ground stations, it is unpacked, formatted and then packed again for the Ground Processing facilities. These ground processing facilities are responsible of the treatment of the satellite data up to L2 (see Section 4. Product Levels).

Apart from the datation, which is assigning a given time value to each pulse or burst, the main ground processing steps are:

- Calibration
- Beam forming
- Multi-looking
- Retracking

5.4.3.1 Calibration

During the on-board processing, the waveforms have been affected by the instrument gains and attenuations and they may have suffered phase variations as well. All these factors have to be accounted on-ground before the Delay-Doppler processing starts.

5.4.3.2 Beam forming

Once the waveforms have been corrected by all the on-board factors, the beam forming starts.

The beam forming consists in dividing the Doppler bandwidth of the pulses of each burst in different Doppler cells, defined by the surface sampling that has been performed previously (see Section 2. Resolution cells). This means that the pulses have been split according to Doppler frequencies. And the remaining waveforms are called beams, each of them being the backscattered contribution of each corresponding resolution cell.

The figure below depicts the beam forming process, with all the Doppler beams obtained from the transmitted burst of pulses.

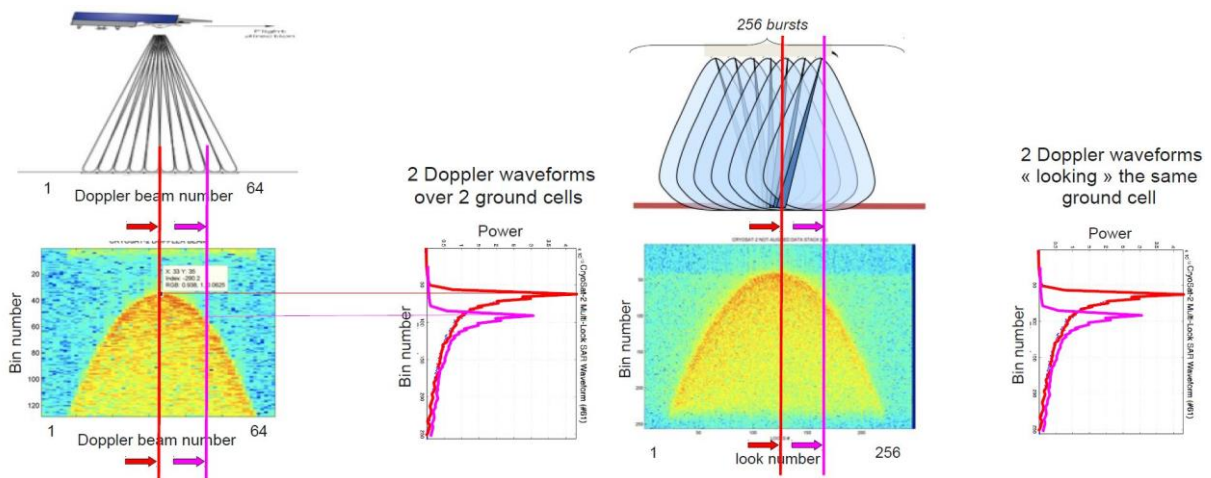


Figure 5.61. Doppler beams obtained from a burst of pulses. Credit: S.Dinardo ESA

5.4.3.3 Multilooking

After the Doppler beams have been created, stacks are formed. A stack is the collection of all the beams that have illuminated the same Doppler cell.

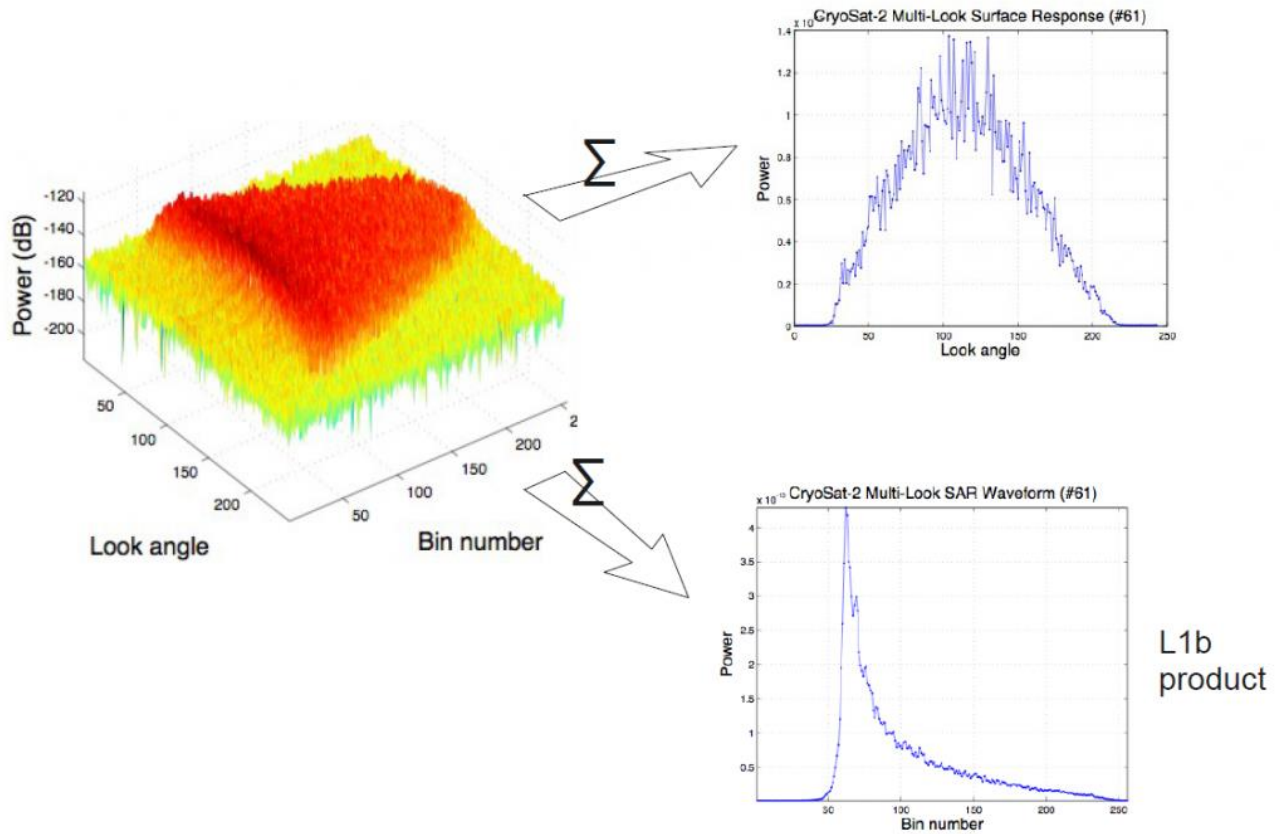


Figure 5.62. Multiple contributions from different bursts conforming to one stack. Credit: S.Dinardo ESA

After the collection, the whole stack is averaged (multi-looking). Note that, before averaging, the stack has been aligned and the beams have been converted to power waveforms. The average should be performed in the along track (beams) dimension in order to get the L1B waveform. If we perform the average on the range dimension we obtain the power distribution along track (top right).

5.4.3.4 Retracking

Retracking is the process that allows extracting scientific parameters characterising the observed scene from the input L1B waveforms. Hence, retracking is a key step in the ground processor chain.

Retrackers can be analytical or empirical. In the analytical ones, a mathematical model emulating the L1b waveform is generated and fitted to the L1B waveform under analysis to extract 3 parameters (epoch, SWH and P_u). In order to do so, the model shall replicate all processing steps that led to the production of the L1B waveform to be retracked.

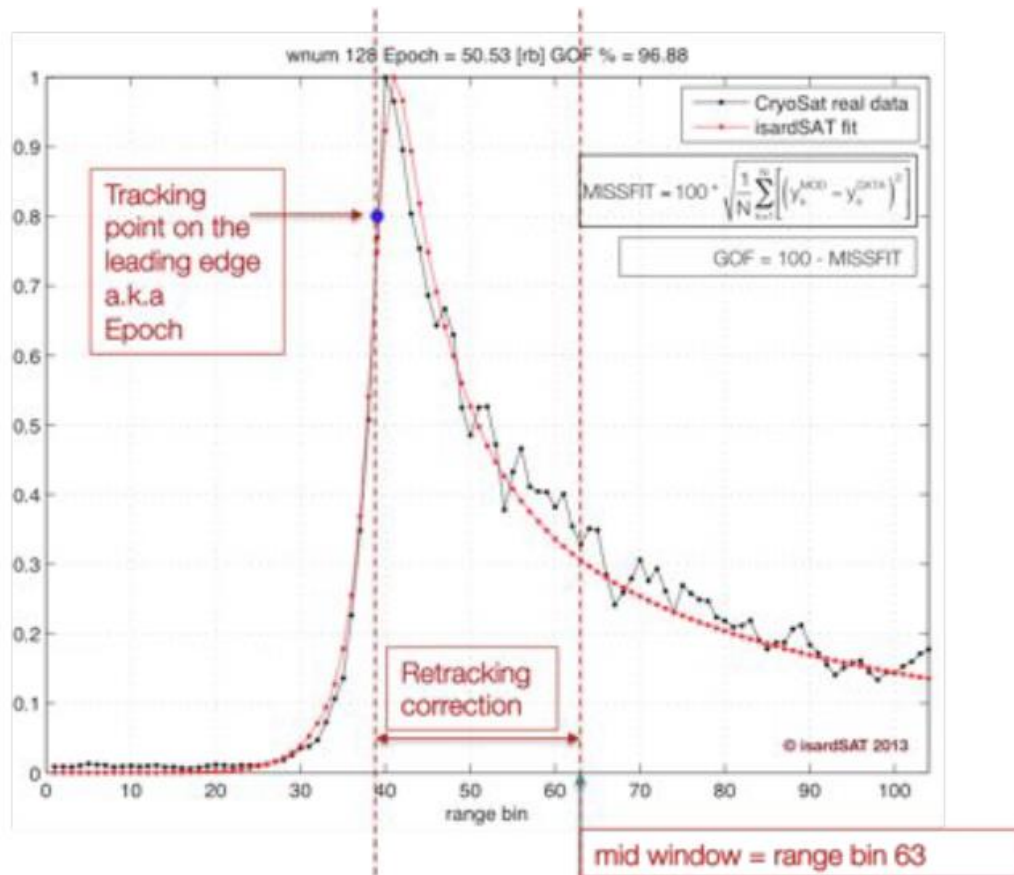


Figure 5.63. Retracking of an Ocean L1B waveform. Credit: isardSAT

In the picture above, an L1B waveform is shown together with the ocean retracker. Outputs of an analytical retracker are:

- Range (from Epoch)
- SWH
- Backscatter coefficient (from amplitude Pu)

Furthermore, wind velocity can also be extracted from the backscattering coefficient.

Empirical retracker focus on the statistics of the waveform not considering the processing from which the L1B waveform has been created. Such retracker follow mathematical formulations to parametrized the waveform and allow to estimate the epoch and the amplitude. Such retracker (e.g. the OCOG, discussed in 5.2.2) provide very good results in the inland water domain (lakes and rivers)

5.4.4 Product levels

There are different data products associated with the three levels of processing of altimeter data:

- Level-0 is the raw telemetered data, geolocated and dated
- Level-1A contains calibrated data before SAR processing.
- Level-1BS is the Level-1A data after the beam forming and the geometry corrections (stack data).
- Level-1B is the Level-1BS data averaged to obtain a single multilooked waveform per record.
- Level-2 is the Level-1B data retracked and corrected for geophysical effects.

5.4.4.1 Level-0

The input data for Level-0 processing is the Instrument Source Packet (ISP). The ISP contains raw data expressed in instrument engineering units, not in international system (SI) units. The first function of the Level-0 processing chain is to extract and decode the ISP raw data and convert it into SI units. The second function of the Level-0 processing chain is to correct the date and time of the measurements and to locate these measurements on the Earth (satellite position and measurement location on the Earth's surface).

5.4.4.2 Level-1A

The L1A is an intermediate output of the SAR processor. L1A complex waveforms should be fully calibrated (including both instrumental gains and calibration corrections) and aligned in range within each burst. The time tag is given at the surface (that is when the middle of the burst reaches the surface). L1A is the starting point for the SAR processing which provides high resolution products.

5.4.4.3 Level-1BS

The L1B-S HR product contains information of Doppler beams data. Hence, it has only been defined for the SAR processing chain.

The Doppler beams associated to a given surface location (also called stack data) are formed through the selection of all the beams that illuminate a given surface location, and that contribute to each L1B HR waveform. Beams are the result of applying a Doppler processing to the waveform bursts, that allows to divide the conventional altimeter footprint in a certain number of stripes and thus create a Delay Doppler Map (DDM). With this, contributions coming from different stripes can be identified and collected separately. When all the contributions from different bursts are collected, a stack is formed. The stack waveforms are provided in I/Q samples (complex waveforms) in the frequency domain.

Apart from the Doppler processing, the beams of a stack have also been fully calibrated and range aligned. The L1B-S also includes characterisation parameters about the stack itself. The time tag is given at each surface location (defined throughout the L1 processing chain).

5.4.4.4 Level-1B

The L1B SAR product contains the same variables as the L1B-S product except for the waveform and the stack characterisation parts. A L1B waveform is the average of each stack and is provided in I2Q2 samples (power waveform) in the frequency domain (range domain).

5.4.4.5 Level-2

The input data for Level-2 processing are the Level-1 products. The first function of the Level-2 processing chain is to apply different re-tracking algorithms to the Level-1 waveforms to calculate the final altimeter range, backscatter coefficient, wind speed over ocean and SWH. There are different types of re-tracking algorithms according to the type of waveforms re-tracked (ocean, ice, sea-ice).

For the Synthetic Aperture Radar Altimeter (SRAL) on board Sentinel-3, the Level-2 processing chain inputs are:

- one Level-1B SRAL product

- one Level-1B MWR product
- a set of dynamic ancillary or auxiliary data.

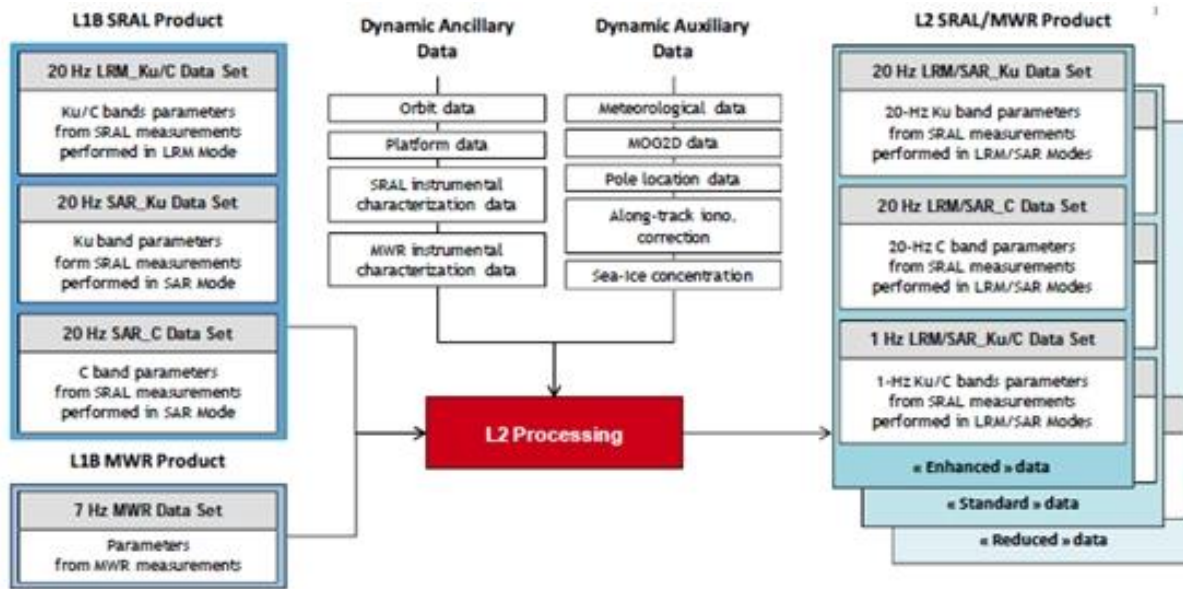


Figure 5.64. SRAL and MWR Level-1B Inputs and SRAL/MWR Level-2 Outputs (Credit: CLS)

The second function of the Level-2 processing chain is to compute and apply all geophysical corrections to the measurements. Examples of geophysical corrections are the tides or the reference surface used (e.g. geoid).

6 Thematic Use Cases

A wealth of applications are possible using radar altimetry measurements, involving most geoscience fields and practised by more than a thousand teams of users around the world. From the 'historical' applications (geodesy, general ocean circulation) to the developing ones (solid Earth and coastal applications, etc) and the ones that have become classic (ocean variability, ice topography, hydrology), altimetry has shown over and over that it is a very productive technique.



Figure 6.1. Example of some use cases

In this section, we propose you with some practical examples of the applications of altimetry data. The type of data to use, the methodology and the main computations are detailed, as well as how to work with data using the Broadview Radar Altimetry Toolbox. Note that these examples are meant to give you the general guidelines, and that some adaptation will be necessary to use them in other contexts.

Ocean

- **Western boundary currents:** [the Gulf Stream and its seasonal variations](#)
- **Altimetry data processing for mesoscale studies:** [Ocean eddies in the Kuroshio current](#)
- **Altimetry data processing for mesoscale studies:** [Computing Geostrophic velocities](#)
- **Altimetry for coastal studies:** [The North Western Mediterranean Sea](#)
- **Altimetry for coastal studies:** [The Agulhas current](#)
- **Altimetry for coastal studies:** [The Florida Keys currents](#)

Ice

- **Sea ice studies:** [Altimetry and radiometry for sea ice classification](#)
- **Ice studies:** [Altimetry for observing polar ice caps](#)
- **Ice studies:** [CryoSat over continental ice](#)
- **Sea ice studies:** [CryoSat over sea ice](#)

Climate

- **Monitoring climate events:** [El Niño and ocean planetary waves](#)

- **Monitoring climate change:** The Mean Sea Level

Atmosphere, wind & waves

- **Wind & waves:** Seasonal distribution of Significant Wave Height
- **Altimetry for extreme weather studies:** Hurricane Katrina

Hydrology & land

- Temporal water surface height variations in enclosed areas: The Amazon Basin
- Hydrology: Aral Sea level
- Land studies: Altimetry over continental surfaces
- Hydrology: Altimetric waveforms for monitoring lakes level
- Hydrology: Altimetry for lake/reservoir studies by using hydrology dedicated products
- Hydrology: Altimetry for wetland studies by using hydrology dedicated products

Geodesy & geophysics

- **Altimetry and gravimetry:** Use of GOCE toolbox in oceanography with altimetry

6.1 Geodesy & geophysics

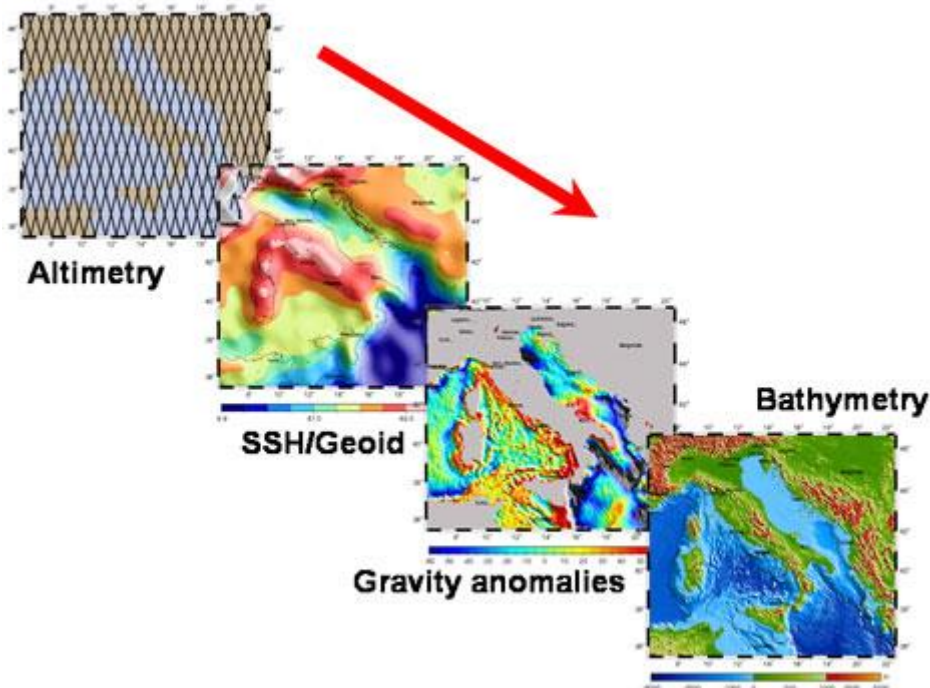


Figure 6.2. Example of geophysical information extracted from altimetry (around Italy) (Credits University of Calgary)

Geophysics is the study of the substances that make up the Earth and the physical processes occurring on, in and above it. Information derived from altimetry data can be used to study the Earth's shape and size, gravity anomalies (geodesy), seafloor relief (bathymetry), tectonic plate motion and rifts (geophysics), etc.

Although often linked to plate tectonics, tsunamis are very different, transient phenomena. However, their impact on the sea surface can be seen by altimeters in some cases, thus helping the study of their propagation.

Further information:

- McAdoo, D., Marine Geoid, Gravity, and Bathymetry: An increasingly clear view with satellite altimetry, 15 years of progress in radar altimetry Symposium, Venice, Italy, 2006

6.1.1 Bathymetry estimate from altimetry

Dense satellite altimeter measurements can be used in combination with sparse measurements of seafloor depth to construct a uniform resolution map of the seafloor topography. These maps do not have sufficient accuracy and resolution to be used for assessing navigational hazards, but they are useful for such diverse applications as locating obstructions/constrictions to the major ocean currents and shallow seamounts where fish and lobster are abundant. Detailed bathymetry also reveals plate boundaries and oceanic plateaus.

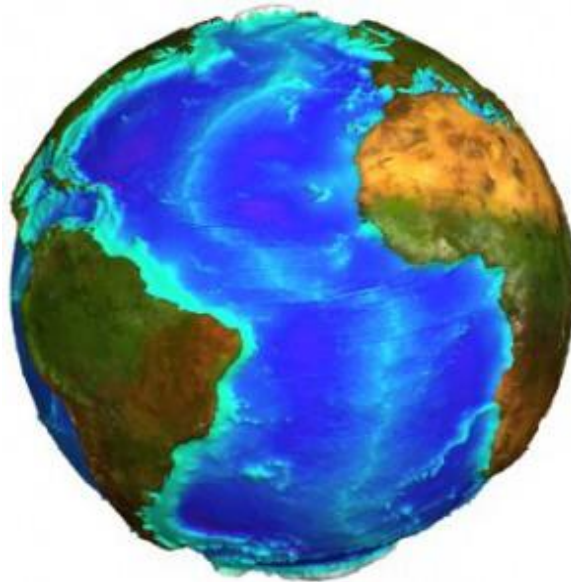


Figure 6.3. Bathymetry can be computed using altimetry together with other data (Credits [CNES](#))

A detailed knowledge of topography is fundamental to the understanding of most Earth processes. In the oceans, detailed bathymetry is essential for understanding physical oceanography, biology and marine geology. Currents and tides are controlled by the overall shapes of the ocean basins, as well as by the smaller, sharp ocean ridges and seamounts. Sea life is abundant where rapid changes in ocean depth deflect nutrient-rich water toward the surface. Because erosion and sedimentation rates are low in the deep oceans, detailed bathymetry also reveals mantle convection patterns, plate boundaries, the cooling/subsidence of the oceanic lithosphere, oceanic plateaus and the distribution of off-ridge volcanoes.

Since it is impossible to map the topography of the ocean basins directly from Space, most seafloor mapping is a tedious process that is carried out by research vessels equipped with echo sounders. However, completely mapping the ocean basins at a horizontal resolution of 100 m would take about 125 ship-years of survey time using the latest technology, with highly non-uniform data. Thus, until recently, our knowledge of the seafloor topography was poor.

Radar altimeters aboard the ERS-1 and Geosat spacecraft have derived the marine gravity field over nearly all of the world's oceans with high accuracy and moderate spatial resolution. In March 1995, ERS-1 completed its dense (~8 km track spacing at the equator) mapping of sea surface topography between the latitudes of 81.5° North and South. These data have been combined and processed to form a global marine geoid or gravity grid [Cazenave et al., 1996; Sandwell and Smith, 1997]. In the wavelength band 15 to 200 km, gravity anomaly variations are highly correlated with seafloor topography and thus, in principle, can be used to recover topography.

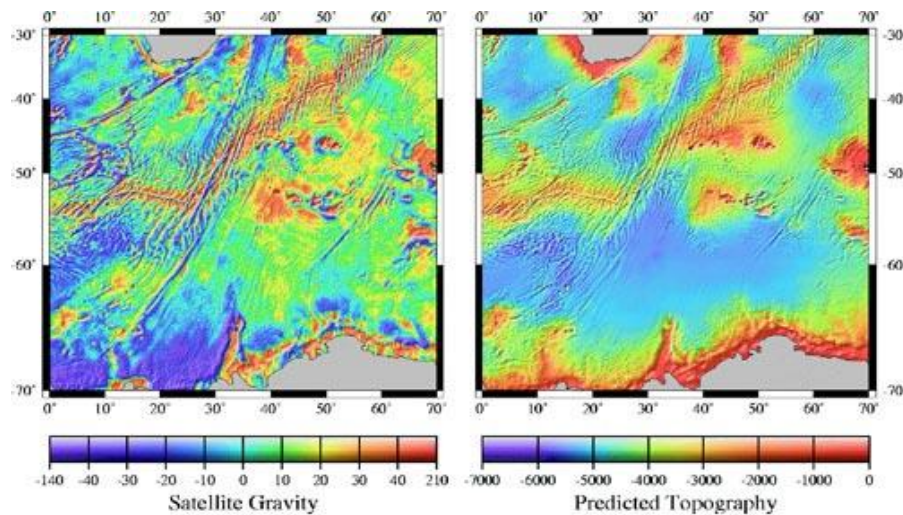


Figure 6.4. Gravity anomalies (left), derived from altimetry, and predicted topography (right) deduced from these gravity anomalies plus *in situ* measurements. (Credits [NOAA/Scripps Institution of Oceanography](#))

The basic theory for predicting seafloor topography from satellite altimeter measurements is summarised in a paper by Dixon et al. [1983]. The conceptual approach uses the sparse depth soundings to constrain the long-wavelength depth while the shorter-wavelength topography is predicted from the downward-continued satellite gravity measurements [Smith and Sandwell, 1994]. There are a number of complications that require careful treatment, e.g.:

- computing bathymetry from gravity anomalies is only possible over a limited wavelength band,
- longer wavelengths in this band are highly dependent on the elastic thickness of the lithosphere and/or crustal thickness,
- sediments favour filling bathymetric lows and can eventually completely bury the pre-existing basement topography.

References:

- Cazenave, A., P. Schaeffer, M. Bergè, and C. Brossier, High-resolution mean sea-surface computed with altimeter data of ERS-1 (Geodetic mission) and Topex/Poseidon, *Geophys. J. Int.*, 125, 696-704, 1996.
- Dixon, T. H., M. Naraghi, M.K. McNutt, and S.M. Smith, Bathymetric prediction from Seasat altimeter data. *J. Geophys. Res.* 88, 1563-1571, 1983.
- Smith, W.H.F., and D.T. Sandwell, Bathymetric prediction from dense satellite altimetry and sparse shipboard bathymetry. *J. Geophys. Res.* 99, 21,803-21,824, 1994.
- Smith, W.H.F., and D.T. Sandwell, Global sea floor topography from satellite altimetry and ship depth soundings. *Science* 277, 1956-1961, 1997.

Further information:

- Sandwell D.T. and W.H.F. Smith, *Bathymetric estimation Satellite altimetry and Earth sciences*, L.L. Fu and A. Cazenave Ed., Academic Press, 2001
- Measured and estimated seafloor topography (UCSD, USA)

6.1.2 Geodesy

Geodesy is the science of the Earth's shape and size. Altimetry makes it possible to compute Mean Sea Surface; such a surface includes the geoid, i.e. the shape of the sea surface, assuming a complete absence of any perturbing forces (tides, winds, currents, etc.). The geoid reflects the Earth's gravitational field. It varies in height by as much as 100 metres over distances of several thousand kilometres due to uneven mass distribution within the planet's crust, mantle and core. Other less pronounced irregularities are also visible over smaller distances. These mostly reflect the ocean bottom topography.

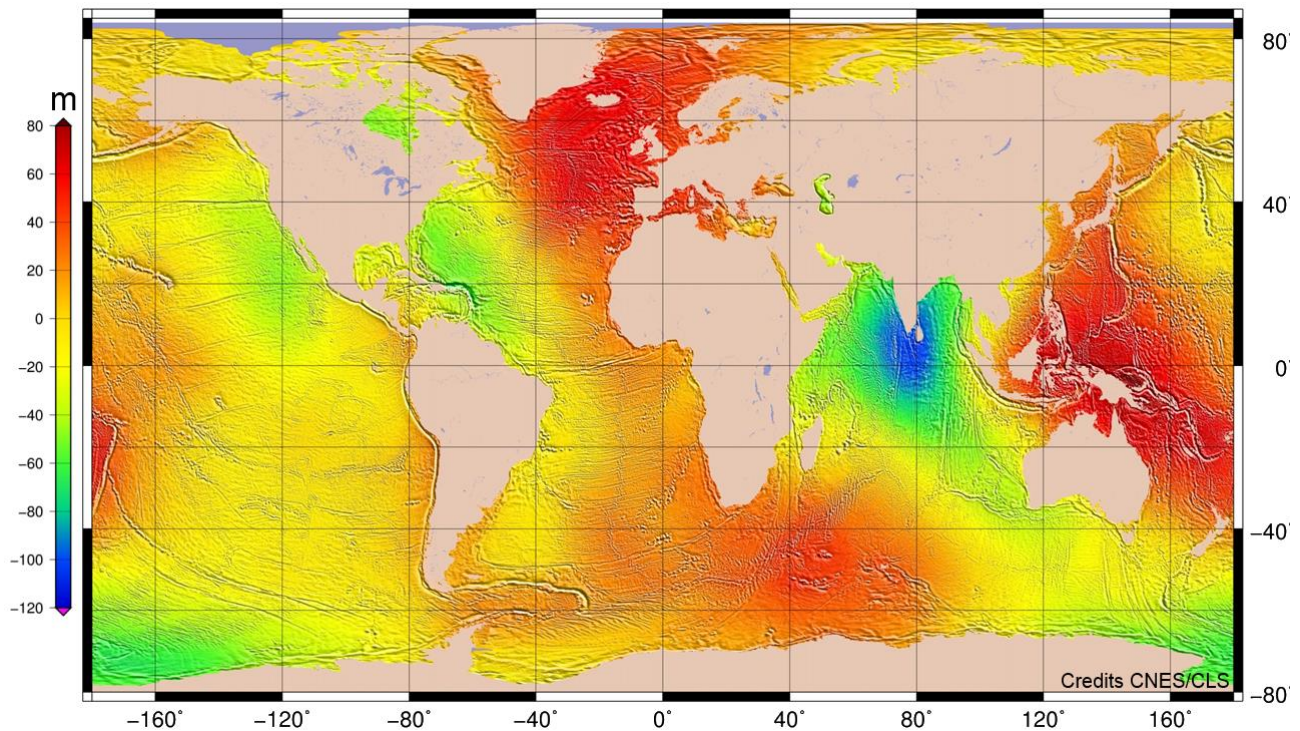


Figure 6.5. Mean Sea Surface, representing the sea level resulting from constant phenomena, computed from 20 years of altimetry data. This Mean Sea Surface is shaped by permanent ocean currents and, above all, by the gravity field. Differences below the surface of the Earth (for example, variations in magma temperature) can generate sea level variations of over 100 metres between two ocean regions thousands of kilometres apart. At smaller scales (a few kilometres), we can also observe on this surface (highlighted here so as to be visible) the influence of ocean floor topography (see [bathymetry](#)) which causes variations of several metres at the ocean surface. (Credits CNES/CLS)

According to the laws of physics, if we set aside any perturbing forces (tides, winds, currents, etc.), the surface of the ocean becomes an equipotential surface of the earth's gravity field. Basically this means that if we could place balls all over the surface of the ocean, none of the balls would roll down the hills of this surface because they would all be on the same "level" (i.e. at the same gravity) and subsequently, that the waters of the currents would not flow due to geoid height variations. This equipotential surface deviates by up to 100 metres from the reference ellipsoid, the ideal shape which fits the rotating Earth most closely. These hills and valleys in the ocean's surface are caused by minute variations in the earth's gravitational field. For example the extra gravitational attraction of a massive mountain on the ocean floor attracts water towards it causing a local bump in the ocean surface; a

2,000-m-tall undersea volcano causes a bump about 2 m high, with a radius of about 20 km. This bump cannot be seen with the naked eye because the slope of the ocean surface is very low. In practice, altimetry data, collected by different satellites over many years, are combined to achieve high data density and to average out sea surface disturbing factors such as waves, winds, tides, and ocean variability. The only other component of mean sea surface that is not the geoid is then the static currents (mean dynamic topography), which have to be explained using different methods and then subtracted (see Altimetry Basic Principles, Large-scale ocean circulation, Applications).

Long wavelengths geoid undulations

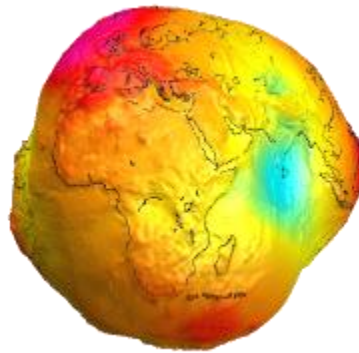


Figure 6.6 EIGEN-CG01C Geoid. (Credits [GFZ Potsdam](#))

The greatest geoid heights and those most visible on a map, reflect deeply-buried density variations.

Gravity anomalies

In order to enhance small-scale features, the high-precision geoid can be converted into a gravity anomaly. Gravity anomaly computations are quite complex, based on laws of physics, geometry and statistics (e. g. see [Sandwell and Smith, 1997]).

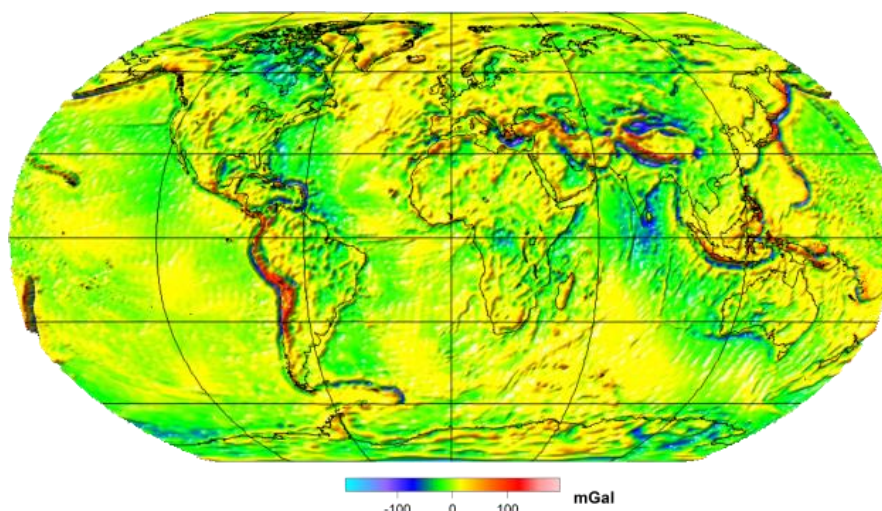


Figure 6.7 EIGEN-CG01C Free Air Gravity Anomalies. (Credits [GFZ Potsdam](#))

References:

- Green, C. M., Fairhead, J. D., and Maus, S., Satellite-derived gravity: Where we are and what's next: *The Leading Edge*, 17, 77-79, 1998.
- Haxby, W. F., Karner, G. D., LaBrecque, J. L., and Weissel, J. K., Digital images of combined oceanic and continental data sets and their use in tectonic studies: *EOS*, 64, 995-1004, 1983.
- Li, Xiong, and Hans-Jürgen Götze, Tutorial: Ellipsoid, geoid, gravity, geodesy, and geophysics, *Geophysics*, vol. 66, no. 6 (november-december 2001); p. 1660-1668, 2001.
- Sandwell, D.T., and Smith, W.H.F., Marine gravity anomaly from Geosat and ERS-1 satellites: *J. Geophys. Res.*, 102, 10039-10054, 1997.
- Yale, M. M., Sandwell, D. T., and Herring, A. T., What are the limitations of satellite altimetry?: *The Leading Edge*, 17, 73-76, 1998.

Further information:

- Tapley, B.D. and M.C. Kim, Applications to geodesy, *Satellite altimetry and Earth sciences*, L.L. Fu and A. Cazenave Ed., Academic Press, 2001

6.1.3 Other geophysical applications

Geophysics is the study of the substances that make up the Earth and the physical processes occurring on, in and above it. Information derived from altimetry data can be used to study tectonic plate motion, rifts, etc.

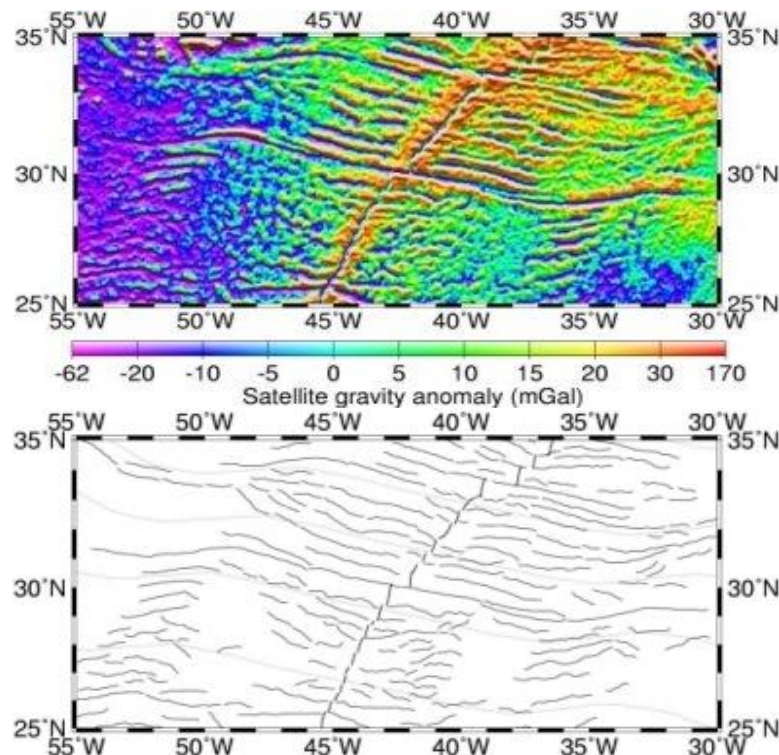
Plate Tectonics

Figure 6.8. Gravity anomalies (top) in the North Atlantic measured in milligals ($1 \text{ mGal} = 10^{-5} \text{ m/s}^2$). Since gravity depends on distribution and density of material, features such as the Mid-Atlantic Ridge and fracture zones show up clearly (Credits [Legos](#)).

Further information:

- Cazenave, A. and J.Y. Royer, Applications to marine geophysics, *Satellite altimetry and Earth sciences*, L.L. Fu and A. Cazenave Ed., Academic Press, 2001

6.1.4 Tsunamis

Tsunamis are waves triggered by the vertical deformation of the ocean bottom, caused by submarine earthquakes or landslides. They lead to waves crossing the oceans at high speed (around 800 km/h), and a potentially enormous quantity of water flooding the coasts when these waves come to shore. Theoretically, sea level anomalies observed by altimetry should reflect these waves. However, observation is difficult, since the additional height is one of the signals of ocean variability. Studying the differences between the few altimetric observations and the tsunami propagation models should enable the scientific community to enhance their understanding of such phenomenon and to fine-tune the models. It is clear that only a multidisciplinary, multi-technique study can grasp all the forces at work here (geophysical, hydrodynamic, energetic etc.).

Until the Indian Ocean tsunami on 26 December 2004, tsunami observations by satellite altimeters had been relatively insignificant. Studies carried out in the past [Okal et al.,1999] show that TOPEX was the only altimeter to detect a tsunami caused by an earthquake in Nicaragua in 1992. The signal was not clearly observed because of its weak amplitude, close to 8 cm, and the great ocean variability in this area. The probability of a satellite altimeter observing a tsunami is low because it requires that the satellite overflies the tsunami wave almost immediately after it originates, due to the tsunami’s great propagation speed (about 800 km/h in an ocean 5,000m deep). Tsunami signals in the open ocean are also quite weak.

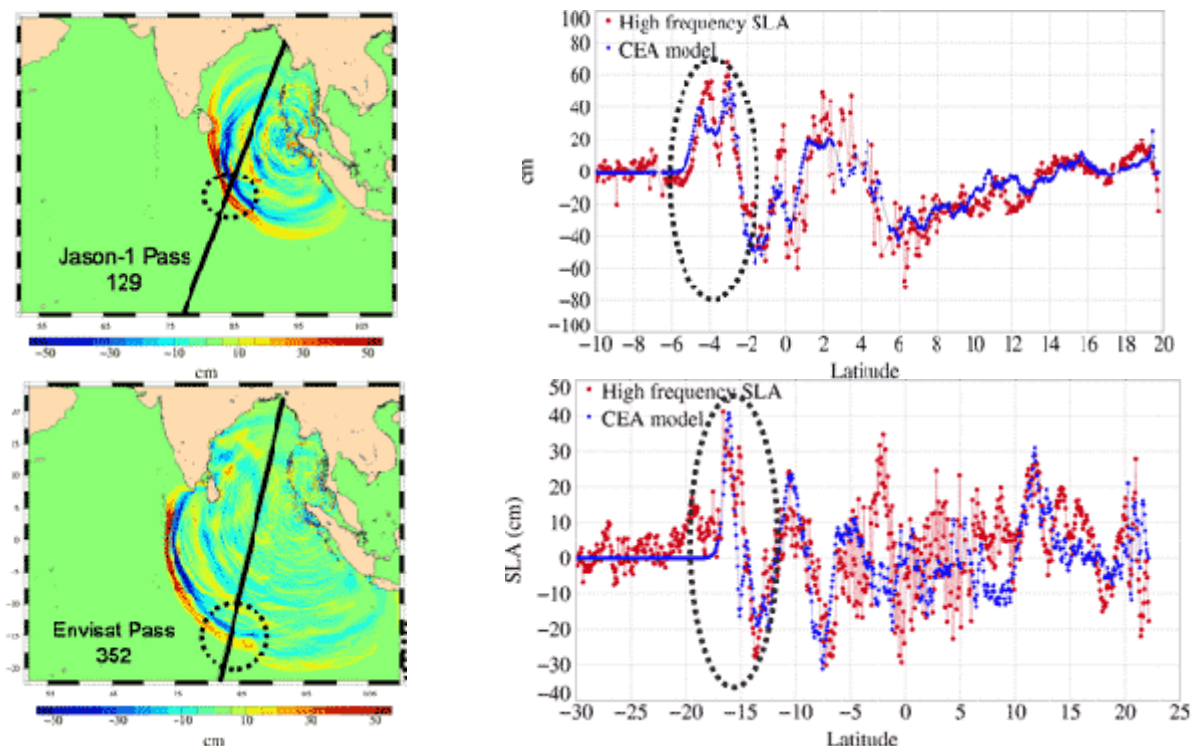


Figure 6.9. Ground track for Jason-1 (top left) and Envisat (bottom left) overlaid by the CEA wave propagation simulation at the time of the satellite’s passage. The area corresponding to the tsunami’s front is circled. Sea level anomalies measured by Jason-1 and Envisat compared to the CEA simulation (top and bottom right) (Credits [CEA](#) & [CLS](#)).

Altimeter Sea Level Anomalies account for many different ocean signals such as large-scale and mesoscale ocean variability. These signals considerably limit our ability to detect tsunami waves, or can at least significantly modify the observed characteristics. Most of these signals can be removed, however, using an ocean variability mapping technique. Note that this is possible only because at the time of the December 2006 tsunami, we had very good space/time sampling of the ocean with four altimeters. Such a configuration is required to describe the ocean's mesoscale variability and thus to extract the signals generated by the tsunami from the background ocean variability signals.

It must be noted that satellite altimetry is not sufficient for the early detection and warning of tsunamis. Even with a four altimeter configuration (as it was the case during the 26 December 2004 Indian Ocean tsunami), the probability of observing a tsunami just after it is triggered remains low [Okal et al., 1999]. This also poses some specific data acquisition and processing issues (data processing time would hardly be compatible with the time required to issue an alert). The unique contribution of satellite altimetry is to better understand and improve the modelling of tsunami propagation and dissipation. In particular, reported observations from the 26 December 2004 Indian Ocean tsunami have been used to refine the initial displacement conditions due to the earthquake, so that observations match model outputs [Ablain, 2006].

Further information:

- Ablain, M., J. Dorandeu, P-Y. Le Traon, A. Sladen, The Indian Ocean Tsunami of December 26, 2004, High Resolution Altimetry Reveals New Characteristics of the December 2004 Indian Ocean Tsunami, *Geophys. Res. Lett.*, submitted, 2006.
- Ablain, M., J. Dorandeu, P-Y. Le Traon, A. Sladen, The Indian Ocean Tsunami of December 26, 2004, Observed by Multi-satellite Altimetry, 15 years of progress in radar altimetry Symposium, Venice, Italy, 2006
- Smith, W.H.F., R. Scharroo, V.V. Titov, D. Arcas, and B.K. Arbic, Satellite altimeters measure tsunamis. *Oceanography*, 18(2), 11-13, 2005.
- Okal, E., A. Piatanesi, and P. Heinrich, Tsunami detection by satellite altimetry. *J. Geophys. Res.* 104 (B1), 1999.

6.2 Ocean applications

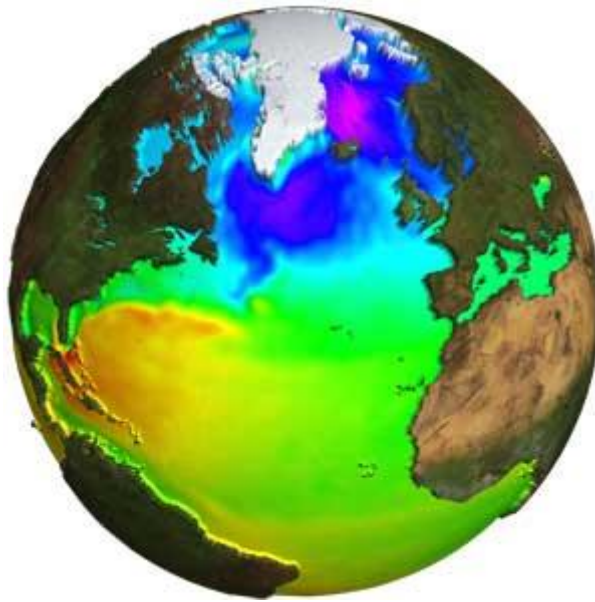


Figure 6.10. Mean Dynamic Topography (Credits [CNES](#))

The ocean is the surface studied by the majority of altimetry applications, and some missions are even optimised for it. Ultimate applications include oceanography itself, as well as the implications of ocean movements on climate (and vice-versa, the effects of climate change on the ocean).

Ocean currents can raise sea surface height by up to a metre higher than the surrounding area. Currents can therefore be mapped by measuring height variations. Satellite altimetry, supplying continuous worldwide observations, has been increasing our knowledge of ocean circulation since the 1978 Seasat mission. The ocean is also a turbulent environment — especially so in the major current areas—, where ‘mesoscale’ eddies (i.e. eddies measuring about 50-500 km across) are generated and move. The goal of operational oceanography is to describe in real-time and to forecast such ocean dynamics, with altimetry supplying the most important data for assimilation.

The tides, another ocean phenomenon seen by altimetry, can now be gauged to within 2 cm, thanks largely to altimetry. This has helped to improve our understanding of Earth-Moon interactions such as the Moon’s impact on the length of the day on Earth, and has given some insight into one of the driving forces of the Earth’s climate system.

Last, but not least, by tracking changes in sea level, altimetry helps us to monitor mean sea level, its time variations and geographical patterns. Many studies are ongoing, in the context of research into the greenhouse effect.

6.2.1 Large-scale ocean circulation

A view of the global ocean circulation shows currents swirling around the hills and valleys at the sea surface. In the Northern Hemisphere, currents flow around hills in a clockwise direction and in an anticlockwise direction (the opposite occurs in the Southern Hemisphere) around valleys. These currents form gyres on either side of the equator. Planetary waves are other large-scale phenomena that are less easy to see on an instantaneous map, but nonetheless they too have a global impact.

Currents

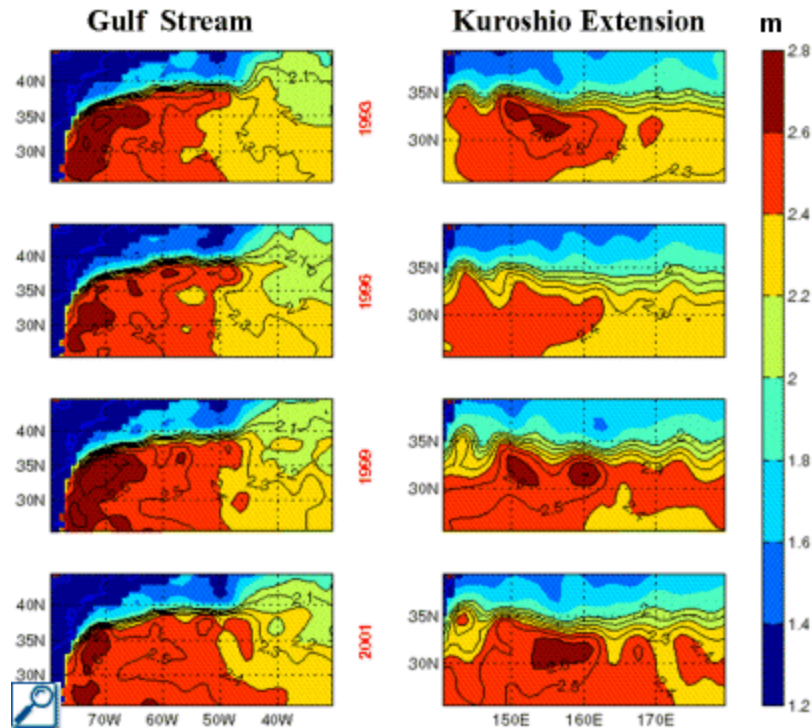


Figure 6.11. Changes in the extent of the Gulf Stream and the Kuroshio, as seen by Topex/Poseidon. The currents were 'elongated' in 1993 and 1999, and contracted in 1996 and 2001. (Credits .University of Washington)

The major ocean currents can raise sea surface height by up to a metre higher than the surrounding area. The deviation of the ocean surface elevation from the geoid is called ocean surface topography. This is used to calculate the speed and direction of ocean currents — provided that the geoid is understood independently with sufficient accuracy, which, since the CHAMP and GRACE gravimetry satellites were launched. This understanding was enhanced further with the GOCE mission. After 4.5 years in orbit, it gathered enough data to map Earth's gravity with unrivalled precision. The 5th gravity field model based, EGM_TIM_RL05, with a mean global accuracy of 2.4 cm in terms of geoid heights and 0.7 mGal for gravity anomalies at a spatial resolution of 100 km.

Even without this knowledge, studies of the large-scale variations have been undertaken since the beginning of altimetry. Among other things, year-to-year variations in the extent of the Gulf Stream and Kuroshio currents have been observed, that can be correlated with changes in upper ocean heat content. These have an impact on ocean-atmosphere heat exchanges, with implications for decadal climate variations.

- Data use case: Western boundary currents: The Gulf Stream and its seasonal variations

Kelvin and Rossby waves

Though the major currents are very important, the ocean and climate are also influenced by phenomena that are more difficult to see. 'Planetary' waves cross the oceans along parallels and interact with general ocean circulation. These are either Rossby waves, which travel from east to west, or Kelvin waves which move in the opposite direction. They intensify currents such as the Gulf Stream or the Kuroshio. In addition, they may be reflected off the continents and return in the opposite direction, or follow coastlines. These waves and their reflections play a key role, in particular in the El Niño phenomenon.

The existence of Rossby waves had been predicted theoretically for over 50 years, but they could not be observed until the advent of high-precision altimetry satellites. Their small amplitude (a few centimetres), extent (an ocean basin) and velocity (a few kilometres per day, depending on the latitude – they take several years to cross the Pacific Ocean at the 30° latitude) made it nearly impossible to observe them using in situ measurements. Now that we know what we are looking for (they can be seen most clearly as a series of straight lines in longitude-time diagrams), we can also detect them in other kinds of satellite measurements. High-precision altimetry, however, remains the best way of detecting these waves.

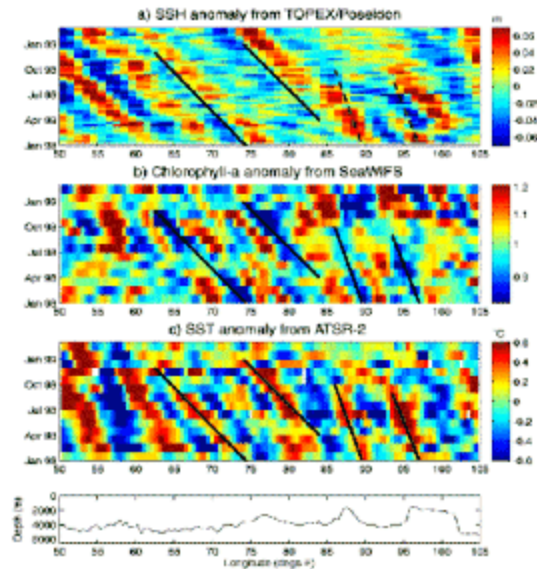


Figure 6.12. Comparison of longitude-time diagrams from three different sensors (altimeter, water colour, surface temperature). (Credits Southampton Oceanography Centre)

Further information:

- Cipollini, P., P.G. Challenor, D. Cromwell, I.S. Robinson, G.D. Quartly, How satellites have improved our knowledge of planetary waves in the oceans, *15 years of progress in radar altimetry Symposium*, Venice, Italy, 2006
- Fu, L.L. and D.B. Chelton, Large-scale ocean circulation, *Satellite altimetry and Earth sciences*, L.L. Fu and A. Cazenave Ed., Academic Press, 2001
- Brockmann, Jan Martin, Norbert Zehentner, Eduard Höck, Roland Pail, Ina Loth, Torsten Mayer-Gürr, and Wolf-Dieter Schuh. "EGM_TIM_RL05: An independent geoid with centimeter accuracy purely based on the GOCE mission." *Geophysical Research Letters* 41, no. 22 (2014): 8089-8099.

6.2.2 Ocean currents and eddies: mesoscale ocean applications

Ocean currents are sometimes compared to ‘sea highways’, because ships follow their flow to gain speed. But this picture is not wholly accurate. In fact, ocean currents are more like secondary roads branching off into narrow country roads and lanes, winding their way around hills and natural obstacles. The main flow of these currents is often disturbed by eddies that form at their edge. So the ocean is really more like a vast, slowly swirling whirlpool bath than a swimming pool divided into perfectly straight lanes.

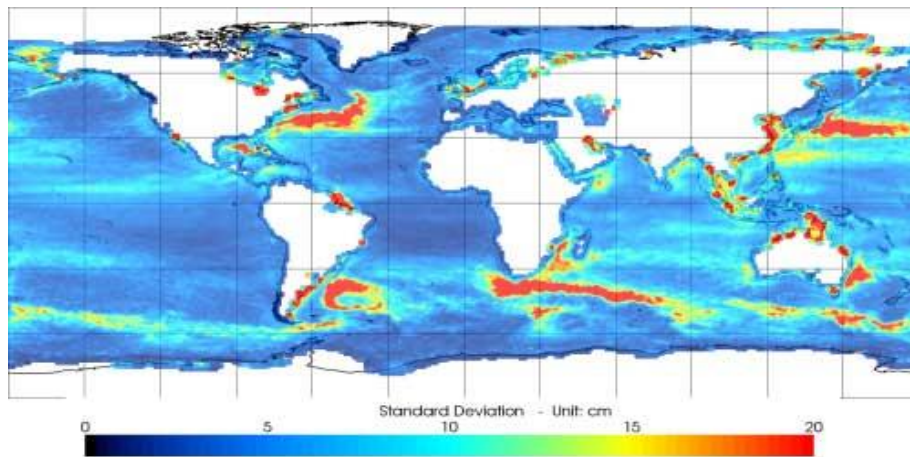


Figure 6.13. Standard deviation computed from 12 years of altimetry data (all available satellites during the 1992-2004 period) (Credits Aviso)

The ocean is a turbulent environment. The most energetic kind of ocean circulation variability is associated with so-called mesoscale variability (eddies, meandering currents or fronts, squirts and filaments), i.e. features on a 50-500 km scale, lasting 10-100 days, with currents of a few kilometres per hour. The energy of these mesoscale processes generally exceeds that of the mean flow by an order of magnitude or more. They also transport heat, salt, carbon and nutrients as they propagate through the ocean. Ocean eddies play an important role in ocean circulation and heat transport, as well as in the ocean's biogeochemical cycles. The ability to monitor them from space has applications in navigation, offshore operations, fisheries, hurricane and climate forecasting, among others.

Before the advent of satellite observations, this turbulence was mostly underestimated, or even ignored. For improved monitoring of such features, altimetry needs merged data from at least two satellites (see: High-precision altimetry with satellites working together).

- Data use case: Ocean eddies as seen by satellite altimetry: the Kuroshio current

Further information:

- Le Traon, P.Y. and R. Morrow, Ocean currents and eddies, *Satellite altimetry and Earth sciences*, L.L. Fu and A. Cazenave Ed., Academic Press, 2001
- Morrow, R. and P.Y. Le Traon, Mesoscale Eddy Dynamics observed with 15 years of altimetric data, *15 years of progress in radar altimetry Symposium*, Venice, Italy, 2006

6.2.3 Operational oceanography

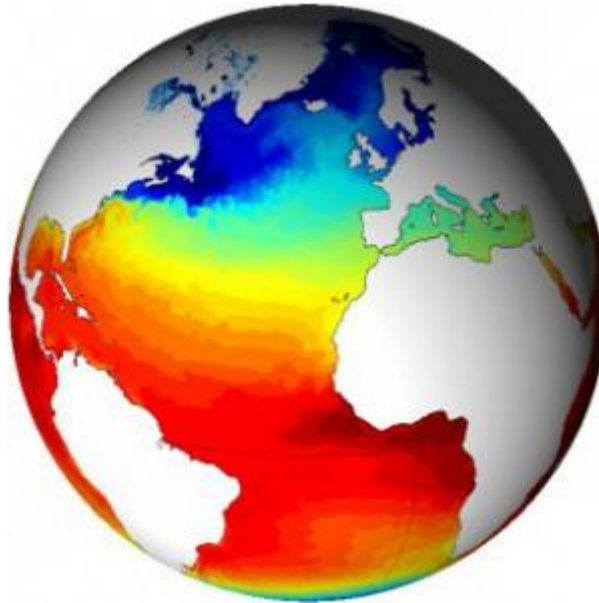


Figure 6.14. Sea Surface Temperature computed by the Mercator global model (Credits Mercator Ocean)

Satellite observations provide a unique opportunity to monitor changes in the ocean in real time, accurately, on a global scale, and with high resolution. As only the properties of the sea surface can be observed from Space, data assimilation systems are needed to improve the consistency between satellite data and model simulations, to dynamically extrapolate and interpolate measurements scattered in space/time, and to better exploit the results of observations.

Ocean models are based on the laws of physics applied to a fluid (Newton's laws, along with thermodynamics). Data assimilation is a procedure that combines actual observations with models. This combination aims to better estimate and describe the state of a dynamic system — the ocean. Estimates of this dynamic system are improved by correcting model errors with the observations on the one hand, and by synthesizing observations with the model on the other.

The vast majority of assimilation methods used in oceanography and meteorology are based on minimising the squared difference between the observations and their modelled equivalents. Several different approaches are used to resolve this problem: they are divided into so-called sequential and variational methods (such as 3D-Var, 4D-Var). Sequential methods, which are more basic but also more robust, enable the density of a water column to be modified in the model in order to correspond to the satellite-observed sea level height. These calculations are performed sequentially and the results are compared with observations at regular intervals, thus allowing the model to be corrected. Other more advanced techniques are costlier and more difficult to adjust due to their complexity. They include the variational method which aims to correct the initial conditions of the numerical model in order to obtain results that best fit the observations made throughout the period studied. At any point in time, therefore, the correction takes into account past and future observations. This technique is useful for controlling large-scale changes in ocean circulation and monitoring phenomena such as equatorial waves.

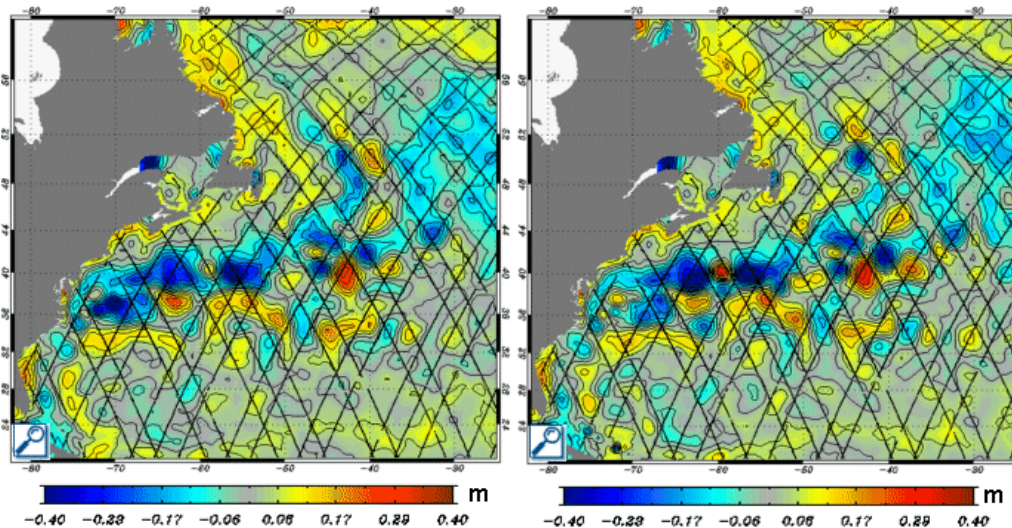


Figure 6.15. Sea level anomalies on 8 January 2003 from the medium-resolution Mercator model ($1/3^\circ$), with assimilation of in situ SST measurements and (left) Jason-1 data only, (right) all available altimetry satellite data (Jason-1, ERS-2 and GFO). More detail can be seen in the right-hand figure (Credits Mercator Ocean).

Ocean models have now improved to the point where they are used to simulate and study the actual circulation of the ocean.

Further information:

- Fukumori, I., Data assimilation by models, Satellite altimetry and Earth sciences, L.L. Fu and A. Cazenave Ed., Academic Press, 2001
- Ocean Weather Forecasting, E. Chassignet and J. Verron Ed., Springer, 2006

6.2.4 Tides

Tides have been studied for longer than most other ocean phenomena; however, for most of this time, the only measurements possible were those made by tide gauges on the coasts, mostly in harbours, which were thus subject to local factors, the geometry of the coasts and, in particular, the bathymetry. Now, satellite altimetry provides measurements of sea surface heights in the open ocean accurate to 2-3 centimetres that are assimilated into mathematical tide prediction models. This has helped to improve tide models (now accurate to within 2 cm in the open ocean), and increase our understanding of Earth-Moon interactions such as the Moon's impact on the length of the day on Earth. In return, tide models are used to remove tidal effects from altimetry data.

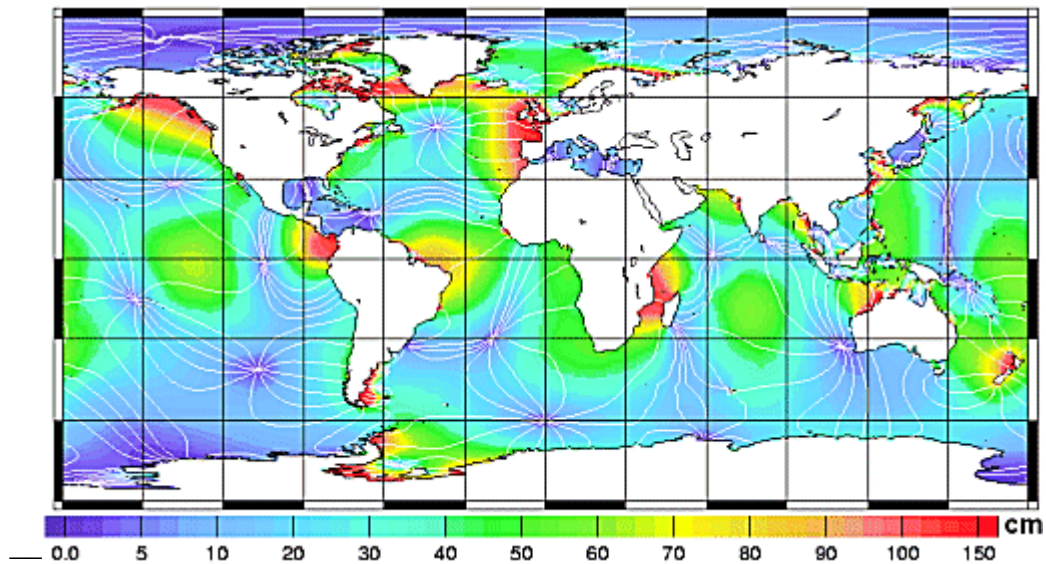


Figure 6.16. Amplitude of the M2 tidal constituent (in centimetres) derived from the FES99 model. Cotidal lines indicating the phase every 30 degrees originate at amphidromic points where the tidal range is zero. (Credits Legos/CNRS)

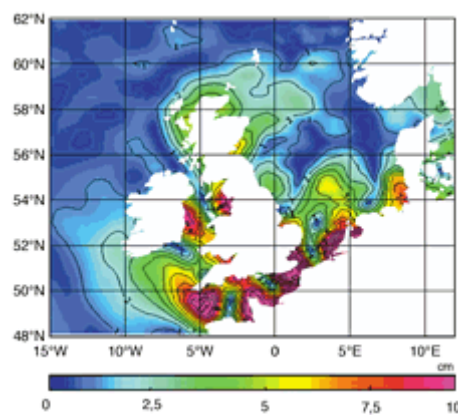


Figure 6.17. Amplitude of the lunar wave for a period of 6 hours (wave M4) in the particularly complex areas of the North Sea and English Channel. A long series of altimetry data, from Topex/Poseidon and then Jason-1, should make it possible to significantly improve forecasting. (Credits KMS)

The combined attraction of the Moon and the Sun generates tides on Earth. Calculating their effects is not as easy as it might seem, as the distance and inclination of the Sun and Moon with respect to Earth, and with respect to each other, have to be factored in. The shape and size of ocean basins is another factor that makes predicting tides such a complex matter. In order to calculate tides, they have to be broken down into sinusoidal waves of given periods, each of which varies in amplitude and represents one component of the problem. Thus, one of the waves, called M2, is due to the attraction of a ‘virtual’ Moon placed on a perfectly circular orbit in the Earth’s equatorial plane. It has two high and two low tides per day (semi-diurnal wave). The K1 wave, with a diurnal period, reflects declination variations of the Moon and Sun. The amplitude of the tide at a given time and place is the

sum of all these sinusoidal waves. In certain areas, a hundred of these waves have to be added together to obtain a precise forecast.

One of the questions that needs solving when using altimetry in tidal studies is the issue of aliasing. Depending on the satellite's repeat period, some tidal constituents are always seen at the same point in their cycle, and thus have not been accurately measured (this is especially true for sun-synchronous satellites, which see semi-diurnal tidal constituents as stationary), whereas other tidal constituents with periods shorter than the satellite's are measured with sparse sampling with respect to their duration, and are thus difficult to piece together.

In addition to their direct effects on maritime and coastal activities, tides appear to have a less well-known impact on the Earth's climate. This discovery, which is based on almost ten years of highly precise altimetry data, has led to a new understanding of the way in which the Moon influences our planet. Ocean waters are stratified according to their density. The different layers mix with difficulty. However the tidal currents coming into contact with the relief of the ocean bottom (even if this is very deep) create waves which are propagated at the interface between two layers of different density (internal waves). It is currently thought that this mechanism contributes more than half of the vertical mixing of water masses. This mixing is fundamental to large-scale ocean circulation (thermohaline circulation) which enables the redistribution of heat from the equator to the poles.

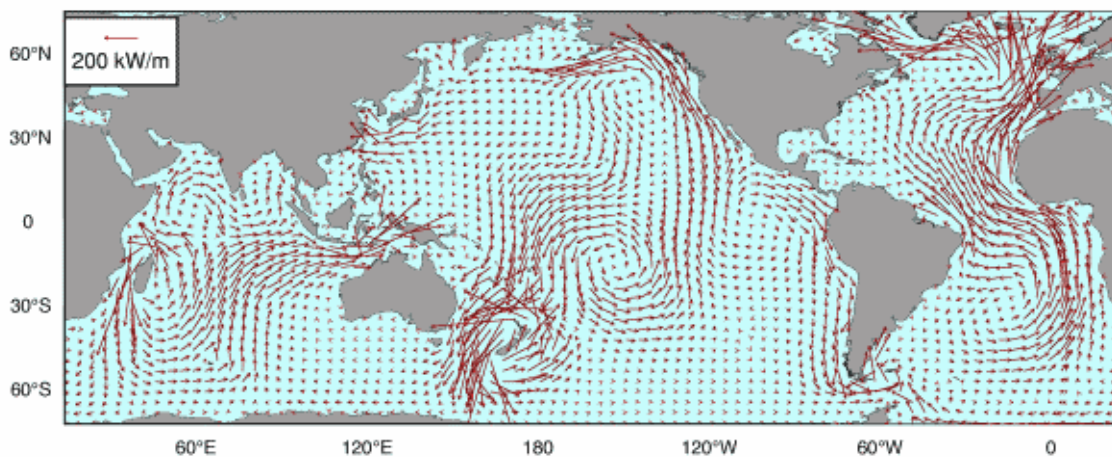


Figure 6.18. Energy flow of the semi-diurnal, lunar tidal wave (M2). The illustration shows the displacement of energy from areas in which it was generated towards dissipation areas. It has been demonstrated, for instance, that the energy dissipated on the Patagonian shelf (to the east of South America), one of the areas where tides are highest, comes from the Pacific and that 40% of the total energy contributed by the Earth/Moon system to ocean tides, is dissipated in the North Atlantic. (Credits NASA/GSFC)

References:

- Cartwright, D. E., Detection of tides from artificial satellites. Tidal Hydrodynamics, *B. Parker*. New York, John Wiley: 547-568, 1991.

- Cartwright, R. E. and R. D. Ray, Oceanic Tides From Geosat Altimetry, *J. Geophys. Res.* 95(C3): 3069-3090, 1990.
- Eanes, R. J. and S. V. Bettadpur, The CSR3.0 global ocean tide model, *Austin, Cent. for Space Res. Univ. of Tex.*, 1996.
- Le Provost, C., A. F. Bennett, et al., Ocean tides for and from TOPEX/Poseidon, *Science* 267: 639-642, 1995.
- Le Provost, C., F. Lyard, et al., A hydrodynamic ocean tide model improved by assimilating a satellite altimeter-derived data set, *J. Geophys. Res.* 103: 5513-5529, 1998.
- Mazzega, P., M2 model of the Global Ocean Tide Drived from SEASAT Altimetry, *Mar. Geod.* 9(335-363), 1985.
- Mènard, Y., E. Jeansou, et al., Calibration of TOPEX/POSEIDON at Lampedusa: additional results at Harvest, *J. Geophys. Res.* 99(C12): 24487-24504, 1994.
- Parke, M. E., R. H. Stewart, et al., On the choice of orbits for an altimetric satellite to study ocean circulation and tides, *J. Geophys. Res.* 92: 11693-11707, 1987.
- Ray, R., A Global Ocean Tide Model From TOPEX/Poseidon Altimetry/ GOT99.2 – NASA/TM-1999-209478. *Greenbelt, MD, Goddard Space Flight Center/NASA*: 58, 1999.
- Schrama, E. J. O. and R. D. Ray, A preliminary tidal analysis of TOPEX/Poseidon altimetry, *J. Geophys. Res.* 99: 24,799-24,808, 1994.

Further information:

- Le Provost C., Ocean tides, Satellite altimetry and Earth sciences, L.L. Fu and A. Cazenave Ed., Academic Press, 2001

6.2.5 Mean Sea Level

Sea level rise and the Greenhouse effect

A large proportion of the world's population lives in coastal areas vulnerable to rising sea levels. Permanent submersion, repeated flooding, faster erosion of cliffs and beaches, increasingly saline estuaries and salt contamination of groundwater are just some of the possible consequences of a rise in sea level in low-lying regions.

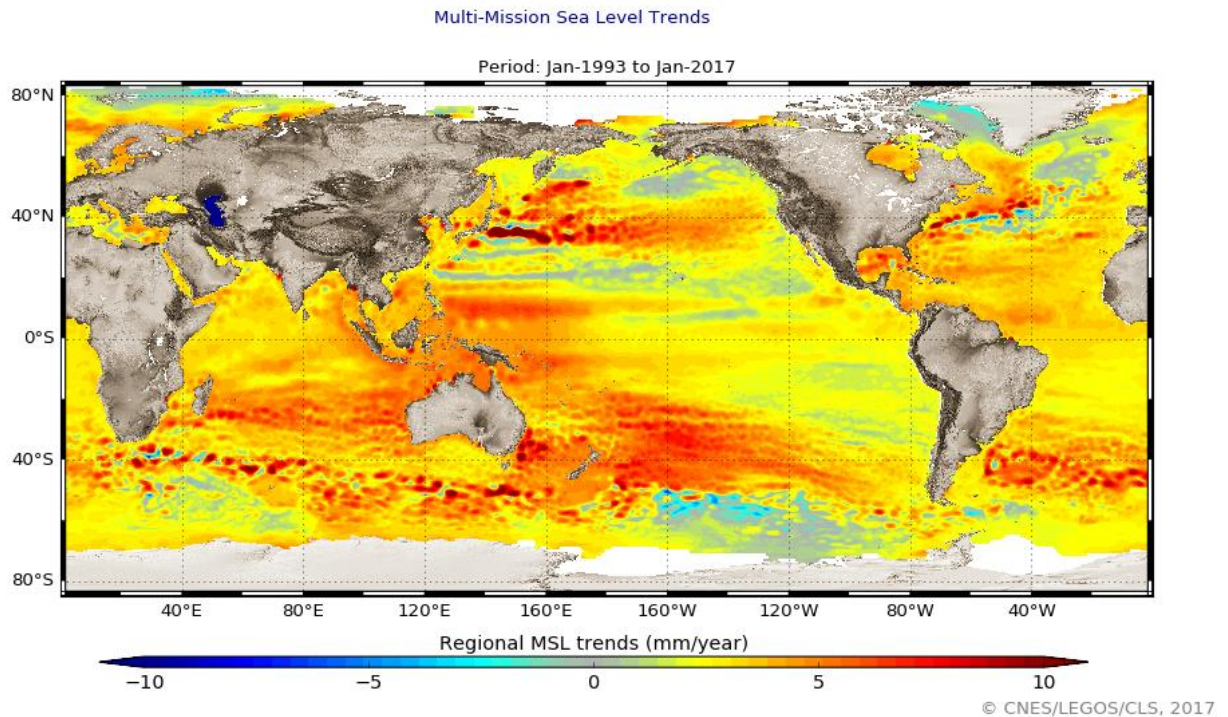


Figure 6.19. Combined map of regional patterns of observed sea level (in mm/year). This map can be obtained using gridded, multi-mission Ssalto/Duacs data since 1993, which enable the local slopes to be estimated with a very high resolution (1/4 of a degree on a Cartesian projection). Isolated variations in MSL are thus revealed, mainly in the major ocean currents and ENSO events (Credits EU Copernicus Marine Service, CLS, Cnes, Legos)

As global temperatures rise, mean sea level is rising with them: all the indicators point to an increase in the mean level of the world's oceans. As far as we can tell from a few isolated measurements taken around 1900, this rise has been continuing for at least a century. Today, thanks to the global coverage of altimetry satellites, estimates of the rise in sea level have improved in accuracy. With time series containing fifteen years of data, we can begin to observe trends and attempt to mitigate their effects.

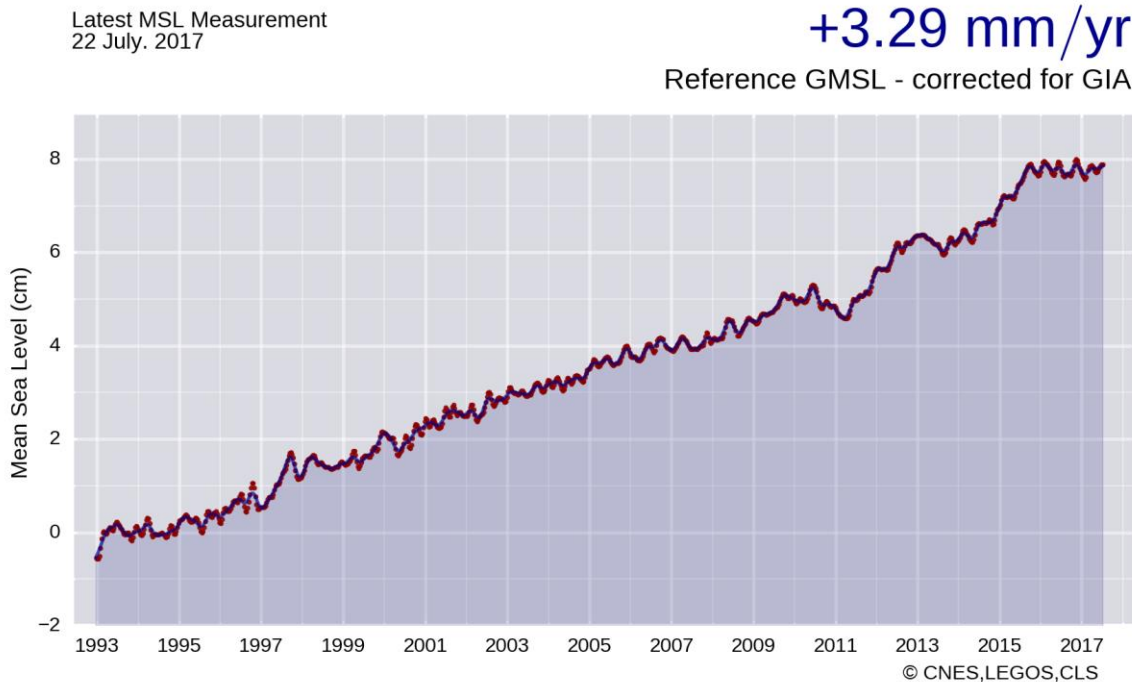


Figure 6.20. Mean Sea Level variation computed from altimetry 1993-2017 (Credits CLS/Cnes/Legos)

Altimetry provides a powerful tool for determining the extent and causes of sea level change. Since early 1993, Topex/Poseidon has been measuring global sea level variations with great accuracy, complemented and followed by Envisat and Jason-1. This long dataset indicates that, in terms of the global mean, sea level is presently rising at a significantly higher rate than the mean rate recorded by tide gauges for the past five or more decades (of the order of 1.8 ± 0.3 mm/yr). The higher rate observed during the 1990s may indicate that sea level rise is accelerating due to greater land ice melting and/or increased ocean warming. Moreover, we cannot exclude the possibility that it at least partly reflects the decadal variability of the combined change in thermal and ocean mass. Longer datasets are needed to discriminate between the different hypotheses and to study this question further.

Estimating mean sea level change and its sources is currently a very active research topic. Many teams are participating in fine-tuning the computations and studying the causes.

Further information:

- Nerem, R.S. and G.T. Mitchum, Sea level change, Satellite altimetry and Earth sciences, L.L. Fu and A. Cazenave Ed., Academic Press, 2001
- Nerem R.S., E; Leuliette and Cazenave A., Present-day sea level change, C.R. Geosciences, in press, 2006.
- A. Cazenave, A. Lombard, R.S. Nerem, and K. DoMinh, Present-day sea level rise: do we understand what we measure?, 15 years of progress in radar altimetry Symposium, Venice, Italy, 2006

- Church, J.A., N.J. White, R. Coleman, K. Lambeck and J.X. Mitrovica, Global and regional sea-level rise, Papers of Note. Bulletin of the American Meteorological Society, 85 (7): 950-952, 2004.
- <http://www.aviso.oceanobs.com/msl/> (Aviso/Altimetry, Mean Sea Level in cooperation between LEGOS, CLS and CNES)
- <http://sealevel.colorado.edu/> (University of Colorado at Boulder, USA)
- <http://copes.ipsl.jussieu.fr/Workshops/SeaLevel/> (Understanding Sea-level Rise and Variability Workshop, June 2006)

6.2.6 Open Ocean - SAR

SAR altimetry over ocean has attracted a lot of attention in the past years and huge progress has been made in a short timespan. CryoSat-2 was the first satellite to provide SAR, also known as delay/Doppler, altimetry data over the ocean, which permitted to demonstrate the significant benefits of SAR mode for ocean altimetry compared to conventional low resolution mode (LRM). Now Sentinel-3 will continue to provide SAR measurements over ocean continuously and globally.

The differences between the SAR mode and LRM in terms of shape of the waveforms and SNR can be appreciated in the figure below where two different echoes have been modelled.

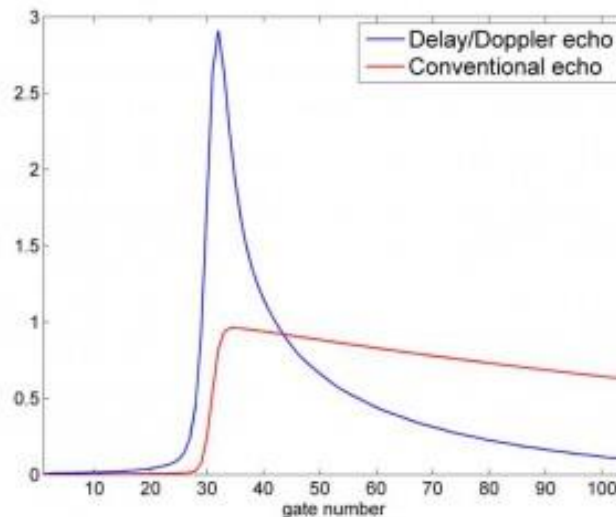


Figure 6.21. Delay/Doppler and conventional echoes for the same altimetric parameters ($P_u = 1$, $\tau = 31$ gates, $SWH = 2$ m; credit: Abderrahim Halimi, ENSEEIHT)

As for the LRM case, the SAR waveform is affected by the state of the ocean: depending on the height of the waves, waveforms will be wider or narrower as it is shown in the figure below.

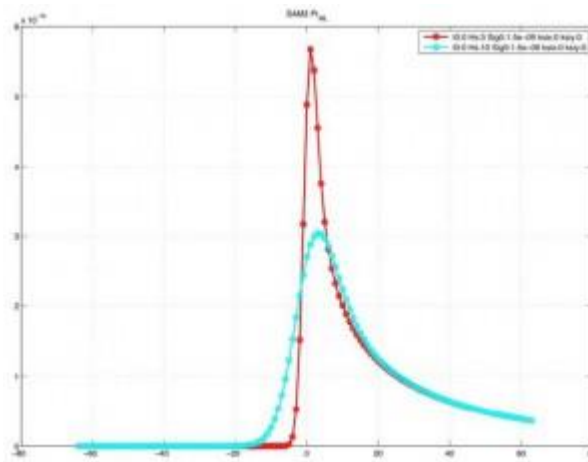


Figure 6.22. SAR waveforms modelled using SAMOSA3 for waves of 3 (red curve) and 10 meters (blue curve), credits NOC

Moreover, new retrackers are needed to process SAR waveforms.

There are different types of retrackers and different groups of people working on them:

- Numerical SAR waveform models, Phalippou & Enjolras, 2007, Phalippou & Demeestere, 2011 from TAS and F.Boy et al., 2012 from CNES.
- Semi-Analytical SAR waveform models, Wingham et al, 2004, Giles et al and Halimi et al., 2012 and different evolutions of the SAMOSA retracker from the ESA-funded project: Martin-Puig et al., 2008, Gommenginger et al., 2012 and Ray et al., 2013.
- Fully-Analytical Physically-Based SAR waveform models.

The convergence of results from different groups indicates a high level of confidence in the retrieval of geophysical information from SAR altimetry over ocean. Improvements **offered** by the SAR mode with respect to the conventional Low Resolution mode are the following:

- Improved precision in range (and derived parameters: SSH, SLA, etc.) with respect to LRM data. In terms of 1Hz noise, improvement from 1.57 cm to 1.22 cm.
- Improved precision in SWH with respect to LRM data. In terms of 1Hz noise, improvement from 11.09 cm to ~ 8.5 cm.
- Improved along track resolution, shown in SLA and SWH spectra, so that scales of less than 100km can be resolved.
- Improved SNR (Fig. 6.21).
- SAR products are consistent with LRM products or have known biases that can be corrected for.

Further information:

- Review of state of knowledge for SAR Altimetry over ocean, EUMETSAT REFERENCE: EUM/RSP/REP/14/749304, [full document link](#).
- CP4O data access
- ESA CP4O project
- ESA SAMOSA Project
- [ESA SCOOP Project](#)
- [ESA SHAPE Project](#)
- [ESA SPICE Project](#)

6.3 Ice: Land and sea ice

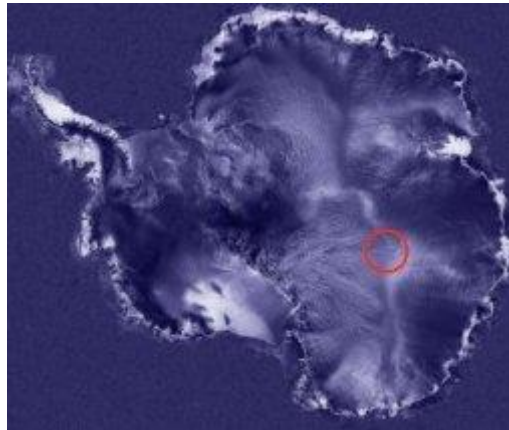


Figure 6.23. Topographic maps of Antarctica and the area around Lake Vostok (red circle), showing the ice plateau capping the lake (three kilometres below the surface). (Credits Legos/CNRS/NASA/GSFC).

Altimetry measurements can also be used to determine sea ice thickness and glacier topography. Ice motion and spread are major indices of global climate change: ice, including sea ice, plays an active role in the climate due to the strong feedback induced by its high albedo, whereas continental ice mostly acts as a huge reserve of fresh water (77% of the Earth's fresh water is frozen in Greenland and Antarctica), that could significantly contribute to sea level rise.

The cryosphere plays an important role in moderating the global climate, and as such, the consequences of receding ice cover due to global warming are far-reaching and complex. While evidence suggests that ice sheets are relatively stable, there are indications that rapid changes are occurring around their margins, where the ice reaches the sea: changes that could weaken the ice sheets.

Altimetry is one of the most powerful tools for observing sea ice and ice sheets. For sea ice, altimetry provides a unique way of measuring its thickness. For ice sheets, their topography can be measured by altimeters, at least by those that can reach high latitudes. Moreover, altimeters also provide other parameters such as backscatter coefficient and waveform shape that give information on surface roughness and snow pack characteristics such as stratification or ice grain size. These parameters are related to relevant unknown quantities affecting the climate, such as snow accumulation rate or snow drift caused by wind.

Further information:

- Remy, F., The new vision of the cryosphere thanks to 15 years of altimetry, 15 years of progress in radar altimetry Symposium, Venice, Italy, 2006
- Zwally, H.J. and A.C. Brenner, Ice sheet dynamics and mass balance, Satellite altimetry and Earth sciences, L.L. Fu and A. Cazenave Ed., Academic Press, 2001

6.3.1 Land Ice

6.3.1.1 Polar Ice Caps

Altimetry is a powerful tool for measuring both the dynamics and mass balance of ice sheets. Continental ice has an impact on sea level: if both of the major Greenland and Antarctica ice sheets were to melt, the sea level would rise by about 80 m.

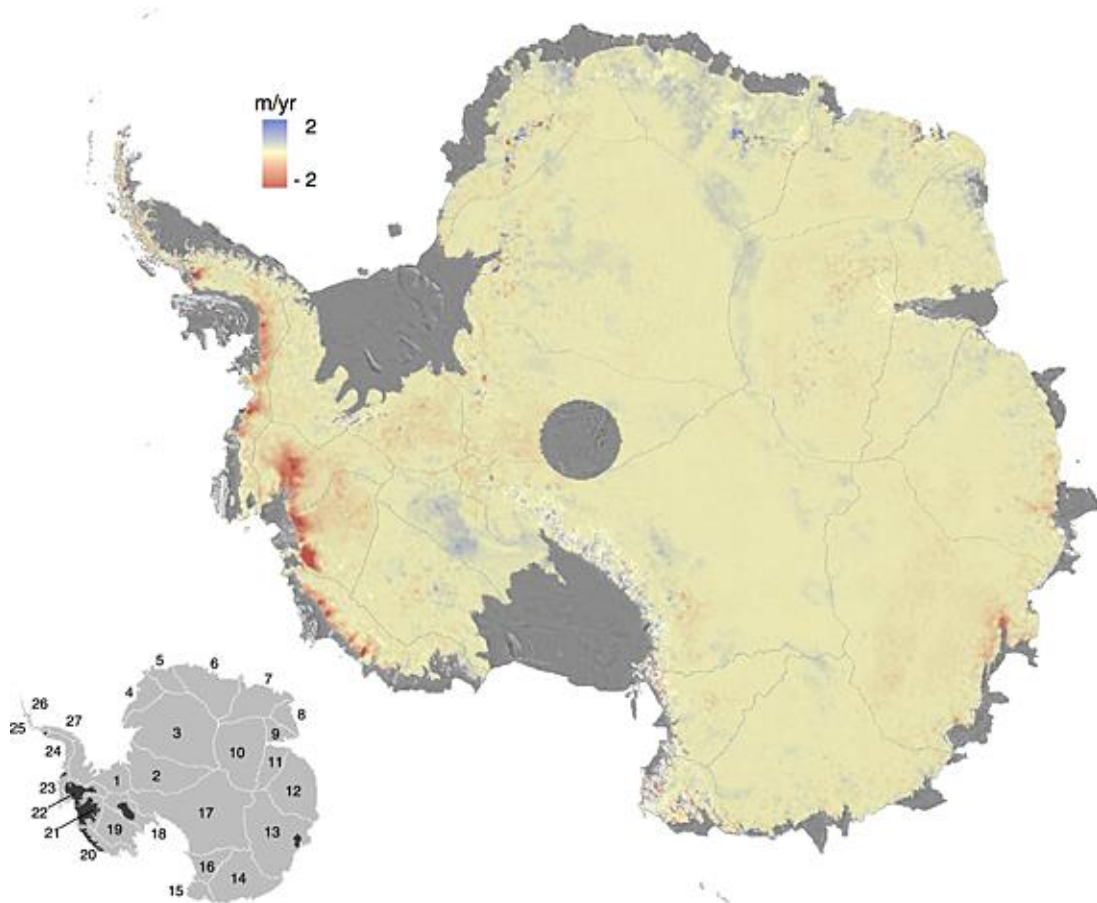


Figure 6.24. Rate of elevation change of the Antarctic ice sheet between 2010 and 2013 determined from CryoSat-2 repeat altimetry and smoothed with a 25 by 25 km median filter. Solid grey and white (inset) lines show the boundaries of 27 ice sheet drainage basins [Zwally et al., 2012]. The CryoSat measurements reach to within 215 km of the South Pole, as compared to 930 and 430 km for the ERS/Envisat and ICESat altimeters, respectively. Also shown (inset) are the numbers used to identify ice sheet drainage basins, with East Antarctica and the Antarctic Peninsula defined as basins 2 to 17 and 24 to 27, respectively, and West Antarctica defined as the remaining basins and the mask developed to identify elevation changes occurring at the density of ice (inset, black regions). Elsewhere, it is assumed that elevation changes are caused by fluctuations in surface mass balance alone, and we therefore applied a density of snow to these signals (inset, grey regions). Ice dynamical imbalance (IDI) is evident as thickening of the Kamb Ice Stream (basin 18) and as widespread thinning across the Amundsen Sea sector (basins 21 and 22), with the latter signal affecting a considerably larger area than at any time in the past two decades [Shepherd et al., 2002, 2004; Wingham et al., 2009]. (Credits CPOM)

Topography is one of the parameters relevant to the processes acting on ice sheets. It contains the signature of the main physical processes (climate and dynamic), that act on an ice sheet on both a small and a large scale, and important information about local anomalies or general trend behaviour. Nowadays topography is also an initial condition for studying future evolution. Large-scale topography controls flow direction and its mapping enables the balance velocity to be derived. Moreover, the deformation and sliding velocities depend on the basal shear stress and thus on surface slopes. Accurate information about topography is, therefore, crucial to predicting future evolution and understanding ice dynamics, either by providing an empirical parameterisation of the flow laws or by pointing out unknown physical processes.

Moreover, altimeters also provide other parameters such as backscatter coefficient and waveform shape that give information on surface roughness and snow pack characteristics, from the global to the kilometre scale. Since ERS-1 was launched, with an orbit as high as 82°N and S, our vision of the ice sheets has been radically transformed. This long series, with ERS-2 and Envisat following ERS-1, has made it possible to discern changes in the shape and volume of both ice sheets, Greenland and Antarctica, which are related to climate change. Moreover, from April 1994 to March 1995, ERS-1 was placed on a geodetic orbit (two shifted cycles with a 168-day repeat) so that the topography of both ice sheets could be mapped with a resolution of 2 km. This precise topography has led to the detection of subglacial lakes, subglacial hydrological networks, outlet glacier anomalies, etc.

The 25 years of data from ERS-1, ERS-2, Envisat and Cryosat-2 have also made it possible to map the ice mass balance. Measurements from CryoSat mission, launched in 2010, have been used to map the height of the huge ice sheets that blanket Greenland and Antarctica and show how they are changing. It carries an interferometer altimeter, called SIRAL, the first of its kind to overcome the difficulties intrinsic to measuring icy surfaces. The instrument allows scientists to determine the thickness of ice floating in the oceans and to monitor changes in the vast ice sheets on land, particularly around the edges where icebergs are calved. Ice sheets gain mass through snowfall and lose it through melting and by glaciers that carry ice from the interior to the ocean.

Examining the ice sheet regions individually we show that the Greenland, West Antarctic and Antarctic ice sheets have all lost mass over the past two decades, whilst the East Antarctic ice sheet has undergone a slight snowfall-driven growth. The Greenland ice sheet has lost the largest mass and accounts for about two-thirds of the combined ice sheet loss over the study period. In Antarctica, the largest mass losses have occurred in the West Antarctic Ice Sheet. However, despite occupying just 4% of the total ice sheet area, the Antarctic Peninsula has accounted for around 25% of the Antarctic mass losses.

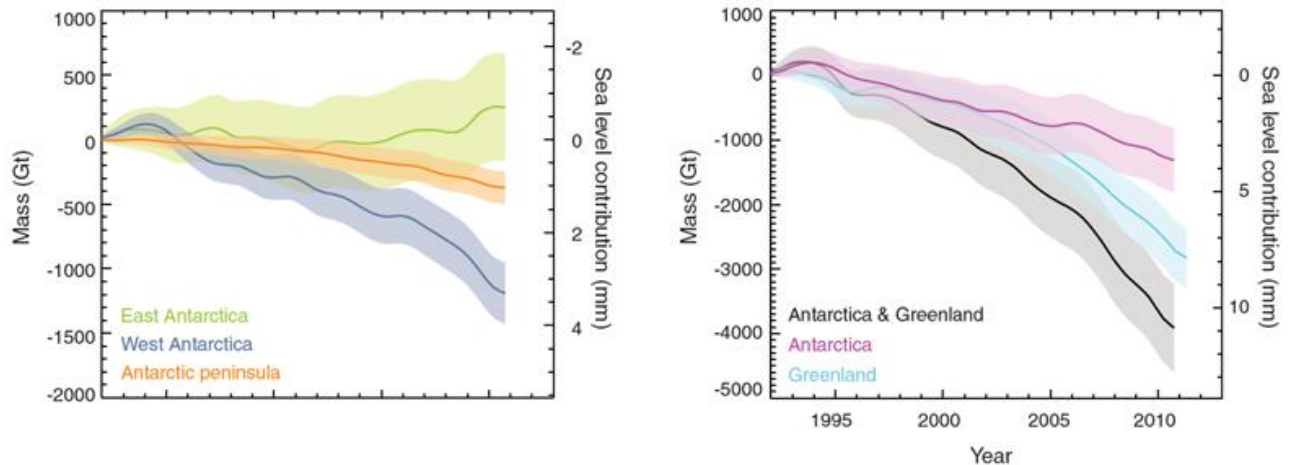


Figure 6.25. Time series of cumulative mass change and sea level contributions from the East, West and Antarctic Peninsula ice sheets (left), and the Antarctic, Greenland, and combined Antarctic and Greenland ice sheets (right). (Credits IMBIE)

Further information:

- Remy, F., The new vision of the cryosphere thanks to 15 years of altimetry, 15 years of progress in radar altimetry Symposium, Venice, Italy, 2006
- Zwally, H.J. and A.C. Brenner, Ice sheet dynamics and mass balance, Satellite altimetry and Earth sciences, L.L. Fu and A. Cazenave Ed., Academic Press, 2001
- McMillan, Malcolm, et al. "Increased ice losses from Antarctica detected by CryoSat-2." *Geophysical Research Letters* 41.11 (2014): 3899-3905.
- Shepherd et al., 2012 A reconciled estimate of ice sheet mass balance.

6.3.1.2 Mountain Glaciers

Satellite altimetry has been used extensively in the past few decades to observe changes affecting large and remote regions covered by land ice such as the Greenland and Antarctic ice sheets. Glaciers and ice caps have been studied less extensively due to the limitation of altimetry over complex topography. However, their role in current sea-level budgets is significant and is expected to impact over the next century and beyond (Gardner et al., 2011), particularly in the Arctic where mean annual surface temperatures have recently been increasing twice as fast as the global average.

Radar altimetry is well suited to monitor elevation changes over land ice due to its all-weather year-round capability of observing ice surfaces. Since 2010, the Synthetic Interferometric Radar Altimeter (SIRAL) on board the European Space Agency (ESA) radar altimetry CryoSat-2 (CS-2) mission has been collecting ice elevation measurements over glaciers and ice caps. Its Synthetic Aperture Radar Interferometric (SARIn) processing mode reduces the size of the footprint along-track and locates the across-track origin of a surface reflector in the presence of a slope. This offers new perspectives for the measurement of regions marked by complex topography.

More recently, data from the CS-SARIn mode have been used to infer elevation beyond the point of closest approach (POCA) with a novel approach known as “swath processing” (Hawley et al., 2009; Gray et al., 2013; Foresta et al., 2016). Together with a denser ground track interspacing of the CS

mission, the swath processing technique provides unprecedented spatial coverage and resolution for space borne altimetry, enabling the study of key processes that underlie current changes of ice caps and glaciers.

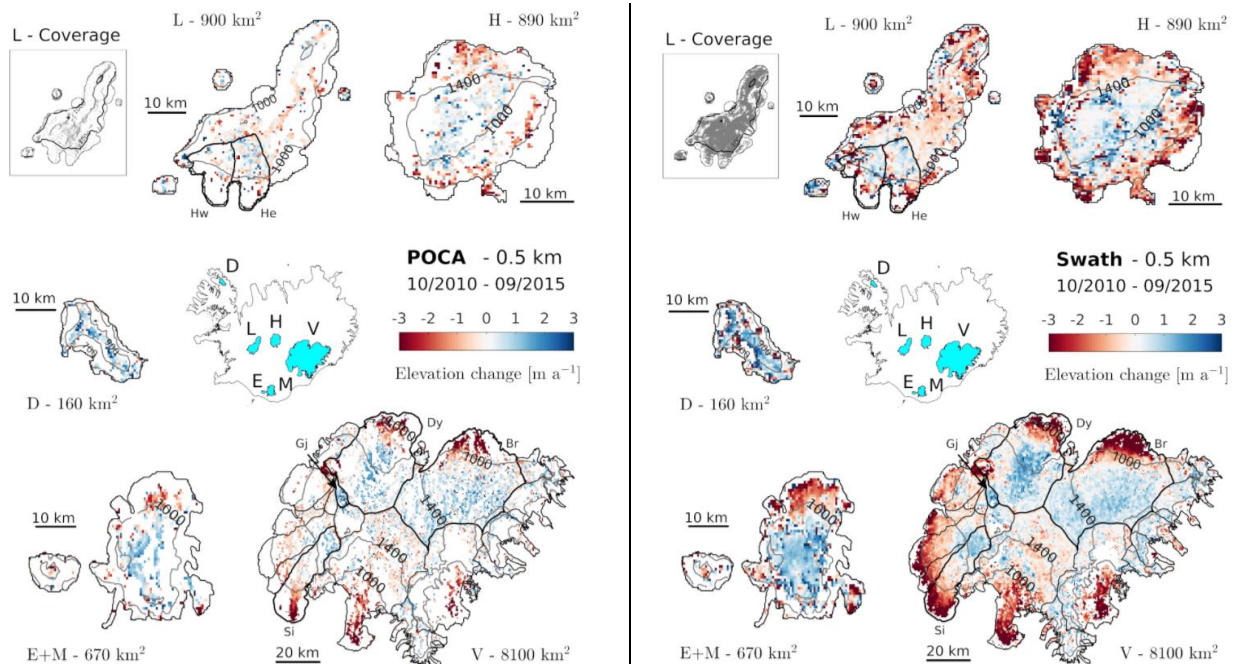


Figure 6.26. Comparison between swath-processed (Swath) and conventional (POCA) surface elevation change rates over the six largest ice caps in Iceland, representing 90% of the glaciated area. V (Vatnajökull), L (Langjökull), H (Hofsjökull), M (Mýrdalsjökull), D (Drangajökull), and E (Eyjafjallajökull). The inset shows the location of individual elevation measurements by using Swath and POCA approaches over Langjökull. [Credit: Luca Foresta et al. (2016).]

Further information:

- Tepes, Paul, et al. "CryoSat swath altimetry to measure ice cap and glacier surface elevation change." AGU Fall Meeting Abstracts. 2016.
- Gardner, A.S., Moholdt, G., Cogley, J.G., Wouters, B., Arendt, A.A., Wahr, J., Berthier, E., Hock, R., Pfeffer, T.W., Kaser, G. and Ligtenberg, S.R., 2013. A reconciled estimate of glacier contributions to sea level rise: 2003 to 2009. *Science*, 340(6134), pp.852-857
- Foresta, L., et al. "Surface elevation change and mass balance of Icelandic ice caps derived from swath mode CryoSat-2 altimetry." *Geophysical Research Letters* 43.23 (2016).

6.3.2 Sea ice

Sea ice is one of the least-known parameters needed for climate modelling. While its extent and age can be measured by other sensors, altimetry is the only one providing sea ice thickness.

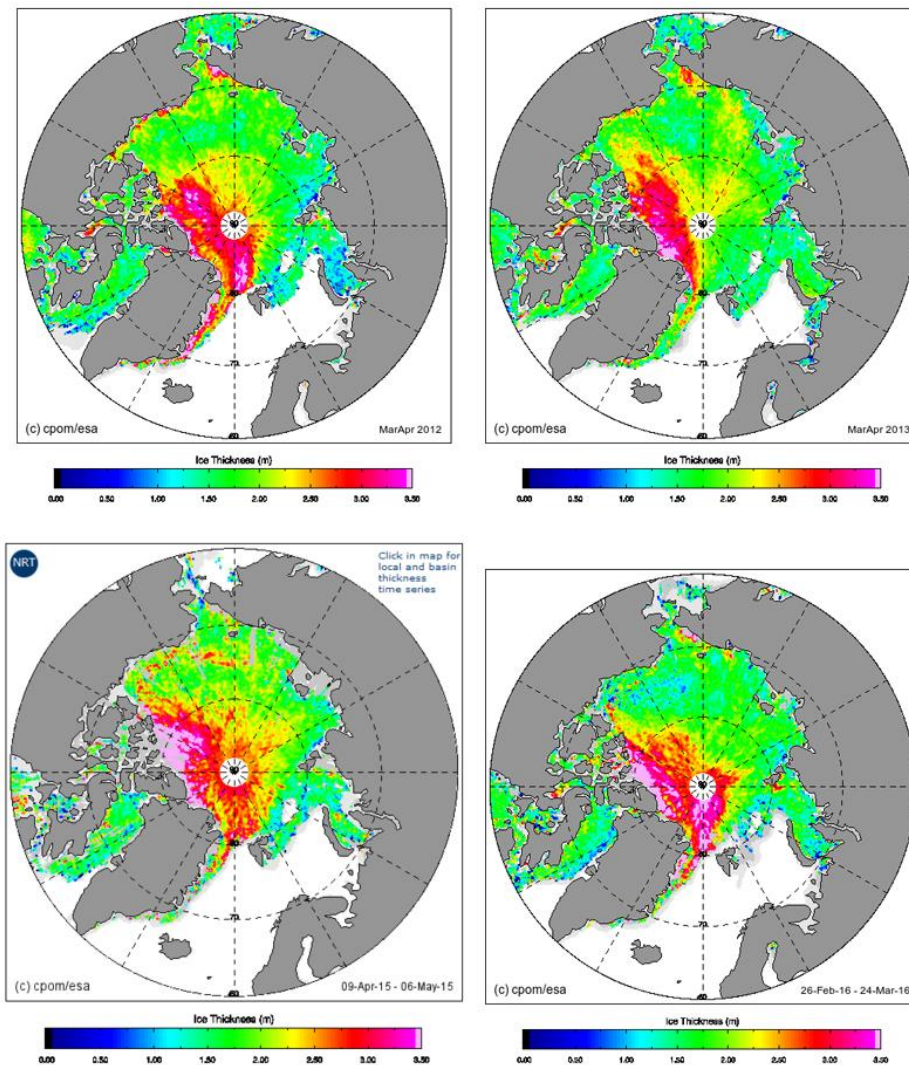


Figure 6.27. Average spring (March-April) Arctic sea ice thicknesses from 2012 to 2016 from satellite altimeter measurements of ice freeboard (height by which the ice extends above the water's surface). Data are not available for the marginal ice zone, or above the ERS latitudinal limit of 81.58°N . Ice freeboard data are converted to thickness using fixed ice, snow and water densities and regional monthly snow depth. The mean thickness excludes thin ice (less than 0.5-1 m) and open water. (Credits University College London/Centre for Polar Observation and Modelling)

Sea ice is seawater that has frozen. It contains little salt as most of it is rejected as it forms. Sea ice covers the Arctic Ocean more or less permanently above the latitude of about 75°N . This permanent ice cap is composed of pack ice, which is kept in continuous motion by the wind, tides and ocean currents. It must be noted that, since sea ice is floating, if it were to melt it would not cause the sea level to rise directly. However, due to its high albedo, ice directly affects the global Earth energy budget by reflecting about 80% of incident sunlight back out to Space. Thus, once formed, ice tends to be maintained. However, if ice cover were to decrease, less solar radiation would be reflected away from the surface of the Earth – causing the ice to absorb more heat and consequently melt faster still. The thickness of Arctic sea ice also plays a central role in the polar climate as it moderates heat exchange by insulating the ocean from the cold polar atmosphere. Moreover, as sea ice forms, the salinity, and therefore the density, of the upper ocean increases. This density increase causes the

surface waters to sink – in essence acting as a pump, driving cold, deep ocean currents from the polar regions towards the equator.

In the Arctic, sea ice typically covers about 14 to 16 million square kilometres at its maximum extent in late winter, and 7 to 9 million km² at its minimum seasonal extent in late summer. In the Antarctic, sea ice at its maximum covers 17 to 20 million square kilometres and only about 3 to 4 million square kilometres at its minimum. Observations show that the mean Arctic ice extent is decreasing at a rate of about 3% per decade while Antarctic ice extent is quite stable. The maximal loss in the Arctic occurs in September, at the end of the summer, and can reach 8%.

Regional sea ice models have been successfully developed over the last decades. However, given the impact that sea ice has on the climate, it is essential to acquire more comprehensive data on sea ice thickness, in order to improve sea ice models for their implementation in general climate studies.

One method of computing sea ice thickness is based on the difference in height between sea and ice surfaces, allowing this parameter to be acquired from altimetry. A careful analysis of individual echoes can distinguish between those backscattered from the open ocean, new ice or multi-year ice. The difference between the elevation of the echoes from snow/sea ice and open water then gives the elevation of the ice above the ocean; the ice thickness can thus be deduced from this.

Further information:

- Laxon, S., N. Peacock, and D. Smith, High interannual variability of sea ice thickness in the Arctic region, *Nature*, 425, 947-950, 2003

6.3.2.1 Iceberg detection

Since the launch of Seasat, the potential of altimeter data to estimate iceberg's freeboard has been explored [McIntyre and Cudlip, 1987] and some examples of freeboard profiles have been published. However, the first generation of altimeters (Seasat, Geosat, Topex/Poseidon) used on-board trackers that frequently lose the surface during rapid transitions of elevation resulting in a several second long loss of data, which greatly hampered the possibility of iceberg freeboard measurement. Since the launch of Jason-1 and Envisat in 2002, the technological progress in altimetry allows to better cope with the rapid elevation changes occurring over a large iceberg or a coast [Gommenginger et al., 2011] opening a new opportunity to measure icebergs freeboards on a quasiroutine basis. To create a database of freeboards, it is necessary first to detect icebergs and then to estimate their characteristics from altimeter data analysis.

Example of waveforms over an Iceberg

On 2 October 2003 Envisat flew over iceberg A43a (Cycle 20 pass 476 descending pass) in the Weddell Sea.

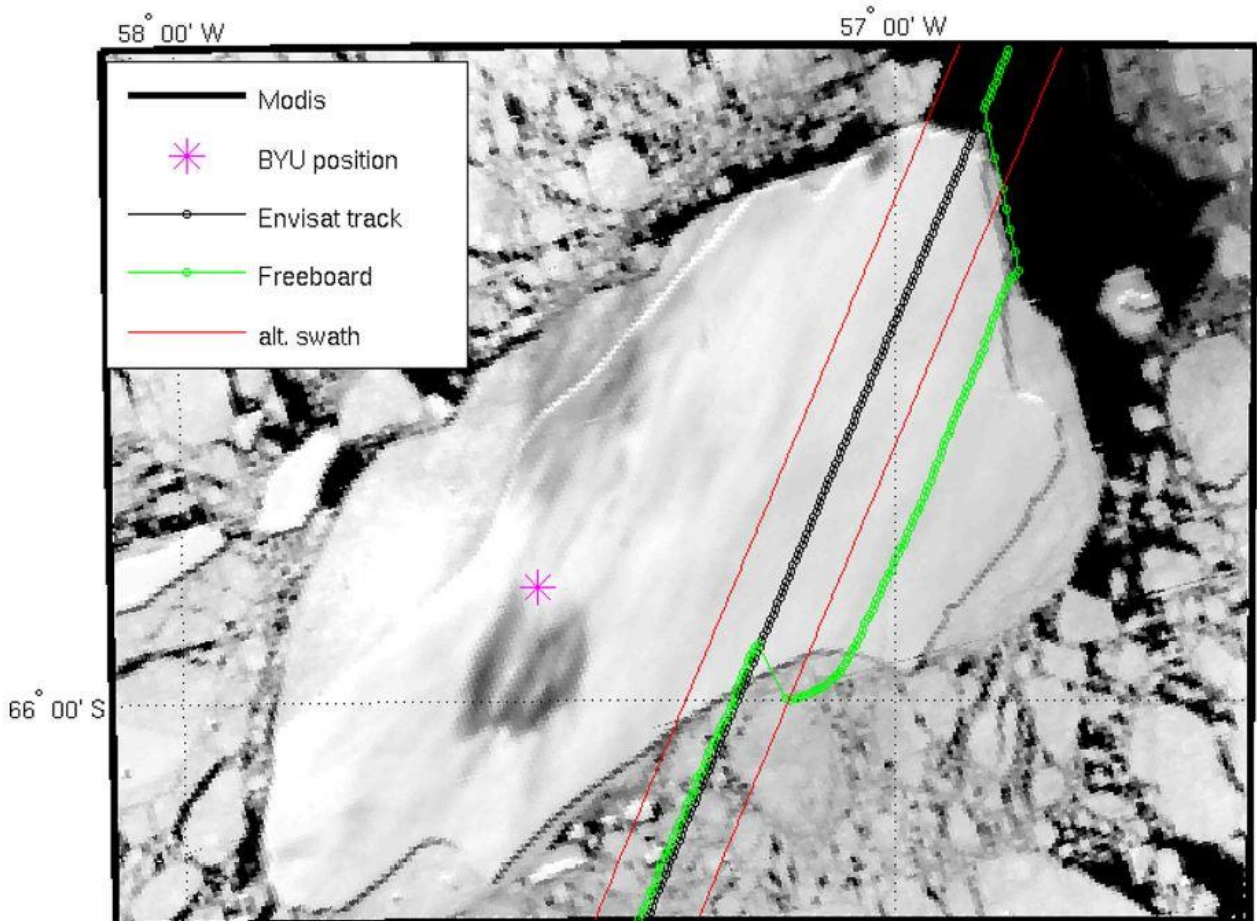


Figure 6.28. MODIS image of iceberg A43A on 2 October 2003 13:20 UT and ENVISAT RA2 ground track (fine black line) and freeboard profile (green line) on 1 October 2003 12:35 UT. The two red lines indicate the width of the altimeter swath and the magenta star the location of the iceberg in the BYU database. (Credits J. Tournade)

The waveforms corresponding to this pass, and the remapped waveforms using the tracker position are presented in the figures. As the altimeter approaches the iceberg from the north near 66° S, the tracker starts to move up mitigating the sea and iceberg surface elevations. As the tracker is not locked on the iceberg surface, the strong echo from the iceberg starts to appear in the first gate of the waveforms then moves toward the nominal track point (0) while the echo from the sea surface moves away from zero. Moving further, the tracker “overshoots” and continues to move up for a few tenth of seconds before locking on the surface. A symmetrical behavior occurs when the altimeter leaves the iceberg. The tracker starts to mitigate the iceberg and sea surface, and then slightly overshoots downward before relocking on the sea surface. In this particular case, it is worth noting that the altimeter ground track is almost perpendicular to the iceberg edge to the north, which gives a sharp elevation transition, while the track intersects the southern edge at a slanted angle resulting in a much longer transition during which the altimeter footprint contains both ocean and iceberg.

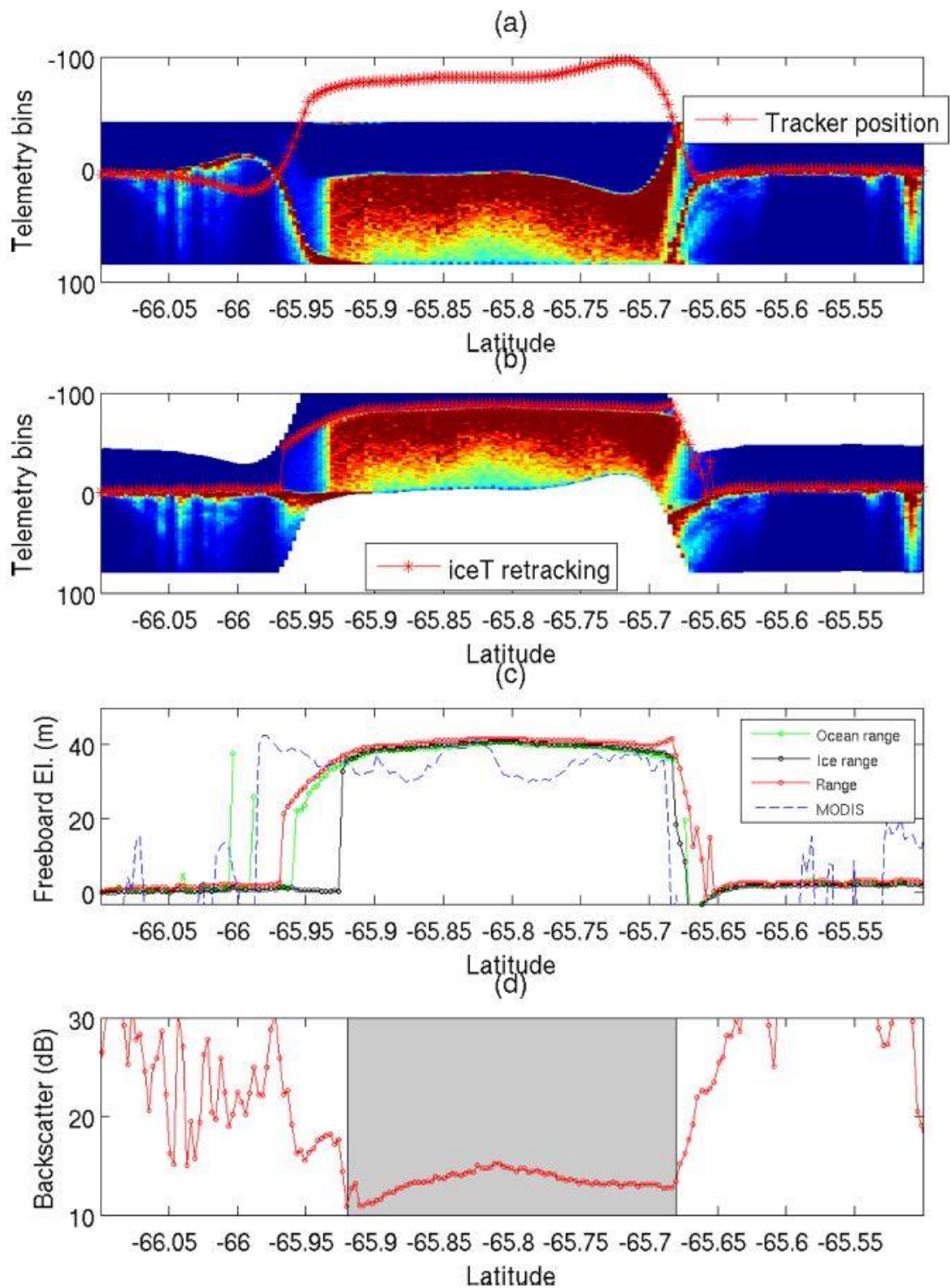


Figure 6.31. Altimeter waveforms for the Envisat pass. The red line indicates the tracker position (a). Retracked waveforms using the tracker position, the red stars represent the iceT freeboard positions (b). Elevations from the MLE3 retracker (green line), the ICE2 retracker (black line), and iceT one (red line), and MODIS brightness (blue line)(c). Measured backscatter (d). The shaded area represents the zone over which only the iceberg surface is seen by the altimeter. (Credits J. Tournade)

Further information:

- Tournadre, J., N. Bouhier, F. Girard-Ardhuin, and F. Remy (2015), Large icebergs characteristics from altimeter waveforms analysis, *J. Geophys. Res.Oceans*, 120, 1954–1974, doi:10.1002/2014JC010502.

6.3.2.2 Sea Ice Freeboard

Sea ice altimetry relies on being able to discriminate between waveforms originating from open water or freshly frozen ice in leads (cracks) in the sea ice and waveforms originating from the sea ice surface. The elevation measured by waveforms originating from leads is taken to be the instantaneous ocean elevation and the sea ice freeboard is estimated by finding the difference between the measured ocean and ice elevations.

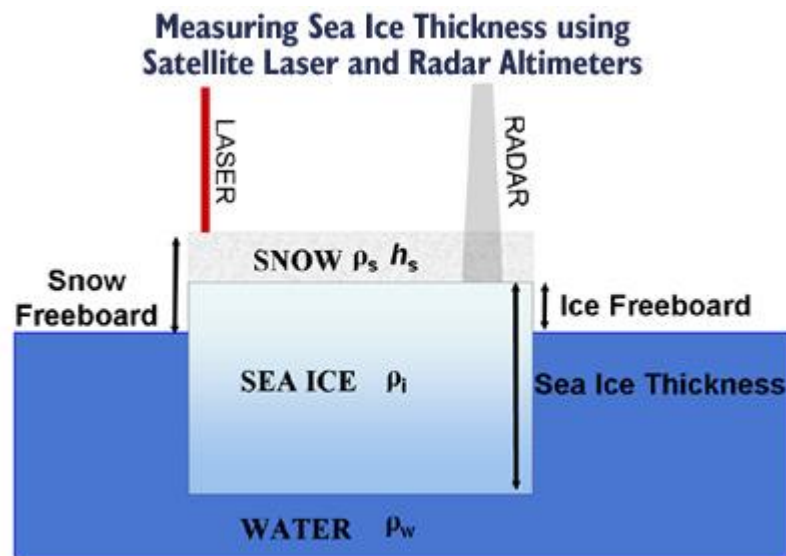


Figure 6.32. Measuring Sea Ice Thickness Using Satellite Laser and Radar Altimeters (Credits NOAA)

Assuming hydrostatic equilibrium (i.e. the ice is floating), the freeboard can then be converted into an ice thickness estimate. By comparing the ocean elevation, as measured by the altimeter, with the mean geoid elevation, the sea ice altimeter processing provides information about the Arctic dynamic topography and also informs models of the Arctic Ocean geoid.

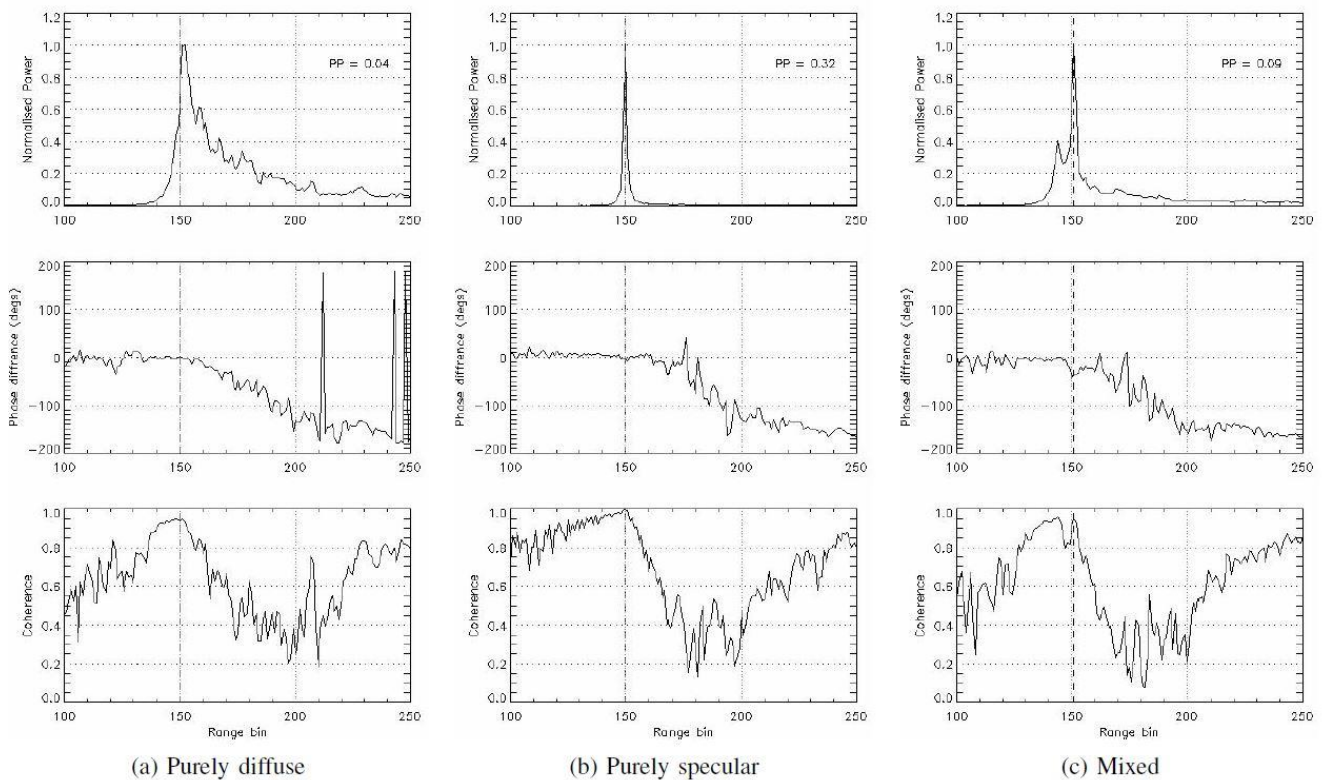


Figure 6.33. CryoSat-2 power waveforms (top row) along with the corresponding phase (middle row) and coherence (bottom row) exhibiting a) purely diffuse behaviour (ice), b) purely specular behaviour (lead) and c) mixed behaviour. The vertical dashed line is the retracking point for the waveform and the pulse peakiness (PP) of each waveform is printed in the top right (Credits T. Armitage)

References:

- Armitage, T.W.K.; Davidson, M.W.J., "Using the Interferometric Capabilities of the ESA CryoSat-2 Mission to Improve the Accuracy of Sea Ice Freeboard Retrievals," IEEE Transactions on Geoscience and Remote Sensing, vol.52, no.1, pp.529,536, Jan. 2014, doi: 10.1109/TGRS.2013.2242082.
- S. L. Farrell, S. W. Laxon, D. C. McAdoo, D. Yi, and H. J. Zwally, "Five years of arctic sea ice freeboard measurements from the ice, cloud and land elevation satellite," J. Geophys. Res., vol. 114, 2009.

6.4 Climate

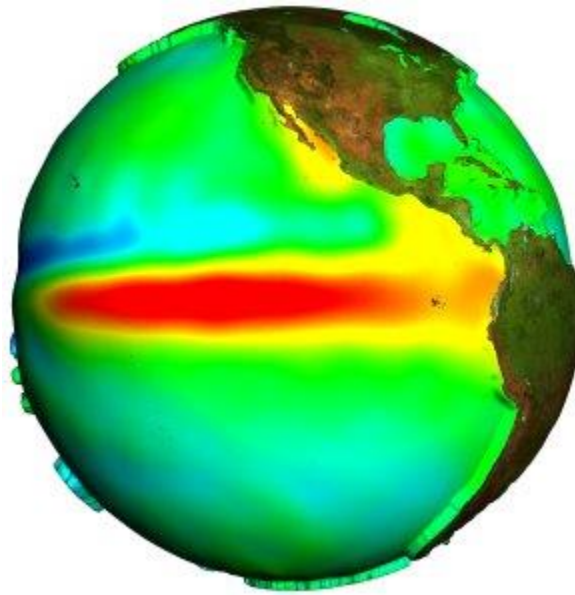


Figure 6.34. El niño event in the Pacific Ocean

The ocean is permanently in motion and exchanges large quantities of heat with the atmosphere, thus playing a major role in climate. It is responsible for around half of poleward heat transport. From the seasonal to the decadal, or even the centennial timeframe, the ocean's influence upon the atmosphere is one of the keys to climate forecasting, including events such as El Niño.

Altimetry is one of the most important tools for monitoring ocean dynamics, and as such is a source of vital data for including in forecasting models of ocean-atmosphere coupled events such as El Niño, monsoons, the North Atlantic Oscillation or decadal oscillations. Seasonal climate forecasting is also beginning to show interesting results. The oceans are in turn affected by climate variations, as the sea level rises and falls in response to their fluctuations.

6.4.1 El Niño - Southern Oscillation (ENSO)

Greater knowledge of ocean circulation is enabling us to better understand and predict the climate, especially natural catastrophes such as El Niño. This phenomenon, caused by the arrival of anomalous warm water on the coast of Peru, brings severe weather patterns such as drought, flooding and cyclones. It is now possible to predict El Niño from ocean data.

For centuries, Peruvian fishermen have feared the sea warming known as El Niño, which every few years around Christmas, drastically reduces their fishing catches. These El Niño events are part of a broader disruption to normal weather patterns which causes drought, flooding and hurricanes around the world. The 1997-98 event gave scientists a chance to analyse the complex relationship between the ocean and the atmosphere. The key to maximising the opportunity was the satellite altimetry missions. Altimetry data are vital for the early detection, analysis and close monitoring of large-scale tropical climate anomalies, in order to predict when and how events will develop and, ultimately, to anticipate and mitigate their impacts.

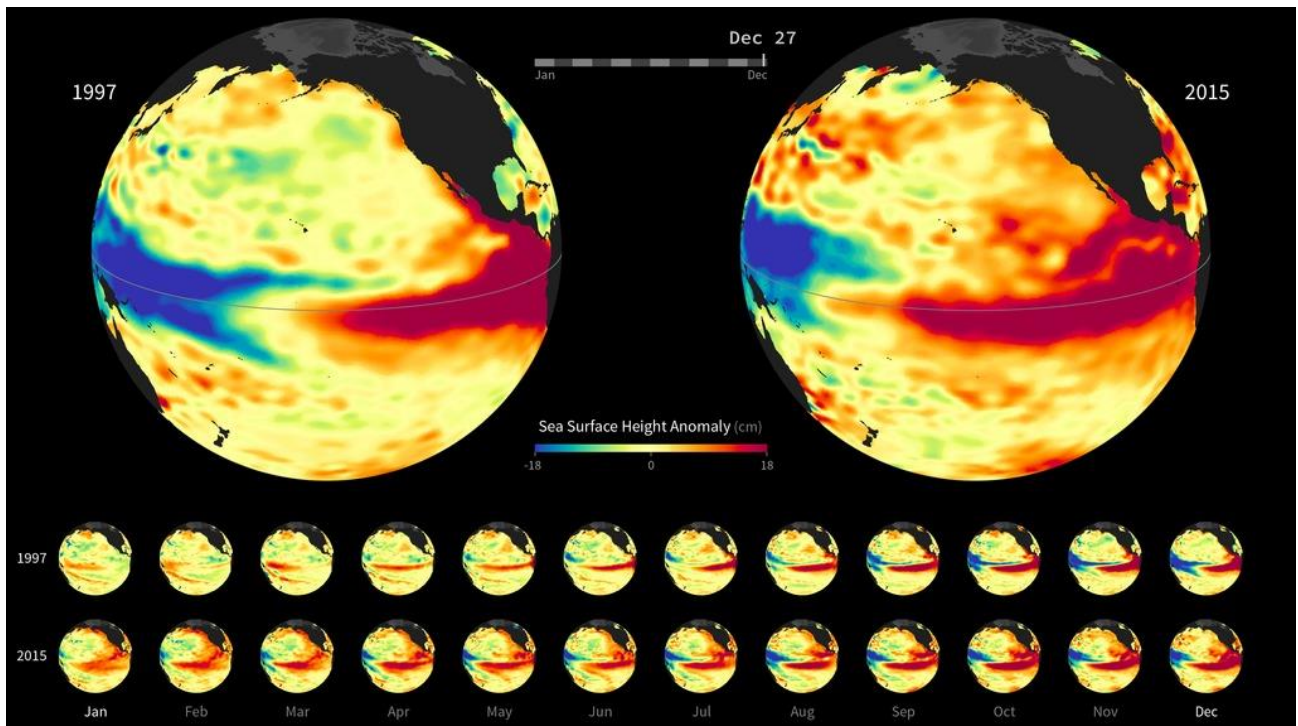


Figure 6.35. Development of 1997 and 2015 El Niño (Credit NASA/JPL).

From February to April 1997, altimeter satellite data pinpointed a large eastward-moving swelling of waters in the central Pacific. This positive sea-level anomaly, over 10 cm high and increasing as the months went by, peaked near the coast. In August 1998, its signature was plain and south-east Asia was hit by severe drought. Topex/Poseidon tracked the development of El Niño, revealing a maximum anomaly of more than 20 cm in the northern winter. By June 1998, surface height was returning to normal. In July 1998, altimeters revealed favourable conditions for La Niña, which developed in 1999.

Ocean circulation in the tropics is closely related to changes in the trade winds. There is a strong seasonal cycle in the significant ocean circulation parameters: temperature, density and dynamic topography. In the equatorial Pacific, the trade winds usually blow westward, pushing surface waters and creating a build-up of warm waters at the western end of the basin. At the end of the year, when the trade winds decrease, the trend reverses and warm waters start to move eastward. Some years, the trade winds are so weak that this eastward current becomes very strong and crosses the Pacific basin in a few weeks. Heat transfers between ocean and atmosphere are considerable and lead to devastating precipitations and storms when reaching South America. This is “El Niño” which has global repercussions on the climate.

Because the tropical ocean can be regarded as consisting of two different layers, sea level is a good indicator of the upper layer’s heat content. Hence the suitability of using altimetry measurements for studying the exchange of warm water in the tropical Pacific Ocean.

References:

- Cheney, R., L. Miller, R. Agreen, N. Doyle, and J. Lillibridge, TOPEX/POSEIDON: the 2-cm solution, *J. Geophys. Res.*, 99, 24 555-24 563, 1994

- Ji, M., R. W. Reynolds, and D. W. Behringer, Use of TOPEX/Poseidon sea level data for ocean analyses and ENSO prediction: some early results, *J. Climate*, 13, 216-231, 2000.
- Picaut, J., E. Hackert, A. J. Busalacchi, R. Murtugudde, and G. S. E. Lagerloef, Mechanisms of the 1997-1998 El Niño-La Niña, as inferred from space-based observations, *J. Geophys. Res.*, 107, 10.1029/2001JC000850, 2002. Picaut, J., M. Ioualalen, C. Menkes, T. Delcroix, and M. J. McPhaden, Mechanism of the zonal displacements of the Pacific warm pool: implications for ENSO, *Science*, 274, 1486-1489, 1996.
- Wang, C., and J. Picaut, Understanding ENSO physics, A review, In: *Earth's Climate: The Ocean-Atmosphere Interaction*. C. Wang, S.-P. Xie, and J. A. Carton, Eds., AGU Geophysical Monograph Series, 147, 21-48, 2004.

Further information:

- Picaut, J., and A.J. Busalacchi, Tropical ocean variability, *Satellite altimetry and Earth sciences*, L.L. Fu and A. Cazenave Ed., Academic Press, 2001

6.4.2 North Atlantic Oscillation (NAO)

One of the Atlantic's most remarkable recurring atmospheric phenomena makes its presence felt in winter. Called the North Atlantic Oscillation (NAO), it is driven by pressure differences between a high-pressure system over the Azores and a low-pressure system over Iceland, which interacts with the ocean.

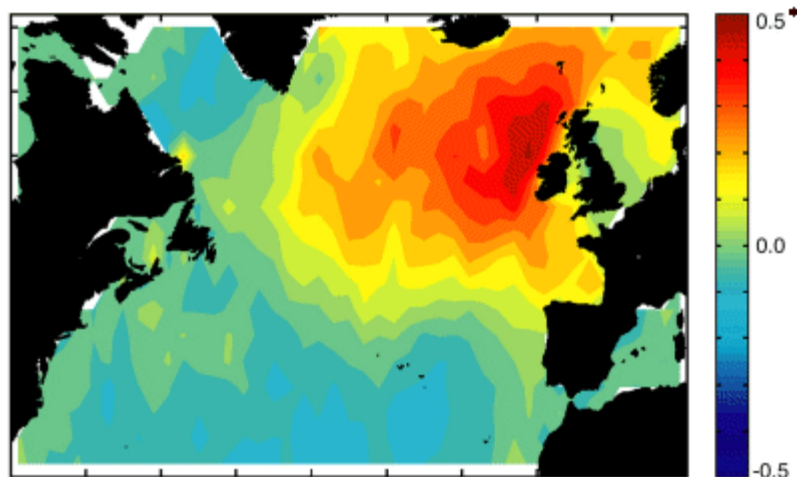


Figure 6.36. Wave heights in winter (in metres per NAO index unit) are very sensitive to pressure variations over the North Atlantic. To the west of Ireland, for example, waves are significantly higher when the NAO index is positive. (Credits SOC)

The weather over the Atlantic exhibits trends that recur over the years in close step with the ocean. From North America to Siberia, regions bordering the Atlantic are exposed in turn to rain or drought, cold or mild temperatures, and strong winds or dead calm. In winter, two air masses influence atmospheric circulation over the North Atlantic: a depression to the north around Iceland, and an anticyclone to the south around the Azores. Their intensity shapes weather conditions on the shores of the ocean. Pressure variations in these air masses, and the associated ocean variations that interact with them, are the driving forces behind the North Atlantic Oscillation (NAO). There are two extremes or 'phases' of the NAO: a positive phase, when the 'Azores high' is especially high and the

‘Icelandic low’ is lower than normal, and a negative phase, when both are weaker. We have been observing these particular weather variations since the 17th century. But it was only when satellites arrived on the scene that we could begin continuous, long-term monitoring of the oceans and atmosphere to unlock the secrets of the mechanisms that control our weather. Improving our understanding of these variations over periods of ten or more years is essential to reliable climate forecasting. In this respect, the permanent ocean-observing capability afforded by altimetry satellites, in combination with other satellites and in-situ measurements, is a vital aid.

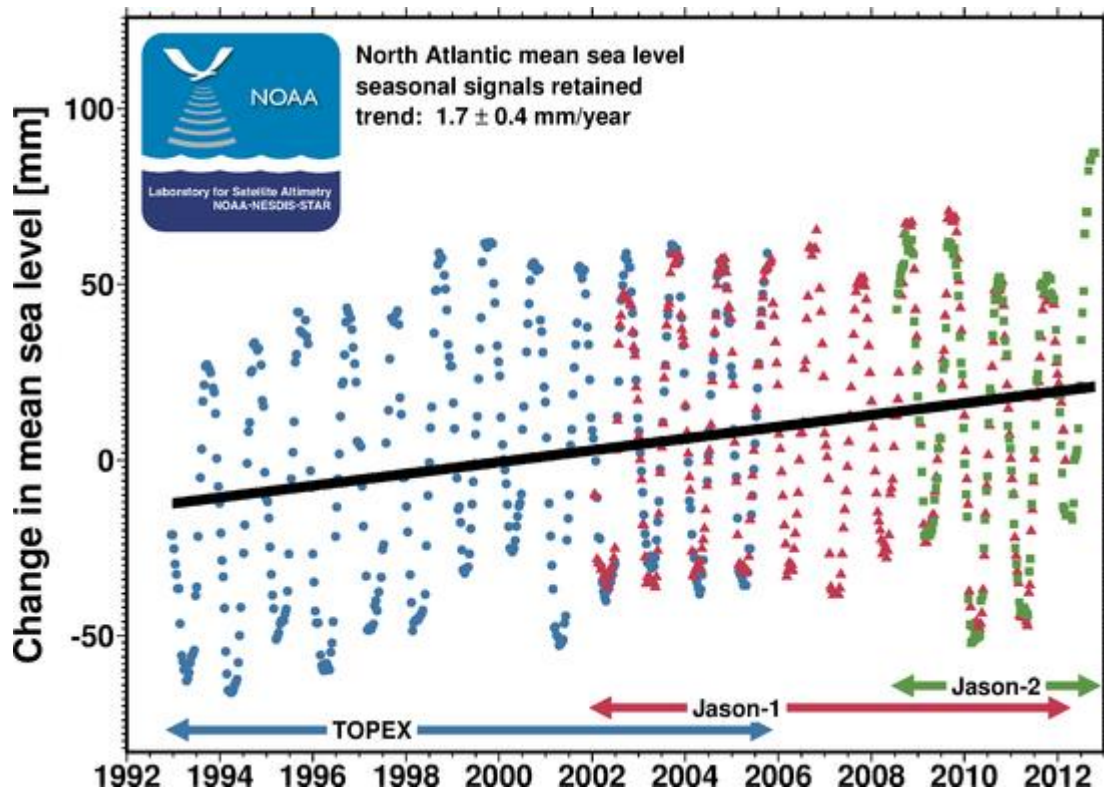


Figure 6.37. Sea level of the north Atlantic jumped from 2011 to 2012 at an apparently unprecedented rate. (Credits NOAA)

Fluctuations in the North Atlantic Oscillation and the temperature variations that go with it lead to changes in sea level. The ocean reacts to shifts in the prevailing winds, which drive the currents, waves, sea surface temperature, etc. Temperature swings also cause sea surface height to vary. We can observe these variations using altimetry satellites. All these measurements can thus serve as indicators of NAO phases and can be used in climate prediction models.

Further information:

- Chafik, L.; Nilsen, J.E.Ø.; Dangendorf, S. Impact of North Atlantic Teleconnection Patterns on Northern European Sea Level. *J. Mar. Sci. Eng.* 2017, 5, 4

6.4.3 Decadal oscillations

The El Niño-Southern Oscillation and the North Atlantic Oscillation are by no means unique. Similar phenomena of greater or lesser intensity, varying over periods of several years, can be observed across the oceans of the globe.

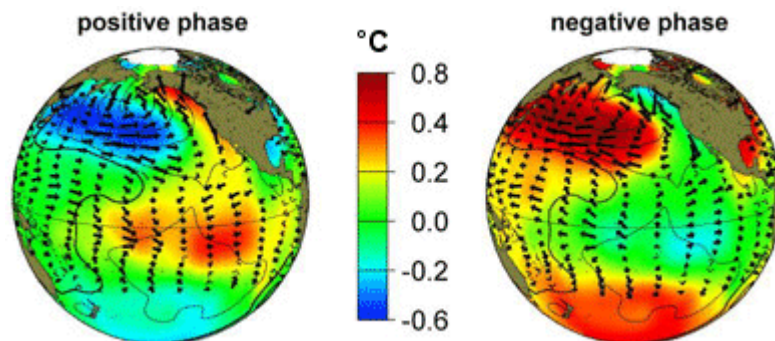


Figure 6.38. Pacific Decadal Oscillation (Credits University of Washington)

Extended time series of satellite data now allow us to study ocean variations over several years. Today, the Pacific Decadal Oscillation (PDO), North Atlantic Oscillation (NAO) and El Niño Southern Oscillation (ENSO) are well documented. The next step will be to predict these phenomena. To achieve this goal, we need to gain a better understanding of how they might be interacting and how they are affected by other ocean and atmospheric variations. Continued monitoring by a permanent series of ocean-observing satellites should yield vital clues.

6.4.4 Seasons

Ocean seasons

One of the most surprising discoveries made by altimeters is the amplitude of seasonal signals. The mean variation in sea level is in fact more than 10 centimetres between cold and warm ocean seasons, and even more in enclosed or semi-enclosed seas. This seasonal cycle is roughly two months out of step with the calendar seasons, due to the inertia of the oceans in propagating heat or cold to deeper waters.

Seasonal forecasting

One of the major questions today in the ocean/atmosphere and climate fields concerns the production of reliable seasonal climate predictions. Even if it will probably be impossible to predict the weather on a given day more than (at the utmost) two weeks in advance, the ocean's influence on the atmosphere should enable the trends of the approaching seasons to be forecasted. This is already providing interesting results in tropical areas. Temperate areas are more difficult, but several projects are underway, which are aiming to predict what the weather will be like next summer – drier or wetter, hotter or colder than the average.

6.4.5 Sea Level CCI

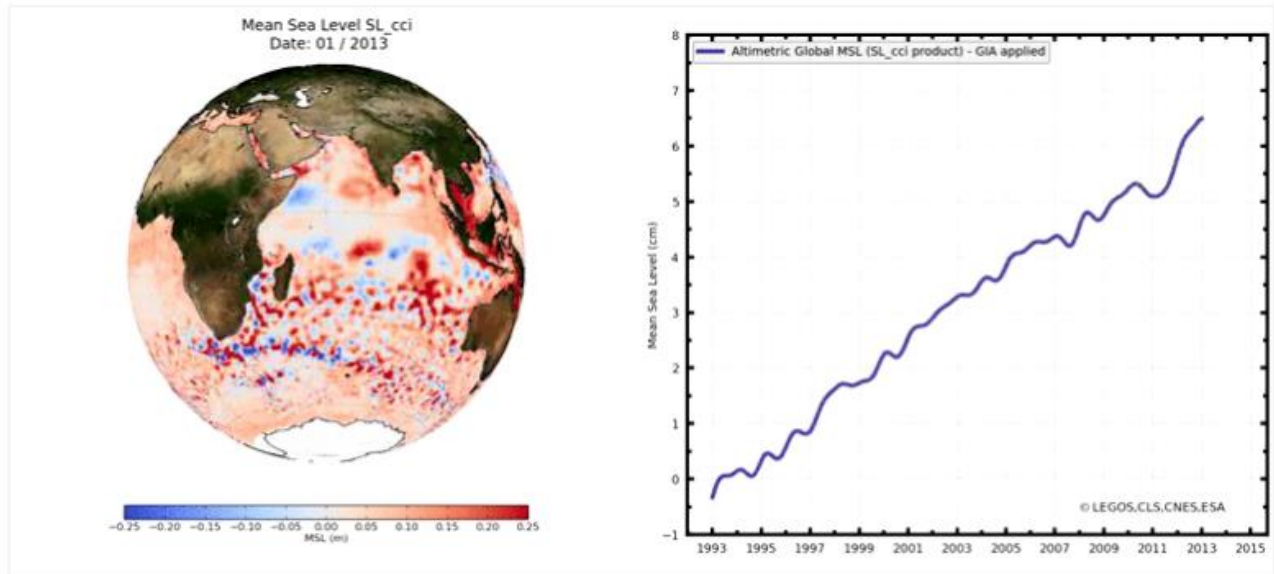


Figure 6.39. Sea level CCI Essential Climate Variable v1.1 1993-2014 Credits LEGOS, CLS, CNES, ESA

Sea level is a very sensitive index of climate change and variability. As the ocean warms in response to global warming, sea waters expand and, as a result, sea level rises. When mountain glaciers melt in response to increasing air temperature, sea level rises because more freshwater glacial runoff discharges into the oceans. Similarly, ice mass loss from the ice sheets causes sea-level rise. The increase of freshwater flowing into the oceans reduces its salinity, decreasing its density and affecting ocean circulation patterns that in turn affect sea level and its spatial variability.

- Why is altimetry important?

With the satellite altimetry missions, the global mean sea level (GMSL) has been calculated on a continual basis since January 1993. ‘Verification’ phases, during which the satellites follow each other in close succession (Topex/Poseidon–Jason-1, then Jason-1–Jason-2), help to link up these different missions by precisely determining any bias between them. Envisat, ERS-1 and ERS-2 are also used, after being adjusted on these reference missions, in order to compute Mean Sea Level at high latitudes (higher than 66°N and S), and also to improve spatial resolution by combining all these missions together. In addition, permanent monitoring of quality during the missions and studies of the necessary corrections of altimetry data regularly add to our understanding and knowledge.

The main objective of the sea level CCI project from ESA is to produce and validate a Sea Level (ECV) product.

To achieve this global objective, the specific objectives for the Sea Level ECV are:

More information

- ESA Sea level CCI project: [web](#)

6.5 Atmosphere, wind & waves

Studying atmospheric effects, marine meteorology and the impact of ocean features and conditions on the weather are all possible using altimetry data.

Altimetry data are used to compute wave height and wind velocity. Today, altimetry makes it possible to access such information in near-real time (within 3 to 48 hours) and to improve weather forecasting models by assimilating these data in them. Moreover, with 25 years of altimetry data, wave height and wind speed statistics, and seasonal and interannual variations can be used to study the whole ocean, or regional areas, for purposes such as offshore industries or navigation.

Using altimetry to study hurricanes is not limited to measuring the very high waves and strong winds, and assimilating them real-time in some forecasting models. It can also help identify the warm features that can cause these storms to intensify. Thus sea surface height anomalies can be used as proxies of the warm currents that provide the hurricanes with their energy source.

Another application of altimetry linked to atmospheric phenomena is the use of dual-frequency altimeters to acquire rain rates over the entire ocean, where there are very few meteorological stations.

6.5.1 Wind & waves as seen by altimetry

Altimeter data are used to compute wave height and wind velocity. The shape and intensity of the reflected radar signal depends on the sea state: a calm sea sends the signal back almost perfectly, like a flat mirror, whereas a rough sea scatters and deforms it (see: Altimetry measurements over the ocean).

Fishermen and other seafarers have an interest in knowing about ocean wave heights and wind velocities. Today, altimetry makes it possible to access such information in near-real time (within 3 to 48 hours) and to improve weather forecasting models. Altimetry cannot supply wave heights for any given location every quarter of an hour – at least not without many, many more satellites, but it is a good technique for identifying trends and computing climatologies, thus giving us information about seasonal and interannual variations, as well as about mean and maximum heights, which are of foremost importance to shipbuilding and offshore structures. Now that we have more than 25 years of continuous altimetry data, wave height and wind speed statistics can be used to achieve such goals with high precision. The link between wave heights in the North Atlantic and the NAO index was discovered in this way [Challenor, 2006]. Altimetry can also help study even very transient phenomena such as rogue waves: if no major significant wave height was observed by altimetry in a particular area, but some ships were nevertheless caught by a very high wave, it was likely to have been a rogue wave [Lefèvre, 2006].

Recent studies show that wave periods can be extracted from altimetry measurements [Caires, 2005, Quilfen, 2005]. This is also of major importance to shipbuilding.

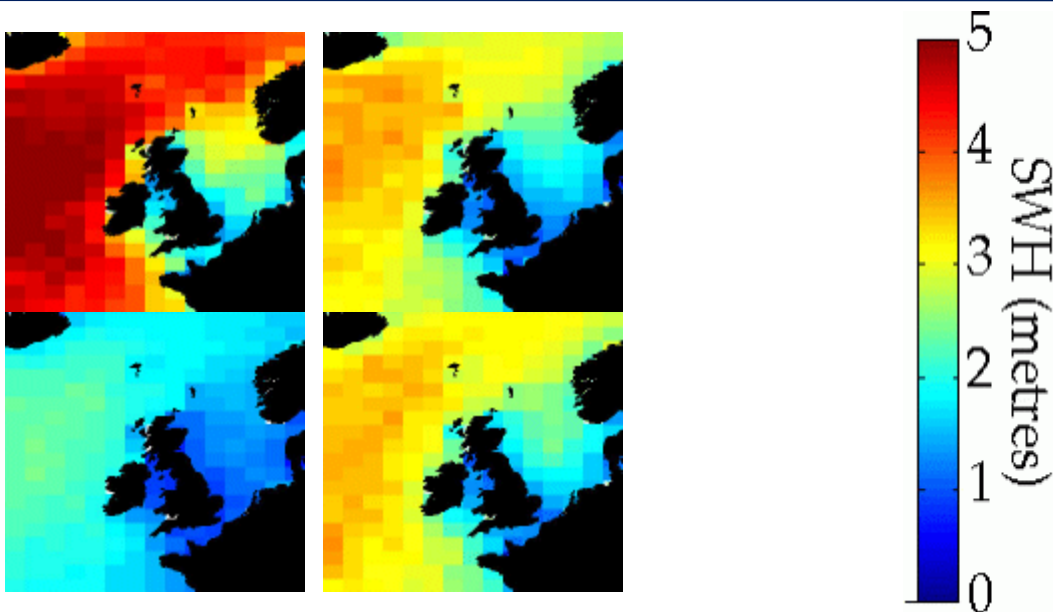


Figure 6.40. Mean wave heights from altimetry off the British Isles in winter (December-February), spring (March-May), summer (June-August) and autumn (September-October) for the years 1993-97. The seasons are very well marked to the west of the Isles, with rough winters (identified by wave heights that can reach 14 metres or even as high as 20 metres), and calm summers. (Credits Southampton Oceanography Centre).

Estimates of air-sea transfer rates of radiatively-active gases are needed for studying regional and global gas cycling and climate change. CO₂ absorption increases with sea surface roughness. Absorption of CO₂ by the ocean thus occurs more rapidly in winter (Northern or Southern) [Frew, 2006]. A rough sea surface also causes reflected radar waves to scatter more, meaning that the return signal received by the altimeter is weaker.

References:

- Caires, S., A. Sterl, and C.P. Gommenginger. Global ocean mean wave period data: Validation and description. *J. Geophys. Res.*, 110(C2), 1-12, 2005.
- Challenor, P., C. Gommenginger, D. Woolf, M. Srokosz, D. Carter, and D. Cotton, Satellite altimetry: A revolution in understanding the wave climate, 15 years of progress in radar altimetry Symposium, Venice, Italy, 2006
- Frew, N., D. Glover, and S. McCue, A Role for Altimeter Radars in Gas Exchange Studies, 15 years of progress in radar altimetry Symposium, Venice, Italy, 2006
- Lefèvre, J.M., L. Aouf, C. Skandrani and P. Queffeulou, Contribution of Satellite Altimetry to Wave Analysis and Forecasting, 15 years of progress in radar altimetry Symposium, Venice, Italy, 2006
- Quilfen, Y., B. Chapron, F. Collard, and M. Serre, Calibration/validation of an altimeter wave period model and application to Topex/Poseidon and Jason-1 altimeters, *Marine Geodesy*, 27, 535-550, 2005.

Further information:

- Lefèvre, J.M. and P.D. Cotton, Ocean surface waves, Satellite altimetry and Earth sciences, L.L. Fu and A. Cazenave Ed., Academic Press, 2001

6.5.2 Cyclones, hurricanes and typhoons

Tropical cyclones (known as hurricanes in the tropical Atlantic, western Pacific and northern Indian oceans; as typhoons in the eastern Pacific Ocean; and as cyclones in the southern Pacific and Indian oceans) are characterised by very high waves and strong winds, that can be measured by altimeters (provided that the satellite flies close enough to the area affected by the cyclone) and assimilated in real-time in some forecasting models. However, altimetry can also help identify the warm features that can cause these storms to intensify. Thus sea surface height anomalies can be used as proxies of the warm currents that provide the hurricanes with their energy source.

Cyclone intensification

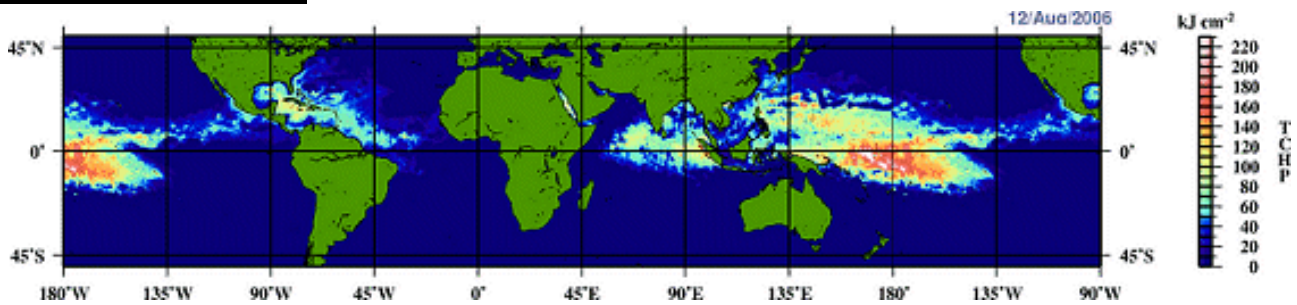


Figure 6.41. Tropical Cyclone Heat Potential field for 12 August 2006. Regions with high (> 50 kJ/cm^2) TCHP values are coloured yellow, green and red. (Credits NOAA/AOML)

Some ocean features, such as warm ocean currents and eddies, have been linked to tropical cyclone intensification [Shay et al]. The intensive heating of the ocean’s upper centimetres which occurs during the summer months usually makes these extensive reservoirs of high thermal energy invisible when observed using sea surface temperature alone. However, they can easily be observed by altimeters as they are also characterised by greater sea surface heights [Goni et al].

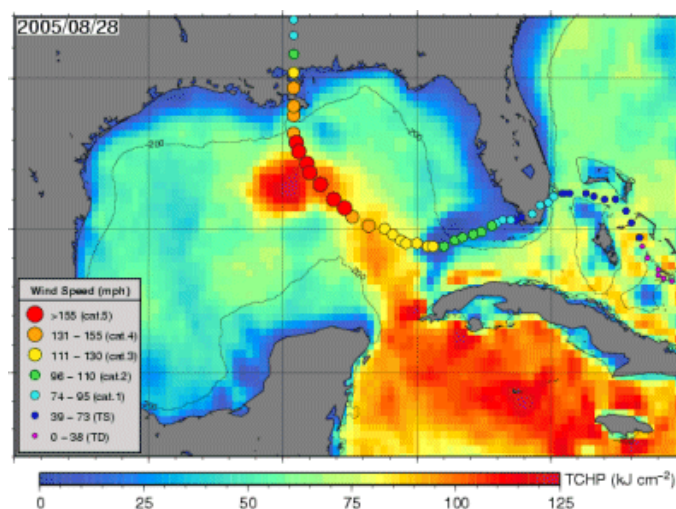


Figure 6.42. Tropical Cyclonic Heat Potential computed from altimetry on 28 August 2005, with Hurricane Katrina’s trajectory and intensity overlaid. Katrina’s intensification seems to coincide with its crossing over the Loop Current. (Credits NOAA/AOML)

Altimetry data in combination with historical hydrographic observations are currently used to estimate synthetic upper ocean temperature profiles. These profiles are then used to compute the

integrated vertical temperature from the sea surface down to the 26°C isotherm, the temperature needed to sustain a tropical cyclone. This quantity is usually referred to as the Hurricane or Tropical Cyclone Heat Potential (TCHP) [Leipper and Volgenau] and represents the amount of heat in the upper ocean available for tropical cyclone intensification.

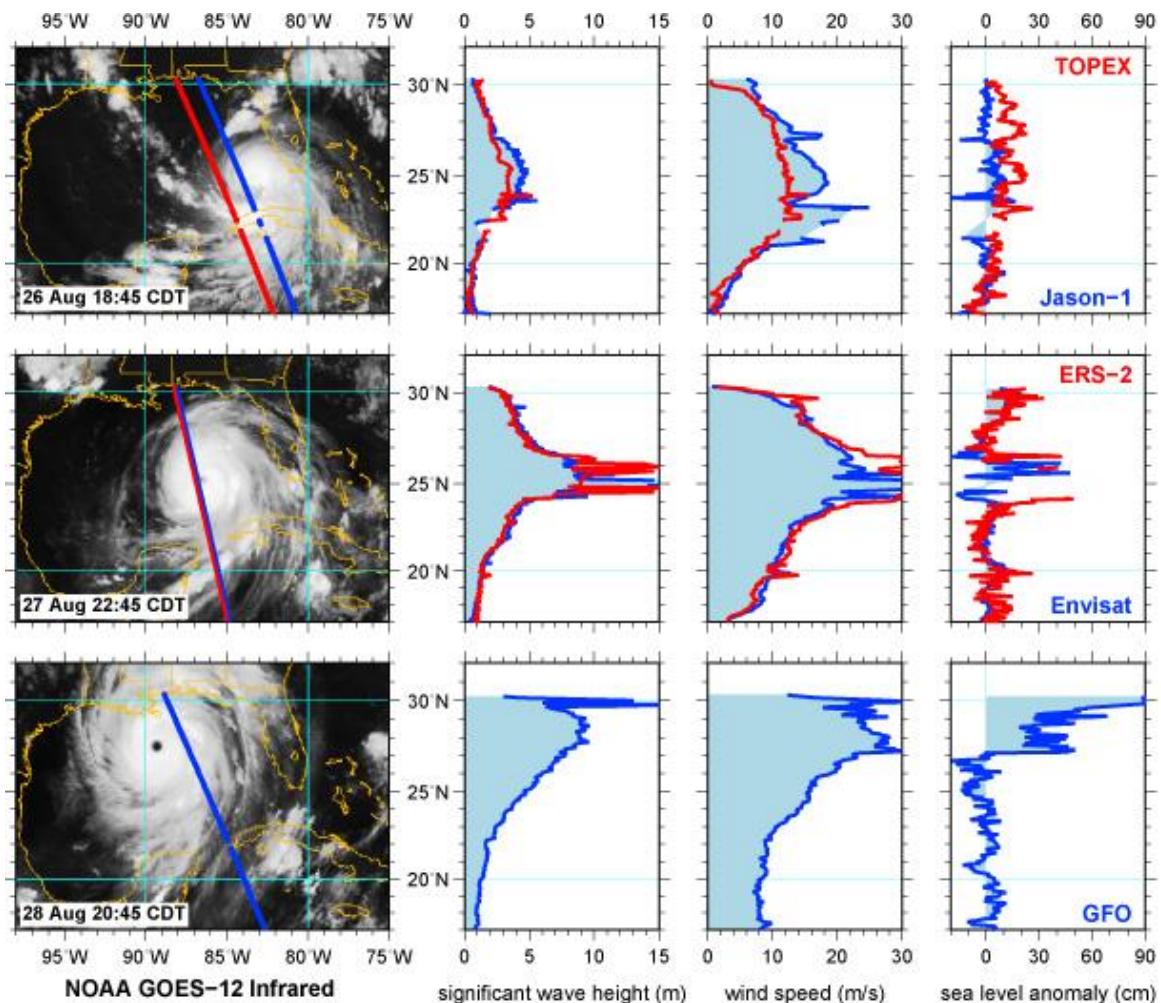


Figure 6.43. NOAA GOES-12 infrared images (left) and wind speed, wave height and sea level anomalies as observed by the different altimetry satellites during Katrina. (Credits NOAA/Altimetrics LLC)

References:

- Goni, G. J., S. L. Garzoli, A. J. Roubicek, D. B. Olson and O. B. Brown. Agulhas ring dynamics from TOPEX/POSEIDON satellite altimeter data, J.Mar. Res., 55, 861-883, 1997.
- Leipper, D. and D. Volgenau. Hurricane heat potential of the Gulf of Mexico, J. Phys. Oceanogr., 2, 218-224, 1972.
- Shay L. K., G. J. Goni and P. G. Black. Effect of a warm ocean ring on hurricane Opal. Mon. Weath. Rev., 128, 1366-1383, 2000.

Further information:

- Goni, G., P. Black, J. Trinanes, Using satellite altimetry to identify regions of hurricane intensification, Aviso Newsletter, 9, 2003

- Scharroo, R., W. H. F. Smith, and J. L. Lillibridge, Satellite altimetry and the intensification of Hurricane Katrina, *Eos Trans. AGU*, 86 (40), 366, 2005.
- <http://www.aoml.noaa.gov/phod/cyclone/data/> (NOAA/AOML)

Assimilation in wave models

Altimetry can also play a part in cyclonic event warnings using significant wave height measurements in near-real time (three hours). Once they have been assimilated in sea state forecast models, wave heights from altimetric satellites significantly improve their predictions. With assimilated data from two satellites, Jason-1 (CNES/NASA) and Envisat (ESA), they become even more accurate.

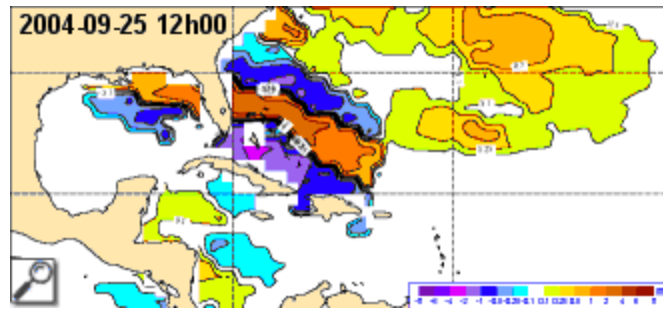


Figure 6.44. Difference between significant wave height from Mètèo France's wave model, with and without assimilation of altimetry data (Jason-1 and ERS-2) on 25 September 2004, with Hurricane Jeanne approaching the Florida coasts. (Credits Mètèo France)

6.5.3 Rain

To be able to use altimetry measurements, we first have to correct them for the effects of atmospheric water – either rain or vapour. One of the side benefits of altimetry satellites is therefore acquiring information about these meteorological parameters, especially rain, for the entire ocean where there are very few meteorological stations. Such studies enable us to gain a better understanding of rain mechanisms and improve altimeter corrections, thus providing increasingly precise data.

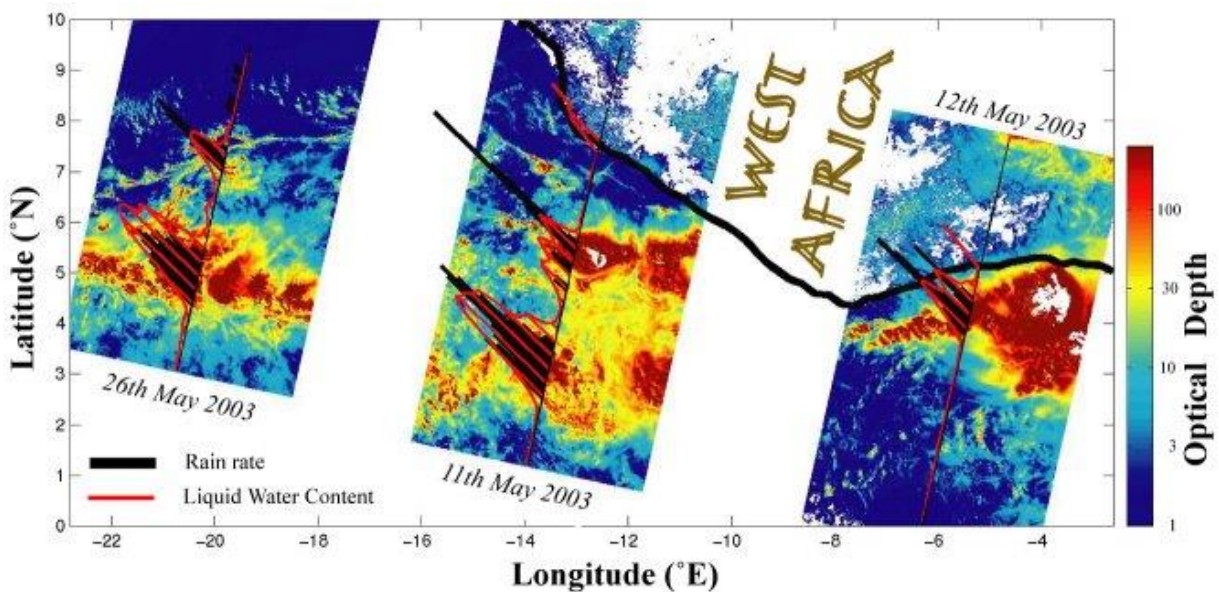


Figure 6.45. Intense storms developing off the coast of West Africa, as seen by several instruments onboard Envisat: background colour map from the AATSR infrared sensor (initially for measuring sea surface temperature), rain rate from the RA-2 altimeter (black along-track curves) and liquid water content from the MWR radiometer (red along-track curves). The optical depth is a measure of cloud thickness. With all three instruments operating simultaneously, it can be noted that rain occurs where the optical depth is greatest, although the spread of active ‘rain cells’ is narrower than the expanse of dense clouds. (Credits National Oceanography Centre, Southampton/Rutherford Appleton Laboratory)

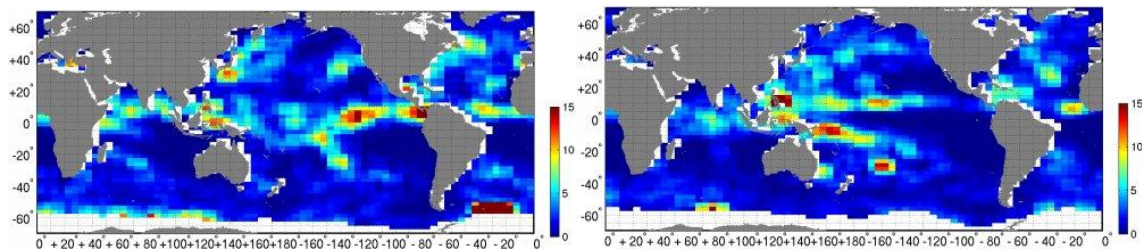


Figure 6.46. Monthly mean rain rate computed from Topex/Poseidon, for November 1997 (top, at the height of the 1997-1998 El Niño) and November 1999 (bottom, during La Niña). During El Niño rains are more abundant over the warm water pushed toward the South American coasts, whereas during La Niña most rains are over Indonesia and the ‘Warm Pool’. (Credits Ifremer/Cersat)

References:

- Cailliau, D. and V. Zlotnicki, Precipitation detection by the TOPEX/Poseidon dual-frequency radar altimeter, TOPEX microwave radiometer, Special Sensor Microwave/ Imager and climatological ship reports, *IEEE Trans. Geosci. Remote Sens.*, 38, 205-213, 2000.
- Chen, G., B. Chapron, J. Tournadre, K. Katsaros, and D. Vandemark, Global oceanic precipitations: a joint view by Topex and the TopexMicrowave Radiometer, *J. Geophys. Res.*, 102, 10, 457-10471, 1997.

- McMillan, A.C., G.D. Quartly, M.A. Srokosz and J. Tournadre, 2002. Validation of TOPEX rain algorithm: Comparison with ground-based radar, *J.Geophys. Res.*, 107 (D4), 3.1-3.10. (DOI10.1029/2001JD000872).
- Quartly, G., M. Srokosz, and T. Guymer, Global precipitation statistics from dual-frequency TOPEX altimetry. *J. Geophys. Res.*, 31,489-31,516, 1999.
- Tournadre, J. and J. Morland, The effect of rain on Topex/Poseidon altimeter data: a new rain flag based on Ku and C band backscatter coefficients, *IEEE Trans. Geosci. Remote Sens.*, 1117-1135, 1997.
- Tournadre, J., Improved Level-3 oceanic rainfall retrieval from dual frequency spaceborne radar altimeter systems, *J. Atmos. Ocean. Tech.*, (submitted).

Further information

- Quartly, G.D., Development in rain altimetry from Seasat to Envisat and Jason, *15 years of progress in radar altimetry Symposium*, Venice, Italy, 2006

6.6 Hydrology and land applications



Figure 6.47. Inland waters over America

The earliest altimetry missions were dedicated to studying the open ocean and some ice measurements. However, as scientists always like to see ‘what happens if...’, they began looking at the levels of lakes, then rivers as measured by altimeters. Some experiments have also been conducted over solid land, to observe and analyse the signal sent back to the altimeter.

Altimetry has the advantage of taking being able to take global, homogeneous, repeated measurements (thus enabling systematic monitoring to be carried out over several years), unhindered by clouds, night or even vegetation. The measured surface heights are referenced to the same frame. However, this technique is mainly optimised for the ocean (but although specific land re-tracking can be applied) and takes measurements only at the nadir (i.e. just under below the satellite), with a rather narrow footprint — and averaging everything in that footprint. Over non-ocean surfaces (wet or dry), the accuracy of the altimetry measurements can be degraded by several centimetres or tens of centimetres, mainly because of the heterogeneity of the reflecting surface (a mix of water and emerged landland surfaces). Another important source of error lies in the signal’s propagation through the atmosphere. The satellites’ repeat-orbits are rather long (10 to 35 days), which do not suit real-time monitoring of river or lake level variations (e.g. flood alerts), but agree do work well with seasonal or interannual monitoring.

References:

- Alsdorf, D., Birkett, C.M., Dunne, T., Melack, J., Hess, L., Water level changes in a large Amazon lake measured with spaceborne radar interferometry and altimetry. *Geophys. Res. Lett.*, 28 (14), 2671-2674, 2001.
- Berry P. A. M., J. D. Garlick, J. A. Freeman, E. L. Mathers, Global inland water monitoring from multi-mission altimetry, *Geophys. Res. Lett.*, 32, L16401, doi:10.1029/2005GL022814, 2005.
- Birkett, C.M. The contribution of TOPEX/POSEIDON to the global monitoring of climatically sensitive lakes. *J. Geophys. Res.* 100 (C12), 25179-25204, 1995.
- Birkett, C.M., Contribution of the TOPEX NASA radar altimeter to the global monitoring of large rivers and wetlands. *Water Resour. Res.*, 34 (5), 1223-1239, 1998.

- Maheu, C., Cazenave, A., Mechoso, C.R., Water level fluctuations in La Plata basin (South America) from TOPEX/Poseidon satellite altimetry. *Geophysical Research Letters*, 30.3, 2003.
- Mercier, F., Cazenave, A., Interannual lake level fluctuations in Africa (1993-1999) from Topex-Poseidon: connections with ocean-atmosphere interactions over the Indian Ocean. *Global and Planetary Change*, 32, 141-163, 2002.
- Stanev, E.V., Peneva, E.L., Mercier, F., Temporal and spatial patterns of sea level in inland basins : Recent events in the Aral Sea. *Geophysical Research Letters* Vol 31 N°15, 2004.

6.6.1 Lake level monitoring

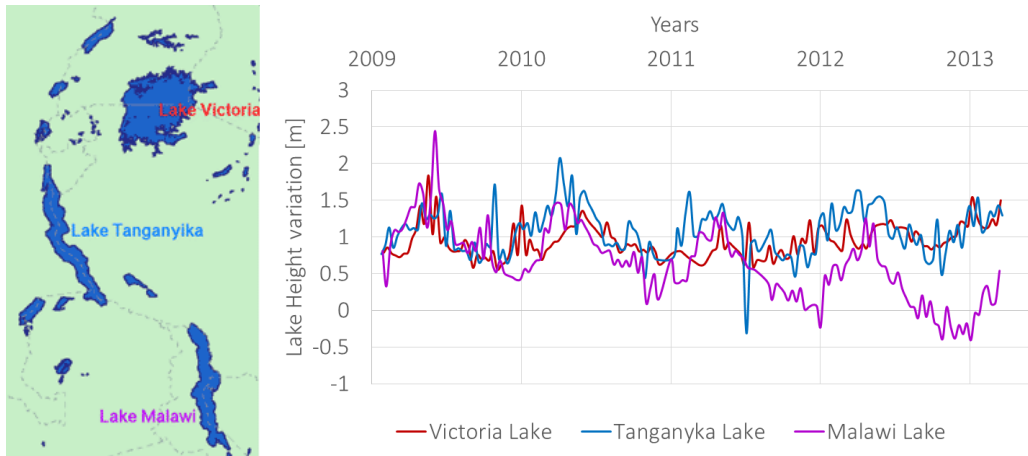


Figure 6.48. Level of the African Great Lakes, as seen by altimeters. (Credits De Montfort University, ESA)

The level of lakes (such as the American and African Great Lakes, etc) varies through the seasons according to inputs (rain rates, snow melting, etc) and outputs (evaporation, withdrawal, etc), and is thus a very sensitive indicator of regional climate variations. Moreover, the level of enclosed seas (Aral Sea, Caspian Sea, etc) is a major indicator of their good (or bad) health. Altimetry enables us to continually monitor these levels, even in areas which are difficult to access.

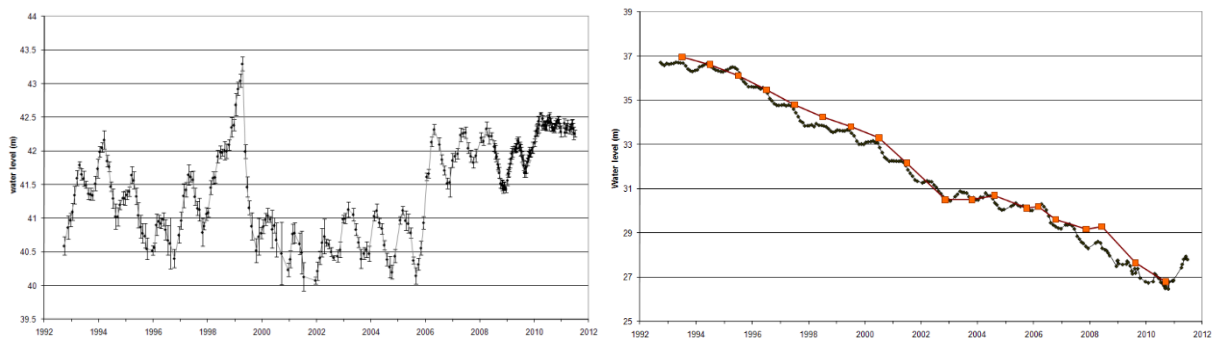


Figure 6.49. Sea level in both basins of the Aral Sea measured by altimeters (multi-satellite data collected between 1993 and 2012 and some in situ measurements) (left: North Aral, right: South Aral). (Credits CNES/Legos)

Studying altimetry over lakes was first undertaken to validate altimeter measurements, lakes having few dynamics compared to the ocean, and many of them being monitored. Today, a great number of lakes of all sizes are monitored by altimetry. However, in situ data (river runoff, temperature, or precipitation) are still critically needed for studying the evolution of each lake's water mass balance. 43 lake systems can be observed by Topex/Poseidon or Jason-1, and 215 by ERS-2 or Envisat, out of a total global population of 842 lake systems of more than 100 km².

6.6.2 Land applications

The radars on altimetry satellites, even those optimised for the ocean, continue to emit pulses while flying over land. Reception of the return echoes is more complex, since a field or a forest does not reflect radar pulses as well as water, but some conclusions can still be drawn. The amount of power received after reflection (or more precisely the backscatter coefficient) in itself yields interesting information, since the backscatter coefficient depends on the state of the observed surface, according to whether it is covered by snow, vegetation, flooded areas, etc.

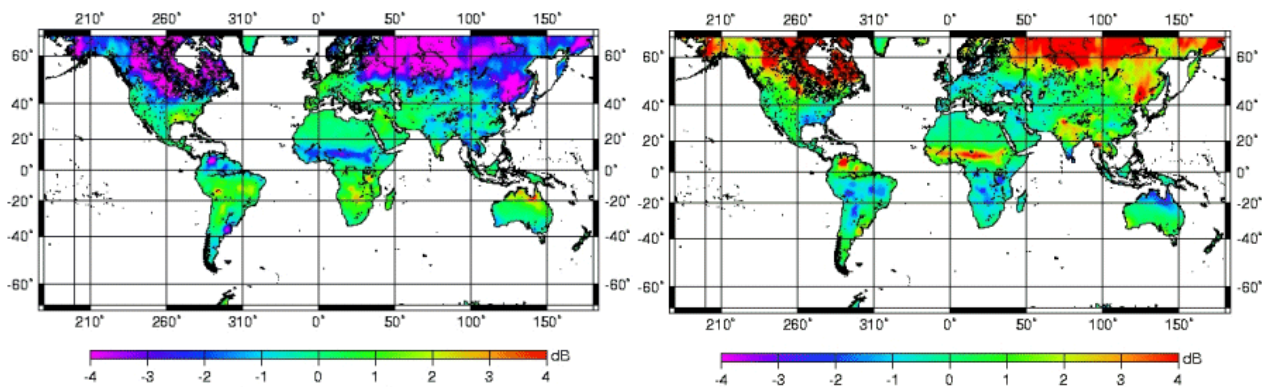


Figure 6.50. Seasonal anomalies of the backscatter coefficient (return rate of the radar wave to the altimeter antenna) for Topex in Ku band, in winter (top) and summer (bottom) for the first ten years of measurements. Significant variations can be seen, especially in regions which are covered by snow in winter (higher than 55°N), or which have a marked rainy season (equatorial regions, India). (Credits Legos/CNRS)

Many of the other unique characteristics of radar altimeters over continents are now beginning to be exploited, such as retracked waveform parameters, dual-frequency measurements or synergies with the radiometer that operates simultaneously on most altimeter platforms. These can contribute to monitoring forests, deserts and boreal regions, and their seasonal variations, e.g. information about snow beginning and end dates, and the thickness of snow or plant cover in relation to the season. This new field of altimetry should grow in importance over the next few years, as a complement to other satellite observation techniques.

6.6.3 River monitoring

For certain major rivers and wetlands, hydrological information can often be difficult to obtain due to a region's inaccessibility, the sparse distribution of gauge stations, or the slow dissemination of data. Satellite radar altimeters can potentially monitor height variations of inland waters [Birkett, 1998]. Hydrological products from satellites are unaffected by political and logistical considerations and can provide accurate height measurements not only for lakes but also for large rivers such as the Amazon, which has been a primary target of study over the last ten years.

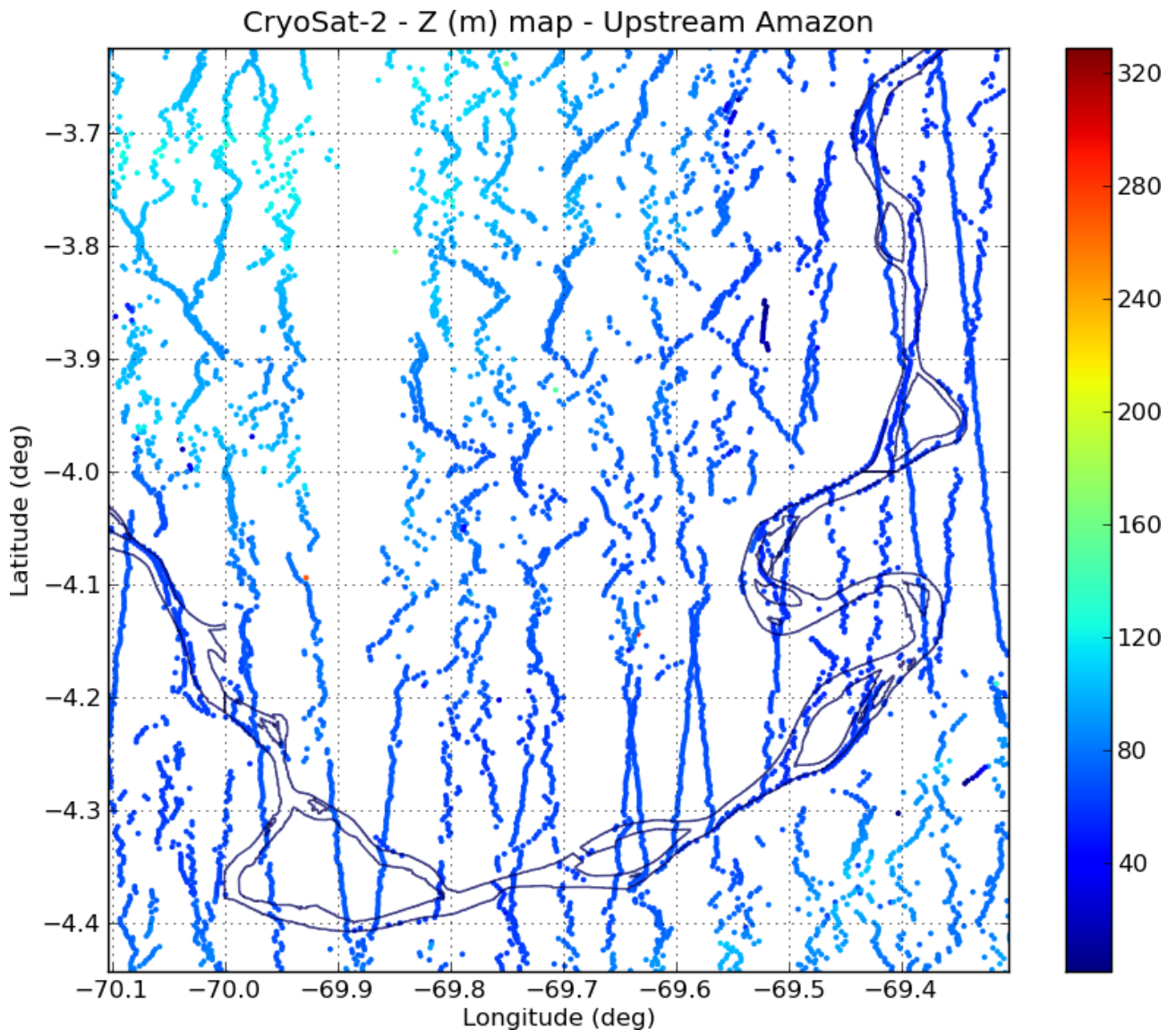


Figure 6.51. Map of surface topography, derived from ESA Cryosat-2 SARin L2 products over the Solimões river (Brazil). A lot of the SARin measurements are focused on the river network sometimes kilometers away from the satellite's ground track (Credits Along-Track)

Monitoring now covers at least 15 major rivers in all the world's continents, and a wealth of others are possible, especially with the high-resolution altimetric range (20 Hz) available, or with altimetric waveform-specific retracking. Recent studies (Berry et al 2012) using individual echoes ('bursts') should give access to even more new targets. The assimilation of altimetry data in hydrodynamic models should also lead to advances in knowledge and ultimately even in forecasting hydrological systems.

- Data use case: Temporal water surface height variations in enclosed areas: the Amazon Basin

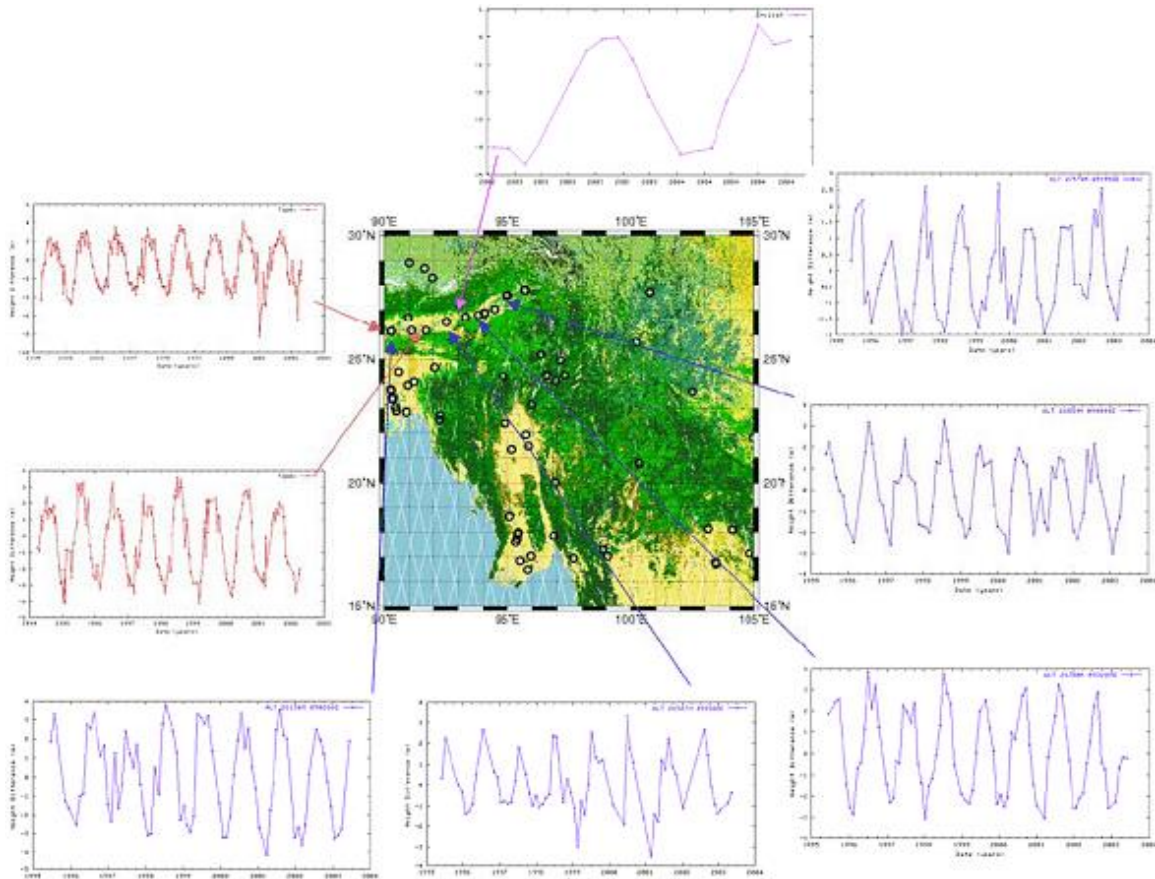


Figure 6.52. Sample multi-mission time series over the Brahmaputra: red Topex, blue ERS-2, pink Envisat. Circles show all possible targets from ERS-2. (Credits De Montfort University)

Reference:

- Birkett, C.M., Contribution of the TOPEX NASA radar altimeter to the global monitoring of large rivers and wetlands. *Water Resour. Res.*, 34 (5), 1223-1239, 1998.
- Berry, P.A., Smith, R.G., Salloway, M.K. and Benveniste, J., 2012. Global analysis of EnviSat burst echoes over inland water. *IEEE Transactions on Geoscience and Remote Sensing*, 50(5), pp.1980-1985.

6.6.4 Inland Water – SAR

CryoSat-2 is the first altimeter offering SAR mode, and is being followed by the Sentinel-3 family. The improved along-track resolution is accompanied by a naturally reduced land contamination thanks to the increased along-track resolution.

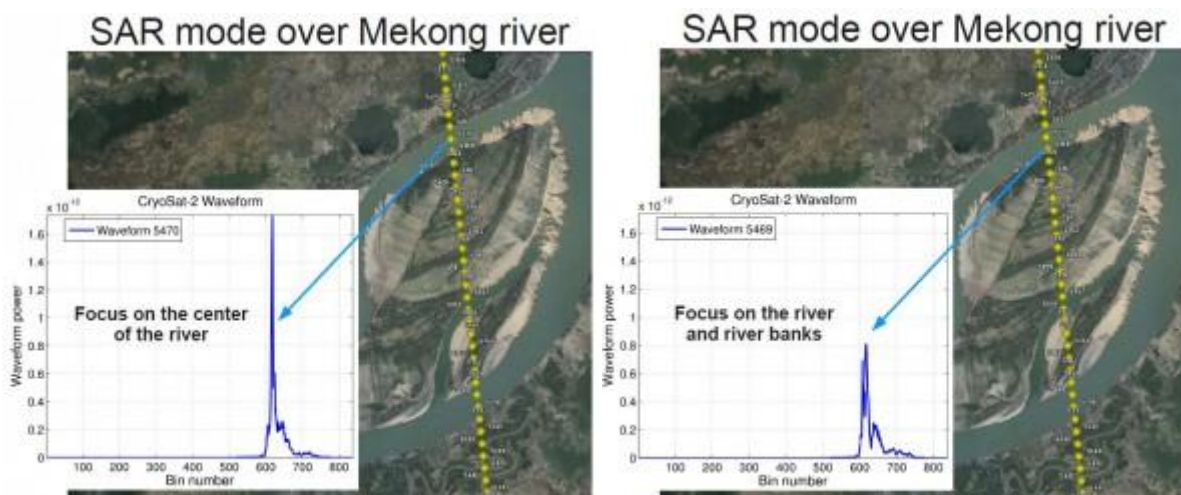
The great advantages of the SAR mode with respect to the conventional (LRM) altimetry are:

- The enhanced resolution along-track (e.g. ~300 m compared to few km) due to Delay-Doppler processing [Raney1998, Wingham2006];

- The possibility of beam steering that enables to focus the measurement at a desired place, thus enables the determination of the height from the processing of echoes returned by a narrow band centred within the river (benefiting of water masks a priori information);
- The accumulation of looks from the same footprint which shall allow to increase the signal to noise ratio, thus achieve better precision of the altimetric measurements and characterize surface response according to the look angles.

It is foreseen that future major investigations will focus on the optimal exploitation of L1B-S data (direction dependent masking, etc.) in order to produce decontaminated waveforms for inland waters.

An example of L1B waveforms over the river is shown below. It can be appreciated that the record located in the centre of the river is much clearer and peakier while the record near the border presents some land contamination.



http://www.altimetry.info/wp-content/uploads/2016/09/Mekong_profile.jpg

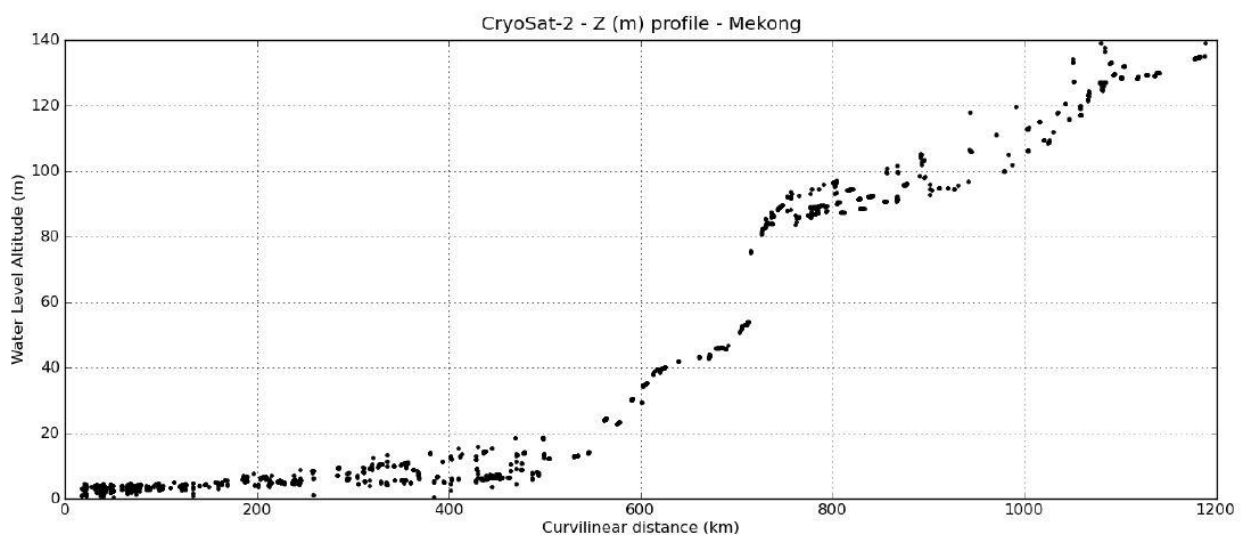


Figure 6.53. Illustration of SAR waveforms over the Mekong river, left and river profile compute from SAR data, Bercher et. al.

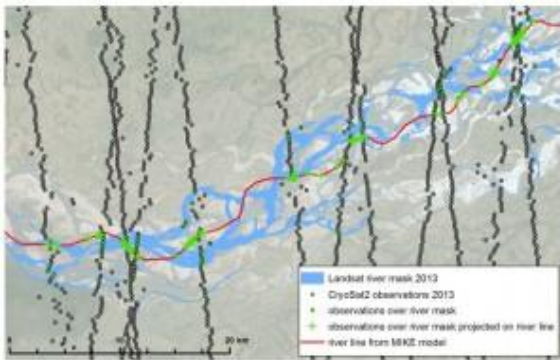


Figure 6.54. Section of the Brahmaputra in the Assam Valley showing the Landsat river mask, the CryoSat-2 observations and their mapping to the 1D river model, all for 2013. Schneider et. at. EGU 2016

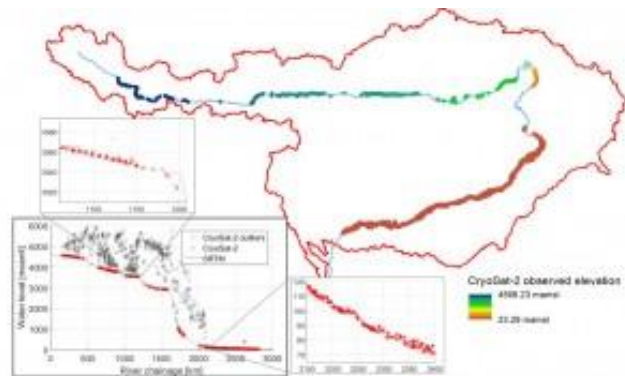


Figure 6.55. CryoSat-2 observations along the Brahmaputra River from 2010 to 2013. The map only displays the outlier-filtered observations, the longitudinal profiles show both outliers and the outlier-filtered data. Schneider et. at. EGU 2016

References:

- Lotus project
- CRUCIAL project
- Schneider, Raphael, et al. "Application of CryoSat-2 altimetry data for river analysis and modelling." *Hydrology and Earth System Sciences* 21.2 (2017): 751.
- [Bercher2013a] – Bercher N., Dinardo S., Lucas B. M., Fleury S., Calmant S., Crétaux J.-F., Femenias P., Boy F., Picot N. et Benveniste, J. (2013a). Applications of CryoSat-2 SAR & SARin modes for the monitoring of river water levels. In Proceedings of the “CryoSat Third Users Workshop”, 12-14 March, Dresden, Germany. Oral communication and paper. Download from chronos.altihydrolab.fr.

6.7 Coastal applications

Many current studies are attempting to enhance the quality of altimetry data close to the coasts. New processing methods and applications can then be developed for litoral and shallow-water regions, some of the most fragile and important areas of the oceans.

The shortage of altimetry data near the coasts (or their inferior quality) is due to several factors:

- the technique itself, since the radar echoes reflected off water, and off a combination of water and land are not identical, and basically only the former undergo processing by the ground segments. Other altimetry satellite measurements also suffer from the same problem, such as those from the radiometer (at a distance of about 50 km from the coast)
- the fact that the basic distributed data (GDR) are mainly average over one second, thus covering about 7 km on the ground.
- the computation of some corrections. Tides, in particular, are much more complex near the shores than in the open sea, and require a highly precise knowledge of the coastal geography to be accurately computed. Moreover, rapid variations (“high frequency”) must be taken into account in those areas (for the tides as well as for the atmospheric pressure). Wet tropospheric corrections, computed from radiometer measurements are also less precise, or even missing, near the coasts.

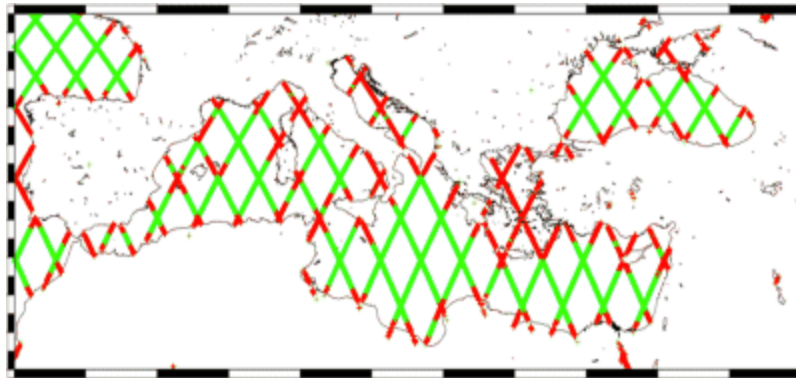


Figure 6.56. For Jason-1 or Topex/Poseidon, areas where radiometer measurements are typically edited out (ie disregarded) by standard processing (in red) and ones where they are retained (in green). The Aegean Sea, in particular, is completely overlooked.

Such studies are leading to advances that will soon make it possible to use altimetry data close to the coasts. With new possibilities such as the use of individual altimetry echoes (as opposed to averaged ones today), we can at last hope for real coastal data.

6.7.1 Coastal Ocean - SAR & SARIn

CryoSat-2 offered the first ever possibility to perform coastal altimetric studies using SAR/SARIn altimetry. With this technological leap forward it is now possible to observe sea level in very small water bodies and also to provide coastal sea level very close to the shore. The advantage of the SAR data compared with conventional altimetry is the fact that the increased spatial resolution of SAR, along-track, provides valuable sea level observations.

Different ESA-EU funded projects have been carried out to evaluate the performances of the CryoSat-2 data near the coast (LOTUS, CP4O), some of them (SCOOP) already aimed at Sentinel-3. The main conclusions are being presented each year in the Coastal Altimetry Workshop series.

Evaluation of CryoSat SAR Data in the Coastal Zone

ESRIN implemented a number of versions of the SAMOSA retracker for validation in CP40, as described in Table 6.1. Some of them are available to the public through [GPOD](#). Additional info can be found in the following [link](#).

Table 6.1 Summary of versions of SAMOSA SAR L2 Data sets produced by ESRIN

Run Reference	C2 L1B Product	L2 SAR retracker model	Alphap LUT	Peel Effect applied	Motivation
ESRIN R1	CPP	ESRIN SAM2	Yes	Yes	Full SAMOSA analytical model (Gaussian waves statistics)
NOC R2	CPP	NOC SAM3	No	No	Consistent with Sentinel 3 DPM except for treatment of Thermal Noise. Only small data set available for benchmarking
ESRIN R3	CPP	ESRIN SAM3	Yes	Yes	To quantify impact on retrieval of omitting f1 term in SAMOSA3
ESRIN R4	CPP	ESRIN SAM3	Yes	No	Consistent with Sentinel 3 DPM but with inclusion of alpha_p LUT
ESRIN R5	ESRI N FBR	ESRIN SAM2	Yes	Yes	Possible impact of L0 – > L1B processing
ESRIN R6	CPP	ESRIN SAM3	No	No	Consistent with Sentinel 3 DPM baseline

In addition to the evaluation of SAR altimeter data in the open ocean, NOC carried out an assessment of capabilities of SAR altimetry in the coastal ocean (Gommenginger et al, 2014, CP40 Technical Note, WP4000). This validation study was carried out on the ESRIN R1 data set (the full implementation of the SAMOSA-2 model), at locations close to the sites of UK coastal tide gauges. The data set available was limited in time and was not long enough to include any repeat visits to any of the locations, and an initial attempt at match ups showed large offsets which varied from pass to pass. The analysis was therefore limited to assessing the availability of valid data, and of the noise levels on these data. An analysis of a longer times series will be needed to allow a comparison between tide gauge and SAR data measurements (e.g. of Total Water level Envelope – a parameter relevant to tidal surge studies).

Segments of the R1 (see Table 6.1) CryoSat SAR validation dataset that lay within 100 km of the UK coast were extracted, and values for the Total Water Level Envelope (TWLE) calculated at 20 Hz intervals (TWLE is calculated as the SSH, with all relevant atmospheric corrections applied, and inclusive of ocean tides and atmospheric forcing). The noise level on the TWLE estimates was calculated as the absolute difference between consecutive measurements. This is believed to provide a good proxy for measurement noise, as the spatial separation between consecutive measurements will be ~300m, so the sea level should only be different by an order of mm.

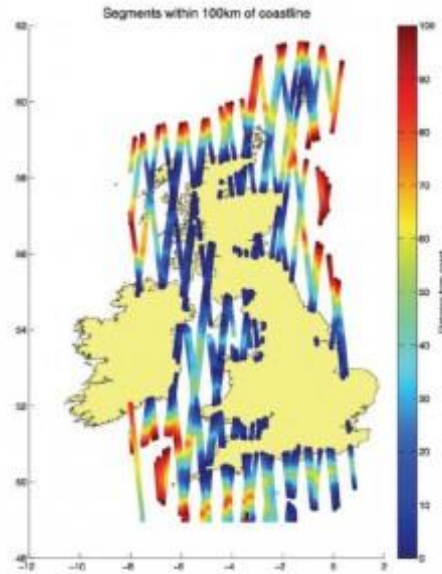


Figure 6.57. Segments of along track CryoSat SAR data within 100 km of UK tide gauge locations (Credits NOC).

The figure below shows the results, for all data, and for data selected according to waveform misfit < 3.

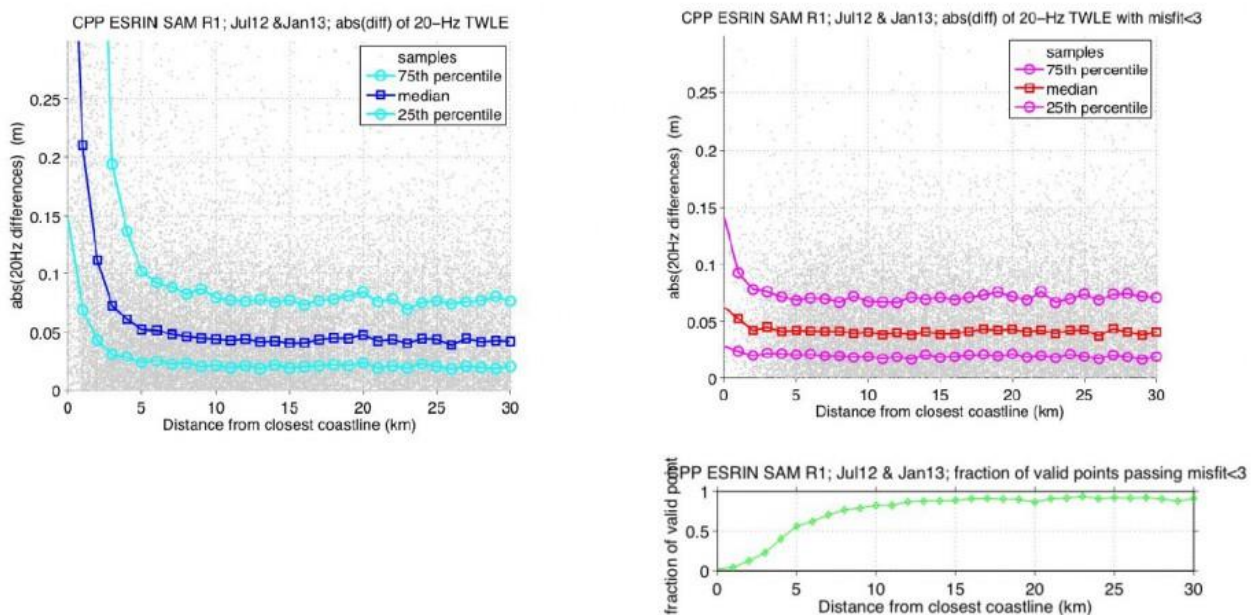


Figure 6.58. 20Hz “Noise” on TWLE (see text) against distance from the coastline. (left) all data passing normal data flags; (top right) as left but further selected for misfit < 3; (bottom right) number of data points in top right panel (Credits NOC)

In the left panel, it can be seen that the median of the absolute differences remains at 5 cm to within 5 km of the coast. Assuming that the noise is Gaussian, with variance of $2\sigma^2$, then the difference

between adjacent samples will have a variance of $2\sigma^2$. Thus a median absolute difference of 5cm is equivalent to a noise level of 3.5 cm for 20 Hz data, or 0.8 cm for 1 Hz data. This remarkable low noise level can be achieved to within 1km of the coast if the data are more carefully filtered according to waveform misfit < 3 (right panel), though of course the number of data being included in the calculation becomes significantly less (under 25% at 3km from the coast – see bottom right panel).

Raynal et al (2014, Validation Report: CP4O WP5000) also looked at the performance of the different SAR products close to the coast, and found very little difference between R1 (see Table 6.1), and R6 (see Table 6.1) SAMOSA products and the CPP product, in terms of the mean calculated Sea Level Anomaly, the number of valid points (per km), and the standard deviation (figure below).

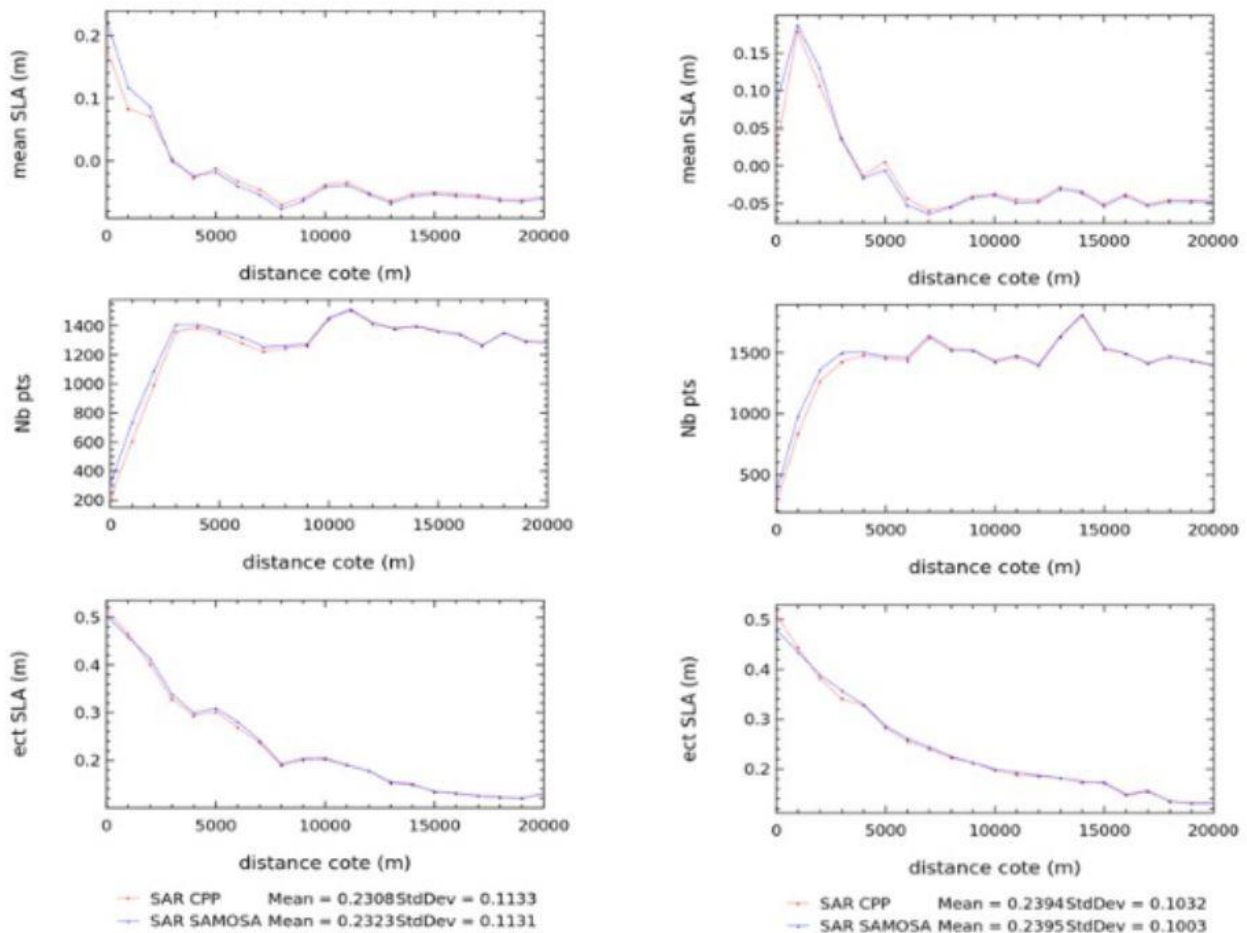


Figure 6.59. Sea Level Anomaly (top), number of points (middle), and standard deviation of SLA (bottom), for CPP SAR (red) and SAMOSA R1 SAR (blue) data with distance from the coast. For ascending (left) and descending (right) passes on tracks close to the UK.

Note that Dinardo et al., (2014) also assessed the capability of CryoSat SAR mode data in the German Bight, using data processed with the SAMOSA retracker. This work was carried out outside the CP4O project, but was reported to CP4O. The study found that CryoSat SSH, SWH and wind speed measurements were consistent with those in the RDSAR products, and the SWH and wind speed measurements were also consistent with buoy and model data.

Conclusions for CryoSAT SAR Coastal Zone Data

Although further work on a larger data set is necessary, it can be concluded from the CP40 analyses that the SAR product can provide low noise estimates of Sea Surface Height, and parameters derived from SSH (SLA, TWLE) to within 1 km of the coast, if the data are filtered appropriately. It has not been yet possible to investigate the relative performance of different processing schemes in this aspect.

The following recommendations for SAR (coastal ocean) are highlighted:

- A comprehensive evaluation of CryoSat SAR data in the coastal area should be carried out.
 - This is one of the objectives of the SCOOP project, using CryoSat data processed following the Sentinel-3 baseline.

Coastal Ocean – SARin

Garcia et al. (2014) describes the short scientific study that was carried out into the use of SARin data from CryoSat to provide insight into the potential for SAR altimetry in the coastal zone. This study made use of data from the SAR Interferometric (SARin) mode of CryoSat, whereby a second antenna is used to receive the reflected signals. The two antennas are mounted perpendicular to the direction of flight, so the across track information is provided. The relative phase information from the two antennas allows the angle of arrival (AoA) of off-nadir across track echoes to be derived. In the example of the figure below, the SIRAL has received a direct nadir echo from the ocean surface and an off nadir echo from a reflector on land. Because of the elevation and brightness of the reflecting facet on the land, the land echo arrives earlier, and has a similar power, to that of the nadir ocean echo.

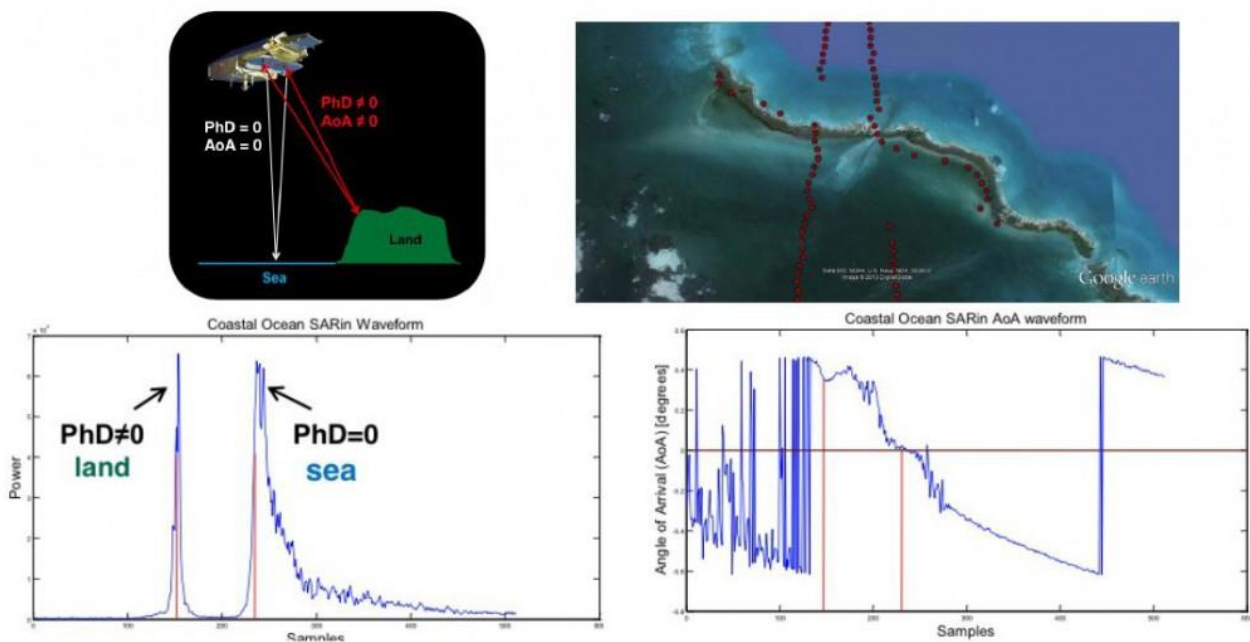


Figure 6.60. Off nadir returns in SARin mode. (Top left) Schematic of the geometry of a nadir ocean and off nadir land echo. (Top Right), Examples of non-nadir echoes received on pass close to Cuba, with true echoing locations identified. (Bottom Left) Power waveform, showing land echo received before ocean echo, and (Bottom right) phase waveform. The two red lines identify the position of the first echoes from the land and ocean reflectors.

The purpose of the study described in Garcia et al., (2014) is to build an approach that can be used for processing SAR mode data which will distinguish and minimise the effect of the contaminating land echo. SARIN for two areas was requested, one region covering the Cuban Archipelago, which includes coastal cliffs and offshore cays, in general lying roughly perpendicular to the CryoSat subsatellite track, and a second region close to the Chilean coast, where the coastline (predominantly cliffs) lies closer to parallel to the CryoSat sub-satellite track.



Figure 6.61. The two SARin regions considered, (left) the Cuban archipelago, (right) the Chilean coastal strip.

The existing L2 processing often selects and retracks the off-nadir land echo, which can arrive earlier and be of similar higher power, and so returns an erroneous range. Thus a modified L2 processing scheme was developed that took as input L1 power, phase difference and coherence waveforms and through an iterative process identified the true nadir echoing point. The processor then used this true echoing point to provide a “seed” to a purpose-built retracker which returns the true range of the nadir echo, together with the latitude and longitude of the nadir echoing point.

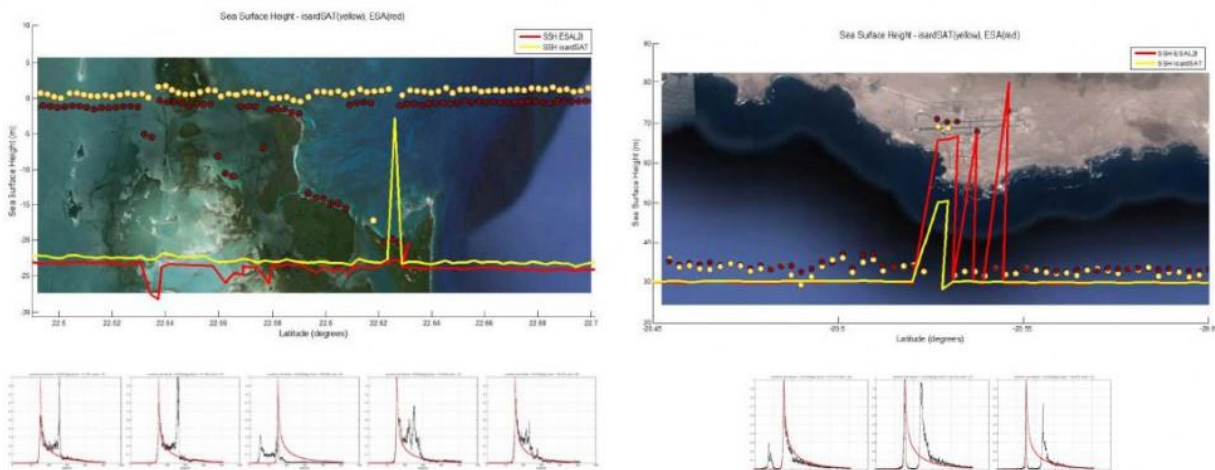


Figure 6.62. Reprocessed SARin data from passes over (left) Cuba, and (right) Chile. The top panels show the locations of the originally processed echo points in red dots, and the echo points identified by the isardSAT processor in yellow dots. The solid lines give the retrieved Sea Surface Height in m (scale on the left) with the same colour code. The bottom panels show a selection of the power waveforms (in black). The retracking fitted waveform is shown in red.

The figure above shows the result of using this modified processor on two sections of SARin data, the first across the Cuban Coast and the second close to the Chilean coast. In both cases the original processing wrongly tracked off nadir echoing points and so returned SSH values that could be ~10m in error (red). The new scheme provided much improved retracking (yellow), though not with a 100% success rate. The algorithm was tuned by running it across a large number of tracks, selecting processing tolerances that provide the best results in most circumstances. As some trade offs were necessary, it was not possible to design a general scheme that worked for all cases. This activity therefore demonstrated that the existing SARin processing scheme was returning incorrect SSH values, by retracking on non-nadir echoes, in a significant number of cases in the coastal zone, and has developed an improved scheme to minimise the contamination from non-nadir echoes.

Further work was recommended to:

- Further improve the modified SARin processing scheme to fine-tune the retracker seed production and the retracking solution itself.
- Produce a test data set for coastal zones to support the development of improved SAR coastal zone retracking solutions.
- Adapt the SARin processing approach for application to SAR data to improve retrieval of ocean parameters (especially sea surface height) from tracks over complex coastal topography.

Further information:

- [CP4O final report](#)
- [CP4O Homepage](#)
- [CP4O data](#)
- [SCOOP Homepage](#)
- [SAMOSA Project](#)

References:

- Dinardo S., Fenoglio-Marc L., Scharroo R., Lucas B., Becker M. and Benveniste J. (2014). Validation of Open-Sea CryoSat-2 Data in SAR model in the German Bight from 2010 to 2014. Poster at the OSTST meeting, Lake Constance, 28-31 October 2014
- Garcia, P., 2014, "Algorithm Theoretical Basis Document (ATBD): SARin for Coastal Ocean. CP4O Technical Note, WP4000
- Gommenginger C., P. Cipollini and H Snaith, 2014, "Product Validation Report (PVR) for SAR Altimetry over the Open Ocean and Coastal Zone". CP4O Technical Note, WP4000
- Raynal, M., T. Moreau. 2014b. "Validation Report: WP5000 Global wet tropospheric correction (U Porto)", CLS-DOS-NT-14- 081 CP4O Technical Note
- Raynal, M., T. Moreau. 2014c. "Validation Report: WP5000 Regional tidal correction (Noveltis)", CLS-DOS-NT-14- 083. CP4O Technical Note
- Raynal, M., T. Moreau. 2014d. "Validation Report: WP5000 Assessment of SAMOSA SAR Solution (ESRIN)", CLS-DOS-NT-14- 084 CP4O Technical Note
- Raynal, M., T. Moreau. 2014e. "Validation Report: WP5000 Ionospheric correction (Noveltis)", CLSDOS-NT-14-082. CP4O Technical Note

6.8 Examples of altimetry data use

6.8.1 Western boundary currents: The Gulf Stream and its seasonal variations

Ocean circulation at subtropical latitudes is made up of large cells known as anticyclonic gyres; the famous Gulf Stream basically corresponds to the western boundary of the North Atlantic subtropical gyre.

Data used

Merged Maps of Sea Level Anomalies (MSLAs) and Maps of Absolute Dynamic Topography (MADTs) are required. (See [description](#) on the [Aviso website](#)).

- both are already gridded and easy to use, moreover no specific data reprocessing is required here,
- both provide their own view of the sea surface current, furthermore their aspects are complementary,
- both have been merged, to provide the most precise dataset available,
- up-to-date ('Upd') data offer better quality for a given date, whereas reference ('Ref') data are more suited to long temporal studies (see the second part: 'Seasonal variations').

You can get access to these products by subscribing and by filling the form on the [Aviso website](#). Then a user account will be sent and you will be able to download the relevant data.

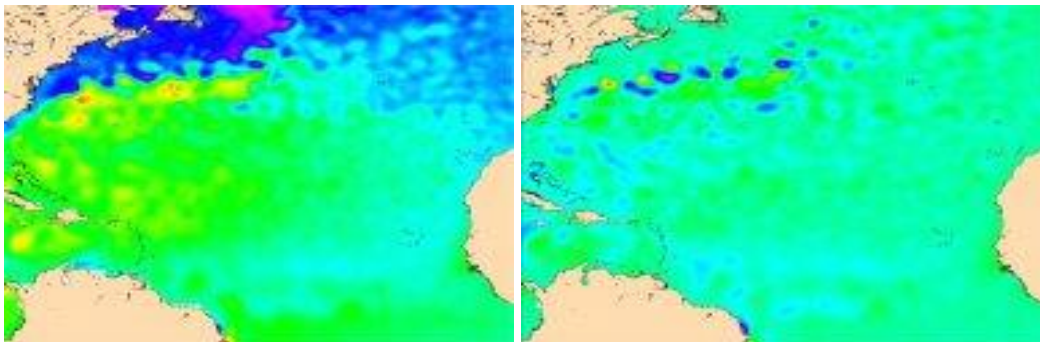


Figure 6.63. Maps of Absolute Dynamic Topography (left) and Sea Level Anomaly (right), North Atlantic

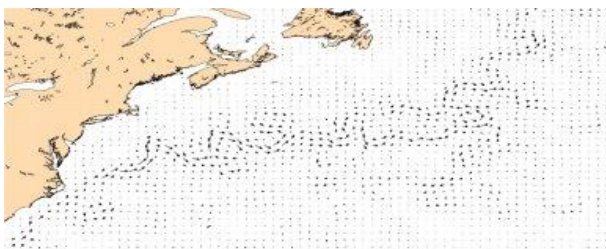


Figure 6.64. Map of absolute geostrophic velocity

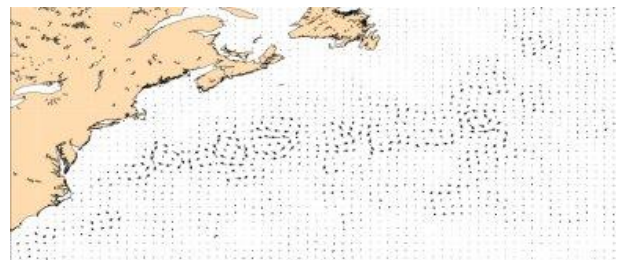


Figure 6.65.: Map of geostrophic velocity anomalies

Methodology

Temporal extraction

From the authenticated service, download up-to-date ("Upd") MSLA and MADT files for November 2, 2005, in `global/dt/upd/msla/merged/h/` or in `global/dt/upd/madt/merged/h/`
Then download reference ("Ref") MSLA and MADT files from 2001 to 2005 (See description) in `global/dt/ref/msla/merged/h/` or in `global/dt/ref/madt/merged/h/`.

Geographic extraction

Our area of interest is defined by the following coordinates: 0°N-50°N,10°W-80°W.

Four different points of view

Select a date, for example here 2 November 2005 and then plot:

- the Absolute Dynamic Topography map corresponding to your chosen file,
- the Sea Level Anomaly map corresponding to your chosen file,
- the absolute geostrophic velocity map provided with your MADT file,
- the geostrophic velocity anomalies map provided with your MSLA file.

On the MADT map, an area with significant contrasts is visible, where the topography varies by approximately 80 centimetres within quite a short distance, all along what seems to be a front.

On the MSLA map, no such frontal area appears, but there are some separated spots in the same place. On the absolute geostrophic velocity map, vector fields plot a continuous structure: vectors join together to form a significant surface current.

On the velocity anomalies map, vectors still plot a major current in the North Atlantic Ocean, but with more eddies.

These maps correspond with a significant current that flows along the coasts of North America towards European shelves. Eddies in its wake show that a lot of energy seems to be carried by this current.

Previous maps provided just a 'snapshot' of the Gulf Stream system. With a larger time scale, it becomes possible to see that this current does not always flow in the same location, nor with the same intensity: it changes with the seasons, and for seasonal or interannual studies, such maps are obviously not enough to quantify its variability.

The Gulf Stream, season by season

Here we are considering two seasons: autumn (October-November) and Spring (April-May). For each one we:

- compute the temporal average of the absolute dynamic topography all along a cross-section in longitude (70°W),
- plot diagrams showing how these averaged dynamic heights vary with latitude.

Seen in this way, the Gulf Stream appears at approximately 37°N , and seems further north in October (black curves) than in April (red curves), as well as appearing more intense. These differences could mirror a seasonal or inter-annual signal.

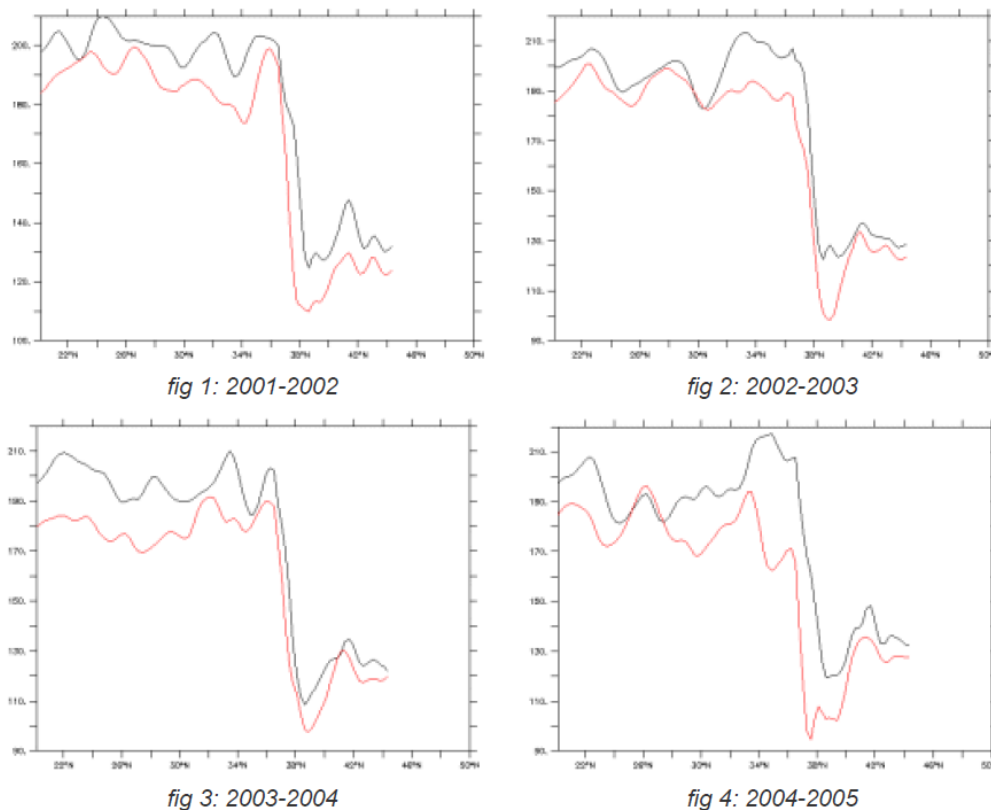


Figure 6.66. Gulf Stream Seasonal variation Autumn (black) vs Spring (April) MDT along the Gulf Stream at 70°W

6.8.2 Ocean eddies as seen by satellite altimetry: the Kuroshio current

Mesoscale variability typically refers to oceanic signals with space and time scales of 50 km to 500 km and 10 days to 100 days, respectively. An example of this are ocean eddies, fronts, and meanders. The Kuroshio is a strong western boundary current in the North Pacific Ocean, similar to the Gulf Stream in the North Atlantic. In this western boundary current, there is considerable mesoscale variability which tends to be dominated by meanders and eddies. Satellite altimetry offers a high-performance technique for studying such phenomena.

Data used

Merged Maps of Sea Level Anomalies (MSLAs) have been used in this study:

- they are already gridded and easy to use, moreover no specific data reprocessing is required here,
- they have been specifically processed for mesoscale studies, i.e they have been filtered from small-scale signals and long wavelength errors, and have been sub-sampled,
- merged datasets provide a better description of mesoscale activities thanks to improved accuracy.

Methodology

Geographic extraction

Extracting data from MSLAs will strongly simplify our study as the MSLAs are available by from FTP. Our area of interest is defined by the following coordinates: 25°N-40°N, 135°E-180°E (Figure 6.67 and Figure 6.68).

Computation of geostrophic currents

The components of geostrophic currents are deduced from the geostrophic balance hypothesis:

$$u = -(g/f) \times d(SLA)/dy - Eq. 5$$

$$v = (g/f) \times d(SLA)/dx - Eq. 6$$



Figure 6.67. Area for data extraction

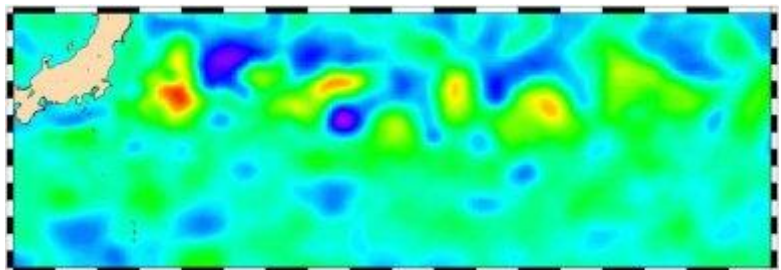
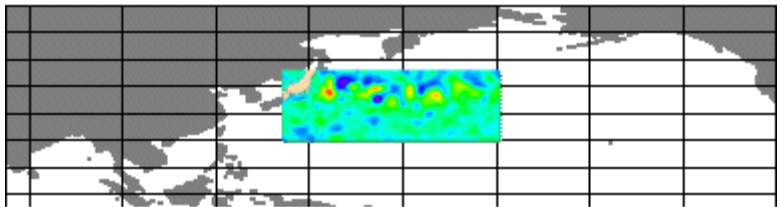


Figure 6.68. Maps of Sea Level Anomaly, Kuroshio area, cm

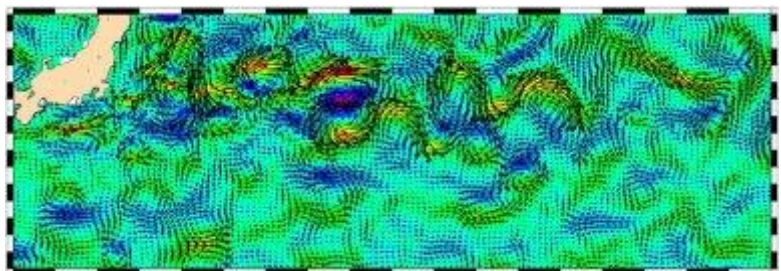


Figure 6.69. Maps of geostrophic velocity anomalies, Kuroshio

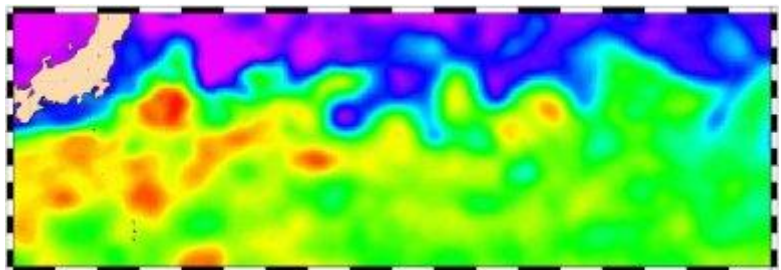


Figure 6.70. Maps of Absolute Dynamic Topography, Kuroshio area

where g is gravity and f the Coriolis parameter. To generate a map of geostrophic currents from SLA fields, algorithms can be based on a centred finite difference method (Figure 6.69).

Computation of MADTs

Maps of Absolute Dynamic Topography (MADT) are obtained using:

$$\text{MADT} = \text{MSLA} + \text{MDT} \qquad \text{Eq. 7}$$

Where MDT is the Mean Dynamic Topography. There are several MDT models, some of which are available on Aviso web site.

‘Absolute Dynamic Topography’ represents the general ocean dynamics, whereas ‘Sea Level Anomalies’ focus on its variable component (Figure 6.70).

Western boundary currents such as the Kuroshio convey a lot of energy and generate strong turbulence systems. While SLAs and geostrophic currents illustrate eddies, EKE (Eddy Kinetic Energy) fields allow us to focus on mesoscale variability; statistics are especially necessary to quantify these phenomena.

6.8.3 Geostrophic velocities: The Antarctic Circumpolar Current, due East around the Earth

The geostrophic circulation is the ocean circulation generated by the balance between the horizontal pressure gradient forces exerted by water masses and the effect of acceleration due to the Earth's rotation.

Geostrophic velocities can be computed using the slope of the surface (available from altimetry data), and the Coriolis force. See e.g. [Surface Geostrophic Currents From Altimetry](#) (Introduction to Physical Oceanography, Texas A&M University) for more precise information.

Data used

We will compute geostrophic velocities from Sea level anomalies.

Compute geostrophic velocities from gridded data

In this case, the best is to use pre-computed multi-mission gridded data (e.g. Aviso MSLA), since the resolution will be better than if you smooth out along-track data as a grid. But you can also use a SLA map created using BRAT from GDR data.

In this case, you can compute both meridional and zonal velocities (U and V; note that if you compute geostrophic velocities directly from along-track data, without gridding them beforehand, the only available slope is the one along the track. Thus the geostrophic velocity computed would be “only” its component perpendicular to the track since the geostrophic velocities are perpendicular to the slope).

Methodology

We will use the “geostrophic velocities” algorithm available in BRAT (version 3 or higher of the software).

Temporal/Geographic extraction

Operations

Define a dataset with a gridded SLA file.

For the gridded data:

In the “Operations” tab, define longitude as X, latitude as Y.

Create two expressions as “Data expression”, one you can call “U” (zonal), the other “V” (meridional). Click in the box for the first one, then click on the “insert algorithm” button. A pop-up window opens. There you will find three existing algorithms. One is for the along-track geostrophic velocity computation, the other two are for U and V, respectively. Choose the appropriate one. A function-like expression is inserted in the Data Expression box. You have only to check that longitude and latitude match the existing variables within your datasets (sometimes they can be called “lon” and “lat”), and to insert the height you want to compute geostrophic velocities from (here SLA) in place of the indication ‘height’ within the function variables.

Create a second operation with only longitude as X, latitude as Y and the SLA as Data expression

In the “set resolution” pop-up window, restrict your area of computation to 45-65°S. Execute this.

Go to the “Views” tab, create a new View.

Take U and plot it (Execute). Take V and plot it (Note that in the View tab, by choosing Plate Carree or Mercator projection, you can pre-define your zoom, which will enable you to keep it for future use).

Create again a new View, with the same projection and zoom (or erase the previous choice and replace it as follow, if you do not want to keep the previous view for future references).

Select the SLA height to serve as background, then the “U” AND the “V” components. Click on the selected U expression and below, click on the box “East component”; click on the selected V and below, click on the box “North component”. Execute.

6.8.4 The North Western Mediterranean Sea by using coastal dedicated products

Satellite altimetry is limited near the coastlines due to a loss of quality in the measurements. These errors are caused by the land contamination in the altimetry and radiometric footprints (10 km and 50 km of footprint diameter, respectively) but also by inaccurate geophysical corrections. Despite this, the altimetric measurements are present and may contain useful information for coastal studies.

This data use case proposes to give some instructions on how to use the Coastal experimental products distributed by Aviso (PISTACH) products over the Northwestern Mediterranean coasts.

Data used

Jason-2 along-track experimental Coastal products produced by the PISTACH project, a coastal (and hydrology)-dedicated processing applied to the Jason-2 mission.

These products derive from the Jason-2 S-IGDR products and include new retracking solutions, several state-of-the-art geophysical corrections as well as higher resolution global/local models. Numerous extra fields derived from the various PISTACH processes are then added to build the products. These products are based on a 20-Hz along-track sampling rate (vs 1-Hz for the official Jason-2 IGDR) but the nomenclature of their variables and files is similar to Jason-2 IGDRs one.

Download freely coastal data files on the [FTP server](#). Files are in the sub-directories named cycle_XXX/. Each cycle lasts about 10 days, the first one (in the cycle_001/ directory) was acquired early July 2008.

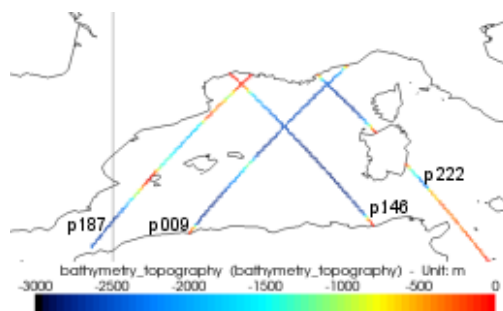


Figure 6.71. Bathymetry (in meters) below four Jason-2 tracks in the North Western Mediterranean Sea. This map is plotted using the BRAT from the PISTACH coastal products (variable bathymetry_topography).

Methodology

We use the Broadview Radar Altimetry Toolbox to observe the data and do some computation.

Data chosen

To limit the volume of data to download, it is better to determine the ground tracks numbers over the area of interest (here, the western Mediterranean Sea). These ground track numbers are available in the pass locator on Aviso website (download the .kml file for the [Jason-2 referenced orbit](#) to visualize it on Google Earth). Here, the Jason-2 interesting passes are: #009, #146, #187 and #222.

A data selection based on the latitudes (36.5°N, 44°N) enables to extract the Mediterranean Sea.

The time series used for this data use case stretches out from the cycle_003 (August 2008) to cycle_084 (September 2010).

Data editing

6.8.4.1 to represent the SSHA as a function of latitude

Once the relevant files are all downloaded, create a dedicated workspace and then, a new dataset. In a first Dataset, named dataset_raw_cy5_tr222, we have added one file corresponding to the coastal PISTACH product for the cycle_005 and the pass 222.

In the “Operations” tab, we have created an operation for the SSHA (Sea Surface Height Anomaly) computation, named Operations_raw_cy5_tr222. For a Y=F(X) representation of the SSHA, select latitude for “X” and for the “Data expression”, type the SSHA formula with the following combination:

SSHA= satellite altitude - Range (from one retracking) -Sea Surface Bias - Atmospheric corrections (iono, wet, dry) - tides (pole, land and ocean) - HF dynamics – Mean Sea Surface

In practice, for coastal oceans, several combinations are interesting. One of them is (with the full names of the NetCDF product variables):

- SSHA1 = alt – range_red3_ku – iono_corr_gim_ku – model_dry_tropo_corr – decontaminated_wet_tropo_corr – solid_earth_tide – ocean_tide_sol3 – pole_tide – inv_bar_corr – hf_fluctuations_corr – mss1

The range term (range_red3_ku) is actually estimated with a retracking algorithm dedicated to signal affected by the land above water (distance to coast < 10 km). Nevertheless, its drawback is to be biased compared to the classical open ocean computation (range_ku) and to have no sea state bias estimate. The sea state bias in Ku-band is not coherent with the RED3 retracking. But for areas very close to the coastline it could improve the SSHA.

The wet tropospheric 'decontaminated' solution has been developed for the coastal ocean. The effect of lands is retrieved using the quantity of land seen by the radiometer. Another wet tropospheric

correction is also useful near the coast: the `composite_wet_tropo_corr` which mixes modelled and radiometer corrections.

No particular editing is computed, only a selection on the extreme values between the `alt - range_red3_ku` is done: `is_bounded(-130,(alt-range_red3_ku),100)`.

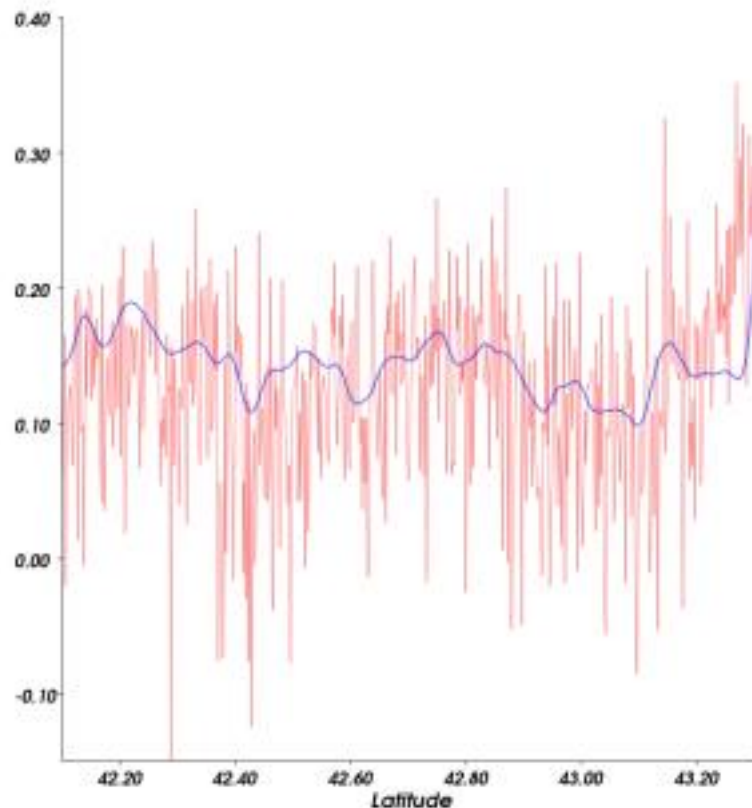


Figure 6.72. Along-track SSHA – Cycle 005 – Track 222 near the coast, made from the raw 20 Hz PISTACH coastal products (in red) and from the filtered SSHA (blue) computed from the coastal products.

Nevertheless, this raw 20 Hz PISTACH SSHA appears too noisy. To study the variation of the ocean surface, a post-processing (filtering + editing) is needed.

To filter and select data at the same time, an iterative strategy has been tested. Both a median filter and a Low-Pass filter (cut-off length $L=7$ km), associated with a 3-sigma data selection on the difference (filtered-non filtered), have been applied on the raw 20 Hz PISTACH SSHA data.

Applying this method provides high-resolution SSH anomalies along the tracks without instrumental noise nor erroneous data but with more pronounced meso-scale signals than its classical products (see Figure 6.72).

The filtered data represented here cannot be directly computed with the Broadview Radar Altimetry Toolbox (yet). After its computation, they were inserted in another Dataset named `dataset_filtered_cy5_tr222`. Another operation, `operations_filtered_cy5_tr222`, is created to compute the SSHA (on the base of the SSHA1 formula above). The two operations are displayed on the same graph. On the Views menu, a view name is created with both operations, by ticking “group expressions in the same plot” (NB: in the Operations menu, both operations must have exactly the same name as “X” to be used on the same plot).

Representing the SSHA on a latitude-time diagram

Two new datasets are created, one per track: named `dataset_filtered_cy1_cy55_tr146` and `dataset_filtered_cy1_cy55_tr222`, they contain all the coastal filtered data between cycle 3 (August 2008) and cycle 55 (January 2010). The operations (one per track) are defined as above for the field Data expression (see SSHA1). The “X” is the latitude and the “Y” is the time. Here in our filtered reprocessed data, the variable time is the cycle (for the raw PISTACH product, the cycle is not a variable; but its variable “time” in seconds can be chosen. In this case, an appropriate expression can change the time in seconds in days: `round(time/24/60/60)`).

In “Set Resolution/Filter” (still in the Operations menu), the X resolution sets to $1/15^\circ$.

Results and comments

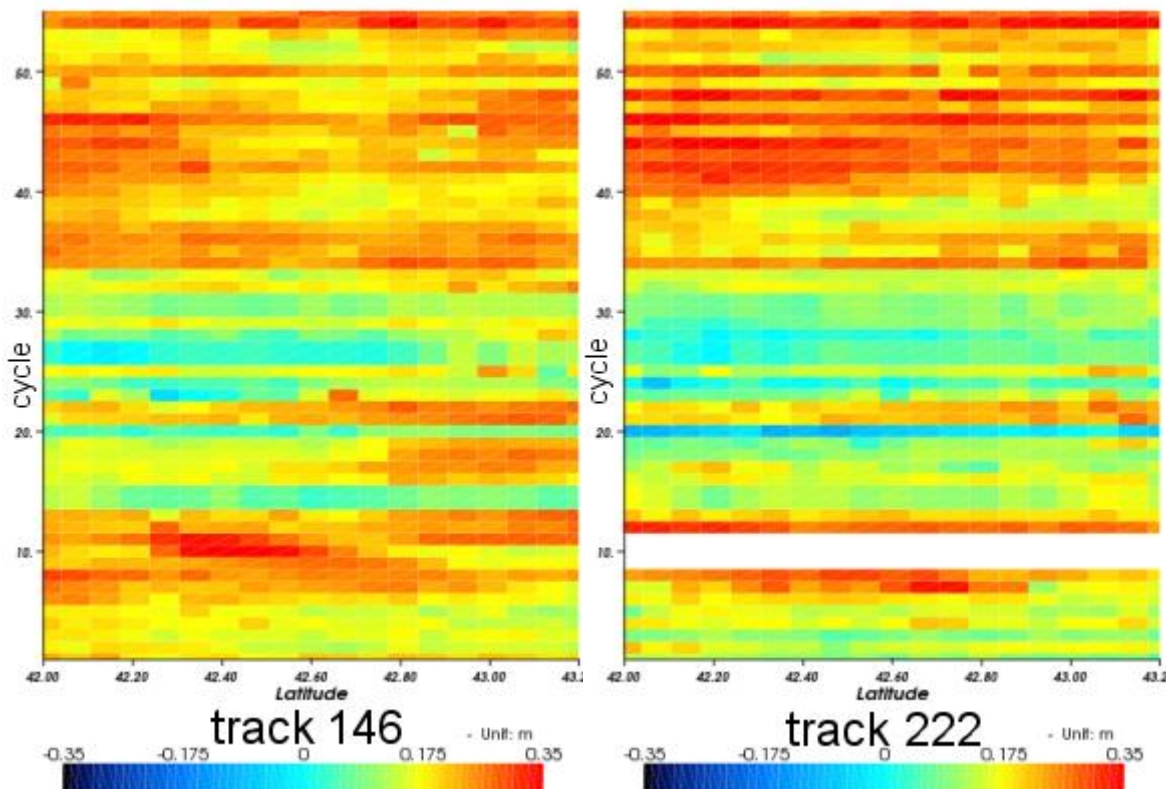


Figure 6.73. Latitude-time diagram of coastal filtered Sea Surface Height Anomalies, between 42°N and 43.2°N , between August 2008 (cycle 1) and January 2010 (cycle 55).

The coastal filtered data are used to try and monitor the variability of the coastal current in the Northwestern Mediterranean Sea. The large scale currents of the Northwestern Mediterranean Sea are dominated by a cyclonic gyre. The Western (WCC) and Eastern Corsica Current (ECC) join to form the Northern Current (also named the Ligurian-Provençal Current, LPC) in the Ligurian Sea.

The LPC flows along the continental slope of the Ligurian Sea and the Gulf of Lion down to the Catalan coasts. If the continental shelf is wide in the Western part (Gulf of Lion, tracks 146 and 187), it is narrow in the Eastern part (Ligurian Sea, tracks 009 and 222). The signature of this LPC current in the altimeter data may be located nearer the coasts (~10 km) in the Eastern part, which is the strong interest for the coastal PISTACH data.

Further information:

- Coastal and Hydrology Altimetry product (PISTACH) handbook (pdf).
- Dufau C., et *al.*, 2010, Use of Pistach Products in Coastal Studies. Oral presentation at the 4th Coastal Altimetry Workshop, Porto, Portugal.
- Mercier F. et *al.*, 2010, The Pistach project for coastal and hydrology altimetry: 2010 project status and activities (pdf). Poster presentation at the OSTST 2010 Lisbon, Portugal

6.8.5 The Agulhas current by using coastal dedicated products

Satellite altimetry is limited near the coastlines due to land contamination in the altimetry and radiometric footprints (10 km and 50 km of footprint diameter, respectively) but also to inaccurate geophysical corrections. Despite this, the altimetric measurements are present and may contain useful information for coastal studies.

This data use case proposes to give some instructions on how to use the Coastal along-track Delayed Time Sea Level Anomaly (CoastalDT-SLA) products distributed by Aviso over the South African coasts, in the Agulhas current.

We will show that more altimetry data are recovered in coastal areas and that this high resolution products allow retrieving small scale oceanic structures, like the Natal Pulse signature. Later, some comparisons with independent data (SAR and *in situ* measurements: current meters, tide gauges data) will show the good correlation.

Data used

The Jason-2 Coastal along-track Delayed Time Sea Level Anomaly (CoastalDT-SLA) product over the Agulhas area is used here.

The CoastalDT-SLA are Level-3 products, conceived as an evolution of the Jason-2 Level-2 coastal products, commonly called PISTACH products. The Level-2 products rather address altimetry experts' needs, and therefore are quite difficult to be used by non-expert users.

The CoastalDT-SLA products are easier-to-use and offer high resolution (20-Hz sampling rate) sea surface height on reference tracks. Differently from Level-2 products, the CoastalDT-SLA products are only computed over specific ocean areas (see details on the Aviso website).

Download CoastalDT-SLA data files from the Aviso FTP server for the Agulhas area. An authentication is required to access products. It can be obtained by filling in the form on [Aviso](#) and by selecting the CoastalDT-SLA product on the second page. Once connected to the server, files are in the sub-directories named /experimental/coastal_dt_sla_j2.

Ssalto/Duacs Along-Track Sea level anomalies are used here for comparison with the CoastalDT-SLA products. They are also distributed by Aviso and can be downloaded from the same authenticated ftp server with the same login/password (see details on the Aviso website and in the dedicated [User Manual](#)). Once connected to the server, files are in sub-directories named

/global/dt/upd/sla/j2_cf and files are typically named dt_upd_global_j2_sla_vvxc_20090805_20090812_20110329.nc.gz

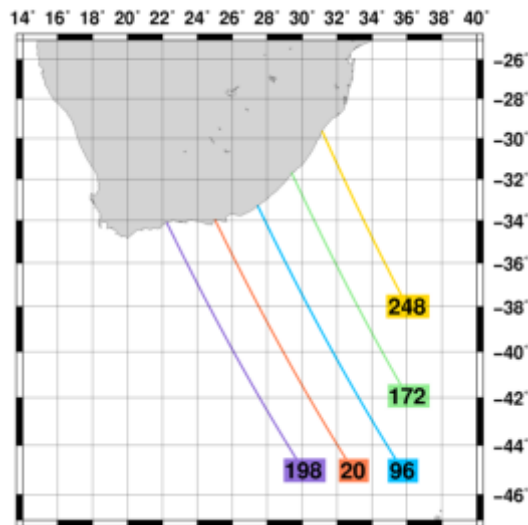


Figure 6.74. Jason-2 ground tracks over the Agulhas area included in the CoastalDT-SLA product.

Methodology

We use the Broadview Radar Altimetry Toolbox to observe the data and do some computation.

Data chosen

For the CoastalDT-SLA product, three Jason-2 passes are used in this data use case:

- the Jason-2 interesting passes over the Agulhas area are descending passes: #020, #096, #172 (one file per pass). The descending track alignment is almost perpendicular to the Agulhas Current flow, this presents a good configuration for repeat-track analysis of the system with altimetry.
- the time series used for this data use case stretches out from the cycle_001 (July 2008) to the cycle_110 (July 2011) (all the cycles are included in a given file).

Ssalto/Duacs Along-track Sea level anomalies used for comparison with the CoastalDT-SLA products contain all the available passes during a 7-days period. The downloaded time series stretches out from the cycle_011 (October 2008) to the cycle_110 (2011-07-08). Although BRAT can handle numerous files, it appeared preferable in terms of efficiency for BRAT to perform an extraction of the files based on a portion of the given track. We performed this extraction with the following script, based on the use of the 'ncdump', 'ncgen' and 'ncea' commands. The latter needs the installation of NCO (NetCDF operators) on the computer. The [NCO](#) homepage contains more information. Here, the extraction is done between -45°S and -33°S.

More altimetry data close to the coasts

Dataset

Once the relevant files are all downloaded, create a dedicated workspace in BRAT and then, create two datasets in the “Dataset” tab:

- a first one, named “agulhas_coastal_096” includes the CoastalDT-SLA product with only one file: coastal_dt_sla_j2_agulhas_096.nc. It contains all the time serie between 2008-07-17 to 2011-07-07.
- the second, named “agulhas_duacs_096” includes the 101 Duacs SLA files between 2008-10-18 to 2011-07-08.

Operations

On “Operations” tab, we create one operation for each dataset, CoastalDT-SLA and Duacs-SLA, in order to plot an hovmöller diagram, i.e a latitude-cycle diagram. These operations are respectively named “Op_agulhas_coastal_096” and “Op_agulhas_duacs_096”.

- Operation “Op_agulhas_coastal_096”: in “Operations” tab, click on “New” button to define a new operation, give the choosen operation name in the “Operation name” box.
- In Data expression, drag and drop the variables “cycle” in “X”, the latitude in “Y” and the “SLA_Filtered_41pts_MLE4” in “Data”.
- The spatial resolution for this dataset is $\sim 1/106^\circ$ in latitude. But as the resolution is set to $1/3^\circ$, by default, in BRAT, we have to change it to reflect the native resolution of the CoastalDT-SLA product. In “Set Resolution/Filter” (still in the Operations menu on the bottom right), the “Step” in Y resolution sets to $1/99^\circ$ (note that a such small spatial resolution as $1/106^\circ$ doesn’t work).
- Operation “Op_agulhas_duacs_096”: The previous Operation can be copied to create the operation corresponding to the “agulhas_duacs_096” dataset. To do that, select the previous operation (“Op_agulhas_coastal_096”) and click on the “Duplicate” button. Change the name to refer to the new operation name (“Op_agulhas_duacs_096”) and be aware to well select the corresponding Dataset with the corresponding Operation.
- In Data expression, drag and drop the variables “cycle” in “X”, the latitude in “Y” and the “SLA” in “Data”. Since the file resolution is different, change the “Step” in Y resolution at $1/20^\circ$.

Once each Operation has been defined, click on the “Execute” button.

Views

Once the Operations finished, define one View per Operation in the “Views” tab:

- View “Vi_agulhas_coastal_096”: Drag and drop the corresponding operation “Op_agulhas_coastal_096” from the list of operations in the “Available” box, on the left, to the “Selected” box on the right. Finally, click on 'Execute'. For comparison between both dataset, the SLA limits are set to -0.9 and 0.9 m in the “Range” boxes.
- View “Vi_agulhas_duacs_096”: Do the same for the operation “Op_agulhas_duacs_096”.

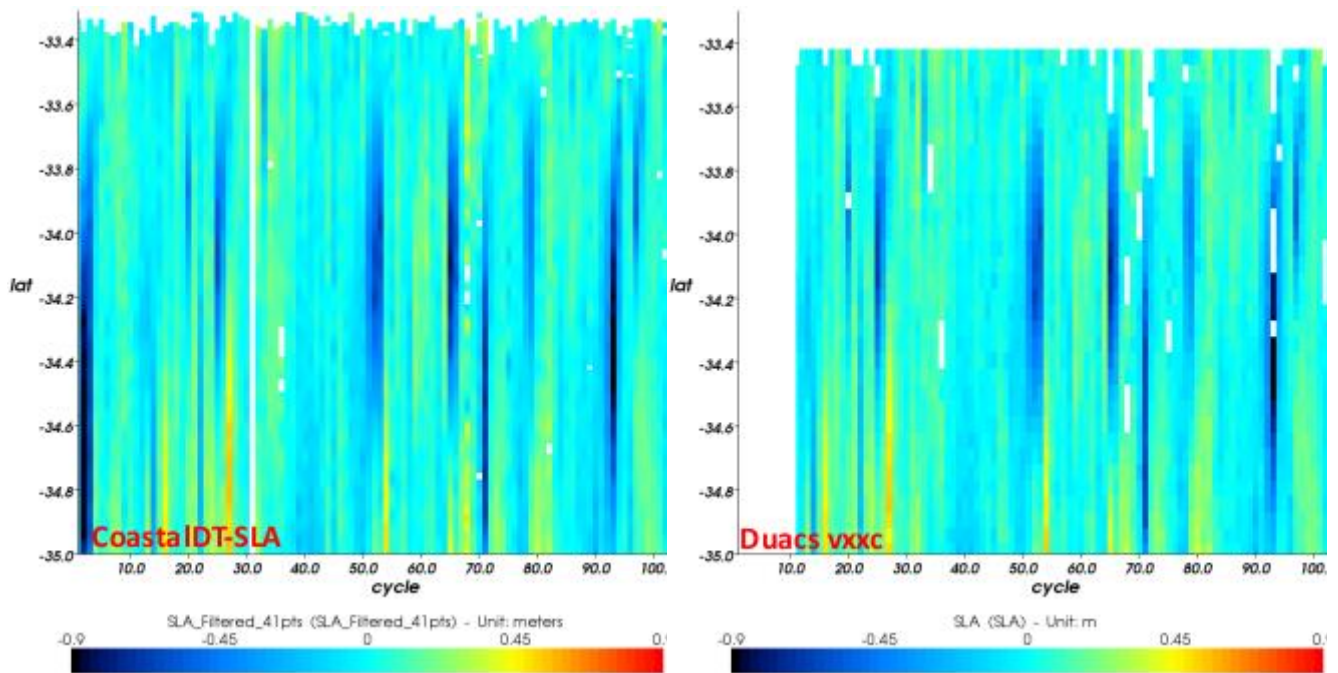


Figure 6.75. Latitude-time (cycle) diagram of Sea Level Anomalies, from -35°S up to the nearest point to the coast, for the Jason-2 pass #096. LEFT: CoastalDT-SLA product between August 2008 (cycle 1) and July 2011 (cycle 110). RIGHT: Ssalto/Duacs Along-track product between October 2008 (cycle 11) and July 2011 (cycle 110). The vertical white areas represent missing data.

The northern limit of the CoastalDT-SLA product reaches -33.32°S whereas it is -33.42°S for the Ssalto/Duacs Along-track product.

Thanks to CoastalDT-SLA product, a better along-track sampling is obtained and more data are recovered in coastal areas compared to the Ssalto/Duacs Along-track product, by roughly 11 km.

Signature of small structures

The aim is to plot the geostrophic currents with hovmöller diagrams for several passes and retrieve the small oceanic structures near the coast.

Dataset

Create new datasets in the “Dataset” tab, one per pass:

- The previous dataset defined for the CoastalDT-SLA product, pass #096 is also used here : “agulhas_coastal_096”. It includes the CoastalDT-SLA product with only one file: coastal_dt_sla_j2_agulhas_096.nc. It contains all the time serie between 2008-07-17 to 2011-07-07.
- On the basis of this dataset, do the same for the following passes by creating the datasets “agulhas_coastal_020” and “agulhas_coastal_172”.

Operations

On “Operations” tab, we create a first operation for a given dataset, by filtering the variable SLA. Then, this operation is exported and integrated in a new dataset. A second operation will compute the geostrophic currents from the filtering SLA which will be plotted as a hovmöller diagram, i.e a latitude-cycle diagram. These steps are detailed below for only one pass. They will be done again for all the passes in order to obtain one plot hovmoeller diagram for each pass.

- **Operation #1**

“Op_agulhas_coastal_096_Filt”: in “Operations” tab, click on “New” button to define a new operation, give the choosen operation name in the “Operation name” box.

In Data expression, drag and drop the variable “time” in “X”, nothing is reported in the optional “Y” field. Then drag and drop the following variables in “Data”: SLA_Filtered_41pts_MLE4, cycle, latitude, longitude.

Then, a Lanczos filter is applied to the SLA. Select the “SLA_Filtered_41pts_MLE4” in the Data expressions and click on the grey box “Expression”. Then click on the “Insert algorithm” button. A pop-up window opens. Define the Lanczos filter computation from the proposed algorithms: BratAlgoFilterLanczosAtp. Click on “OK” to close the pop-up window. A function-like expression is inserted in the Expression box. You have to check that the variable “Expr” matches the existing variables within your dataset (here, you have to drag and drop the “SLA_Filtered_41pts_MLE4” from “Fields” up to the “Expr” field). The Window Length, the Cut-Off and the minimum of valid points have to be defined. We respectively set 41,30 and 1. Finally, the filtered SLA computation is :
`exec(“BratAlgoFilterLanczosAtp”,SLA_Filtered_41pts_MLE4,41,30,1, 0)`

- **Export:** this “Op_agulhas_coastal_096_Filt” operation is exported by clicking on the “Export” button (upper right). A pop-up window opens. Set the “NetCDF format”, define the “Output file” name “Op_agulhas_coastal_096_Filt.nc” (don’t change the path). Click on “Execute operation before export” and on “Execute”. Once finished, the output file is available in the sub-directory “Operations” of your workspace.

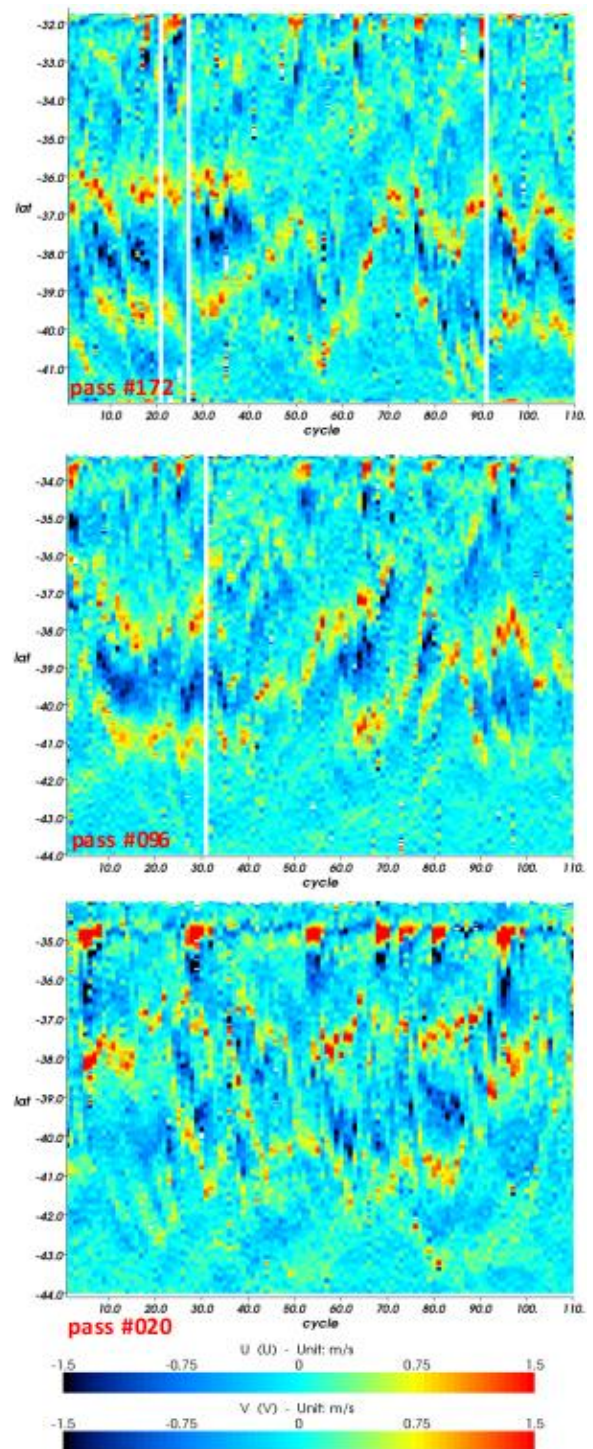


Figure 6.76. Latitude-time (cycle) diagram of coastal filtered geostrophic velocity anomalies, perpendicular to the track, up to the nearest point to the coast, for the Jason-2 passes #020 (bottom), #096 (middle) and #172 (top), between August 2008 (cycle 1) and July 2011 (cycle 110). The vertical white areas represent missing data.

- In the “Dataset” tab, create a new dataset “agulhas_coastal_096_Filt” by retrieving the previous operation saved in the the sub-directory “Operations” of your workspace.
- Operation #2: create a new operation named “Op_agulhas_coastal_096_UV” corresponding to the dataset “agulhas_coastal_096_Filt”. In Data expression, drag and drop the variable “cycle” in “X”, the “latitude” in “Y” and the “SLA_Filtered_41pts_MLE4” in “Data”. With a right-mouse click on Data, select ”Insert empty expression”, and rename this new expression with “U” (for East component). Click on the grey box “Expression” and then on the “Insert algorithm” button. A pop-up window opens. Choose the BratAlgoGeosVelAtp algorithm. A function-like expression is inserted in the Expression box. You have to check that the variable “Height” matches the existing variables within your dataset (here, you have to drag and drop the “SLA_Filtered_41pts_MLE4” from “Fields” up to the “Height” field). Finally, the expression for “U” is:
`exec(“BratAlgoGeosVelAtp”, latitude, longitude, SLA_Filtered_41pts_MLE4)`
 The “Y” spatial resolution is set to 1/99° in latitude in “Set Resolution/Filter”.
 Do the same for the North component. Execute the operation “Op_agulhas_coastal_096_UV”.

Views

Once the Operation finished, define a View in the “Views” tab:

- Create a new view and name it “Vi_agulhas_coastal_096_UV”. Then, drag and drop the U and V of the operation “Op_agulhas_coastal_096_UV” from the list in the “Available” box, under the Z=F(X,Y) section, located on the left, to the “Selected” box on the right. Click on the “Selected” U expression and below, click on the box “East component”. Define the Min/Max for “U” under “Display Expression Properties”: -1.5/1.5 (unit=m/s). Then click on the “Selected” V expression and below, click on the box “North component”. Define the same Min/Max for “V”. Finally, click on 'Execute'.
- The display window opens, and your hovmöller diagram is created.

Results

The Agulhas current is a major western boundary current flowing in the southwestern Indian Ocean. Near the South African coasts, it follows the narrow continental shelf where is characterized by stable flow conditions. Nevertheless, some variability patterns occurs during the “Natal Pulses”, some solitary cold cyclonic meanders. These meanders are generated at the Natal Bight (off Durban), close to the coast, and move downstream along the Agulhas Current by going away from the coast.

Natal pulses can be identified with satellite altimetry as depressions in the sea surface topography (see also negative sea level anomalies on Figure 6.75 left) and as negative flow anomalies in the geostrophic velocity anomalies, describing southwestward flow anomalies (Figure 6.76). Evidence of such variability are several times plotted on the latitude-time diagrams, in the northern extremes of each figure: around -35.5°S for pass #020, around -34.5°S for pass #096 and around -33.3°S for pass #172. The Natal Pulse is well observed either on the western part of the area (on the pass #020) when it comes off the coast, or in the eastern part (pass #172) when it flows closer to the coast.

Validation

To assess the quality of the CoastalDT-SLA product, some comparisons with external data have been done (note that these figures have not been plotted with BRAT).

SAR

The small scale structures (50 km wavelength) observed with the CoastalDT-SLA product are confirmed by the SAR currents. The coastal anomalies retrieved with CoastalDT-SLA in the last 50 km are confirmed by SAR data.

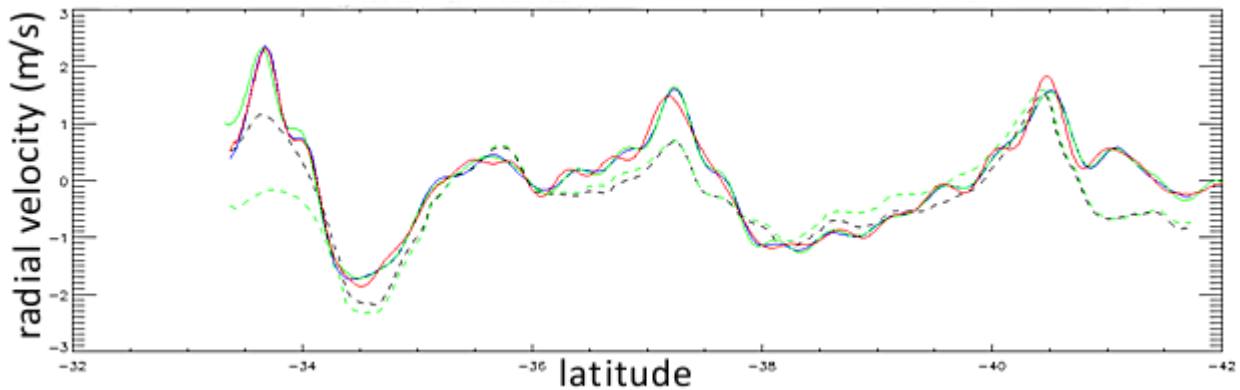


Figure 6.77. Comparison of velocity anomalies during cycle 65 (April 2010) between SAR projected velocities and CoastalDT-SLA product, Jason-2 pass #096 (note that the coast is on the left). SAR velocities anomalies are plotted in dashed lines: the green one corresponds to the original data (total current) and the black one corresponds to the SAR minus the mean current (MDT CNES-CLS09_v1.1). CoastalDT-SLA velocities anomalies are plotted in solid lines: the blue one corresponds to the MLE4 retracking, the green corresponds to RED3 and the red one corresponds to the OCE3 retracking. Credits CLS.

ADCP

The strong negative current anomaly ($\sim -34.5^{\circ}\text{S}$) occurred during a Natal Pulse event is coherent in position and amplitude between the CoastalDT-SLA product and ADCP *in situ* measurements. The same Natal Pulse event is also observed with the SAR currents the same day (see Figure 6.77).

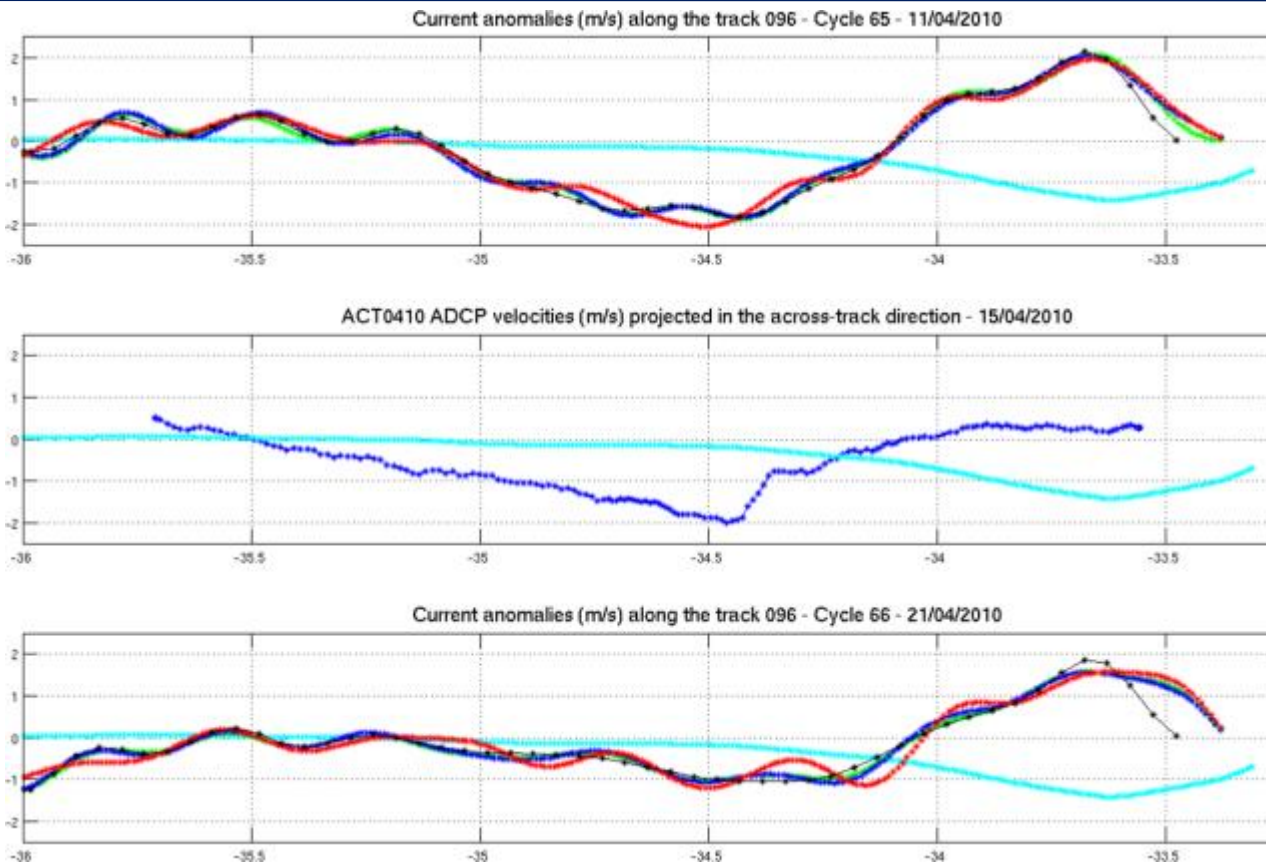


Figure 6.78. Comparison of velocity anomalies between ADCP projected velocities (middle) and CoastalDT-SLA product, Jason-2 pass #096 (top and bottom) on April 2010 (note that the coast is on the right). Cyan lines correspond to the mean current (over the 3 figures). Green lines (top and bottom) correspond to the MLE4 retracking, the blue lines correspond to RED3 and the red lines correspond to the OCE3 retracking. Blue line (middle) corresponds to ADCP in situ measurements. Credits Noveltis, ADCP data provided by ACT oceanographic cruise (RSMAS Univ. of Miami).

Tide gauge

By approaching the coast, the CoastalDT-SLA product provides additional data which are consistent with tide gauge observations (correlation >0.85)

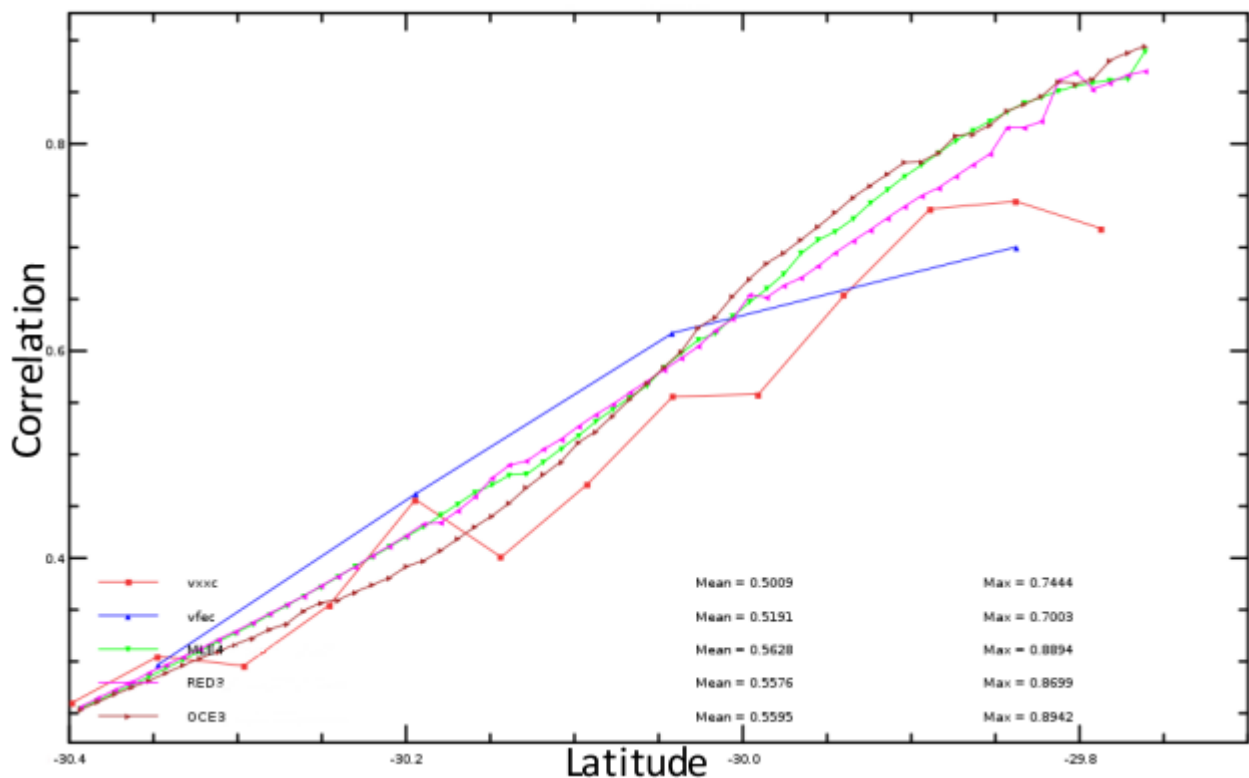


Figure 6.79. Correlation between the altimeter data (Jason-2 pass #248) and tide gauge measurements done in Durban (see details on the tide gauge identification, on the Aviso website). Blue line corresponds to Ssalto/Duacs Along-Track SLA vfec altimeter data, red line correspond to vxxc, green line correspond to MLE4 retracking in CoastalDT-SLA product, red line correspond to RED3 retracking in CoastalDT-SLA product and brown line correspond to OCE3 retracking in CoastalDT-SLA product. Credits CLS.

Further information:

- Other Data Use Case using CoastalDT-SLA products: [The Florida Keys by using coastal dedicated products](#)
- User Handbook: [CoastalDT-SLA User Manual](#)
- S.Labroue et al.: Level-3 PISTACH Products for Coastal Studies ([pdf](#), Presentation at the San Diego Coastal meeting, 2011)
- C.Dufau et al.: The PISTACH product: altimeter data for coastal ocean, Presentation at the 2012 EGU meeting (EGU2012-12649).
- J.Tournadre et al.: Agulhas Current Estimation from High Resolution Altimetry ([pdf](#), Presentation at the San Diego Coastal meeting, 2011)
- F.Collard et al.: Surface Current in the Coastal Region of the Agulhas Current. ([pdf](#), Presentation at the San Diego Coastal meeting, 2011)

6.8.6 The Florida Keys currents by using coastal dedicated products

Satellite altimetry is limited near the coastlines due to land contamination in the altimetry and radiometric footprints (10 km and 50 km of footprint diameter, respectively) but also to inaccurate geophysical corrections. Despite this, the altimetric measurements are present and may contain useful information for coastal studies.

This data use case proposes to give some instructions on how to use the Coastal along-track Delayed Time Sea Level Anomaly (CoastalDT-SLA) products distributed by Aviso in the Florida Keys area, a chain of little islands and reefs in South of the Florida Strait. We will obtain a map with the filtered across-track geostrophic velocities anomalies for a given date.

Data used

The Jason-2 Coastal along-track Delayed Time Sea Level Anomaly (CoastalDT-SLA) product over the Florida Keys area is used here.

The CoastalDT-SLA are Level-3 products, conceived as an evolution of the Jason-2 Level-2 coastal products, commonly called Pistach products. The Level-2 products rather address altimetry experts and are quite difficult to use for non expert users.

The CoastalDT-SLA products are easier-to-use and offer high resolution (20-Hz sampling rate) sea surface height on reference tracks. Differently from the Level-2 products, the CoastalDT-SLA products are only computed over specific ocean areas (see details on the Aviso website and in the dedicated User Manual).

Download CoastalDT-SLA data file on the Aviso FTP server for the Florida Keys area. An authentication is required to access it. It can be obtained by filling in the form on Aviso and by selecting the CoastalDT-SLA product on the second page. Once connected to the server, files are in the sub-directories named /experimental/coastal_dt_sla_j2.

Ssalto/Duacs Along-Track Sea level anomalies are used here for comparison with the CoastalDT-SLA products. They are also distributed by Aviso and can be downloaded from the same authenticated FTP server with the same login/password (see details on the Aviso website and in the dedicated User Manual). Once connected to the server, files are in sub-directories named /global/dt/upd/sla/j2_cf and files are typically named dt_upd_global_j2_sla_vxxc_20090805_20090812_20110329.nc.gz. We choose here to plot the cycle 42 which corresponds to 2009/08/26 (use the tool conversion on the Aviso website to recover the cycle at a given date and vice versa). Download the corresponding file included the cycle 42: dt_upd_global_j2_sla_vxxc_20090826_20090902_20110329.nc

Methodology

We use the Broadview Radar Altimetry Toolbox to observe the data, do some computation and plot the across-track geostrophic velocities anomalies.

Data chosen

- For the CoastalDT-SLA product, the Jason-2 interesting pass over the Florida Keys area is a descending pass: #102. The time series used for this data use case stretches out from the cycle_001 (July 2008) to the cycle_110 (July 2011) (all the cycles are included in the file).
- Ssalto/Duacs Along-track Sea level anomalies used for comparison with the CoastalDT-SLA products contain all the available passes during a 7-days period. A selection based on the pass number (#102) is shown in BRAT (in Operations tab, see the following step).

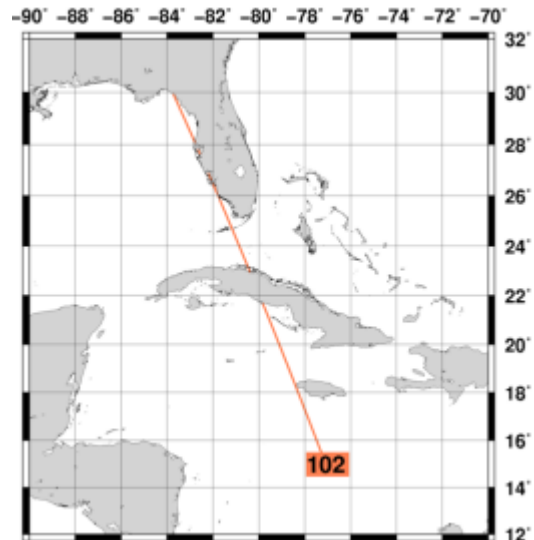


Figure 6.80. Jason-2 ground track over the Florida Keys area included in the CoastalDT-SLA product.

More altimetry data close to the coasts

Dataset

Once the relevant files are all downloaded, create a dedicated workspace in BRAT and then, create two datasets in the “Dataset” tab:

- a first one, named “flokeys_coastal_102” includes the CoastalDT-SLA product with only one file: coastal_dt_sla_j2_agulhas_102.nc. It contains all the time series between 2008-07-17 and 2011-07-07.
- the second, named “flokeys_duacs_102” includes the Ssalto/Duacs SLA file between 2009-08-26 and 2009-09-02.

Operations

On “Operations” tab, we create one operation for each dataset, CoastalDT-SLA and Duacs-SLA, in order to plot the map of filtered across-track geostrophic velocities. These operations are respectively named “Op_flokeys_coastal_102” and “Op_flokeys_duacs_102”.

- Operation “Op_flokeys_coastal_102”: in “Operations” tab, click on “New” button to define a new operation, give the chosen operation a name in the “Operation name” box.
- In Data expression, drag and drop the variables “longitude” in “X”, the latitude in “Y” and the “SLA_Filtered_41pts_RED3” in “Data”.
- With a right-mouse click on Data, select 'Insert empty expression', and rename this new expression with 'U' (for East component). Click on the grey box 'Expression' and then on the “Insert algorithm” button. A pop-up window opens. Choose the BratAlgoGeosVelAtp algorithm. A function-like expression is inserted in the Expression box. You have to check that the variable “Height” matches the existing variables within your dataset (here, you have to drag and drop the “SLA_Filtered_41pts_RED3” from “Fields” up to the “Height” field).

- Then, a Lanczos filter is applied to “U”. Always by hovering your mouse cursor on the grey box 'Expression', click on the “Insert algorithm” button. The same pop-up window opens. Define the Lanczos filter computation from the proposed algorithms: BratAlgoFilterLanczosAtp. Click on “OK” to close the pop-up window. A function-like expression is inserted in the Expression box. The Window Length, the Cut-Off and the minimum of valid points have to be defined. We respectively set 41,30 and 1. Finally, the filtered geostrophic velocity “U” computation is :
- `exec(“BratAlgoFilterLanczosAtp”,exec(“BratAlgoGeosVelAtp”, % {lat}, % {lon}, SLA_Filtered_41pts_RED3),41,30,1, 0)`
- The “Y” spatial resolution is set to 1/99° in latitude in “Set Resolution/Filter” (it corresponds to the inverse of the difference between two consecutive latitudes).
- Do the same for the North component. Set the “X” spatial resolution to 1/211°.
- A selection criteria is applied to only select a given date by choosing the cycle 42. By clicking on “Selection criteria”, move your mouse cursor on the grey box “Expressions” and write: `cycle==42`.
- Execute the operation “Op_flokeys_coastal_102”.
- Operation “Op_flokeys_duacs_102”: The previous Operation can be copied to create the operation corresponding to the “flokeys_duacs_102” dataset. Then, it will adapted to this new operation. To do that, select the previous operation (“Op_flokeys_coastal_102”) and click on the “Duplicate” button. Change the name to refer to the new operation name (“Op_flokeys_duacs_102”) and be aware to select well the corresponding Dataset with the corresponding Operation.
- In Data expression, we have the variables “longitude” in “X”, the latitude in “Y”. Delete the field under “Data” corresponding to the previous Operation (field “SLA_Filtered_41pts_RED3”) and drag and drop the “SLA” variable in “Data”. For the “U” and “V” expressions, only change the SLA field. Since the file resolution is different, change the “Step” in “X” resolution at 1/11° and the “Y” resolution at 1/19°. Select the unique pass #102 in Selection criteria by deleting the previous criteria (`cycle==42`) and by writing: `track==102`.
- Once the Operation has been defined, click on the “Execute” button.

Views

Once the Operation finishes, define one View per Operation in the “Views” tab:

- View “Vi_flokeys_coastal_102”: drag and drop the U and V of the operation “Op_flokeys_coastal_102” from the list in the “Available” box to the “Selected” box on the right. Click on the “Selected” U expression and, below, click on the box “East component”. Then click on the “Selected” V expression and, below, click on the box “North component”. Finally, click on 'Execute'.
- View “Vi_flokeys_duacs_102”: Do the same for the operation “Op_flokeys_duacs_102”.

Displays

Once the Views are ready, define one Display per View in the “Display” window.

- Display for CoastalDT-SLA product: choose your projection, the vector scale (here we have taken 1) and the range (0 to 2). Then, you can save the figure.
- Display for Duacs-vxxc product: choose your projection, the vector scale (here we have taken 1) and the range (0 to 0.6). Then, you can save the figure.

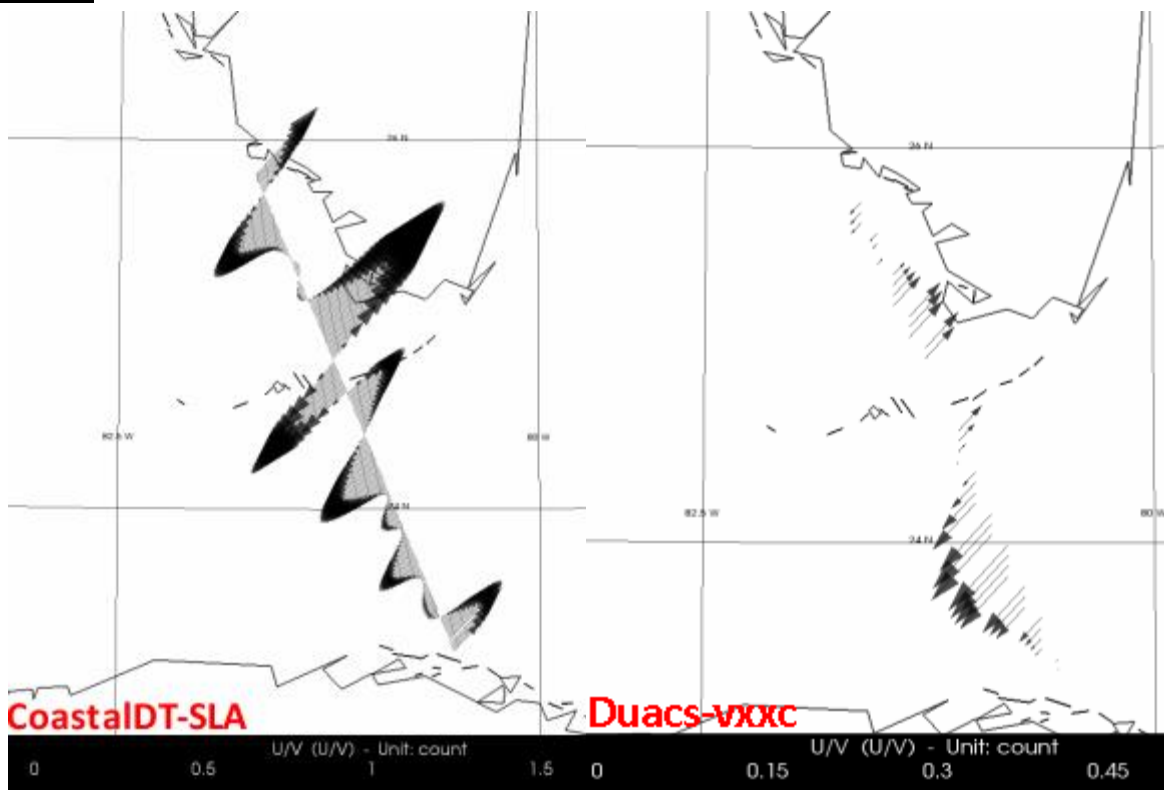
Results

Figure 6.81. Map of filtered across-track geostrophic velocities anomalies for the CoastalDT-SLA product (left) and the Ssalto/Duacs Along-Track “vvxc” product (right), along the Jason-2 pass #102, for the cycle 42 (2009/08/26), around the Florida Keys. Note that the vectors scale are not the same in the two panels.

Thanks to the CoastalDT-SLA processing associated to 20Hz processing, a better along-track sampling is obtained, more data are recovered near the coasts, on both sides of the islands, compared to Ssalto/Duacs along-track “vvxc” products.

Further information:

- Other Data Use Case using CoastalDT-SLA products: [The Agulhas current by using coastal dedicated products](#)
- User Handbook: [CoastalDT-SLA User Manual](#)
- M.Cancet et al.: Anomalies Derived from the PISTACH Products: the Loop Current Case ([pdf](#), Presentation at the San Diego Coastalt meeting, 2011)
- S.Labroue et al.: Level-3 PISTACH Products for Coastal Studies ([pdf](#), Presentation at the San Diego Coastalt meeting, 2011)
- V.Kourafalou et al.: Modeling and in Situ Observations around the Florida Keys Coral Reefs: Potential Applications of Coastal Altimetry ([pdf](#), Presentation at the San Diego Coastalt meeting, 2011)
- Y.Liu et al.: Altimetry on the West Florida Shelf ([pdf](#), Presentation at the San Diego Coastalt meeting, 2011)

6.8.7 Ice applications: Combined altimetry and radiometry for sea ice classification

Using both altimeter and radiometer, ocean surfaces potentially covered by sea ice can be classified into several sea ice types and age intervals.

The cryosphere plays an important role in moderating the global climate, in part due to its high albedo. Sea ice is seawater that has frozen (not to be mistaken with icebergs that are shed from continental ice).

Data used

Both altimeter and radiometer data are included in Geophysical Data Records. By giving a good overview of Polar Regions (-82.5°S / 82.5°N), Envisat mission is well adapted. However, since the period cycle is 35-days, the sea ice distribution can vary due to processes of formation, motion or melting. Envisat altimeter (RA-2) and radiometer (MWR) data are delivered on DVD-ROMs or by FTP and can be obtained from [EOHelp](#).

This dataset has another advantage. The Envisat GDR brings the opportunity to use algorithms other than the classical ocean-oriented ones that are better suited for non-ocean surfaces. One of them is optimized for sea ice, the so-called sea ice retracker. We used the brightness temperature from the MWR which is a dual-channel radiometer operating at 23.8 GHz and 36.5 GHz and whose primary goal is to measure tropospheric water vapor path delay correction for RA-2 altimeter.

Methodology

The earliest altimetry missions were dedicated to studying the open ocean, but since then the ability of radar altimetry to monitor ice surfaces has also been demonstrated. We use the Broadview Radar Altimetry Toolbox to observe sea ice changes through time.

Temporal extraction

We use data spanning the period of winter 2004 (Envisat cycle 025) and summer 2004 (Envisat cycle 029) in order to get seasonal variability.

Geographic extraction

In order to compute some statistical parameters for the brightness temperatures only on Polar Regions, we limit the coordinates between 50°N and 82.5°N and between 50°S and 82.5°S. We also apply the land mask here to exclude all data over continents.

Data editing

In the “Datasets” tab, click on “Add Dir” to download the numerous files for cycles 025 and 029 from the GDR Envisat in the same dataset (and use a meaningful name for the dataset to easily identify it later on, for example, Datasets_025_029).

A specific operation is made for statistical computation on each polar region. Select

longitude for “X”,

latitude for “Y”

and for the “**Data Expression**“, make the difference between the two brightness temperature ($\Delta TBs = \text{interpole_365_temp_mwr} - \text{interpole_238_temp_mwr}$).

In the “**Selection criteria**” box:

The data editing uses the formula as follows: **altim_landocean_flag** ≤ 1 , in order to apply a land mask. To compute expression on either Arctic or Antarctic region, we add (still in the selection criteria) a selection based on latitude coordinates as defined above ($\&\& \text{is_bounded}(50, \text{lat}, 82.5)$), for example, for the Arctic).

Finally, click on “Compute statistics” button. A file result gives the statistical value for Number of valid data, Mean, Standard deviation, Minimum and Maximum.

For a given cycle (here we choose the cycle 025), a second operation is created with the previous mean and the standard deviation values to normalize the ΔTBs as follows: $\Delta TBs\text{-norm} = (\Delta TBs - \text{mean } \Delta TBs) / \text{standard_deviation}$, ΔTBs corresponds to our new data expression. For the Arctic region, we have $\Delta TBs = (\Delta TBs - 4.82) / 10.77$.

In the views menu, we plot the file with the previous operation.

To map the backscatter coefficient (σ_0) for a given cycle (here we choose the Envisat cycle 025), we choose the backscatter coefficient computed from the sea ice retracking in the Ku-band and at 18 Hz. No statistical value is computed for this parameter. So, the operation can directly be made selecting longitude for “X”, latitude for “Y” and for the “Data expression”: 18 Hz Ku-band sea ice backscatter coefficient. The data editing uses the formula as follows: **altim_landocean_flag** ≤ 1 $\&\& \text{is_bounded}(0, \text{hz18_ku_seaice_bscat}, 45)$.

Results and comments

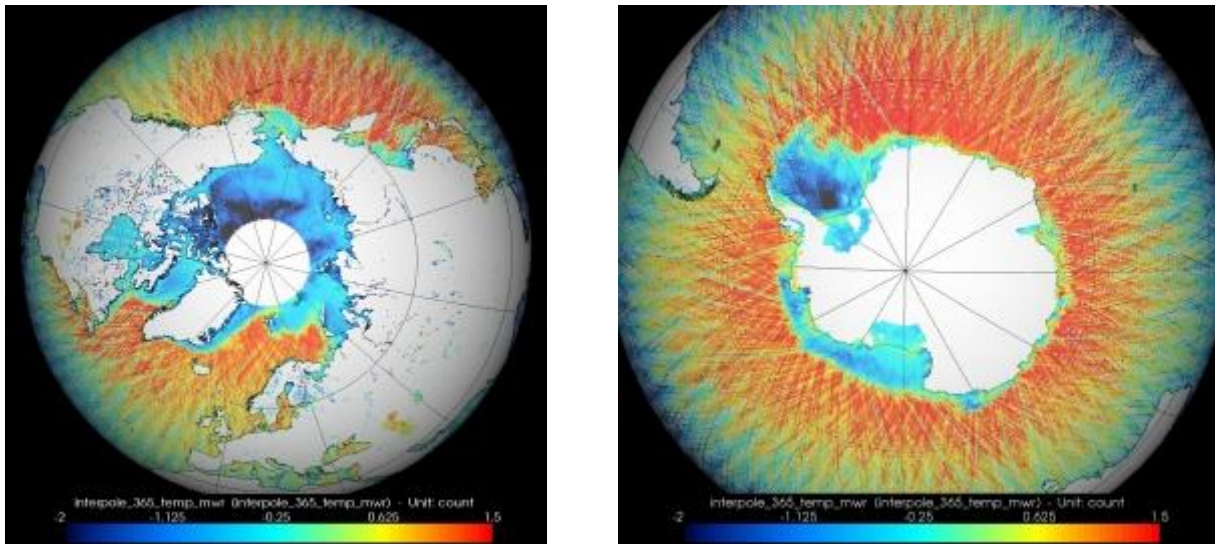


Figure 6.82. Difference of the two brightness temperatures normalized, for the Envisat cycle 025 (2004/03/09 – 2004/04/12) over the polar regions.

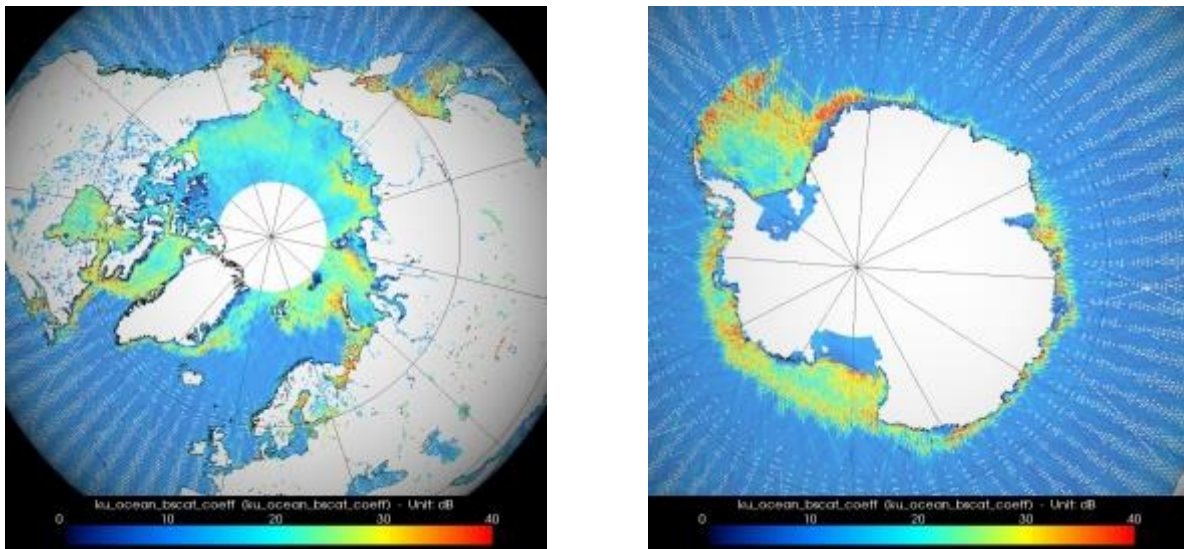


Figure 6.83. Backscatter coefficient in Ku-band (ocean retracking) for the Envisat cycle 025 (2004/03/09 – 2004/04/12) over the polar regions.

The distribution of the ΔTB s normalized values displays several structures with negative values (in dark colours), with neutral values (in light-blue colours) and positive values (in red colours). These structures are in accordance with those shown in Tran et al., 2009. Based on clustering method and reference maps, their study describe several sea ice types from Envisat altimetry and radiometry data. By using their conclusion, we can easily retrieve some of these sea ice categories over our maps:

- ice-free ocean for the highest positive ΔTB s-norm values and the lowest sigma0 values (<10 dB),
- multi-year sea ice for the lowest ΔTB s-norm values and low sigma0 values (0-15 dB),
- first year sea ice for neutral ΔTB s-norm values and the highest sigma0 values (20-30 dB).

Further information:

- Tran, N., Girard-Ardhuin, F., Ezraty, R., Fenf, H., Fèmèniàs, P., Defining a Sea Ice Flag for Envisat Altimetry Mission, in *IEEE Geoscience and Remote Sensing Letters*, Vol. 6, No. 1, January 2009.

6.8.8 Ice caps applications: Altimetry for observing polar ice caps

Altimetry is one of the most powerful tools for monitoring ice sheets.

The cryosphere plays an important role in moderating the global climate. Rapid changes are occurring on ice caps margins that can significantly contribute to sea level rise. Altimeter data is a powerful tool for measuring both the dynamics and mass balance of ice sheets. Moreover, altimeters also provide other parameters such as backscatter coefficient and waveform shape that give information on surface roughness and snow pack characteristics.

Data used

By giving a good overview of Polar Regions (-82.5°S / 82.5°N), the Envisat mission is well adapted and able to accurately map 80% of Antarctica and almost all the Greenland. Envisat altimeter (RA-2) data are supplied on DVD-ROMs and by FTP and can be obtained from [EOHelp](#).

This dataset has another advantage. The Envisat GDR directly offers the opportunity to use other algorithms that are better suited for non-ocean surfaces. One of them is optimized for ice surfaces, the so-called ICE-2 retracker.

The RA-2 altimeter on Envisat platform is a dual-frequency radar operating at Ku-band (13.575 GHz) and at S-band (3.2 GHz). This dual-frequency can be used for better quantify wave penetration in the snowpack and improve the knowledge of the ice sheets surface topography evolution.

Methodology

Two parameters were used to map ice sheets: the radar altimetric backscatter coefficient, which corresponds to the waveform integrated power and gives information on surface characteristics and the leading edge width, which is related to the penetration into the medium and the surface roughness.

Temporal extraction

We use data spanning the period of summer 2005 (Envisat cycle 040).

Data editing

In the “Datasets” tab, we have selected both cycles 034 and 040 in two different datasets and named them: Dataset_cy034 and Dataset_cy040.

In the “Operations” tab, we have created a first operation for the backscatter coefficient for each Dataset_cycle. Select longitude for “X”, latitude for “Y”. For the “Data expression”, use the difference between the two bands S-Ku: `hz18_s_ice2_bscat – hz18_ku_ice2_bscat`. The following selection criterium limits the backscatter coefficient boundaries to exclude the most erroneous data and applies an ocean mask: `((altim_landocean_flag > 0) && (is_bounded(0, hz18_s_ice2_bscat, 45))) && (is_bounded(0, hz18_ku_ice2_bscat, 45))`. This first operation is duplicated to be applied on the second cycle but be careful to select the corresponding dataset.

In order to give you several examples, we choose to represent two different geographic resolutions for each cycle: 1/3° for cycle034 and 1° for cycle040. This is done by clicking on “Set Resolution/Filter AND selecting the “step” in X resolution and Y resolution.

The second operation is applied to the difference S-Ku band on the leading edge width: select longitude for “X”, latitude for “Y”. For the “Data expression”, use: `hz18_s_ice2_edge_width – hz18_ku_ice2_edge_width`. A selection criterium masks the data over the oceans and tends to eliminate most of the bad data: `((altim_landocean_flag > 0) && (is_bounded(0, hz18_ku_ice2_edge_width, 7.7))) && (is_bounded(0, hz18_s_ice2_edge_width, 7.7))`.

In the “Views” tab, select each operation to be plotted and “execute” it.

Results and comments

In the S-band, the radar waves penetrate deeper in the snow and ice than the Ku-band and it is less sensitive to the slope effect than the Ku-band. From this known physical properties, we are able to see differences on high altitude areas: over West Antarctica, the S-band waves are less constrained by the slope effect and less attenuated by the snow grain, providing a stronger return echo than the Ku-band. This is clearly visible on the map below for the cycle 040 (Aug.-Sep.2005) where, over West Antarctica, a long area with a north-south direction shows a positive difference between the two bands.

On the contrary, the Ku-band gives higher values over Central-East Antarctica .

In southern winter (Envisat cycle 034, Jan.-Feb. 2005) and in southern summer (Envisat cycle 040, August-Sept. 2005), the figures below are quite similar (except for the resolution), we find essentially the same distribution for the backscatter difference.

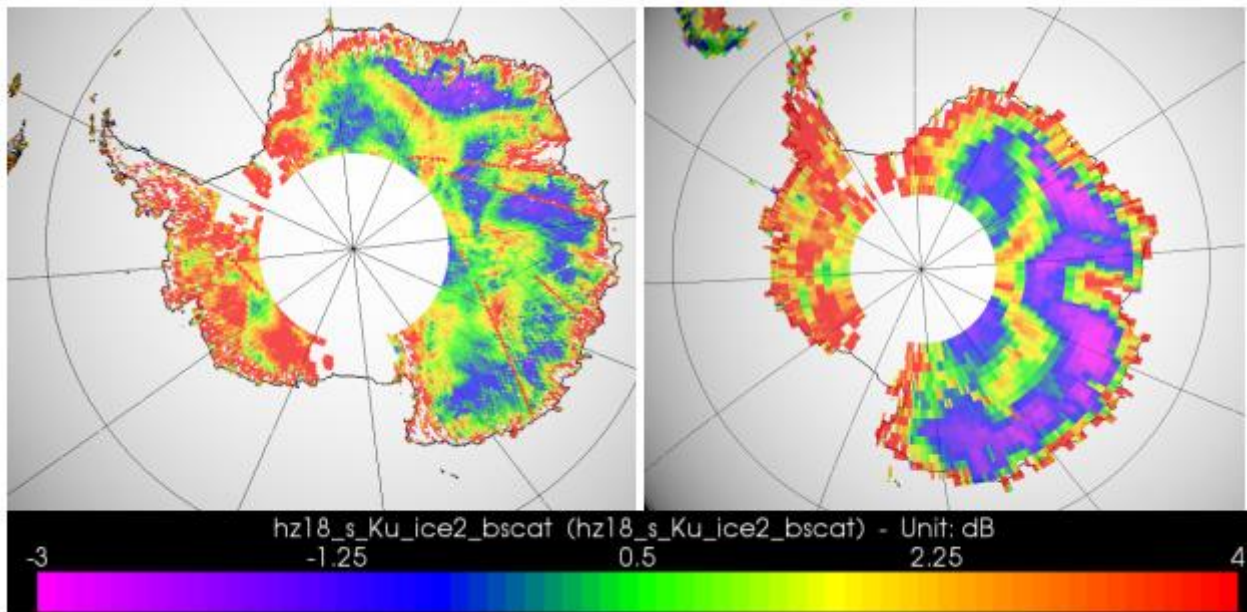


Figure 6.84. Backscatter coefficient difference (in dB) between the S and the Ku-bands over Antarctica, from Envisat cycle 034 (left) and 040 (right). As explained above, we give an example with two different geographical resolutions: $1/3^\circ$ on the left and 1° on the right.

The leading edge width in S-band tends to have smaller values than the Ku-band one toward the coastal areas over Greenland. On the contrary, the leading edge width in S-band has higher values on the plateau and its distribution seems to be lightly larger during winter (Envisat cycle 034 -below, left-).

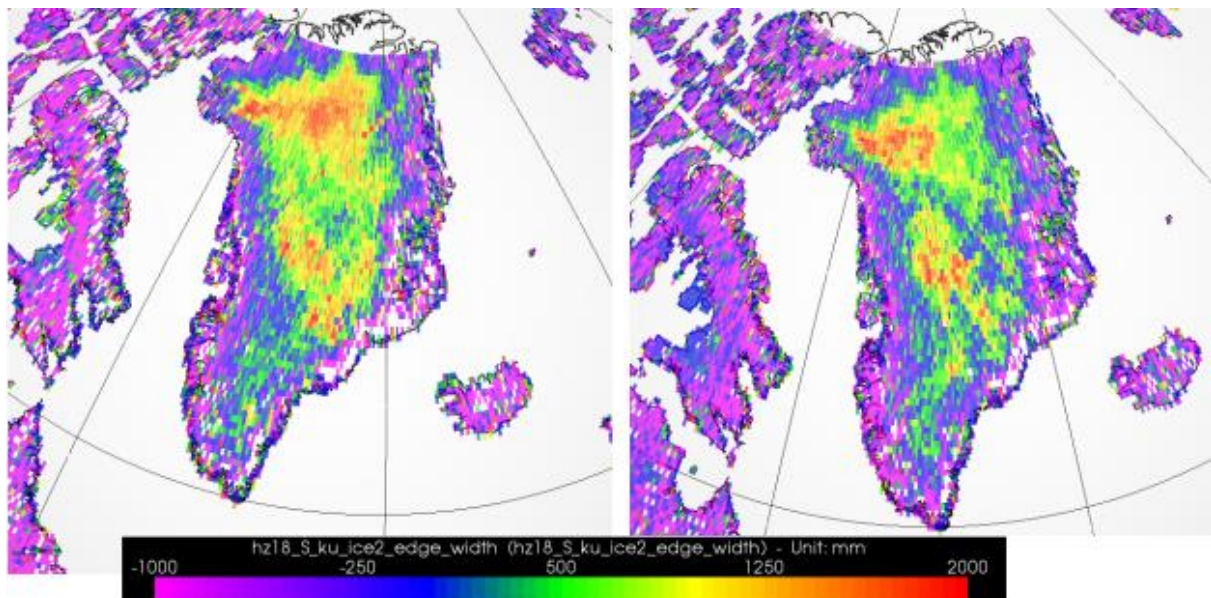


Figure 6.85. Leading edge width difference (in m) between the S and the Ku-bands over Greenland, from Envisat cycle 034 (left) and 040 (right).

Further information:

- Legrèsy, B., Papa, F., Remy, F., Vinay, G., Van Den Bosch, M., Zanife, O-Z., Envisat radar altimeter measurements over continental surfaces and ice caps using the ICE-2 retracking algorithm, in *Remote Sensing of Environment*, Vol. 95 (2005), 150-163.

6.8.9 Ice applications: CryoSat over continental ice

The cryosphere plays an important role in moderating the global climate. Altimeter data is a powerful tool for measuring both the dynamics and mass balance of ice sheets (and sea ice). The CryoSat mission was specifically designed to study such phenomena.

Data used**Low Resolution Mode (LRM) data**

The Low Resolution Mode (LRM) is in the most classical (pulse-limited) altimeter mode. This mode is generally selected for CryoSat wherever no margins are expected (outside some test areas), i.e. on ocean and in the interior of ice lands, including Greenland and Antarctica.

Methodology

Two parameters are used here to map ice sheets:

- the radar altimetric backscatter coefficient which corresponds to the waveform integrated power and gives information on surface characteristics.
- the surface height with respect to the reference ellipsoid (i.e. altitude – (satellite-surface distance), corrected for instrument effects, propagation delays, measurement geometry, and other geophysical effects such as tides).

Time period

We use data measured during the period September 10 – October 9, 2010 (roughly one CryoSat 30 days pseudo-cycle).

For comparison, we took the Envisat IGDR data over the same period.

Operations

We use the Broadview Radar Altimetry Toolbox to read and visualize the CryoSat and Envisat data.

CryoSat Low resolution Mode (LRM) data

In the “**Datasets**” tab, we have selected a series of files from September 10, 2010 to October 9, 2010. All are “LRM” data, so mostly over ocean and inland the ice caps.

Select longitude for “X”, latitude for “Y”.

As Data expression, we choose:

– surf_height (note that this is a high-resolution (20 Hz) data)

– bkscat_sigma_0 (note that this is a high-resolution (20 Hz) data). The following selection criterium limits the backscatter coefficient boundaries to exclude the most erroneous data and applies an ocean mask: (surf_type_flags > 0) && (is_bounded(0, bkscat_sigma_0, 45)).

Envisat IGDR data

For Envisat, we make a second operation, and take the corresponding variables in Ku band.

– corrected height: alt_cog_ellip – hz18_ku_band_ocean – mod_dry_tropo_corr – solid_earth_tide_ht – geocen_pole_tide_ht – ra2_ion_corr_ku – mod_wet_tropo_corr

– hz18_ku_ice1_bscat (the “ice1” or “OCOg” retracking being the closest to CryoSat one, and the Ku band the frequency used by CryoSat; note that this is a high-resolution (18 Hz) data)

And the selection criteria: ((altim_landocean_flag > 0) && (is_bounded(0, hz18_ku_ice1_bscat, 45))) && (is_bounded(0, hz18_ku_ice2_bscat, 45)).

In the “Views” tab, select each variable to be plotted and click on “Execute”, one after the other.

Results

Once plotted, the two parameters can be looked at over Greenland and over Antarctica. Note that the margins of those lands are not visible within CryoSat, since we are using “only” LRM data. The borders of those lands are measured using the SAR-interferometric mode.

NB. Results illustrate just the methodology as much more work is needed to study these phenomena with CryoSat (including the use of longer time series).

Sigma0 gives an indication of surface roughness: the rougher the surface, the less signal will be received by the altimeter. Monitoring this quantity thus enables to follow surface roughness variations (e.g. snow melt or fall, freezing of surfaces or breaking of the ice, flooding...)

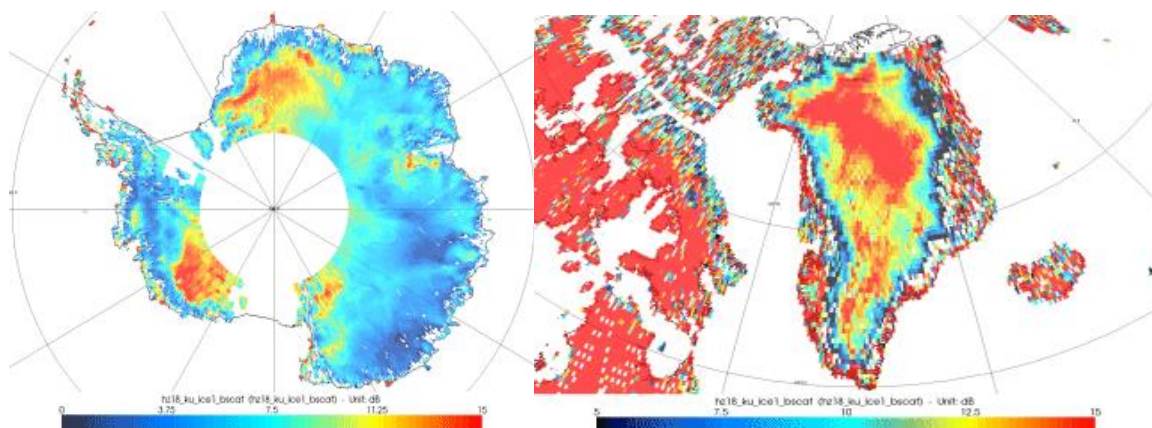


Figure 6.86. Sigma0 in Ku band over Greenland and Antarctica from Envisat (ice1) IGDRs.

(Corrected) Surface height is one of the fields available within the CryoSat Level 2 data, and can be computed in Envisat.

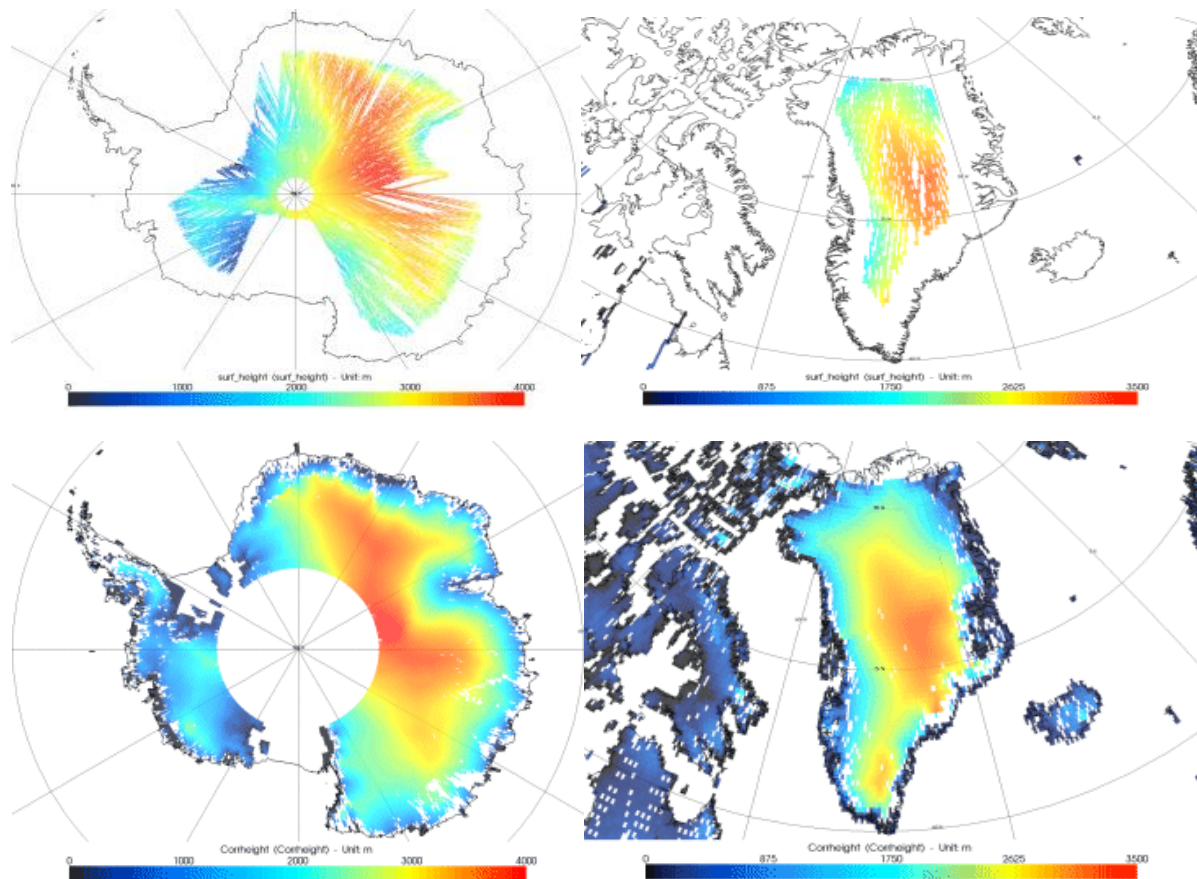


Figure 6.87. Surface height in Ku band over Greenland and Antarctica from CryoSat LRM mode (top) and from Envisat (ice1) IGDRs (bottom). Note that CryoSat gives measurements much closer to the pole (margins of the iced lands being in SARIn mode, these are not represented in the plot even though the satellite was measuring over the whole Earth).

6.8.10 Ice applications: CryoSat over sea ice

The cryosphere plays an important role in moderating the global climate. Altimeter data is a powerful tool for measuring both sea ice as well as the dynamics and mass balance of ice sheets). The CryoSat mission was specifically designed to study such phenomena.

Data used

Low Resolution mode data

The Low Resolution Mode (LRM) is in the most classical (pulse-limited) altimeter mode. This mode is generally selected for CryoSat wherever no margins are expected (outside some test areas), i.e. on ocean and in the interior of ice lands, including Greenland and Antarctica.

SAR and SAR-In mode

SAR mode enables to increase along-track resolution, and thus allows to better capture abrupt height variations (including those due to sea ice). Note that this is not an imagery mode as the SAR data may be.

SAR interferometry enables to retrieve slope values where measurements were taken and are mainly used over ice caps margins/glaciers.

We will look at waveform data in SAR and LRM mode (L1b data)

Methodology

To compare, we will use the Broadview Radar Altimetry Toolbox to infer waveform shapes over the Arctic, in SAR mode, and over the ocean, in SAR and LRM modes.

Geographical / Temporal extraction

We will use one file over the Arctic, one over the Atlantic off Portuguese coasts (SAR mode) and one over the Atlantic (LRM mode). Note that CryoSat L1b data are not provided as tracks or half-orbits, since the mode may change (L2 “GDR” data include, however, a flag to indicate the mode). Files are the following:

- CS_OFFL_SIR_LRM_1B_20101111T084452_20101111T085219_A001.DBL (LRM mode data, taken on 2010/11/11, in the Atlantic)
- CS_OFFL_SIR_SAR_1B_20101111T001539_20101111T002242_A001.DBL (SAR mode data, taken on 2010/11/11, in the Arctic)
- CS_OFFL_SIR_SAR_1B_20101111T195241_20101111T195604_A001.DBL (SAR mode data, taken on 2010/11/11, off the coast of Portugal)

Operations

In the “Datasets” tab, we select the three files, each in a different dataset.

In the “Operations” tab, we create four operations as follows: one using LRM mode data, one SAR mode data off the coast of Portugal and **two** using SAR mode data in the Arctic.

For all four operations, select the latitude that is in the for “X” **within the “time_orb_data” record** (in order to have high-resolution latitude), and as “Data expression”, the field “avg_pow_echo_wavf” (in the “wavf_data” record), which contains the 128 Ku-band waveform samples for each waveform.

In the “Selection criteria” expression, the geographical boundaries are limited as follows for the SAR mode data in the Arctic (CS_OFFL_SIR_SAR_1B_20101111T001539_20101111T002242_A001.DBL):

- is_bounded(-180, lon, -90) (for the first part of the track)
- is_bounded(110, lon, 180) (for the second part of the track)

This is needed in order to see the waveforms vs latitude in a chronological sequence (since the satellite goes from (-90°E, 82°N) to (110°E, 72°N) through 88°N. Otherwise, you can put in “mdsr_time” as X, but you will not be able to localize immediately your waveforms in the plot.

Execute the Operations

In the “View” tabs, you can choose between two different kinds of graphs:

- $Y=F(X)$ which plots the waveforms individually and represents the return echo power in function of time every 1/20th of a second.
- $Z=F(X,Y)$ which plots a set of cumulated waveforms as a function of latitude, as if seen from above.

Results

We are showing here a few examples of CryoSat waveforms over ocean (for comparison purposes), and over sea ice.

Over ocean

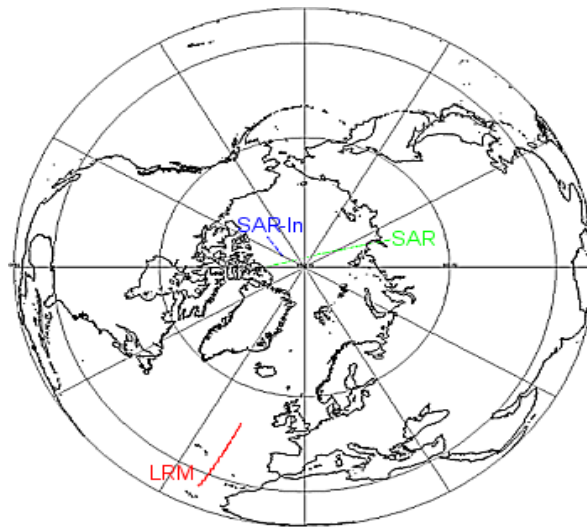


Figure 6.88. The three ground tracks visualized here (red LRM, green SAR, blue SARIn)

Since the best-known shape of a waveform is over ocean here is a comparison between one “LRM” (i.e. pulse-limited, or the “classical” altimetry) waveform and one “SAR” waveform, both collected in the Atlantic off the coasts of Portugal, and plotted in a $Y=F(X)$ mode. Most waveforms for either mode are looking like this (you can try and look at the whole series for each file, either by using the arrows to increase the index or by clicking on the “animate” button that browses automatically through the whole series). As expected, the SAR waveform is peakier than the LRM one (respecting the Brown-model waveform, see SAR Tutorial)

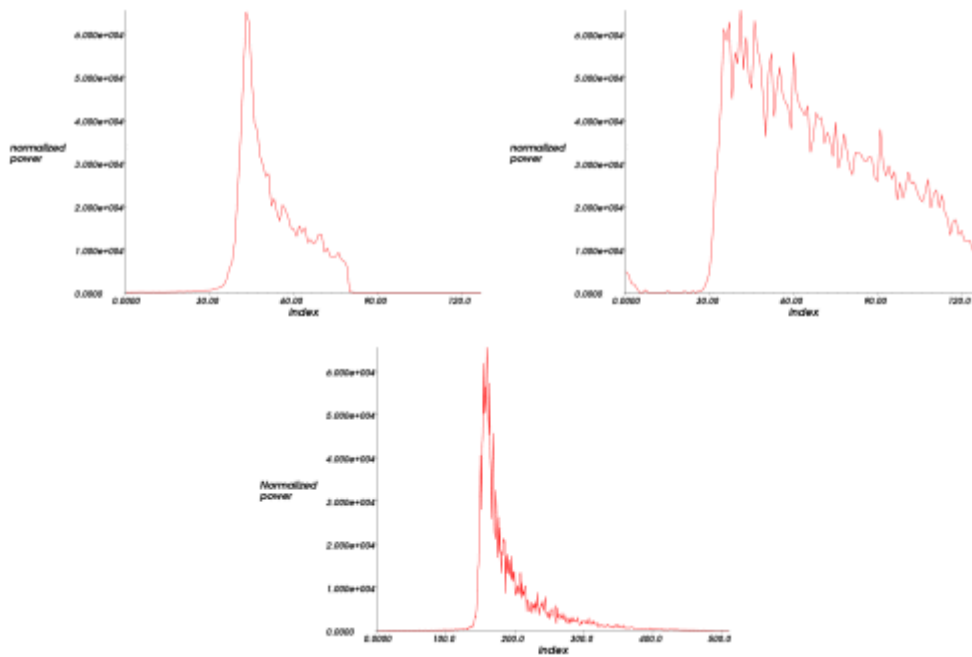


Figure 6.89. Three waveforms over ocean: in SAR mode (left) and, for comparison since it is the most usual shape of a waveform, in LRM mode (middle). (right) A waveform in SAR-In mode over ocean (South of Iceland). The number of gates in the SAR-In mode is 512 (vs 128 in the other two modes).

Over ice

We look at the SAR waveforms over the Arctic. In November, most of the surface of the Arctic Sea is frozen except a small area near the coasts of Siberia (Taimyr Peninsula). Compared with ocean SAR waveforms, the ones over sea ice are much rougher, since the surface where the radar wave reflects is more irregular than water. In the second part of the track (180°E-110°E), note that the data between 72°N and 76.75°N are over land, and much rougher.

Some waveforms seem to feature little peeks just before the main one. This might be the signature of a surface higher than the surrounding areas where the wave is reflected before being reflected by the main surface (this typically occurs when the ground track of the altimeter overflies an iceberg).

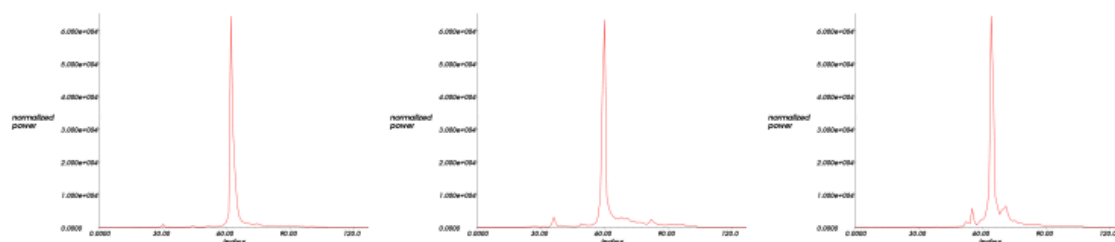


Figure 6.90. Waveforms over ice (Arctic) in SAR mode. Left, a very specular waveform. Middle and right two consecutive waveforms showing the signature of an early reflection with a small peak just before the main one.

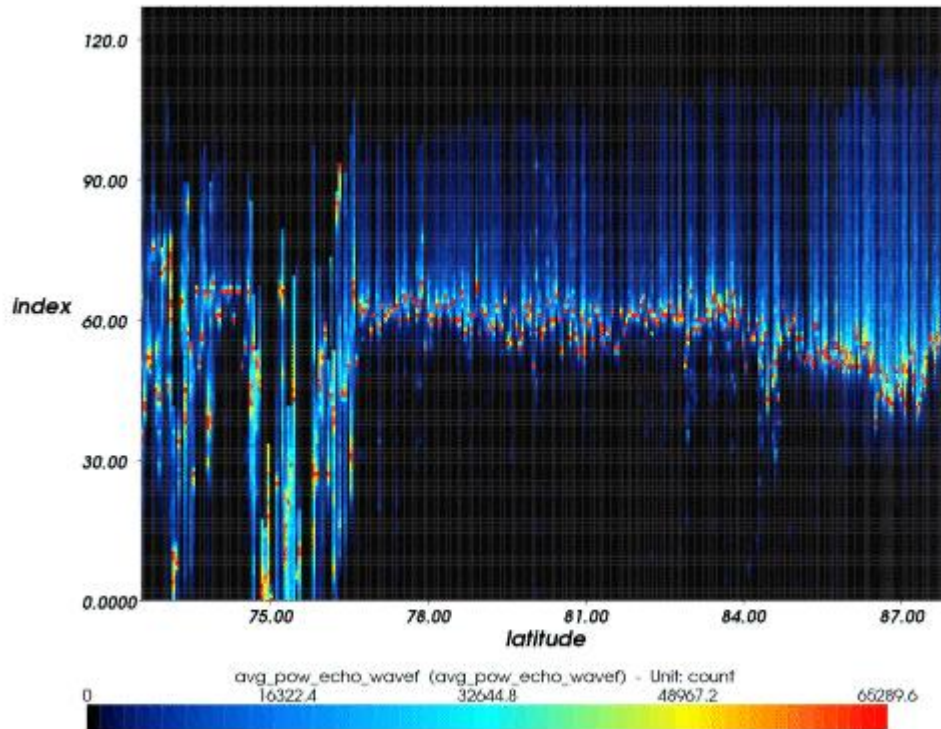


Figure 6.91. Part of the Arctic SAR track waveforms: the left side (up to about 76.7°N) corresponds to measurements over land. This representation also shows the specular quality of the SAR waveforms with respect to classical mode (see Hydrology data use case: Altimetric waveforms for monitoring lakes level)

Future developments

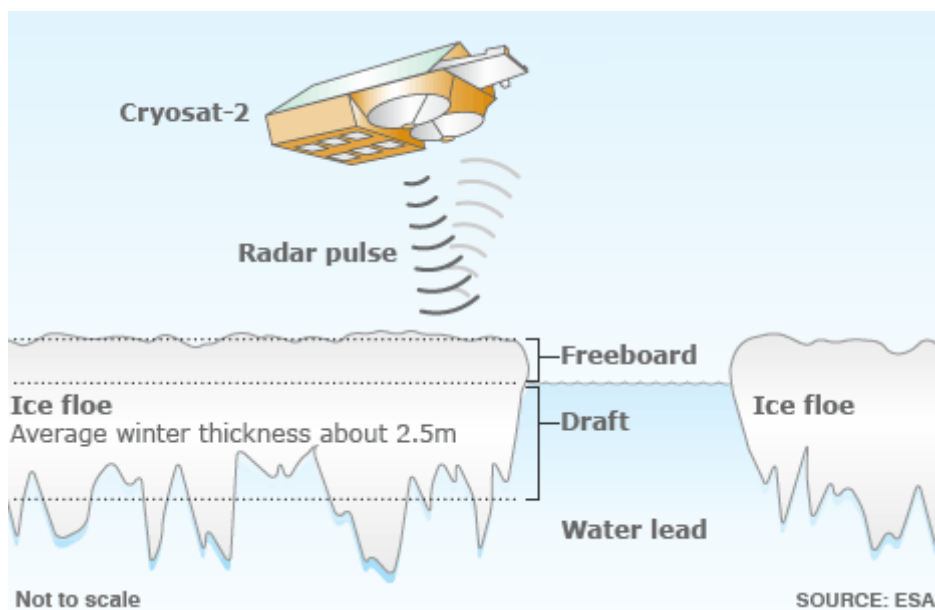


Figure 6.92. Ice Freeboard measurement

The sea ice freeboard can be computed, by subtracting the ice height to the MSS (subtracting snow thickness also, if need be). From this freeboard, since the ice is floating, taking into account ice and snow density and following Archimedes principle, sea ice thickness can be computed.

6.8.11 Monitoring El Niño: Rossby and Kelvin waves

El Niño is a climatic phenomenon occurring in the Pacific Ocean every two to ten years. During an El Niño event, a few months before Christmas, anomalous warm water accumulates off the coast of Peru. The El Niño event that occurred in 1997 was a good example of where satellite altimetry made a major contribution to monitoring such phenomenon.

Data used

No particular reprocessing of altimeter data is necessary in this case, so it is possible to use ready-made maps of Sea Level Anomalies. As combined data offer the best quality, and delayed-time the optimal orbit, we have chosen the merged DT-MSLA dataset, up-to-date ('Upd') data for better quality for a given date, and reference ('Ref') data for long temporal studies (see the second part: 'Ocean planetary waves').

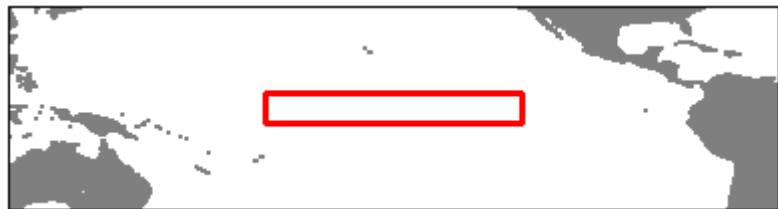


Figure 6.93. Area for data extraction

Methodology

Temporal extraction

Download MSLAs from 1992 to 2005. This could take some time (!), if necessary you can reduce the data period to 1996-2000. The main advantage of selecting such a long time period is to put the El Niño event into context.

Geographic extraction

Data selection concerns the Pacific Ocean, and specifically the following coordinates:

30°S-30°N,170°W-120°W (fig 1).

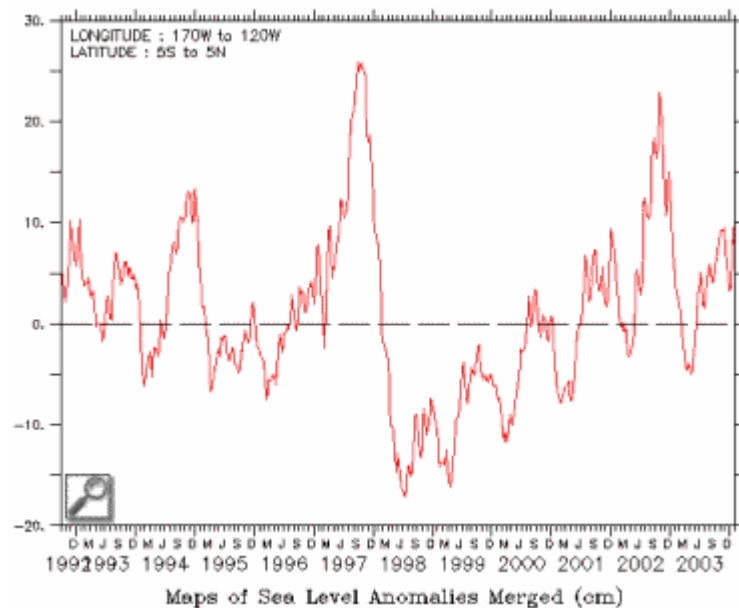


Figure 6.94. Temporal series of MSLAs in the El Niño area

Temporal series of MSLA

- Compute the geographic average for SLAs corresponding to the area defined by (5°S-5°N, 170°W-120°W). The value obtained, for a given time, represents the mean sea level anomaly over the equator in the Pacific Ocean. This averaged SLA shall now be referred to as M .

- Plot the curve $M=f(t)$ in order to show the temporal variations in M all along the chosen period.

The diagram shows periodic oscillations in M and illustrates the annual variability in sea surface heights. Moreover M 's value significantly increased in 1997 to over 25 cm: the signature of an occurring El Niño. Then, from summer 1998, sea surface height oscillations began again.

1997 El Niño

Focusing on 1997 enables us to consider specifically the month of November as an indicator of El Niño's intensity. Using only the four MSLA datasets available for November 1997, a new monthly mean map can be plotted (Figure 6.95 simply re-enlarge the selected area to $30^{\circ}\text{S}/30^{\circ}\text{N}$). This gives an overview of El Niño's distribution throughout the Equatorial Pacific Ocean during the month of November.

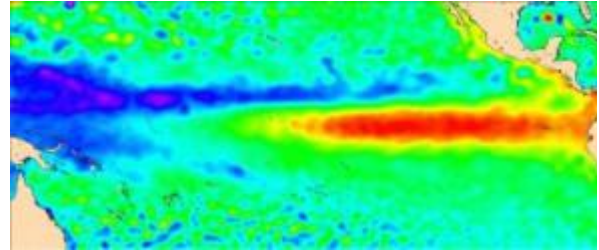


Figure 6.95. Monthly Mean of Maps of Sea Level Anomalies, El Niño area, during November 1997

It is now acknowledged that an El Niño event is caused by significant changes in wind stress; it thus provides a good example of existing interactions between ocean and atmosphere. However, sea surface slope changes, in terms of space and time scales, involving planetary waves (i.e. those with long wavelengths that can travel thousands of kilometres). These are known as Kelvin waves and Rossby waves.

Kelvin waves

Kelvin waves propagate eastwards in response to wind stress.

In the same way as for November, plot SLA maps for December and January. The resulting diagrams show the situation at successive monthly intervals: the maximum SLA values (i.e Kelvin waves) progress towards the South American coast and divide into two poleward Kelvin waves.

Rossby waves

One part of the Kelvin wave is deflected westwards: this is a Rossby wave, which propagates across the rise in thermocline at lower speeds (by a factor of approximately 3) than Kelvin waves. Space and time features of planetary waves suggest another approach to their study, as plotting maps for each month would be ineffective and tedious. Other diagrams, such as Hovmoller diagrams, can be useful.

Hovmöller diagram

In a Hovmöller diagram, SLA variations are plotted for time and longitude at a fixed latitude, which highlights the role of waves.

To plot such a diagram on the area (5°N-5°S, 135°E-75°W), select your time period (in the example the datasets go from the beginning of 1996 to the end of 1999), then compute the averaged SLA for latitude. Then plot this mean SLA for longitude and for the whole time period.

On this diagram, SLA appears to be streaked with colours: these straight lines represent ocean waves. The red stretch shows the El Niño event, where maximum values reached 40 centimetres around 125°W at the end of 1997.

Planetary waves transport heat and energy across the oceans, and satellite altimetry allows us to detect them because of the variations in sea level they generate.

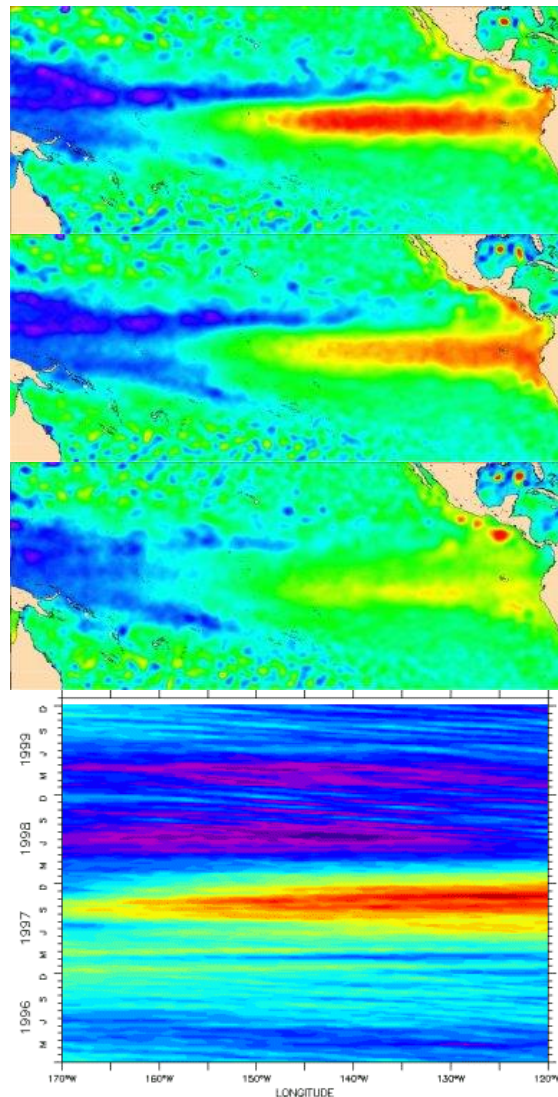


Figure 6.96. SLA Hovmöller diagram

6.8.12 Mean sea level

The long term sea level change is a crucial indicator of our climate, for example in response to increasing greenhouse gases. The spatial sampling offered by satellite altimetry and its continuity during the last 25 years are major assets to provide an improved vision of the mean sea level.

Data used

We use the gridded merged Ssalto/Duacs products, even if it is possible to compute the mean sea level directly from along-track monosatellite data like the Geophysical Data Records (GDRs). If you aim to process it with your own geophysical corrections, like tide or inverted barometer, we recommend you to use GDR-like datasets.

Methodology

Temporal analysis: the global Mean Sea Level (MSL) is directly computed on each individual map from an equi-area average of all the grid values. The MSL variations can then be plotted as a function of time. The MSL trend is estimated by the slope of the curve, after filtering higher frequency signals like 60-day and seasonal signals.

Geographical analysis: The sea level slope is computed at each individual grid point using a temporal analysis. The geographic distribution of the slopes can then be plotted on a map.

We propose to use the Ferret software combined with an Opendap access; Ferret is a free software widely used by oceanographers and meteorologists. Using the Ferret software allows us to perform a temporal analysis.

Temporal extraction

Launch Ferret, then type :

```
use
"http://opendap.aviso.oceanobs.com/thredds/dodsC/dt_upd_global_merged_msla_h"
```

Now you are “connected” to the merged maps of sea level anomalies FTP directory. Within Ferret, the command *show data* will provide file characteristics. The variable is named “grid_0001”, this is the parameter we are interested in.

Geographic extraction

No specific focus here, we are going to plot the mean sea level for the whole entire world.

Computing the mean sea level

Type the command *let mean = GRID_0001[x=-180:180,y=-82:82@AVE]*: this is to define a new variable “mean” that we are going to plot after.

Here Ferret has an interesting advantage: the average that Ferret is computing is already weighted with the cosine of the latitude. In ocean areas of lowest latitudes there are fewer points due to the Mercator grid, but of course they should not be less accounted for.

The command *plot mean[01-DEC-1992:20-SEP-2006]* now displays the temporal evolution of what we called “mean”, i.e the temporal series of each mean MSL estimation from December 1992 to September 2006.

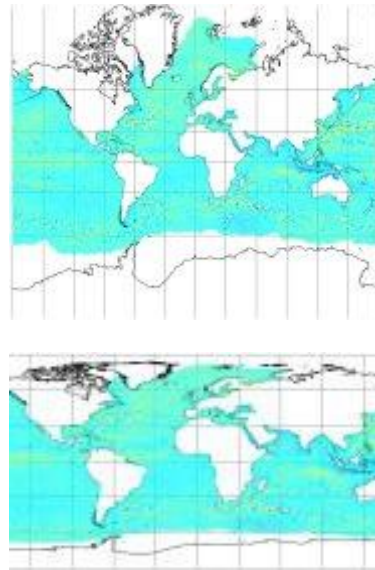


Figure 6.97. Example of sea level anomaly grids, September 20th, 2006. The maps are respectively on a Mercator grid and on a regular grid. To compute the global mean sea level, it would not make any sense not to attach the same weight for each ocean grid cell; that is why in considering the Mercator grid each value has to be weighted in latitude.

Results and comments

The mean sea level is dominated by several harmonics:

- annual signal
- semi-annual signal
- 60 days signal.

Actually if we want to really focus on the sea level rise we have to filter out these signals. Filtering these signals is a complex procedure not implemented here, but the final result is already available in NetCDF format on the AVISO web site ([link](#)). For example, you can plot and superimpose the two curves to observe the differences between filtered and non filtered MSL estimations.

The rate of the mean sea level rise as seen by satellite altimetry appears to be about 3 mm/year. This information has to be further quantified to estimate the contribution of each climate component (ice regions, ocean atmosphere exchanges...).

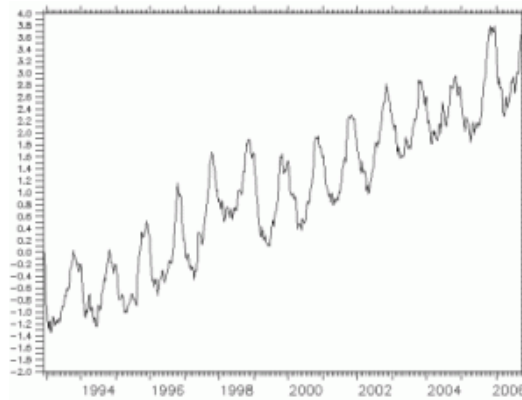


Figure 6.98. Mean sea level rise, computed using 14 years of altimetry data.

6.8.13 Seasonal distribution of Significant Wave Height

The global coverage and continuity made possible by satellite altimetry enables scientists to provide ocean wave climatology and to study large-scale patterns of wave variability. Below is a short example based on one year's satellite altimetry datasets using the Broadview Radar Altimetry Toolbox (BRAT)

Data used

We have focused on 2004 and have used gridded Jason-1 Near-Real Time (NRT) Significant Wave Height (SWH) datasets. Merged gridded SWHs (with improved quality) are not included as they have only been available since the end of 2005. It is also possible to use historical along-track SWH datasets and then grid them.

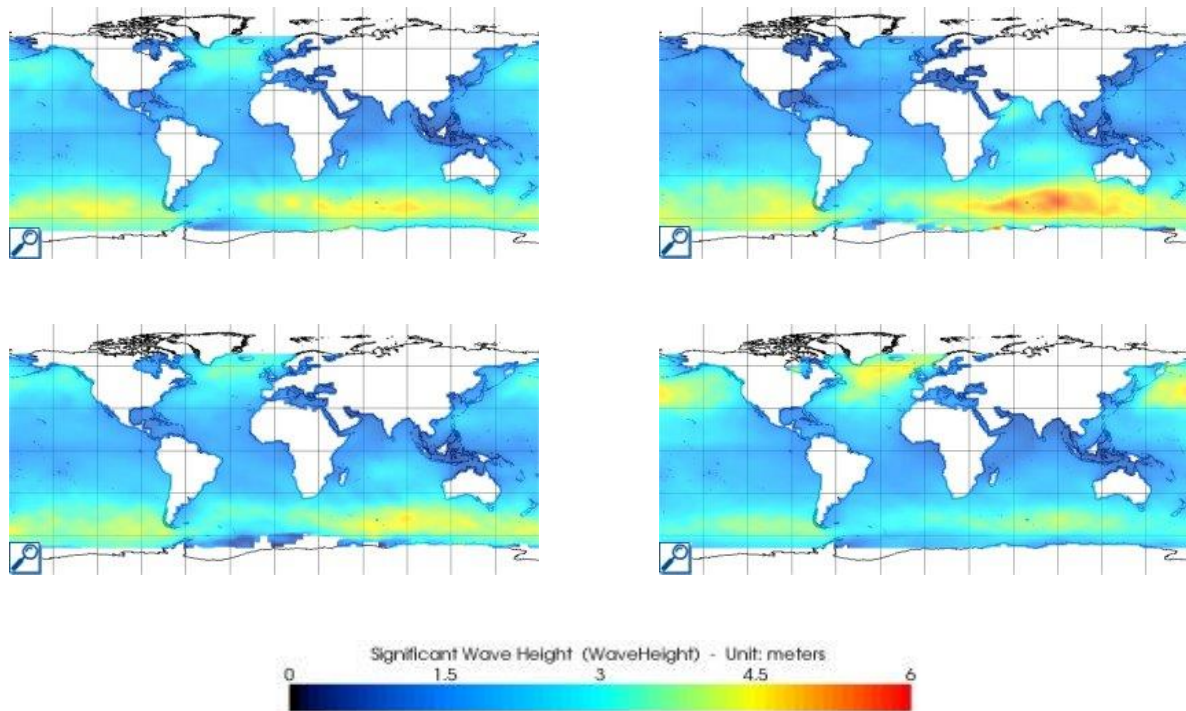


Figure 6.99. Seasonal map of global significant wave height derived from Jason-1 data acquired from March 2004 to March 2005. From top to bottom: spring (March-May), summer (June-August), autumn (September-November) and winter (December-February).

Methodology

Name the dedicated BRAT workspace you are using for this job. Within this workspace, name your dataset: as the study is based on four seasons, you can for example name your dataset ‘winter_swh’, ‘summer_swh’ etc., which will allow you to easily identify the kind of file in your dataset.

Temporal extraction

Download Jason-1 NRT MSWH. The time period ranges from early March 2004 (nrt_mswh_j1_19783.nc.gz) to the end of February 2005 (nrt_mswh_j1_20089.nc.gz).

Geographic extraction

No specific focus here.

Mapping the distribution of SWH

In the ‘Operations’ tab, name your computation (for example, ‘seasonal_mean’), then select your dataset and data. In ‘Data Computation’ keep ‘MEAN’ selected.

Enter your data expression: specify to BRAT that the data field is Grid_0001 and rename it ('MeanSWH'). For the X field the variable is 'Longitude', and for Y it is 'Latitude'. In both X and Y field options, enter 1 as the step value to obtain a 1°x1° map (which is the original resolution of this NetCDF file). Now your output file is ready to be executed.

In the 'Views' menu, you now only have to name your plot file, give the plot a title, select your NetCDF computed file and click on 'execute' to view it.

Results and comments

The global distribution of significant wave height displays a zonal structure, with a large band of high waves in the Southern Oceans that reaches its maximum around 50°S.

In the Northern Hemisphere's winter, the highest waves are located in the mid-latitudes, both in the central North Atlantic and North Pacific Oceans.

In the Northern Hemisphere's summer, high waves disappear in the North while they become stronger and larger in the Southern band.

Spring and autumn maps appear as transitional periods between the two previous ocean states.

Note also the signature of the monsoon in the Arabian Sea, where the increasing wave height reaches up to 3 metres in summer.

Wave climatology suggests possible links between the state of the oceans on inter-annual and seasonal scales (for example, are the wave climates of the North Atlantic and North Pacific connected?). It has also now been proved that North Atlantic wave climatology is linked to North Atlantic Oscillation.

Using more than 25 years of altimeter data, this investigation is still ongoing.

6.8.14 Observing wind and waves: hurricane Katrina

Data used

We will take advantage of the fact that several satellites were providing data at the time (August 2005), and use the GDRs from Envisat, Jason-1, Topex/Poseidon and GFO.

Methodology

We will use the Broadview Radar Altimetry Toolbox to have a look at significant wave heights and wind speed modulus as provided in the standard datasets.

Geographic extraction

We will be looking at individual ground tracks (one for each satellite), between 17°N and 30°N

Data selection and BRAT Datasets definition

To select the right tracks, you can have a look at the pass locator using Google Earth available through Aviso.

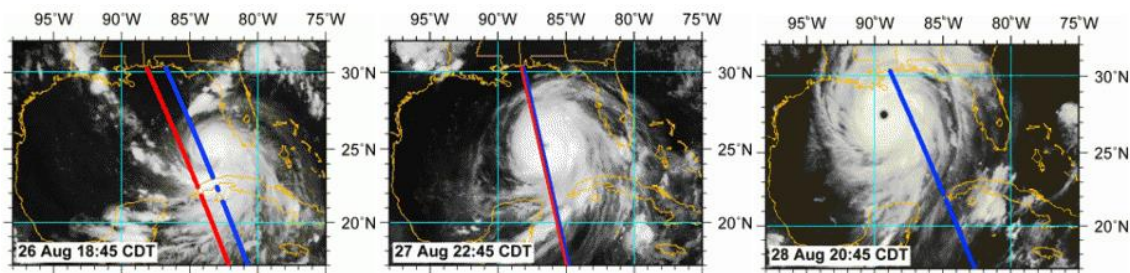


Figure 6.100. Katrina at different dates with T/P (red) and Jason-1 (blue) passes, Envisat (and ERS-2), and GFO passes. The images were taken within 20 minutes of the altimeter passes. (Credits NOAA/Altimetrics LLC)

The tracks and cycles closest to hurricane Katrina are:

- Envisat, cycle 040, pass #351
- Jason-1, cycle 134, pass #026
- Topex/Poseidon, cycle 477, pass #026
- GFO, cycle 157, pass #409

Name the dedicated BRAT workspace you are using for this job. Within this workspace, name your datasets. We will need 4 datasets: one for each satellite, with one file in each of them.

BRAT Operations definition

In the ‘Operations’ tab, name your operation (you will need 4 operations, too, one for each satellite), then select your dataset and data record. In ‘Data mode’ keep $Y=F(X)$ for a plot.

Enter your data expression:

We will define two data fields, one for Significant Wave Height in Ku-band, one for Wind speed modulus.

For the X field the variable is the latitude (beware that default is longitude, so you have to change it, and change the data type).

The only thing we will put in ‘Selection criteria’ is the ocean flag. “Classical” data editing (the one provided as pre-defined formula within BRAT) is not in order here, since we are dealing with a phenomena out of the ordinary (and thus over usual thresholds). Optionally, you can constrain the number of values used to compute a 1-Hz value (depending on the satellite; see the ocean data editing for ideas of significant values) and the wet tropospheric correction (between -1 and 1 m).

Results

Once the different operations are executed, you can plot them in the “Views” tab. Define minimum and maximum X for the plot (between 17 and 30°N); you can also use maximum Y at 15 m for SWH or 30 m/s for wind speed (minimum being 0). You can define two views: one for SWH, one for wind speed. Resulting plots should look like the ones below:

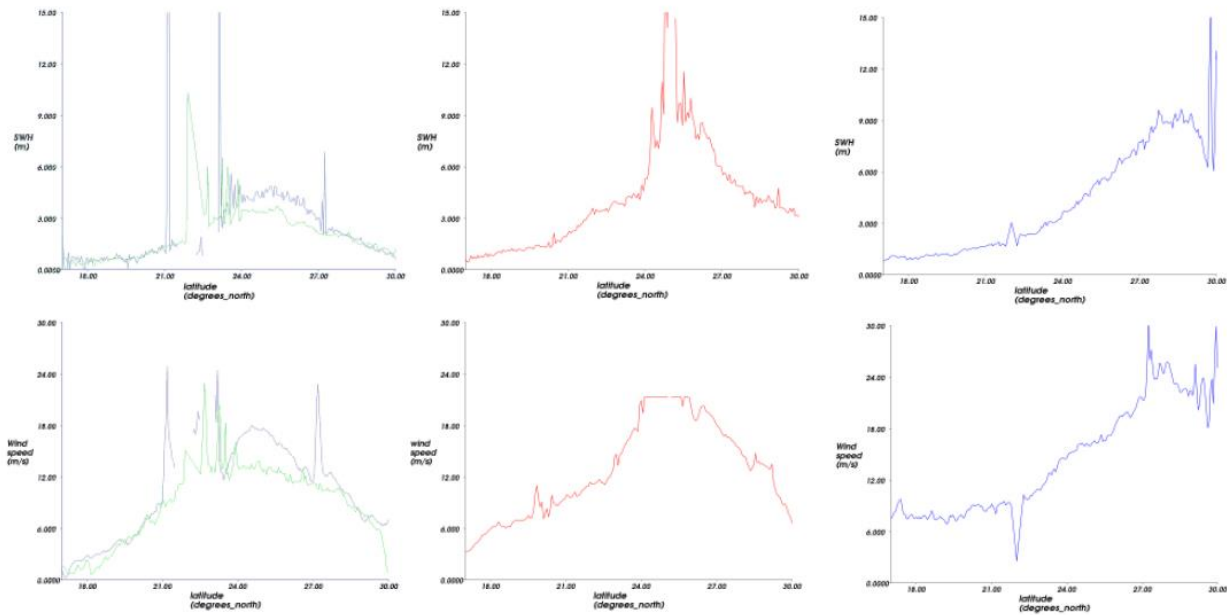


Figure 6.101. First three plots are SWH, second three are wind speed. T/P and Jason-1 are together on the first (T/P in green, Jason-1 in blue-grey), Envisat on the second (red) and GFO is on the third (blue).

Comments

- Topex and Jason-1 recorded significant wave heights up to 5 metres, and wind speeds around 20 m/s.
- Envisat crossed Katrina very near the eye of the storm and measured wave heights well beyond 10 metres and wind speeds around 30 m/s (wind speeds higher than 20 m/s can not be measured reliably; the algorithm used at that time in Envisat processing is making the plateau in the wind speed line).
- GFO caught up with Katrina shortly before making land fall. Wave heights and wind speeds sustained at 10 metres and near 30 m/s, respectively, with higher values measured near the coast.
- Wind speeds and wave height distributions appear asymmetric, with higher values measured windward of the eye.

See Figure 6.43 in the Application about Cyclones, hurricanes and typhoons

Scharroo, R., W. H. F. Smith, and J. L. Lillibrige, The impact of dynamic topography on the intensification of hurricanes, *15 years of progress in radar altimetry Symposium*, Venice, Italy, 2006

6.8.15 Temporal water surface height variations in enclosed areas: the Amazon Basin

Satellite altimetry was originally intended for open oceans. Monitoring river water levels using altimetry data presents a number of problems:

- the along-track ground resolution: each radar echo is separated by approximately 580 metres, meaning that satellite altimetry is not suited to studying narrow rivers,

- environmental and geophysical corrections models (such as the wet tropospheric correction) have been optimised for open oceans, and may sometimes be nonexistent for continents,
- lastly, radar echoes are subject to perturbations from surrounding terrain (vegetation canopy, topography). When considering the Amazon basin, we have to distinguish floodplain and wetlands water from the main river.

Data used

For studying water surface heights in the Amazon Basin, we are using altimetry measurements over land with the following parameters: geoid model, dry tropospheric correction, wet tropospheric correction and ionospheric correction.

Range values should preferably be computed from waveforms to obtain improved altimetric datasets: for processing radar echoes, retracking algorithms may be adapted to the ground type under study (this is not the intention of this particular 'Data Use Case').

Here we are using altimetry measurements from Topex/Poseidon Geophysical Data Records (GDR-M). Other suitable products include Envisat or Jason-1 GDRs, which provide altimetry measurements directly over land, unlike the ERS-1 and 2 missions for which only waveforms are available.

There are a few advantages and disadvantages to these datasets:

- The temporal period for Envisat is 35 days, and for Jason-1 is 10 days (like T/P); consequently, Envisat's spatial coverage is better than Jason-1,
- On the other hand, T/P was launched in 1992, which means that data series as far back as 1992 are available.

It is not possible to use CorSSH (Corrected Sea Surface Height) data here because only valid ocean measurements are available for this product.

Methodology

Initial geographic extraction for GDR-M

The first step is to limit the volume of altimetry data to our area of interest.

We therefore select and extract all the available data in GDR-M within the study area (5°S-10°S, 48°E-80°E), from October 1992 to December 2000 (Figure 6.102).

T/P GDR-M are supplied on DVD-ROM.

Distinguishing dry land data from water surface data

Waveforms are perturbed by interfering reflections due to water from wetlands, the vegetation canopy, floodplains and the main river. In this case, we have to identify water surfaces on the satellite ground track and discriminate rivers from flood areas.

6.8.15.1 Evaluating the measurement density parameter

Along with a given satellite track, all valid data are counted for the whole set of cycles over the entire period. For this purpose, we consider all available measurements (at 10-day intervals) inside successive circles of a 3 km radius; circles with less than 50% valid measurements are rejected. The

result is a ‘measurement density’ parameter, which is useful as an indicator of the availability of valid measurements (Figure 6.103).

6.8.15.2 Precise geographic extraction for the Manaus area

We next focus on the T/P ground track near the Rio Negro-Solimoes confluence, where we need to know the location of the land/water boundary as precisely as possible.

To do this, we have to locate intersections of T/P ground tracks and shore boundaries. In this case, accurate and ‘up-to-date’ georeferenced datasets are essential. Information is provided either from satellite images (SPOT for example) or a GIS (Figure 6.104).



Figure 6.102. T/P ground tracks in the Amazon Basin

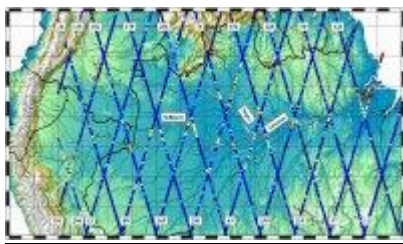


Figure 6.103. T/P density measurement in the Amazon Basin



Figure 6.104. Manaus area; white rectangle shows geographic extraction, T/P track 63 is in orange

We now know:

- the measurement density distribution for each ground track during the period,
- the location of T/P ground tracks, especially in the Rio Negro-Solimoes confluence area, using the most precise georeferenced geographic sources available.

Methodology

Computing water surface heights

Water level h' is computed from GDR-M using:

$$h' = s - r \quad \text{Eq. 8}$$

where s is the satellite's altitude (orbit) and r the range value.

Subtracting geoid and geophysical effects

Altimetry data must be corrected for geoid and propagation effects as follows:

$$h = h' - g - i - d - w \quad \text{Eq. 9}$$

where g is the geoid value, i the ionospheric correction, d the dry tropospheric correction and w the wet tropospheric correction. NB: For T/P GDR-M, the wet tropospheric correction is not available for continents; thus in the present study we are unable to take this parameter into account [de Oliveira Campos et al., 2001]. Note also that depending on the area being studied, the dry tropospheric correction is fairly static, which means that sometimes it is possible to compute water surface heights without applying this correction.

Computing a mean water level

For each ground track, a mean water surface height is computed using

$$h_{mean} = (\text{sum of } h_i)/n \quad \text{Eq. 10}$$

where h represents the value corresponding to the index i and n the number of altimetry measurements.

Mean water level variations in Manaus

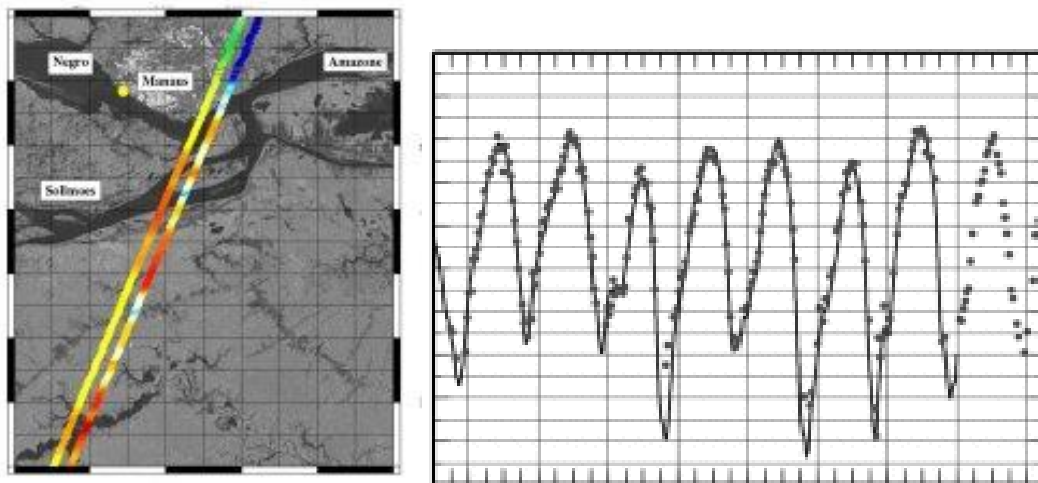


Figure 6.105. Right: Water level time series in the Amazon for T/P track 63 (3.21°S-3.14°S), in metres; dots represent in situ data from the Manau station. Left: Overview of the geographic window showing the stations; the backscatter coefficient and measurement density parameter have been computed along T/P track 63.

6.8.16 Monitoring Aral Sea level:

The Aral Sea level has been shrinking since the 60s, due to irrigation. The recession is estimated as nearly half of its volume over the last fifteen years. In 1989, the Sea split into two basins, the Great and the Small Aral. The small Aral is now stabilized, due to a dam, and its level may even be rising,

but the Great Aral is still drying up. Altimetry satellites measure sea level continuously over the long term and thus enable us to monitor variations in the Aral Sea.

Data used

We will take advantage of the more than 10 years continuous Topex/Poseidon dataset, and use the GDR-M 1Hz data, since the Aral Sea is (still) a big enough body of water that high-resolution data are not absolutely mandatory to study its variations.

Methodology

We will use the Broadview Radar Altimetry Toolbox to have a look at the Aral sea level variations along the years.

Geographic extraction

The exact coordinates of the actual Aral Sea have changed through the years, and the land mask provided with the data is no longer valid (i.e. places flagged as “water” are now dry). Roughly, the Big (South) Aral is between 59°N to 61°N, and 44°E to 46°E

Data selection and BRAT Datasets definition

We have to select the track(s) we wish to work on (we do not need the whole cycles of T/P data).

To select the right track, you can have a look at the ground track maps that may be provided with the data handbook. You can also use a [pass locator](#) using Google Earth available through Aviso.

The “best” Topex/Poseidon track that passes over the Aral Sea is the #107 (up till cycle 365, when the satellite orbit was changed). We took all available pass 107 data file from cycle 010 to cycle 364.

For Envisat, you could use pass #126 or 253.

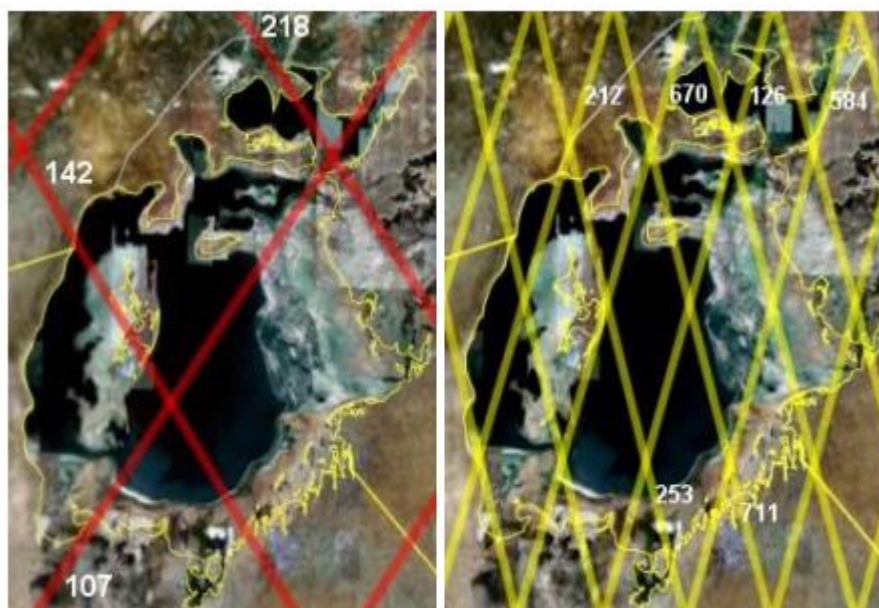


Figure 6.106. T/P (left) and Envisat (right) tracks over the Aral Sea

Name the dedicated BRAT workspace you are using for this job. Within this workspace, name your datasets; we will need 3 datasets: one for a cycle in 1992-1993 (e.g. cycle 010), one for a cycle in 2002 (e.g. 360), and one with the whole series of the pass #107.

BRAT Operations definition

In the ‘Operations’ tab, name your operation, then select your dataset and data. In ‘Data Computation’ keep ‘MEAN’ selected.

Enter your data expression: you will be computing the sea level with respect to the geoid, as for the “Amazon” data use case. The expression using T/P GDR field names is:

sat_alt – h_alt – h_geo – h_set – h_pol – iono_cor – dry_corr – wet_h_rad

(satellite altitude – altimetric range – corrections)

Eq. 11

name it, e.g., LLH (for “Lake Level Height”).

For the X field, the variable is ‘Lon_Tra’ when looking at one cycle and tim_moy_1 when working with the whole series.

Data editing

As we will see, data editing is needed to remove some less accurate data. The formula we will be using is:

```
geo_bad_1.water_land_distribution == 0 && is_bounded(-130,(sat_alt-h_alt),100) && nval_h_alt
>= 5 && is_bounded(0,rms_h_alt,0.1) && is_bounded(-2.5,dry_corr,-1.9) && is_bounded(-
0.500,wet_h_rad,-0.001) && is_bounded(-0.400,iono_cor,0.040) && is_bounded(7,sigma0_k, 30)
&& is_bounded(-1,h_set,1) && is_bounded(-0.150,h_pol,0.150) && is_bounded(0,att_wvf,0.4)
```

It is an adaptation of the Ocean data editing (provided within BRAT), with some fields removed.

Aral Sea level along the track: need of data editing

We will have a look at what we can see when plotting LLH for (e.g.) cycle 010 with respect to longitude.

If we plot “just” the level wrt longitude, in fact, we see more than the Aral Sea level. Even using the land/water flag (geo_bad_1.water_land_distribution == 0, which means that the data are considered as taken over open seas), we still have unwanted data — in part because of the changes of the Aral Sea extent, but not only.

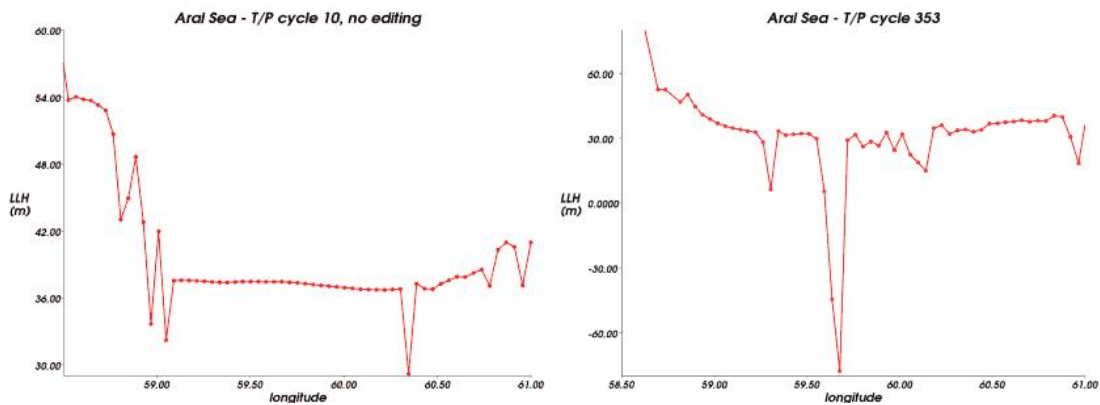


Figure 6.107. Lake level height for the Aral sea without data editing, T/P cycle 010 (left); The measurements over the sea is the “flat” area in the middle of the curve (between, roughly, 59.1° and 60.3°N). Right, a more problematic cycle, cycle 353, for which no clear signal can be seen.

We will have a look at some of the data fields that are used in data editing:

- RMS of altimetric range, which measures the variability of the altimetry measurement: over an open body of water, this variability should be rather low (between 0 and 0.1 m)
- Antenna mispointing, which can come from a change in surface, the radar sensing pulse previously reflected off-nadir
- sigma0, the backscatter coefficient, which is the ration of the altimeter radar pulse power that is reflected on the surface and measured by the radar. Abrupt changes in this coefficient can also come from a change in surface reflection.

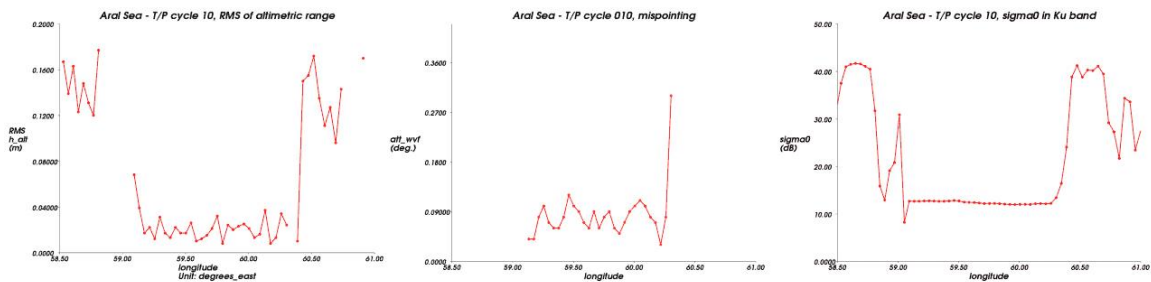


Figure 6.108. Several data fields plotted for T/P cycle 10 over the Aral Sea area: RMS of the signal, antenna mispointing, Sigma0. They all show abrupt differences between the measurements outside and over the Sea.

Depending on the water body, fine tuning of the threshold condition used in data editing has to be done.

Aral Sea level along the track at two different time

Here we will have a look at the Aral Sea level along the track in December 1992 (cycle 010) and June 2003 (cycle 360). We compute LLH for both cycles, using the editing given in the previous page. In the 'Views' menu, you name your plot, give the plot a title, select both computed LLH fields and click on 'execute' to view them (you can restrict X from 58.5 to 61°N).

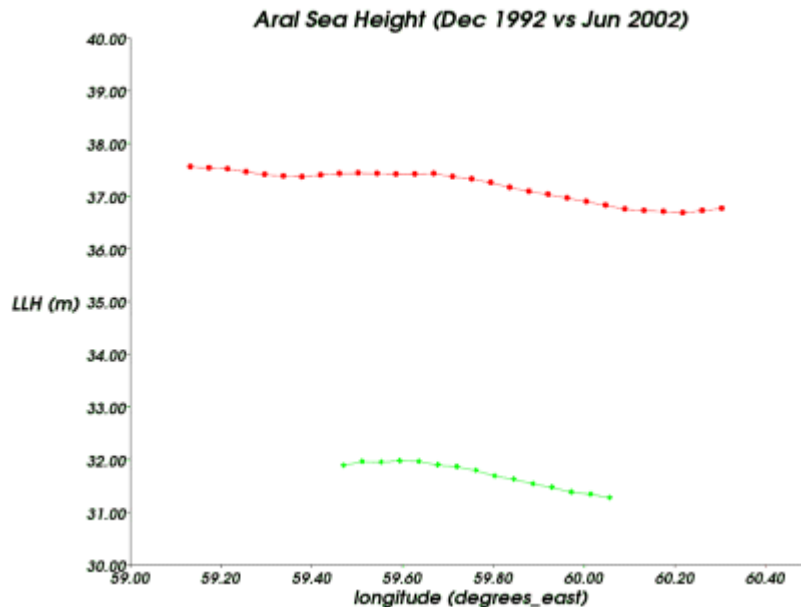


Figure 6.109. Topex/Poseidon along-track LLH over the Aral Sea for cycle 010 (December 1992, red) and cycle 360 (June 2002, green). The slight curvature of the height is due to the geoid model inaccuracies over this area. The level is obviously much lower in 2002, and the extent of the Sea is also much smaller.

Compute the Aral sea level variation over 10 years

Using the dataset with all the pass #107 from cycle 010 to 364, we will be able to plot the evolution of the Aral Sea over the whole period.

By using the time in days ('tim_moy_1') as abscissa, a mean is automatically done for each day for all available data on this day. We will use geographical selection to restrict the data averaged to the Aral Sea (add '&& is_bounded(59.06,lon_tra,60.32) && is_bounded(44.11,lat_tra,45.52)' in the Select expression box)

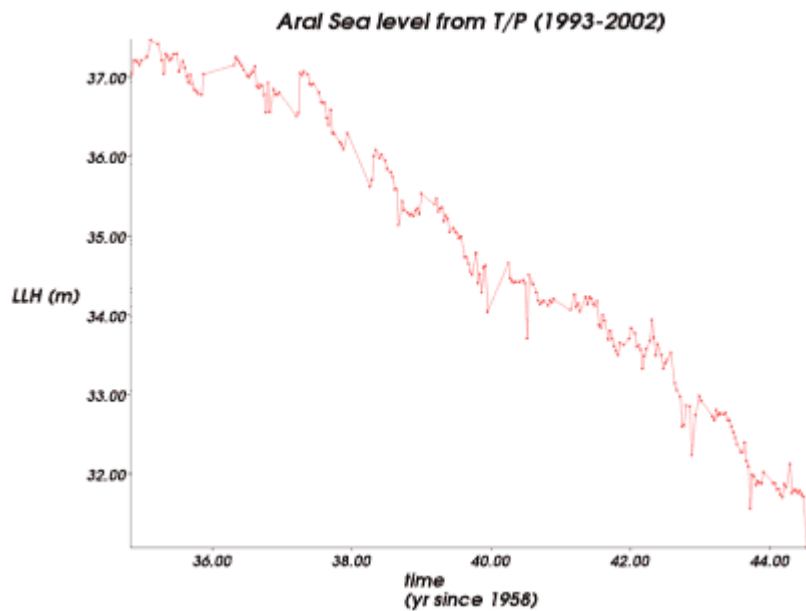


Figure 6.110. Aral Sea level variations from Dec 1992 to June 2002 from BRAT. Some more editing should be done to obtain a completely “clean” curve.

6.8.17 Land applications: Monitoring continental surfaces

While earliest altimetry missions were dedicated to studying the open ocean, various continental surfaces can also provide valid data, offering a new opportunity to monitor their temporal variability.

Data used

By giving a good overview of polar regions ($-82.5^{\circ}\text{S} / 82.5^{\circ}\text{N}$), Envisat mission is well adapted. Envisat altimeter (RA-2) data are delivered on DVD-ROMs or by FTP and can be obtained from [EOHelp](#).

This dataset has another advantage. The Envisat GDR brings the opportunity to use algorithms other than the classical ocean-oriented ones that are better suited for non-ocean surfaces. One of them is optimized for continental surfaces, the so-called ICE-2 retracker.

The RA-2 altimeter on Envisat platform is a dual-frequency radar operating at Ku-band (13.575 GHz) and at S-band (3.2 GHz).

Methodology

By using the Broadview Radar Altimetry Toolbox (BRAT), we map the radar altimeter backscattering coefficient in S-band in order to classify major global surface properties and to study their temporal evolution: date of the first snows, thickness of snow or vegetal cover in relation to the season, inundated areas, etc.

Temporal extraction

We use data spanning from cycle 30 (2004/08/31- 2004/10/04) to cycle 40 (2005/08/16) – 2005/09/19) that allows a yearly study with seasonal variability.

Geographical extraction

This example is made on a global scale without any geographical limits.

Data editing

In the “Datasets” tab, we have selected one cycle per dataset, carefully named (from Datasets_cy30 to Datasets_cy40) from the DVD GDR Envisat. Finally, we have 11 datasets, each with ~980 files (up to 1002).

A first operation is created, selecting longitude for “X”, latitude for “Y” and for the “Data expression”, we use the S-band ICE-2 backscatter coefficient at 18 Hz (hz18_s_ice2_bscat field).

The data editing limits the backscatter coefficient boundaries to eliminate the most erroneous data. An ocean mask is also applied to keep data only on continental areas: (altim_landocean_flag > 0) && (is_bounded(0, hz18_s_ice2_bscat, 45)).

Next operations are created from the first one using the “Duplicate” button but be careful to link up each operation to the good cycle dataset.

In the “Views” tab, we add each operation-cycle in the same plot. Click on “With Animation” in the “General Plot Properties” and “Execute”. In the Display screen, you can change the speed for each frame to be displayed or you can stop on each frame and save it independently.

Results and comments

At a global scale, the backscatter coefficient values mainly ranges from 0 to 20 dB in S-band. The backscatter coefficient is high (~20 dB and more) on very flat surfaces: deserts, river basins or wetlands due to the specularly of the return echo. But it is low over mountainous regions. Strong variations can be seen, especially for regions which are covered by snow in winter or with a contrasted rainy season.

The backscattering coefficient results from a surface scattering echo and a volume scattering echo inside a medium. Over land surfaces, three different cases can be described:

- the return signal is only due to the surface echo: water surfaces, inundated soils, melting snow,
- the return signal is due to reflecting surfaces located under volumetric scatterers: sparse forests, inundated forests, dry snow,
- the return signal is due to reflecting surfaces located above volumetric scatterers: dry or arid areas, wet snow.

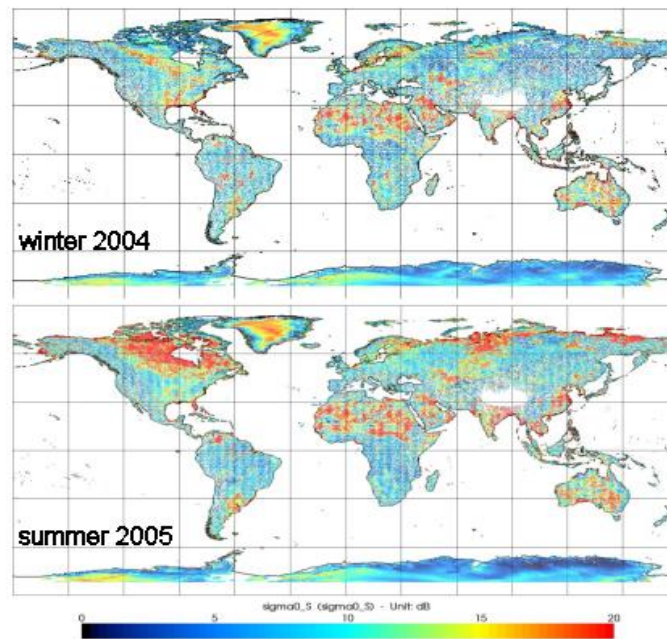


Figure 6.111. Backscatter coefficient Σ_0-S from ICE-2 retracker for Envisat cycle 034 (top) and 040 (bottom): several river basins such as Orinoco, Mississippi, Amazon, Parana, Lena, etc, and areas with melting snow during boreal summer are clearly visible.

Further information:

- Legrèsy, B., Papa, F., Remy, F., Vinay, G., Van Den Bosch, M., Zanife, O-Z., Envisat radar altimeter measurements over continental surfaces and ice caps using the ICE-2 retracking algorithm, in *Remote Sensing of Environment*, Vol. 95 (2005), 150-163.

6.8.18 Altimetric waveforms to monitor lakes level: Lake Issyk-kul

Satellite altimetry is an efficient tool to monitor the level of enclosed seas, lakes and even large rivers as long as the satellite flies over them.

The Issyk-kul Lake is a great salted mountain lake in Central Asia, in Kyrgyzstan. Its name means “warm lake” since it never freezes. It is located around 77.40°E and 42.20°N.

Data used

Contrary to the “Aral Sea” Data Use Case, we will not use the altimetric height in order to plot its sea level variations along the years. For this example on the Issyk-kul Lake, we directly use the altimetry waveforms which are the records of the reflected echoes over time. From this waveform, several parameters are computed using several algorithms (retrackers) which describe its shape (leading edge width, trailing edge, epoch at mid-height, skewness, etc.) and provide the satellite-ground range.

We use here the OSTM/Jason-2 SIGDR which can be obtained from Aviso and contain the 20 Hz along-track waveform information. OSTM/Jason-2 offers the opportunity to use an algorithm enabling a better tracking over lake or over non-ocean surfaces. Its altimeter is equipped with an open-loop tracking technique for which a Digital Elevation Model (DEM) has been developed. The altimeter’s onboard memory contains the elevation values of areas overlayed by the ground tracks. These data, combined with DORIS, are used to position the receiving window in advance, in order to

anticipate the contrasts of the topography and to give priority to measurements over water. This one corresponds to the DIODE/DEM tracker. During the OSTM/Jason-2 validation phase, two others trackers were used: the Split Gate Tracker (SGT) and the Median Tracker. The SGT tracker is equivalent to the Poseidon-2 tracker on Jason-1. The Median tracker works on the barycenter of the waveform shape and improves data availability on coastal zones (water/land transitions) and on continental water areas (lakes).

Methodology

We will use the Broadview Radar Altimetry Toolbox to have a look at waveform shapes over the lake and at the land/water transitions with three different OSTM/Jason-2 trackers.

Temporal extraction

We only use the three first cycles of OSTM/Jason-2 (during its validation phase):

- from 2008/07/12 to 2008/07/21 for OSTM/Jason-2 cycle 001 and corresponding to the SGT tracker,
- from 2008/07/21 to 2008/07/31 for OSTM/Jason-2 cycle 002 and corresponding to the Median tracker
- and from 2008/07/31 to 2008/08/10 for OSTM/Jason-2 cycle 003 and corresponding to the DIODE/DEM tracker.

Geographical extraction

To select the right track, you can have a look at the pass locator using Google Earth available through Aviso. Thus, we can directly download the pass #131 we wish to work on (and we do not need the whole cycles of OSTM/Jason-2 data) in the “Datasets” tab. After that, in the “Operations” tab we limit the geographical boundaries around the lake from the latitudes: 41°N – 45°N, so a 4°-segment.

Data editing

In the “Datasets” tab, we have selected the three first OSTM/Jason-2 cycles, each in a different dataset: Datasets_wvf_c001, Datasets_wvf_c002 and Datasets_wvf_c003.

First, in the “Operations” tab, create three operations. From the native OSTM/Jason-2 SIGDR files, create one operation per cycle as follows: select the latitude at 20 Hz that is to say the field “lat_20hz” for “X”, and select in the “Data”, the field “waveforms_20hz_ku” which contains the 104 Ku-band waveform samples for each waveform.

In the “Selection criteria” expression, the geographical boundaries are limited as follows: `is_bounded(41, lat_20hz, 45)`. Execute this first operation for a given cycle from the native OSTM/Jason-2 SIGDR files.

In the “View” tabs, you can choose between two different kind of graphs:

- $Y=F(X)$ which plots the waveforms individually and represents the return echo power in function of time.
- $Z=F(X,Y)$ which plots a set of cumulated waveforms in function of latitude, as if seen from above.

For the $Y=F(X)$ graph, you have just to select the operation and execute it.

In order to properly plot the $Z=F(X,Y)$ graph, a second step is necessary. The Broadview Radar Altimetry Toolbox fits the pixels of this kind of figures to span the space between two values. However, when there are gaps in the values, this leads to extending artificially some data over those gaps. So, to have a figure with gaps correctly plotted, we first have to compute the date, then instead of plotting the Data expression directly from the Operation result, we use the NetCDF file thus created by the Broadview Radar Altimetry Toolbox in a new dataset.

You can select in the “Dataset” tab this NetCDF output, from the location where you have saved your workspace on your computer, in the “Operations” folder (named CreateOperations_wvf_c001.nc). This file contains three different fields that we integrate again into a new operation. Be careful to give a new, meaningful, operation name mentioning the NetCDF format. Select the field “lat_20hz” for “X”, the “wvf_ind” for “Y” and the “waveforms_20hz_ku_c001” for the “Data”. No expression is described here, but a new resolution is given according to the total number of waveforms for one-degree of latitude. Since one-degree of latitude is about 111 km, and since the ground distance covered by OSTM/Jason-2 during 1/20 s, is about 0.350 km, the step for the X resolution is $0.350/111 = 0.00315$. This last value must be filled in the “Operations” tab, by clicking on the “Set Resolution filter” button. The number of intervals is computed and gives the total number of waveforms for your pass segment.

In the “Views” tab, select this last operation made from the BRAT NetCDF output file and execute it. The same steps are performed for others cycles by duplicating the operations.

Results and comments

On the first kind of graph, $Y=F(X)$, each waveform can be seen either individually, by browsing one by one, or through an animation, displaying all the selected waveforms. This animation cannot be saved, but each frame/waveform can be. We have selected and saved 5 waveforms per cycle, which are the closest ones to a given location from one cycle to another (altimetry measurements are not taken exactly at the same point from one cycle to another). We observe many waveform shapes along the lake: Brown echoes, specular, multi-peaked, etc (see From radar pulse to altimetry measurements). But the waveform shapes are also quite different for the same location, due to the kind of tracker used or due to a change of surface conditions between the cycles.

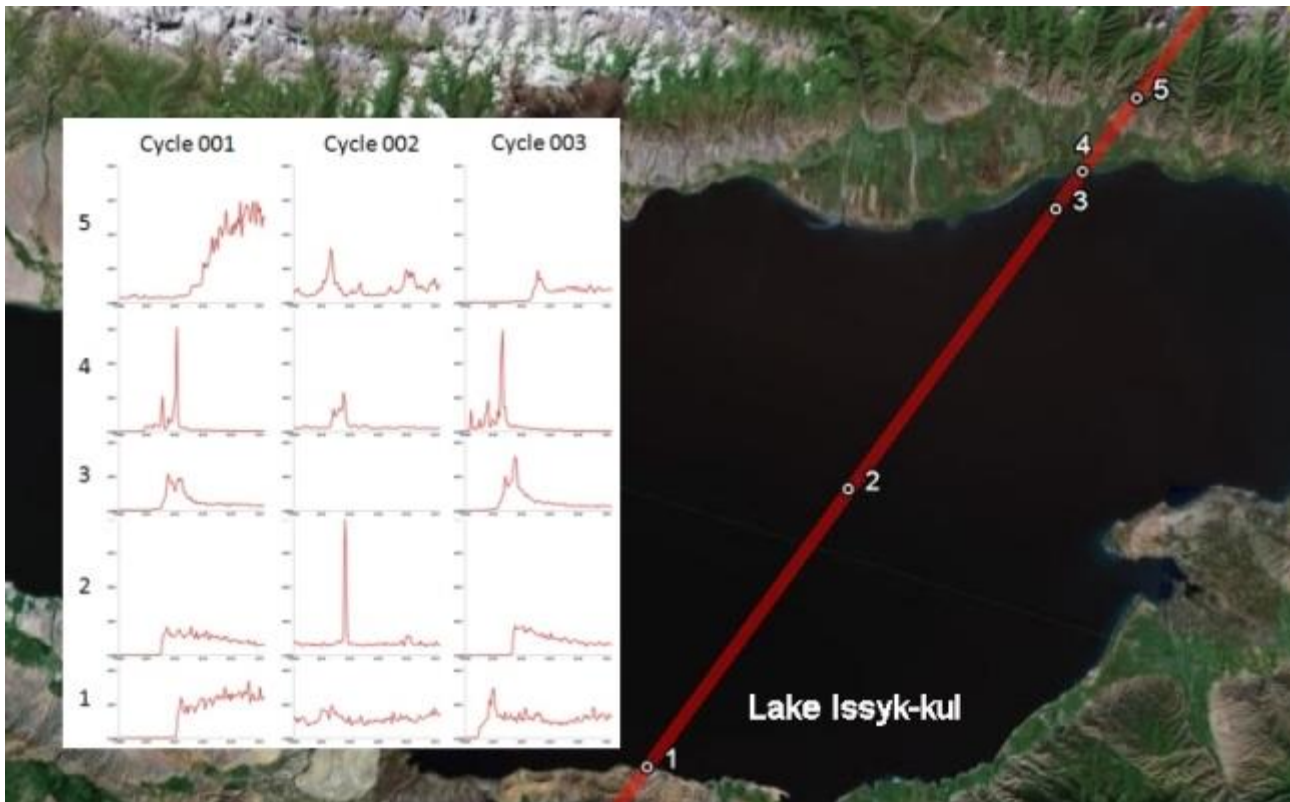


Figure 6.112. Individual waveforms along five given points over the lake Issyk-kul for the three first cycles of OSTM/Jason-2 (maps from Google Earth). X-axis represents the 104 waveforms samples (gates) in Ku-band, so the time. The Y-axis represents the return echo power.

On the second kind of graph, $Z=F(X,Y)$, we observe a set of juxtaposed waveforms as a function of latitude, as if seen from above. The segment pass is covering approximatively 520 km, from 41°N to 45°N , so a long segment before and after the lake.

The altimetric signal is not present all over the segment, there are a lot of missing values (white areas on the graph) corresponding to the mountainous land. The signal loss is different in function of the tracker used : the Median tracker (middle) seems to be locked and gives a signal more often.

The Southern boundary of the Lake Issyk-kul is detected for the three trackers at the same time, around 42.15°N . But the Median tracker (middle) seems to give a longer tracking over (or beyond) the Northern boundary of the lake.

Over the lake, the thermal noise of the waveforms corresponds to black areas. The leading edge position corresponds to the black/dark blue transition and follows the thermal noise. The leading edge position varies a lot over the lake for the trackers SGT and Median: a difference of 20 gates can be seen for the Median tracker, corresponding to a range difference of almost 10 m. Such discrepancies are corrected using the adapted retracking algorithm.

Another feature can be underlined with the red area measured over the lake by all the three trackers and at the same time, around 42.7°N . This feature might correspond to a highly reflecting surface nearly the Northern coast.

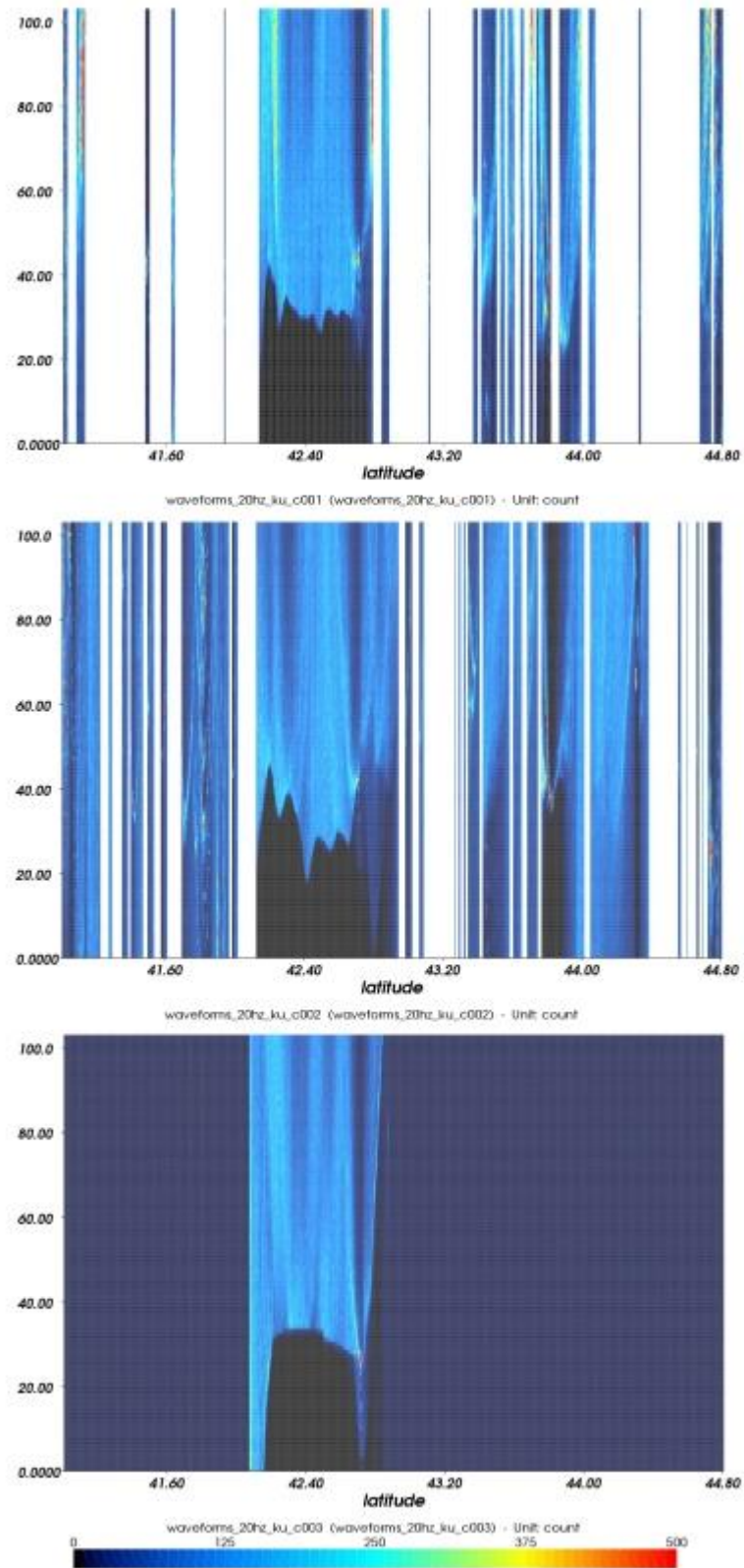


Figure 6.113. Set of juxtaposed waveforms as a function of latitude ($41^{\circ}\text{N} - 45^{\circ}\text{N}$, pass #131) and as seen from above for the first three cycles of OSTM/Jason-2. Each cycle corresponds to a different tracker: SGT for cycle 001, Median tracker for cycle 002 and Diode+MNT for cycle 003

6.8.19 Altimetry for lake/reservoir studies by using hydrology dedicated products.

Satellite altimetry dedicated to hydrology.

The purpose of this Data Use Case is twofold:

- Provide an overview of the information contained in Jason-2 experimental PISTACH products over non-ocean areas, based on the example of the monitoring of the Sathanur Reservoir (India),
- Provide newcomers to altimetry with a generic approach for studying a given water body using BRAT and Level 2 (Geophysical Data Records) altimetry products.

Selection of the target area

First of all, and since satellite altimetry missions are optimized for open ocean studies with limited nadir footprint (a few kilometer radius circle) and repeat orbital cycles, one has to be lucky to have a suitable coverage over a specific inland water body of limited extent! To investigate, the pass locator on Aviso website (download the .kml file for the [Jason-2 referenced orbit](#)) gives a quick and easy access to the precise ground track coverage of the various altimetry missions on Google Earth.

In our case, we have decided to look for a lake or reservoir in India. We found the Sathanur Reservoir located in the Tamil Nadu State, south-east India, around 100 km West of Pondicherry city. This reservoir is roughly located between 12.15°N and 12.25°N below Jason-2 track #079. This is an ascending track, the satellite flying from the south-west to the northeast.

In Google Earth, it is useful to fly over and around the lake with the mouse to get an idea of the topography of the lake surroundings. It is important to realize that the surrounding terrain of an inland water body can have a significant impact on the accuracy of altimetric estimates over the lake: for example, reflections of the radar signal over surrounding mountains can strongly alter the shape of the waveforms and induce inaccurate or even erroneous range measurements. For the Sathanur Reservoir, we notice that the topography is rather flat around the water body, with an altitude of:

- ~235 m below the track a few kilometers south-west (i.e. 'before') of the lake,
- ~221 m over the lake,
- ~250 m below the track a few kilometers northeast (i.e. 'after') of the lake.

Some hills nevertheless appear on a 3D view on Google Earth, both in the South and North directions.



Figure 6.114. Jason-2 pass 079 overlaid on Google Earth in the vicinity of Sathanur Reservoir, India. Different views on Google Earth give important details on topography.

In addition, in Google Earth, the urbanization of the immediate surroundings of the lake seems rather limited (hydropower plant), and therefore, polluted waveforms should be limited. So, we reasonably expect acceptable quality of the altimetric data over the reservoir.

Download and preparation of the data

In order to study inland water bodies with the PISTACH products, one has to download the 'hydro' product found (free access) on the [FTP server](#). After reading the 'Readme.txt' file, then go to the J2/IGDR/hydro/ directory.

The PISTACH products have the same organization (and format) as the standard official Jason-2 Level Products: one file per track and per cycle. Therefore, 254 files are found in each of the 'cycle_CCC' directories. For that example, we only downloaded the files corresponding to the track #079 (example: the file ftp://ftpsedr.cls.fr/pub/oceano/pistach/J2/IGDR/hydro/cycle_009/JA2_IPH_2PTP009_079_20081002_102440_20081002_110916.nc.gz corresponds to the track #079 of orbital cycle #009, corresponding to an acquisition date between 10h24 and 11h09 on the 2nd of October 2008).

A shell script can be used on a Unix/Linux computer to download a series of files for a given track number (#079 here) and several cycles.

Of course, the files need to be unzipped before using them within BRAT.

To elaborate this Data Use Case, we downloaded track #079 for the first 100 cycles. Although BRAT can handle 100 files or more, it appeared preferable in terms of efficiency for BRAT to perform an extraction of the files over a portion of track. We performed that extraction with the following script, based on the use the 'ncdump', 'ncgen' and 'ncea' commands. The latter needs the installation of NCO (NetCDF operators) on the computer. The [NCO homepage](#) contains more information. Here, the extraction is done between 12.15°N and 12.25°N, i.e. over the Sathanur Reservoir.

First and quick look at the data with BRAT

The first objective is to check whether the quality of the data is acceptable to perform the monitoring of the level of Sathanur Reservoir. In BRAT, performed the following actions:

- Create a new workspace.
- In “Datasets” tab, create a new dataset that we name 'PISTACH_IGDR_Hydro_T079'.
- Add of the PISTACH product NetCDF files in the dataset.

We then obtain the following screen, with:

- the list of data files in the 'dataset' window,
- the display of the header of the selected file in the 'File description' window,
- the list of the variables of the selected file in the 'product' window (upper right),
- the description of the selected field in 'Fields description' window (lower right),

The most simple operation to do for checking the data is to visualize the 'orbit - range' difference along the track. To do so:

- In “Operations” tab, create a new operation (named 'OrbitMinusRange', for example)
- Select the latitude field ('lat') and drop it on the 'X' in the 'Data expression frame'
- Select the orbit height field ('alt') and drop it on the 'Data' in the 'Data expression frame'
- Type the '-' operator sign after 'alt' in the 'Expression' frame
- Select the range field ('range_ku') and drop it in the 'Expression' frame' to form the 'alt-range_ku' expression.
- Rename the 'alt' name in the 'Data Expression' frame with 'AltMinusRangeKu'

If the data files have not been 'reduced' in the preparation step, it is useful to introduce a selection criterion (copy into the Expression grey box: `is_bounded(12.15,lat,12.25)`). On the example below, only the data points with latitudes between 12.15°N and 12.25°N are selected.

Now click on 'Execute'. BRAT computes this operation on each data point of each cycle for track #079 on the selected track portion.

Once the computation is completed (a few seconds to a few minutes, depending on your computer), go to the 'Views' menu to create a graphical representation of the result of this operation:

- Creation and naming of a new view.
- Selection of the data to draw among the 'Available' operation results (only one choice at this stage of the Data Use Case).
- Click on the '==>' button to introduce it in the 'Selected' frame (or drag&drop).
- Click on 'Execute'.

The Figure 6.115 appears (after masking the lines and drawing the points). Interpretation: no evident information can be extracted from that plot!

Does it mean that the PISTACH products do not contain any useful information over the Sathanur Reservoir?

In fact, this plot mainly illustrates that the 'range_ku' field (i.e. the 'ocean' range field of the standard Jason-2 products) is not the most appropriate for that purpose, because the waveform over that area are not ocean-like waveforms.

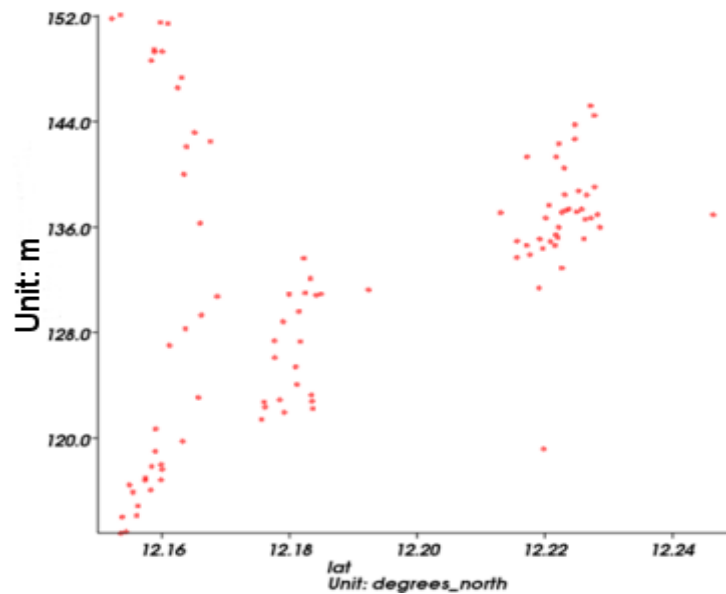


Figure 6.115. First look on data, computation of the “orbit - range” with the “range_ku” (i.e. the “ocean” range).

Let us then plot the 'Ice1' range. It is necessary to create a new operation (or use the 'duplicate' button), and replace the 'range_ku' field with the 'ice_range_ku' (results of the 'Ice1' retracking). After creating a new plot with both operations, we obtain the Figure 6.116(left). Here, the 'alt-ice_range_ku' values are in red and the 'alt-range_ku' in blue. We now observe a coherent and dense set of points (with some outliers). The 'cloud' seems particularly coherent between 12.18°N and 12.21°N, i.e. over the reservoir.

Let us now add the result of the PISTACH Ice3 retracking (field: 'range_ice3_ku') on that plot (after creating once again a new operation and a new view). The result appears on Figure 6.116 (right).

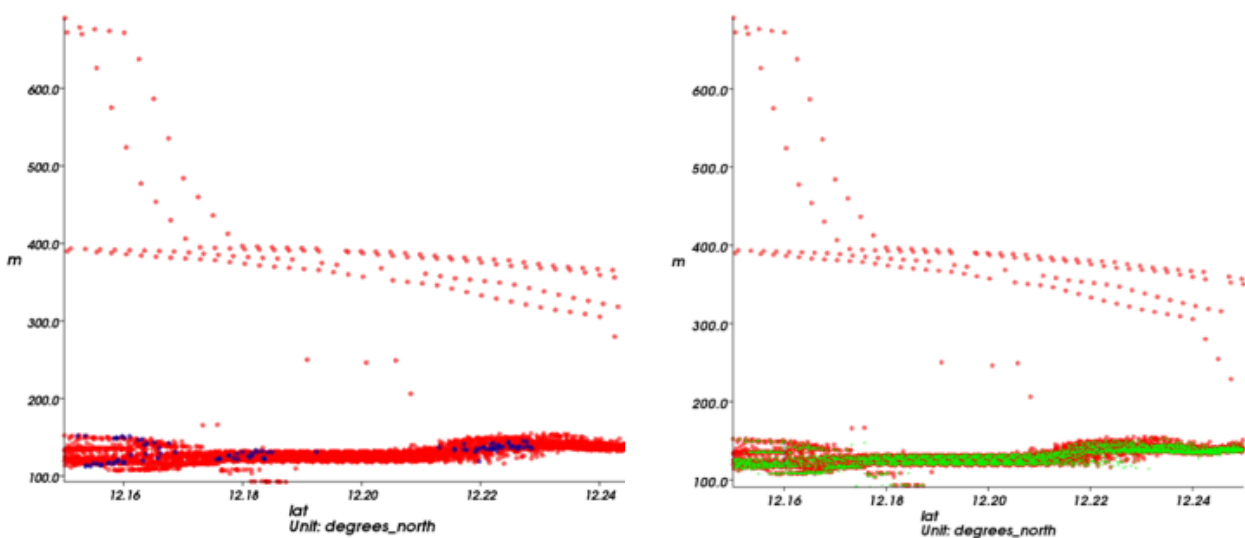


Figure 6.116. Computation of the “orbit – range” with the Ice1 retracking (left, in red) and with the Ice3 retracking (right, in green). The “orbit – range” with the ocean retracking is plotted in blue on both.

The data set now appears even more coherent, with very few outliers. This indicates that a coherent set of data is present in the PISTACH products over the Sathanur Reservoir, when using the results of the **Ice3 retracking algorithm**.

A representation as a function of time (Figure 6.117) should also give a coherent signal: this is verified with a new operation (replacing 'lat' with 'time' in the X coordinate). We can easily distinguish a temporal fluctuation of more than a 10 m peak to peak amplitude. Outliers on that representation probably correspond to measurements acquired over emerged lands surrounding the reservoir. Now that we are sure that exploitable information is contained in the PISTACH data set, it is necessary to precisely compute the water surface height and to refine the data selection.

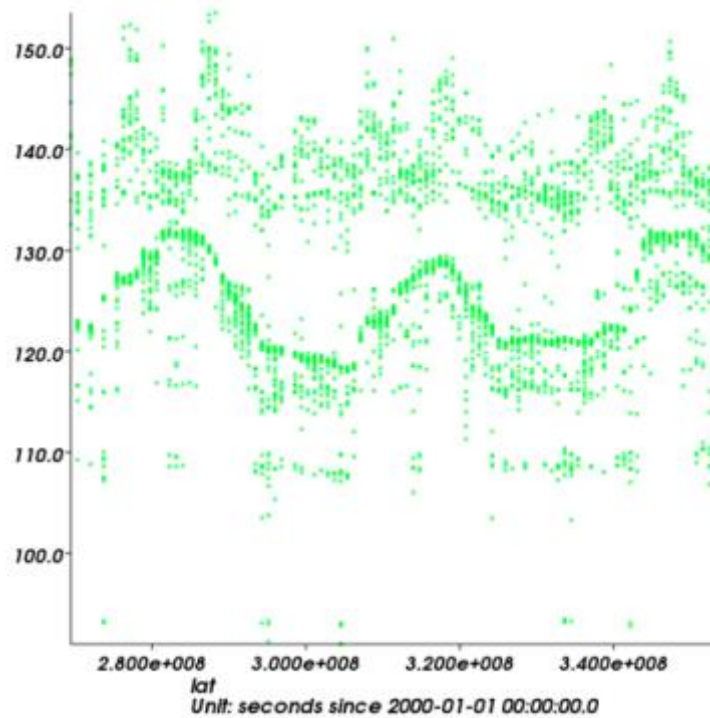


Figure 6.117. Computation of the “orbit – range” with the Ice3 retracking vs time.

Computation of a precise water surface height

Taking into account the geoid

Up to this point, we only computed a raw surface height. Since the position of the satellite on its orbit is referenced to an ellipsoid, the raw surface height is also referenced to the ellipsoid. The terrain altitude, as observed in Google Earth for example, is referenced to the geoid. Thus we need to take into account the height of the geoid to compare satellite and *in situ* measurements. Note that over India, the Geoid is far (~80 m) below the ellipsoid. The PISTACH products contains the values of the EGM96 geoid height (above the reference ellipsoid), as in the standard Jason-2 Level2 products, but also the more precise values from the EGM2008 model. Values from both geoid models (data fields 'geoid_EGM96' and 'geoid_EGM2008' are shown along the considered portion of track #079 on the figure 5.

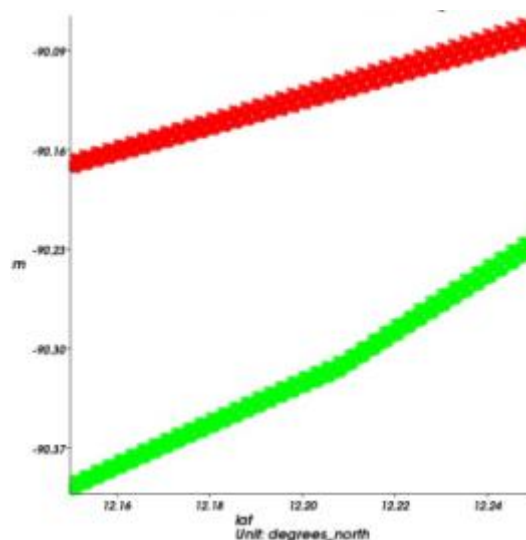


Figure 6.118. Geoids heights (EGM96 model in red and EGM2008 model in green) over the Jason-2 pass #079 on the vicinity of the Sathanur reservoir.

Taking into account the propagation corrections

It is also necessary to take into account the propagation delays of the radar signal through the troposphere and ionosphere since their temporal fluctuations may be on the same order of magnitude as the fluctuations of the surface of the water bodies. These temporal fluctuations are shown on the figure 6 (data fields: 'model_dry_tropo_corr', 'model_wet_tropo_corr', and 'iono_corr_gim_ku').

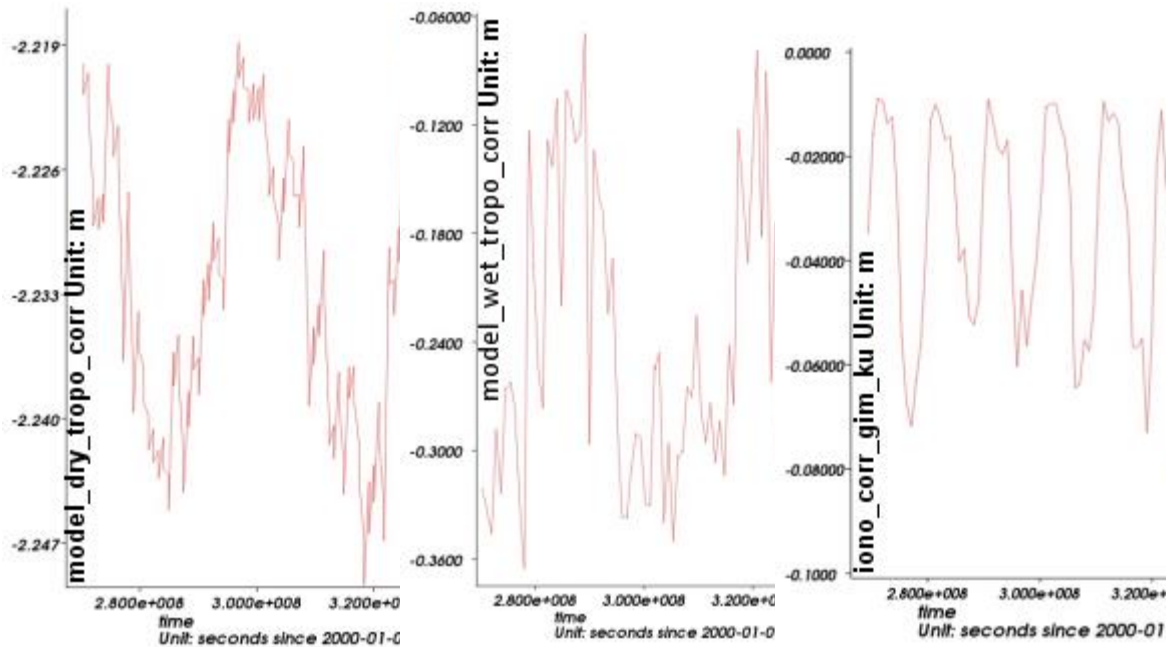


Figure 6.119. Amplitudes in metres of the dry tropospheric correction derived from model (left), of the wet tropospheric correction derived from model (middle) and of the ionospheric correction derived from the GIM model (right).

Dry Tropospheric correction: as over the oceans, this correction is always a model correction, mainly computed from the surface pressure. Over non ocean areas, most of the error of this correction comes from inaccurate values of the real surface elevation along the track. In the PISTACH project, a new computation has been developed, based on the estimation of the surface elevation using the altimeter range measurements. However, this correction (data field 'model_dry_tropo_corr_direct_sol') has not been activated in the first version of the PISTACH since this requires a direct link with ECMWF model outputs.

Wet Tropospheric correction: It is usually computed from the radiometer measurements over the oceans. However, the radiometer is highly perturbed by emerged lands and cannot be used over inland water bodies (unless very large). So, a model correction is used. Same comments as above for the dry tropo corrections apply.

Ionospheric correction: The dual frequency correction cannot be used over inland water bodies when the radar echoes are not ocean-like waveforms. It happens mainly over small water bodies (Fernandes MJ., 2014). We use the correction computed from the GIM model.

Taking into account the geophysical corrections

Finally, we also have to consider the solid earth tide and pole tide that induce a vertical deformation of the earth surface (data fields 'solid_earth_tide' and 'pole_tide') on Figure 6.120

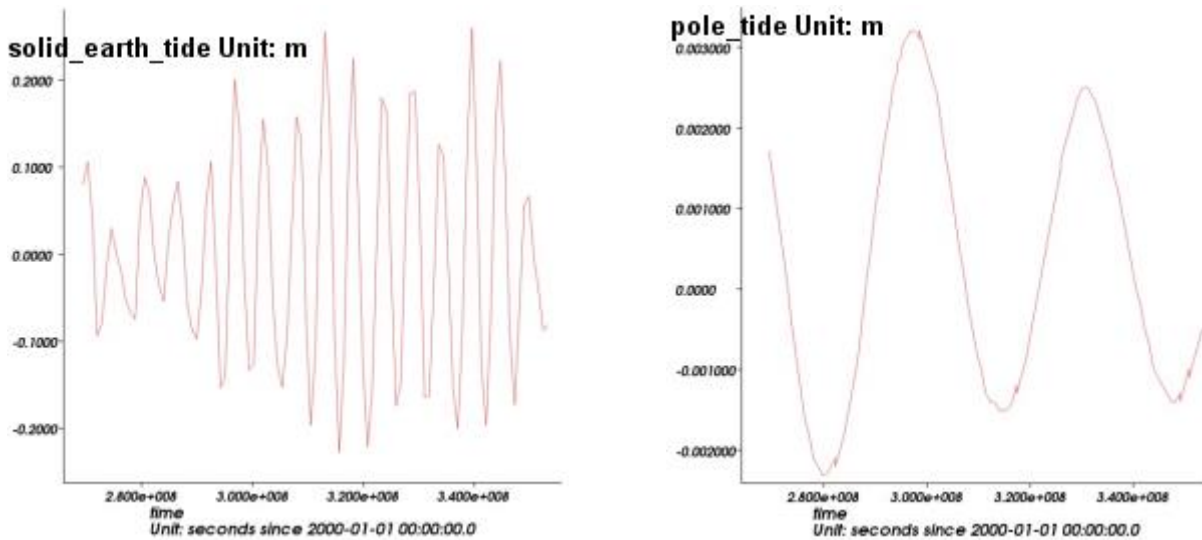


Figure 6.120. Amplitudes in metres of the solid Earth tide (left) and the pole tide right).

Computation of a precise water level

As a conclusion, a more precise formula for the retrieval of the real water surface altitude (WSA) over inland water bodies can be written as follows:

$$WSA = alt - range_ice3_ku - model_dry_tropo_corr - model_wet_tropo_corr - iono_corr_gim_ku - pole_tide - solid_earth_tide - geoid_EGM2008$$

When applying this formula, we obtain the Figure 6.121 as a function of latitude (left) and time (right). On the left plot, we have superimposed the topography information found in the PISTACH products:

- In red: the topography as found in the standard Jason-2 GDR,
- In green: the topography computed for PISTACH using the Digital Elevation Model SRTM_CGIAR (and ACE2 in the future version 2 of the products),
- In blue: WSA as detailed above.

We observe a rather good agreement between green and blue curves, i.e. between the topography derived from the SRTM and the WSA computation; especially between 12.18° and 12.20 °N, i.e. on the water surface. These values are also coherent with the values observed in Google Earth.

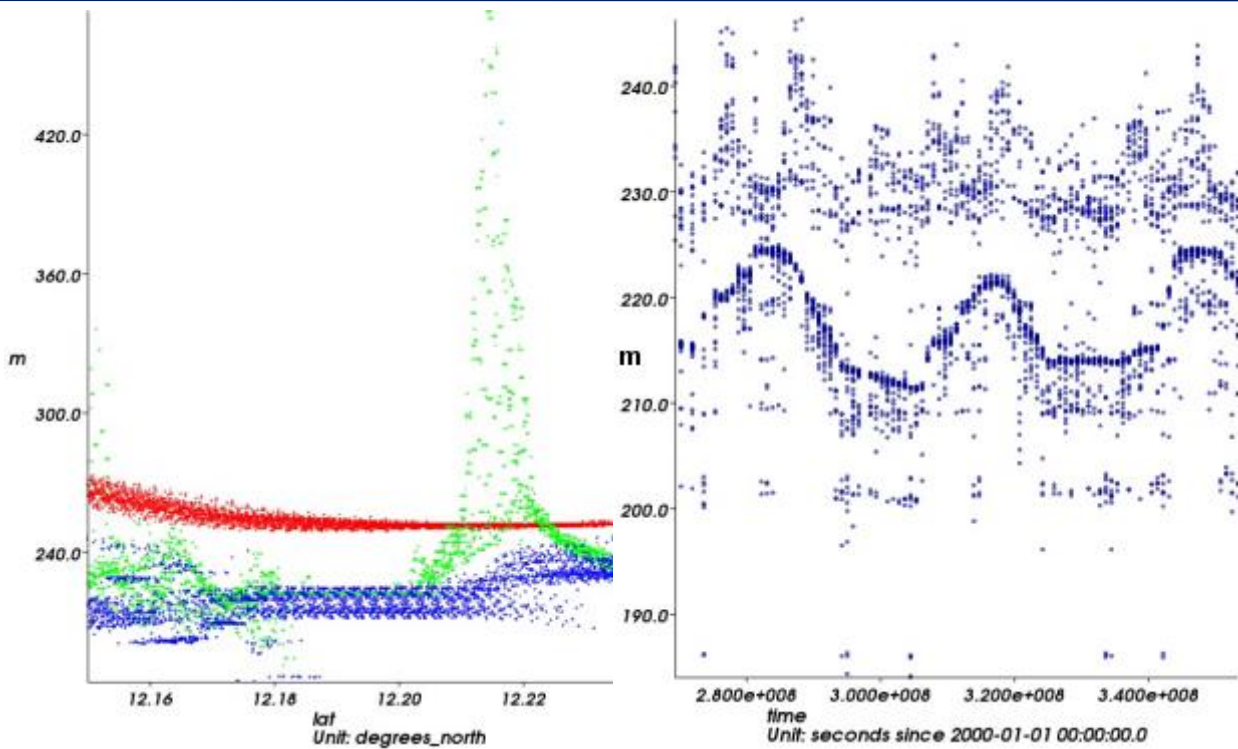


Figure 6.121. Water Surface Altitudes (WSA) in metres in function of the latitude (left) and the time (right).

From these 2 plots on Figure 6.121, we clearly see that it is necessary to make a more accurate selection of the data, and in priority, the extraction has to be restricted to the water body.

Selection of the data

On the Figure 6.122, we see that the along-track selection of the data can be restricted to the interval 12.1875°N to 12.2025°N. Note that on this 1.5 km track segment, the satellite passes over small islands. This plot also shows that the surface area of the Sathanur Reservoir also changes with time.

In PISTACH products, we find new information describing the shape of the waveforms (waveforms are not included in the PISTACH products): data field 'wf_class_ku' (see PISTACH products handbook) for more explanations. Class 1 corresponds to ocean-like waveforms, class 2 to peaky waveforms, etc. Since the Ice3 retracking is conceived to deal to peaky waveforms, it is possible to introduce the waveform class values as a selection criterion.

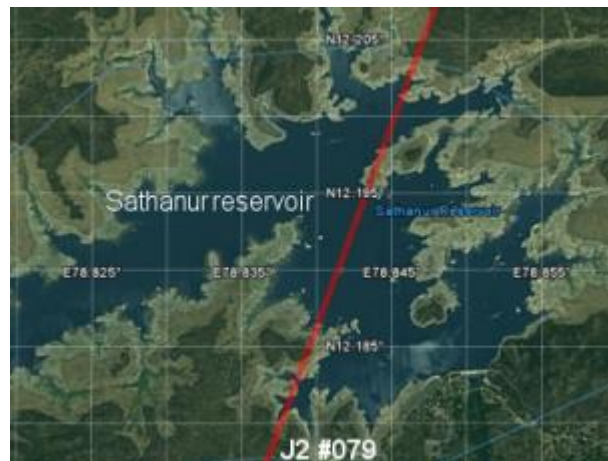


Figure 6.122. Zoom view with Google Earth on the Sathanur Reservoir to restrict the data over the water.

Waveform classification

Figure 6.123 on the left ('wf_class_ku' as a function of 'lon' and 'lat' with BRAT) shows the geographical along-track distribution of the waveforms classes between 12.15°N and 12.25°N. The lateral distribution of the pixels illustrates the +/- 1km orbit control with respect to the theoretical track. We observe 2 main areas with peaky (class 2 in deep blue) waveforms: one over the Reservoir and the other one a few km north of the lake.

Another representation of the waveforms is shown in Figure 6.123 (right): Class 23 corresponds multi-peak waveforms. Note that there are less multi-peaked waveforms over the water body.

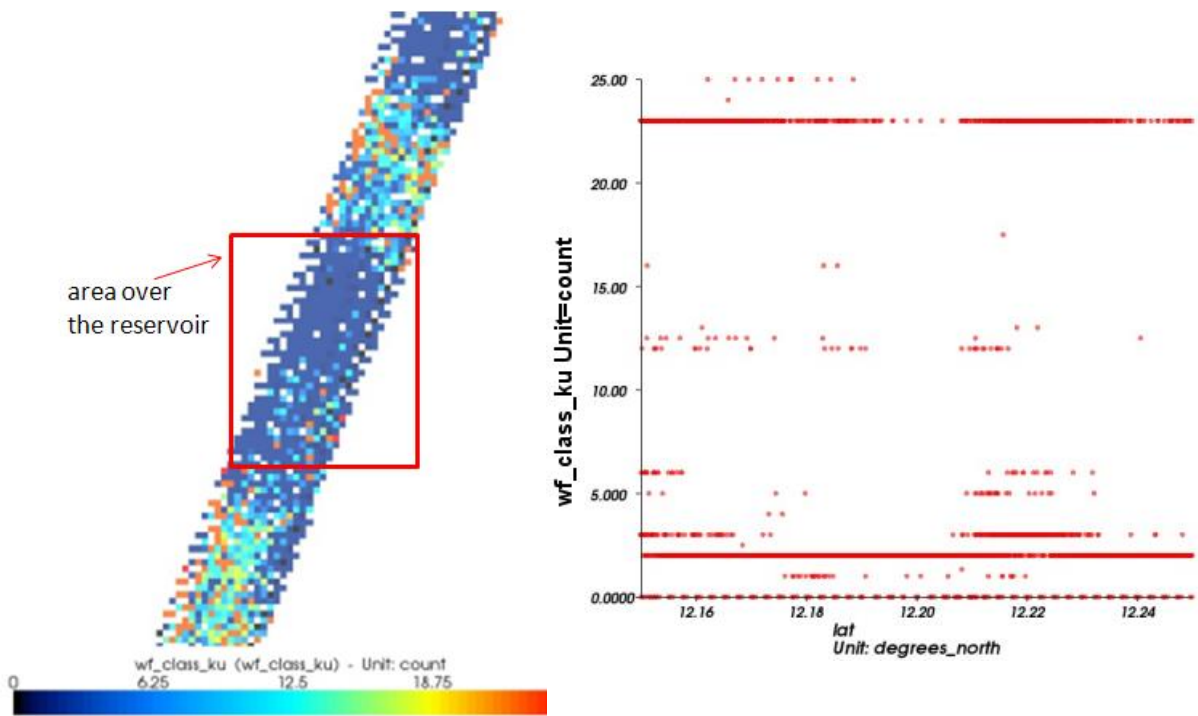


Figure 6.123. Distribution of the waveform classes between latitudes 12.15°N and 12.25°N, along the track (left: as a function of longitude/latitude) and on a diagram (right: as a function of the latitude). The value of each waveform class is detailed in the PISTACH products handbook). Here we mainly see waveform class 2 (peaky) and 23 (multi-peak).

Backscattering coefficient

The backscattering coefficient ('ice_sig0_ku' corresponding to the Ice1 retracking sigma0) can also bring useful information with respect to the data selection (Figure 6.124).

We observe higher sigma0 values over the water body: it is possible to introduce this specificity in the data selection. However, this criterion is not very discriminating and probably has to be adapted to each water body with respect to its environment.

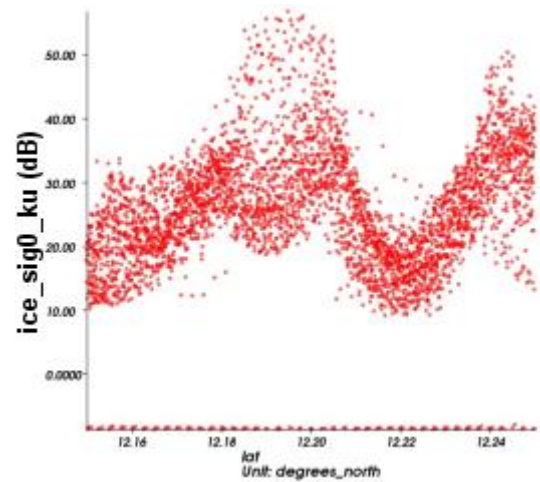


Figure 6.124. Backscattering coefficient in dB between latitudes 12.15°N and 12.25°N.

Finally, we used the following selection criteria in BRAT, adding a test on the latitudes, on the waveform classes, on the model topography, on the backscattering coefficient and on a processing flag associated with the Ice3 retracking:

```
((is_bounded(12.1875, lat, 12.2025)) && (wf_class_ku == 2)) && (is_bounded(210, topography, 228))) && (is_bounded(20, ice_sig0_ku, 60)) && (retracking_flag_ice3_ku == 0)
```

We obtain the time series shown on Figure 6.125 for the period July 2008 to March 2011.

The water level fluctuations are clearly seen, with very few outliers remaining at the end of the selection process. This reservoir exhibits very large fluctuations (~14 m peak to peak). Given these large interannual fluctuations, the dispersion of the surface height estimation for each cycle appears negligible. It remains however on the order of +/- 15 cm.

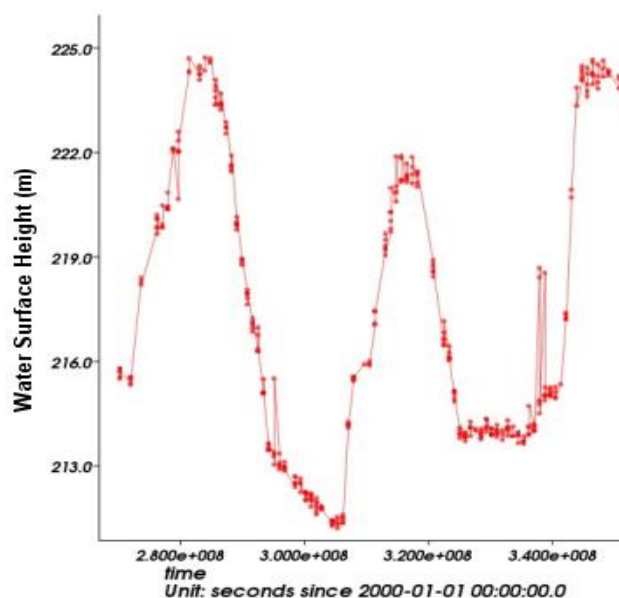


Figure 6.125. Water surface altitude of the Sathanur reservoir from the Pistach “hydro” products, after selection of the data.

Further information:

- Other Data Use Cases using hydrology dedicated products: Altimetry for wetland studies
- Aviso website: Posters and presentations at the Towards High-Resolution of Ocean Dynamics and Terrestrial Surface Waters from Space 2010 workshop.
- Coastal and Hydrology Altimetry product (PISTACH) handbook
- Fernandes MJ, Lázaro C, Nunes AL, Scharroo R. Atmospheric Corrections for Altimetry Studies over Inland Water. *Remote Sensing*. 2014; 6(6):4952-4997' (<http://www.mdpi.com/2072-4292/6/6/4952>).

6.8.20 Altimetry for wetland studies by using hydrology dedicated products.

Satellite altimetry is limited over continental areas due to a loss of quality in the measurements. These errors are caused both by the heterogeneity of the reflecting surface (a mix of water and emerged land surfaces) in the altimetry and radiometric footprints (extending 10 km and 50 km, respectively) and also by inaccurate geophysical corrections. Despite this, the altimetric measurements are present and may contain useful information for hydrology studies.

This data use case proposes to give some instructions on how to use the Hydrology experimental products distributed by Aviso (PISTACH) products over a large wetland, the Sudd Marshes (southern Sudan).

Data used

Jason-2 along-track experimental Hydrology products produced by the PISTACH project, a hydrology (and coastal) -dedicated processing applied to the Jason-2 mission.

These products derive from the Jason-2 S-IGDR products and include new retracking solutions, several state-of-the-art geophysical corrections as well as higher resolution global/local models. Numerous extra fields derived from the various PISTACH processes are then added to build the products. These products are based on a 20-Hz along-track sampling rate (vs 1-Hz for the official Jason-2 IGDR) but the nomenclature of their variables and files is similar to Jason-2 IGDRs one.

Download freely coastal data files on the FTP server. Files are in the sub-directories named cycle_XXX/. Each cycle lasts about 10 days, the first one (in the cycle_001/ directory) was acquired early July 2008.

Methodology

We use the Broadview Radar Altimetry Toolbox to observe the data and do some computation.

Over continental areas, the altimeter waveforms are highly perturbed by emerged land within the radar footprint. Numerous kind of echoes are encountered: Brown, peaky, Brown/peaky, multi-peaked... Dedicated retracking algorithms are required to properly retrieve the altimetric range. First, we propose to localise the waveform classes onto Google Earth to appreciate their repartition according to surface type (land/water). Finally, we will be able to choose an appropriate retracker to plot the water level fluctuations.

Data chosen

To limit the volume of data to download, it is better to determine the ground tracks numbers over the area of interest (here, the Sudd Marshes). These ground track numbers are available in the pass locator

on Aviso web site (download the .kml file for the Jason-2 referenced orbit to visualize it on Google Earth). Here, the Jason-2 interesting passes is: #120.

The time series used for this data use case stretches out from the cycle_001 (July 2008) to cycle_094 (January 2011).

Although BRAT can handle numerous files, it appeared preferable in terms of efficiency to perform an extraction of files over a portion of the track. We performed this extraction with the following script, based on the use of the 'ncdump', 'ncgen' and 'ncea' commands. The latter needs the installation of NCO (NetCDF operators) on the computer. The NCO homepage contains more information. Here, the extraction is done between 7°N and 9°N.

Operation

To extract the waveforms classes

Once the relevant files are all downloaded, create a dedicated workspace and then, a new dataset in the “Dataset” tab: in dataset_tr120, we have added the whole time series defined above.

On “Operations” tab, we create one operation for each waveform class mainly encountered in our area. Each waveform is classified according to its main shape and a number is assigned to each class. You can retrieve these classes in the Coastal and Hydrology Altimetry product (PISTACH) handbook in the session “Classification of the waveforms”. In our case, four operations are created:

- 1) operation_120_wvf1 for ocean (Brown) echoes
- 2) operation_120_wvf2 for specular echoes
- 3) operation_120_wvf12 for Brown+peaky echoes
- 4) operation_120_wvf23 for multi-peaked echoes

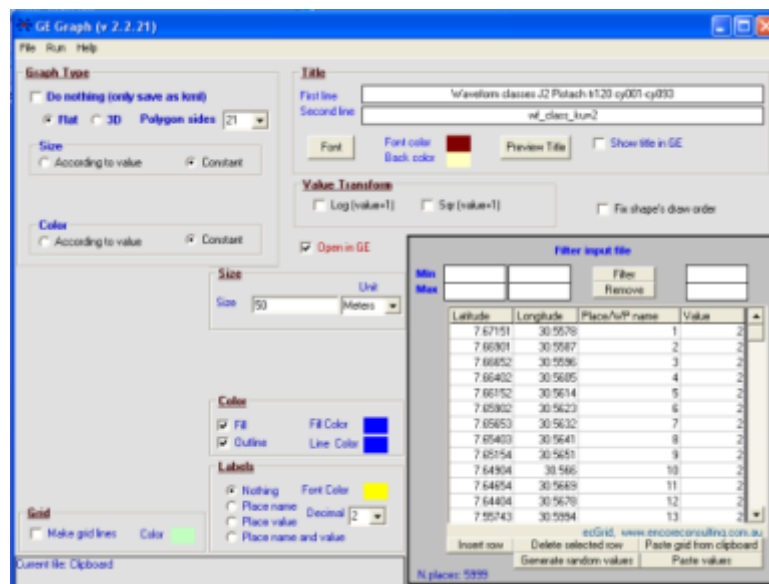


Figure 6.126. Screen of the GE-Graph software to export from BRAT, the longitude/latitude points corresponding to each waveform class on Google Earth.

For the first operation above, drag and drop the longitude (ie the field “lon”) on “X”, the latitude (ie “lat”) on “Y” and the field wf_class_ku on “Data”. Define the selection criteria to only have the data

for the considered waveform class (here for ocean echoes) over a narrow segment: (is_bounded(7.35, lat, 7.7)) && (wf_class_ku == 1).

Click on the “Export” button to obtain an ASCII output file. Rename the .txt file as ExportAsciiOperations_120_wf_class1.txt. Then do the same previous steps for each waveform class by duplicating the first operation (rename it and change the waveform class value in the selection criteria).

Then, we use a free software to export on Google Earth, the longitude/latitude points corresponding to each waveform class. Download this GE-Graph software [here](#) and proceed as follow:

- retrieve the output files in the Operation folder in your workspace and open them in MS Excel. A three-row file (with latitude, longitude, waveform class) is opened per each waveform class file.
- in MS Excel, add the first row to insert an index corresponding to the value number and corresponding to the Place/WP name in GE-Graph. So in MS Excel, four rows are created (per file): index, lat, lon, waveform class value. Select and copy all the data.
- open Ge-Graph, and click on “Paste grid from clipboard” button. Note that the row order is changed: Latitude, Longitude, Place/WP name and Value. Parameter the shape, size (constant), the color (different for each waveform class), the title.
- Save the .kml file from GE-Graph and open it in Google Earth.

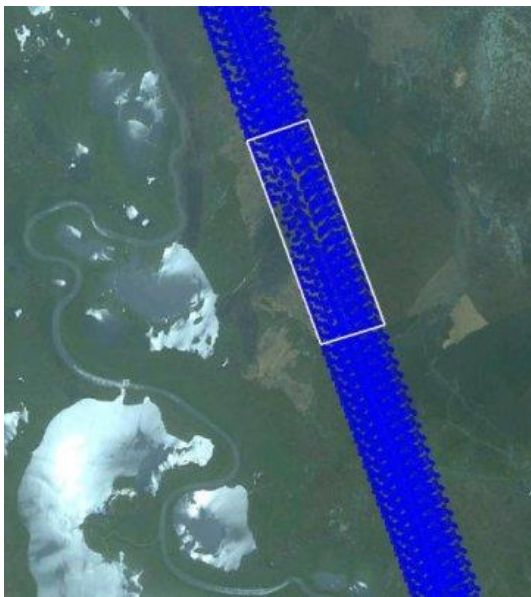


Figure 6.127. LEFT: Waveform class = 2 corresponding to Specular echoes

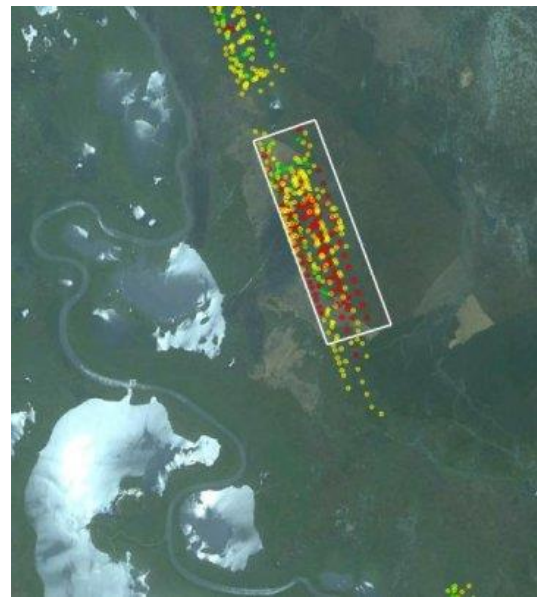


Figure 6.128. RIGHT: Waveform class = 1 (red), 12 (yellow) and 23 (green) respectively corresponding to Ocean(Brown), Brown+Peaky and Multi-peaked echoes

To represent the water level variations

The distribution of echo shape over our selected area ($7.35^{\circ} < \text{lat} < 7.7^{\circ}$) is dominated by echoes conforming to the Specular class with high-power narrow echoes (almost 96%, in blue on fig.2). The Brown+Peaky echoes class (in yellow on Fig.3) is then represented (almost 3%). The two last waveform classes represented here are less represented (Brown echoes and Multi-peaked echoes). An appropriate retracker has to be chosen taking into account the specific narrow shape of the echoes. In

the “Operation” tab, create a new operation to plot the water level variations with all the available retracking algorithms (named `Operations_p120_retrackers_vs_time`) by using the same Dataset, `dataset_tr120`. Drag and drop the field `time` on “X”. The time is expressed in seconds, to convert it in day, write in the gray box: `round(((time / 24) / 60) / 60)`.

Then insert nine new expressions in Data (an expression per RETRACKING): `ice_range_ku`, `range_c`, `range_ku`, `range_ice3_c`, `range_ice3_ku`, `range_oce3_c`, `range_oce3_ku`, `range_red3_c`, `range_red3_ku`. For each expression, insert the following operation to compute the Water Surface Altitude (WSA):

$$\text{WSA} = \text{alt} - \text{RETRACKING} - \text{geoid_EGM2008} - \text{model_dry_tropo_corr} - \text{model_wet_tropo_corr} - \text{pole_tide} - \text{solid_earth_tide} - \text{iono_corr_gim_ku}$$

The typical computation of a Water Surface Altitude for hydrologic areas (height of the surface of a given water body above the geoid) is calculated by subtracting the corrected range from the satellite altitude. The corrections are: wet troposphere, dry troposphere, ionosphere corrections and geoid, tides (pole, solid earth). The radiometer and the difference between the altimeter dual-frequency are usually perturbed by emerged lands. Thus, the wet troposphere and the ionosphere corrections are computed from models.

Click on “Execute”. In the “Views” tab, click on “New” and rename the plot in “View name”. The previous operation (`Operations_p120_retrackers_vs_time`) is displayed on the left box; unfold it to see all the expressions and put all of them on the right. The mark “Group expressions on the same plot” is ticked off. Click on “Execute”.

The retracking responses are quite different over the same surface. While `Oce3` and `Red3` retracking give a large dispersion and numerous data gaps, the `Ice1` and `Ice3` retracking in Ku-band give a similar response (black and magenta points on Figure 6.129). `Ice1` and `Ice3` differ each other by the portion/position of the window selected around the main leading edge of the waveform. We cannot identify the “best” retracking but `Ice1` and `Ice3` standards altimeter range solution seem to suit to this area and can be used over medium-size water targets with specular echoes.

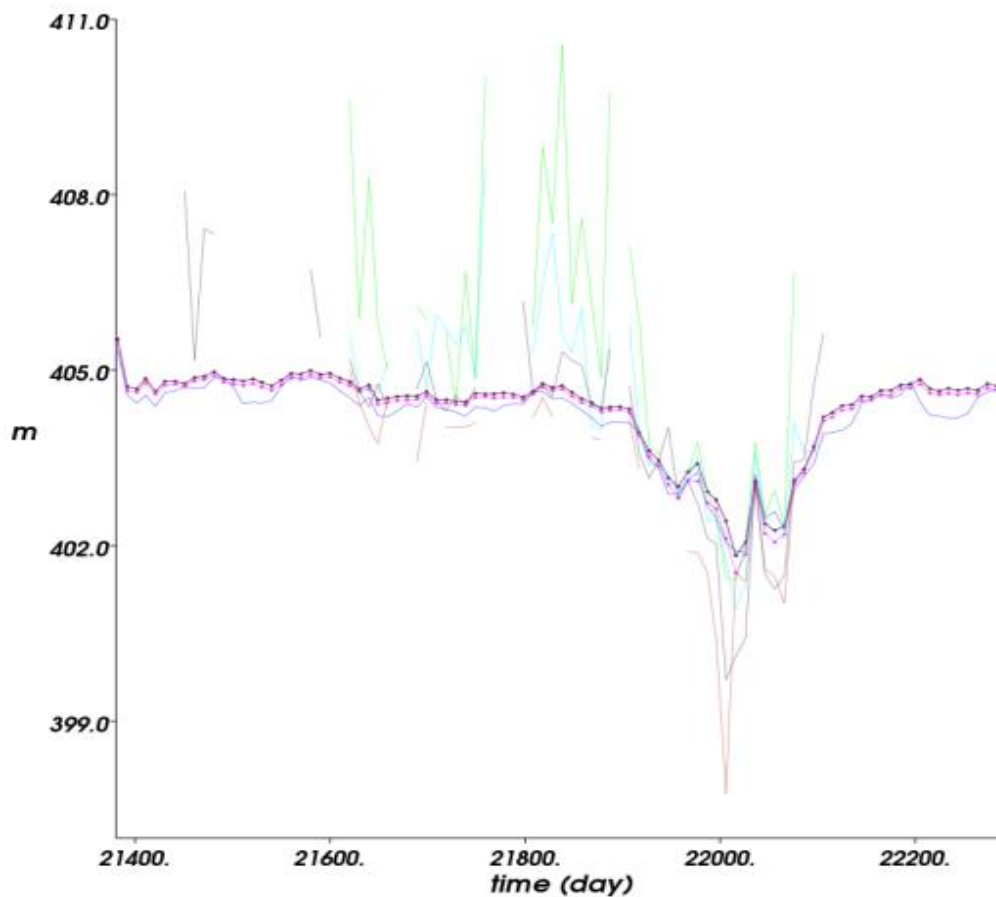


Figure 6.129. Water Surface Altitude time series (in meter and Julian days) derived from the 20 Hz Jason-2 along the pass 120 ($7.492^{\circ} < \text{lat} < 7.533^{\circ}$), computed from all the available retracking algorithms in c. The retracking `ice_range_ku` (black) and `range_ice3_ku` (magenta) are drawn with points. The others are: `range_c` (green), `range_ice3_c` (blue), `range_ku` (light brown), `range_oce3_ku` (black – no point), `range_red3_c` (light blue), `range_red3_ku` (dark brown). The `range_oce3_c` retracking gives no output point on this area.

Further information:

- Other Data Use Cases using hydrology dedicated products: [Altimetry for lake/reservoir studies](#).
- [Aviso website](#): Posters and presentations at the Towards High-Resolution of Ocean Dynamics and Terrestrial Surface Waters from Space 2010 workshop.
- [Coastal and Hydrology Altimetry product \(PISTACH\) handbook](#)

6.8.21 Use of the GOCE toolbox (GUT) in oceanography along with altimetry

Knowledge of the gravity field, and more specifically of the geoid is of foremost importance to use altimetry data in oceanography.

Dynamic topography and altimetry

Dynamic topography is the sea level driven by thermodynamic processes in the ocean. It includes a “static” part (taking into account features like the main currents, etc.), and a variable part. Altimetry

gives access to the sea surface height with respect to an ellipsoid reference. However, this sea surface height includes features from several different sources: geoid, ocean variability, main currents, etc.

SSH = Geoid height + dynamic topography

= Mean Sea Surface + Sea Level Anomalies

= (Geoid height + Mean Dynamic Topography) + Sea Level Anomalies

Variations of the Sea Surface Height can be computed (Sea Level Anomalies, i.e. sea surface height with respect to the Mean Sea Surface), using long period of altimetry data to define a mean sea surface or a mean profile under the satellite track.

Warnings

Geoid, MSS, MDT and SLA data are not immediately compatible. Meaning:

- they must be referenced on the same surface (Reference ellipsoid),
- they must be homogeneous with respect to tides
- and, last but not least, their spectral content must be the same. If one data include small-scale phenomena and not the other, the addition will miss some information (and the same for a comparison between different datasets).

GOCE and GOCE User Toolbox

GOCE (Gravity Field and Steady-State Ocean Circulation) is an ESA mission dedicated to the determination of the Earth's gravity field and the geoid height at a spatial resolution of 100 km with unprecedented accuracy.

The GOCE User Toolbox (GUT) is a compilation of tools for the utilisation and analysis of GOCE Level 2 products. GUT supports applications in Geodesy, Oceanography and Solid Earth Physics. GUT consists of a series of advanced computer routines that carry out the required computations. It may be used on Windows PCs, UNIX/Linux Workstations, and Mac.

Data used

“A priori” data provided with GUT v1.1, including GOCE EGM_GOC_2 Level-2 Spherical Harmonic Potential Product File (DIRECT SOLUTION – First HPF Delivery) data, MSS_CNES_CLS10, MDT_CNES_CLS_09, and also gridded and along-track SLA from Aviso

Methodology

We will use both GUT and BRAT to compute a MDT then use it with altimetry data.

GUT processing: create a satellite-only MDT

GOCE spherical harmonics data are provided with GUT. Once retrieved, you can compute a geoid, then you have to harmonize this geoid with the Mean Sea Surface you wish to use. Once done, you can subtract the two and get a Mean Dynamic Topography.

The steps to follow to calculate the mean dynamic topography in spatial domain are:

– **Compute a geoid from GOCE spherical harmonics data**

Step 1: Create a geoid height, into the same reference system as the MSS

```
gut                                geoidheight_gf                                -InFile
GO_CONS_EGM_GOC_2__20091101T000000_20100110T235959_0002.HDR -Ellipse TOPEX -
T mean-tide -OutFile geoidheight_TP_MT.nc
```

– **Grid adaption between geoid and MSS**

Step 2: Interpolate the MSS file onto the same grid as the geoid height

```
gut adapt_gf -InFile MSS_CNES_CLS_10_2M.nc -Gf geoidheight_TP_MT.nc -OutFile
MSS_adapt.nc
```

– **Subtraction of geoid from MSS**

Step 3: Subtract both files by typing:

```
gut subtract_gf -InFileLhs MSS_adapt.nc -InFileRhs geoidheight_TP_MT.nc -OutFile
MSS_geoidheight_TP_MT.nc
```

– **Masking the Difference**

Step 4: Remove the values on continents by typing:

```
gut landmask_gf -InFile MSS_geoidheight_TP_MT.nc -InLsmFile GUT_LSM.nc -OutFile
MSS_geoidheight_TP_MT_lmsk.nc
```

– **Filtering in space domain (at 2°)**

Step 5 : Filter the resulting file by typing:

```
gut filter_gf -InFile MSS_GOCE_TP_MT_lmsk.nc -Fhan 2 -OutFile
MSS_geoidheight_TP_MT_lmsk_fhan2.nc
```

Note that a built-in workflow within GUT enables you to do the same in one instruction:

```
gut                                geoidheight_gf                                -InFile
GO_CONS_EGM_GOC_2__20091101T000000_20100110T235959_0002.HDR -Ellipse TOPEX -
R 0.5:359.5,-89.5:89.5 -I 1:1 -OutFile geoidheight.nc
```

It was split in different steps here to highlight the important points of the processing.

GUT is using the BRAT Display as a viewer, so you can use directly this by entering “BratDisplay *yourfile.nc*” in a command window.

BRAT processing:

BRAT can be used in combination with GUT. For example:

- to compute SLA, either from GDRs or from higher level datasets, along-track or gridded, or extract them from pre-computed datasets
- to compute geostrophic velocities, and plot them (See Data Use Case on [Geostrophic velocities](#))
- to compute Kinetic energy from those (or from similar GUT outputs)
- to overlay on other altimetry data or data available within altimetry datasets (e.g. bathymetry)
- to select/edit relevant data by using thresholds, or flag values, etc.

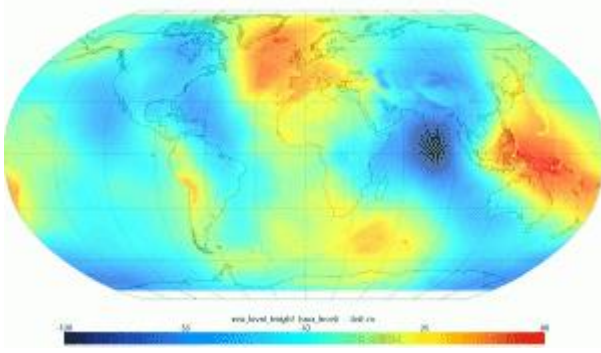


Figure 6.130. Compute a geoid from GOCE spherical harmonics data

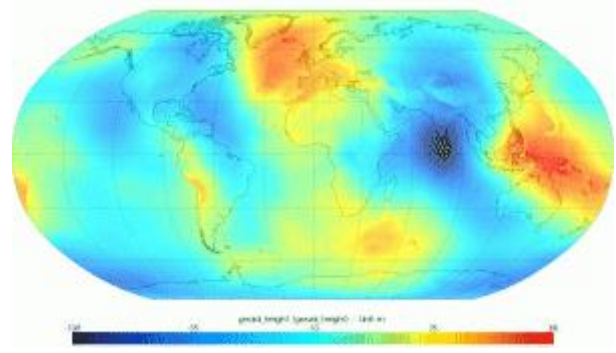


Figure 6.131. Grid adaption between geoid and MSS

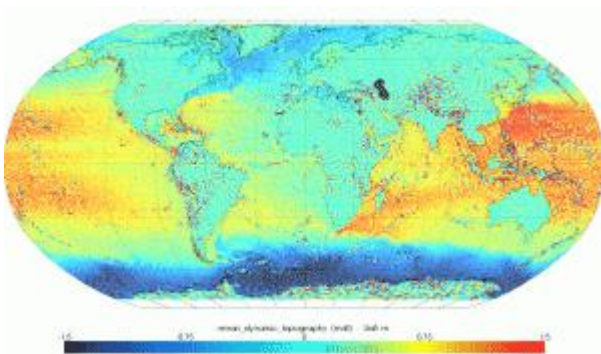


Figure 6.132. Subtraction of geoid from MSS

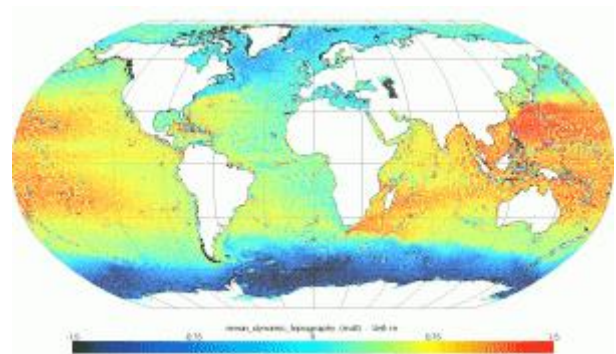


Figure 6.133. Masking the Difference

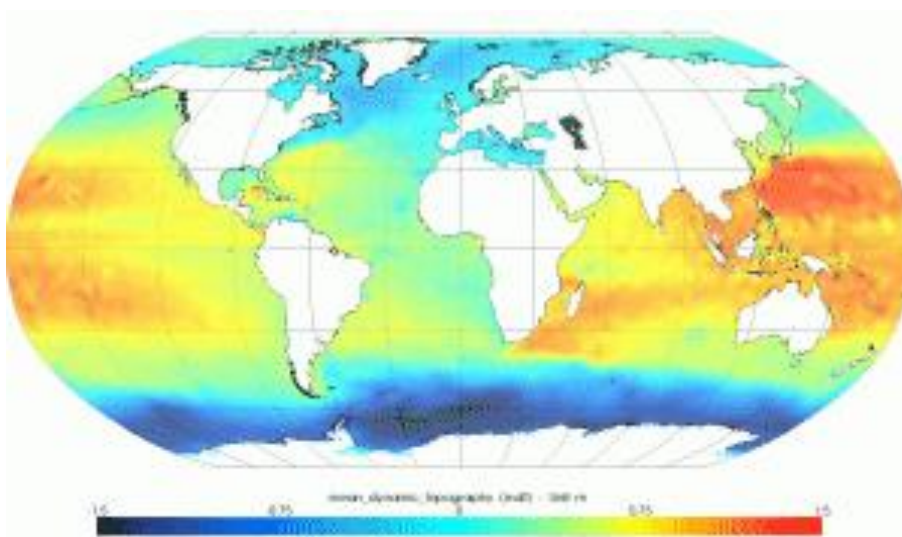


Figure 6.134. Resulting MDT after filtering in space domain (at 2°)

Dynamic topography and altimetry

Once your MDT computed, you can use again GUT to add it to different SLAs computed within BRAT.

The main point to remember is that you must compute SLA in m (the same than MDT), and adapt the SLA grid to the MDT one (using the `adapt_gf` workflow)

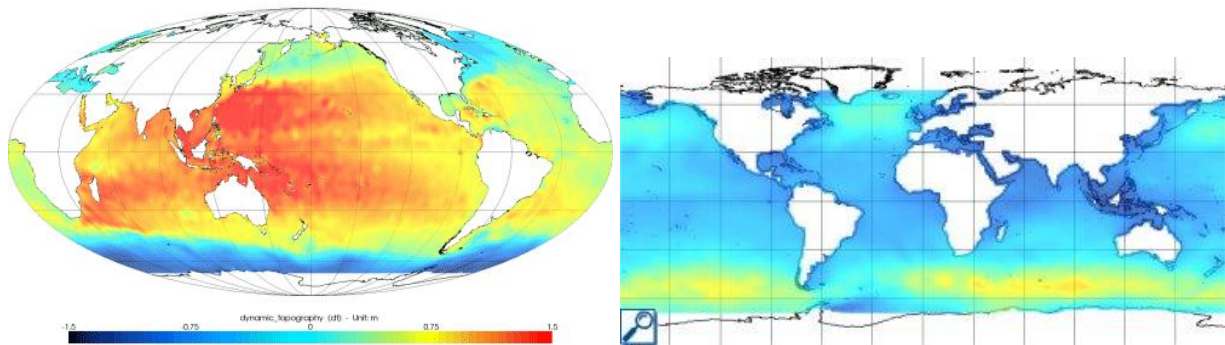


Figure 6.135. Jason-2 SLA added to the above computed MDT

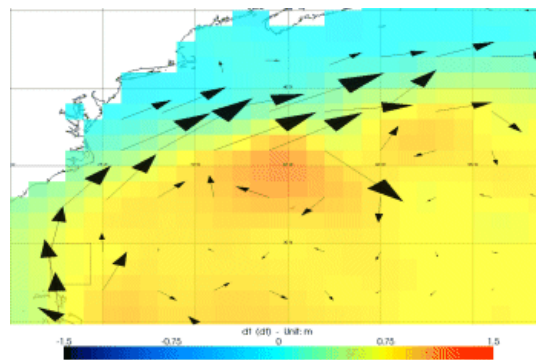


Figure 6.136. Geostrophic velocities computed from this Dynamic Topography over the Gulf Stream region using BRAT (see relevant Data Use Case).

References

- The GOCE User Toolbox can be downloaded in <https://earth.esa.int/gut>.

7 Missions

Precise satellite altimetry missions have transformed the way we view Earth and its oceans. Highly accurate altimetry measurements give us the ability to observe sea surface height systematically.

The earliest altimeters were intended to demonstrate proof of concept. With Seasat (1978), the first scientific results were shown. Since 1986 (Geosat), these missions have been providing vital information for an international user community. Besides international programs dedicated to studying global oceans and climate, such as WOCE, WCRP, Clivar and GOOS, and others working on the El Niño phenomenon (TOGA), ocean forecasting projects such as GODAE are now getting underway. All these programs call for high-quality altimetry measurements, which are merged with other data to obtain the broadest picture possible of the underlying mechanisms at work, and assimilated into ocean and climate prediction models.

Past altimetry missions

- The first altimetric satellites: Skylab, GEOS 3, Seasat
- Geosat
- ERS-1
- Topex/Poseidon
- GFO
- ERS-2
- Envisat
- Jason-1

Current altimetry missions

- Jason-2
- CryoSat-2
- HY-2A
- SARAL
- Sentinel 3
- Jason-3

Future missions altimetry missions

- Jason-CS/Sentinel-6
- SWOT
- See also future technology improvements

Planetary Missions

- MARSIS-Mars
- SHARAD-Mars
- RIME-Jupiter Moons
- SRS- Venus

7.1 Past missions

Altimetry was announced as a priority at the Williamstown Symposium in 1969. The 1970s saw the development of accurate satellite altimeter systems, with Skylab (which produced the first measurements of undulations in the marine geoid due to seafloor features), GEOS-3 and Seasat, whose data were widely and freely distributed to scientists throughout the world, laying the foundations for a new generation of ocean satellites. In the 1980s, only Geosat was launched, whose data was at first classified.

In the 1990s, with ERS-1 and Topex/Poseidon, altimetry began providing vital information to a growing international user community (more than 1,000 teams of users around the world in 2006). In the 2000s, more than a breakthrough in ocean observation, Jason-1 and Envisat opened a new pathway for radar altimetry, and it has helped to build up a 20-year time series of continuous sea surface measurements.

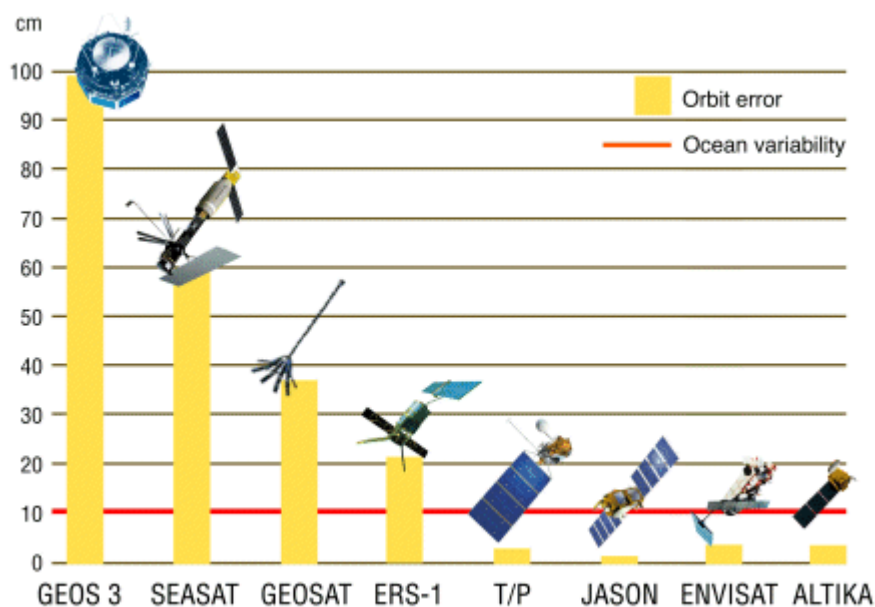


Figure 7.1. Improvements in measurement accuracy since the first satellite altimetry missions has enabled us to observe ocean variations at close quarters since 1992. (Credits [CNES](#))

The first altimetric satellites: [Skylab](#), [GEOS 3](#), [Seasat](#)

7.1.1 Skylab



Figure 7.2. Skylab (Credits NASA)

Skylab, America's first experimental Space station, was launched in May 1973 and visited by crews three times in 1973 and 1974. It carried a generalised general active and passive microwave measurement system called S193. This instrument carried the first spaceborne altimeter, for the purpose of "providing ocean state effects on pulse characteristics." Using a pulse width of 0.1 microseconds this system was able to get achieve a resolution of 15 m. It only operated over short orbital segments only but was able to demonstrate the measurement of coarse features of the marine geoid, such as major ocean trenches.

Satellite	Skylab
Launched	May 1973
Mission	acquiring new knowledge in Space to improve life on Earth
Altitude	435 km
Inclination	50°

Further information on [NASA/KSC website](#)

7.1.2 GEOS 3



Figure 7.3. GEOS 3 (Credits NASA)

Satellite	GEOS 3
Launched	9 April 1975
Mission	Geodesy
Altitude	845 km
Inclination	115°

GEOS 3 (Geodynamics Experimental Ocean Satellite) was launched in April 1975, and ended its mission in December 1978. It carried the first instrument to yield useful measurements of sea level and its variability over time.

When a satellite flies at higher altitudes, this reduces the strength of the altimeter's return signal (which is proportional to the cube of the height) and alters the size of the footprint on the ground. Because the satellite is incapable of emitting a more powerful signal, the pulse compression technique must be used above a certain altitude to compensate for the weakened return signal. Since GEOS 3 (1974), which flew at an altitude of 840 km, all altimeters have used pulse compression, and the resolution made possible by this compression has been enhanced. GEOS 3 offered significant improvements over Skylab's altimeter, including improved performance as well as greater global coverage, but this performance was still not good enough to enable useful science to be extracted from its measurements.

Further information on [International Laser Ranging Service \(ILRS\) web site](#) (NASA/GSFC)

7.1.3 Seasat



Figure 7.4. Seasat (Credits NASA)

Satellite	Seasat
Launched	26 June 1978
Mission	study Earth and its seas
Altitude	800 km
Inclination	108°

Seasat (SEAfaring SATellite) was launched by NASA in June 1978, and ended its mission in October 1978, due to a malfunction. Seasat's experimental instruments included a synthetic aperture radar, which provided the first ever highly-detailed radar images of ocean and land surfaces from Space; a radar scatterometer, which measured near-surface wind speed and direction; a radar altimeter, which measured ocean surface and wave heights; and a scanning multi-channel microwave radiometer measuring surface temperatures, wind speeds and sea ice cover. Seasat carried a range of sensors selected for remote sensing of the oceans, including the first high-performance altimeter. The improvement required for Seasat could not be achieved by simply upgrading the GEOS 3 design. Although video circuitry could be designed to process higher bandwidth signals, at the expense of increasing power, the pulse compression filters required for direct implementation of the required waveform were simply not available. A new approach was devised: the full-deramp technique. With this technique, no compression filter is required in the receiver. From Seasat onwards, all altimeters have been using this technique, achieving a significant improvement in resolution. In oceanography, Seasat gave us our first global view of ocean circulation, waves and winds, providing new insights into the links between the ocean and atmosphere that drive our climate. For the first time, the state of an entire ocean could be seen all at once. Seasat's altimeter mapped ocean topography, allowing scientists to determine ocean circulation and heat storage. The data also revealed new information about the Earth's gravity field and the topography of the ocean floor. Since Seasat, advanced ocean altimeters on JPL's Topex/Poseidon and Jason missions have been making precise measurements of sea surface height which are used to study climate phenomena such as El Niño and La Niña. Ocean altimetry has since become part of weather and climate models and many other applications.

Further information on [Seafaring Satellite Sets 25 Year Trend](#) (NASA/JPL website)

7.1.4 Geosat

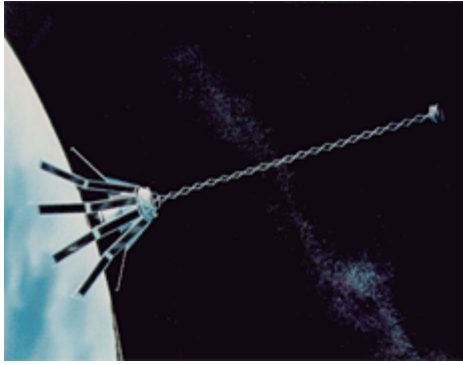


Figure 7.5. Geosat (Credits US Navy)

Geosat (GEOdetic SATellite) was launched in March 1985, and ended its mission in January 1990. Its primary task was to measure the marine geoid for the US Navy, but it also provided measurements of sea state and winds which proved to be useful for operational Navy purposes. Once this 18-month mission was over, the satellite was put on a 17-day repeat orbit (Exact Repeat Mission: ERM) which began on 8 November 1986, retracing Seasat's ground tracks, and providing the scientific community, through NOAA, with altimeter data for over three years. Geosat was the first mission to provide long-term high-quality altimetry data.

Satellite	Geosat
Launched	12 March 1985
Mission	Describe the marine geoid
Altitude	800 km
Inclination	108°(non-sun-synchronous)

Further information on the [data](#) (NOAA website)

7.1.5 ERS-1



Figure 7.6.ERS-1 (Credits ESA)

Satellite	ERS-1
Launched	17 July 1991
Mission:	Observe Earth and environment
Altitude:	785 km
Inclination:	98.52°

The ERS-1 satellite's main mission was to observe Earth, in particular its atmosphere and ocean. Built by ESA, it carried several instruments, including a radar altimeter.

ERS-1 was launched in July 1991, switched off in June 1996 and retired in March 2000. ERS-2, the follow-on from ERS-1, was launched in April 1995. It was used in tandem with ERS-1 from August 1995 to June 1996, their identical orbits (35 days) having a one-day shift.

ERS-1 flew on three different orbits:

- a 3-day period for calibration and sea ice observation,
- a 35-day period for multi-disciplinary ocean observations,
- a 168-day period for geodetic applications.

Further information on:

- ERS missions [Home Page](#) (ESA website),
- [ERS-1](#) (Cersat website)

7.1.5.1 ERS-1 Instruments

The ERS satellites carry instrumentation consisting of a core set of active microwave sensors supported by additional, complementary instruments:

- AMI – active microwave instrument consisting of a synthetic aperture radar (SAR) and a wind scatterometer
- RA – radar altimeter
- ATSR – along-track scanning radiometer
- Gome (ERS-2) – global ozone monitoring experiment
- MWS – microwave sounder
- PRARE – precise range and range rate equipment
- LRR – laser retroreflector

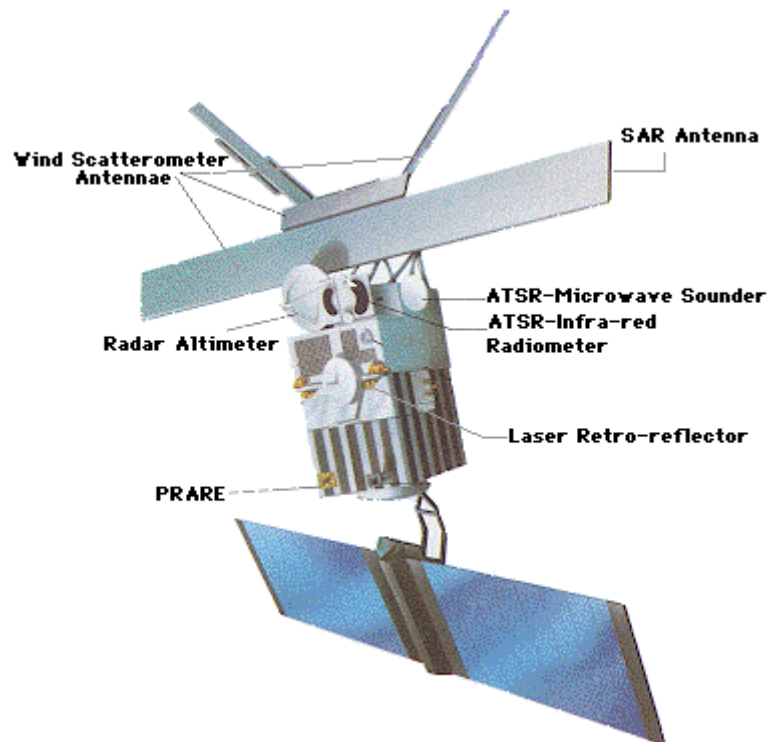


Figure 7.7. ERS-1 instruments (Credits ESA)

The satellite concept is based on reusing the Multi-mission Platform, developed within the French SPOT programme. This platform provides the major services for satellite and payload operations, in particular attitude and orbit control, power supply, monitoring and control of payload status, and telecommunications with the ground segment.

RA altimeter

The Radar Altimeter (RA) is a Ku-band (13.8 GHz) nadir-pointing active microwave sensor designed to measure the return trip time for echoes from ocean and ice surfaces. Functioning in one of two operational modes (ocean or ice) the Radar Altimeter provides information on significant wave height, surface wind speed, sea surface elevation, relating to ocean currents, the surface geoid and tides, and various parameters over sea ice and ice sheets.

MicroWave Sounder

The Along-Track Scanning Radiometer (ATSR) combines an infrared radiometer and a microwave sounder for measuring sea surface temperature, cloud top temperature, cloud cover and atmospheric water vapour content. This is used, among other things, to correct altimetry data from path delay due to atmospheric water.

Location systems

The ERS sensor location system includes two instruments – the Precise Range and Range-rate Equipment (PRARE) and the Laser Retroreflectors (LRR) to provide precise orbit determination for the referencing of height measurements made by the Radar Altimeter. The PRARE has been non-operational since launch, but a description of it is included here for completeness.

PRARE

The Precise Range and Range-rate Equipment (PRARE) is included for the accurate determination of the satellite's position and orbit characteristics, and for precise position determination (geodetic fixing).

LRR

The LRR is highly accurate but it requires ground stations that are complex to operate, and its use can be restricted by adverse weather conditions. It is used to calibrate the other location system so that the satellite's orbit can be determined as accurately as possible.

Further information on [ERS instruments](#) (ESA website)

7.1.5.1.1 Radar Altimeter

The Radar Altimeter (RA) is a Ku-band (13.8 GHz) nadir-pointing active microwave sensor designed to measure the return trip time for echoes from ocean and ice surfaces. Functioning in one of two operational modes (ocean or ice) the Radar Altimeter provides information on significant wave height, surface wind speed, sea surface elevation (relating to ocean currents, the surface geoid and tides) and various parameters over sea ice and ice sheets.

Function

The Radar Altimeter is a Ku-band (13.8 GHz) nadir-pointing active microwave sensor designed to measure the time return echoes from ocean and ice surfaces. Functioning in one of two operational modes (ocean or ice) the Radar Altimeter provides information on significant wave height; surface wind speed; sea surface elevation, which relates to ocean currents, the surface geoid and tides; and various parameters over sea ice and ice sheets.

Principle

The altimeter emits a radar beam that is reflected back to the antenna from the Earth's surface. RA operates at a single frequency (13.6 GHz in the K_u-band).

The Radar Altimeter operates by timing the two-way delay for a short-duration radio frequency pulse, transmitted vertically downwards. The level of accuracy required for range measurement (better than 10 cm) calls for a pulse compression (full deramp) technique. In ocean mode a chirped pulse of 20 microseconds duration is generated with a bandwidth of 330 MHz. For tracking in ice mode an increased dynamic range is used, obtained by reducing the chirp bandwidth by a factor of four to 82.5 MHz, though this also results in a coarser resolution (see [how altimetry works](#) for details).

Technical data

Emitted Frequency (GHz)	Single-frequency (Ku) – 13.8
Pulse Repetition Frequency (Hz)	1020
Pulse duration (microseconds)	20
Bandwidth (MHz)	330 and 82.5
Antenna diameter (m)	1.2
Antenna beamwidth (degrees)	1.3

Power (W)	50
Redundancy	Yes
Specific features	2 bandwidths for ocean and ice measurements

Further information on [RA instrument](#) (ESA website)

7.1.5.1.2 MWS: Microwave Sounder

The main objective of the microwave radiometer (MWS) is to measure the integrated atmospheric water vapour column and cloud liquid water content, which are used as correction terms for the radar altimeter signal. In addition, MWS measurement data are useful for determining surface emissivity and soil moisture over land, for surface energy budget investigations to support atmospheric studies, and for ice characterisation.

Function

The MWS measures water vapour content in the atmosphere so that we can determine how it impacts radar signal propagation. Its measurements can also be used directly for studying precipitable water and cloud liquid content along the satellite track.

Principle

The MWS is a passive receiver that collects radiation reflected by the oceans at frequencies of 23.8 GHz and 36.5 GHz.

Radiation measured by the radiometer depends on surface winds, ocean temperature, salinity, foam, absorption by water vapour and clouds, and various other factors. To determine atmospheric water vapour content accurately, we need to eliminate sea surface and cloud contributions from the signal received by the radiometer. This is why the MWS uses different frequencies, each of which is more sensitive than the others to one of these contributions. The frequencies 23.8 GHz and 36.5 GHz are the result of a trade-off between the instrument (reflector) size required to cover a horizontal area on the Earth's surface comparable to the altimeter beam, and the maximum sensitivity to water vapour change in the atmosphere. These frequencies are used to measure the strength of the weak water-vapour emission-line at 22 GHz. In order to eliminate microwave radiation emitted by the Earth's surface, differential measurements at two frequencies must be made. The optimal choice is to use one frequency at the peak of the line and one at the lowest point.

With one feed horn for each frequency, the MWS points via an offset reflector at an angle close to nadir. The instrument is configured in such a way that the 23.8 GHz channel is pointing in the forward direction, the 36.5 GHz channel in the backward direction, with a footprint of about 20 km diameter for each beam.

Further information on [MWS instrument](#) (ESA website)

7.1.5.1.3 PRARE

Precise Range and Range-rate Equipment (PRARE) is included for the accurate determination of the satellite's position and orbit characteristics, and for precise position determination (geodetic fixing). It is a satellite tracking system which provides two-way microwave range and range-rate measurements to ground-based transponder stations.

The PRARE system was developed by the Institut für Navigation (INS) at the University of Stuttgart, Kayser-Threde GmbH, Munich and the Deutsches Geodätisches Forschungsinstitut, Munich, as a German national experiment.

Function

The system was designed to:

- * provide, in all weather conditions, precise satellite-to-ground or satellite-to-satellite range and range-rate information,
- * very reliable measurements through cross-checks and calibration procedures,
- * ensure highly effective operation of the ground segment through data collection and dissemination via the satellite itself, and control of the global network via one central ground station,
- * allow rapid generation of products at an archiving, processing and distribution centre.

Principle

The PRARE measurement principle involves two signals sent from the sensor on board the satellite, one signal in the S-band (2.2 GHz) and the other in the X-band (8.5 GHz). Both signals are modulated with a PN code (pseudo-random noise). The time delay in the reception of the two simultaneously-emitted signals is measured at the ground station with great accuracy (<1 ns) and retransmitted to the on-board memory for ionospheric data correction. Collection of meteorological data by the ground station allows corrections to be applied for tropospheric refraction.

Further information on [PRARE instrument](#) (ESA website)

7.1.5.1.4 Laser RetroReflector

The LRR is an array of mirrors that provides a target for laser tracking measurements from the ground. By analysing the round-trip time of the laser beam, we can locate where the satellite is on its orbit.

Function

A laser retroreflector is attached to a mount on the nadir panel close to the RA antenna.

The LRR is a passive device which is used as a reflector by ground-based SLR (Satellite Laser Ranging) stations using high-power pulsed lasers. In the case of ERS-1, tracking using the LRR was mainly performed by the International Laser Ranging Service (ILRS).

The ILRS provides tracking for the satellite from its global network of laser ranging stations. Laser stations fire short laser bursts at ERS and time the interval before the pulse is reflected back. These ILRS stations are relatively few, but because their positions are very accurately known, they provide a set of independent reference measurements of ERS's position, which contribute to the satellite's precise orbit determination.

Principle

The operating principle of the LRR is therefore to measure on the ground the return trip time of laser pulses reflected from an array of corner cubes mounted on the Earth-facing side of the satellite. The corner cubes ensure that the laser beam is reflected back parallel to the incident beam. The detailed design of the cubes includes compensation for the aberration of the laser beam caused by the satellite's

velocity: the satellite moves almost 40 metres between the emission and reception of the laser pulse from the SLR station, and this is compensated for by slight nonparallelism of the reflected beam.



Figure 7.8. ERS-1 LRR (Credits ESA)

The corner cubes are made of the highest-quality fused silica and work in the visible spectrum. Their performance is optimised at the two wavelengths (694 nm and 532 nm) commonly used in SLR stations. The corner cubes are symmetrically-mounted on a hemispherical surface with one nadir-pointing corner cube in the centre, surrounded by an angled ring of eight corner cubes.

This allows laser ranging in the field of view angles of 360° in azimuth and 60° in elevation around the perpendicular to the satellite’s Earth-facing panel (positioned on the axis at point -Zs with respect to the satellite’s centre of mass).

Orbit performance

Figure shows the history of the ground track for ERS-1

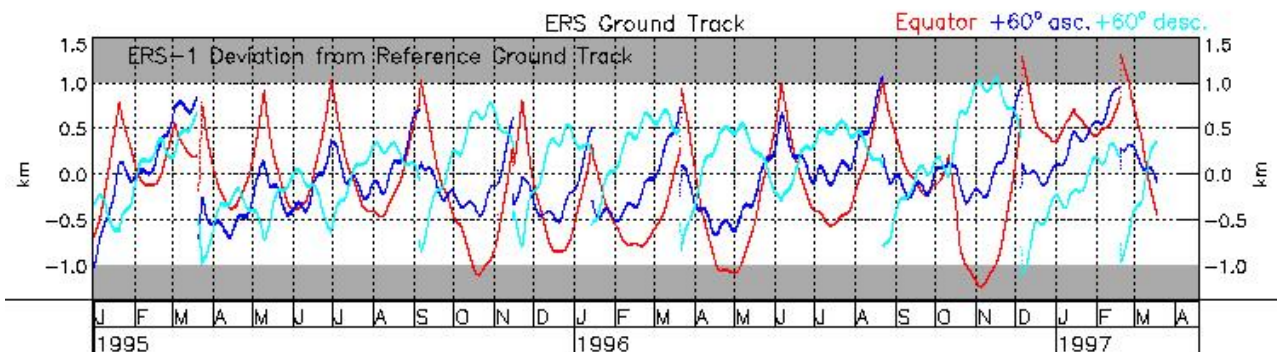


Figure 7.9. R. Zandbergen et.al. , Progress in ERS Orbit and Tracking Data Analysis

Further information on ERS (ESA website)

7.1.5.2 ERS-1 orbits

To carry out its mission ERS-1's orbit had to enable its instruments to scan along predetermined paths designed to give optimum coverage for a set number of orbits. To achieve this, ERS-1 was a three-axis-stabilised, Earth-pointing satellite in yaw steering mode (YSM). The elliptical orbit was sun-synchronous, near-polar, with a mean altitude of 785 km, an inclination of 98.5° and a local solar time at the descending node of 10:30 a.m.

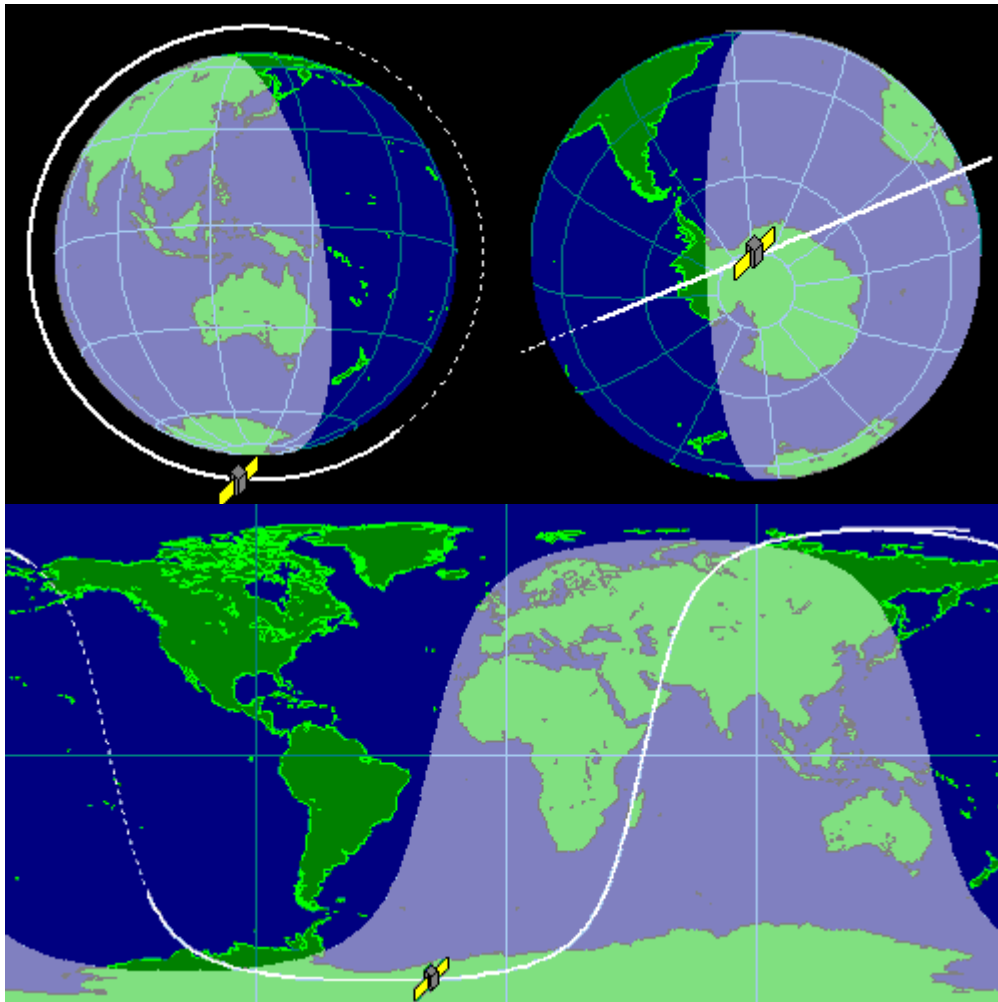


Figure 7.10. ERS-1 orbit

Orbit parameters

35-day orbit

Table 7.1 ERS -1 Orbit Main characteristics

Semi-major axis	7159.5 km
Eccentricity	0.0001042
Argument of perigee	92.4836°

Table 7.1 ERS -1 Orbit Main characteristics

Inclination (sun-synchronous)	98.543°
-------------------------------	---------

Table 7.2 ERS -1 Orbit Auxiliary data

Mean altitude	782 km
Nodal period	50 min 25.5 s
Repeat cycle	35 days
Number of passes per cycle	1002
Ground track separation at Equator	80 km
Acute angle at Equator crossings	
Longitude at Equator of pass 1	
Orbital velocity	7.45 km/s
Ground scanning velocity	

For the other repeat periods:

	3-day	35-day	168-day
semi major axis	7153.138	7159.496	7147.191
inclination	98.516 deg.	98.543 deg.	98.491 deg.
mean altitude	785 km	782 km	770 km
orbits per cycle	43	501	2411

Further information on [ERS](#) (ESA website)

7.1.6 Topex/Poseidon

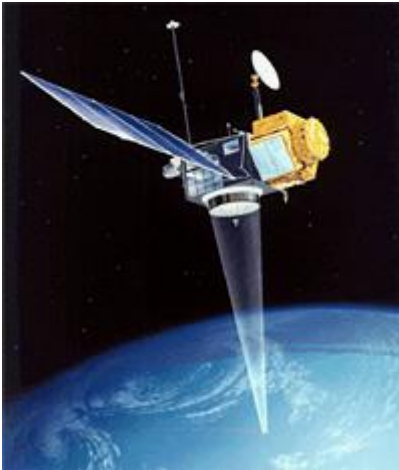


Figure 7.11. Topex/Poseidon

Satellite	Topex/Poseidon
Launched	10 August 1992
Mission	Measure sea surface height
Altitude	1336 km
Inclination	66° (non-sun-synchronous)

The Topex/Poseidon satellite was launched on 10 August 1992 with the objective of “observing and understanding the ocean circulation”. A joint project between NASA, the US space agency, and CNES, the French space agency, it carried two radar altimeters and precise orbit determination systems, including the DORIS system.

To be useful for studying ocean circulation, especially on gyre and basin scales, numerous improvements had been made to Topex/Poseidon compared with previous altimetry systems (Seasat, Geosat), including a specially-designed satellite, suite of sensors, satellite tracking systems and orbit configuration, as well as the development of an optimal gravity model for precision orbit determination and a dedicated ground system for mission operations.

Topex/Poseidon laid the foundation for long-term ocean monitoring from Space. Every ten days, it supplied the world’s ocean topography, or sea surface height, with unprecedented accuracy.

On 15 September 2002 Topex/Poseidon assumed a new orbit midway between its original ground tracks. The former Topex/Poseidon ground tracks were overflown by Jason-1. This tandem mission demonstrated the scientific capabilities of a constellation of optimised altimetry satellites. The last data were acquired on October 2005, due to a failure in a pitch reaction wheel. The mission ended on 18 January 2006.

Further information on:

- [Topex/Poseidon \(Aviso\)](#)
- [Ocean surface topography from space \(NASA/JPL\)](#)
- [Physical Oceanography Distributed Active Archive Center \(NASA/JPL\)](#)
- [Topex/Poseidon, the beginnings of satellite oceanography \(CNES\)](#)

7.1.6.1 T/P Instruments

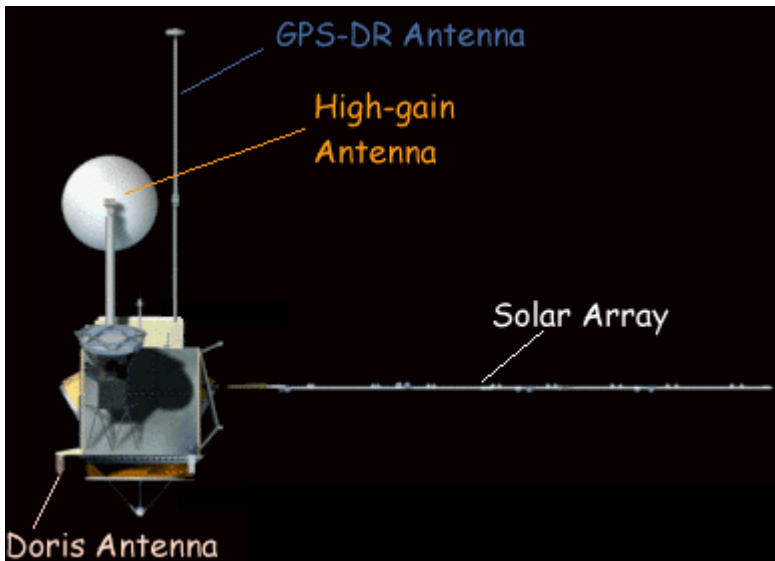


Figure 7.12. Topex/Poseidon instruments (Credits NASA/CNES)

The Topex/Poseidon satellite was an adaptation by Fairchild Space of the existing Multimission Modular Spacecraft (MMS) which successfully carried the payloads of the Solar Maximum Mission, Landsat 4 and Landsat 5. The MMS design was modified to meet Topex/Poseidon's requirements: a 2,400 kg mass carrying six science instruments – four operational and two experimental.

Topex (Topography Experiment) altimeter, or NRA (NASA Radar Altimeter)

The NRA is a radar altimeter that emits pulses at two frequencies (13.6 and 5.3 GHz, the second frequency is used to determine the electron content in the atmosphere) and analyses the return signal reflected by the surface. The signal's round-trip time is estimated very precisely in order to calculate the range, after applying the necessary corrections (Instrument supplied by NASA).

Poseidon-1 altimeter, or SSALT (Single frequency Solid State radar ALTimeter)

Poseidon-1 is an experimental instrument. It is a compact, low-power, low-mass instrument offering a high degree of reliability. Poseidon-1 is a radar altimeter that emits pulses at a single frequency (13.65 GHz – Ku-band) and analyses the return signal reflected by the surface. It shares the same antenna as the NRA; thus only one altimeter operates at any given time. It operates about 10% of the time, or one cycle in ten (Instrument supplied by CNES).

TMR (Topex Microwave Radiometer)

This instrument measures radiation from the Earth's surface at three frequencies (18, 21 and 37 GHz). Measurements acquired at each frequency are combined to determine atmospheric water vapour and liquid water content. Once the water content is known, we can determine the correction to be applied for radar signal path delays (Instrument supplied by NASA).

Location systems

Altimetric measurements are referred to geodetic coordinates by means of a precise orbit determination system. Two precise orbit determination teams, one operated by CNES and one by NASA, use a combination of LRA and DORIS tracking data.

The location systems on board Topex/Poseidon complemented each other to measure the satellite's position on orbit to within two centimetres on the radial component. The LRA is highly accurate, but it requires ground stations that are complex to operate, and its use can be restricted by adverse weather conditions. It is used to calibrate the other two location systems so that the satellite orbit can be determined as accurately as possible. The TRSR (a GPS receiver) acquires data that complement

DORIS measurements in order to determine the orbit in real time and to support precise orbit determination.

DORIS (Doppler location)

The DORIS system uses a ground network of orbitography beacons spread around the globe, which send signals at two frequencies to a receiver on the satellite. The relative motion of the satellite generates a shift in the signal's frequency (called the Doppler shift) that is measured to derive the satellite's velocity. These data are then assimilated in orbit determination models to keep permanent track of the satellite's precise position (to within three centimetres) on its orbit (Instrument supplied by CNES).

GPSDR (GPS location)

The GPSDR uses the Global Positioning System (GPS) to determine the satellite's position by triangulation, in the same way that GPS fixes are obtained on Earth. At least three GPS satellites determine a mobile object's (in this case, the satellite's) exact position at a given instant. Positional data are then integrated into an orbit determination model to track the satellite's trajectory continuously (Instrument supplied by NASA).

LRA (laser tracking)

The LRA (Laser Retroreflector Array) is an array of mirrors that provides a target for laser tracking measurements from the ground. By analysing the round-trip time of the laser beam, we can locate where the satellite is on its orbit (Instrument supplied by NASA).

Further information on [Topex/Poseidon](#) (Aviso website)

7.1.6.1.1 Topex altimeter, or NRA

The Topex altimeter (206 kg including redundancy, 237 W), operating simultaneously at 13.6 GHz (Ku-band) and 5.3 GHz (C-band) was provided by NASA. It is a fifth generation altimeter, whose design is based on the previous Seasat and Geosat altimeters with significant improvements including the 5.3 GHz channel for the ionospheric measurement. It was the main sensor on the Topex/Poseidon mission. The measurements made at both frequencies were combined to obtain the altimetry height of the satellite above the sea (satellite range), wind speed modulus, significant wave height and ionospheric correction.

Function

Topex measures range (the distance from the satellite to the Earth's surface), wave height and wind speed.

Principle

The altimeter emits a radar beam that is reflected back to the antenna from the Earth's surface (see [how altimetry works](#) for details). Topex operates at two frequencies (13.6 GHz in the Ku-band and 5.3 GHz in the C-band) to determine atmospheric electron content, which affects the radar signal path delay. These two frequencies also serve to measure the amount of rain in the atmosphere.

Technical data*Table 7.3 Topex altimeter main parameters*

Emitted Frequency (GHz)	Dual-frequency (Ku, C) – 13.575 and 5.3
Pulse Repetition Frequency (Hz)	4200 (Ku), 1220 (C)
Pulse duration (microseconds)	102.4 (Ku), 102.4 or 32 (C)
Bandwidth (MHz)	320 (Ku), 320 or 100 (C)
Antenna diameter (m)	1.5
Antenna beamwidth (degrees)	1.1 (Ku), 2.7 (C)
Power (W)	237
Redundancy	Yes
Specific features	Dual-frequency for ionospheric correction

Further information on [Instrument Description: Altimeter\(s\)](#) (NASA/JPL website)

7.1.6.1.2 Poseidon-1

SSALT, also called Poseidon-1, has validated the technology of a low-power (49 W), lightweight (23 kg without redundancy) altimeter for future Earth observing missions. It was supplied by the French Space Agency (CNES). It shares the same antenna as the NRA; thus only one altimeter operates at any given time (on Topex/Poseidon it operated about 10% of the time, or one cycle in ten).

SSALT operates at a single frequency of 13.65 GHz (Ku-band). Its measurements give the same geophysical information as NRA's. However since this sensor uses a single frequency, an external correction for the ionosphere must be supplied (see the [DORIS](#) instrument).



Figure 7.13. Poseidon-1 (Credits CNES/Alcatel)

Function

Poseidon-1 measures range (the distance from the satellite to the Earth's surface), wave height and wind speed.

Principle

The altimeter emits a radar beam that is reflected back to the antenna from the Earth's surface (see How altimetry works for details). Poseidon-1 operates at a single frequency (13.6 GHz in the Ku band).

Technical data

Poseidon-1, or SSALT (for Solid State ALTimeter), uses solid-state amplification techniques.

Table 7.4 Poseidon-1 main parameters

Emitted Frequency (GHz)	Single-frequency (Ku) – 13.65
Pulse Repetition Frequency (Hz)	1718
Pulse duration (microseconds)	105
Bandwidth (MHz)	320
Antenna diameter (m)	1.5
Antenna beamwidth (degrees)	1.1
Power (W)	5
Redundancy	No
Specific features	Solid-State Power Amplifier (low power, low mass)

Further information on Topex/Poseidon (Aviso website)

7.1.6.1.3 TMR : Topex Microwave Radiometer

The TMR acquires measurements via three separate frequency channels to determine the path delay of the altimeter's radar signal due to atmospheric water vapour.

The TMR (50 kg including partial redundancy, 25 W) measures the microwave emissivity (brightness temperatures) of the sea surface at three frequencies (18, 21 and 37 GHz) to provide the total vapour content in the troposphere along the altimeter beam. The 21 GHz channel is the primary channel for water vapour measurement. The 18 and 37 GHz channels are respectively used to remove the effects of wind speed and cloud cover (liquid water contribution) from the water vapour measurement. Measurements are combined to obtain the error in the satellite range measurements caused by pulse delay due to water vapour, and to obtain the sigma naught correction for liquid water absorption.

Function

The TMR measures water vapour content in the atmosphere so that we can determine how it impacts radar signal propagation. Its measurements can also be used directly for studying other atmospheric phenomena, particularly rain.

Principle

The TMR is a passive receiver that collects radiation reflected by the oceans at frequencies of 18.7, 23.8 and 34 GHz.

Radiation measured by the radiometer depends on surface winds, ocean temperature, salinity, foam, absorption by water vapour and clouds, and various other factors. To determine atmospheric water vapour content accurately, we need to eliminate sea surface and cloud contributions from the signal received by the radiometer. This is why the TMR uses different frequencies, each of which is more sensitive than the others to one of these contributions. The main 23.8 GHz frequency is used to measure water vapour, the 34 GHz channel provides the correction for non-rainbearing clouds, and the 18.7 GHz channel is highly sensitive to wind-driven variations in the sea surface. By combining measurements acquired at each of these frequencies, we can extract the water vapour signal.

Further information on [Instrument Description: Radiometer\(s\)](#) (NASA/JPL website)

7.1.6.1.4 DORIS



Figure 7.14. DORIS antenna

The DORIS instrument onboard Topex/Poseidon provided precise orbit determination. DORIS measurements are also used for geophysical studies, in particular through the [International DORIS Service \(IDS\)](#). DORIS is a dual- frequency instrument able to determine atmospheric electron content.

Functions

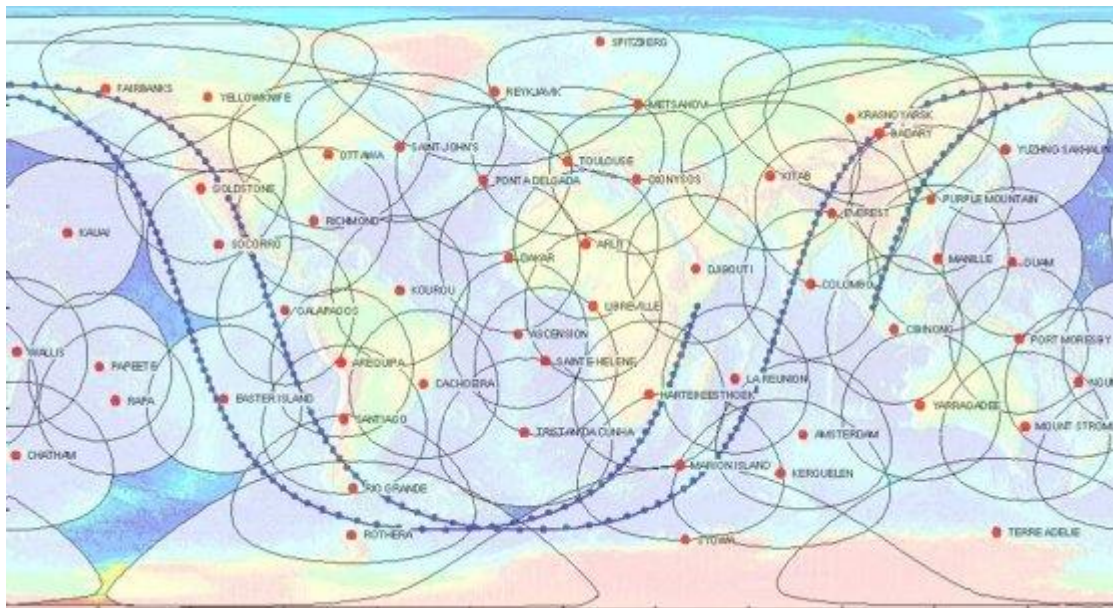


Figure 7.15. The DORIS network of orbitography beacons and their spatial coverage (Credits CNES)

Precise orbit determination

DORIS measurements are used for precise orbit determination (POD).

Ionospheric electron content

By measuring and comparing the path delay of signals transmitted at two separate frequencies, DORIS is able to calculate the electron content in the atmosphere. This information is then used to determine perturbations acting on the altimeter's radar signal.

This function complements the Topex dual-frequency altimeter function.

Principle



Figure 7.16. DORIS Beacon

DORIS orbitography beacons transmit signals at two separate frequencies (2,036.25 MHz and 401.25 MHz) to the satellite. The receiver on board the satellite analyses the received signal frequencies to calculate its velocity relative to Earth. This velocity is fed into orbit determination models to derive the satellite's position on orbit to within two centimetres on the radial component.

For Further information, see [the International DORIS Service \(IDS\)](#) and [DORIS, the space surveyor \(Aviso\)](#)

7.1.6.1.5 GPSDR GPS tracking receiver

The GPSDR (Global Positioning System Demonstration Receiver) is a tracking system that uses the GPS constellation of satellites to determine the exact position of a transmitter.

The GPSDR (28 kg without redundancy, 29 W), operating at 12,227.6 MHz and 1,575.4 MHz, receives signals from up to six GPS satellites. The GPS antenna is mounted on a long boom to reduce multipath effects which can severely corrupt the measurements.

These satellite data plus GPS tracking data from ground sites allow nearly geometric solutions. Precise tracking of the satellite is made possible by using the Kalman filtering technique and a new GPS differential ranging technique.

Function

The GPSDR supports precise orbit determination by the DORIS system. It also helps to improve gravity field models and provides data for satellite positioning accurate to about 50 metres and 50 nanoseconds.

Principle

The GPSDR receives dual-frequency navigation signals continuously and simultaneously from 16 GPS satellites. It uses these signals to acquire phase measurements accurate to about one millimetre and pseudo-range measurements accurate to about 10 centimetres.

Technical data

The onboard system consists of two independent receivers operating in cold redundancy, each with an omnidirectional antenna, low-noise amplifier, quartz oscillator, sampling converter and a baseband digital processor communicating via the bus interface.

Further information on [Instrument Description: GPS](#) (NASA/JPL website)

7.1.6.1.6 LRA: Laser Retroreflector Array

The LRA or Laser Retroreflector Array (29 kg) reflects laser signals from a network of 10 to 15 ground laser tracking stations (Satellite Laser Ranging stations, SLR) to provide tracking data for precise orbit determination and the altimeter bias calibration.

The LRA is an array of mirrors that provides a target for laser tracking measurements from the ground. By analysing the round-trip time of the laser beam, we can locate very precisely where the satellite is on its orbit.

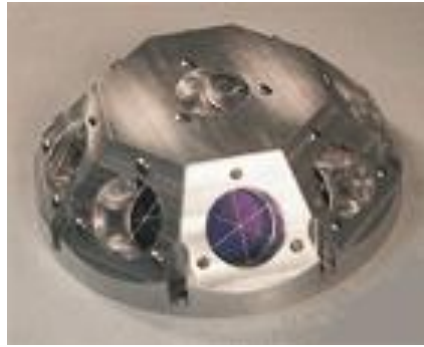


Figure 7.17. LRA (Credits [ATSC](#))

The LRA is used to calibrate the other location systems on the satellite with a very high degree of precision.

Principle

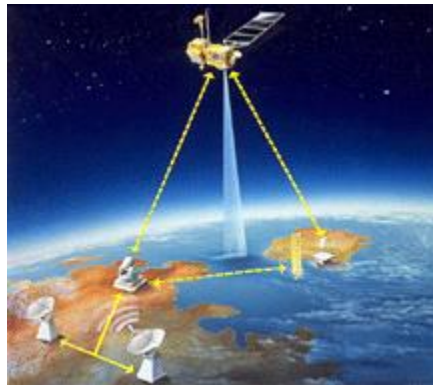


Figure 7.18. Laser Retroreflector diagram

The LRA is a passive instrument that acts as a reference target for laser tracking measurements performed by ground stations. Laser tracking data are analysed to calculate the satellite's altitude to within a few millimetres. However, the small number of ground stations and the sensitivity of laser beams to weather conditions make it impossible to track the satellite continuously. This is why other onboard location systems are needed.



Figure 7.19. LRA station in action

Technical data

The retroreflectors are placed on the nadir side of the satellite. The totally passive unit consists of nine quartz corner cubes arrayed as a truncated cone, with one cube in the centre and the others arranged azimuthally around the cone. This arrangement allows laser ranging at field-of-view angles of 360 degrees in azimuth and 60 degrees in elevation around the perpendicular. The retroreflectors are optimised for a wavelength of 532 nanometres (green), offering a field of view of about 100 degrees. Topex/Poseidon's LRA was built by ITE Inc. under contract to NASA's Goddard Space Flight Center.

Further information on [Instrument Description: LRA](#) (NASA/JPL website), and ILRS (International Laser Ranging Service)

7.1.6.2 T/P orbit

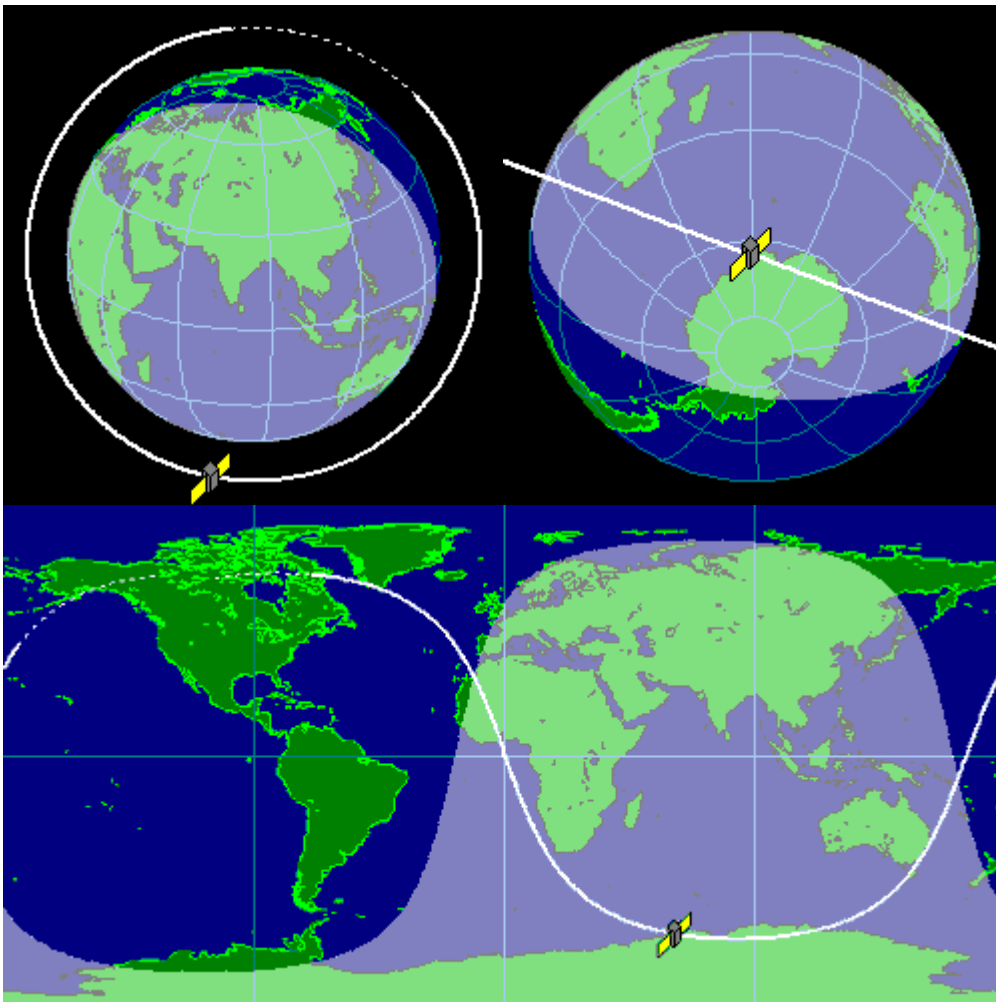


Figure 7.20. Topex/Poseidon orbit

The orbit configuration was chosen to optimise the study of temporal large-scale ocean variability and avoid aliasing different tidal constituents to the same frequency.

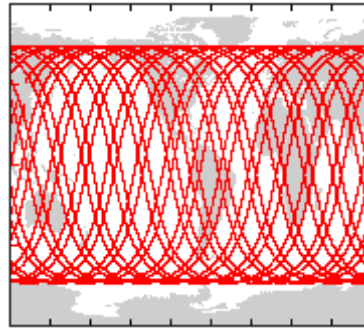


Figure 7.21. Topex/Poseidon altimeter tracks

A high orbit altitude was also selected to minimise atmospheric drag and gravity forces acting on the satellite, and to make orbit determination easier and more accurate.

On 15 September 2002 Topex/Poseidon assumed a new orbit midway between its original ground tracks. The former Topex/Poseidon ground tracks were overflown by Jason-1. This tandem mission demonstrated the scientific capabilities of a constellation of optimised altimetry satellites.

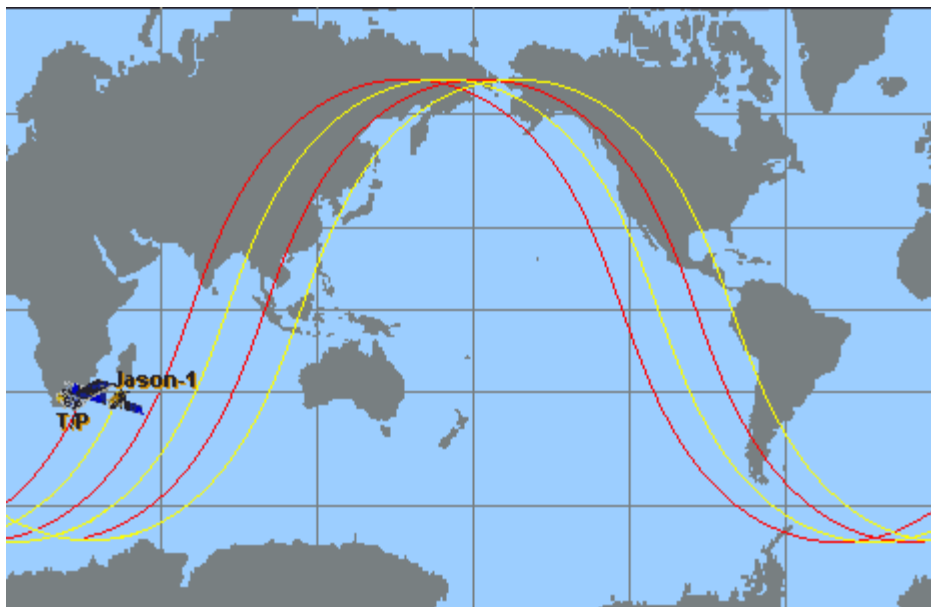


Figure 7.22. T/P on its new orbit, situated at one half the Jason-1 track spacing to the west of Jason-1. Cycle 369, which began on Friday 20 September, was the first full cycle in the new orbit. (Credits [Aviso](#))

Orbit parameters

Table 7.5 Topex Orbit Main characteristics

Semi-major axis	7714.4278 km
Eccentricity	0.000095
Argument of perigee	270.8268°
Inclination (non-sun-synchronous)	66.039°

Table 7.6 Topex Orbit Auxiliary data

Reference altitude (equatorial)	1,336 km
Nodal period	6,745.72 seconds (112'42" or 1h52')
Repeat cycle	9.9156 days
Number of passes per cycle	254
Ground track separation at Equator	315 km
Acute angle at Equator crossings	39.5°
Longitude at Equator of pass 1	99.92° 98.51° since Sept. 2002
Orbital velocity	7.2 km/s
Ground scanning velocity	5.8 km /s

The exact altitude enabling the orbit to satisfy these constraints and flying over two verification sites located in the Mediterranean Sea (Lampedusa Island, Italy) and at the Harvest oil rig platform (California, USA) was 1,336 km. An inclination of 66° was selected – i.e. the inclined orbit sampled from 66° north to 66° south – so as to cover most of the world's oceans (~ 90%). The orbit was non-sun-synchronous and prograde. A repeat period of 9.916 days was chosen (ie; the satellite passed vertically over the same location, to within 1 km, every ten days) as the best compromise between spatial and temporal resolutions. The distance between successive tracks was of the order of 315 km at the equator. The local time of successive passes shifted by nearly two hours per cycle.

A satellite orbit slowly decays due to air drag and has long-period variability due to the Earth's inhomogeneous gravity field, solar radiation pressure, and other lesser forces. Periodic manoeuvres are therefore required to keep the satellite on its orbit. The frequency of these manoeuvres depends primarily on the solar flux affecting the Earth's atmosphere, but there is generally expected to be one manoeuvre (or series of manoeuvres) every 40 to 200 days. The process usually takes from 20 to 60 minutes. Manoeuvres should wherever possible be performed at the end of a 10-day cycle, preferably when the satellite is overflying land in order not to disrupt precise orbit determination. Science data are not acquired when orbit maintenance manoeuvres are being performed.

Further information on [Topex/Poseidon](#) (Aviso website).

7.1.6.3 T/P objectives

The objectives of the Topex/Poseidon mission, as announced in 1992, were:

- to study ocean circulation on a large scale including its interaction with the atmosphere, to improve our knowledge of the role of the ocean in the global climate,
- to increase our understanding of heat transport in the ocean,
- to model the tides,

- to improve the geophysical study of the marine geoid by analysing altimetry measurements and the accurate location of ground beacons,
- to calculate variation trends in mean sea level on a global scale (an indicator of the greenhouse effect).

The first research proposals for Topex/Poseidon data were therefore mainly focused on large-scale ocean circulation, with another being the modelling of tides offshore (the orbit was deliberately chosen to measure all tidal components, whichever their period), as well as several geodesy studies.

Further information on [Topex/Poseidon](#) (Aviso website)

7.1.7 Geosat Follow-On

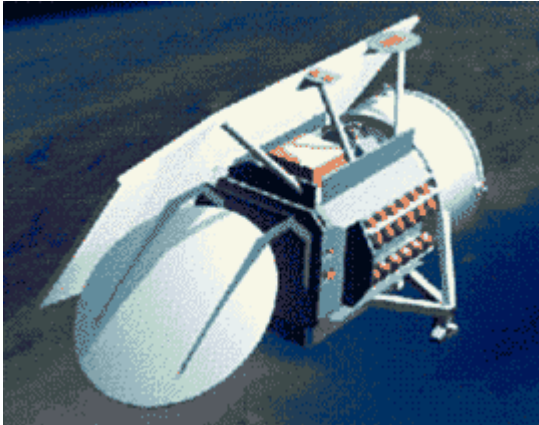


Figure 7.23. Credits US Navy

GFO, Geosat Follow-On was launched in February 1998, and retired in November 2008. Its mission is to provide real-time ocean topography data to the US Navy. Scientific and commercial users have access to these data through NOAA (National Oceanic and Atmospheric Administration). Its primary payload is a radar altimeter.

GFO follows the 17-day repetitive orbit of Geosat.

Satellite	Geosat Follow-On
Launched	February 10, 1998
Mission	Mesure ocean topography
Altitude	880 km
Inclination	108° (non-sun-synchronous)

Further information on:

- [mission and operations](#) (US Navy website)
- [data](#) (NOAA website)

7.1.8 ERS-2



Figure 7.24. ERS-2 (Credits ESA)

Satellite	ERS-2
Launched	21 April 1995
Mission:	Observe Earth and its environment
Altitude:	785 km
Inclination:	98.52°

The ERS-2 satellite's main mission is to observe Earth, in particular its atmosphere and ocean. Built by ESA, the European Space Agency, it carries several instruments, including a radar altimeter.

ERS-2 was launched in April 1995 as the follow-on from ERS-1, with which it was used in tandem from August 1995 to June 1996. Their identical orbits (35 days) had a one-day shift. Since 22 June 2003, ERS-2's onboard tape recorder used to collect altimeter data experienced a number of failures. This means that altimeter data were unavailable except for the time when the satellite was within visibility of ESA's ground stations over Europe, North Atlantic, the Arctic and western North America.

In July 2011, ERS-2 operations were terminated by lowering the orbit of the satellite. These deorbiting procedures are done while the fuel is still sufficient to perform careful manoeuvres.

Further information on:

- ERS missions [Home Page](#) (ESA website),
- [ERS-2](#) (Cersat website)

7.1.8.1 ERS-2 Instruments

The ERS satellites carry instrumentation consisting of a core set of active microwave sensors supported by additional, complementary instruments:

- AMI – active microwave instrument consisting of a synthetic aperture radar (SAR) and a wind scatterometer
- RA – radar altimeter
- ATSR – along-track scanning radiometer
- Gome (ERS-2) – global ozone monitoring experiment
- MWS – microwave sounder
- PRARE – precise range and range rate equipment
- LRR – laser reflector

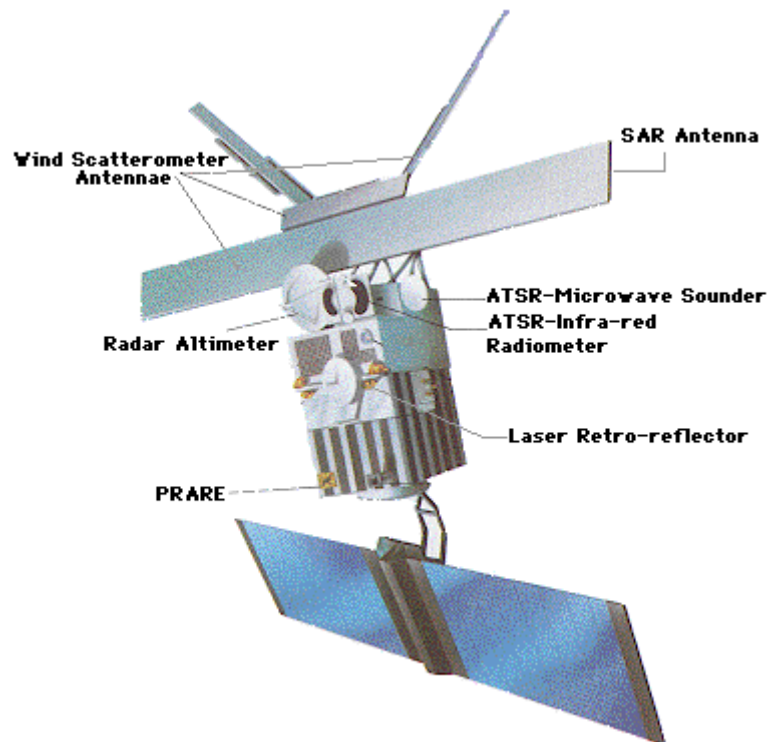


Figure 7.25. ERS-2 instruments (Credits ESA)

The satellite concept is based on reusing the Multi-mission Platform, developed within the French SPOT programme. This platform provides the major services for the satellite and payload operation, in particular attitude and orbit control, power supply, monitoring and control of payload status, telecommunications with the ground segment.

RA altimeter

The Radar Altimeter (RA) is a Ku-band (13.8 GHz) nadir-pointing active microwave sensor designed to measure the return trip time for echoes from ocean and ice surfaces. Functioning in one of two operational modes (ocean or ice) the Radar Altimeter provides information on significant wave height, surface wind speed, sea surface elevation, which relates to ocean currents, the surface geoid and tides, and various parameters over sea ice and ice sheets.

MicroWave Sounder

The Along-Track Scanning Radiometer (ATSR) combines an infrared radiometer and a microwave sounder for measuring sea surface temperature, cloud top temperature, cloud cover and atmospheric water vapour content. This is used to correct altimetry data from path delay due to atmospheric water.

Location systems

The ERS sensor location system includes two instruments – the Precise Range and Range-rate Equipment (PRARE) and the Laser Retroreflectors (LRR) to provide precise orbit determination for the referencing of height measurements made by the Radar Altimeter. The PRARE has been non-operational since launch, but a description of it is included here for completeness.

PRARE

The Precise Range and Range-rate Equipment (PRARE) is included for the accurate determination of the satellite's position and orbit characteristics, and for precise position determination (geodetic fixing).

LRR

The LRR is highly accurate but it requires ground stations that are complex to operate, and its use can be restricted by adverse weather conditions. It is used to calibrate the other location system so that the satellite orbit can be determined as accurately as possible.

Further information on ERS instruments (ESA website)

7.1.8.1.1 RA

The Radar Altimeter (RA) is a Ku-band (13.8 GHz) nadir-pointing active microwave sensor designed to measure the return trip time for echoes from ocean and ice surfaces. Functioning in one of two operational modes (ocean or ice) the Radar Altimeter provides information on significant wave height, surface wind speed, sea surface elevation (relating to ocean currents, the surface geoid and tides) and various parameters over sea ice and ice sheets.

Function

The Radar Altimeter is a Ku-band (13.8 GHz) nadir-pointing active microwave sensor designed to measure the time return echoes from ocean and ice surfaces. Functioning in one of two operational modes (ocean or ice) the Radar Altimeter provides information on significant wave height; surface wind speed; sea surface elevation, which relates to ocean currents, the surface geoid and tides; and various parameters over sea ice and ice sheets.

Principle

The altimeter emits a radar beam that is reflected back to the antenna from the Earth's surface. RA operates at a single frequency (13.6 GHz in the Ku-band).

The Radar Altimeter operates by timing the two-way delay for a short duration radio frequency pulse, transmitted vertically downwards. The level of accuracy required for range measurement (greater than 10 cm) calls for a pulse compression (full deramp) technique. In ocean mode a chirped pulse of 20 microseconds duration is generated with a bandwidth of 330 MHz. For tracking in ice mode an increased dynamic range is used, obtained by reducing the chirp bandwidth by a factor of four to 82.5 MHz, though this also results in a coarser resolution (see [how altimetry works](#) for details).

Technical data

Table 7.7 ERS-2 RA Main parameters

Emitted Frequency (GHz)	Single-frequency (Ku) – 13.8
Pulse Repetition Frequency (Hz)	1020
Pulse duration (microseconds)	20
Bandwidth (MHz)	330 and 82.5

Table 7.7 ERS-2 RA Main parameters

Antenna diameter (m)	1.2
Antenna beamwidth (degrees)	1.3
Power (W)	50
Redundancy	Yes
Specific features	2 bandwidths for ocean and ice measurements

Further information on [RA instrument](#) (ESA website)

7.1.8.1.2 MWS: Microwave Sounder

The main objective of the microwave radiometer (MWS) is to measure the integrated atmospheric water vapour column and cloud liquid water content, which are used as correction terms for the radar altimeter signal. In addition, MWS measurement data are useful for determining surface emissivity and soil moisture over land, for surface energy budget investigations to support atmospheric studies, and for ice characterisation.

Function

The MWS measures water vapour content in the atmosphere so that we can determine how it impacts radar signal propagation. Its measurements can also be used directly for studying precipitable water and cloud liquid content along the satellite track.

Principle

The MWS is a passive receiver that collects radiation reflected by the oceans at frequencies of 23.8 GHz and 36.5 GHz.

Radiation measured by the radiometer depends on surface winds, ocean temperature, salinity, foam, absorption by water vapour and clouds, and various other factors. To determine atmospheric water vapour content accurately, we need to eliminate sea surface and cloud contributions from the signal received by the radiometer. That is why the MWS uses different frequencies, each of which is more sensitive than the others to one of these contributions. The frequencies 23.8 GHz and 36.5 GHz are the result of a trade-off between instrument (reflector) size required to cover a horizontal area on the Earth's surface comparable to the altimeter beam, and the maximum sensitivity to water vapour change in the atmosphere. These frequencies are used to measure the strength of the weak water-vapour emission-line at 22 GHz. In order to eliminate microwave radiation emitted by the Earth's surface, differential measurements at two frequencies must be made. The optimal choice is to use one frequency at the peak of the line and one at the lowest point.

With one feed horn for each frequency, the MWS points via an offset reflector at an angle close to nadir. The instrument is configured in such a way that the 23.8 GHz channel is pointing in the forward direction, the 36.5 GHz channel in the backward direction, with a footprint of about 20 km diameter for each beam.

Further information on [MWS instrument](#) (ESA website).

7.1.8.1.3 PRARE

Precise Range and Range-rate Equipment (PRARE) is included for the accurate determination of the satellite's position and orbit characteristics, and for precise position determination (geodetic fixing). It is a satellite tracking system which provides two-way microwave range and range-rate measurements to ground based transponder stations.

The PRARE system was developed by the Institut für Navigation (INS) at the University of Stuttgart, Kayser-Threde GmbH, Munich and the Deutsches Geodätisches Forschungsinstitut, Munich, as a German national experiment.

Function

The system was designed to:

- * provide, in all weather conditions, precise satellite-to-ground or satellite-to-satellite range and range-rate information,
- * guarantee very reliable measurements through cross-checks and calibration procedures,
- * ensure highly effective operation of the ground segment through data collection and dissemination via the satellite itself, and control of the global network via one central ground station,
- * allow rapid generation of products at an archiving, processing and distribution centre.

Principle

The PRARE measurement principle involves two signals sent from the sensor on board the satellite, one signal in the S-band (2.2 GHz) and the other in the X-band (8.5 GHz). Both signals are modulated with a PN code (pseudo-random noise). The time delay in the reception of the two simultaneously-emitted signals is measured at the ground station with great accuracy (<1 ns) and retransmitted to the on-board memory for ionospheric data correction. Collection of meteorological data by the ground station allows corrections to be applied for tropospheric refraction.

Further information on [PRARE instrument](#) (ESA website)

7.1.8.1.4 Laser RetroReflector

The LRR is an array of mirrors that provides a target for laser tracking measurements from the ground. By analysing the round-trip time of the laser beam, we can locate where the satellite is on its orbit.

Function

A laser retroreflector is attached to a mount on the nadir panel close to the RA antenna.

The LRR is a passive device which is used as a reflector by ground-based SLR (Satellite Laser Ranging) stations using high-power pulsed lasers. In the case of ERS-1, tracking using the LRR is mainly performed by the [International Laser Ranging Service \(ILRS\)](#).

The ILRS provides tracking for the satellite from its global network of laser ranging stations. Laser stations fire short laser bursts at ERS and time the interval before the pulse is reflected back. These ILRS stations are relatively few, but because their positions are very accurately known, they provide a set of independent reference measurements of ERS's position, which contribute to the satellite's precise orbit determination.

Principle

The operating principle of the LRR is therefore to measure on the ground the return trip time of laser pulses reflected from an array of corner cubes mounted on the Earth-facing side of the satellite. The corner cubes ensure that the laser beam is reflected back parallel to the incident beam. The detailed design of the cubes includes a compensation for the aberration of the laser beam caused by the satellite's velocity: the satellite moves almost 40 metres between the emission and reception of the laser pulse from the SLR station, and this is compensated for by slight nonparallelism of the reflected beam.



Figure 7.26. ERS-2 LRR (Credits ESA)

The corner cubes are made of the highest-quality fused silica and work in the visible spectrum. Their performance is optimised at the two wavelengths (694 nm and 532 nm) commonly used in SLR stations. The corner cubes are symmetrically-mounted on a hemispherical surface with one nadir-pointing corner cube in the centre, surrounded by an angled ring of eight corner cubes.

This allows laser ranging in the field of view angles of 360° in azimuth and 60° in elevation around the perpendicular to the satellite's Earth-facing panel (positioned on the axis at point with respect to the satellite's centre of mass).

Orbit performance

Figure shows the history of the ground track for ERS-2

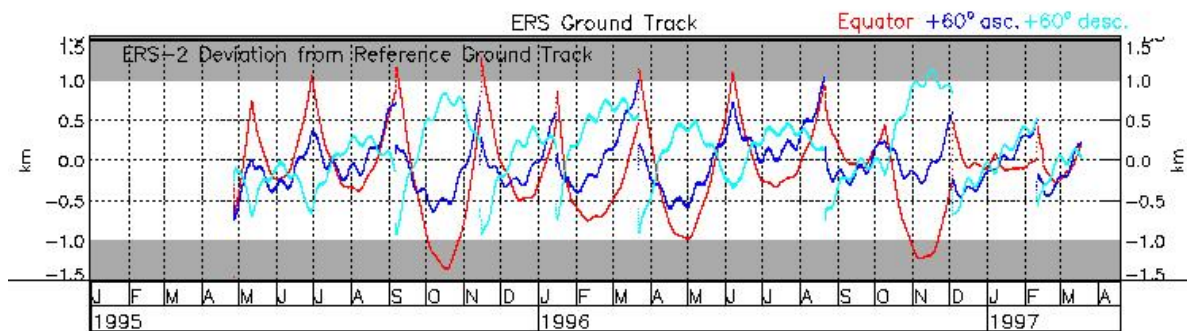


Figure 7.27. R. Zandbergen et.al. , Progress in ERS Orbit and Tracking Data Analysis

7.1.8.2 ERS-2 orbit

To carry out its mission ERS-2's orbit must enable its instruments to scan along predetermined paths designed to give optimum coverage for a set number of orbits. To achieve this, ERS-2 is a three-axis-stabilised, Earth-pointing satellite in yaw steering mode (YSM). The elliptical orbit is sun-synchronous, near-polar, with a mean altitude of 785 km, an inclination of 98.5° and a local solar time at the descending node of 10:30 a.m.

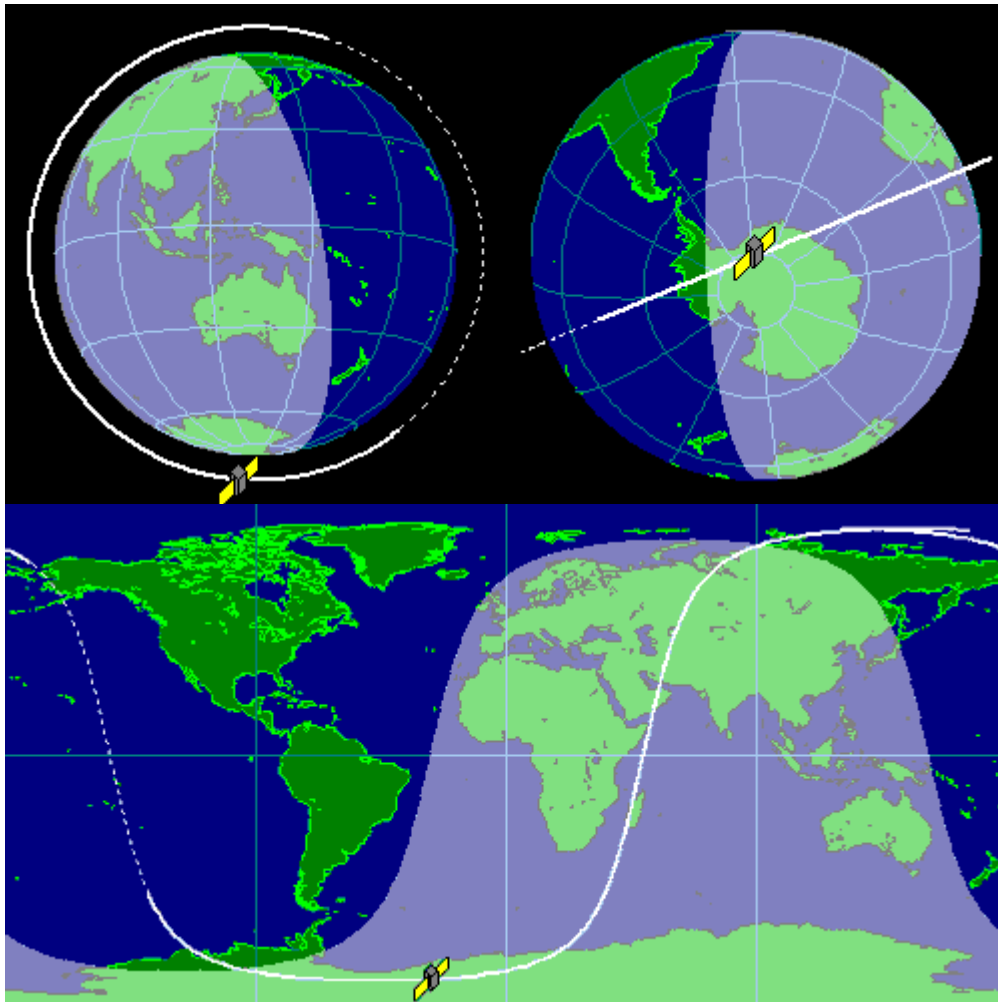


Figure 7.28. ERS-2 orbit

Orbit parameters

35-day orbit

Table 7.8 ERS-2 Orbit Main characteristics

Semi-major axis	7159.5 km
Eccentricity	0.0001042
Argument of perigee	92.4836°
Inclination (sun-synchronous)	98.55°

Table 7.9 ERS-2 Orbit Auxiliary data

Reference altitude (equatorial)	799.8 km
Nodal period	50 min 25.5 s
Repeat cycle	35 days
Number of passes per cycle	1002
Ground track separation at Equator	80 km
Orbital velocity	7.45 km/s

7.1.9 Envisat

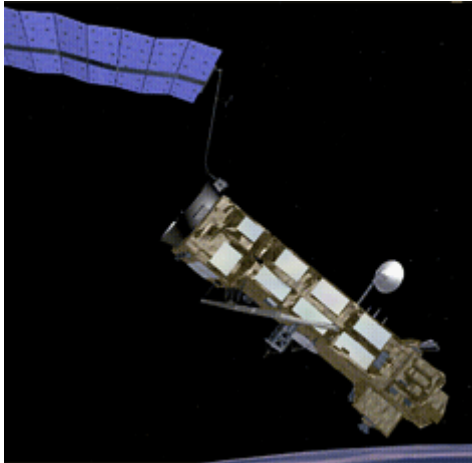


Figure 7.29. Envisat (Credits ESA)

Satellite	Envisat
Launch	March 1st, 2002
Mission	Observe Earth's atmosphere and surface
Altitude	800 km
Inclination	98.55°

Envisat (Environmental Satellite) is the follow-on to ERS-1 and ERS-2. Devoted to environmental studies, and climate change in particular, its mission is to observe Earth's atmosphere and surface. Built by ESA, the European Space Agency, Envisat is carrying ten complementary instruments for observing parameters ranging from the marine geoid to high-resolution gaseous emissions. Among these instruments are a radar altimeter, and the DORIS orbitography and precise location system.

Envisat's orbital period is 35 days, like ERS-2 and some of the ERS-1 phases. As it is integrated in new international climate study programmes such as GOOS and GODAE. Envisat thus forms part of the coming operational era in oceanography, offering near-real-time data access.

Envisat changes its orbit from the October 22, 2010 to ensure an additional 3 years lifespan. After these orbit manoeuvres, the ground track change and consequently the repeat cycle change: 30 days with 431 orbits per cycle instead of 35 days-501 orbits per cycle.

7.1.9.1 Envisat instruments

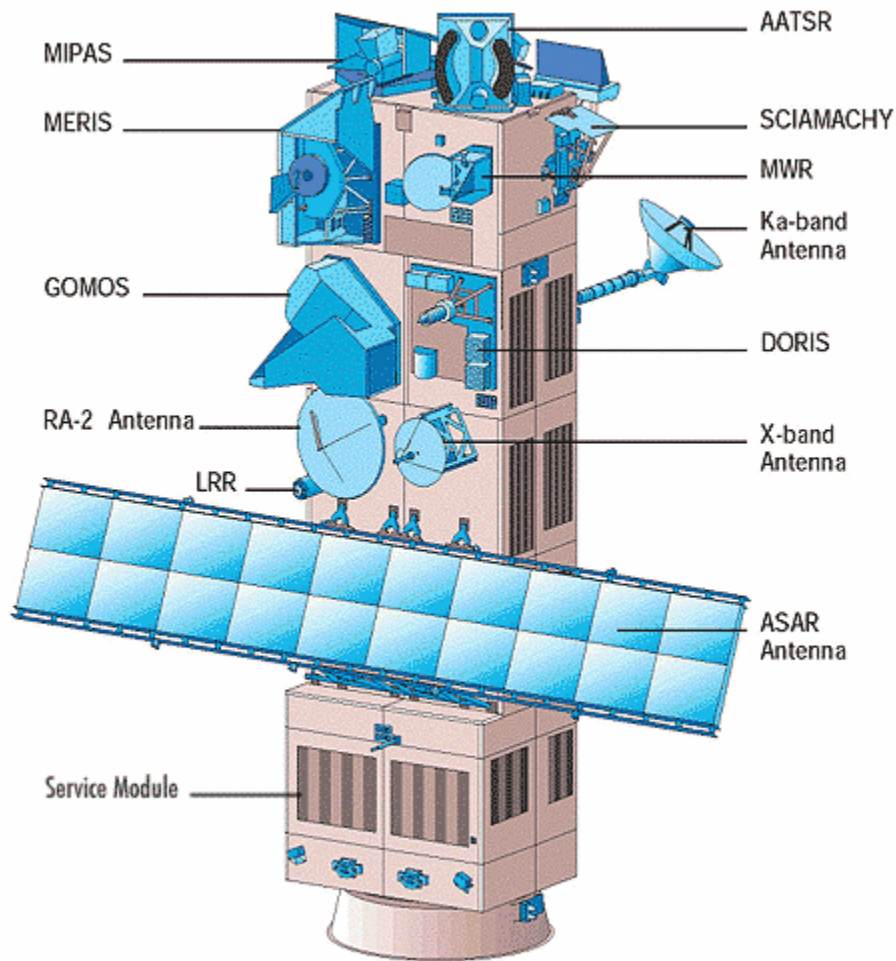


Figure 7.30. Figure 7.31. Envisat instruments

RA-2 altimeter

The Radar Altimeter 2 (RA-2) is an instrument for determining the two-way delay of the radar echo from the Earth's surface to a very high precision: less than a nanosecond. It also measures the power and shape of the reflected radar pulses. The RA-2 is derived from the ERS-1 and 2 radar altimeters, providing improved measurement performance and new capabilities. Operating over oceans, its measurements are used to determine the ocean topography, thus supporting research into ocean circulation, bathymetry and marine geoid characteristics. Furthermore, the RA-2 is able to map and monitor sea ice, polar ice sheets and most land surfaces. Measurement of the radar echo's power and shape enables wind speed and significant wave height at sea to be determined, thus supporting weather and sea state forecasting.

MWR (Microwave Radiometer)

The main objective of the microwave radiometer (MWR) is to measure the integrated atmospheric water vapour column and cloud liquid water content, which are used as correction terms for the radar altimeter signal. Once the water content is known, we can determine the correction to be applied for radar signal path delays for the altimeter. In addition, MWR measurement data are useful for determining surface emissivity and soil moisture over land, for surface energy budget investigations to support atmospheric studies, and for ice characterisation.

Location systems

The location systems onboard Envisat complement each other to measure the satellite's position on orbit to within two centimetres on the radial component. The LRR is highly accurate, but it requires ground stations that are complex to operate, and its use can be restricted by adverse weather conditions. It is used to calibrate DORIS so that the satellite orbit can be determined as accurately as possible. DORIS measurements determine the orbit in real time to support precise orbit determination.

DORIS (Doppler location)

The DORIS system uses a ground network of orbitography beacons spread around the globe, which send signals at two frequencies to a receiver on the satellite. The relative motion of the satellite generates a shift in the signal's frequency (called the Doppler shift) that is measured to derive the satellite's velocity. These data are then assimilated in orbit determination models to keep permanent track of the satellite's precise position (to within three centimetres) on its orbit.

LRR (laser tracking)

The LRR (Laser Retroreflector Array) is an array of mirrors that provides a target for laser tracking measurements from the ground. By analysing the round-trip time of the laser beam, we can locate where the satellite is on its orbit.

Further information on the [instruments](#) (ESA website)

7.1.9.1.1 RA-2

The Radar Altimeter 2 (RA-2) is an instrument for determining the two-way delay of the radar echo from the Earth's surface to a very high precision: less than a nanosecond. It also measures the power and shape of the reflected radar pulses. The RA-2 is derived from the ERS-1 and 2 radar altimeters, providing improved measurement performance and new capabilities.

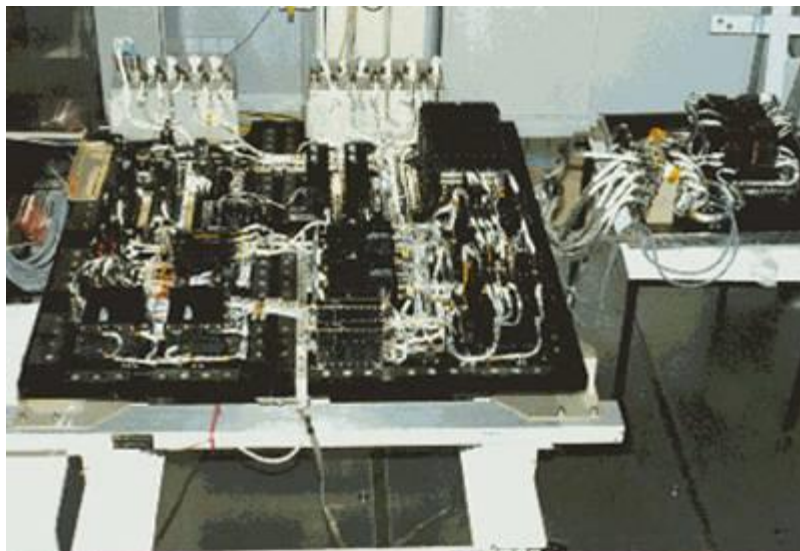


Figure 7.32. RA-2 during integration on Envisat (CreditsESA)

Function

Operating over oceans, RA-2 measurements are used to determine the ocean topography, thus supporting research into ocean circulation, bathymetry and marine geoid characteristics. Furthermore, RA-2 is able to map and monitor sea ice, polar ice sheets and most land surfaces. Measurement of the radar echo power and shape enables wind speed and significant wave height at sea to be determined, thus supporting weather and sea state forecasting.

Principle

The altimeter emits a radar beam that is reflected back to the antenna from the Earth's surface (see [how altimetry works](#) for details). RA-2 operates at two frequencies (13.57 GHz in the Ku-band and 3.2 GHz in the S-band) to determine atmospheric electron content, which affects the radar signal path delay. These two frequencies can also serve to measure the amount of rain in the atmosphere.

Technical data

Table 7.10 Envisat RA Main parameters

Emitted Frequency (GHz)\	Dual-frequency (Ku, S) – 13.575 and 3.2
Pulse Repetition Frequency (Hz)	1795 (Ku), 449 (S)
Pulse duration (microseconds)	20
Bandwidth (MHz)	320, 80 and 20 (Ku) – 160 (S)
Antenna diameter (m)	1.2
Antenna beamwidth (degrees)	1.29 (Ku), 5.5 (S)
Power (W)	161
Redundancy	Yes
Specific features	Dual-frequency for ionospheric correction, 3 bandwidths in Ku-band

Further information on the [RA2 instrument](#) (ESA website)

7.1.9.1.2 MWR: Microwave Radiometer

Figure 7.33. MWR integration (CreditsESA)

The main objective of the microwave radiometer (MWR) is to measure the integrated atmospheric water vapour column and cloud liquid water content, which are used as correction terms for the radar altimeter signal. In addition, MWR measurement data are useful for determining surface emissivity and soil moisture over land, for surface energy budget investigations to support atmospheric studies, and for ice characterisation.

The Envisat MWR has evolved from the instruments previously flown on ERS-1 and ERS-2. It is a dual-channel nadir-pointing radiometer, operating at frequencies of 23.8 GHz and 36.5 GHz. For Envisat the design of the MWR had to be modified in some areas compared to its ERS predecessors, in order to comply with the different platform and mission requirements.

Function

The MWR measures water vapour content in the atmosphere so that we can determine how it impacts radar signal propagation. Its measurements also can be used directly for studying precipitable water and cloud liquid content along the satellite track.

Principle

The MWR is a passive receiver that collects radiation reflected by the oceans at frequencies of 23.8 GHz and 36.5 GHz.

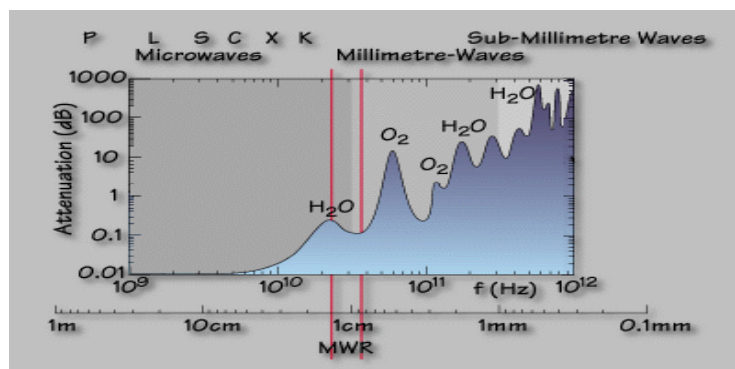


Figure 7.34. Electromagnetic spectrum and MWR frequencies

Radiation measured by the radiometer depends on surface winds, ocean temperature, salinity, foam, absorption by water vapour and clouds, and various other factors. To determine atmospheric water vapour content accurately, we need to eliminate sea surface and cloud contributions from the signal received by the radiometer. This is why the MWR uses different frequencies, each of which is more sensitive than the others to one of these contributions. The frequencies 23.8 GHz and 36.5 GHz are the result of a trade-off between instrument (reflector) size required to cover a horizontal area on the Earth's surface comparable to the RA-2 beam, and the maximum sensitivity to water vapour change in the atmosphere. These frequencies are used to measure the strength of the weak water-vapour emission-line at 22 GHz. In order to eliminate microwave radiation emitted by the Earth's surface, differential measurements at two frequencies must be made. The optimal choice is to use one frequency at the peak of the line and one at the lowest point.

With one feed horn for each frequency, the MWR points via an offset reflector at an angle close to nadir. The instrument is configured in such a way that the 23.8 GHz channel is pointing in the forward

direction, the 36.5 GHz channel in the backward direction, with a footprint of about 20 km diameter for each beam.

Further information on the [MWR instrument](#) (ESA website)

7.1.9.1.3 DORIS



Figure 7.35. DORIS antenna

The DORIS instrument onboard Envisat provides real-time location and precise orbit determination. DORIS measurements are also used for geophysical studies, in particular through the International DORIS Service (IDS). DORIS is a dual-frequency instrument able to determine atmospheric electron content.

To perform its missions of satellite orbit restitution and ground beacon location, the DORIS system comprises an onboard package, a network of beacons, and the DORIS Control and Data Processing Centre. For operational aspects, the DORIS control centre provides an interface with the satellite flight operation segment. The orbit determination beacons are deployed throughout a dense worldwide network. This network is deployed and maintained by the IGN (French national geographic institute). The time reference for the system is provided by master beacons located in Toulouse, France and Kourou, French Guiana, which are connected to atomic clocks. The DORIS onboard instrument package consists of:

- a redundant receiver with two receiving chains;
- an ultrastable crystal oscillator (USO) identical to the USOs employed in the DORIS ground segment;
- an omnidirectional dual-frequency antenna;
- an Instrument Control Unit (shared with the MWR).

The receivers can track two beacons simultaneously.

The Doppler measurements are also processed on board to obtain real time orbit data with lower accuracy.

Function

DORIS is based upon the accurate measurement of the Doppler shift of radio frequency signals transmitted from ground beacons and received on board the satellite. Measurements are made at two frequencies: 2.03625 GHz for precise Doppler measurements and 401.25 MHz for ionospheric correction of the propagation delay. The 401.25 MHz frequency is also used for measurement time-tagging and auxiliary data transmission. The selection of an uplink-only system allows fully automated operation of the beacons and easy communication links for the overall system, data being centralised through the satellite and its ground segment to the DORIS data processing centre. The control and data processing centre is located in Toulouse, France, and operated by CLS.

Precise orbit determination

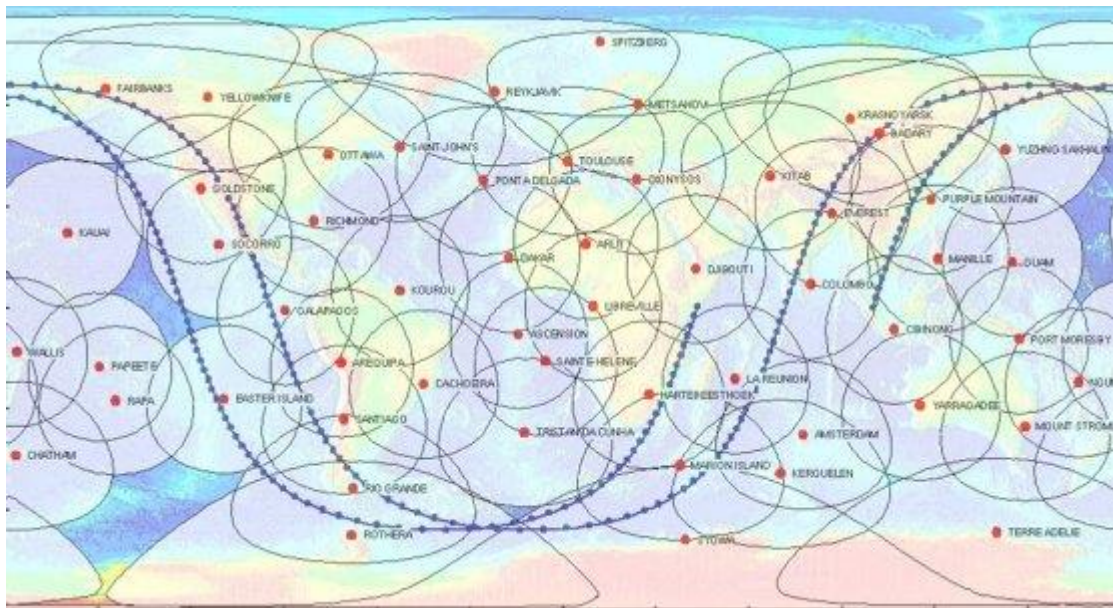


Figure 7.36. The DORIS network of orbitography beacons and their spatial coverage (Credits CNES)

DORIS measurements are used for precise orbit determination (POD). Onboard measurements of the Doppler shift are performed every 10 seconds. The resulting radial velocity values (accurate to the order of 0.4 mm/s) are used on the ground in combination with a dynamic model of the satellite’s trajectory to perform precise orbit determination with an accuracy of greater than 5 cm in altitude. These orbit data are available with a time lag of 1.5 months, with the delay being mainly due to the availability of external data, such as solar flux

Real-time location: Diode

The Doppler measurements are also processed on board to obtain real-time orbit data with lower accuracy. The Diode onboard navigator locates the satellite on orbit in real time. This information is essential for providing altimetry data in real time or near-real time.

Ionospheric electron content

By measuring and comparing the path delay of signals transmitted at two separate frequencies, DORIS is able to calculate the electron content in the atmosphere. This information is then used to determine perturbations acting on the altimeter's radar signal.

This function complements the [dual-frequency altimeter](#) function.

Principle

DORIS orbitography beacons transmit signals at two separate frequencies (2,036.25 MHz and 401.25 MHz) to the satellite. The receiver onboard the satellite analyses the received signal frequencies to calculate its velocity relative to Earth. This velocity is fed into orbit determination models to derive the satellite's position on orbit to within two centimetres on the radial component.

Every 10 seconds the receiver measures the Doppler shift of the signals continuously transmitted from the ground beacons at the two frequencies of 2,036.25 MHz and 401.25 MHz. The onboard ultra-stable oscillator provides the reference for this measurement with a stability of 5×10^{-13} over 10 to 100 seconds. Both frequencies are susceptible to group-delay caused by propagation through the ionosphere, but the effects are much greater at the lower VHF frequency (being inversely proportional to the square of the frequency). Thus these measurements can be used to obtain a correction for the higher frequency.

Further information on

- the [DORIS instrument](#) onboard Envisat (ESA website)
- For Further information, see the International [DORIS Service](#) (IDS) and [DORIS, the space surveyor](#) (Aviso)

7.1.9.1.4 Laser RetroReflector

The LRR is an array of mirrors that provide a target for laser tracking measurements from the ground. By analysing the round-trip time of the laser beam, we can locate where the satellite is on its orbit.

Function

A laser retroreflector is attached to a mount on the nadir panel close to the RA-2 antenna.

The LRR is a passive device which is used as a reflector by ground-based SLR (Satellite Laser Ranging) stations using high-power pulsed lasers. In the case of Envisat, tracking using the LRR is mainly performed by the International Laser Ranging Service (ILRS). The ILRS provides tracking for the satellite from its global network of laser ranging stations. Laser stations fire short laser bursts at Envisat and time the interval before the pulse is reflected back. These ILRS stations are relatively few, but because their positions are very accurately known, they provide a set of independent reference measurements of Envisat's position, which contribute to the satellite's precise orbit determination.

Principle

The operating principle of the LRR is therefore to measure on the ground the return trip time of laser pulses reflected from an array of corner cubes mounted on the Earth-facing side of the satellite. The corner cubes ensure that the laser beam is reflected back parallel to the incident beam. The detailed design of the cubes includes a compensation for the aberration of the laser beam caused by the

satellite's velocity: the satellite moves almost 40 metres between the emission and reception of the laser pulse from the SLR station, and this is compensated for by slight nonparallelism of the reflected beam.



Figure 7.37. ERS-1 LRR, which is identical to the Envisat model. (Credits ESA)

The corner cubes are made of the highest-quality fused silica and work in the visible spectrum. Their performance is optimised at the two wavelengths (694 nm and 532 nm) commonly used in SLR stations. The corner cubes are symmetrically-mounted on a hemispherical surface with one nadir-pointing corner cube in the centre, surrounded by an angled ring of eight corner cubes. This allows laser ranging in the field of view angles of 360° in azimuth and 60° in elevation around the perpendicular to the satellite's Earth-facing panel (positioned on the axis at point -Zs with respect to the satellite's centre of mass). The design is identical to the very successful reflectors used on ERS-1 and ERS-2.

Instrument characteristics

Wavelength: 350-800 nm optimised for 532 nm

Efficiency: less or equal than 0.15 end-of-life

Reflection Coefficient: less or equal than 0.80 end-of-life

Field of view: elev. half-cone angle 60 degrees; azimuth 360 degrees

Diameter: more or equal than 20 cm

Further information on the [LRR instrument](#) (ESA website)

7.1.9.2 Envisat orbit

Choice of orbit

The selection of a sun-synchronous orbit was of primary importance and has driven the satellite's physical configuration. The total altitude range, within a few tens of kilometres of 800 km, was also critical to the design. Apart from this, there was a certain degree of freedom in the choice of parameters. Many of the choices were examined during the ERS-1 mission preparation and the concept of the multidisciplinary orbit, with a 35-day cycle, evolved. Envisat flies this same high-inclination, sun-synchronous, near-circular orbit with the same ground track.

Orbit maintenance

The orbit maintenance requirements are that the deviation of the actual ground track from the nominal one is kept below 1 km and that the mean local nodal crossing time matches the nominal one to within five minutes. The orbit maintenance strategy aims for minimum disturbance of the payload operation. In-plane manoeuvres are used for altitude adjustment to compensate for the effects of air-drag. This altitude decay affects the ground-track repeatability, mainly in the equatorial regions. The frequency of these manoeuvres is determined by the rate of orbital decay, which in turn is determined by the air density, and this is a function of solar activity. The nominal rate for these in-plane manoeuvres is twice a month. They do not interrupt the operations of most sensors. Out-of-plane corrections are used to rectify the steady drift of inclination mainly caused by solar and lunar gravity perturbations. The solar wind also influences inclination, but its contribution is typically an order of magnitude smaller than the one made by solar and lunar gravity. Inclination drift degrades ground-track maintenance at high latitudes. The drift rate does not depend on air density and corrections are required every few months. As they are out-of-plane they require a 90 degree rotation of the spacecraft, to align the thrusters with the required thrust direction, so these manoeuvres are performed in eclipse to avoid the risk of optical sensors viewing the sun.

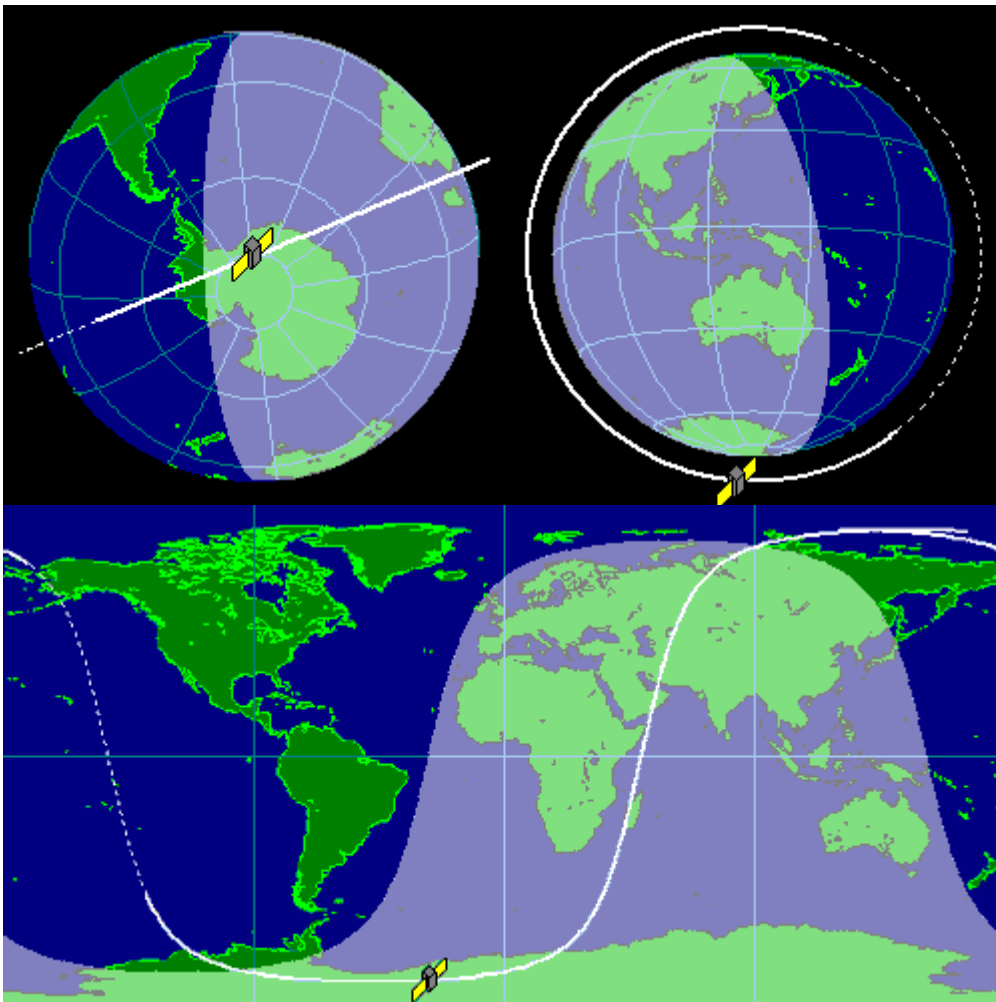


Figure 7.38. Envisat orbit

Orbit parameters*Table 7.11 Envisat Orbit Main characteristics*

Semi-major axis	7159.5 km
Inclination (sun-synchronous)	98.55°

Table 7.12 Envisat Orbit Auxiliary data

Reference altitude (equatorial)	799.8 km
Nodal period	100.59 min
Repeat cycle	35 days
Number of passes per cycle	1002
Ground track separation at Equator	80 km
Orbital velocity	7.45 km/s

Further information on the [mission's orbit](#) (ESA website)

7.1.9.3 Envisat objectives

The Envisat satellite has an ambitious and innovative payload designed to ensure the continuity of the data measurements from ESA's ERS satellites. Envisat data supports Earth science research and allows monitoring of the evolution of environmental and climate changes. Furthermore, the data facilitates the development of operational and commercial applications.

Introduction

The main objective of the Envisat programme is to provide Europe with an enhanced capability for remote sensing observation of Earth from Space, with the aim of furthering the ability of participating states to take part in the studying and monitoring of the Earth and its environment.

Its primary objectives are:

- to provide for continuity of the observations begun with the ERS satellites, including those obtained from radar-based observations;
- to enhance the ERS mission, notably the ocean and ice missions;
- to extend the range of parameters observed to enable us to learn more about the factors determining the environment;
- to make a significant contribution to environmental studies, notably in the area of atmospheric chemistry and ocean studies (including marine biology).

These are coupled with two related, secondary objectives:

- to allow the Earth's resources to be more effectively monitored and managed;
- to improve our understanding of solid Earth processes.

The mission intends to continue and improve upon measurements initiated by ERS-1 and ERS-2, and to take into account the requirements related to the global study and monitoring of the environment.

The mission is an essential element in providing long-term continuous data sets that are crucial for addressing environmental and climatological issues. At the same time it further promotes the gradual transfer of applications of remote sensing data from experimental to pre-operational and operational exploitation.

Envisat, as an undertaking of ESA member states plus Canada, constitutes a major contribution to the effort of Space agencies worldwide to provide the data and information required to further the understanding, modelling, and prediction of environmental and climate changes.

This mission includes both global and regional mission objectives (see below) with the corresponding need to provide data to scientific and applications users (see below) within various time scales.

Global mission objectives

Some global applications require near-real-time data delivery (within a few hours to one day of acquisition). Specific examples include:

- forecasting the sea state conditions at various scales;
- monitoring sea surface temperature;
- monitoring some atmospheric species (e.g., ozone for warning purposes);
- monitoring some atmospheric variables (e.g., temperature, pressure, water vapour, cloud top height, earth radiation budget, etc.);
- monitoring ocean colour for supporting fisheries and pollution monitoring (complementing the regional missions).

Some of the global objectives require products available in off-line mode (days to weeks of acquisition). Specific examples include quantitative monitoring of:

- radiative processes;
- ocean-atmosphere heat and momentum exchange;
- interaction between the atmosphere and land or ice surfaces;
- composition of the atmosphere and associated chemical processes;
- ocean dynamics and variability;
- ice sheet characteristics and sea ice distribution and dynamics;
- large-scale vegetation processes in correlation with surface energy and water distribution;
- ocean primary productivity;
- natural and man-made pollution over the oceans;
- support for major international programmes (GCOS, IGBP, etc.).

Regional mission objectives

Continuous and coherent regional data sets are needed by the scientific and application user community for a variety of objectives such as:

- sea ice off-shore applications;
- detecting and mapping snow and ice;
- monitoring coastal processes and pollution;
- monitoring ship traffic;

- monitoring agriculture and forests;
- monitoring soil moisture and large-scale vegetation processes;
- geological features and mineral resources;
- applications linked to SAR interferometry (DEM generation, hazard monitoring, etc.);
- hydrological research and applications;
- support for fisheries in coastal waters.

Some of the regional objectives (e.g., sea ice applications, marine pollution, maritime traffic, hazard monitoring, etc.) require near-real-time data products (within a few hours of acquisition) generated according to user requests. Others (e.g., agriculture, soil moisture, etc.) require fast turnaround data services (a few days). The remainder are generally satisfied with off-line (few weeks) data delivery.

Further information on the [mission's objectives](#) (ESA website)

7.1.9.4 Envisat Ground segment

The Envisat ground segment provides the means and resources for managing and controlling the mission, receiving and processing the data produced by the instruments, and disseminating and archiving the products generated. Furthermore, it provides a single interface to the users to allow optimum utilisation of the system's resources in line with their needs.

The ground segment can be divided into two major parts:

- the flight operation segment (FOS), which is responsible for command and control of the satellite;
- the payload data segment (PDS), which is responsible for exploiting the instrument data.

The satellite-to-ground communication links rely on various ground stations (Kiruna, Fucino, Svalbard and Villafranca – the latter as TT&C back-up) and the ESA data relay satellite system, Artemis, which provides direct communication between Envisat and the ground even when the satellite is out of sight of the ground stations. This enables the use of high-rate sensors whose data cannot be stored on board, optimally managed tape dumps, and enhanced visibility for command and control. Additional national and ESA ground stations are involved.

Payload Data Segment (PDS)

The PDS comprises all the ground segment elements related to payload data acquisition, processing and archiving. It also includes the user interface facilities which offer Envisat services to the user community.

For more detailed information see the PDS Detailed Description.

Role of the PDS

The PDS provides all services related to the exploitation of data produced by the instruments carried on the Envisat satellite:

- all payload data acquisition for the global mission;
- all regional data acquisition performed by ESA stations;
- processing and delivery of ESA near-real-time products;

- archiving, processing and delivery of ESA offline products with the support of processing and archiving centres (PACs);
- interfaces with national and foreign stations acquiring regional data;
- interfaces with the user community from order handling to product delivery.

Architectural elements

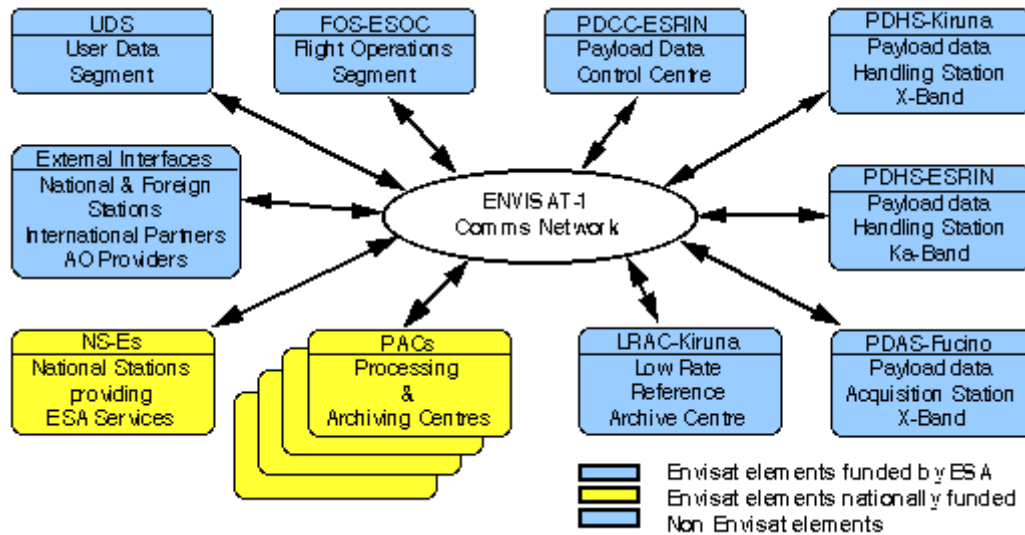


Figure 7.39. Overview of the PDS architectural elements

The PDS comprises:

ESA provided centres and stations:

- the payload data control centre (PDCC) at Esrin;
- the payload data handling station (PDHS) at Esrin and Kiruna;
- the payload data acquisition station (PDAS) at Fucino;
- the low-rate reference archive centre (LRAC) at Kiruna.

Centres and stations procured nationally:

- the processing and archiving centre (PAC's) located at ESA member states;
- the national stations providing ESA services (NSES) and located in programme participating states.

The PDS also interfaces with national and foreign stations duly authorised to receive Envisat regional data.

All PDS centres and stations is coordinated by the payload data control centre (PDCC) which is in charge of instrument and ground segment planning and of the overall PDS monitoring and control. The PDCC interfaces with the flight operation control centre (FOCC) for all mission planning activities.

PDS product distribution

Two categories of product distribution services are provided by the PDS:

Near real time services

- Typically three hours from acquisition for data used in forecasting or tactical operations (global and regional products produced and distributed systematically);
- Typically one to three days from acquisition for applications requiring high-resolution images (agriculture, forestry, soil moisture, etc.) with production and delivery to users on request.

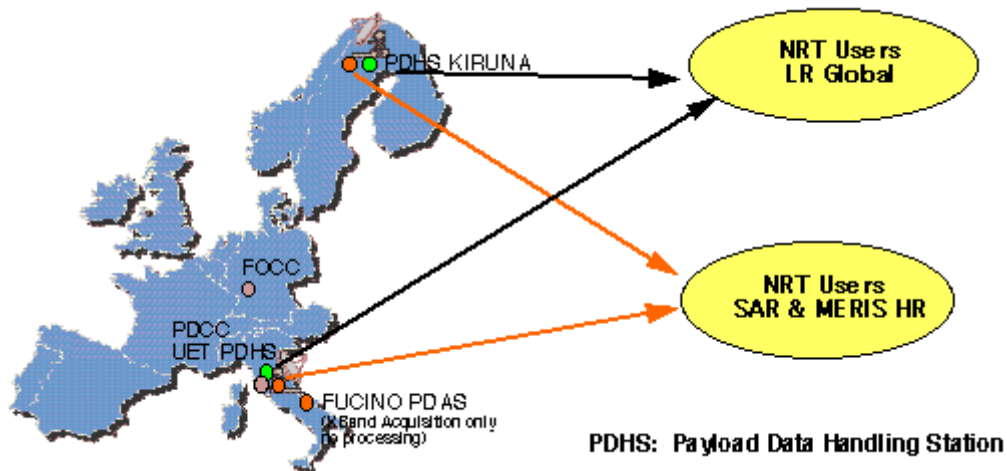


Figure 7.40. Payload data handling stations for Near real time

Off-line service

Continuity of services from near real time to off-line

- Delivery a few days to weeks from data acquisition
- Product commonalities (same format, same processing algorithms whenever possible)
- Off-line products benefit from a posteriori knowledge of calibration, auxiliary data, and precise orbit

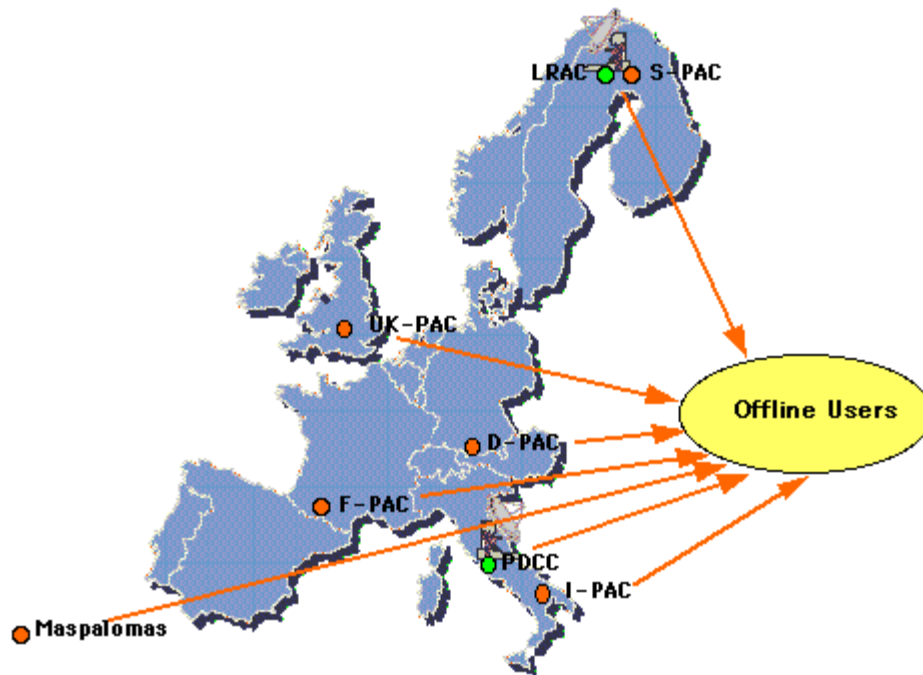


Figure 7.41. Payload data handling stations for off-line users

Processing and archiving centres (PAC)

The processing and archiving centres, located in ESA member states, archive and process off-line high rate data and generate off-line geophysical products for the regional high-rate and full-resolution instruments and for the global low-rate instruments. Altimetry processing and archiving centre is located at F-PAC

Further information on [Envisat ground segment](#) (ESA website)

7.1.10 Jason-1



Figure 7.42. Jason-1 (Credits [CNES/NASA](#))

Satellite	Jason-1
Launched	7 December 2001
End Date	1 July 2013
Mission	Measure sea surface height
Altitude	1336 km
Inclination	66° (non-sun-synchronous)

Jason-1 is the follow-on to [Topex/Poseidon](#), whose main features it has inherited (orbit, instruments, measurement accuracy, etc.), and is being developed jointly by CNES and NASA. Satellite control and data processing operations are performed by a new ground segment.

On mid-February, 2009 (on the beginning of cycle 262), The Jason-1's orbit is shifted midway between its original ground tracks (corresponding to those of Topex/Poseidon after 2002) while OSTM/Jason-2 still keeps the original ground tracks (those of Topex/Poseidon before 2002 and Jason-1 before February 2009). OSTM/Jason-2 and Jason-1 have also a time lag of approximately 5-days. This new tandem configuration better is better suited for real-time applications.

Contact was lost with the Jason-1 spacecraft on 21 June 2013. At the time of the last contact, the spacecraft its payload instruments were in nominal health and there were no indications of any alarms or anomalies. All attempts to re-establish communications with the Jason-1 spacecraft over the ten days from 21 June to 01 July, from both US and French ground stations, were unsuccessful.

Jason-1 was passivated and decommissioned on 01 July 2013, terminating the Jason-1 mission after 11.5 years of operations.

Further information on:

- [Jason-1 \(Aviso/CNES\)](#)
- [Ocean surface topography from space \(NASA/JPL\)](#)
- [Physical Oceanography Distributed Active Archive Center \(NASA/JPL\)](#)
- [Jason-1 and 2, the ocean observatory \(CNES\)](#)

7.1.10.1 Jason-1 Instruments

Jason-1 is carrying a payload of five instruments: the Poseidon-2 altimeter, the mission's main instrument, which measures range; the JMR radiometer, which measures perturbations due to atmospheric water vapour; and three location systems: DORIS, LRA and TRSR.



Figure 7.43. Jason 1 instruments

Poseidon-2 altimeter

Poseidon-2 is the mission's main instrument, derived from the experimental Poseidon-1 altimeter on Topex/Poseidon. It is a compact, low-power, low-mass instrument offering a high degree of reliability. Poseidon-2 is a radar altimeter that emits pulses at two frequencies (13.6 and 5.3 GHz, the second frequency is used to determine the electron content in the atmosphere) and analyses the return signal reflected by the surface. The signal's round-trip time is estimated very precisely in order to calculate the range, after applying the necessary corrections (Instrument supplied by CNES).

JMR (Jason-1 Microwave Radiometer)

This instrument measures radiation from the Earth's surface at three frequencies (18.7, 23.8 and 34.0GHz). Measurements acquired at each frequency are combined to determine atmospheric water vapour and liquid water content. Once the water content is known, we can determine the correction to be applied for radar signal path delays (Instrument supplied by NASA).

Location systems

The location systems onboard Jason-1 complement each other to measure the satellite's position on orbit to within two centimetres on the radial component. It is highly accurate but it requires ground stations that are complex to operate, and its use can be restricted by adverse weather conditions. It is used to calibrate the other two location systems so that the satellite orbit can be determined as accurately as possible. The TRSR (a GPS receiver) acquires data that complement DORIS measurements in order to determine the orbit in real time and to support precise orbit determination.

DORIS (Doppler location)

The DORIS system uses a ground network of orbitography beacons spread around the globe, which send signals at two frequencies to a receiver on the satellite. The relative motion of the satellite generates a shift in the signal's frequency (called the Doppler shift) that is measured to derive the satellite's velocity. These data are then assimilated in orbit determination models to keep permanent track of the satellite's precise position (to within three centimetres) on its orbit (Instrument supplied by CNES).

TRSR (GPS location)

The TRSR uses the Global Positioning System (GPS) to determine the satellite's position by triangulation, in the same way that GPS fixes are obtained on Earth. At least three GPS satellites determine a mobile object's (in this case, the satellite's) exact position at a given instant. Positional data are then integrated into an orbit determination model to track the satellite's trajectory continuously (Instrument supplied by NASA).

LRA (laser tracking)

The LRA (Laser Retroreflector Array) is an array of mirrors that provide a target for laser tracking measurements from the ground. By analysing the round-trip time of the laser beam, we can locate where the satellite is on its orbit (Instrument supplied by NASA).

Further information on [Jason-1](#) (Aviso website)

7.1.10.1 Poseidon-2

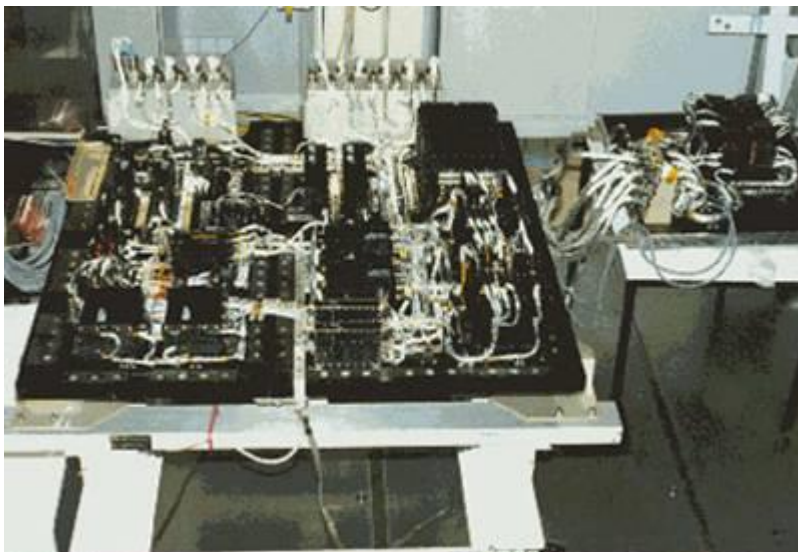


Figure 7.44. Poseidon-2 being integrated on Jason-1 (Credits CNES/Alcatel)

The Poseidon-2 altimeter is the main instrument on the Jason-1 mission. Derived from the Poseidon-1 altimeter on Topex/Poseidon, it measures sea level, wave heights and wind speed. It operates at two frequencies and is also able to estimate atmospheric electron content.

Function

Poseidon-2 measures range (the distance from the satellite to the Earth's surface), wave height and wind speed.

Principle

The altimeter emits a radar beam that is reflected back to the antenna from the Earth's surface (see [how altimetry works](#) for details). Poseidon-2 operates at two frequencies (13.6 GHz in the Ku band and 5.3 GHz in the C band) to determine atmospheric electron content, which affects the radar signal path delay. These two frequencies also serve to measure the amount of rain in the atmosphere.

Technical data

Poseidon-2, or SSALT (for Solid State ALTimeter), uses solid-state amplification techniques.

Table 7.13 Poseidon-2 Main parameters

Emitted Frequency (GHz)	Dual-frequency (Ku, C) – 13.575 and 5.3
Pulse Repetition Frequency (Hz)	2060 interlaced {3Ku-1C-3Ku}
Pulse duration (microseconds)	105
Bandwidth (MHz)	320 (Ku and C)
Antenna diameter (m)	1.2
Antenna beamwidth (degrees)	1.28 (Ku), 3.4 (C)
Power (W)	7
Redundancy	Yes
Specific features	Solid-State Power Amplifier. Dual-frequency for ionospheric correction, High resolution in C band (320 MHz)

7.1.10.1.2 JMR: Jason-1 Microwave Radiometer

Figure 7.45. JMR antenna

The JMR acquires measurements via three separate frequency channels to determine the path delay of the altimeter's radar signal due to atmospheric water vapour.

Function

The JMR measures water vapour content in the atmosphere so that we can determine how it impacts radar signal propagation. Its measurements also can be used directly for studying other atmospheric phenomena, particularly rain.

Principle

The JMR is a passive receiver that collects radiation reflected by the oceans at frequencies of 18.7, 23.8 and 34 GHz.

Radiation measured by the radiometer depends on surface winds, ocean temperature, salinity, foam, absorption by water vapour and clouds, and various other factors. To determine atmospheric water vapour content accurately, we need to eliminate sea surface and cloud contributions from the signal received by the radiometer. This is why the JMR uses different frequencies, each of which is more sensitive than the others to one of these contributions. The main 23.8 GHz frequency is used to measure water vapour; the 34 GHz channel provides the correction for non-rainbearing clouds, and the 18.7 GHz channel is highly sensitive to wind-driven variations in the sea surface. By combining measurements acquired at each of these frequencies, we can extract the water vapour signal.

Further information on [Instrument Description: Radiometer\(s\)](#) (NASA/JPL website).

7.1.10.1.3 DORIS



Figure 7.46. DORIS antenna

The DORIS instrument onboard Jason-1 provides real-time location and precise orbit determination. DORIS measurements are also used for geophysical studies, in particular through the International DORIS Service (IDS). DORIS is a dual-frequency instrument able to determine atmospheric electron content.

Function

Real-time location: Diode

The Diode onboard navigator locates the satellite on orbit in real time. This information is essential for providing altimetry data in real time or near-real time.

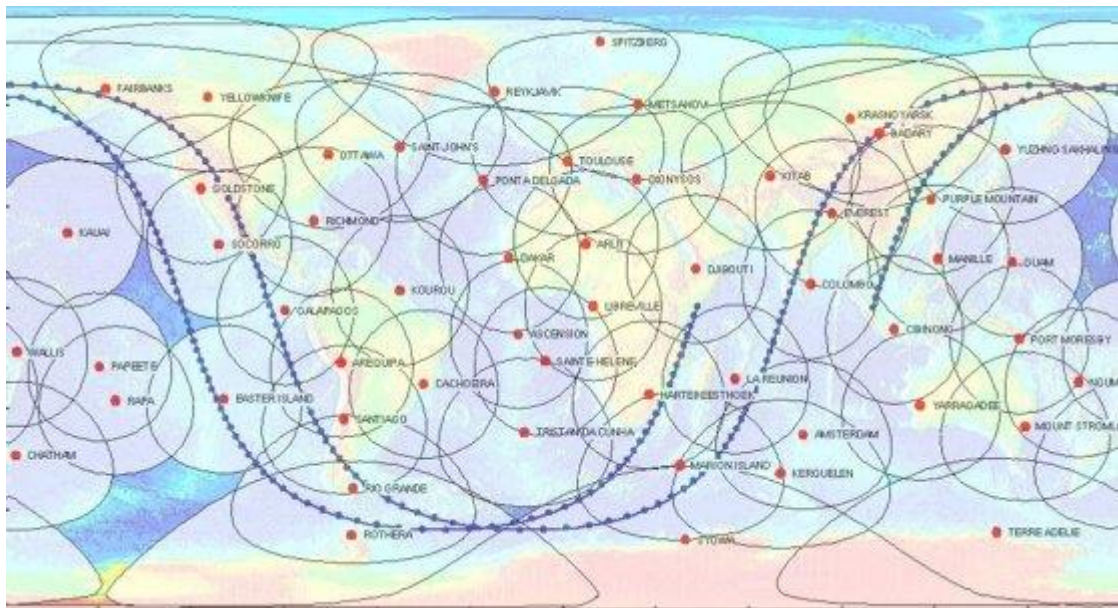


Figure 7.47. The DORIS network of orbitography beacons and their spatial coverage from Jason-1's orbit

Precise orbit determination

DORIS measurements are used for precise orbit determination (POD).

Ionospheric electron content

By measuring and comparing the path delay of signals transmitted at two separate frequencies, DORIS is able to calculate the electron content in the atmosphere. This information is then used to determine perturbations acting on the altimeter's radar signal.

This function complements the dual-frequency altimeter function.

Principle



Figure 7.48. DORIS Beacon

DORIS orbitography beacons transmit signals at two separate frequencies (2,036.25 MHz and 401.25 MHz) to the satellite. The receiver on board the satellite analyses the received signal frequencies to calculate its velocity relative to Earth. This velocity is fed into orbit determination models to derive the satellite's position on orbit to within two centimetres on the radial component.

For Further information, see the [International DORIS Service \(IDS\)](#) and [DORIS, the space surveyor \(Aviso\)](#)

7.1.10.1.4 TRSR GPS tracking receiver

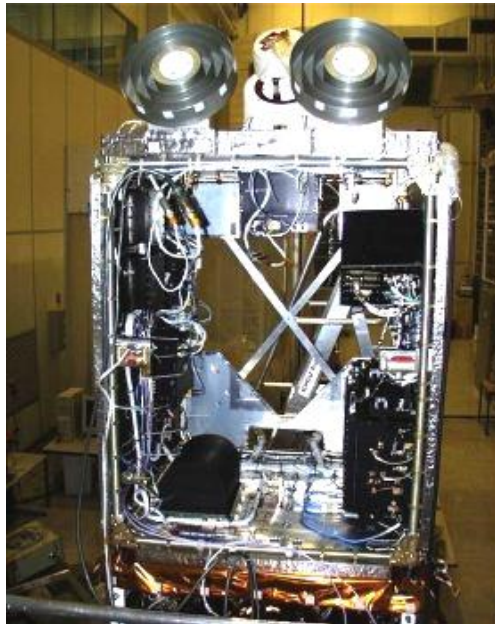


Figure 7.49. TRSR GPS System

The TRSR (Turbo Rogue Space Receiver) is a tracking system that uses the GPS constellation of satellites to determine the exact position of a transmitter.

Function

The TRSR supports precise orbit determination by the DORIS system. It also helps to improve gravity field models and provides data for satellite positioning accurate to about 50 metres and 50 nanoseconds.

Principle

The TRSR receives dual-frequency navigation signals continuously and simultaneously from 16 GPS satellites. It uses these signals to acquire phase measurements accurate to about one millimetre and pseudo-range measurements accurate to about 10 centimetres.

Technical data

The onboard system consists of two independent receivers operating in cold redundancy, each with an omnidirectional antenna, low-noise amplifier, quartz oscillator, sampling converter and a baseband digital processor communicating via the bus interface.

For Further information see [International GPS Services](#).

7.1.10.1.5 LRA: Laser Retroreflector Array



The LRA is an array of mirrors that provide a target for laser tracking measurements from the ground. By analysing the round-trip time of the laser beam, we can locate very precisely where the satellite is on its orbit.

Figure 7.50. LRA (Credits ATSC)

Function

The LRA is used to calibrate the other location systems on the satellite with a very high degree of precision.

Principle

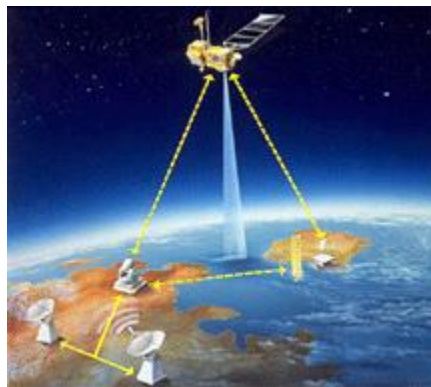


Figure 7.51. Laser Retroreflector diagram

The LRA is a passive instrument that acts as a reference target for laser tracking measurements performed by ground stations. Laser tracking data are analysed to calculate the satellite's altitude to within a few millimetres. However, the small number of ground stations and the sensitivity of laser beams to weather conditions make it impossible to track the satellite continuously. That is why other onboard location systems are needed.

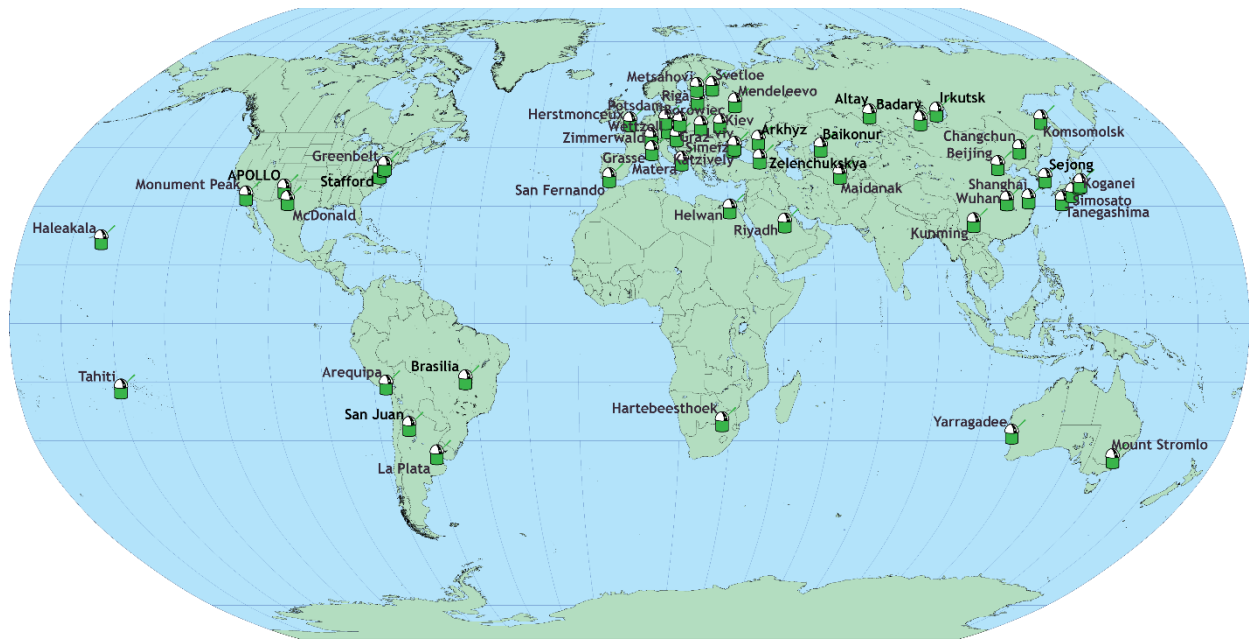


Figure 7.52. Network of laser ranging stations (Credits: ILRS (International Laser Ranging Service))

Technical data

The retroreflectors are placed on the nadir side of the satellite. The totally passive unit consists of nine quartz corner cubes arrayed as a truncated cone, with one cube in the centre and the others arranged azimuthally around the cone. This arrangement allows laser ranging at field-of-view angles of 360 degrees in azimuth and 60 degrees in elevation around the perpendicular. The retroreflectors are optimised for a wavelength of 532 nanometres (green), offering a field of view of about 100 degrees. Jason-1’s LRA was built by ITE Inc. under contract to NASA’s Goddard Space Flight Center.

Further information on

- Instrument Description: LRA (NASA/JPL website),
- [ILRS](#) (International Laser Ranging Service)

7.1.10.2 Jason-1 orbit

Jason-1’s orbit is identical to that of Topex/Poseidon. It is optimised to study large-scale ocean variability and to provide coverage of 90% of the world’s oceans over a ten-day cycle.

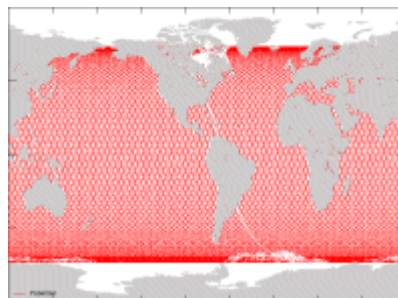


Figure 7.53. Jason-1 ground tracks, before February 2009

Choice of orbit

Jason-1's high altitude (1,336 kilometres) reduces interactions with the Earth's atmosphere and gravity field to a minimum, thus making orbit determination easier and more precise. The orbit inclination of 66 degrees North and South enables the satellite to cover most of the globe's unfrozen oceans. The orbit's repeat cycle is just under 10 days (9.9156 days to be precise, i.e. 10 days minus two hours) – in other words, the satellite passes over the same point on the Earth's surface (to within one kilometre) every ten days. This cycle is a trade-off between spatial and temporal resolution designed for the study of large-scale ocean variability. The fact that the orbit is prograde and not sun-synchronous also avoids aliasing of different tide components at the same frequency.

Furthermore, using the same orbit as Topex/Poseidon ensures better intercalibration and data continuity. The orbit is also designed to pass over two dedicated ground calibration sites: Cap Senetosa in Corsica and the Harvest oil rig platform in California, USA.

Jason-1 has undergone an orbit change at the end of OSTM/Jason-2's calibration phase in February 2009. Currently, Jason-2 is located on the former orbit of Topex/Poseidon (before 2002) and Jason-1 (before February 2009). The Jason-1's orbit is shifted midway between its original ground tracks (corresponding to those of Topex/Poseidon after 2002). Jason-1 and OSTM/Jason-2 also have a time lag of 5 days.

Manoeuvres

A satellite's orbit parameters tend to change over time as a result of atmospheric drag. In the long term, more or less periodic variations also occur due to instabilities in the Earth's gravity field, solar radiation pressure and other forces of smaller magnitude.

Orbit manoeuvres are performed every 40 to 200 days. Intervals between manoeuvres depend chiefly on solar flux and each manoeuvre lasts from 20 to 60 minutes. Wherever possible, they are performed at the end of the orbit cycle, and above solid earth, so that lost data acquisition time is reduced to a minimum.

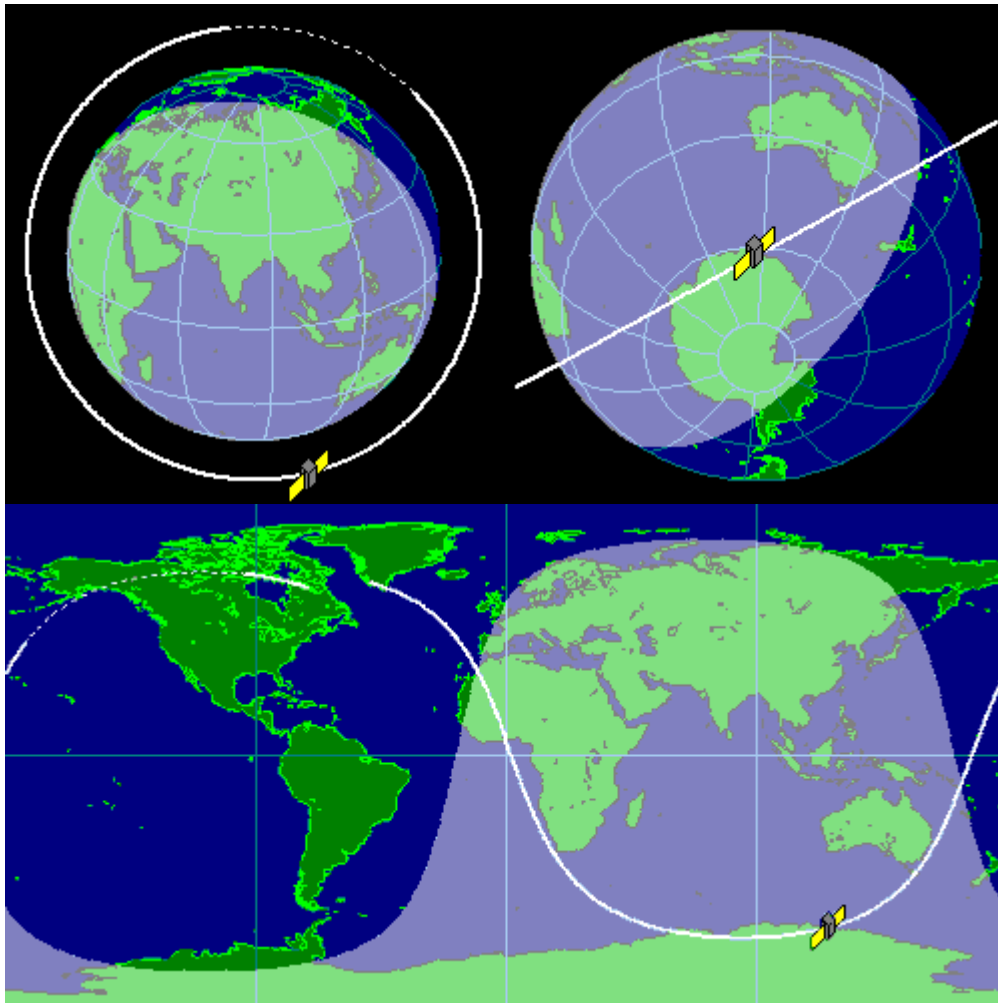


Figure 7.54. Jason-1 orbit

Orbit parameters

Table 7.14 Jason-1 Orbit Main characteristics

Semi-major axis	7714.4278 km
Eccentricity	0.000095
Inclination (non-sun-synchronous)	66.039°

Table 7.15 Jason-1 Orbit Auxiliary data

Reference altitude (equatorial)	1,336 km
Nodal period	6,745.72 seconds (112'42" or 1h52')
Repeat cycle	9.9156 days
Number of passes per cycle	254
Ground track separation at Equator	315 km

Table 7.15 Jason-1 Orbit Auxiliary data

Acute angle at Equator crossings	39.5°
Orbital velocity	7.2 km/s
Ground scanning velocity	5.8 km/s

7.1.10.3 Jason-1 Mission objectives

Is the Earth getting warmer? What do the ocean currents hold in store for tomorrow? What are the underlying processes driving ocean movements? The Jason series of satellites sustain radar altimetry observations in the coming decades, providing continuous data on sea surface height (SSH) accurate to within a few centimetres all over the globe, to tell us more about variations in surface and deep-water ocean circulation. Designed to follow on from Topex/Poseidon, Jason-1's instruments and data processing systems have drawn extensively on the lessons learned from its predecessor. Jason-1 is a true ocean observatory that supplies SSH and sea-state measurements in near-real time to an international user community.

Oceanography and ocean forecasting

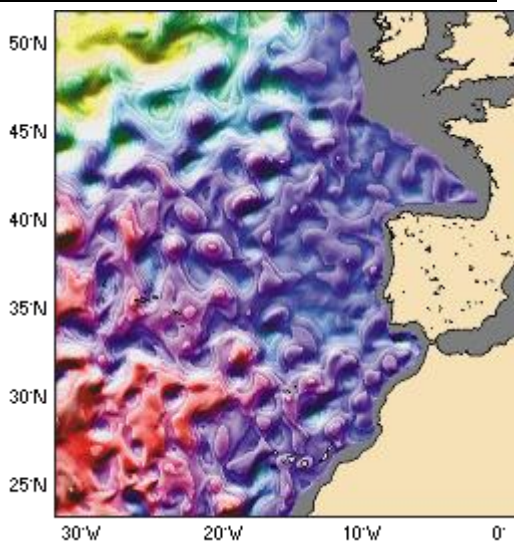


Figure 7.55. Forecasts of ocean circulation and its eddies (Credits SHOM/CLS)

Ocean variability is the central focus of the Jason-1 mission. The satellite's orbit – identical to Topex/Poseidon – has been defined to cover 90% of the world's ice-free oceans every ten days. Real-time data delivery makes it possible to issue ocean bulletins in much the same way as we do weather forecasts today.

Climatology and climate prediction

Altimetry data yield vital information for studying and predicting climate, in particular climatic phenomena such as El Niño. Jason-1's ability to measure mean sea level with millimetre accuracy is a key asset for monitoring climate change.

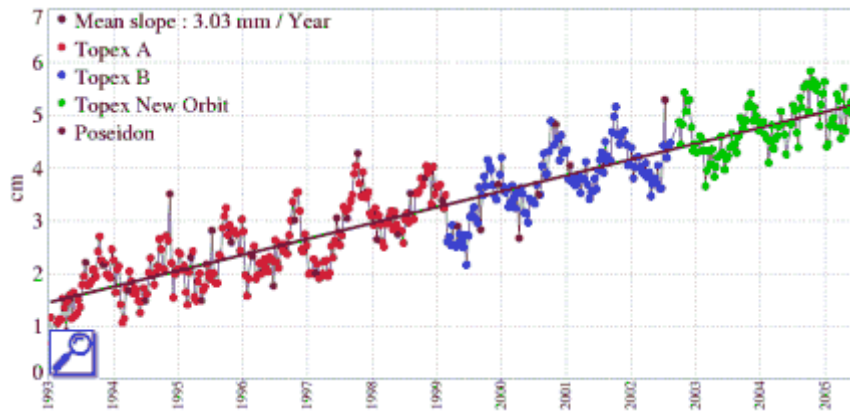


Figure 7.56. Figure 7.57. Global variations in mean sea level measured by Topex/Poseidon. (Credits [Aviso](#))

Marine meteorology

Jason-1 delivers sea-state data (wave heights and wind speed) within three hours. This information helps us to better understand and predict weather conditions over the oceans.

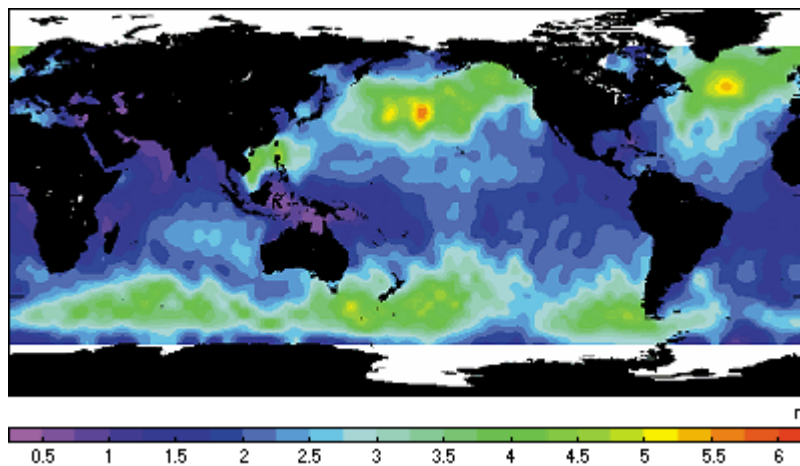


Figure 7.58. Wave heights measured by Topex/Poseidon in December 1999. (Credits [Aviso](#))

Geophysics

The Earth's gravity field affects sea level. By measuring the ocean's dynamic topography, we can learn more about plate tectonics, bottom topography, movements of the Earth's mantle and many other geophysical phenomena. Altimetry data are also used to study ice, lakes and rivers, and relief in desert regions.

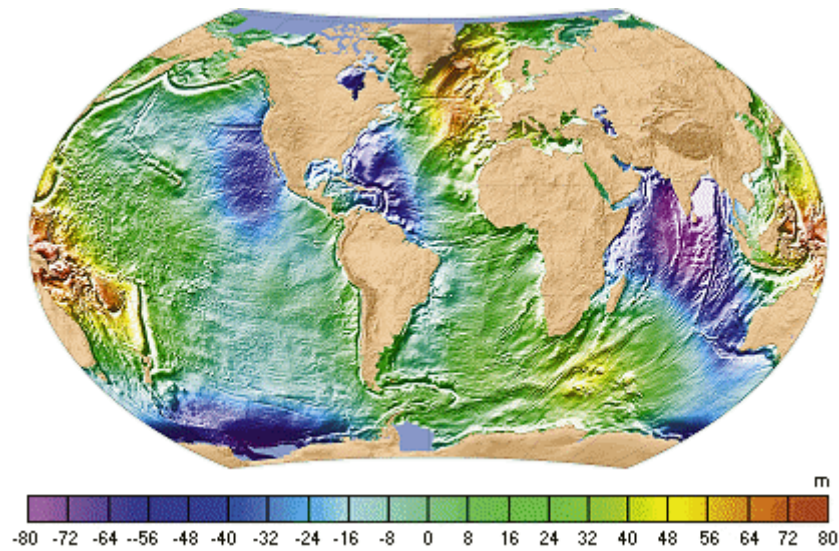


Figure 7.59. The mean sea surface shows how the Earth's gravity field affects the oceans. (Credits SHOM/CLS)

See the scientific objectives in Y. Mènard, L.L. Fu, 2000: Jason-1, on the tracks of Topex/Poseidon, *Aviso Newsletter*, 7, January 2000.

7.1.10.4 Ground segment

The Jason-1 ground segment is made up of three components providing the human (teams) and equipment resources required to ensure the mission's success:

- The Proteus Generic Ground Segment (PGGS, based in Toulouse, France)
- The Project Operation Control Centre (POCC, based in Pasadena, California, USA)
- The SSALTO multimission ground segment (based in Toulouse, France).

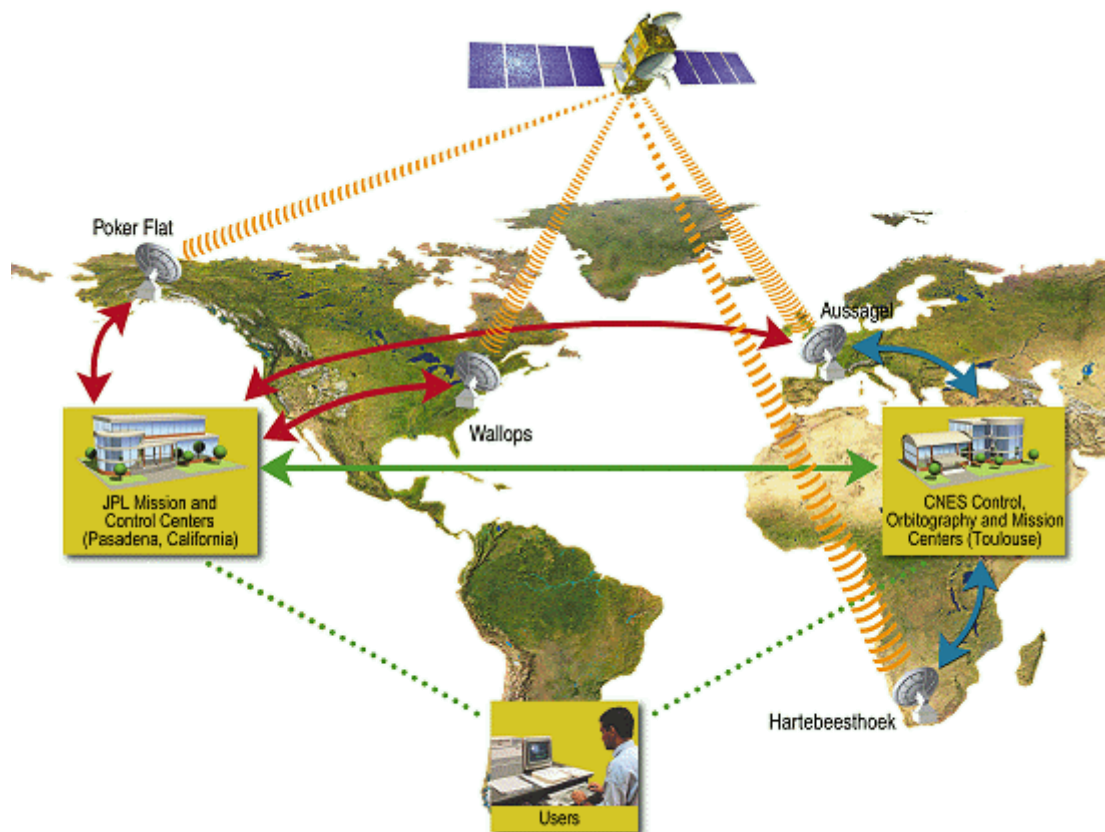


Figure 7.60. Ground Segment components

Mission operations

This comprises the Proteus Generic Ground Segment (PGGS) located in Toulouse, France, and the Project Operations Control Centre (POCC) located in Pasadena, Ca, USA.

PGGS

The Proteus Generic Ground Segment provides the necessary capability for operating a Proteus spacecraft. It includes an Earth terminal, a command and control centre and a data communications network. Proteus adapted its facilities to meet Jason-1's requirements. It was used to perform satellite operations during the early phase of the mission (launch, station acquisition, in-orbit acceptance) and then performed spacecraft analysis and navigation functions when the POCC took over routine satellite operations. The PGGS is broken down into three main components: the TTCET Earth terminal, the command control centre (CCC) and the data communications network (DCN). Development of the generic product and the specific adaptation to the Jason-1 mission were managed by the same team.

POCC

The POCC provided the capability for operating Jason-1 during its routine phase, including 1) real-time telemetry and command (JTCC), 2) sequence generation (JSEQ), 3) Earth terminal (ET), 4) science processing and distribution (JSDS), and 5) data archiving (PODAAC) functions. It was derived from the Topex/Poseidon POCC and simultaneously supported Topex/Poseidon and Jason-1

SSALTO

The SSALTO multimission ground segment (Segment Sol multimissions d'ALTimétrie, d'Orbitographie et de localisation précise) encompasses ground support facilities for controlling the DORIS and Poseidon instruments, processing data from DORIS and the altimeters onboard Topex/Poseidon, Jason-1 and Envisat-1, and providing user services and expert altimetry support.

SSALTO was designed by CNES, the French space agency, in partnership with its subsidiary CLS and local French industry. SSALTO serves as a common ground segment for the DORIS/Spot, DORIS/Envisat, Topex/Poseidon, Jason-1 and Envisat missions. It thus responds to a growing commonality of user needs and supports the continued operation of DORIS instruments and altimetry payloads flying simultaneously on different satellites.

SSALTO encompasses the resources for:

- controlling onboard DORIS and Poseidon instruments, and the DORIS orbitography beacon network (CCI)
- obtaining precision orbits (POD)
- processing altimeter and radiometer data (CMA)
- providing user services, and archiving and managing data (Aviso)

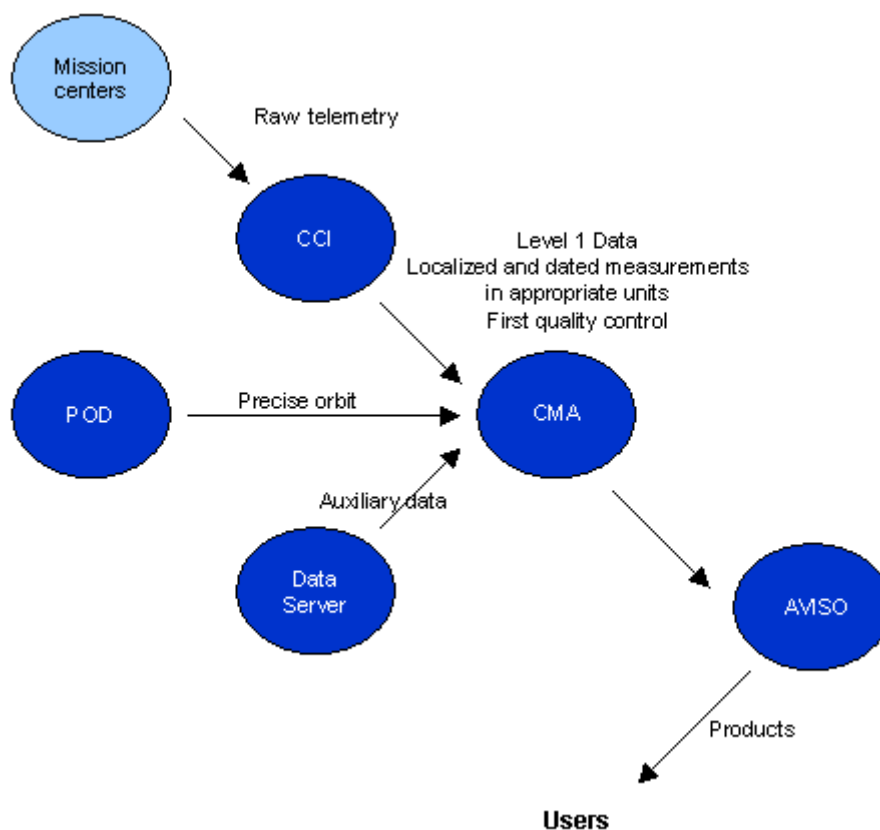


Figure 7.61. SSALTO data flow

The CMA (Multi-mission Altimetry Centre) processes altimetry data from Jason-1 and Envisat, and from SSALTO components that control the instruments (CCI) and determine precise orbits. Other components process Topex/Poseidon and DORIS data from other satellites (SPOT, Envisat) and distribute data ([Aviso](#)).

See also S. Coutin-Faye et al., 2000: SSALTO: a new ground segment for a new generation of altimetry satellites, *Aviso Newsletter*, n°7 January 2000.

7.2 Current missions

There are six altimetry satellites currently in service:

- Jason-2 – with a relatively short repeat cycle (10 days), able to observe the same spot on the ocean frequently but with relatively widely-spaced ground tracks (315 kilometres at the equator). Jason-2 is on the same orbit as their predecessors, Topex/Poseidon (1992-2005) and Jason-1 (2001-2013).
- Saral – The orbit is similar to the orbit of ENVISAT allowing continuation of the ERS/ENVISAT time series.. The repeat cycle is 35 days and the ground track spacing is 90 kilometres at the equator, complementary to the Jason-2 orbit.
- CryoSat-2 – with an altimeter (Siral) able to work with an interferometric mode, with a high orbit inclination of 92° to satisfy the scientific requirements for observing the poles and the ice sheets, and with an orbit non-sun-synchronous (commonly used for remote-sensing satellites).
- HY-2 – with a 14-day orbit.
- Jason-3 – To ensure continuity of the global sea level record, Jason-3 is flying in the same 9.9 day repeat track orbit as all previous Jason missions, meaning the satellite is making observations over the same ocean point once every 9.9 days. The orbital parameters are: 66.05 degree inclination, 1380 km apogee, 1328 km perigee, 112 minutes per revolution around the earth.
- Sentinel-3 – The Sentinel-3 mission is based on a constellation of two satellites to fulfill revisit and coverage requirements, providing robust datasets for Copernicus Services. Sentinel-3 is a multi-instrument mission to measure sea-surface topography, sea- and land-surface temperature, ocean and land colour with high-end accuracy and reliability. The orbit is a near-polar, sun-synchronous orbit with a descending node equatorial crossing at 10:00 h Mean Local Solar time. In a sun-synchronous orbit, the surface is always illuminated at the same sun angle. The orbital repeat cycle is 27 days ($14+7/27$ orbits per day, 385 orbits per cycle). The mission will support ocean forecasting systems, as well as environmental and climate monitoring. Sentinel-3A was launched on 16 February 2016. Sentinel-3B is scheduled for launch in 2017. Sentinel-3C and D are already planned.

7.2.1 Jason-2



Figure 7.62 Jason-2

Satellite	Jason-2
Launch	20 June 2008
Mission	Measure sea surface height
Altitude	1336 km
Inclination	66° (non-sun-synchronous)

Jason-2 is taking over and continuing the missions of Topex/Poseidon and Jason-1, in the framework of a cooperation between CNES, NASA, Eumetsat and NOAA. It carries the same kind of payload as its two predecessors for a high-precision altimetry mission: a Poseidon-class altimeter, a radiometer and three location systems. The orbit is also identical.

The Jason-2 payload includes the next generation of Poseidon altimeter (Poseidon-3, with the same general characteristics as Poseidon-2, but with a lower instrument noise and an algorithm enabling better tracking over land and ice), and the DORIS location system. The accuracy should be about 2.5 cm for the altimeter measurements.

Further information on:

- [Jason-2 \(Aviso\)](#)
- [Ocean surface topography from space \(NASA/JPL\)](#)
- [Jason-1 and 2, the ocean observatory \(CNES\)](#)

7.2.1.1 Jason-2 Instruments

Jason-2 is carrying a main payload of five instruments: the Poseidon-3 altimeter, the mission's main instrument, which measures range; the AMR radiometer, which measures perturbations due to atmospheric water vapour; and three location systems: DORIS, LRA and GPSP. These instruments provides full redundancy and measurements for at least three years. There are also three experimental instruments (Carmen-2, LPT and T2L2) onboard.

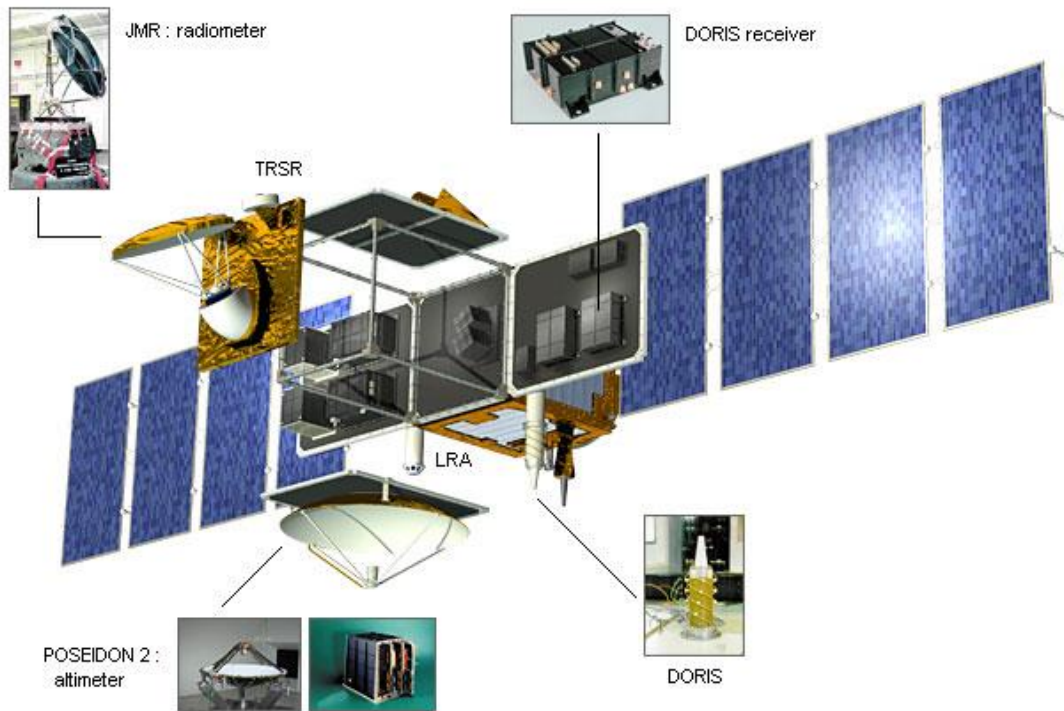


Figure 7.63. Jason 2 instruments

Poseidon-3 altimeter

Poseidon-3 is the mission's main instrument, derived from the Poseidon-2 altimeter on Jason-1. It is a compact, low-power, low-mass instrument offering a high degree of reliability. Poseidon-3 is a radar altimeter that emits pulses at two frequencies (13.6 and 5.3 GHz, the second frequency is used to determine the electron content in the atmosphere) and analyses the return signal reflected by the surface. The signal round-trip time is estimated very precisely to calculate the range, after applying the necessary corrections (Instrument supplied by CNES).

Advanced Microwave Radiometer (AMR)

This instrument measures radiation from the Earth's surface at three frequencies (18, 21 and 37 GHz). Measurements acquired at each frequency are combined to determine atmospheric water vapour and liquid water content. Once the water content is known, we can determine the correction to be applied for radar signal path delays (Instrument supplied by NASA).

Location systems

The location systems onboard Jason-2 complement each other to measure the satellite's position on orbit to within two centimetres on the radial component. The LRA is highly accurate but it requires ground stations that are complex to operate, and its use can be restricted by adverse weather conditions. It is used to calibrate the other two location systems so that the satellite's orbit can be determined as accurately as possible. The GPSP (a GPS receiver) acquires data that complement DORIS measurements in order to determine the orbit in real time and to support precise orbit determination.

DORIS (Doppler location)

The DORIS system uses a ground network of orbitography beacons spread around the globe, which send signals at two frequencies to a receiver on the satellite. The relative motion of the satellite generates a shift in the signal's frequency (called the Doppler shift) that is measured to derive the satellite's velocity. These data are then assimilated in orbit determination models to keep permanent track of the satellite's precise position (to within three centimetres) on its orbit (Instrument supplied by CNES).

GPSP (GPS location)

The GPSP uses the Global Positioning System (GPS) to determine the satellite's position by triangulation, in the same way that GPS fixes are obtained on Earth. At least three GPS satellites determine the mobile object's (in this case the satellite's) exact position at a given instant. Positional data are then integrated into an orbit determination model to track the satellite's trajectory continuously (Instrument supplied by NASA).

LRA (laser tracking)

The LRA (Laser Retroreflector Array) is an array of mirrors that provide a target for laser tracking measurements from the ground. By analysing the round-trip time of the laser beam, we can locate where the satellite is on its orbit (Instrument supplied by NASA).

7.2.1.1.1 Poseidon-3

The Poseidon-3 altimeter is the main instrument on the Jason-2 mission. Derived from the Poseidon-1 altimeter on Topex/Poseidon and Poseidon-2 on Jason-1, it measures sea level, wave heights and wind speed. It operates at two frequencies and is also able to estimate atmospheric electron content.



Figure 7.64. . Poseidon-2 being integrated on Jason-1. Poseidon-3 on Jason-2 is similar. (Credits CNES/Alcatel)

Function

Poseidon-3 measures range (the distance from the satellite to the Earth's surface), wave height and wind speed.

Principle

The altimeter emits a radar beam that is reflected back to the antenna from the Earth's surface (see [how altimetry works](#) for details). Poseidon-3 operates at two frequencies (13.6 GHz in the K_u band and 5.3 GHz in the C band) to determine atmospheric electron content, which affects the radar signal path delay. These two frequencies also serve to measure the amount of rain in the atmosphere.

Technical data

Poseidon-3, or SSALT (for Solid State ALTimeter), uses solid-state amplification techniques.

Table 7.16 Poseidon-3 Main parameters

Emitted Frequency (GHz)	Dual-frequency (Ku, C) – 13.575 and 5.3
Pulse Repetition Frequency (Hz)	2060 interlaced {3Ku-1C-3Ku}
Pulse duration (microseconds)	105
Bandwidth (MHz)	320 (Ku and C)
Antenna diameter (m)	1.2
Antenna beamwidth (degrees)	1.28 (Ku), 3.4 (C)
Power (W)	7
Redundancy	Yes
Specific features	Solid-State Power Amplifier. Dual-frequency for ionospheric correction, High resolution in C band (320 MHz)

7.2.1.1.2 AMR



Figure 7.65. AMR antenna

The AMR (Advanced Microwave Radiometer) acquires measurements via three separate frequency channels to determine the path delay of the altimeter's radar signal due to atmospheric water vapour.

Function

The AMR measures water vapour content in the atmosphere so that we can determine how it impacts radar signal propagation. Its measurements can also be used directly for studying other atmospheric phenomena, particularly rain.

Principle

The AMR is a passive receiver that collects radiation reflected by the oceans at frequencies of 18.7, 23.8, and 34 GHz.

Radiation measured by the radiometer depends on surface winds, ocean temperature, salinity, foam, absorption by water vapour and clouds, and various other factors. To determine atmospheric water vapour content accurately, we need to eliminate sea surface and cloud contributions from the signal received by the radiometer. This is why the AMR uses different frequencies, each of which is more sensitive than the others to one of these contributions. The main 23.8 GHz frequency is used to measure water vapour, the 34 GHz channel provides the correction for non-rainbearing clouds, and the 18.7-GHz channel is highly sensitive to wind-driven variations in the sea surface. By combining measurements acquired at each of these frequencies, we can extract the water vapour signal.

7.2.1.1.3 DORIS



Figure 7.66. DORIS antenna

The DORIS instrument onboard Jason-2 provides real-time location and precise orbit determination. DORIS measurements are also used for geophysical studies, in particular through the International DORIS Service (IDS). DORIS is a dual-frequency instrument able to determine atmospheric electron content.

The main changes from the previous DORIS instruments are:

Principle

DORIS orbitography beacons transmit signals at two separate frequencies (2,036.25 MHz and 401.25 MHz) to the satellite. The receiver onboard the satellite analyses the received signal frequencies to calculate its velocity relative to Earth. This velocity is fed into orbit determination models to derive the satellite's position on orbit to within two centimetres on the radial component.



Figure 7.67. DORIS Beacon

For further information, see the [International DORIS Service \(IDS\)](#) and [DORIS, the space surveyor \(Aviso\)](#)

7.2.1.1.4 GPSP

The GPSP is a tracking system that uses the GPS constellation of satellites to determine the exact position of a transmitter.

Function

The GPSP supports precise orbit determination by the DORIS system. It also helps to improve gravity field models and provides data for satellite positioning accurate to about 50 metres and 50 nanoseconds.

Principle

The GPSP receives dual-frequency navigation signals continuously and simultaneously from 16 GPS satellites. It uses these signals to acquire phase measurements accurate to about one millimetre and pseudo-range measurements accurate to about 10 centimetres.

Technical data

The onboard system consists of two independent receivers operating in cold redundancy, each with an omnidirectional antenna, low-noise amplifier, quartz oscillator, sampling converter and a baseband digital processor communicating via the bus interface.

7.2.1.1.5 LRA

The LRA is a totally passive reflector designed to reflect laser pulses back to their point of origin on Earth. It is used for calibrating the satellite's Precise Orbit Determination system.

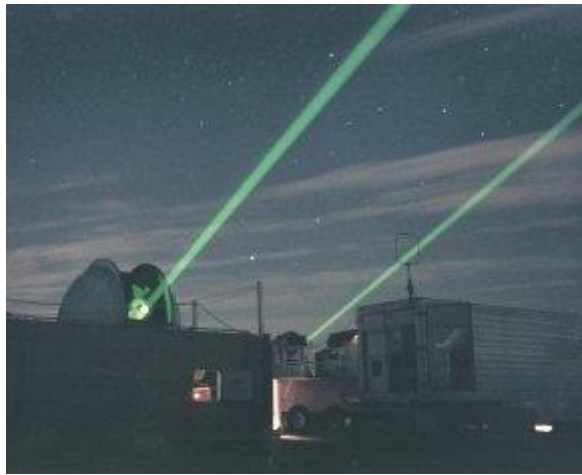


Figure 7.68. LRA ground station.

Function

The LRA (Laser Retroreflector Array) is an array of mirrors that provides a target for laser tracking measurements from the ground. By analysing the round-trip time of the laser beam, we can locate very precisely where the satellite is on its orbit. The LRA is used to calibrate the other location systems on the satellite (DORIS, GPSP) with a very high degree of precision.

Principle

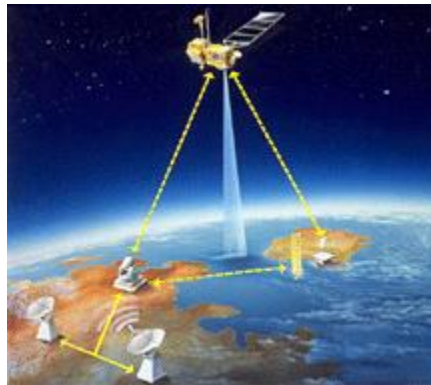


Figure 7.69. Laser Retroreflector diagram

The LRA is a passive instrument that acts as a reference target for laser tracking measurements performed by ground stations. Laser tracking data are analysed to calculate the satellite's altitude to within a few millimetres. However, the small number of ground stations and the sensitivity of laser beams to weather conditions makes it impossible to track the satellite continuously. This is why other onboard location systems are needed.

Technical data



Figure 7.70. LRA reflectors (Crédits [ATSC](#))

The retroreflectors are placed on the nadir side of the satellite. The totally passive unit consists of nine quartz corner cubes arrayed as a truncated cone, with one cube in the centre and the others arranged azimuthally around the cone. This arrangement allows laser ranging at field-of-view angles of 360 degrees in azimuth and 60 degrees in elevation around the perpendicular. The retroreflectors are optimised for a wavelength of 532 nanometres (green), offering a field of view of about 100 degrees.

7.2.1.2 Jason-2 Orbit

Jason-2's orbit is identical to that of Jason-1 (and that of Topex/Poseidon previously). It is optimised to study large-scale ocean variability and to provide coverage of 90% of the world's oceans over a ten-day cycle.

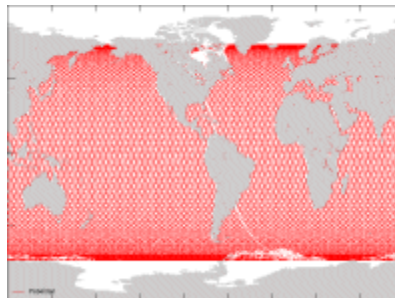


Figure 7.71. Topex/Poseidon ground tracks

Choice of orbit

Jason-2's high altitude (1,336 kilometres) reduces interactions with the Earth's atmosphere and gravity field to a minimum, thus making orbit determination easier and more precise. The orbit inclination of 66 degrees North and South enables the satellite to cover most of the globe's unfrozen oceans. The orbit's repeat cycle is just under 10 days (9.9156 days to be precise, i.e., 10 days minus two hours) – in other words, the satellite passes over the same point on the Earth's surface (to within one kilometre) every ten days. This cycle is a trade-off between spatial and temporal resolution designed for the study of large-scale ocean variability. The fact that the orbit is prograde and not sun-synchronous also avoids aliasing of different tidal components at the same frequency.

Furthermore, using the same orbit as Topex/Poseidon ensures better intercalibration and data continuity. The orbit is also designed to pass over two dedicated ground calibration sites: Cap Senetosa in Corsica and the Harvest oil rig platform in California, USA.

Manoeuvres

A satellite’s orbit parameters tend to change over time as a result of atmospheric drag. In the long term, more or less periodic variations also occur due to instabilities in the Earth’s gravity field, solar radiation pressure and other forces of smaller magnitude.

Orbit manoeuvres are performed every 40 to 200 days. Intervals between manoeuvres depend chiefly on solar flux and each manoeuvre lasts from 20 to 60 minutes. Wherever possible, they are performed at the end of the orbit cycle, and above solid earth, so that lost data acquisition time is reduced to a minimum.

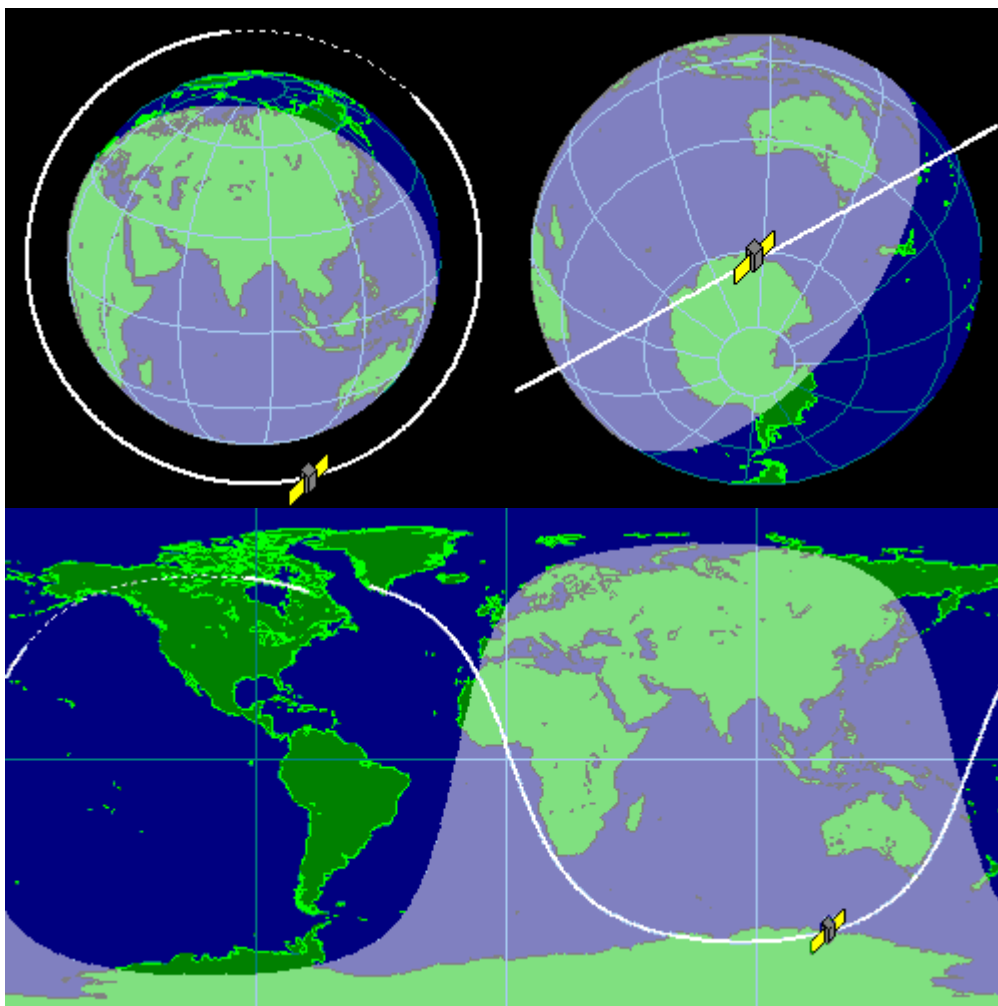


Figure 7.72. Jason-2 orbit

Orbit parameters

Table 7.17 Jason-2 Orbit Main characteristics

Semi-major axis	7714.4278 km
Eccentricity	0.000095
Inclination (non-sun-synchronous)	66.039°

Table 7.18 Jason-2 Auxiliary data

Reference altitude (equatorial)	1,336 km
Nodal period	6,745.72 seconds (112'42" or 1h52')
Repeat cycle	9.9156 days
Number of passes per cycle	254
Ground track separation at Equator	315 km
Acute angle at Equator crossings	39.5°
Longitude at Equator of pass 1	99.9242°
Orbital velocity	7.2 km/s
Ground scanning velocity	5.8 km/s

7.2.1.3 Jason-2 Objectives

- To have high-precision altimetric measurements in near-real time for integration into ocean forecasting models (operational oceanography)
- To continue Topex/Poseidon – Jason-1 time series, in order to benefit from data over a period long enough to study ocean long-term variations (including mean sea level variations), and decadal variations (decadal oscillations)
- To have quality data nearer to the coasts, and over lakes and rivers.
- Expected applications are also Topex/Poseidon and Jason-1's :
 - ocean study,
 - climate study, seasonal forecasting (including El Niño and such phenomena),
 - wind speed and wave height measurements, in real-time for weather forecast models, and over the long term (climatologies) for studies and model improvements,
 - better knowledge of the geoid, in combination with geodetic satellites (Grace, GOCE),
 - Tide models improvements,

7.2.1.4 Jason-2 Ground Segment

Jason-2's ground segment is a distributed system between NASA, CNES, Eumetsat and NOAA. On the terms and conditions specified with the quadripartite agreement for the Jason-2 project:

- raw data of the Poseidon3 altimeter, DORIS and the radiometer are processed by the NOAA and Eumetsat centres to product near-real time altimetry data (OGDR);
- raw data of the *Poseidon-3 altimeter and the radiometer are only processed by the mission centre at CNES to product delayed time altimetry data (IGDR; S-IGDR, GDR and S-GDR);*

- the production of preliminary and precise orbits of the satellite is provided by the CNES from data of DORIS system, and for the precise orbite determination, data are supplemented by GPS and laser systems;
- all Jason-2 products are permanently archived and distributed by CNES and NOAA. Thus, all scientific telemetry, delayed time products, near-real time products and all Jason-2 auxiliary data are archived and distributed by the mission centre at CNES that these data come from NOAA, Eumetsat or the CNES;
- value-added products generated by CNES are archived and distributed in stages by the CNES.

The data processing is integrated to the SALP (*Service d'Altimètrie et de Localisation Prècise* with the SSALTO ground segment, which already operates Topex/Poseidon, Jason-1 and Envisat altimetry missions.

7.2.2 CryoSat-2

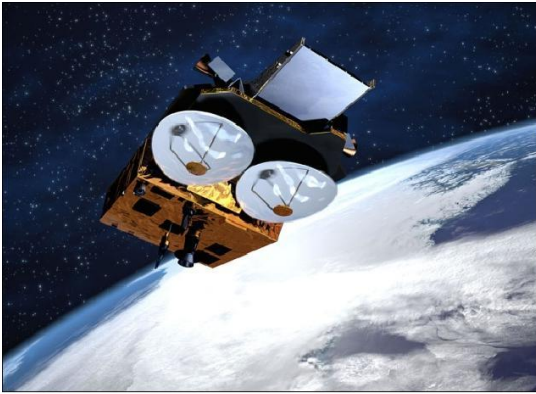


Figure 7.73. CryoSat-2 (Credits EADS Astrium)

CryoSat-2 is an altimetry satellite built by the European Space Agency and dedicated to polar observation. It embarks on a three-and-a-half-year mission to determine variations in the thickness of the Earth's continental ice sheets and marine ice cover, and to test the prediction of thinning Arctic ice due to global warming.

Satellite	CryoSat-2
Launch	2010/04/08
Mission	polar observation
Altitude	717 km
Inclination	92° (non-sun-synchronous)

The CryoSat orbit, at an inclination of about 92 degrees and an altitude of 717 kilometres, covers almost all the Polar Regions. CryoSat carries an altimeter/interferometer called SIRAL and a DORIS instrument, but no radiometer. SIRAL is a Ku-band instrument (13.575 GHz) operating in three modes:

- Low-resolution, nadir-pointing altimeter mode
- SAR mode
- SAR interferometer mode

Current plans are for CryoSat to operate over the oceans for validation purposes in low-resolution mode. This means that the ground segments are able to process ocean altimetry measurements acquired by SIRAL. Direct radiometric corrections, however, are not possible. Dynamic topography data of medium quality, but from a new orbit, may therefore be available. These data could be combined with measurements from other dedicated altimetry missions.

The first CryoSat satellite was lost on launch, on 8 October 2005, due to an anomaly in the launch sequence.

Further information:

- [ESA's ice mission CryoSat](#) (ESA website)

7.2.2.1 CryoSat-2 Instruments

CryoSat-2's primary payload is the SAR/Interferometric Radar Altimeter (SIRAL), which has extended capabilities to meet the measurement requirements for ice-sheet elevation and sea-ice

freeboard. CryoSat-2 also carries three star trackers for measuring the orientation of the baseline. In addition, a radio receiver called Doppler Orbit and Radio Positioning Integration by Satellite (DORIS) and a small laser retroreflector ensures that CryoSat-2's position is accurately tracked.

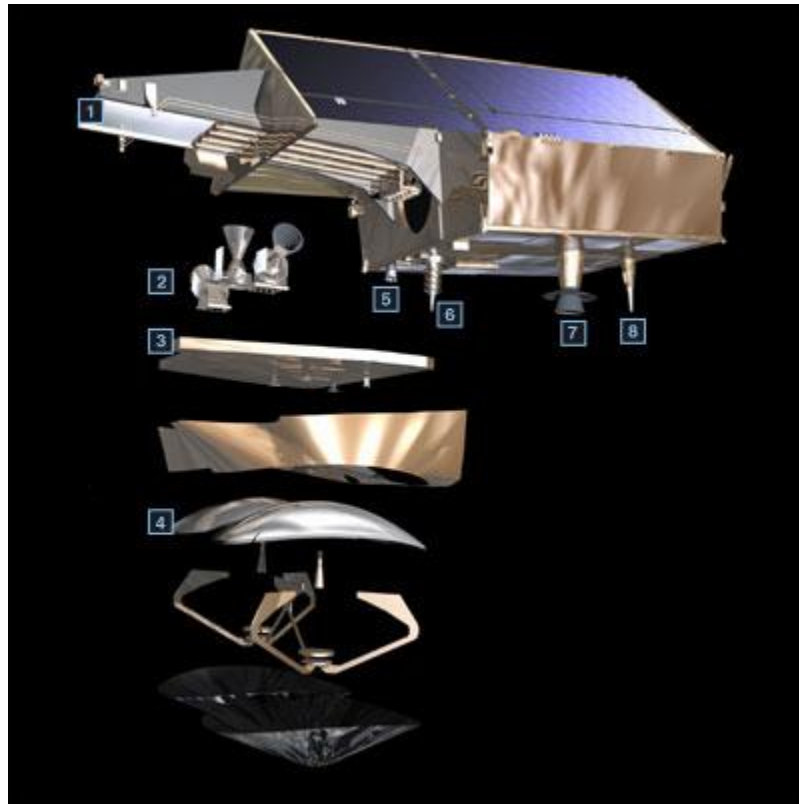


Figure 7.74. CryoSat platform decomposition. 1 Magnetometer, 2 Star Trackers, 3 Thermal radiator, 4 SITAL Antennas, 5 Laser retroreflector, 6 DORIS antenna, 7 X-band downlink antenna, 8 S-band communications antenna.

SIRAL altimeter

SIRAL is an altimeter/interferometer operating in Ku-band (13.575 GHz) in three modes:

- Low-resolution, nadir-pointing altimeter mode

The altimeter measures the distance between the satellite and the surface of the Earth.

- SAR mode

Unlike conventional radar altimeters, where the interval between pulses is about 500 microseconds, the CryoSat altimeter sends a burst of pulses with an interval of only 50 microseconds between them. The returning echoes are correlated, and by treating the whole burst of pulses in one operation, the data processor can separate the echo into strips arranged across the track by exploiting the slight frequency shifts (caused by the Doppler effect) in the forward- and aft-looking parts of the beam.

– SAR interferometer (SarIn) mode

In order to measure the arrival angle, a second receive antenna is activated so that the radar echo is received by two antennas simultaneously. When the echo comes from a point not directly beneath the

satellite there is a difference in the path-length of the radar wave, which is measured. Simple geometry provides the angle between the baseline joining the antennas and the echo direction.

Location systems

The location systems onboard CryoSat-2 complement each other to measure the satellite's position on orbit to within two centimetres on the radial component. The LRR is highly accurate but it requires ground stations that are complex to operate, and its use can be restricted by adverse weather conditions. It is used to calibrate DORIS measurements in order to determine the orbit in real time and to support precise orbit determination.

DORIS (Doppler location)

The DORIS system uses a ground network of orbitography beacons spread around the globe, which send signals at two frequencies to a receiver on the satellite. The relative motion of the satellite generates a shift in the signal's frequency (called the Doppler shift) that is measured to derive the satellite's velocity. These data are then assimilated in orbit determination models to keep permanent track of the satellite's precise position (to within three centimetres) on its orbit.

LRR (laser tracking)

The LRR is an array of mirrors that provide a target for laser tracking measurements from the ground. By analysing the round-trip time of the laser beam, we can locate where the satellite is on its orbit.

Further information: [CryoSat-2 satellite](#) (ESA website)

7.2.2.1.1 SIRAL

CryoSat-2's primary payload is the SAR/Interferometric Radar Altimeter (SIRAL), which has extended capabilities to meet the measurement requirements for ice-sheet elevation and sea-ice freeboard.

Derived from Poseidon altimeters, Siral included important evolutions to operate on rough surfaces:

- Low-resolution mode like a conventional altimeter, on land ice or sea which are composed of few rough surfaces,
- SAR mode operating a high resolution measurement on sea ice,
- SAR interferometer (SARIn) mode operating on rough surfaces like on the sea ice/land limit.

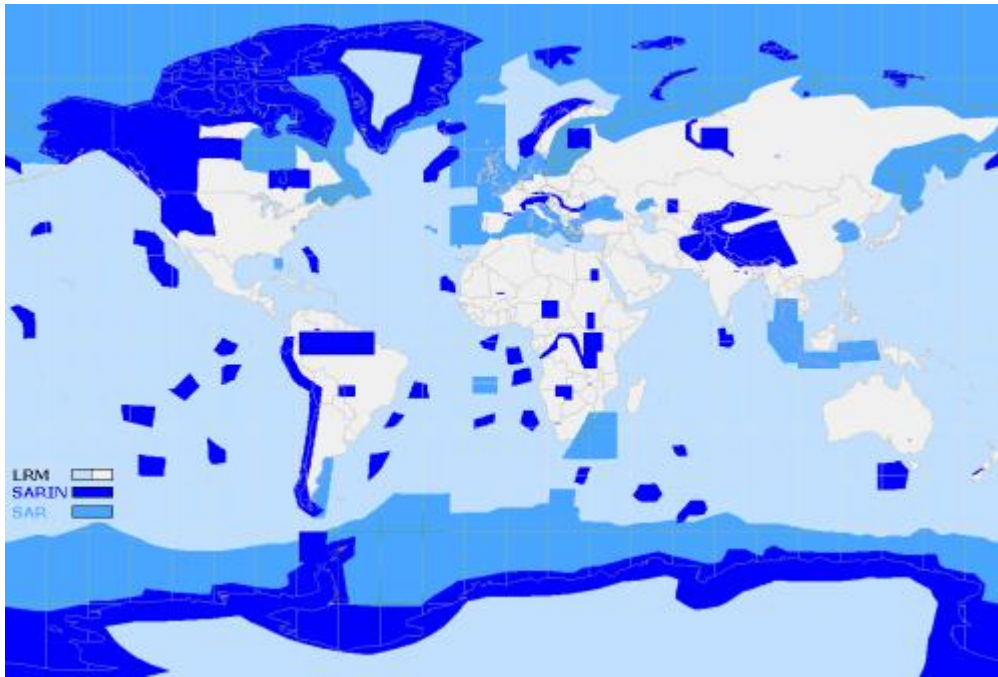


Figure 7.75. Surfaces operated by the 3 modes of Siral (also available on Google Earth, download the kml [here](#)). Credits ESA.

Unlike conventional radar altimeters, where the interval between pulses is about 500 microseconds, the CryoSat altimeter sends a burst of pulses with an interval of only 50 microseconds between them. The returning echoes are thus correlated, and by treating the whole burst of pulses in one operation, the data processor can separate the echo into strips arranged across the track by exploiting the slight frequency shifts (caused by the Doppler effect) in the forward- and aft-looking parts of the beam. Each strip is about 250 m wide and the interval between bursts is arranged so that the satellite moves forward by 250 m each time. The strips laid down by successive bursts can therefore be superimposed on each other and averaged to reduce noise. This mode of operation is called Synthetic Aperture Radar, or SAR mode.

Phase difference between returning radar waves: in order to measure the arrival angle, a second receive antenna is activated so that the radar echo is received by two antennas simultaneously. When the echo comes from a point not directly beneath the satellite there is a difference in the path length of the radar wave, which is measured. Simple geometry provides the angle between the baseline joining the antennas and the echo direction.

Knowledge of the precise orientation of the baseline and the two receiving antennas are essential for the success of the mission. CryoSat is to measure this baseline orientation using the oldest and most accurate of references – the position of the stars in the sky. Three star trackers are mounted on the support structure for the antennas. Each one contains a camera, which takes up to five pictures per second. The images are analysed by a built-in computer and compared to a catalogue of star positions.

The altimeter measures the distance between the satellite and the surface of the Earth. This measurement cannot be converted into the more useful measurement of surface height until the position of the satellite is accurately known.

Function

SIRAL measures range (the distance from the satellite to the Earth's surface).

Further information: [CryoSat mission overview](#) (ESA website)

7.2.2.1.2 DORIS

Figure 7.76. DORIS antenna

A radio receiver called DORIS (Doppler Orbit and Radio positioning Integration by Satellite) detects and measures the Doppler shift on signals broadcast from a network of radio beacons spread around the world. Although the full accuracy of this system is only obtained after ground processing, DORIS is able to provide a real-time estimate onboard, good to about half a metre.

The DORIS instrument onboard CryoSat-2 provides real-time location and precise orbit determination.

Function**Real-time location: Diode**

The Diode onboard navigator locates the satellite on orbit in real time. This information is essential for providing altimetry data in real time or near-real time.

Precise orbit determination

DORIS measurements are used for precise orbit determination (POD).

Ionospheric electron content

By measuring and comparing the path delay of signals transmitted at two separate frequencies, DORIS is able to calculate the electron content in the atmosphere.

Principle

DORIS orbitography beacons transmit signals at two separate frequencies (2,036.25 MHz and 401.25 MHz) to the satellite. The receiver onboard the satellite analyses the received signal frequencies to calculate its velocity relative to Earth. This velocity is fed into orbit determination models to derive the satellite's position on orbit to within two centimetres on the radial component.

For Further information, see the [International DORIS Service \(IDS\)](#) and [DORIS, the space surveyor \(Aviso/CNES\)](#)

7.2.2.1.3 LRR

A small laser retroreflector is attached to the underside of CryoSat-2. This compact device has seven optical corner cubes, which reflect light back in exactly the direction it comes from. A global network of laser tracking stations fires short laser pulses at CryoSat-2 and time the interval before the pulse is reflected back. These stations are relatively few, but because their position is very accurately known from their routine work of tracking geodetic satellites, they provide a set of independent reference measurements of CryoSat-2's position.

Function

The LRR is used to calibrate the other location system on the satellite (DORIS) with a very high degree of precision.

Principle

The LRR is a passive instrument that acts as a reference target for laser tracking measurements performed by ground stations. Laser tracking data are analysed to calculate the satellite's altitude to within a few millimetres. However, the small number of ground stations and the sensitivity of laser beams to weather conditions make it impossible to track the satellite continuously. This is why other onboard location systems are needed.

Technical data

The retroreflectors are placed on the nadir side of the satellite. The totally passive unit consists of nine quartz corner cubes arrayed as a truncated cone, with one cube in the centre and the others arranged azimuthally around the cone. This arrangement allows laser ranging at field-of-view angles of 360 degrees in azimuth and 60 degrees in elevation around the perpendicular. The retroreflectors are optimised for a wavelength of 532 nanometres (green), offering a field of view of about 100 degrees.

7.2.2.2 CryoSat-2 Orbit

CryoSat is a satellite with a single mission objective – the selection of its orbit and basic characteristics have therefore been entirely driven by the scientific requirements. Consequently, the orbit has a high inclination of 92°, taking it just 2° short of the poles. This orbit is non-sun-synchronous (commonly used for remote-sensing satellites) and drifts through all angles to the Sun in eight months. This has presented some challenges in the satellite design; all parts are at some time exposed to the full heating power of the Sun, while at other times half the satellite are in permanent shadow for weeks on end.

The science requirements for sea ice demand spatial sampling at 105 km² (~ 300 km by 300 km). The effect of snowfall variability requires that the measurements of sea ice for the primary mission goal

fall within one month in any one year. This places an upper limit on the temporal sampling. This sampling is also suitable for the secondary sea ice objectives. For land ice, the requirements dictate spatial sampling at 104 km² (~ 100 km by 100 km). There is no specific temporal sampling requirement, although the accuracy of the trend estimate depends on the number of temporal samples. To maximise coverage over ice caps and glaciers, dense spatial sampling consistent with the temporal sampling for the primary mission goal should be achieved.

The spatial pattern of samples need not repeat, provided it retains a constant temporal and spatial sampling density. Sea ice is a moving mass field. Were the sample pattern to repeat itself, measurements would still observe different ice. The land ice measurement uses crossovers of the orbit, and in doing so removes the effect of the topography.

Why doesn't won't CryoSat fly in a 90° inclination orbit, which would take it directly over the poles to observe all of the Polar Regions? The choice of orbit is a compromise, as a 90° orbit would be beneficial for the survey of surveying Arctic sea-ice, but would seriously degrade the monitoring of the Greenland and Antarctic ice masses. Such measurements are made at orbit crossovers, where the north-going satellite track crosses over an earlier (or later!) south-going track. With a 90° inclination orbit, crossovers would be few, only occurring due to the Earth's rotation, since the orbit tracks are otherwise directly along the lines of longitude and do not cross. The 2° offset from a true polar orbit is enough to ensure an adequate density of crossovers over the ice sheets.

Further information: [CryoSat mission overview](#) (ESA website)

7.2.2.3 CryoSat-2 Objectives

CryoSat's mission is dedicated to monitoring very precise changes in the elevation and thickness of polar ice sheets and floating sea ice over a three-year period. The observations made by CryoSat determine whether or not our ice masses are thinning due to global warming.

The question of whether global climate change is causing the polar ice caps to shrink is one of the most hotly-debated environmental issues we currently face. By monitoring precise changes in the thickness of the polar ice sheets and floating sea ice, the CryoSat mission aims to answer this question.

Cryosphere's role

Almost 80% of the Earth's fresh water is locked up in the cryosphere, i.e. in snow, ice and permafrost. The cryosphere plays an important role in moderating the global climate, and as such, the consequences of receding ice cover due to global warming are far-reaching and complex. Due to their high albedo, ice masses directly affect the global energy budget by reflecting about 80% of incident sunlight back out to Space. Thus, once formed, ice tends to be maintained. However, if ice cover were to decrease, less solar radiation would be reflected away from the surface of the Earth – causing the ice to absorb more heat and consequently melt faster still. Around the North Pole, an area of sea ice the size of Europe melts away every summer and then freezes again over the winter. The thickness of Arctic sea ice plays a central role in the polar climate as it moderates heat exchange by insulating the ocean from the cold polar atmosphere.

The cryosphere has a central role in the Earth's radiation budget. Loss of sea ice is predicted to cause greater greenhouse-gas warming in the Arctic than the rest of the Earth. Ice sheets and glaciers are a control on sea level. They are the largest uncertainty factor in determining the source of the present

rise in sea level. The central questions concerned with the cryosphere are: How is deepwater formation and polar and sub-polar ocean exchange affected by sea ice? What are the imbalances in the Antarctic and Greenland ice sheets? Ocean-atmosphere-ice models and ocean-ice-solid Earth models demand spatially- and temporally-continuous estimates of ice mass fluxes on regional and global scales. Current observations are deficient and only satellites can eliminate this deficiency. The CryoSat mission and various international programmes are undertaking a decade of focused study on the roles of the cryosphere.

To meet the challenges of measuring ice, CryoSat reaches latitudes of 88° and carries a sophisticated radar altimeter called SIRAL (Synthetic Aperture Radar Interferometric Radar Altimeter). It is based on the heritage of existing instruments, but incorporates several major enhancements designed to overcome the difficulties intrinsic to the precise measurement of ice surfaces.

Cyrosat measurements

Fundamentally, there are two types of polar ice: the ice that floats in the oceans and the ice that lies on land. Not only do these two forms of ice have different consequences for our planet and its climate, they also pose different challenges when trying to measure them from Space.

Floating sea ice

Sea ice is relatively thin – up to a few metres thick, but it influences regional temperature and the circulation of ocean currents, and consequently the Earth's climate. CryoSat acquires precise measurements of the thickness of floating sea ice so that annual variations can be detected.

CryoSat determines the thickness of floating sea ice by measuring the freeboard of ice floes; that is the height by which the ice extends above the water's surface. This technique was demonstrated with the ERS-1 radar altimeter, but that instrument, as with all conventional radar altimeters, was hampered by its relatively low spatial resolution of about 5 km. CryoSat achieves improved spatial resolution of 250 m in the along-track direction using the Synthetic Aperture technique.

Ice-shelf break up

In contrast, the ice sheets that blanket Antarctica and Greenland are several kilometres thick. The growth and shrinkage of these ice masses have a direct influence on sea level. The approach used for measuring these vast thicknesses is to determine the height of the surface accurately enough to detect small changes.

The improved resolution of CryoSat's radar compared with that of its pulse-limited predecessors, coupled with its interferometric capability, allows for the first time spatially- and temporally-continuous measurements of the ice-sheet margins and smaller ice masses.

Further information:

- [CryoSat science overview](#) (ESA website)

7.2.2.4 CryoSat-2 Ground segment

The CryoSat Ground Segment is organised around a single ESA ground station, located in Kiruna-Salmijarvi, in Northern Sweden. This is where contact is established with the satellite, for about 10

minutes at a time, 11 times a day, during which commands are sent to the satellite and data downloaded.

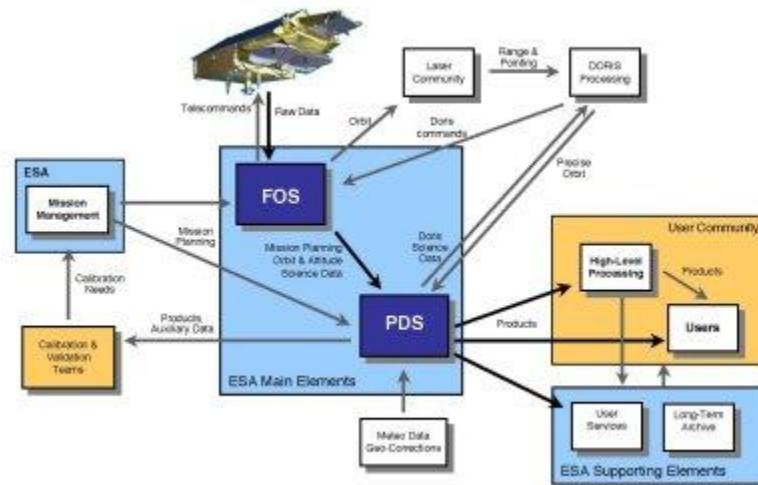


Figure 7.77. CryoSat ground segment

Mission planning, however, is performed in ESA-ESRIN for all matters relating to the payload (mainly instrument activity planning) and in ESA-ESOC for everything concerning the platform (mainly orbit maintenance through manoeuvres). The detailed plan is uploaded weekly to the satellite from Kiruna-Salmijarvi.

It is worth noting that the activity of the CryoSat instruments is very repetitive, and is based on ground topology (ice boundaries evolving through the year) and a few specific user demands, recorded before launch.

The large amount of data received from the payload, and in particular from the altimeter, is processed at Kiruna-Salmijarvi. Data products at Level-1b (radar echoes geolocated and corrected for instrument features) and Level-2 (ground elevation and ice freeboard, corrected for atmospheric and geophysical effects) are systematically produced by ESA, based on the repetitive data acquisition activity planned above. There is no ‘on-demand’ data processing in the routine data production; however, provision has been made for troubleshooting needs.

All external auxiliary data needed for data processing, in particular the Precise Orbit data, is received from the SSALTO centre operated by CNES in Toulouse, with one exception – dynamic sea ice concentration is received from UCL in London.

Data is routinely distributed to users using ftp service

An important aspect of the CryoSat Ground Segment is that it has been designed for low manpower operations. Furthermore, operations and troubleshooting are performed remotely for all systems located in Kiruna-Salmijarvi.

Further information:

- [CryoSat ground segment](#) (ESA website)

7.2.3 HaiYang-2



Figure 7.78. (Credits China Academy of Space Technology)

HY-2 (HaiYang means ‘ocean’ in chinese) is a marine remote sensing satellite series planned by China (HY-2A, then HY-2B (2012), HY-2C (2015), HY-2D (2019)).HY-2 belongs to a series of ocean-oriented satellites :

- HY-1A and HY-1B (respectively launched on May, 2002 and April, 2007) are designed to measure the ocean colour and temperature with the visible and infrared sensor,
- HY-2 is focused on the marine dynamic environment,
- HY-3 combines visible/infrared and microwave sensors.

Satellite	HY-2
Launch	Aug. 2011
Mission	observe the ocean dynamics
Altitude	963 km
Inclination	99.3°

The objective of HY-2 is monitor the dynamic ocean environnement with microwave sensors to detect sea surface wind field, sea surface height and sea surface temperature. It includes an altimeter dual-frequency in Ku and C-bands, a scatterometre and a microwave imager.

7.2.3.1 HaiYang -2 Instruments

HY-2 satellite is equipped with radar altimeter, microwave scatterometer, scanning microwave radiometer and calibration microwave radiometer as well as DORIS, dual-band GPS and laser range reflector. The radar altimeter is used for measuring the sea surface height, significant wave height and wind speed etc; the microwave scatterometer is mainly used for observing the global sea surface wind field; the scanning microwave radiometer is mainly used for observing global sea surface temperature, sea surface wind field, water vapor content in the atmosphere, cloud moisture, sea ice and rainfall amount etc; and the calibration microwave radiometer measures atmospheric water vapor necessary for altimeter measurement calibration

Radar altimeter technical data

Table 7.19 HY-2 Radar altimeter technical specifications

Emitted Frequency (GHz)	Dual-frequency (Ku, C) – 13.58 and 5.25
Pulse limited footprint	≤ 2 km
Height measuring accuracy	≤ 4 cm
Effective wave height measuring range	0.5-20m
Effective wave height measuring accuracy	0.5m

7.2.3.2 HaiYang -2 Orbit

The orbit of HY-2 satellite is sun-synchronous with a 14-day cycle in the first half of its lifetime at an altitude of 971 km, while the last half of lifetime at an altitude 973 km with a 168-day cycle. The objective of HY-2 is monitoring the dynamic ocean environment by using microwave sensors onboard. It is used to detect global sea surface wind field, sea surface height, significant wave height and sea surface temperature in all-weather.

Table 7.20 HY-2 satellite orbit parameters

Orbit	Sun synchronous
Inclination	99.34 degrees
Repea Cycle	Phase I mission : 104.46 min., Phase II : 104.50 min.

7.2.3.3 HaiYang -2 data applications

Ocean surface wind prediction

Sea surface winds obtained by HY-2 microwave scatterometer are added into China's marine wind prediction model system, and thus provide better initial conditions and improve prediction skills. The use of HY-2 scatterometer wind observations in marine prediction marks a new era in marine environmental prediction without using other sources of wind observations. The application of HY-2 scatterometer winds in numerical models improves China's marine environmental prediction abilities and thus meets the needs of national economics and security.

Sea level rise decision support

The long time-series of HY-2 satellite altimeter measurements of sea surface height, combined with data from China's coastal and polar stations, are used to establish sea level rise decision support system to support sea level rise hazards and prevention.

Ocean waves prediction and assimilation

The significant wave height and sea surface wind derived from HY-2 satellite are assimilated into China's numerical wave model to improve marine environmental prediction skills

Data assimilation in ocean model

The sea surface temperature and height data of HY-2 satellite are assimilated into 3-D ocean numerical model to improve ocean model prediction accuracy and skills.

Storm surge monitoring

The sea surface height and winds data of HY-2 satellite as well as data from coastal stations and buoys are used for the storm surge hazards prevention decision support system. The use of these data improves China's ability in storm surge hazard prevention and decision making.

Sea ice monitoring and forecasting

The brightness temperature of HY-2 microwave radiometer, together with sea ice observations from other satellites and in situ observations, is used to monitor and predict sea ice hazards, and to improve sea ice hazard prevention and decision making.

Oceanic gravity field

The variations of sea surface dynamic height observed by the HY-2 satellite and ship measurements are used to compute and monitor oceanic gravity field.

Air-sea interaction

The HY-2 satellite measurements of sea surface temperature and winds and in situ measurements of sea surface fluxes are used to study air-sea interaction. The HY-2 satellite data is used to quantify air-sea interaction and monitor its variations, and thus provide observations to study climate change and global warming.

Oceanic fishery

The combined use of measurements of sea surface temperature, winds and waves from HY-2 satellite and ocean color from HY-1 satellite is important in the open ocean fishery application system. Measurements of HY-2 radar altimeter and scanning microwave radiometer may identify oceanic fronts and mesoscale eddies, and detect the ocean fishing ground. The radar altimeter, microwave scatterometer and microwave radiometer are useful for improving the weather forecasting accuracy for ocean fishing.

7.2.3.4 HaiYang -2 Ground segment

The HY-2 satellite data are received by three ground stations located in China including Beijing, Sanya and Mudanjiang Station. HY-2 satellite observes global oceans in one day. Data within ground views of the three stations are received in real time and data over the other parts of the global oceans are dumped from onboard memory.

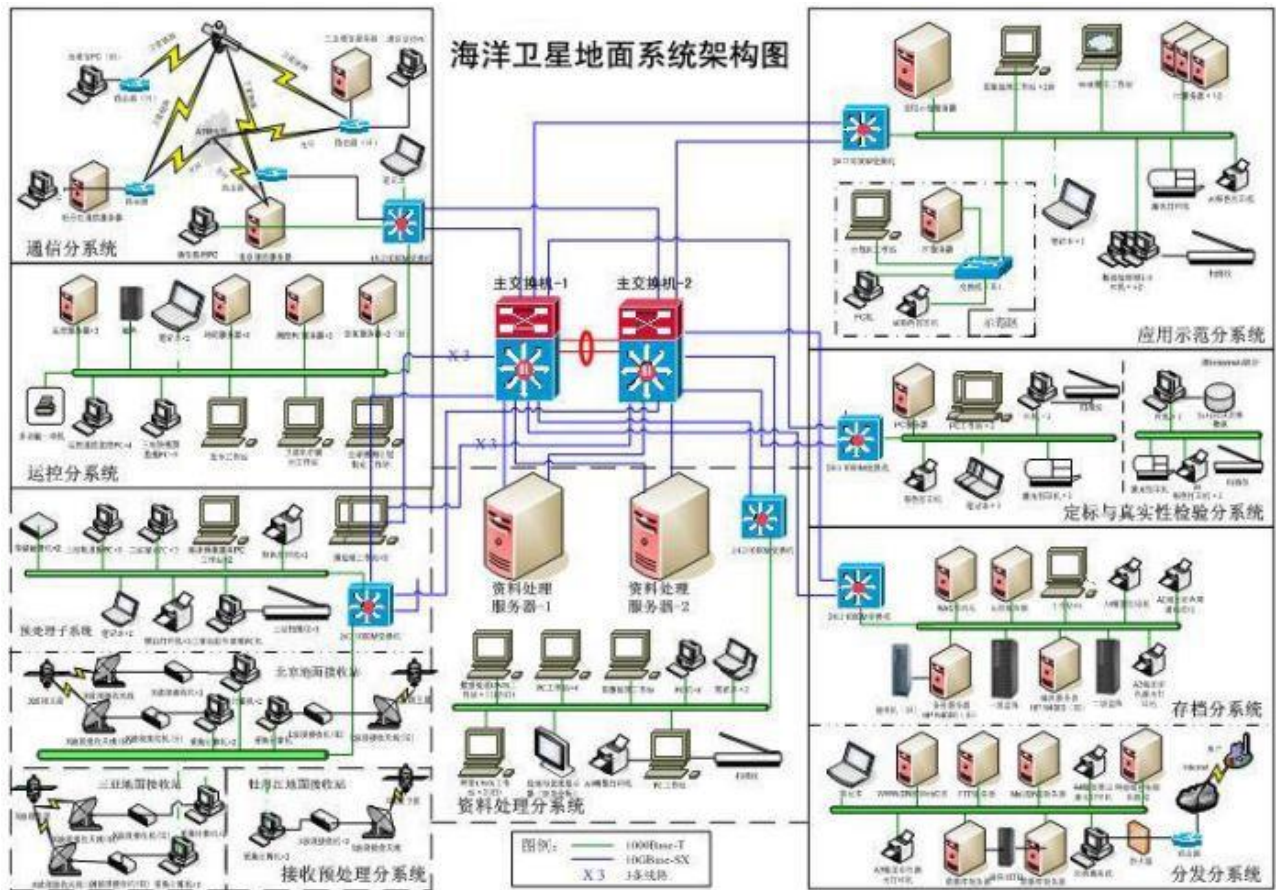


Figure 7.79. HY-2 satellite ground system framework (Credit NSOAS)

References:

- HY-2A Satellite User's Guide NSOAS 2013

7.2.4 Saral



Figure 7.80. (Credits Geko)

An Isro (Indian Space Research Organization) satellite, Saral (Satellite with ARgos and ALtika), embarks the AltiKa altimeter (working in Ka-band, 35 GHz), built by Cnes, as well as a Doris instrument. Signal frequencies in the Ka-band enables better observation of ice, rain, coastal zones, land masses (forests, etc.), and wave heights.

Satellite	Saral
Launch	2013/02/25
Mission	Measure sea surface height
Altitude	~800 km
Inclination	98.55°

The Saral mission is complementary to Jason-2. Its objectives are:

- to carry out precise, repetitive global measurements of sea surface height, significant wave heights and wind speed, for:
 - developing operational oceanography;
 - improving understanding of the climate and developing forecasting capabilities;
 - operational meteorology.
- to ensure, in association with Jason-2, the continuity of the service currently provided by the altimeters onboard Envisat and Jason-1,
- to meet the requirements expressed by various international ocean and climate study programmes, and contribute to building a global ocean observing system.

The payload integrates:

- a high-resolution AltiKa altimeter that incorporates a dual-frequency radiometric function,
- the DORIS precise orbitography system, in association with a laser retroreflector (LRA).

The launch of this mission on 2013/02/25, is planned with a life of 3 years (2 year for the nominal phase, and one year for the extended phase). This mission is a cooperation between Cnes and Isro.

Further information:

- the [AltiKa instrument](#)

- Saral/AltiKa on the [Space Scientific Missions](#) of the Cnes (SMSC) website

7.2.4.1 SARAL Instruments

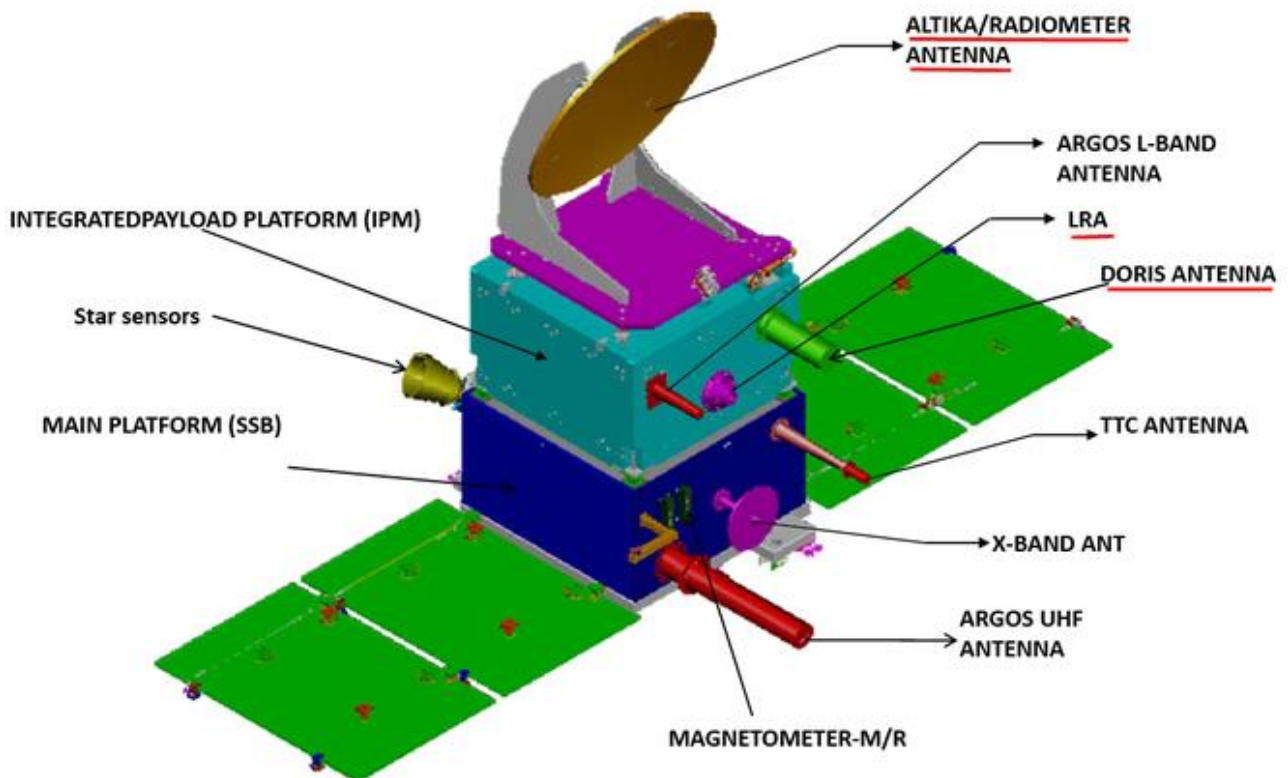


Figure 7.81. SARAL instruments (Credits ISRO)

7.2.4.1.1 AltiKa

AltiKa is a Ka-band altimeter (35 GHz) developed by CNES that can be flown on a microsatellite or as an auxiliary passenger on other missions. Signal frequencies in the Ka-band enable better observation of ice, rain, coastal zones, land masses (forests, etc.) and wave heights.

AltiKa is aiming to observe the ocean in as much detail and as accurately as current missions, only at lower cost, by flying the altimeter on a microsatellite that is cheaper to design, build and launch. Experience has shown that an altimetry platform must comprise an altimeter, radiometer and precise orbit determination system, with sufficient redundancy, as well as enough fuel to keep the satellite orbiting on a repeating ground track – at least with a ‘conventional’ altimetry mission.

The AltiKa altimeter is a single-frequency Ka-band altimeter (operating at 35.75 GHz, weighing less than 20 kg and consuming less than 50 Watts). Alcatel Space developed a Ka-band altimeter between 1998 and 2000 which was based on the same technologies as those used for the Poseidon-1 and Poseidon-2 altimeters.

7.2.4.1.2 Dual frequency microwave radiometer

The bi-frequency (23.8 GHz / 37 GHz) radiometer is used to correct altimetry measurements from wet troposphere crossing effects. The 23.8 GHz channel is the primary water vapor sensing channel, meaning higher water vapor concentrations will lead to larger 23.8 GHz brightness temperature values. The addition of the 37 GHz channel, which has less sensitivity to water vapor, facilitates the removal of the contributions from cloud liquid water, which also act to increase the 23.8 GHz brightness temperature

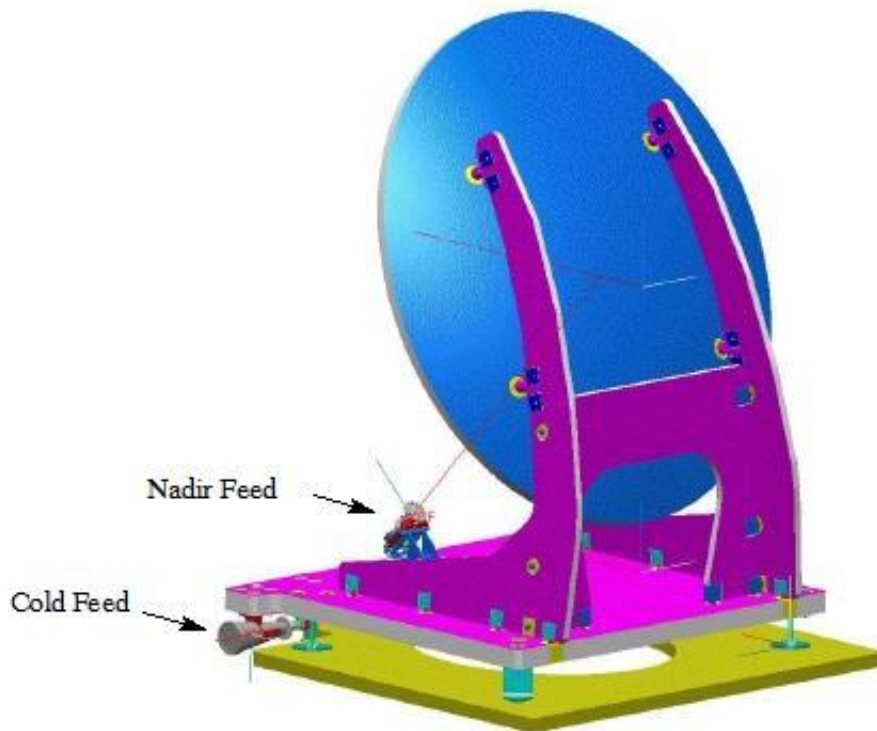


Figure 7.82. Illustration of the AltiKa & Radiometer antenna (CAD model), image credit: CNES

7.2.4.1.3 DORIS System

The complete DORIS system includes the DORIS on-board package, a network of approximately 60 beacons located around the world and a ground system. The on-board package includes the electronic box hosting the receiver itself and the ultra stable oscillator and an omnidirectional antenna. The DORIS on-board package is of the same version as the one embarked on Jason-2. It includes a 7-beacon receiving capability and an on-board real time function (DIODE for Détermination Immédiate d'Orbite par DORIS Embarqué) to compute the orbit ephemeris in real time. The DORIS on-board package is dual string (in cold redundancy), each DORIS chain is automatically connected to the single antenna through a switching box inside the DORIS unit. Each receiver is connected to its own ultra-stable oscillator.



Figure 7.83. SARAL/AltiKa DORIS Receiver Antenna and Instrument

7.2.4.1.4 Laser Reflector Array LRA

It is used for precise calibration of other POD instruments, through analysis of laser shots from the ground then reflected by the LRA mirrors. The laser reflector array is placed on the nadir face of the satellite. It consists of several quartz corner cubes arrayed as a truncated cone with one in the center and the others distributed azimuthally around the cone.

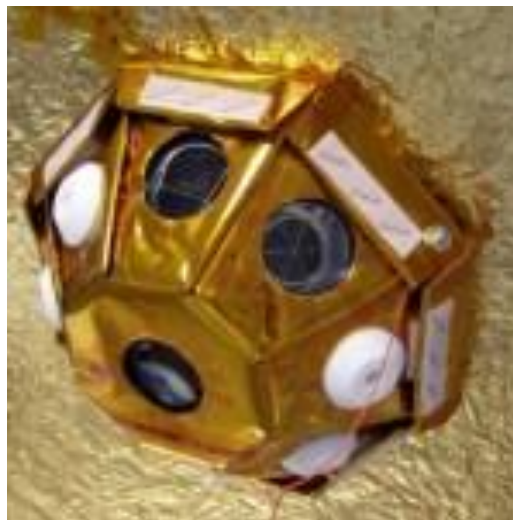


Figure 7.84. SARAL/AltiKa Laser Reflector Array

7.2.4.1.5 Argos-3 (Data Collection System)

The objective is to collect data from remote terminals in the ground segment referred to as PPTs (Platform Transmitter Terminals).

The Argos-3 onboard package represents the newest generation of the Argos system. The major improvement of the new Argos-3 system is that it will now be able to send orders to its terminals whereas before the onboard instruments were only capable of receiving data (up to Argos-2 inclusive). The MetOp-A spacecraft of EUMETSAT (launch Oct. 19, 2006) is carrying the first Argos-3 instrument demonstrator package. In comparison to previous generations, system performance is enhanced via a unique downlink and a high data uplink (4800 bit/s versus 400 bit/s), while ensuring complete compatibility with existing systems in the ground segment. Thanks to digital

processing, the new instrument is lighter and more compact than its predecessors on analog basis. Argos-3 is capable of receiving messages from over 1000 PTTs (Platform Transmitter Terminal) simultaneously within the satellite's FOV (Field of View).



Figure 7.85. SARAL UHF antenna

7.2.4.2 SARAL Orbit

The SARAL/AltiKa satellite flies on the same ground-track as ENVISAT with a 501-orbit, 1002-pass, 35-day exact repeat cycle. Orbital characteristics and the equator crossing longitudes for SARAL/AltiKa are given in orbit tables below.

At the beginning of the mission, the orbit was NOT exactly on the ENVISAT repetitive ground track. A deviation of the order of 2.5 km at high latitudes was observed. It has been corrected by several inclination manoeuvres performed by ISRO. The nominal ENVISAT repetitive ground has been reached only late October 2013.

A satellite orbit slowly decays due to air drag, and has long-period variability because of the inhomogeneous gravity field of Earth, solar radiation pressure, and smaller forces. Periodic manoeuvres are required to keep the satellite in its orbit. The frequency of manoeuvres depends primarily on the solar flux as it affects the Earth's atmosphere, and there are expected to be one manoeuvre (or series of manoeuvres) every 15 to 30 days.

Each orbit maintenance manoeuvre is performed using only one thrust to minimize impacts on the ground orbit solution. Orbit computation is optimized to minimize the orbit error during such periods. Science data are taken during orbit maintenance manoeuvres and are distributed (an orbit state flag is provided in the products).

7.2.4.3 SARAL Objectives

The overall objectives are to realize precise, repetitive global measurements of sea surface height, significant wave heights and wind speed for:

- The development of operational oceanography (study of mesoscale ocean variability, coastal region observations, inland waters, marine ecosystems, etc.)
- Understanding of climate and developing forecasting capabilities
- Operational meteorology.

The SARAL mission is considered to be complementary to the Jason-2 mission of NASA/NOAA and CNES/EUMETSAT (it is also regarded a gap filler mission between Envisat and the Sentinel-3 mission of the European GMES program). The combination of two altimetry missions in orbit has a considerable impact on the reconstruction of SSH (Sea Surface Height), reducing the mean mapping error by a factor of 4.

7.2.4.4 SARAL Ground segment

According to the CNES-ISRO agreement:

- CNES is responsible for the production, the archiving and the distribution of near-realtime altimetry products (OGDR: Operational Geophysical Data Record) and delayed products (GDR: Geophysical Data Record, IGDR, S-IGDR and S-GDR) to users outside India.
- Production of the mission preliminary and precise orbits is realized by CNES, from DORIS system data, completed by the laser system data, for the precise orbit. The operational upkeep of DORIS components and system is ensured by CNES.
- CNES uses EUMETSAT support for the operation of ground stations in Sweden, as well as to produce, archive and distribute near-realtime products to users outside India
- CNES supplies the near-realtime data processor to EUMETSAT and ISRO, as well as a support for its integration, test and operation
- CNES supplies the processor for delayed products to ISRO, as well as a support for its integration, test and operation
- ISRO is responsible for the production, the archiving and the distribution to Indian users of near-realtime and delayed-time altimetry products
- ISRO is responsible for the command-control operations of the satellite.
- All housekeeping and scientific telemetry as well as auxiliary data are archived by CNES and ISRO
- CNES and ISRO are responsible for the product enhanced value and the support to their respective users.
- CNES is responsible for the coordination of AltiKa with the other altimetry missions. The enhanced value products of DUACS (Data Unification and Altimeter Combination System) generated by CNES are archived and distributed under CNES responsibility.
- CNES is responsible for the expertise and the long term CalVal.

More info

CNES web page <https://altika-saral.cnes.fr/en/>

ISRO web page <http://www.isro.gov.in/Spacecraft/saral>

SARAL/AltiKa Product Handbook SALP-MU-M-OP-15984-CN

7.2.5 Jason-3



Figure 7.86 Jason-3

Jason-3 is proposed to take over and continue the missions of Topex/Poseidon, Jason-1 and 2, in the framework of a cooperation between CNES, NASA, Eumetsat and NOAA. It carries the same kind of payload as its three predecessors for a high-precision altimetry mission: a Poseidon-class altimeter, a radiometer and three location systems. The orbit is also identical.

Satellite	Jason-3
Launch	17/01/2016
Mission	Measure sea surface height
Altitude	1336 km
Inclination	66° (non-sun-synchronous)

7.2.5.1 Jason-3 Instruments

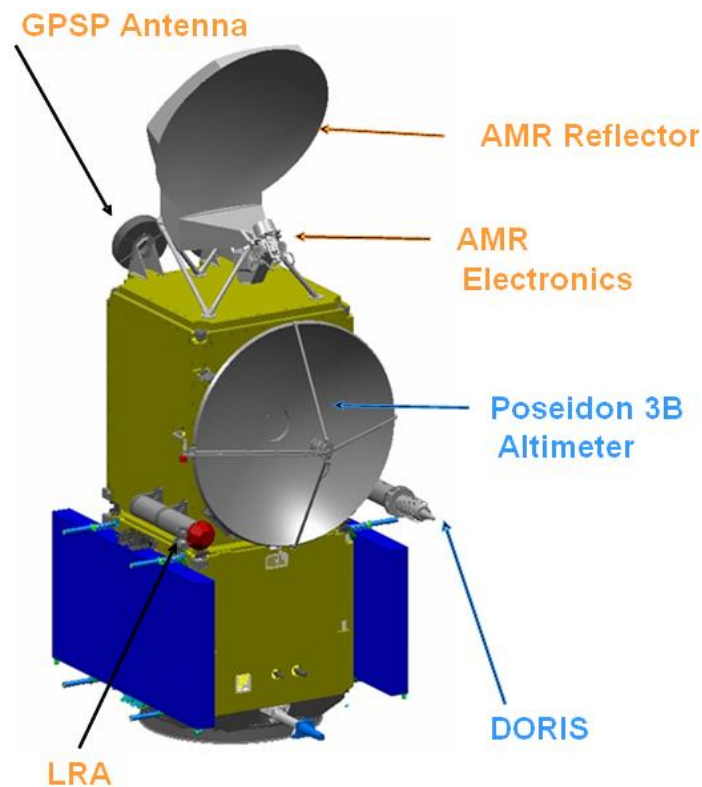


Figure 7.87. Jason-3 instruments

7.2.5.1.1 The Poseidon-3B altimeter

The Poseidon-3B is the mission's main instrument. It allows measuring the range (the distance from the satellite to the Earth's surface), wave height and wind speed. This new altimeter implements a mixed mode allowing on-board automatic transitions between the Diode/DEM mode and the acquisition/tracking mode with respect to the satellite position. Indeed, Jason-2 uses the two altimeter modes, the "autonomous tracking" and the Diode/DEM modes, to improve measurements over coastal areas, inland waters and ice. But these modes have the disadvantage to be exclusive.

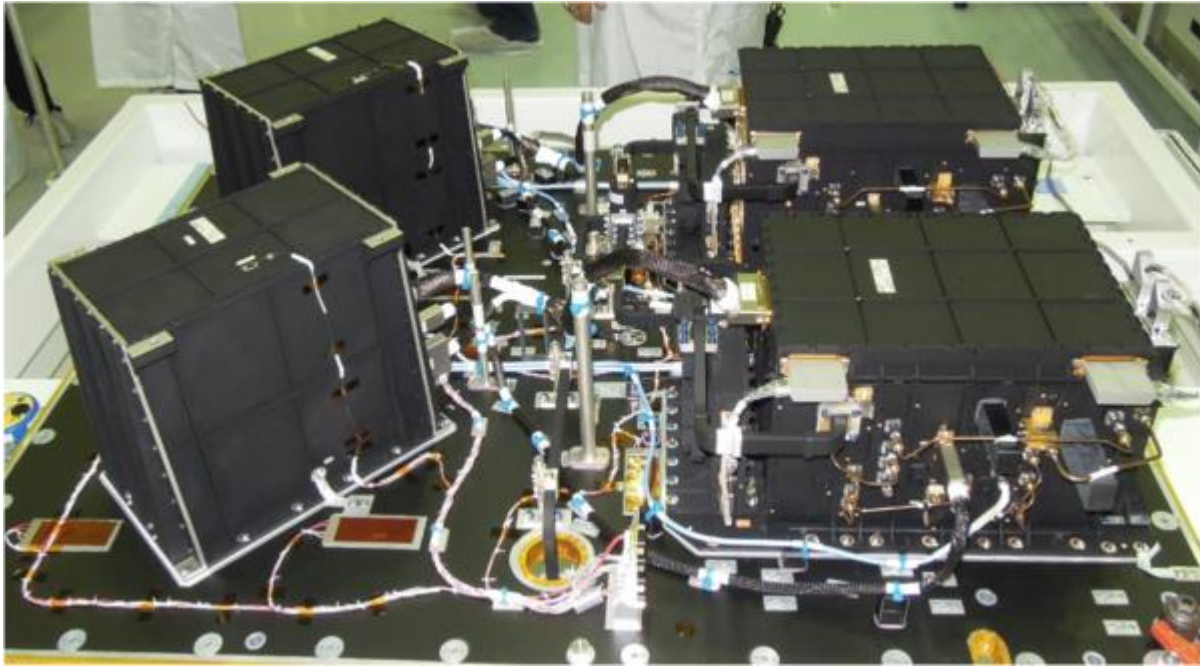


Figure 7.88. Poseidon-3B being integrated on Jason-3 (Credits CNES)

New features wrt Poseidon-3 onboard Jason-2

This new altimeter implements a mixed mode allowing on-board automatic transitions between the Diode/DEM mode and the acquisition/tracking mode with respect to the satellite position, while Jason-2 altimeter requires a ground telecommand to switch from one mode to the other, thus being much less flexible.

Moreover, Poseidon-3B DEM upload is now possible without mission interruption.

Technical data

Poseidon-3, or SSALT (for Solid State ALTimeter), uses solid-state amplification techniques.

Table 7.21 Poseidon-3B Main parameters

Emitted Frequency (GHz)	Dual-frequency (Ku, C) – 13.575 and 5.3
Pulse Repetition Frequency (Hz)	2060 interlaced {3Ku-1C-3Ku}
Pulse duration (microseconds)	105

Bandwidth (MHz)	320 (Ku and C)
Antenna diameter (m)	1.2
Antenna beamwidth (degrees)	1.28 (Ku), 3.4 (C)
Power (W)	7
Redundancy	Yes
Specific features	Solid-State Power Amplifier. Dual-frequency for ionospheric correction, High resolution in C band (320 MHz)

7.2.5.1.2 The Advanced Microwave Radiometer (AMR)

Developed by NASA, it measures radiation from the Earth's surface. Each frequency is combined to determine atmospheric water vapor and liquid water content. Once the water content is known, the correction to be applied for radar signal path delays is determined. It performs thorough lesson learned review from Jason-2 experience with: account for parts obsolescence, improve the instrument thermal control and stability, small design updates to retire residual implementation risks on Jason-2. Unlike the radiometers of its predecessors, the calibration of the Jason-3 AMR should be completed with pitch manoeuvres in order to perform cold-space measurements at regular intervals (every 30 to 60 days).

7.2.5.1.3 Locations systems

GPS Receiver (GPSP)

The GPSP uses the Global Positioning System (GPS) to determine the satellite's position by triangulation, in the same way that GPS fixes are obtained on Earth. At least three GPS satellites determine the mobile's exact position at a given instant. Positional data are then integrated into an orbit determination model to track the satellite's trajectory continuously.

Supplied by NASA, it is a different receiver but with same basic (blackjack) design as on Jason-1 and 2. No changes to data processing or products with expect same or better performance as on Jason-2.

DORIS (Doppler Location)

The DORIS system uses a ground network of 60 orbitography beacons around the globe, which send signals at two frequencies to a receiver on the satellite. The relative motion of the satellite generates a shift in the signal's frequency (called the Doppler shift) that is measured to derive the satellite's velocity. These data are then assimilated in orbit determination models to keep permanent track of the satellite's precise position (to within three centimeters) on its orbit.

This instrument is supplied by CNES with a new generation (DGXXS) taking into account lessons learned from Jason-2. Improvement in modelling solar panels position has been made. Model improvements has also been integrated: albedo and infra-red pressure, new ITRF, pole prediction, Hill along-track empirical acceleration, on-board USO frequency prediction, allowing a more and more accurate Diode navigation tool.

LRA (Laser Tracking)

The LRA instrument, provided by NASA, is an array of mirrors that provides a target for laser tracking measurements from the ground. By analyzing the round-trip time of the laser beam, the satellite's orbit location can be determined.

7.2.5.2 Jason-3 Orbit**Choice of orbit**

Jason's high altitude (1 336 kilometers) reduces interactions with the Earth's atmosphere and gravity field to a minimum, thus making orbit determination easier and more precise. The orbit inclination of 66 degrees north and south enables the satellite to cover most of the globe's unfrozen oceans. The orbit's repeat cycle is just under 10 days (9.9156 days to be precise, i.e., 10 days minus two hours).

Further, using the same orbit as Jason-2 will ensure better intercalibration and data continuity. The orbit is also designed to pass over two dedicated ground calibration sites: Cap Senetosa in Corsica and the Harvest oil rig platform in California, USA.

Orbit parameters*Table 7.22 Jason-3 Orbit Main characteristics*

Inclination (sun-synchronous)	66.04°
-------------------------------	--------

Table 7.23 Jason-3 Orbit Auxiliary data

Reference altitude (equatorial)	1336 km
Repeat cycle	9.92 days
Number of passes per cycle	254
Ground track separation at Equator	315 km

(Source Aviso)

7.2.5.3 Jason-3 Objectives

Jason-3 mission's objectives are mostly the same than Jason-2, with an emphasis on:

- Data continuity for climate applications: Jason-3 should enable to reach the 30-year time.
- Contribute to "Copernicus" program, with its marine service CMEMS distributing operationally ocean data, altimetry in particular for operational applications and assimilation in ocean forecasting models such as Mercator Ocean.
- To have quality data nearer to the coasts, and over lakes and rivers.

Expected applications are also Topex/Poseidon, Jason-1 and Jason-2's :

- Ocean study,
- Climate study, seasonal forecasting (including El Niño and such phenomena),
- Wind speed and wave height measurements, in real-time for weather forecast models, and over the long term (climatologies) for studies and model improvements,

- Better knowledge of the geoid, in combination with geodetic satellites (Grace, Goce),
- Tide models improvements,

7.2.5.4 Jason-3 Ground segment

The Jason-3 mission was determined as part of an agreement between four partners: CNES, NASA, NOAA and EUMETSAT.

The Jason-3 Programme is led by the operational agencies EUMETSAT and NOAA, with CNES making a significant in-kind contribution and acting at technical level as the system coordinator. NASA in conjunction with EUMETSAT, NOAA and CNES will support science team activities.

Further information:

- JPL website <https://sealevel.jpl.nasa.gov/missions/jason3/>
- Aviso website <https://www.aviso.altimetry.fr/en/missions/current-missions/jason-3.html>

Figure 7.90. Sentinel-3 instruments

SLSTR: Sea and Land Surface Temperature Radiometer

SRAL: Synthetic Aperture Radar Altimeter (derivative of SIRAL on CryoSat-1 and -2)

OLCI: Ocean and Land Colour Instrument

MWR: MicroWave Radiometer

LRR: Laser Retro-Reflector

7.2.6.1.1 SRAL altimeter

SRAL (Synthetic Aperture Radar Altimeter) is a redundant dual-frequency (C-band and Ku-band) instrument for determining the two-way delay of the radar echo from the Earth's surface to a very high precision: less than a nanosecond. It also measures the power and shape of the reflected radar pulses. SRAL is derived from the CryoSat SIRAL altimeter, and from Jason-2 Poseidon-3 altimeter.

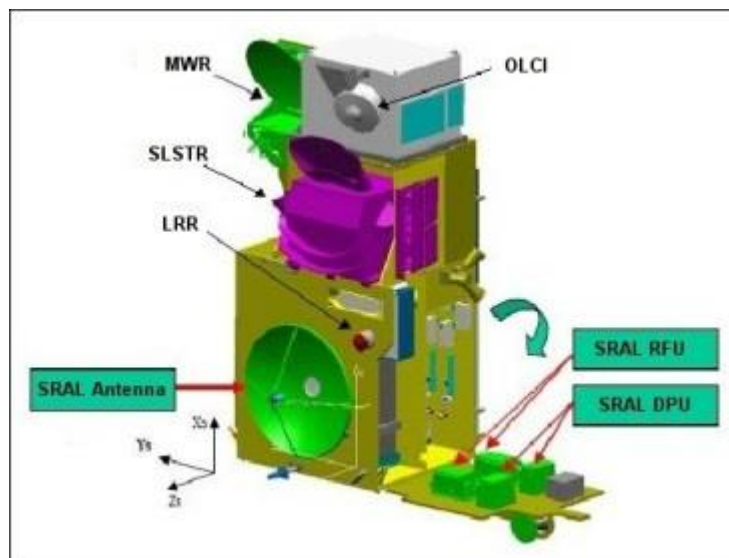


Figure 7.91. Conceptual view of SRAL altimeter on Sentinel-3 (Credits [ESA](#))

Function

Operating over oceans, SRAL measurements are used to determine the ocean topography, thus supporting research into ocean circulation, bathymetry and marine geoid characteristics. Furthermore, SRAL also facilitate operation in coastal and inland waters and the gauging of the flow of large rivers. Measurement of the radar echo power and shape enables wind speed and significant wave height at sea to be determined, thus supporting weather and sea state forecasting. SRAL has a strong heritage of the instrument techniques implemented for the Poseidon-3 altimeter on Jason-2 and for SIRAL (SAR Interferometer Radar Altimeter) on CryoSat.

Principle

The altimeter emits a radar beam that is reflected back to the antenna from the Earth's surface (see [how altimetry works](#) for details). SRAL operates at two frequencies (13.575 GHz in the Ku-band and 5.41 GHz in the C-band) to determine atmospheric electron content, which affects the radar signal path delay. These two frequencies can also serve to measure the amount of rain in the atmosphere.

The SRAL instrument includes measurement modes, calibration modes and support modes. The measurement modes are composed of two radar modes associated to two tracking modes:

- LRM (Low Resolution Mode). It refers to the conventional altimeter pulse-limited resolution mode (so far, the LRM mode is being used on all altimetry missions). It consists of regular emission/reception sequences at a fixed PRF (Pulse Repetition Frequency) of around 1920 Hz leading to an ambiguity rank of 10.
- SAR mode: This is a high along-track resolution mode composed of bursts of Ku-band pulses.

These modes are associated to two tracking modes which consist of the following:

- Closed-loop mode: refers autonomous positioning of the range window (ensures autonomous tracking of the range and gain by means of tracking loop devices implemented in the instrument).
- Open-loop mode: refers to the positioning of the range window based on a-priori knowledge of the terrain height from existing high-resolution global digital elevation models.

The open-loop is intended to be used (on coastal ocean, sea ice ice sheet margins or rivers/lakes) instead of the more conventional closed-loop tracking over some surfaces, to improve the acquisitions over inhomogeneous or rough topography. While in open-loop, the setting of the tracking window of the altimeter is driven by predetermined commands, stored on board, combined with real-time navigation information available from the GNSS receiver. The main advantage is that the measurements are continuous, avoiding the data gaps typical of closed-loop tracking, which has problems in tracking the rapid topographic changes at coastal margins and in mountainous regions.

Technical data

Table 7.24 SRAL Main parameters

Emitted Frequency (GHz)	Dual-frequency (Ku, C) – 13.575 and 5.41
Pulse Repetition Frequency (Hz)	1920 (Ku)
Pulse duration (microseconds)	20
Bandwidth (MHz)	350 (Ku) – 320 (C)
Redundancy	Yes
Specific features	Dual-frequency for ionospheric correction

7.2.6.1.2 MWR (Microwave Radiometer)

The main objective of the microwave radiometer (MWR) is to measure the integrated atmospheric water vapour column and cloud liquid water content, which are used as correction terms for the radar

altimeter signal. Once the water content is known, we can determine the correction to be applied for radar signal path delays for the altimeter. In addition, MWR measurement data are useful for determining surface emissivity and soil moisture over land, for surface energy budget investigations to support atmospheric studies, and for ice characterisation.

7.2.6.1.3 Location systems

The location systems onboard Sentinel 3 complement each other to measure the satellite's position on orbit to within two centimetres on the radial component. The LRR is highly accurate, but it requires ground stations that are complex to operate, and its use can be restricted by adverse weather conditions. It is used to calibrate the GNSS receiver so that the satellite orbit can be determined as accurately as possible. A Doris receiver will also be onboard.

7.2.6.1.4 DORIS (Doppler location)

The DORIS system uses a ground network of orbitography beacons spread around the globe, which send signals at two frequencies to a receiver on the satellite. The relative motion of the satellite generates a shift in the signal's frequency (called the Doppler shift) that is measured to derive the satellite's velocity. These data are then assimilated in orbit determination models to keep permanent track of the satellite's precise position on its orbit.

7.2.6.1.5 GNSS receiver

The GNSS receiver uses the Global Navigation Satellite System (including the Global Positioning System (GPS) and its European civil counterpart, Galileo) to determine the satellite's position by triangulation, in the same way that GPS fixes are obtained on Earth. At least three GNSS satellites determine the mobile object's (in this case the satellite's) exact position at a given instant. Positional data are then integrated into an orbit determination model to track the satellite's trajectory continuously.

7.2.6.1.6 LRR (laser tracking)

The LRR (Laser Retroreflector Array) is an array of mirrors that provides a target for laser tracking measurements from the ground. By analysing the round-trip time of the laser beam, we can locate where the satellite is on its orbit.

7.2.6.2 Sentinel-3 Orbit

Choice of orbit

The Sentinel-3 orbit provides an optimal compromise between spatial and temporal sampling for capturing mesoscale ocean structures, offering an improvement on SSH mapping error of up to 44% over Jason due to improved spatial sampling and 8% over the Envisat 35-day orbit due to better temporal sampling.

Orbit parameters

Table 7.25 Sentinel-3 Orbit Main characteristics

Inclination (sun-synchronous)	98.5°
-------------------------------	-------

Table 7.26 Sentinel-3 Orbit Auxiliary data

Reference altitude (equatorial)	814 km
Repeat cycle	27 days
Number of passes per cycle	~770
Ground track separation at Equator	104 km

(Source ESA)

7.2.6.3 Sentinel-3 Objectives

The pair of Sentinel-3 satellites will routinely monitor ocean and land surfaces to generate valuable information for the European Union (EU) and its Member States as part of the Global Monitoring for Environment and Security (GMES) programme.

The MyOcean project is the EU Marine Core Service (MCS). Operational oceanography services have been developed within the MERSEA 6th Framework Programme and through the ESA GSE Marcoast and Polarview projects. The MyOcean will deliver regular, systematic products on sea-surface topography and sea-state and ecosystem characteristics over the oceans and the European regional and shelf seas. The information from Sentinel-3 will be assimilated into models in near-realtime to provide routinely the best-available estimate of the state of the oceans, together with forecasts (from days to weeks) and reanalyses ('hindcasts' of ocean state over long time-series in the past).

Sentinel-3 will deliver routine operational services to policy-makers and marine and land service users:

- Marine and Coastal Environment
 - Sea-surface topography
 - Mesoscale circulation
 - Water quality
 - Sea-surface temperature
 - Wave height and wind speed
 - Sediment load and transport
 - Eutrophication (excessive plant growth in water bodies)
- Polar Environment
 - Sea-ice thickness
 - Ice surface temperature
- Maritime Security
 - Ocean-current forecasting
 - Water transparency
 - Wind and wave height
- Global Change Ocean
 - Global sea-level rise
 - Global ocean warming
 - Ocean carbon dioxide flux
- Land Cover & Land-Use Change
 - Land-use mapping
 - Vegetation indices

- Forest Monitoring
 - Forest cover mapping
- Food Security Early Warning
 - Regional land-cover mapping
 - Drought monitoring
- Humanitarian Aid
 - Land-use mapping
- Air Pollution (local to regional scales)
 - Aerosol concentration
 - Risk Management (flood and fires)
 - Burned scar mapping
 - Fire detection
- Global Change Land
 - Forest-cover change mapping
 - Soil degradation mapping

7.3 Future altimetry missions

Thanks chiefly to Topex/Poseidon, satellite altimetry has proven a valuable source of data for a broad range of applications. Looking beyond the missions in operational service today, future satellites will need to provide better spatial and temporal coverage so that we can study in particular mesoscale variations and other phenomena more closely.

Missions envisioned

Several options are being considered for 2013 and beyond. The currently foreseen missions (still in discussion) are:

- Jason-CS/Sentinel-6 (2020)
- SWOT (2021)

For the medium term, consideration is now being given to altimetry missions capable of ‘scanning’ the ocean surface to acquire data at scales of a few tens of kilometres, passing over the same spots every few days. Other projects on the drawing board are based on constellations of dedicated, low-cost microsatellites.

Looking further into the future, the goal will be to monitor relatively rapid ocean variations with a period of less than 10 days at scales below 100 kilometres.

Beyond 2010, ‘conventional’ operational missions are still envisaged, especially for operational purposes (Sentinel-3, Jason-3).

7.3.1 Jason-CS / Sentinel-6

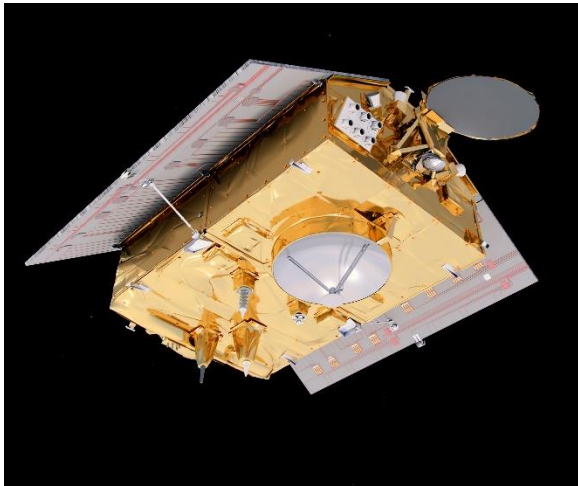


Figure 7.92. (Credits [ESA/ATG medialab](#))

Satellite	Jason-CS / Sentinel-6
Launch	2020 and 2026
Mission	Measure sea surface height
Altitude	1 336 km
Inclination	66°

Jason-CS is envisioned for 2020 to ensure adequate overlap with Jason-3 in a joint project including United States and Europe.

The satellite bus will be based on CryoSat and the altimeter will take advantage of recent developments of CryoSat and Sentinel. This new altimeter will integrate new modes compared to Jason-3 (SAR mode, interleaved mode).

Given the importance of maintaining the precise climate record of sea surface height, Jason-CS / Sentinel-6 should maintain the 1336 km reference orbit flown by Topex/Poseidon and Jason-1, 2 and 3.

7.3.1.1 Jason-CS / Sentinel-6 Objectives

The main objective of the SENTINEL-6 mission is to measure sea surface topography with high accuracy and reliability to support ocean forecasting systems, environmental monitoring and climate monitoring. The mission definition is driven by the need for continuity in provision of TOPEX and JASON missions, with improvements in instrument performance and coverage.

The SENTINEL-6 mission will be a multi-agency partnership comprising ESA, EU, EUMETSAT, NASA-JPL, NOAA, and CNES, to deliver operational ocean and land observation services.

The spacecraft carries one main instrument:

- The Synthetic Aperture Radar Altimeter (POSEIDON-4)

It is complemented by,

Four instruments for Precise Orbit Determination (POD):

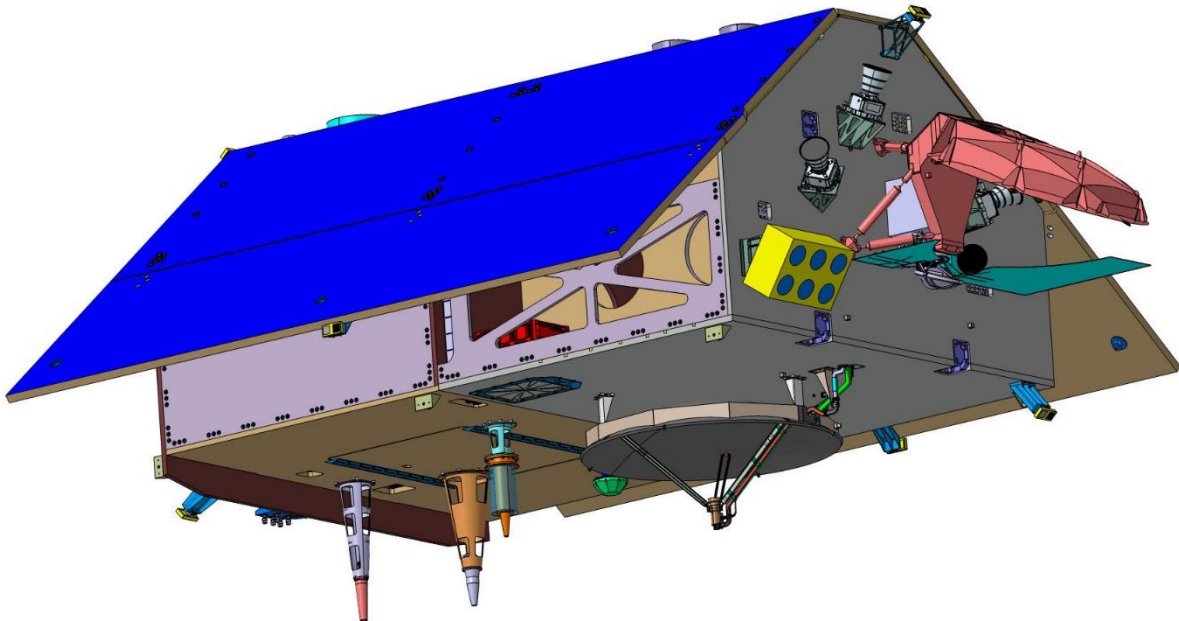
- DORIS: Doppler Orbit Radio positioning system
- GNSS-POD: GPS/Galileo receiver, providing data for precise orbit determination
- Star trackers used in support of POD and knowledge of the altimeter pointing
- LRA: to accurately locate the satellite in orbit using a Laser Retro-reflector Array system

One instrument for water vapour corrections:

- AMR-C (Climate Quality Advanced Microwave Radiometer): this radiometer is a 3-frequency radiometer complemented by several higher frequency channels to support high-resolution coastal geophysical parameter retrieval provided by NASA-JPL

As a secondary mission objective:

- GNSS-RO is an instrument provided by NASA-JPL for the purpose of allowing derivation of atmospheric profiles of pressure and temperature as a function of height by means of radio occultation of GPS signals.



0.082

Figure 7.93 Sentinel-6 Satellite and Payloads (Credit: Airbus Defence and Space)

More info

- [ESA web page](#)

7.3.2 SWOT

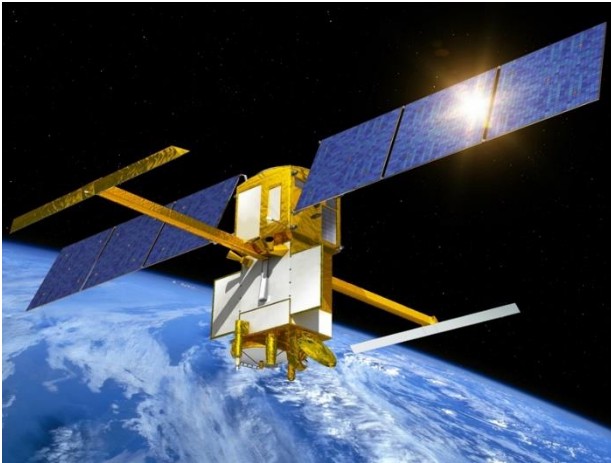


Figure 7.94. (Credits CNES)

SWOT (Surface Water Ocean Topography) is envisioned for 2020 in a joint project including Nasa and Cnes. It would combine the concepts of WaTER (Water and Terrestrial Elevation Recovery) and the Hydrosphere Mapper missions into a single one to address the objectives of both land hydrology and oceanography. The technology for Swot should be a Ka-band Radar INterferometer (KaRIN, 0.86 cm wavelength).

Satellite	SWOT
Launch	April 2021
Mission	Measure sea surface height
Altitude	857-890 km
Inclination	78°

7.3.2.1 SWOT Objectives

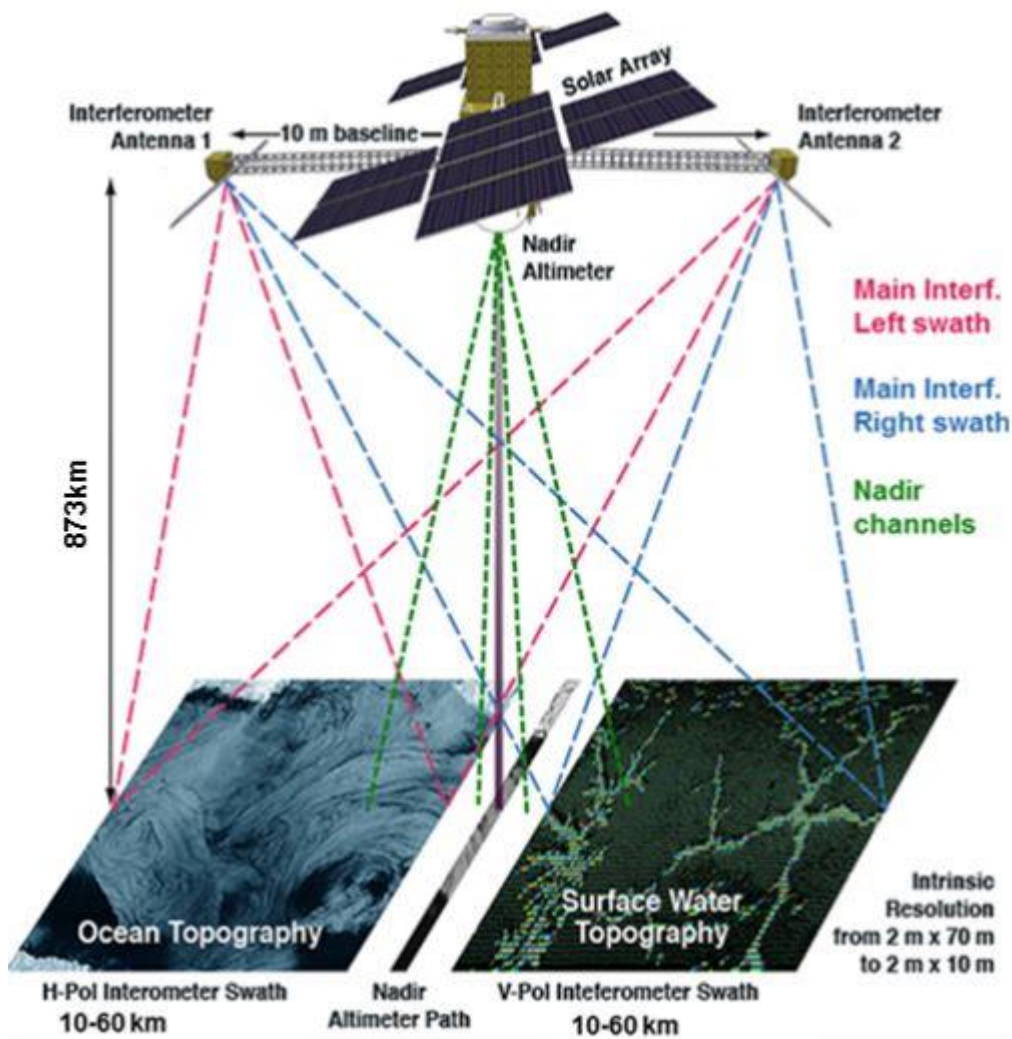


Figure 7.95 SWOT Dual-swath Ka-band radar interferometry system. (Credit: CNES/JPL)

The primary oceanographic objectives of the SWOT mission are to characterize the ocean mesoscale and submesoscale circulation determined from the ocean surface topography at spatial resolutions of 15 km (for 68% of the ocean). (Spatial resolution is defined to be wavelength in the oceanographic context.)

Current altimeter constellations can only resolve the two-dimensional ocean circulation at resolutions larger than 200 km. Fundamental questions on the dynamics of ocean variability at scales shorter than 200 km, the mesoscale and submesoscale processes, such as the formation, evolution, and dissipation of eddy variability (including narrow currents, fronts, and quasi-geostrophic turbulence) and its role in air-sea interaction, are to be addressed by the new observations.

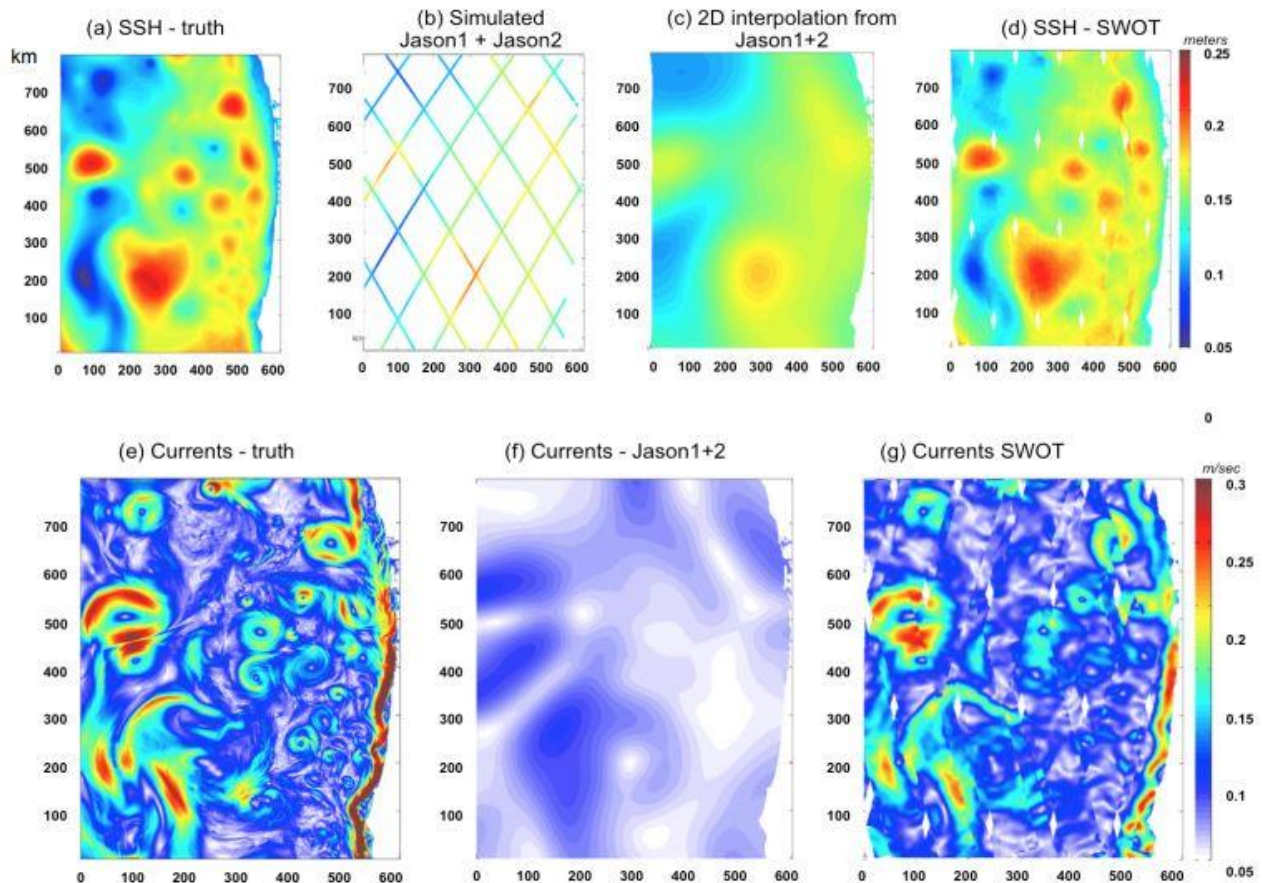


Figure 7.96 Simulated SWOT ocean observations (Credit: CNES/JPL)

The SWOT mission will provide measurements of water storage changes in terrestrial surface water bodies and will provide estimates of discharge in large (wider than 100 m, baseline, or 170 m, threshold), rivers, globally.

The hydrologic science measurement objectives of the SWOT mission are:

- To provide a global inventory of all terrestrial surface water bodies whose surface area exceeds $(250\text{m})^2$ (goal: $(100\text{m})^2$, threshold: 1km^2) (lakes, reservoirs, wetlands) and rivers whose width exceeds 100m (goal: 50m, threshold: 170m).
- To measure the global storage change in terrestrial surface water bodies at sub-monthly, seasonal, and annual time scales.
- To estimate the global change in river discharge at sub-monthly, seasonal, and annual time scales.

More information:

- Science Requirements Document JPL D-61923 2016
https://swot.oceansciences.org/docs/D-61923_SRD_Rev_A_20160318.pdf
- List of publications and documents: <https://swot.oceansciences.org/documents.htm?>

7.4 Altimetry in planetary missions

Radar subsurface sounders have been also designed to measure the surface characteristics and access the buried structures of different planets in the Solar System.

In the context of planetary missions, radars operating at extremely different frequencies have been used. The choice of the frequency is of the uppermost importance since it will drive the penetration depth. Moreover, because the bandwidth is limited by the central frequency, this choice will also set the range resolution (i.e. its ability to distinguish between two targets at different distances of the instrument). Radars designed to perform deep soundings of the subsurface must operate at low center frequencies and consequently have a poor vertical resolution.

7.4.1 MARSIS - Mars



Figure 7.97 Mars Express Credit: ESA/Alex Lutkus.

The MARSIS (Mars Advanced Radar for Subsurface and Ionosphere Sounding) orbital radar sounder, onboard ESA's Mars Express spacecraft launched in 2003, was designed to investigate the Martian ionosphere and the geological and hydrological structure of the subsurface, with a particular emphasis on the detection of deep bodies of solid or liquid water

Satellite	Mars Express
Launch	2 June 2003
Altitude	298 - 10107 km
Inclination	86.3 degrees

MARSIS is a low frequency, nadir-looking pulse limited radar sounder and altimeter with ground penetration capabilities, which uses synthetic aperture techniques and a secondary receiving antenna to isolate subsurface reflections.

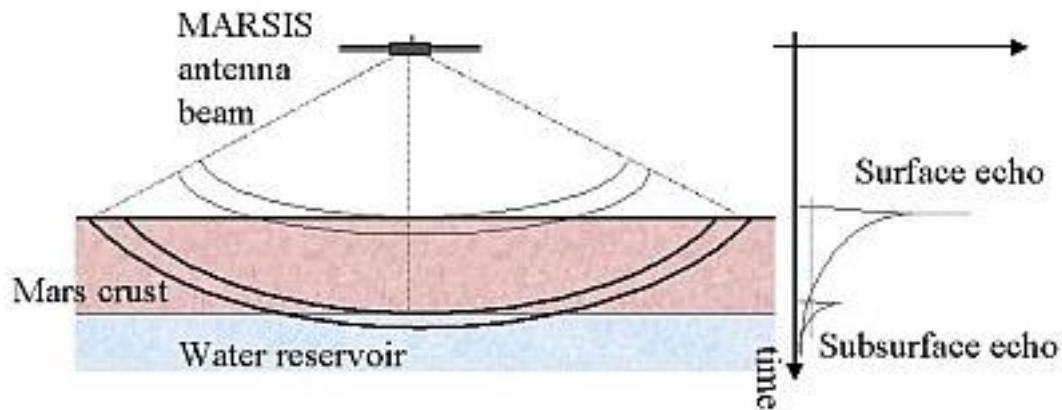


Figure 7.98. MARSIS Principle of Operation (Credits ESA)

The operation altitudes for MARSIS are up to 800 km above the Martian surface for subsurface sounding and up to 1200 km for ionospheric sounding. In its standard operating mode, the instrument is capable of making measurements in 1 MHz wide bands centred at 1.8, 3.0, 4.0 and 5.0 MHz.

MARSIS operates in the following modes:

- Subsurface Sounding
- Active Ionospheric Sounding
- Receive Only
- Calibration

The particularly low frequencies used by the instrument give it a theoretical ability to detect the presence of liquid water, under ideal sounding conditions, at depths of up to ~3–5 km beneath the Martian surface. It has achieved this level of sounding performance only in a number of specific environments, which include the ice-rich North and South Polar Caps, where it provided estimates of the thickness of ice deposits, as well as several other sites at lower latitudes.

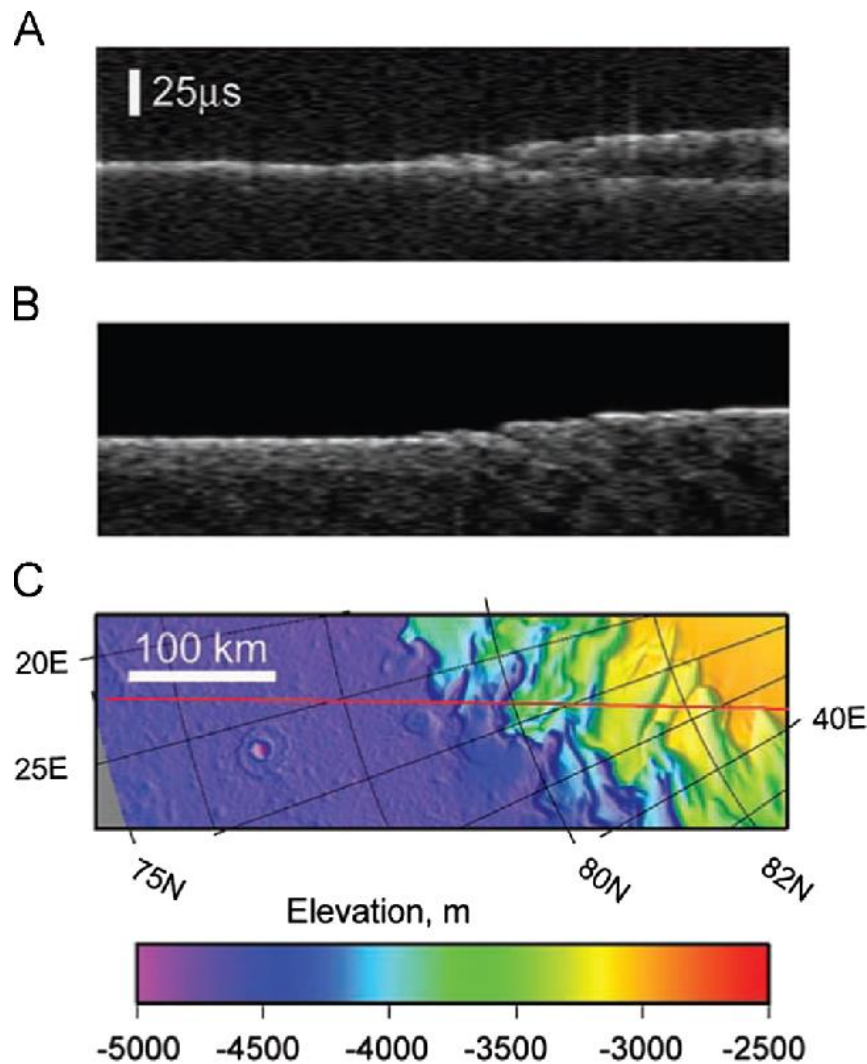


Figure 7.99. (A) MARSIS data in radargram format for orbit 1855 as it crosses the margin of the north polar layered deposits. (B) Simulated MARSIS data if echoes are only from the surface (nadir and off-nadir clutter). (C) MOLA (Mars Orbiter Laser Altimeter) topography along the ground track (red line); elevation is relative to the mean planetary radius. MARSIS data at 5 MHz show a split of the strong return into two as the ground track reaches the NPLD (higher terrain to the right). Maximum time delay to the second reflector is 21 μ s, equivalent to 1.8 km depth in water ice (from Picardi et al., 2005).

More information

- ESA website <http://sci.esa.int/mars-express/34826-design/?fbodylongid=1601>

References

- Orosei, R., et al. "Mars Advanced Radar for Subsurface and Ionospheric Sounding (MARSIS) after nine years of operation: A summary." *Planetary and Space Science* 112 (2015): 98-114.
- Dieval, Catherine, et al. "MARSIS remote sounding of localized density structures in the dayside Martian ionosphere: A study of controlling parameters." *Journal of Geophysical Research: Space Physics* 120.9 (2015): 8125-8145.

- Ciarletti, Valérie. "A variety of radars designed to explore the hidden structures and properties of the Solar System's planets and bodies." *Comptes Rendus Physique* 17.9 (2016): 966-975.

7.4.2 SHARAD - Mars

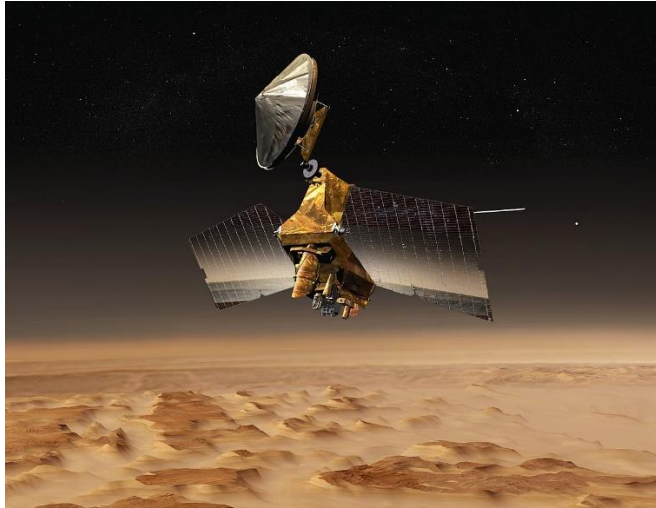


Figure 7.100. Mars Reconnaissance Orbiter (MRO):
NASA.

SHARAD (SHAllow-RADar) is one of the main instruments on board the Mars Reconnaissance Orbiter (MRO), NASA's planetary exploration spacecraft launched in August 2005 and operating in Mars' orbit since the end of 2006. The purpose of the MRO mission is global mapping of the surface (in visible and near infrared), investigation of the subsurface, identification of future landing sites for spacecraft and future communications and navigation support to Martian missions.

Satellite	Mars Express
Launch	12 August 2005
Altitude	250 to 316 km
Inclination	93 degrees

SHARAD was designed to complement the capabilities and performance of MARSIS by operating at higher frequencies around 20 MHz to better resolve variations in near-surface composition, stratigraphy and structure – particularly with regard to resolving the internal layers of the polar caps. The horizontal resolution of the instrument is between 0.3 and 3 km and the vertical resolution is about 15 m (10 times better than MARSIS).

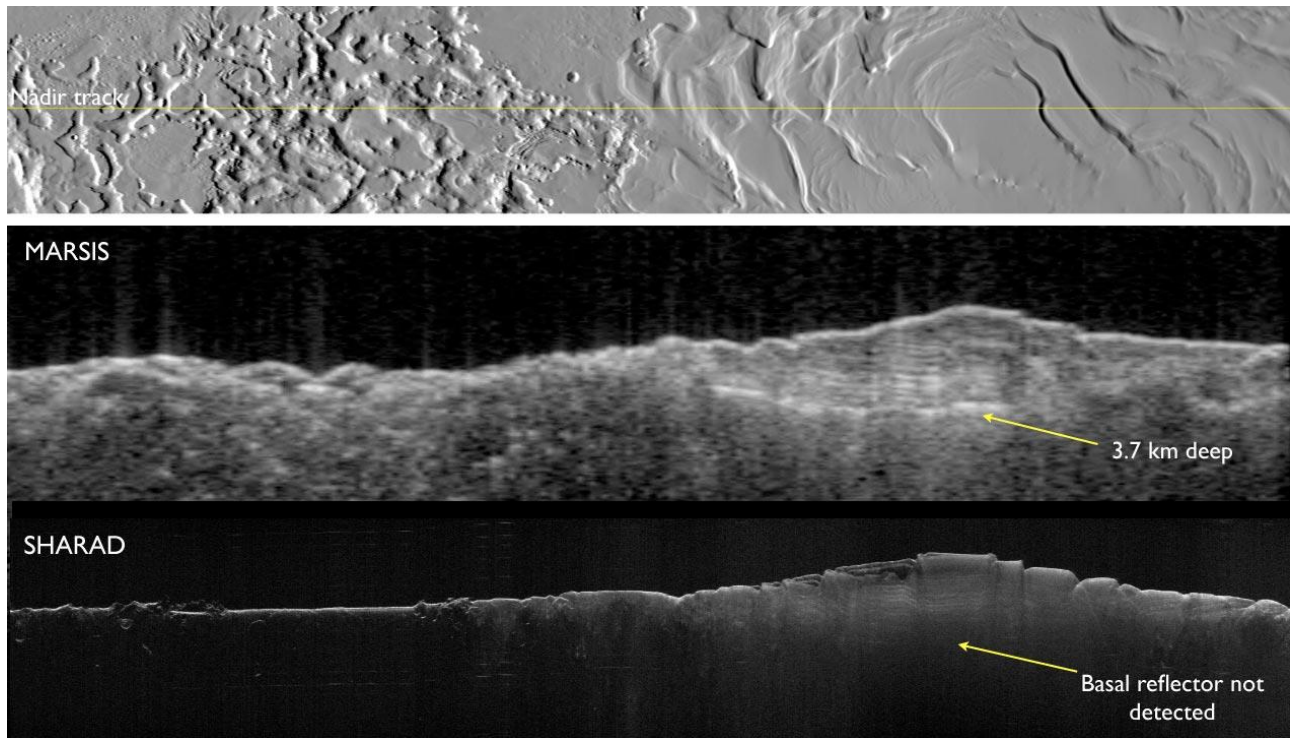


Figure 7.101. Comparison between MARSIS and SHARAD radargrams over the South Polar Layered Deposits on Mars. (Credit NASA/ESA/JPL-Caltech/University of Rome/Washington University in St. Louis)

The SHARAD radar penetrated the north polar layered ice deposits of Mars and revealed a relatively small (about 100 meter) maximum deflection of the underlying rock, which suggests a strong lithosphere greater than 300 kilometers thick. Radar results consistent with massive deposits of water ice in middle latitudes support a debris-covered glacier hypothesis.

On November 22, 2016, NASA reported finding a large amount of underground ice in the Utopia Planitia region of Mars using SHARAD. The volume of water detected has been estimated to be equivalent to the volume of water in Lake Superior, the largest of the Great Lakes of North America, .

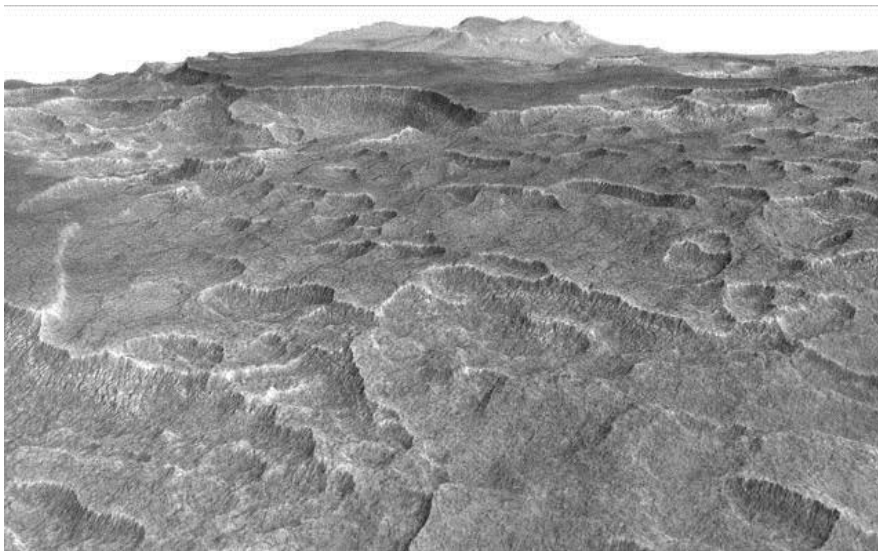


Figure 7.102. Mars - Utopia Planitia. Scalloped terrain led to the discovery of a large amount of underground ice enough water to fill Lake Superior

More information

- NASA website https://www.nasa.gov/mission_pages/MRO/spacecraft/sc-instru-sharad.html
- ASI website <http://www.asi.it/en/activity/solar-system-exploration/sharad>

References

- Seu, Roberto, et al. "SHARAD sounding radar on the Mars Reconnaissance Orbiter." *Journal of Geophysical Research: Planets* 112.E5 (2007).
- Campbell, Bruce, et al. "SHARAD radar sounding of the Vastitas Borealis Formation in Amazonis Planitia." *Journal of Geophysical Research: Planets* 113.E12 (2008).

7.4.3 RIME – Jupiter Moons



*Figure 7.103. JUICE explorer illustration
Copyright: Spacecraft: ESA/ATG medialab;
Jupiter: NASA/ESA/J. Nichols (University of
Leicester); Ganymede: NASA/JPL; Io:
NASA/JPL/University of Arizona; Callisto and
Europa: NASA/JPL/DLR*

In May 2012 the European Space Agency approved the JUPITER ICy moons Explorer (JUICE) mission. This is the first Large-class mission chosen as part of the ESA's Cosmic Vision 2015-2025 programme. JUICE is aimed to study Jupiter and to investigate the potentially habitable zones in the Galilean icy satellites: Ganymede, Europa and Callisto. One of the most important sets of science goals for JUICE is related to the study of the subsurface geology and geophysics of icy moons and to detect possible subsurface water.

RIME (Radar for Icy moon Exploration) is a radar sounder optimized for the penetration of the Galilean icy moons, Ganymede, Europa and Callisto, up to a depth of 9 km. This is a nadir-looking active instrument which transmits radio waves with the unique capability to penetrate deeply into the subsurface.

Satellite	JUICE
Launch	2022

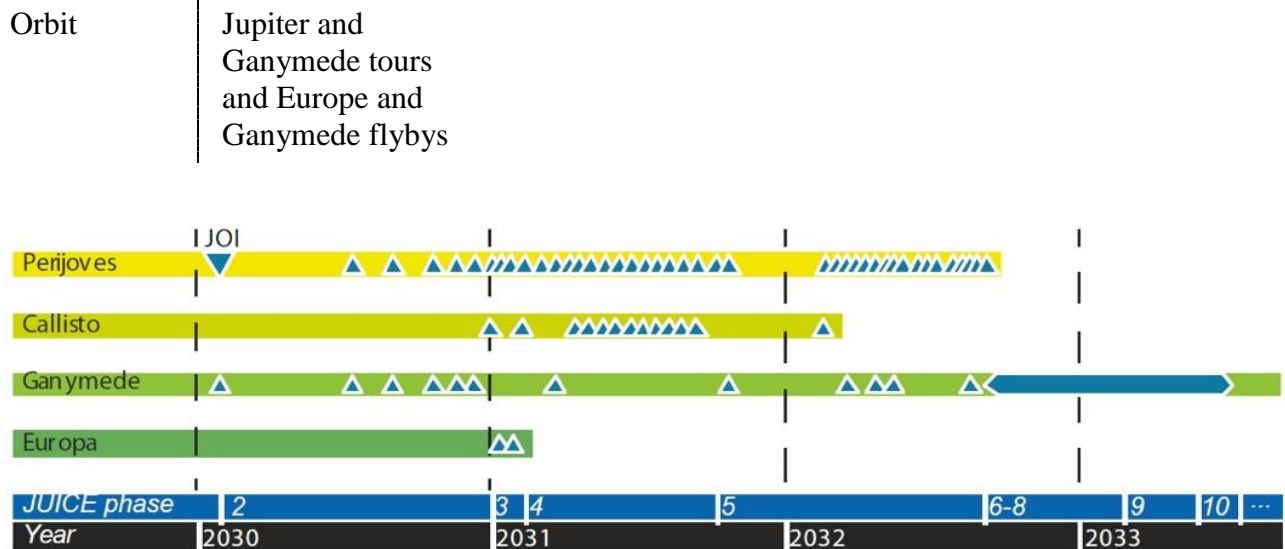


Figure 7.104. Illustrative timeline of the JUICE baseline mission. Credit: ESA

Two main operation scenarios are foreseen for RIME: flyby observations of Europa, Ganymede and Callisto and circular orbital operations around Ganymede at the end of the mission. According to these scenarios, RIME will explore the icy shell of the Galilean icy satellites by characterising the wide range of compositional, thermal, and structural variation found in the subsurface of these moons. These subsurface observations will provide insight into the dynamic history of the satellites, test models of the formation of their surface features, and constrain the distribution of deformation in their ice shells as well as global and regional surface ages.

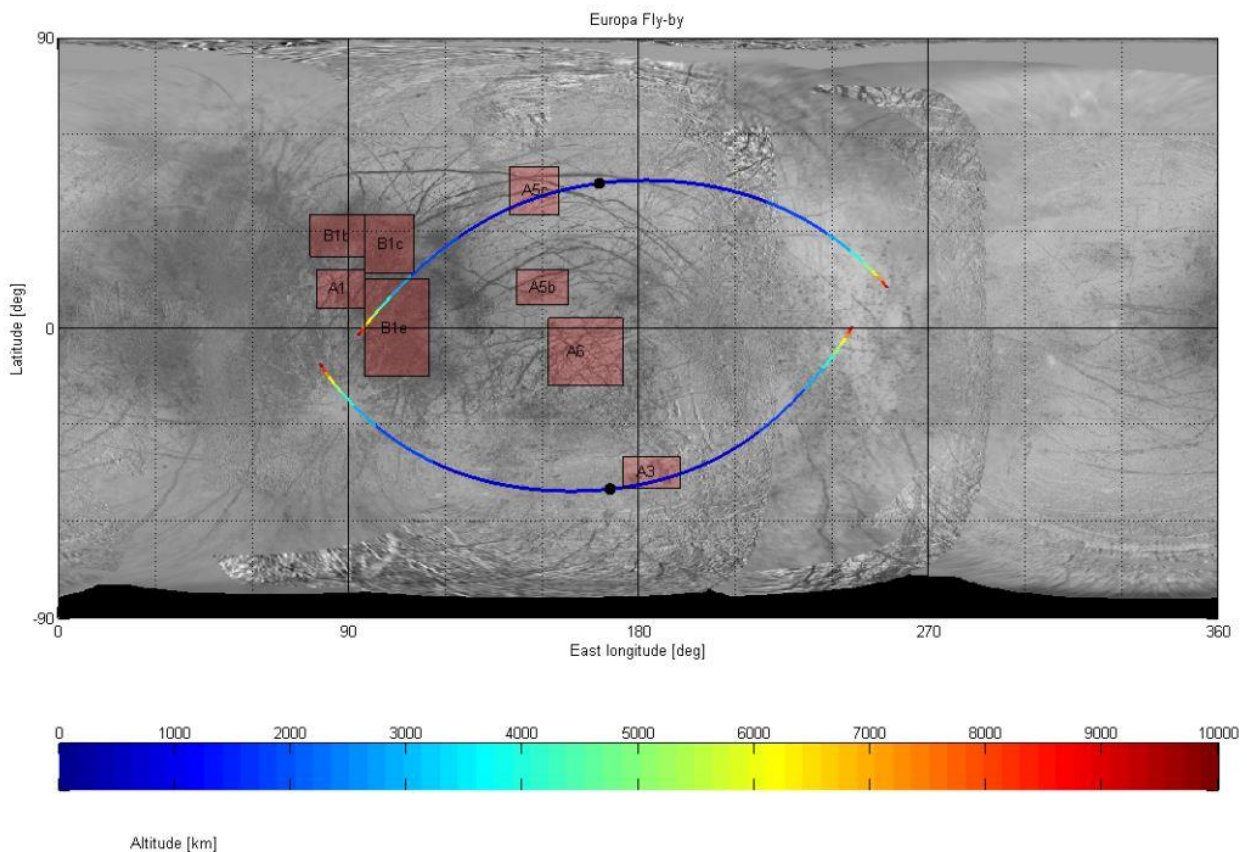


Figure 7.105. Ground track of the spacecraft during Europa flybys. The image shows a Europa surface map with the areas of specific interest indicated by colour rectangles. The ground tracks of the two flybys are indicated in coloured lines, with the colour indicating the altitudes in 1000 km (see colour bar). Credit: ESA

Scientific measurements can be performed in two different resolution modes: high resolution and low resolution (using 3 and 1 MHz chirp bandwidth, respectively). The low resolution mode will be used to reduce data volume when observing deep sounding targets. RIME offers a wide flexibility in terms of acquisition parameters during measurements. Moreover, it foresees a calibration mode (receive-only) in which no pulse is transmitted and the instrument only records the output of the receiver. Within the high and low resolution modes, parameters can be adjusted to change the output data rate. In particular, the on-board pre-summing can be set to values between 1 and 8, providing a corresponding factor in data rate reduction, at a potential cost of along-track resolution and sensitivity to sloping subsurface interfaces. In addition, if depth of detectable features can be anticipated, the receive window size can be adjusted to receive echoes only for the period of interest to further manage the data rate. For high-priority flybys, such as the two of Europa, the high resolution mode (3 MHz bandwidth) will be used, with no pre-summing, and a receive window of 226 μ s.

References

- ESA Web page <http://sci.esa.int/juice/>
- Bruzzone, Lorenzo, et al. "RIME: Radar for icy moon exploration." *Geoscience and Remote Sensing Symposium (IGARSS), 2013 IEEE International*. IEEE, 2013.

7.4.4 SRS - Venus

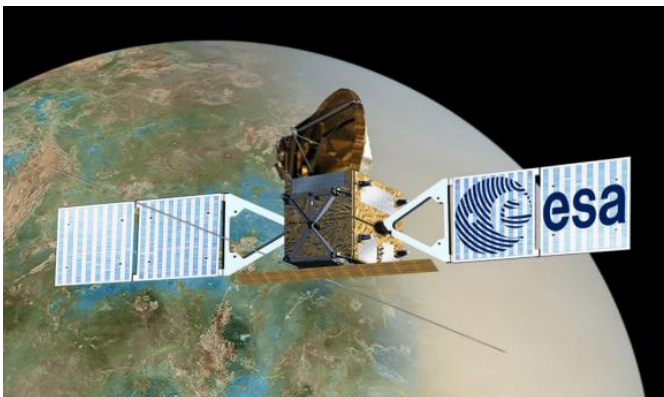


Figure 7.106. EnVision concept

EnVision is a proposed ESA medium class mission to determine the nature and current state of geological activity on Venus, and its relationship with the atmosphere, to understand how Venus and Earth could have evolved so differently.

It will use a subsurface radar sounder to obtain profiles of the upper few hundred metres, and an IR mapper and spectrometer to detect volcanic eruptions and a world-leading European phased array synthetic aperture radar, VenSAR, to obtain global topography at 27m and imagery at up to 1m resolution, and us InSAR to detect changes of < 1cm/yr

Satellite	EnVision
Launch	2029
Altitude	259 km

The use of a low frequency nadir looking radar sounder provides the ideal complementary information to the SAR data acquired by the S-band VenSAR, enabling a full and detailed investigation of the surface and subsurface geology of Venus. The combination of InSAR data (intensity, topography and displacement variables) with the sounder data results in an exceptional ability to understand the link between the surface and subsurface processes on Venus.

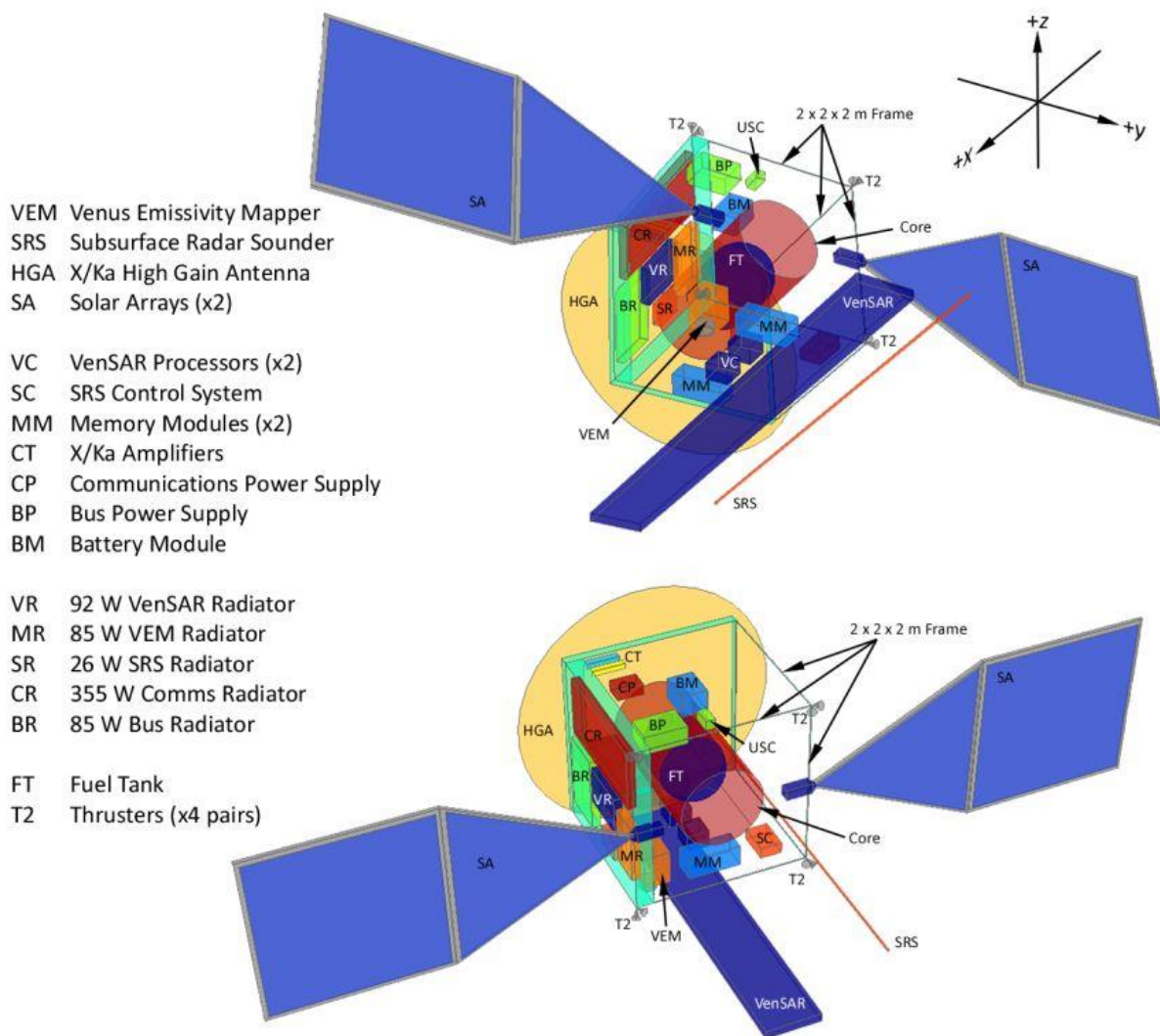


Figure 7.107. Nominal Spacecraft Layout. Credits EnVision Team.

To achieve the science requirements, the radar shall be designed to work with a central frequency in the range 9 to 30 MHz for optimal ground penetration capability. The radar bandwidth shall be of

several MHz to achieve adequate range resolution. The SRS maximum penetration depth, which has been inferred from the various dielectric measurements in different types of basaltic rocks.

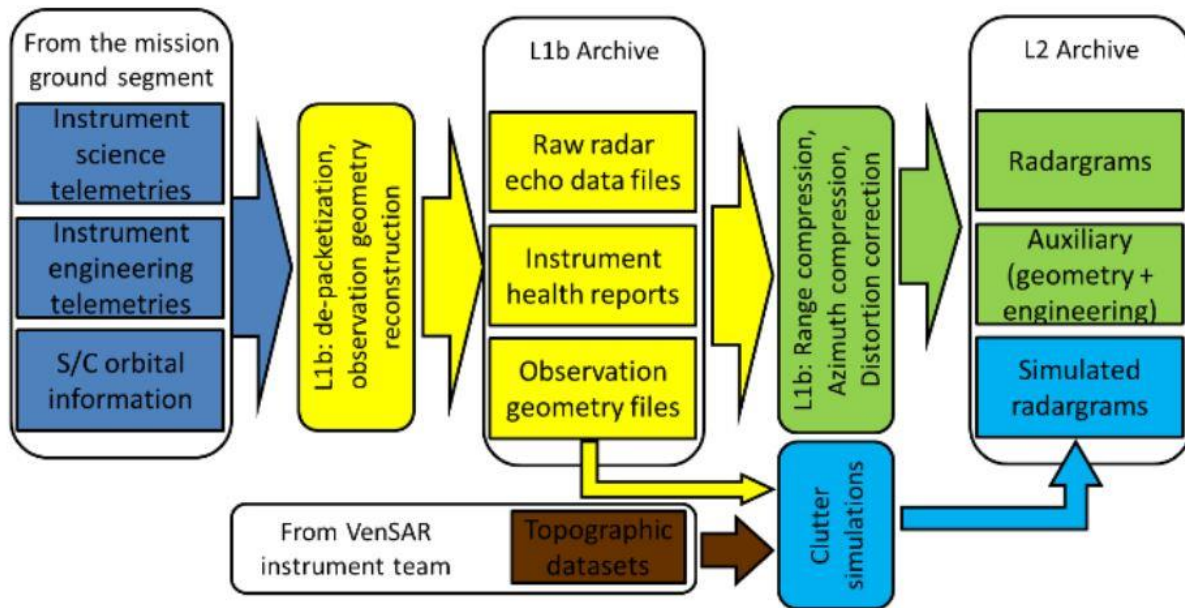


Figure 7.108. Scheme illustrating data processing flow and related data products. Credits EnVision Team.

The pipeline for Level 1b (L1b) processing will use as input both scientific and engineering telemetry of the instrument, and the orbital information of the spacecraft. Data will be split into individual files, one for each type of telemetry and for every observation, with packets arranged in time order, and corrupted or duplicated packets removed. For scientific telemetry packets, a set of parameters describing the geometry of observation will be computed using orbital information of the spacecraft

SRS heritage includes RIME (Radar for Icy Moon Exploration) onboard JUICE (Jupiter Icy Moon Explorer), MARSIS (Mars Express) and SHARAD on NASA’s Mars Reconnaissance Orbiter.

References

- Ghail, Richard, et al. "EnVision: understanding why our most Earth-like neighbour is so different." arXiv preprint arXiv:1703.09010 (2017).

8 Glossary

- ACC: Antarctic Circumpolar Current

- Cold current encircling the Antarctic, driven by westerly winds between 40° and 50° South. The flow of the ACC is not checked by the continents. It thus links the Atlantic, Indian and Pacific Oceans.
- **ADT**: Absolute Dynamic Topography. Ocean topography with respect to the geoid
- **AGC**: Automatic Gain Control
- **Along-track**: Along-track data are data chronologically ordered, following the satellite “ground track”, i.e. the virtual track left by the radar beam on the ground.
- **Altimetry**: Technique for measuring height. Satellite altimetry measures the time taken by a radar pulse to travel from the satellite antenna to the surface and back to the satellite receiver. Combined with precise satellite location data, altimetry measurements yield sea-surface heights.
- **ASCII**: American Standard Code for Information Interchange
- **ASIC**: Application Specific Integrated Circuit
- **ATSR**: Along-Track Scanning Radiometer instrument measuring sea-surface temperatures (ESA)
- **Aviso**: Archiving, Validation and Interpretation of Satellite Oceanographic data. French data distribution and archiving centre for altimetry satellites and Doris data.

- **Bathymetry**: Measurement of the ocean depths.
- **Backscatter coefficient**: The amplitude of the useful radar altimeter echo signal with respect to the emission amplitude gives the backscatter coefficient, σ_0 . The backscatter coefficient can be related to wind speed.
- **Brown model**: Over an ocean surface, the radar altimeter echo waveform has a characteristic shape that can be described analytically (the Brown model).

- **Calval**: CALibration – VALidation
- **CCI**: Centre de Contrôle des Instruments. Instruments control centre (Jason-1)
- **CD Rom**: Compact Disk Read Only Memory
- **Cersat**: Centre ERS d’Archivage et de Traitement French Processing and Archiving Facility [Website](#)
- **CHAMP**: CHAllenging Minisatellite Payload
- **Clivar**: Climate Variability and Predictability (WCRP)
- **CLS**: Collecte, Localisation, Satellites
- **CMA**: Centre Multimissions Altimétrique CNES altimetry multi-mission ground segment
- **CNES**: Centre National d’études Spatiales French Space Agency
- **CryoSat**: ESA’s altimetry mission, to determine variations in the thickness of the Earth's continental ice sheets and marine ice cover
- **CTRS**: Conventional Terrestrial Reference System
- **Cycle**: Satellite repetitivity, or repeat orbit

- **DAS**: Data Assimilation System
- **Data assimilation**: Use of data as initial input to a model and during computation to yield results that fit/approximate reality as closely as possible. For example, assimilation of readings from meteorology stations into weather forecasting models generates more reliable results.
- **Data processing**: Antennas on the ground receive raw telemetry from satellites. These raw data must be processed by applying corrections and combining them with complementary data before they are usable. Data are processed to different levels:
- Level 0: raw telemetry

- Level 1: time-tagged data located and corrected for perturbing effects (level 1, 1.5 and 1b data fall into this category)
- Level 2: geophysical data (GDR-M) time-tagged, precisely located and corrected for environment effects. Data at this level are used by specialists with a close knowledge of their subject.
- Level 3: data ready for immediate use in applications, corrected and/or inter-calibrated.
- Level 4: gridded or model output data.
- Depending on the mission, retracking is performed at level 1 or 2.
- **DEOS**: Delft Institute for Earth-Oriented Space research
- **DHU**: Data Handling Unit
- **DIODE**: Dètermination Immèdiate d’Orbite par DORIS Embarquè
- DORIS onboard navigator, processing orbit in real time.
- **Doppler effect (Doppler-Fizeau effect)**: The pitch of a sound emitted by a moving object appears to be higher the faster it approaches, and lower the faster it moves away. A good analogy is a stream into which leaves are thrown at regular intervals. As we move upstream towards the source, leaves will flow past us more often. The faster we go, the more leaves we will see. Conversely, as we move downstream away from the source leaves will flow past less often-to the point where we would only see a single leaf when moving at the same speed as the current. High-pitched sounds have high frequencies, which means we “meet” the sound wave often-as if we were moving towards the source (or it was approaching us); low-pitched sounds have lower frequencies-as if we were moving away. The same principle applies to light rays, which shift towards the longer wavelengths as they move away, and towards the shorter wavelengths as they approach. (Adapted from Evry Schatzmann, Les Enfants d’Uranie)
- We can thus determine the velocity of a moving object emitting sound or light waves by measuring the shift between the transmitted and received frequencies. The DORIS system achieves precise orbit determination and location by measuring the Doppler shift in this way.
- **DORIS**: Doppler Orbitography and Radiopositioning Integrated by Satellite. Precise orbit determination and location system using Doppler shift measurement techniques. A global network of orbitography beacons has been deployed. DORIS was developed by CNES, the French space agency, and is operated by CLS.
- **Dry tropospheric correction**: Permanent gases in the atmosphere (oxygen, nitrogen) slow the radar pulse, generating an error on altimetry measurements of the order of 2.30 metres. The value of the correction is determined from atmospheric pressure data supplied by a meteorological model.
- **DT**: Delayed Time: data used to compute the product were processed using precise orbit
- **DUACS**: Data Unification and Altimeter Combination System (as part of the SSALTO processing system) (previously Developing Use of Altimetry for Climate Studies, in the EU project frame)
- **DVD Rom**: Digital Versatile Disk Read Only Memory.
- **Dynamic topography**: Sea level driven by thermodynamic processes in the ocean.
- **ECMWF**: European Centre for Medium-range Weather Forecasting [Website](#)
- **Eddies**: Hydrodynamic instabilities in the oceans that form in the wake of currents or are generated by winds. Eddies may persist for weeks or months, and may be tens to hundreds of kilometres across. They penetrate quite deep below the ocean surface and transport heat, salts and nutrients. Electromagnetic Bias (EMB) Perturbation of the altimeter radar pulse due to the fact that wave troughs reflect more energy than wave crests.
- **EM**: Electromagnetic

- **ENSO:** El Niño - Southern Oscillation El Niño Southern Oscillation Climatic phenomenon occurring in the Tropics that involves transports of warm (El Niño) or cold (La Niña) water masses from west to east across the Pacific basin. This displacement of water is accompanied by a shift of atmospheric cells, and therefore of winds and monsoons across the Tropics. This oscillation, which has been occurring at irregular intervals for thousands of years, has a global effect on climate. The phenomenon is named “El Niño” (meaning the Christ Child or the Little Boy in Spanish) because warm waters often reach the coast of Peru around Christmas time, often severely disrupting local fisheries.
- **Environmental corrections:** The radar pulse used to measure altimetry is subjected to a number of disturbances as it passes through the atmosphere and when it is reflected by the sea surface.
- **Envisat:** ENVironmental SATellite Earth-observing satellite (ESA)
- **ERM:** Exact Repeat Mission (Geosat) Phase of the Geosat mission during which the satellite was put into a 17-day repeat orbit to study the oceans.
- **ERS:** European Remote Sensing satellites (ERS-1, ERS-2) Earth-observing satellites (ESA)
- **ESA:** European space Agency
- **ESOC:** European Space Operations Centre
- **ESRIN:** ESA Centre for Earth Observation
- **ESTEC:** European Space Research and Technology Centre
- **EU:** European Union
- **Eumetsat:** European Organisation for the Exploitation of METeorological SATellites

- **F-DAC:** French-Distribution and Archiving Centre (F-DAC)
- **F-PAC:** French-Processing and Archiving Centre (F-PAC)
- **FDP:** Fast Delivery Product
- **FM:** Frequency Modulation
- **FNMOC:** Fleet Numerical Meteorological & Oceanographic Center (US Navy)
- **FNOC:** Fleet Numerical Oceanographic Center
- **Full-deramp:** The full-deramp technique concept consists in mixing this incoming signal with a replica of the transmitted chirp, slightly shifted in frequency. This circumvents problems of power necessary for the emitted pulse, and of the very short duration that would be needed to obtain requested accuracy.

- **GDR:** Geophysical Data Record(s) Geodesy The science of measuring the Earth, its shape and gravitational field.
- **Geoid:** The shape of the sea surface assuming a complete absence of perturbing forces (tides, wind, currents, etc.). The geoid reflects the Earth’s gravitational field (it is an equipotential surface) and varies in height by as much as 100 metres over distances of several thousand kilometres due to uneven mass distribution within the planet’s crust, mantle and core. Other, less pronounced, irregularities are also visible over smaller distances. These reflect the ocean’s bottom topography.
- **Geophysical corrections:** The radar pulse used to measure altimetry is subjected to a number of disturbances as it passes through the atmosphere and when it is reflected by the sea surface.
- **GEOS 3:** Geodynamics Experimental Ocean Satellite Altimetric satellite (NASA)
- **Geosat:** Geodetic & Oceanographic SATellite Altimetric satellite (US Navy)
- **Geostrophic circulation:** Ocean circulation generated by the balance between the horizontal pressure gradient forces exerted by water masses and the effect of acceleration due to the Earth’s rotation.
- **GFO:** Geosat Follow-On Altimetric Satellite (US Navy).

- **GM:** Geodetic Mission (Geosat). Phase of the GEOSAT mission during which the satellite's orbit was designed to study the geoid.
- **GOCE:** Gravity field and steady-state Ocean Circulation
- **GODAE:** Global Ocean Data Assimilation Experiment.
- **GPS:** Global positioning System.
- **GPSDR:** Global Positioning System Demonstration Receiver. One of three positioning systems on Topex/Poseidon that uses the GPS to determine the satellite's position.
- **GRACE:** Gravity Recovery and Climate Experiment
- **Greenhouse effect:** A good proportion of the heat penetrating the Earth's atmosphere is not reflected back into space but is "trapped" by clouds and water vapor. This heat is thus returned to the surface, maintaining an average temperature of 15°C on Earth. Without it, the temperature would be nearer -18°C. Increasing quantities of certain gases in the atmosphere-called greenhouse gases-such as carbon dioxide are thought to amplify this phenomenon, leading to an increase in temperature on the surface of the globe.
- **Ground Segment:** The teams, hardware and software involved in controlling a satellite and in retrieving and processing its data.
- **Gulf Stream:** Western boundary current of the subtropical gyre. The Gulf Stream is a strong current that transports warm waters from the Gulf of Mexico up the south coast of the United States to the Mid-Atlantic Ocean.

- **H_s or H_{1/3}:** See Significant Wave Height.

- **IAT:** International Atomic Time
- **IDS:** International DORIS Service
- **IERS:** International Earth Rotation Service
- **IGDR:** Interim Geophysical Data Record(s) or rapid-delivery products (48 hours after acquisition)
- **IM:** Instrument Module
- **Inverted Barometer (IB):** Correction applied to allow for atmospheric forcing of the ocean surface. The sea level is lower when atmospheric pressure is high, and higher when atmospheric pressure is low.
- **Ionosphere:** Layer of the upper atmosphere where electron and ionisation activity is particularly high. Electromagnetic waves are subjected to a number of perturbing effects as they pass through the ionosphere.
- **Ionospheric correction:** The altimeter radar signal is delayed as it travels through the ionosphere. Free electrons slow the radar pulse, causing an error on altimetry measurements of the order of 0 to 30 centimetres. The value of this correction is determined by combining range measurements acquired at two different frequencies (Topex and Poseidon-2 altimeters), as it is inversely proportional to the square of the frequency. For mono-frequency altimeters such as that used on the ERS satellites, this value is determined using a statistical model of the ionosphere.
- **ISRO:** Indian Space Research organisation
- **ITRF:** International Terrestrial Reference Frame.

- **Jason-1:** Altimetric satellite (CNES/NASA), follow-on of Topex/Poseidon
- **JGM:** Joint Gravity Model
- **JMR:** Jason-1 Microwave Radiometer
- **JPL:** Jet Propulsion Laboratory (NASA)

- **Kuroshio Current:** Western boundary current of the subtropical gyre. The Kuroshio Current is a strong current that transports warm waters from the China Sea and the Philippines up past Japan to the Mid-Pacific Ocean. It is the counterpart of the Gulf Stream in the North Atlantic.
- **La Niña:** See ENSO
- **LEO:** Low Earth Orbit
- **LOD:** Length-Of-Day
- **LRA:** Laser Retroreflector Array; One of three positioning systems on Topex/Poseidon and Jason. The LRA uses a laser beam to determine the satellite's position by measuring the round-trip time between the satellite and Earth to calculate the range.
- **LRR:** Laser RetroReflector; One of three positioning systems on ERS-1 and 2, Envisat and CryoSat. The LRR uses a laser beam to determine the satellite's position by measuring the round-trip time between the satellite and Earth to calculate the range.
- **MADT:** Maps of Absolute Dynamic Topography
- **MMS:** Multimission Modular Spacecraft
- **Modelling:** Modelling a phenomenon involves identifying its main characteristics and expressing them mathematically to better understand and, above all, predict how the phenomenon is likely to evolve.
- **MOE:** Medium Orbit Ephemeris
- **Mean Sea Level (MSL):** The sea surface height averaged across all the oceans of the globe. An increase in the mean sea level is an indicator of a possible global warming. MSLAMaps of Sea Level Anomalies
- **MSS:** Mean Sea Surface. Permanent component of the sea surface height. The mean sea surface comprises a geoid contribution (~100 m) and a permanent circulation contribution (~1 m).
- **MWR:** MicroWave Radiometer (onboard Envisat) MWSMicroWave Radiometer Sounder (onboard ERS-1 and 2).
- **nadir:** point of the celestial sphere representing the downward vertical direction, in one place (as opposed to the zenith)
- **NASA:** National Aeronautics and Space Administration
- **NAO:** North Atlantic Oscillation
- **NAVOCEANO:** NAVal OCEANographic Office
- **Niña (La):** See ENSO
- **Niño (El):** See ENSO
- **NOAA:** National Oceanic and Atmospheric Administration
- **Noise:** Statistical quantity used to estimate the inherent error on measurements induced by the instrument itself.
- **NPOESS:** National Polar-orbiting Operational Environmental Satellite System
- **NRA:** NASA Radar Altimeter, other name for the Topex altimeter
- **NRCS:** Normalised Radar Cross Section NRTNear-Real Time: data using preliminary orbit (produced in 2 or 3 days)
- **Ocean-atmosphere coupling:** The ocean and atmosphere are mutually interdependent. In particular, water that evaporates from the ocean causes the atmosphere to become hotter and more humid. This phenomenon affects atmospheric movements (winds), which in turn affect ocean circulation and so on: the temperature of air masses in contact with the ocean is modified and, conversely, ocean currents are driven by dominant winds. These ocean-

atmosphere interactions are a major factor in weather forecasting and a key element in our understanding of climate.

- **Orbitography:** The study of satellite orbits. Very precise determination of a satellite's exact position is a key factor in altimetry. Depending on the satellite, two or three orbit determination systems are used.
- **OSDR:** Operational Sensor Data Record(s) (Jason-1)
- **PAC:** Processing and archiving centres (ESA)
- **PCU:** Processing and Control Unit
- **PDS:** Payload Data Segment, responsible for exploiting the Envisat instrument data
- **Permanent circulation:** Steady state of ocean currents in an idealised unchanging atmospheric system.
- **POCC:** Project Operation Control Centre (Jason-1)
- **PO-DAAC:** Physical Oceanography - Distributed Active Archive Center (NASA/JPL)
- **POD:** Precise Orbit Determination
- **POE:** Precise Orbit Ephemeris
- **Poseidon:** One of the two altimeters onboard Topex/Poseidon (Cnes); Poseidon-2 is Jason-1 altimeter.
- **PRARE:** Precise Range and Range-rate Equipement (ERS-1 & 2)
- **PRF:** Pulse Repetition Frequency
- **PROTEUS:** Plate-forme Réutilisable pour l'Observation, les Telecommunications et les Usages Scientifiques. Minisatellite bus developed in France for Jason-1 and other missions.
- **Radar Altimeter:** RA is the altimeter onboard ERS-1 and 2; RA-2 is onboard Envisat.
- **Radiometer:** Passive instrument that detects and measures radiant energy, usually in the microwave, infrared and near-infrared wavebands. Radiometers flown on altimetry satellites help us to measure water vapor and liquid water content in the atmosphere. These measurements are used to apply corrections to altimetry data. The radiometer's antenna collects radiation reflected by the ocean. The amount measured depends on surface winds, ocean temperature, salinity, foam, absorption by water vapor and clouds, and other factors. To determine atmospheric water vapor content accurately, the surface and cloud contributions must be filtered out from the signal received by the radiometer. For this reason, different signal frequencies are used to increase sensitivity to each of these parameters. By combining measurements acquired at both frequencies, we can extract the water vapor signal.
- **Range:** the altimeter satellite-to-surface distance, deduced from the return echo time delay.
- **Reference ellipsoid:** Arbitrary reference surface that is a raw approximation of the Earth's shape, which is basically a sphere "flattened" at its poles. The length of one of the axes at the Equator is chosen so that the ellipsoid coincides at this latitude with the mean sea level. For example, the ellipsoid used by the Topex/Poseidon mission has a radius of 6378.1363 km and a flattening of 1/298.257.
- **Retracking:** Retracking altimetry data is done by computing the departure of the waveform's leading edge from the altimeter tracking gate and correcting the satellite range measurement (and surface elevation) accordingly.
- **RF:** Radio Frequency
- **RFU:** Radio Frequency Unit
- **RMS:** Root Mean Square.
- **SAR:** Synthetic Aperture Radar
- **SFDU:** Standard Formatted data Unit
- **SGDR:** Sensor Geophysical Data Record(s)

- **Sigma 0:** or sigma-naught, or backscatter coefficient, reflexivity coefficient of the radar wave on the surface.
- **Significant Wave Height (SWH):** Symbol H_s or $H_{1/3}$. The significant wave height is obtained by analyzing the shape and intensity of the altimeter radar beam reflected from the sea surface (radar echo). A long time delay in the return signal indicates that waves are high and, conversely, a short delay indicates that the sea surface is calm.
- **SIRAL:** altimeter onboard CryoSat.
- **SLA:** Sea Level Anomalies or SSHA (Sea Surface Height Anomalies)
- Difference between the observed sea surface height and the mean sea level. The SLA allows us to monitor ocean variability due to seasonal variations and climatic phenomena such as El Niño. Sea level variability (the standard deviation over time) is somewhere between 2-3 cm and 60 cm, depending on energy levels in different parts of the ocean. For altimetry data, these anomalies are not usually computed with respect to a seasonal mean, but to a multi-annual mean.
- **SLH:** Sea Level Height
- **SLR:** Satellite Laser Ranging
- **SSALT:** Solid State radar ALTimeter
- **SSALTO:** Segment Sol multimissions d'ALTimètrie, d'Orbitographie et de localisation précise. CNES multimission ground segment
- **SSB:**Sea State Bias due to the sea-surface state, which consists of two components: electromagnetic bias and tracker bias.
- **SSDP:**Segment Sol DORIS/Poseidon, DORIS/Poseidon ground segment
- **SSDT:** Sea Surface Dynamic Topography
- **SSH:**Sea Surface Height measured by altimetry. Not the sea's depth (i.e., the distance from the surface to the ocean floor), but a height measured with respect to an arbitrary reference level, called the reference ellipsoid. The sea surface height includes the geoid and the dynamic topography, which is the height due to ocean circulation. This dynamic topography includes a permanent component (permanent circulation) and a highly variable component driven by variations in currents, winds, tides, surface temperatures, and so on.
- **SSHA:** Sea Surface Height Anomalies see Sea Level Anomalies (SLA)
- **SSS:** Sea Surface Salinity
- **SST:** Sea Surface Temperature Water temperature at the ocean surface. The SST can be measured by satellite-based infrared radiometers.

- **TDRS:** Tracking and Data Relay Satellite System
- **TGS:** Topex Ground Segment
- **Thermocline:** Zone between the colder water of the ocean depths and warmer surface water. Large temperature variations occur with depth in the thermocline zone. Near the surface, however, where water is always in motion, and in the ocean depths where there is no source of heat, the water temperature is fairly uniform.
- **Thermohaline circulation:** Large-scale global ocean circulation driven by variations in the temperature and salinity of water masses. Cooled and saline waters downwell at high latitudes (off the coast of Norway and Greenland). Waters warmed in the Tropics upwell to the surface, where they are cooled, and so on. It is estimated that a single water molecule takes about 1,000 years to complete the circuit.
- **Tide:** Variation in sea level due to the gravitational attraction of the Sun and Moon. Tides can be higher than seven metres in certain harbours. As well as ocean tides, Earth tides describe variations in the solid Earth caused by these gravitational forces.
- **TMR:** Topex Microwave Radiometer, Radiometer onboard Topex/Poseidon

- **Topex:** Ocean TOPOgraphy Experiment. One of the 2 altimeters (Nasa) onboard Topex/Poseidon.
- **Topex/Poseidon:** Altimetric satellite (Nasa/Cnes)
- **T/P:** Topex/Poseidon
- **TRSR:** Turbo Rogue Space Receiver. One of three positioning systems on Jason-1 that uses the GPS to determine the satellite's position.

- **UTC:** Universal Time Coordinated. Timekeeping system that relies on atomic clocks to provide accurate measurements of the second, while remaining coordinated with the Earth's rotation, which is much more irregular. To stay synchronised, UTC has to be adjusted every so often by adding one second to the day, called a leap second, usually between June 30 and July 1, or between December 31 and January 1. This is achieved by counting 23h59'59", 23h59'60" then 00h00'00". This correction means that the Sun is always at its zenith at noon exactly (accurate to the second)
- **UCL:** University College London

- **Waveform:** The magnitude and shape of the radar altimetry return echoes
- **Wet tropospheric correction:** Water vapor in the atmosphere slows the radar pulse. This effect can generate mean errors of the order of 15 centimetres on altimetry measurements. The value of the correction applied is determined using measurements by radiometer on the satellite.
- **WITTEX:** Water Inclination Topography and Technology Experiment
- **WOCE:** WOWorld Ocean Circulation Experiment
- **WSOA:** Wide-Swath Ocean Altimeter

- **ZWD:** Zenith Wet Delay